Geochemistry of mine and spoil drainage in the Durham Coalfield

Elizabeth Louise Ander

Submitted for the degrees of

Doctor of Philosophy
of the University of London

&

the Diploma
of Imperial College

September 1998

Environmental Geochemistry Research Group
T.H. Huxley School of Environment, Earth Science & Engineering
Royal School of Mines
Imperial College of Science, Technology & Medicine
University of London

Abstract

The run down of the coal industry in Britain has resulted in the abandonment of many mines. The drainages from such abandoned workings are frequently characterised by high concentrations of metal ions, SO_4 and low pH values at their point of discharge into surface waters, and are a cause of environmental concern. The Durham coalfield with its long history of mining is typical of the old mining areas with a large number of abandoned mines and spoil heaps. The aim of this research was to describe the chemistry of abandoned coal mine and spoil heap discharges, the chemical data then being used to understanding the processes controlling the hydrogeochemistry of the discharge points and the receiving streams

Suitable sites were used for sampling of waters and sediments to determine dissolved and suspended aqueous chemistry and stream sediment chemistry and mineralogy. The sampling program was carried out on 6 occasions, allowing the collection of data under flood, low flow and intermediate conditions. Eight points of discharge were selected for sampling and at 3 of these monitoring continued downstream from the point of discharge. Samples were analysed in the field and laboratory and a method of determining the Fe^{II} /Fe^{III} couple in natural waters was developed. Hydrogeochemical modelling was undertaken using PHREEQ-C.

Comparison of results between the points of discharge showed that the broad characteristics of spoil heap drainage are different to those of deep mines. The deep mine discharge sites were characterised by the temporally consistent chemical compositions of the drainages, the dissolved phase being characterised by Fe and SO_4 water types. The exact composition of the waters varied spatially between sampling locations, but were stable temporally over the 2 years in which sampling was undertaken. The precipitation of ferrihydrite has been postulated to control the chemistry of the aqueous phase, with the formation of goethite as an ageing product.

The spoil heap discharge chemistries, in contrast were found to be variable in composition over several orders of magnitude. The variation in the discharge chemistries was found (qualitatively) to be related to the stream flow volumes. Low flow conditions were associated with the lowest pH and highest concentrations of ions such as Fe, SO_4, Al, Zn and Cu: the converse was true for periods of high flow. A more complex assemblage of precipitated minerals was found to form from the low pH high ion concentration waters, otherwise the precipitate was dominated by ferrihydrite. Sampling took place on a temporal scale of months, over a period of 2 years, and the fluctuations observed were responses to short term precipitation events.

Concentration of ions downstream from the point of discharge were controlled by dilution and reaction. The rate of reaction removing Fe from solution was found to be greater when the concentrations of ions were highest, and stream flow lowest. This is attributed to the higher temperature and more extreme conditions leading to a greater rate of reaction, and the lower competence of the stream resulting in more rapid removal of ions from solution. Another factor could be the increased surface area to volume ratio of a stream in low flow allowing more rapid oxidation of Fe^{II} by aqueous O_2 derived from equilibrium with the atmosphere and thus increasing the rate of reaction of Fe, which controls the stream chemistry.

Acknowledgements

I should like to thank all the people who have helped me complete this research. Firstly my supervisors, Iain Thornton and Margaret Farago for their help. This project was funded by a NERC CASE award, and Rio Tinto were the industrial partners. I should like to thank Chris Cross and Dave Richards (Rio Tinto) for their assistance, particularly with setting up the project and Chris for his logistical support throughout the duration of the PhD. Lorraine Webber and Kelly Dibble (formerly Anamet Services) were very helpful to me on my visits to Avonmouth. Paul Younger and Julia Sherwood (University of Newcastle-upon-Tyne) are thanked for their help, which was instrumental in selecting study sites in the Durham Coalfield.

I should like to acknowledge Ron Fuge (University of Wales, Aberystwyth) for his invaluable enthusiasm in the collaborative research we undertook in Aber and presented in Utah, and when reading parts of this thesis and engaging in discussion over aspects of the results with me. Oh, and the vast numbers of beers in "The Mill"!

The use of analytical facilities in the (former) Geology Department at Imperial was made possible by the help of Alban Doyle, Dick Giddens, Martin Gill, Krys St Clair Gribble, Lizzie Morris, Mike Ramsey and Pete Watkins. I should also like to particularly thank Barry Coles who not only ran all ICP analyses, but was also a source of knowledgeable assistance and infinite patience with my many computing problems and understanding of statistics.

I would like to thank the other members, past and present, of EGRG who helped in a multitude of ways whilst I was studying, particularly Peter Kavanagh, Walter Daesslé Heuser, Clare Gee, Emma Tristán, Keith Whitehead, Myung-Chae Jung, and John Watt. I should also like to thank Barry, Emma, Paul Schofield and Dave Dewhurst for their help in the production of this thesis.

The preservation of my sanity owes much to the social life which exists in the Geology Department here and, in addition to those already mentioned above, Sarah Gleeson, Gary Hampson, Richard Jolly, Jamie Wilkinson and Matt Jackson are among those who made sure it was never a case of "all work and no play". Cheers!!

Elizabeth, Staffan and Rebecca are thanked, as always, for their continued support.

Contents

Abstract i

Acknowledgements ii

Contents iii

List of tables viii

List of figures ix

List of plates xii

List of equations xiii

1.0 Introduction 1

1.1 Introduction to the research 1

1.2 Aims and objectives of the research 2

1.3 Structure of the thesis 4

2.0 Coal mine and spoil drainage geochemistry and management issues 5

2.1 Hydrogeochemistry of coal mine drainage 5

2.1.1 Comparison of coal and metalliferous mine and spoil drainage in Britain 5

2.2.1a Pyrite occurrence in coal and associated sediments 16

2.2.1b Iron(II) sulphates 17

2.2.2 Buffering of H^+ generated in pyrite oxidation 17

2.2.2a Occurrence of potential buffering minerals in coal and associated sediments 20

2.2.2b Aqueous speciation and mineral saturation 21

2.2.3 Fe^{II} oxidation 22

2.2.3a Chemical and electrode determination of Eh 23

2.2.3b Determination of the dissolved component of aqueous samples 25

2.2.4 Fe^{III} hydrolysis 27

2.2.5 Fe^{III} precipitate mineralogy 27

2.2.5a Goethite 28

2.2.5b Ferrihydrite 29

2.2.5c Schwertmannite 30

2.2.5d Jarosite minerals 31

2.3 Minor and trace ion geochemistry in mine and spoil drainage 31

2.3.1 Sources of aqueous minor and trace ions 31

2.3.2 Aluminium precipitation 32

2.3.3 Manganese precipitation 34

2.3.4 Sorption of trace and minor ions on suspended material in stream waters 34

2.4 Management of abandoned mine and spoil drainage in Britain 35

2.4.1 Legislative context 35

2.4.2 Effects of mine and spoil drainage 36

2.4.3 Remedial options for abandoned coal mine and spoil heap drainage 38

2.5 Summary 38

3.0 Regional and local context of study sites **40**
3.1 Location and physical setting of the Durham Coalfield **40**
3.2 Geology of the Durham Coalfield **42**
3.2.1 Carboniferous Period *42*
3.2.1a Coal Measures 42
3.2.1b Mineralisation in the Coal Measure sediments 43
3.2.2 Post-Carboniferous *47*
3.2.2a Permian 47
3.2.2b Quaternary 47
3.2.2c Igneous 48
3.2.3 Structure *48*
3.3 Hydrology of the Durham Coalfield **48**
3.3.1 Physical hydrology *48*
3.3.2 Physical hydrogeology *48*
3.3.3 Hydrogeochemistry of surface water and stream sediments *50*
3.3.4 Hydrogeochemistry of groundwater *50*
3.3.4a Chemistry of waters in an undisturbed Coal Measures aquifer 50
3.3.4b Chemistry of waters in an actively mined Coal Measures aquifer 52
3.3.4c Chemistry of waters in an abandoned, mined Coal Measures aquifer 52
3.4 Description of the study sites **53**
3.4.1 Deep mine drainage *54*
3.4.1a Broken Banks (BB) 54
3.4.1b Edmondsley Yard Drift (EY) 54
3.4.1c Low Lands (LL) 54
3.4.1d Stony Heap (SH) 54
3.4.1e Tindale Colliery (TC) 55
3.4.2 Spoil heap drainage *55*
3.4.2a Helmington Row (HR) 55
3.4.2b Quaking Houses (QH) 55
3.4.2c Willington (WG) 56
3.5 Historical and Present management of the Durham Coalfield **56**
3.6 Summary **56**

4.0 Sample collection and analytical methods **64**
4.1 Field sampling protocol **64**
4.1.1 Site Selection *64*
4.1.2 Sampling Location Selection *64*
4.1.3 Sampling Frequency *64*
4.2 Sample collection methods **65**
4.2.1 Waters *65*
4.2.2 Suspended Sediment *66*
4.2.3 Stream Sediment Samples *66*

4.3 Analytical Methods **66**
4.3.1 Stream Waters: Physico-chemical analyses *67*
4.3.1a Eh and pH 67
4.3.1b Dissolved oxygen 67
4.3.1c Major cations 67
4.3.1d Minor and trace ions 67
4.3.1e Arsenic, Sb and Bi 68
4.3.1f Sulphate and Cl^- 68
4.3.1g Alkalinity 68
4.3.1h Iron(II) and Fe^{III} by colorimetry 69
4.3.2 Stream Waters: Discharge measurements *70*
4.3.3 Suspended Sediment *70*
4.3.4 Stream Sediments and minewater precipitates *71*
4.4 Data Quality Control **71**
4.4.1 Detection Limit *71*
4.4.2 Bias *72*
4.4.3 Precision *73*
4.5 Mineralogical analysis of sediments and iron rich precipitates **75**
4.5.1 X-ray powder diffraction *75*
4.5.2 Scanning electron microscopy *77*
4.5.2a Compositional analysis 77
4.5.2b Topographical analysis 80
4.6 Hydrogeochemical modelling of water data **82**
4.6.1 PHREEQ-C modelling package *82*
4.6.2 Advantages and limitations of using a hydrogeochemical modelling package *82*
4.7 Summary **84**

5.0 Characteristics of the discharge localities **85**
5.1 Deep mine drainage **85**
5.1.1 Physical characteristics *85*
5.1.2 Aqueous chemistry: Major ions *85*
5.1.3 Aqueous chemistry: Minor and trace ions *94*
5.1.4 Suspended sediment *96*
5.1.5 Minewater precipitate mineralogy *96*
5.1.6 Ochre cores *99*
5.1.7 Deep mine summary *104*
5.2 Spoil heap drainage **106**
5.2.1 Physical characteristics *106*
5.2.2 Aqueous chemistry: Major ions *106*
5.2.4 Suspended sediment *114*
5.2.5 Spoil heap discharge precipitate mineralogy *116*

5.3 Measurement of Fe^{II} and Fe^{III} in different filter fractions 122
5.3.2 Eh measurement, comparison of results by different methods 123
5.3.3 Sensitivity analyses of modelling, with respect to filter pore size and Eh measurement method 125
5.3.4 Summary of filtering and modelling results 126
5.4 Summary 126

6.0 Hydrogeochemistry of ferruginous drainage from abandoned coal mines and spoil heaps 127
6.1 Controls on major ion chemistry of deep mine drainage 127
6.1.1 Conceptual model of local hydrogeological conditions in the aquifers of the mines studied 127
6.1.2 Major ion chemistry 128
6.1.3 Pyrite oxidation 131
6.1.4 Buffering of water chemistry 135
6.1.5 Precipitation of ochre from mine drainage 137
6.1.6 Deep mine drainage summary 140
6.2 Spoil heap discharge geochemistry 141
6.2.1 Pyrite oxidation & buffering of pH 141
6.2.2 Mineralogy of precipitates 146
6.2.3 Spoil heap discharge summary 148
6.3 Minor and trace element hydrogeochemistry from mine and spoil workings 149
6.3.1 Effect of Eh and pH 149
6.3.2 Effect of SO_4 on trace and minor ions 152
6.4 Hydrogeochemical modelling 152
6.5 Summary 154

7.0 Results of geochemistry downstream from discharge points 156
7.1 Stony Heap 156
7.1.1 Physical characteristics 156
7.1.2 Aqueous chemistry: major ions 156
7.1.3 Aqueous chemistry: minor & trace ions 166
7.1.4 Stream sediment chemistry 169
7.2 Helmington Row 171
7.2.1 Physical characteristics 171
7.2.2 Aqueous chemistry: major ions 171
7.2.3 Aqueous chemistry: minor and trace ions 181
7.2.4 Stream sediments 188
7.3 Quaking Houses 191
7.3.1 Physical characteristics 191
7.3.2 Aqueous chemistry: major ions 191
7.3.3 Aqueous chemistry: minor and trace ions 201
7.3.4 Stream precipitate chemistry 201
7.4 Summary 204

8.0 Processes controlling chemistry downstream from coal mine and spoil water discharge 205
8.1 Controls on major ion chemistry downstream from mine and spoil discharge 205
8.1.1 Dilution 205
8.1.2 Reactive loss from the aqueous phase 210
8.1.4 Major ion summary 224
8.2 Factors affecting minor and trace element chemistry 225
8.2.1 Mechanisms controlling Al, Zn and Cu 225
8.2.2 Mechanisms controlling Mn concentrations 228
8.2.3 Minor and trace ion summary 232
8.3 Factors controlling the toxicity of the waters 232
8.3.1 Consideration of results obtained in this study in a statuary water quality context 233
8.3.2 Comparison of the water and stream sediment quality in relation to background concentrations 233
8.4 Disequilibria observed in this study 234
8.4.1 Chemical disequilibria 234
8.4.2 Aqueous - solid phase disequilibria 235
8.4.3 Aqueous disequilibria as a result of sampling artefacts 235
8.5 Summary 236
9.0 Summary, conclusions and future research 237
9.1 Summary 237
9.2 Conclusions 239
9.3 General considerations 244
9.4 Recommendations for further work 244
References 246
Appendices 263
Appendix I: Summary information on sampling locations 264
II.i Analytical Techniques - Water 265
II.ii Analytical Techniques - Suspended sediment 270
II.iii Analytical Techniques - Sediments and Soils 272
III Data quality analysis results 274
IV Analytical results 275

List of tables

Table 2.1: Comparative chemical data for abandoned coal mine drainage in Britain..... 8

Table 2.2: Selected metalliferous mine drainage composition in Britain..... 12

Table 2.3: Selected coal mine drainage composition from studies outside Britain. 12

Table 2.4 : Carbonate contents of some shales in coal measure sediments, Pennsylvania 21

Table 2.5: The maximum permissible concentrations of Zn and Cu in salmonoid rivers. 37

Table 4.1: Diagnostic d-line spacings for commonly occurring minerals in mine drainage waters..... 78

Table 5.1: Iron concentrations and modelled speciation in deep mine water discharge. 92

Table 5.2: The speciation of Ca, Mg and Ba as affected by SO_4 in deep mine drainage. 92

Table 5.3: Trace and minor ion mean concentrations for deep mine drainage sites. 94

Table 5.4: The speciation of Ca, Ba and Al^{III} as affected by SO_4 in spoil heap drainage. 111

Table 5.5: Concentration of selected elements in precipitate at HR spoil heap drainage discharge site..... 116

Table 5.6: Chemical results for HR discharge site using SEM analysis 119

Table 5.7: Selected saturation indices (SI) for Fe in solution..... 121

Table 5.8: Selected saturation indices (SI) for Al in solution..... 121

Table 5.9: Comparison of aqueous chemistry arising from filtering a different nominal pore sizes. 122

Table 5.10: Comparison of different Eh measurement methods on predicted saturation indices..... 124

Table 6.1: Summary of mean chemical composition of discharge at BB, EY and SH. 129

Table 6.2: Modelling of pyrite oxidation using measured deep mine drainage data. ... 134

Table 6.3: Modelling of acidity buffering reactions in deep mine drainage..... 134

Table 7.1: Concentrations of selected ions in precipitates at the discharge and downstream from HR 188

Table 7.2: Iron(II) speciation predicted by PHREEQ-C for QH downstream from the discharge in July 1995..... 199

Table 8.1: The potential acidity due to Fe^{II} at SH and HR discharge localities..... 232

List of figures

Figure 2.1: The coalfields of Britain. 6

Figure 2.2: The major metalliferous mining regions of Britain. 7

Figure 2.3: Chemistry of mine drainage recorded from the South Wales coalfield from the report of NRA (1994a). 10

Figure 2.4: The stability fields of Fe species. 15

Figure 2.5: Speciation of dissolved inorganic carbon (DIC) 18

Figure 2.6: Stability fields of Al-SO_4 phases which may form from acid mine drainage. 33

Figure 2.7: Stability fields of Mn species in natural waters 34

Figure 3.1: Geography and geology of the Durham Coalfield sampling region. 41

Figure 3.2: The lithological sequence of the Durham Coalfield 44

Figure 3.3: Conceptual model of groundwater flow during- and post- mining in County Durham 51

Figure 3.4: Map of Stony Heap stream system and sampling locations 57

Figure 3.5: Map of Helmington Row stream system and sampling locations. Including Willington discharge site. 58

Figure 3.6: Map of Quaking Houses stream system and sampling locations 59

Figure 3.7: Maps of sites monitored only at the point of discharge (a) Broken Banks (b) Edmondsley Yard Drift (c) Low Lands (d) Tindale Colliery 60

Figure 4.1: Robust ANOVA analysis 74

Figure 4.2: XRD plots for sample SH06 used to compare the benefit of different step-times. 76

Figure 4.3: Typical XRD plots for the minerals commonly found in mine drainage waters 79

Figure 5.1: Eh - pH values recorded at mine and spoil discharge sites. 86

Figure 5.2: Triangular plots of major ion chemistry at deep mine discharge locations. . 87

Figure 5.3: Sodium and Cl molar concentrations in mine and spoil drainage. 88

Figure 5.4: Triangular diagram of major cations in deep mine drainage, including Fe. . 89

Figure 5.5: Temporal variability in pH and selected major ions measured in spoil heap and deep mine drainage. 90

Figure 5.6: Deep mine drainage S speciation. 93

Figure 5.7: Temporal variability of Mn and Al concentrations in spoil heap and deep mine drainage at the study sites 95

Figure 5.8: Diffraction pattern of ochreous material at BB 99

Figure 5.9: SEM-EDS spectra for deep mine ochres. 100

Figure 5.10: Downcore chemistry at EY and SH.. 103
Figure 5.11: X-ray diffraction of ochre cores at EY and SH..... 105
Figure 5.12: Triangular plots of major ion chemistry at spoil heap discharge locations.. 108
Figure 5.13: Proportion of dissolved S(VI) predicted to be in the species shown by the program PHREEQ-C. 111
Figure 5.14: Comparison of pH and dissolved Al, Cu and Zn concentrations at the point of discharge. 113
Figure 5.15: Concentrations of selected ions in suspended sediment from spoil heap and deep mine drainage.. 115
Figure 5.16: X-ray diffraction results for ochre at Helmington Row discharge site..... 120
Figure 5.17: Comparison of Fe concentrations in waters filtered at 0.2μm or 0.1μm with filtering at 0.45μm. 123
Figure 5.18: Comparison of the effect of filtering at different pore sizes and measuring Eh by different methods on the predicted SI of amorphous $Fe(OH)_3$..... 125

Figure 6.1: Comparison of Fe and SO_4 concentrations measured in this study with abandoned mine drainage in the South Wales coalfield. 131
Figure 6.2: Comparison of spoil heap Fe and SO_4 with theoretical ratios from pyrite oxidation reactions. 144
Figure 6.3: Comparison of Mn concentrations and DO concentrations in discharge from abandoned spoil heaps and coal mines 149

Figure 7.1: Downstream variations of selected parameters at SH. 157
Figure 7.2: Triangular plot of major ion chemistry at SH..... 159
Figure 7.3: Downstream variations in selected ions. 160
Figure 7.4: Comparison of molar concentrations or ratios at SH.. 164
Figure 7.5: Downstream variations in Fe loading in the stream system at SH..... 165
Figure 7.6: Downstream variations in Mn loading in the stream system at SH. 167
Figure 7.7: Downstream variations in Zn loading in the stream system at SH 168
Figure 7.8: Variations in the concentration of Fe and Mn in stream sediments downstream from SH discharge. 170
Figure 7.9: Downstream variations of selected parameters at HR..... 172
Figure 7.10: Triangular diagram of major ion chemistry at HR. 173
Figure 7.11: Physical and chemical partitioning of Ca in the HR stream system..... 175
Figure 7.12: Downstream variations in selected ions at HR.. 176
Figure 7.13: Molar ratios of conservative and reactive elements downstream from source at HR. 179
Figure 7.14: Downstream variations in Fe loading in the stream system at HR..... 180
Figure 7.15: Downstream variations in selected ions.. 182

Figure 7.16: Downstream variations in Mn and Al loading in the stream system at HR.. 184

Figure 7.17: Molar ratios of selected ions at HR to study reactive loss and dilution from source..... 186

Figure 7.18: Relationship between aqueous and suspended sediment Cu and Zn with Fe_{ss} and pH at HR. 187

Figure 7.19: Concentrations of selected elements in stream sediments downstream from source at HR..... 189

Figure 7.20: XRD diffraction patterns for the discharge point and a downstream location on two sampling occasions. 190

Figure 7.21: Concentrations of Al and Zn in stream sediments downstream from HR 192

Figure 7.22: Downstream variations of selected parameters at QH..... 193

Figure 7.23: Triangular diagram of the major ion chemistry at Quaking Houses 194

Figure 7.24: Composition of waters compared to a NaCl mixing line..... 195

Figure 7.25: Downstream variations in selected ions. 196

Figure 7.26: Downstream variations in Fe loading in the stream system at QH.. 200

Figure 7.27: Downstream variations in selected ions. 202

Figure 7.28: Concentrations of Fe in stream sediments downstream from source at QH. 204

Figure 8.1: Simple inverse modelling results for pH using measured Fe at SH and HR. 216

Figure 8.2: Comparison of the concentrations of pH and selected ions downstream from the points of discharge. 218

Figure 8.3: Reactive loss of Al, Fe and Mn along the stream length of the discharge sites..... 231

List of plates

Plate 3.1: Tindale Colliery discharge. 62
Plate 3.2: Willington discharge 63

Plate 4.1: The ochre loading, without disaggregation, for SEM analysis 81

Plate 5.1: Broken Banks deep mine discharge 97
Plate 5.2: SEM images of ochreous material at SH. 98
Plate 5.3: Edmondsley Yard Drift (EY) core sample 101
Plate 5.4: Stony Heap (SH) location and core collected. 102
Plate 5.5: Quaking Houses (QH) spoil heap drainage, showing the variation in discharge between low flow and high flow conditions. 107
Plate 5.6: Helmington Row (HR) spoil heap discharge. 117

Plate 6.1: Low Lands spoil heap and mine drainage 142

Plate 8.1: Edmondsley Yard Drift discharge in high and low flow of receiving water. 207

List of equations

Eq. 2.1: Oxidation of pyrite by O_2 14
Eq. 2.2: Oxidation of Fe^{2+} 14
Eq. 2.3: Hydrolysis of Fe^{3+} 14
Eq. 2.4: Oxidation of pyrite by Fe^{3+} 14
Eq. 2.5: Proton induced dissolution of calcite 18
Eq. 2.6: Proton induced dissolution of dolomite 18
Eq. 2.7: Oxidation of pyrite in the presence of calcite 18
Eq. 2.8: Proton induced dissolution of siderite, precipitating Fe^{III} 19
Eq. 2.9: Proton induced dissolution of siderite 19
Eq. 2.10: Sulphate reduction 19
Eq. 2.11: The acid dissolution of K-feldspar to form kaolinite) 20
Eq. 2.12: Saturation index calculation 22
Eq. 2.13 The Nernst Equation 23
Eq. 2.14 The Nernst Equation for the Fe^{2+}/Fe^{3+} couple 23
Eq. 2.15: Ageing of schwertmannite to goethite 30
Eq. 2.16: Precipitation of jarosite minerals 31

Eq. 5.1: The molar relation of Na, Ba and Cl mixing 88

Eq. 2.1: Oxidation of pyrite by O_2 132
Eq. 2.4: Oxidation of pyrite by Fe^{3+} 132

Eq. 8.1: Oxidation and hydrolysis of Mn^{II} 230

1.0 Introduction

This chapter introduces the research and the rationale of the work undertaken in the completion of this thesis. A broad introduction to the context of the investigation is contained in section 1.1, which leads on to the specific aims and objectives of the project in section 1.2. Finally the layout of the thesis is shown in section 1.3. This organises the dissemination of the information acquired in this study around the thesis aims.

1.1 Introduction to the research

The geochemistry of drainage from several abandoned coal mines and spoil heaps is investigated. Uncontrolled mine and spoil drainages occur from abandoned coal and metalliferous mines and wastes and are typically of low pH and high metal ion loading in the dissolved phase. Upon entry into a stream they are often characterised by the precipitation of large volumes of ochreous minerals. Whilst such waters are not consumed directly by humans, their impact on aquatic ecosystems, potable (pre-treatment) water supplies, livestock watering, and amenity value of river drainage systems gives cause for concern at their occurrence. Such ferruginous water is also of concern in Britain due to the absence of provision for remedial treatment under English and Welsh or Scottish law. Thus, with a few, generally recent, exceptions in Cornwall, Glamorgan, Ceredigion and County Durham the rivers are usually subject only to self-remediating processes, subsequent to a mine or spoil water entering from an abandoned working.

The processes controlling the chemistry of waters prior to emergence from the mined or spoil aquifer are of interest, in the understanding of their evolution and composition, and their impact on receiving waters. For this reason, a sampling program at eight localities in County Durham was instigated to monitor the chemistry of discharge localities.

County Durham has a long (>300 years) history of coal extraction from deep workings. As regions of the coalfield were exhausted and abandoned, so the local groundwater table was left to rebound, uncontrolled, after the cessation of mining. Many spoil heaps also exist in the area, and whilst many of these have been landscaped and made safe from a ground stability viewpoint, they generate equally ferruginous waters to those emanating from coal mines, thus, both types of discharge are studied in this research.

The discharge localities are of both deep mine and spoil heap types. Sampling was undertaken on up to 6 occasions at each site, over a period of two years. The repeated sampling strategy enables the chemical stability of the discharge sites to be assessed and any similar characteristics between sites to be established.

Concomitant with the sampling of discharge localities was the selection of 3 of these sites to study downstream dispersion in the surface hydrological system. Of these streams, 2 were subject to dilution (in all but the driest weather) as soon as they emerged, whilst one was not subject to dilution within 1 km downstream from the point of emergence.

1.2 Aims and objectives of the research

The research undertaken is thus based on the following rationale: firstly, establishing the controls on the chemical composition of 2 types of ferruginous drainage in differing hydrological conditions; secondly, establishing the factors controlling the chemistry of the discharges downstream from the point of emergence; and finally, the methods used to achieve the above targets. These are divided into 3 aims, which will be reflected in the structure of this report (see below), each of which has specific objectives in achieving that aim. These are listed below (following page):

Aim 1:

To understand the processes controlling the chemistry of deep mine and spoil heap drainage

Specific objectives:

I.a) Describe the chemistry of deep mine drainage, highlighting any characteristics specific to this type of discharge.

I.b) Describe the controls on the observed fluctuations

II.a) Describe the chemistry of spoil heap drainage, highlighting any characteristics specific to this type of discharge.

II.b) Describe the controls on the observed fluctuations

Aim 2:

To understand the controls on the chemical fluctuations observed downstream from coal mine or spoil drainage into receiving water courses

Specific objectives:

I.a) Study the chemical variations observed on a temporal basis at each site

I.b) Compare those fluctuations between different sites

I.c) Describe the controls on the observed fluctuations

II.a) Describe the implications of the fluctuations observed, with respect to toxicity assessment and geochemical monitoring of such streams

Aim 3:

To utilise appropriate techniques for assessing the chemical composition of the aqueous and solid phases studied

Specific objectives:

I.a) Increase the range of protocols used as methods are developed and equipment becomes available, during the study

I.b) Analyse the mineralogical and chemical composition of precipitates formed in the streams

I.c) Use geochemical modelling to assess the aqueous speciation and saturation indices of the aqueous phase samples

1.3 Structure of the thesis

Chapter 2 next provides a brief review to previous work pertinent to this research. This includes research into the evolution of ferruginous waters from mines and spoil heaps, and the typical controls on the ions thus discharged into the surface hydrological environment. Chapter 3 then provides a summary of the physical and chemical characteristics of the specific field location of the Durham Coalfield and the discharge points selected for investigation. The available information on the geochemistry and mineralogy of the hydrogeological system of mined Coal Measure and spoil heap aquifers is summarised. The sampling sites are then described. Chapter 4 reviews the methods used in sampling, analysis and interpretation of data. Here a parallel study into the application of a field sampling technique for subsequent laboratory analysis is briefly reported. This work allowed the studied method to be implemented on a subsequent field sampling session for this research. This section includes the work which achieves aim 3.

The results are then divided according to the first two objectives. Chapter 5 describes the chemistry of abandoned deep mine and spoil heap waters from 8 localities, the discussion of these data can then be found in chapter 6 (aim 1). The description of the chemical data downstream from 3 of the points of discharge can be found in chapter 7 and the data is discussed in chapter 8 (aim 2). The conclusions from this study are then summarised in chapter 9, according to the objectives as described above. Chapter 9 is then completed by an appraisal of future research potential arising from this thesis.

2.0 Coal mine and spoil drainage geochemistry and management issues

This chapter will briefly review the previous literature pertaining to aspects of mine and spoil drainage studied in this research. The chapter begins (section 2.1) with a review of the general chemical composition of coal and metalliferous mine drainage in Britain, highlighting the chemical differences that exist between two types of discharge in Britain. This will be followed (sections 2.2 and 2.3) by a brief review of the processes of pyrite oxidation and the reactions associated with pyrite oxidation, which are expected to take place. There exists a large body of literature on these subjects, reference will be made as appropriate to suitable research and review papers, to which the reader is directed for more information. This chapter concludes with a summary of the management methods which have been used for the amelioration of the impacts of mine and spoil drainage.

2.1 Hydrogeochemistry of coal mine drainage

2.1.1 Comparison of coal and metalliferous mine and spoil drainage in Britain

The coalfields (figure 2.1) and metalliferous mining regions (figure 2.2) of Britain have long been associated with water discharges from abandoned mines (e.g. Carpenter, 1924), which are sources of metal ions and SO_4 (dominantly), and potential lowering of stream pH at, and downstream from, the point of discharge. This section will review some of the large body of literature that exists upon this subject.

The Durham Coalfield has been the subject of much research since the closure of all the deep mines in this region in 1993 (section 3.5). The publications of Younger, in particular, have dealt with this subject and have published geochemical data on the discharges arising from abandoned mine and spoil heap sites in the Durham Coalfield (Younger & Sherwood, 1993; Younger & Bradley, 1994; Younger, 1995a; Younger, 1997a; Younger *et al.*, 1997). The sites which have been studied by those workers, and are also part of this study, are referred in the appropriate sections of chapter 3, as well as being referred to here. These studies have generally shown the pH of the mine drainages to be circum-neutral, with varying concentrations of Fe (1.8-26 mg l^{-1}) and SO_4 (137-325 mg l^{-1}) (Younger, 1995b) and are of samples collected after 1993 from the discharges. These data and other selected data from studies of British coalfields are summarised in table 2.1. These show that discharge chemistries from abandoned coal mines are largely circum-neutral pH, and of moderately high Fe and SO_4, which are the direct products of pyrite oxidation (section 2.2) which causes this ferruginous drainage to



Figure 2.1: The coalfields of Britain (adapted from: Ordnance Survey, 1945a,b; Rae, 1978; Rippon, 1997).

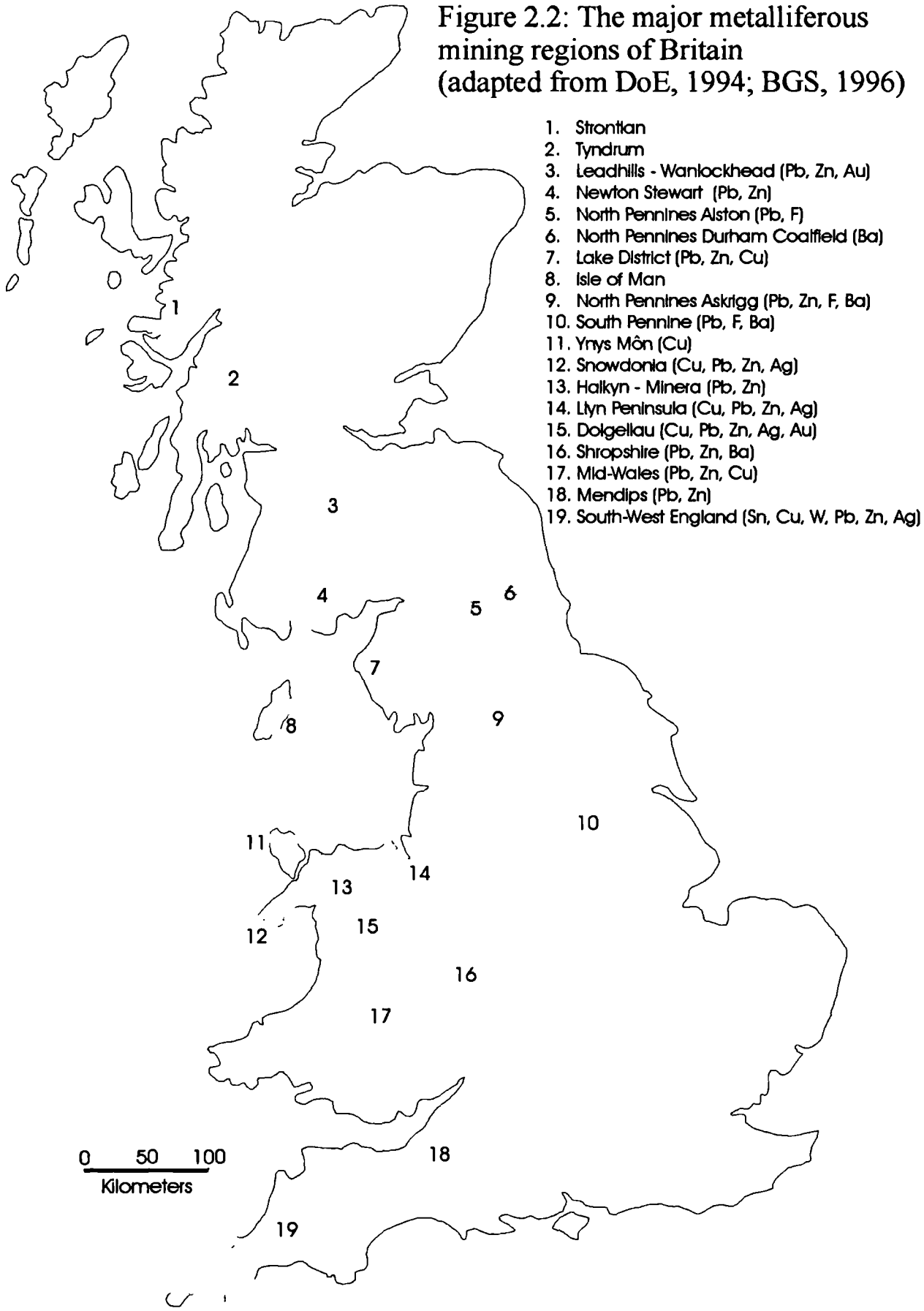


Figure 2.2: The major metalliferous mining regions of Britain (adapted from DoE, 1994; BGS, 1996)

1. Strontian
2. Tyndrum
3. Leadhills - Wanlockhead (Pb, Zn, Au)
4. Newton Stewart (Pb, Zn)
5. North Pennines Alston (Pb, F)
6. North Pennines Durham Coalfield (Ba)
7. Lake District (Pb, Zn, Cu)
8. Isle of Man
9. North Pennines Askrigg (Pb, Zn, F, Ba)
10. South Pennine (Pb, F, Ba)
11. Ynys Môn (Cu)
12. Snowdonia (Cu, Pb, Zn, Ag)
13. Halkyn - Minera (Pb, Zn)
14. Llyn Peninsula (Cu, Pb, Zn, Ag)
15. Dolgellau (Cu, Pb, Zn, Ag, Au)
16. Shropshire (Pb, Zn, Ba)
17. Mid-Wales (Pb, Zn, Cu)
18. Mendips (Pb, Zn)
19. South-West England (Sn, Cu, W, Pb, Zn, Ag)

Table 2.1: Comparative chemical data for abandoned coal mine drainage in Britain.

Coalfield	pH	D.O.	Fe	SO_4	Ca	Alkalinity	Na	Cl	Al	Mn	Zn	Cu	Ref.
		mg l^{-1}	mg l^{-1}	mg l^{-1}	mg l^{-1}	mg l^{-1}	mg l^{-1}	mg l^{-1}	µg l^{-1}	µg l^{-1}	µg l^{-1}	µg l^{-1}	
S. Wales	6.92 (0.78)	6.8 (4.7)	11.9 (24.1)	229 (294)		143 (153)			29	1238	63	1.6	1 2
S. Wales	5.6		43		29			120 ^		1000 ^	45	20 ^	3
Forest of Dean	6.8		3 ^	900 ^	200 - 400 ^	300 ^			100				4
Fife	4	"reducing"	1200	6000				5000					5 6
Kent													7
S. Wales	3.5-5		300-400 "high"							"high"			
S. Wales	2.8			7244					200	1200	22	90	8
Durham	6.3		26	325	84	188	28	102					

Where there is no value recorded the parameter was not reported. (1) NRA (1994a) (mean of 85 data points in South Wales coalfield) (standard deviation in brackets). (2) Sperring (1995) single site at Garnswllt, Ammanford. (3) Aldous (1987) (data for Norchard Drift discharge only, ^ data approximated from figures for the last sampling occasion). (4) Robins (1990) the Dalquharran mine (NS 266 017) in 1979. (5) Headworth *et al.* (1980). The Tilmanstone mine, Kent (Cretaceous coal). Only Cl recorded as that was the potable water supply "contaminant". (6) Younger (1994). Ynysarwed Colliery (SN 808 017) in 1994. (7) Ineson (1967). Ogilvie Colliery abandoned drainage. (8) Younger (1995b) Stony Heap discharge site.

form. Similar data were also shown by Bradley (1993), Jarvis (1994) and Turner (1994) for the Durham Coalfield.

Table 2.1 show that the Dalquharran mine (Robins, 1990) and Ogilvie Colliery (Ineson, 1967) have pH values much lower, and metal and SO_4 ion concentrations much greater than at the other sites. This lower pH and higher metal ion chemistry is one frequently associated with minewaters when the first discharge to surface after groundwater rebound occurs. This has been studied by Frost (1977) and Aldous (1987). These authors have shown that a decrease in Fe and SO_4 concentrations occur with time after initial discharge, and that the underlying trend of this decrease can be approximated by an exponential decline in Fe concentrations. The half-life (T(1/2)) derived by these workers varies, with Aldous (1987) finding a T(1/2) for the Forest of Dean of 5.5 years, and Frost (1977), for mines in County Durham, a T(1/2) ~2-5 years. Frost (1979) found that the decline in a colliery shaft had a T(1/2) of ~1 year, however. These differences must be attributable to the local aquifer conditions (Frost, 1979). A similar type of decline (T(1/2) not quantified) is shown for Dalquharran coal mine by Robins & Younger (1996), and Zn concentrations in abandoned metalliferous mine drainage by Sadler (1998).

The composition of mine waters can also be highly saline, as was the cause for investigation of the hydrochemistry of coal mine water in the Cretaceous coalfield of Kent (Headworth *et al.*, 1980). This site had a Cl concentration of 5000 mg l^{-1} (Headworth *et al.*, 1980). The composition of brines in the Coal Measures of County Durham is described in section 3.3.4.

The largest collection of data on abandoned coal mine data is that for the South Wales coalfield, published by the NRA (National Rivers Authority, now Environment Agency (EA)) (NRA, 1994a). This data has subsequently been discussed by Davies *et al.* (1997), in the context of freshwater impacts (section 2.4.2). As stated above, the data on abandoned coal mine discharge available for Britain, generally shows a circum-neutral pH, with more variation in the Fe and SO_4 concentrations. Figure 2.3 shows the Fe and SO_4 concentrations, and pH values, summarised in graphical form. Figure 2.3a shows that there appears to be a relationship between the Fe and SO_4 concentrations, with both increasing and decreasing simultaneously. Also shown on figure 2.3a are the ratios of Fe and SO_4 which would be expected to be found in solution by two different pyrite oxidation mechanisms. The line with a slope of 0.5 represents pyrite oxidation by

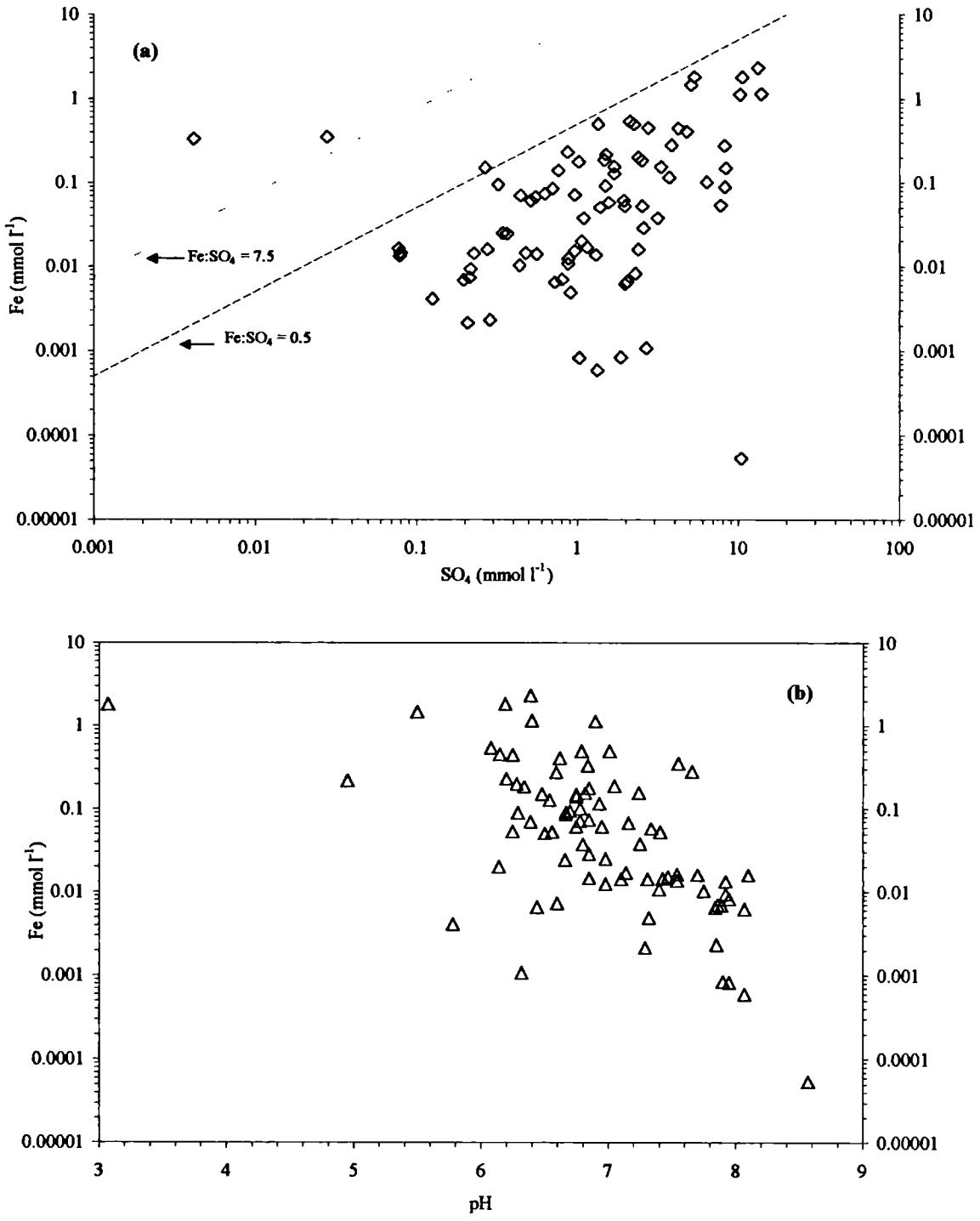


Figure 2.3: Chemistry of mine drainage recorded from the South Wales coalfield from the report of NRA (1994a). (a) The comparison of Fe and SO_4 concentrations at discharge sites. See text for explanation of Fe:SO_4 ratios. (b) Comparison of pH and dissolved Fe concentrations at discharge sites.

oxygen and the line with a slope of 7.5 represents a water chemistry evolved from the oxidation of pyrite by Fe^{3+}. Both these mechanisms are discussed in section 2.2.1. What can be seen directly from this graph is that coal mine drainage in South Wales, generally, shows a SO_4 excess over Fe, from that which would be expected. This will be discussed further in section 6.1.3, and has been noted by Winland *et al.* (1991) who attributed this to Fe^{II} oxidation and consequent Fe^{III} hydrolysis, leaving a SO_4 excess. The chemical composition of deep mine drainages studied in this research are presented in sections 5.1 and 6.1. The data from NRA (1994a) have been summarised in this work, because they represent the largest single database of chemical analyses of coal mine drainage water available. Figure 2.3b shows that the measured pH is the most closely consistent parameter from these drainage, with only 3 sites recording a pH of <5.6, from a total of 85 analyses. The sampling of Sperring (1995) (Ammanford) and Aldous (1987) also showed circum-neutral drainage. Aldous (1987) studied the hydrogeochemical variations over a ~20 year period from the main drainage in the Forest of Dean (Norchard Drift), and described the temporal variations in the chemistry, but the pH recorded and summarised by Aldous (1987) are all >6 from the commencement of surface drainage. Davidson *et al.* (1988) demonstrated the improvement in waters draining colliery spoil heaps with respect to increasing pH values through time.

Few references have been located which specifically deal with the chemistry of waters draining colliery spoil heaps, abandoned or working, in Britain. The drainage from spoil heaps in Yorkshire contains high concentrations of ions in solution (RCEP, 1992), such as 1300-3000 mg l^{-1} Cl, 2600-5500 mg l^{-1} SO_4, 1750-3400 mg l^{-1} Na, 0.1-5.3 mg l^{-1} Fe and 0.1-2.7 mg l^{-1} Mn. These variable chemical compositions are borne out by studies of spoil heaps in the Durham coalfield. Jarvis (1994) noted that the concentrations of other ions could vary immensely at spoil heap discharge, with 66 mg l^{-1} dissolved Al being found by Jarvis (1994), in comparison with 4 mg l^{-1} by Younger & Bradley (1994). The same site (Helmington Row - section 3.4.2) was also sampled by Turner (1994) who found 26 mg l^{-1} Al in solution at the discharge. The chemical composition of spoil heap drainages sampled in this study are presented in section 5.2 and 6.2.

The composition of metalliferous mine drainage is frequently of a much lower pH and concentrations of dissolved ions in solution are much higher (table 2.2), which has caused these to be researched for longer (c.f. Carpenter, 1924) and be of more concern to the regulatory authorities (e.g. DoE, 1994). Metalliferous mining has taken place in carbonate hosted ores (Dunham, 1990) and base poor regions, such as the mineralisation

Table 2.2: Selected metalliferous mine drainage composition in Britain.

Orefield	pH	D.O.	Fe	SO_4	Ca	Alkalinity	Na	Cl	Al	Mn	Zn	Cu	Ref.
		mg l^{-1}	mg l^{-1}	mg l^{-1}	mg l^{-1}	mg l^{-1}	mg l^{-1}	mg l^{-1}	mg l^{-1}	mg l^{-1}	mg l^{-1}	mg l^{-1}	
South-west England	3.4		50								12	1.2	1
Mid-Wales	2.8			441-846	25-32				13.9		38-72	30-68	2
Mid-Wales	5.6			75-78	10-18				0.18		7.8-24	0.005	3
Anglesey	2.5		934	3800	45				174	23	82	74	4

(1) Johnson & Thornton (1987) County Adit discharge. (2) Fuge *et al.* (1991) Lower adit, Cwmrheidol. (3) Fuge *et al.* (1991) Adit, Cwmystwyth. (4) Fuge *et al.* (1994) Lake, Mona Mine

Table 2.3: Selected coal mine drainage composition from studies outside Britain.

Coalfield	pH	D.O.	Fe	SO_4	Ca	Alkalinity	Na	Cl	Al	Mn	Zn	Cu	Ref.
		mg l^{-1}	mg l^{-1}	mg l^{-1}	mg l^{-1}	mg l^{-1}	mg l^{-1}	mg l^{-1}	mg l^{-1}	mg l^{-1}	mg l^{-1}	mg l^{-1}	
Witbank	2.8		193	1440				611	84	9.3			1
Pennsylvannia	2.6		26	2200	150		1.7	13	50	62	9.8		2
Ohio*	4.8		1.44	16	5		4.7	.9	637				3

(1) Bullock & Bell (1997) Witbank coalfield, South Africa. (2) Hem (1985) (2) Ott (1987) Mitchel No. 2 Mine discharge 28/1/82 (3) Winland *et al.* (1991) Ohio coalfield, mean water chemistry analyses *in mmol l^{-1} other than pH

associated with the granite of Cornwall and Devon (BGS, 1996a). The contrasting acid buffering potential gives rise to differing pH values and dissolved ion concentrations. Table 2.2 shows both types of drainage, and demonstrates that ions which are normally at trace (<0.1 mg l^{-1} (Freeze & Cherry, 1979)) concentrations are significantly elevated in some of the examples cited. The dissolved concentrations of elements associated with a carbonate hosted, or carbonate gangue, abandoned mine drainage may be lower than those associated with base poor lithologies (Fuge *et al.*, 1991) and such sites may show a higher pH value (>5) than those often associated with acid mine drainage (<5) (e.g. as shown in table 2.2).

It should be noted that such drainage chemistries as these will cause a negative impact on receiving waters (e.g. Chapman *et al.*, 1983; Fuge *et al.*, 1991; Jarvis, 1994; Johnson, 1986) due to the elevated concentrations of major and minor dissolved ions, which will be controlled by precipitation (section 2.2.5) and sorption (section 2.3) reactions.

2.1.2 Comparison of coal mine drainage in Britain with overseas studies

The hydrogeochemical composition of coal mine waters has most frequently been reported from the eastern coal basin of the USA, of which selected analyses are quoted in table 2.3. What this data shows is that the pH values measured are low (<5) in most cases, and metal ion concentrations are greater than those found for coal mine drainage in Britain (table 2.1). It would seem possible that a geological reason or a mine geometry cause could be invoked, but the other factor which may influence such research publications, is that there will be greater concern over those with lower pH and higher metal loadings than those a circum-neutral pH with metal loadings which are (by comparison) moderate. In their study of sites in the Ohio coalfield, Winland *et al.* (1991) note that the pH was >6 at 20% of the sites they visited, which suggests that preferential reporting may indeed be part of the anomaly between data from Britain and that from the eastern USA and other sites (tables 2.1 & 2.3).

2.2 Pyrite oxidation and associated reactions

The processes described in this section have been the subject of extensive study; reviews and research have recently been published in Nordstrom & Alpers (1997), Alpers & Blowes (1994) and Jambor & Blowes (1994) to which the reader is referred for more detail.

The oxidation of pyrite is responsible for the enhanced concentrations of Fe and SO_4 and the lower pH values frequently encountered in acid mine drainage (table 2.2). The reactions taking place in the oxidation of pyrite can be summarised as shown below:

$$FeS_{2(s)} + \frac{7}{2}O_{2(aq)} + H_2O_{(l)} \longrightarrow Fe^{2+}_{(aq)} + 2SO^{2-}_{4(aq)} + 2H^{+}_{(aq)}$$

Eq. 2.1: Oxidation of pyrite by O_2

$$Fe^{2+}_{(aq)} + \frac{1}{4}O_{2(aq)} + H^{+}_{(aq)} \rightarrow Fe^{3+}_{(aq)} + \frac{1}{2}H_2O_{(l)}$$

Eq. 2.2: Oxidation of Fe^{2+}

$$Fe^{3+}_{(aq)} + 3H_2O_{(l)} \rightarrow Fe(OH)_{3(s)} + 3H^{+}_{(aq)}$$

Eq. 2.3: Hydrolysis of Fe^{3+}

$$FeS_{2(s)} + 14Fe^{3+}_{(aq)} + 8H_2O \longrightarrow 15Fe^{2+}_{(aq)}\ 2SO^{2-}_{4(aq)} + 16H^{+}_{(aq)}$$

Eq. 2.4: Oxidation of pyrite by Fe^{3+}

Equations 2.1-2.4 from Stumm & Morgan (1996)

These equations demonstrate that two different reaction paths for the oxidation of pyrite are possible, and that these are followed by the subsequent oxidation of Fe^{II} and hydrolysis of Fe^{III}. The following review will thus be divided into sections broadly defined by these reactions, but also incorporating other geochemical processes which are associated with pyrite oxidation.

2.2.1 Pyrite oxidation

The two possible pathways of pyrite oxidation are shown in equations 2.1 & 2.4 (Stumm & Morgan, 1996). It can be seen that oxidation of pyrite in the presence of O_2 results in two protons and 2 moles of SO_4^{2-} for each mole of Fe^{2+} and consumes 3.5 moles of O_2 for each mole of FeS_2 oxidised (equation 2.1). The pathway utilising Fe^{3+} as the oxidant, consumes $14Fe^{3+}$ per mole of FeS_2 whilst producing $16H^+$ for each mole of pyrite oxidised (equation 2.4). The stability fields of Fe are shown in figure 2.4 (Appelo & Postma, 1994). This shows that Fe^{II} is stable only in reducing waters (Eh discussed in section 2.2.3a.

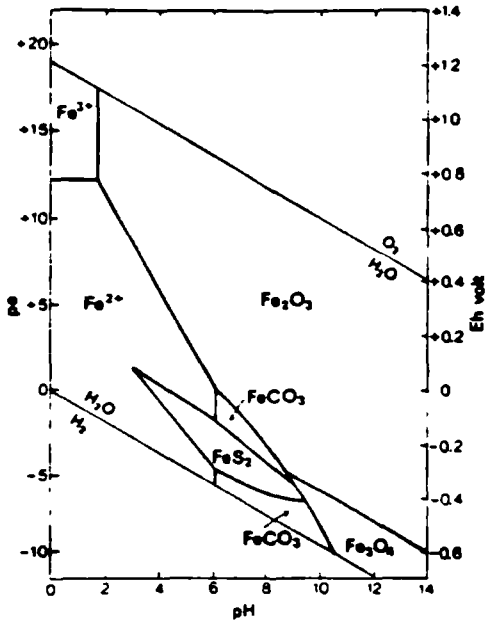


Figure 2.4: The stability fields of Fe species. The Fe-C-O-H system (Appelo & Postma, 1994). Plotted for 25°C, $\Sigma S = 10^{-6}$ and $TIC = 10^{0}$ M.

The oxidation of pyrite has been subject to a large body of research which has been summarised by Lowson (1982), Bierens de Haan (1991) and Nordstrom & Southam (1997) and references therein. Singer & Stumm (1970) showed that the oxidation of pyrite by Fe^{3+} (equation 2.4) is much faster than by O_2 (equation 2.1). However, the oxidation pathway was generally considered to be via equation 2.1 (O_2 oxidation) at circum-neutral pH, until the work of Moses *et al.* (1987) showed that Fe^{III} activity is sufficient even at pH~7 to cause direct pyrite oxidation and that the role of O_2 may be in the regeneration of Fe^{III} (section 2.2.3).

The necessary role of bacterial activity in catalysing these reactions, and those of other sulphides, has also been the subject of extensive study (e.g. Ahonen & Tuovinen, 1989; Bhatti *et al.*, 1992; Tuovinen *et al.*, 1994). The organism *Thiobacillus ferrooxidans* is particularly studied in many of the research papers, and below pH 4.5 is instrumental in determining the rate of pyrite oxidation (Bigham *et al.*, 1992). The review of Nordstrom & Southam (1997) contains an extensive reference list, focusing on the bacterial processes taking place in the oxidation of pyrite and other sulphides, to which the reader is directed.

The S produced by pyrite oxidation is always quoted as SO_4^{2-} (i.e. S^{VI}) because the oxidation of S from pyrite is extremely rapid, with respect to the rate of transport from

the pyrite surface, and thus intermediaries are only observed under experimental conditions (Moses *et al.*, 1987; Taylor *et al.*, 1984a,b).

2.2.1a Pyrite occurrence in coal and associated sediments

Pyrite (FeS_2, cubic) is less reactive than marcasite (FeS_2, orthorhombic) (Deer *et al.*, 1966), however, pyrite is generally more abundant in coal and associated sediments (Stumm & Morgan, 1996) and is thought to be responsible for much of the ferruginous water observed in coal mines (Nordstrom, 1982a).

Pyrite in coals, and therefore the acid generating potential (equations 2.1-2.4) are often associated with marine deposits (Williams & Keith, 1963; Wandless, 1954, 1959; Thomas, 1992). This derives from the fact that, with an average SO_4 concentration of 28 mmol l^{-1} in seawater, sulphide formation is not limited by the availability of SO_4, as is the case in freshwater sediments. (Berner & Raiswell, 1984). In freshwater sediments Fe^{II} is frequently precipitated as siderite ($FeCO_3$) due to this lack of S (Berner & Raiswell, 1984). Thus it is frequently suggested that the occurrence of marine beds in coal mined regions will lead to a greater acid generating potential (Morrison *et al.*, 1990; Younger, 1995b). The pyrite morphology has also been considered as a factor in acid generation, with some research showing a greater reactivity of framboidal pyrite (Caruccio *et al.*, 1977), although this has been disputed (Wiersma & Rimstidt, 1984; Morrison *et al.*, 1990). The concentration of pyritic S has also been shown to vary within a seam (Whately & Tuncali, 1995). That it is only inorganic S (and not that bound within coal macerals) which participates in acidity production has been shown by Casagrande *et al.* (1989) and Helz *et al.* (1987). The relationship between depositional environment of the coal, and the S producing potential has been disputed by Rippon (1997) in a review of literature pertaining (primarily) to British coalfields. Rippon (1997) shows that there is no clear pattern of pyrite occurrence in Carboniferous Coal Measures which can be related to mapped marine facies, although pyrite is known to be found in marine bands (e.g. Land, 1974 in County Durham). The reasons for this are suggested as being that marine incursions of short duration may not be distinguishable by a marine band deposit, but may still increase S concentrations sufficiently to deposit sulphides (Rippon, 1997). What should also be considered in a sedimentary sequence is the post-compactional history, which in County Durham, includes a period of sulphide mineralisation associated with the North Pennines orefield (Dunham, 1990).

The abundance of pyrite within a coalfield is generally mapped by the mining company (e.g. NCB, 1959, 1961) (primarily as concerned with power generation contaminants). The concentrations of pyrite found in the Durham Coalfield are given in section 3.2.1a, but as in other coalfields recorded, are generally in the range up to 3% (NCB, 1959, 1961; Rippon, 1997; Bigham, 1994).

2.2.1b Iron(II) sulphates

The formation of Fe^{II} sulphates such as melanterite ($FeSO_4.7H_2O$) and rozenite ($FeSO_4.4H_2O$) is reviewed by Alpers *et al.* (1994a). These are highly soluble salts which are part of a series which can be represented by $FeSO_4.xH_2O$ (Alpers *et al.*, 1994a). These minerals are able to form in an oxidising atmosphere as efflorescences on sulphide surfaces (Helz *et al.*, 1987), which are flushed out by a waters recharging an aquifer, which cause the transport of Fe^{II} and SO_4 in solution, and frequently result in pH lowering after rainfall (Frost 1978a, b; Johnson & Thornton, 1987; Nordstrom *et al.*, 1992). This has been observed to control the concentrations of minor elements such as Zn and Cu in metalliferous mine drainage by Alpers *et al.* (1994b). Cairney & Frost (1974) suggested that the control of a water table to a constant depth in a mine will minimise the oxidation of pyrite, and thus the subsequent flushing out of products controlled by Fe^{II}-SO_4 salts.

2.2.2 Buffering of H^+ generated in pyrite oxidation

The minerals present in an aquifer or surface water determine the ability of that system to buffer the pH when H^+ or OH^- are introduced to that aquifer. The theory of buffering capacity is reviewed in many publications (e.g. Appelo & Postma, 1994; Hem, 1985) and the carbonate buffering equilibria are particularly explained by Krauskopf & Bird (1995). The dissolved inorganic carbon (DIC), OH^- and H^+ buffering system is particularly important in natural water systems because the reaction rates are fast, and calcite buffers at circum-neutral pH (Hem, 1985). The speciation of DIC is controlled by pH alone, in normal surface temperature and pressure conditions (figure 2.5) with HCO_3- dominating at circum-neutral pH (more details in: Appelo & Postma, 1994; Krauskopf & Bird, 1995)

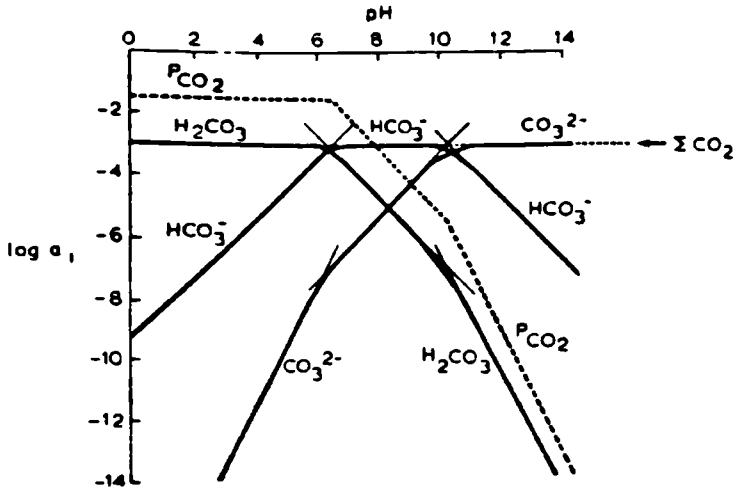


Figure 2.5: Speciation of dissolved inorganic carbon (DIC) (Appelo & Postma, 1994). Total inorganic carbon = 1mmol l^{-1}.

The dissolution of calcite and dolomite will consume acidity when the pH is <6.7 (Morrison *et al.*, 1990) and these processes are shown in reactions 2.5-2.6.

$$2H^+ + CaCO_3 \leftrightarrow Ca^{2+} + CO_2 + 2H_2O$$

Eq. 2.5: Proton induced dissolution of calcite (Krauskopf & Bird, 1995)

$$4H^+ + CaMg(CO_3)_2 \rightarrow Ca^{2+} + Mg^{2+} + 2CO_2 + 2H_2O$$

Eq. 2.6: Proton induced dissolution of dolomite (Morrison et al., 1990)

These reactions show that Ca and Mg may be released into solution, and HCO_3^- will be generated. Several studies of coal mine drainage, where circum-neutral pH has been observed (Sperring, 1995; Winland *et al.*,1991; NRA, 1994a) have attributed this to carbonate buffering of the aqueous pH. The overall reaction of the simultaneous oxidation of pyrite and dissolution of calcite is shown in equation 2.7.

$$FeS_2 + 2CaCO_3 + \frac{15}{4}O_2 + \frac{3}{2}H_2O \rightarrow Fe(OH)_3 + 2SO_4^{2-} + 2Ca^{2+} + 2CO_2$$

Eq. 2.7: Oxidation of pyrite in the presence of calcite (Morrison et al., 1990)

Thus it can be seen that the reaction is incongruent (as is pyrite oxidation when Fe^{III} hydrolysis occurs, c.f. equation 2.3). What should be noted is that the dissolution of Ca and SO_4 may result in the precipitation of gypsum ($CaSO_4.2H_2O$) which has been

suggested as affecting mine drainage chemistry by Aldous (1987), Henton (1976) and Sperring (1995) and the experiments on coal samples by Helz *et al.* (1987).

It has been suggested that the occurrence of siderite ($FeCO_3$) as the dominant carbonate phase will limit the acid neutralisation potential of a Coal Measures sediment (Morrison *et al.*, 1990; Younger, 1995b). As shown below in equation 2.8, when the reaction is written to completion it does not result in a net loss of H^+ from the aqueous system.

$$FeCO_3 + \frac{1}{4}O_2 + \frac{3}{2}H_2O \rightarrow Fe(OH)_3 + CO_2$$

Eq. 2.8: Proton induced dissolution of siderite, precipitating Fe^{III} (Morrison et al., 1990)

However, if this reaction is considered as a congruent process, it can be seen that as long as Fe^{II} is not oxidised and subsequently hydrolysed, the buffering of H^+ is fulfilled (equation 2.9).

$$H^+ + FeCO_3 \rightarrow Fe^{2+} + HCO_3^-$$

Eq. 2.9: Proton induced dissolution of siderite (Morrison et al., 1990)

These reactions (equations 2.5 - 2.7) show that waters undergoing buffering of pH due to carbonate (dominantly calcite) dissolution would be expected to be a Ca-SO_4 water with additional Mg if Mg rich calcite or dolomite is present in an aquifer. Waters of just such a composition have been modelled to form by this mechanism by Bethke (1996) and measured in field studies by Helz *et al.* (1987).

It has been suggested that the high pH in mine water found in County Durham could be attributed to bacterially mediated SO_4 reduction (Younger & Bradley, 1994; Younger, 1997a) consuming acidity according to equation 2.10.

$$SO_4^{2-} + 8e + 10H^+ \rightarrow H_2S + 4H_2O$$

Eq. 2.10: Sulphate reduction (Younger & Bradley, 1994)

However, when the pH of waters is circum-neutral the dissociation of H_2S would be expected, which would act to reduce the pH (Hem, 1985). Another potential conflict with this hypothesis is the large concentrations of SO_4 measured in minewaters, which suggest the equilibria associated with equation 2.10 is far to the left as shown above.

The high concentrations of Al in solution which may exist (e.g. table 2.2) are derived from the acid weathering of aluminosilicates (Nordstrom & Ball, 1986). The reactions associated with these processes are covered by Appelo & Postma (1994), an example of which is shown in equation 2.11. This shows the reaction of K-feldspar to form kaolinite and silicic acid.

$$2KAlSi_3O_8 + 2H^+ + 9H_2O \rightarrow Al_2Si_2O_5(OH)_4 + 2K^+ + 4H_4SiO_4$$

Eq. 2.11: The acid dissolution of K-feldspar to form kaolinite (Appelo & Postma, 1994)

This shows that silicate weathering may release Al and Si into waters, although it should be noted that these reactions tend to be incongruent, with respect to both Al and Si unless the aqueous pH is very low (Appelo & Postma, 1994; Krauskopf & Bird, 1995). The buffering reactions of silicates become important in the absence of carbonate buffering (Appelo & Postma, 1994).

Another mechanism which may act to reduce the metal and SO_4 ion concentration and increase the pH value of waters which have been chemically modified by pyrite oxidation is dilution by fresh infiltrating rainfall. This was shown to be the case by Fuge (1972) who collected infiltrating waters and those which had evolved by dissolution of pyrite oxidation products and showed that these could account for the decrease in concentrations found in the discharging mine waters. The dilution of spoil drainage in County Durham has been shown by Younger *et al.* (1997) to have a similar effect.

Another process which has been suggested for coal mines, which is not a buffering reaction, but one that leads to the cessation of pyrite oxidation, and therefore, acid generation, is that controlled reflooding can result in the resumption of reducing conditions (Cairney & Frost, 1974; Frost, 1978b). This would implicitly be expected to reduce Fe and SO_4 concentrations in solution as well, and seems to be suggested by the data on pumped discharge chemistry shown in Henton (1976) and Younger (1997a), and the exponential decline in aqueous chemistry described in section 2.1.1.

2.2.2a Occurrence of potential buffering minerals in coal and associated sediments

The presence of carbonates has been attributed to causing the elevated pH observed in some British coal mines (e.g. Davies *et al.*, 1997), however there is little data published which provides comparative pyrite and carbonate concentrations to help verify this (see also section 3.2.1). The study of Morrison *et al.* (1990) on shales associated with

Pennsylvanian coals provides such information and the experimental weathering carried out on these sequences found that brackish shales had a greater acidity generating capacity, because the proportion of pyrite to carbonate was higher than for marine or freshwater shales (table 2.4). These authors also note that this buffering was achieved largely by siderite (because Fe^{II} did not oxidise and then hydrolyse in their experimental conditions) and that, where there was up to 3.25% pyrite, acidity production could be effectively neutralised.

Table 2.4 : Carbonate contents of some shales in coal measure sediments, Pennsylvania (after Morrison *et al.*, 1990).

Facies	Number of Samples	Proportion of Carbonate Present (%)	Pyrite (%)
Marine shales			0.95
calcite	16	0.42	
siderite	16	4.85	
dolomite-ankerite	16	0.91	
Brackish shales			2.40
calcite	14	0.01	
siderite	14	1.13	
dolomite-ankerite	14	0.30	
Freshwater shales			0.15
calcite	6	0.29	
siderite	6	3.86	
dolomite-ankerite	6	1.36	

The occurrence of carbonates, particularly ankerite and siderite, has been noted in publications by several authors working on the Carboniferous Coal Measures of Britain (Hawkins, 1978; Hirst & Kaye, 1971; Rippon & Spears, 1989; Spears, 1997; Spears & Sezgin, 1985; Taylor & Spears, 1967). However, these studies are for purposes quite different to the study of potential acid generating and buffering minerals occurrence, and thus the information is of qualitative use only.

2.2.2b Aqueous speciation and mineral saturation

The complexation of ions in natural waters is studied in this thesis using a geochemical modelling package (section 4.6). The calculation of the activity of ions is important in the determination of such parameters as Eh (section 2.23a) and saturation indices (below). The formation of complexes is reviewed in standard texts such as Appelo & Postma (1994) and shall not be reviewed here. What is of note is that the complexation of an ion in solution can lead to changes in the activity of dissolved species as compared with the total measured concentration. The ideal way to calculate these is using a

computer program, such as PHREEQ-C (Parkhurst, 1995) (section4.6), which can simultaneously solve numerous equations and iterate to a solution. The other determinand, once aqueous speciation is calculated, is the saturation indices of mineral phases, with respect to the water studied. These are calculated as shown in equation 2.12 and explained in more detail by Appelo & Postma (1994).

$$SI = \log \frac{[IAP]}{[K_{sp}]}$$

Where: SI = satuaration index; IAP = ion activity product; K_{sp} = solubility product

Eq. 2.12: Saturation index calculation (Appelo & Postma, 1994)

This calculation can be used to assess which minerals the aqueous phase may be in equilibrium with, or which phases may be expected to actively precipitate (Appelo & Postma, 1994). The equilibrium of a phase is demonstrated by a SI = 0; supersaturation (i.e. expected to precipitate) by a SI >0 and undersaturation by SI <0 (Appelo & Postma, 1994).

2.2.3 Fe^{II} oxidation

Singer & Stumm (1970) found that Fe^{II} oxidation is the rate determining step in the overall pyrite oxidation process, but that there is $>10^6$ increase in the rate in natural waters compared with laboratory experiments. This is due to microbial action, which increases the rate of oxidation from ~$1x10^{-6}$ mmol h^{-1}, to ~1 mmol h^{-1} when bacterially catalysed (Singer & Stumm, 1970). Field calculations of the Fe^{II} oxidation rate by Nordstrom (1985) showed that the rate was too fast for abiotic oxidation. *Thiobacillus ferrooxidans* is the strongest catalyst of Fe^{II} oxidation (Nordstrom, 1985) and was invoked for causing the Fe^{II} oxidation rate of 2.4 mmol h^{-1} observed by Nordstrom (1985). More recently Kirby & Brady (1998) have noted field Fe^{II} oxidation rates varying by 4 orders of magnitude in field measurement trials. Nordstrom (1985) noted that dilution due to rainfall could reduce the rate of oxidation (to 0.65 mmol h^{-1}) due to the dilution of bacteria and Fe^{II}. *T. ferrooxidans* have been observed in acid mine drainage by Walton & Johnson (1992). The optimal pH range for *T. ferrooxidans* is 2-4, above this pH the abiotic rate is so rapid that bacterial catalysis is not essential to understand the oxidation rates seen in natural samples (Nordstrom & Southam, 1997). A comprehensive review of the physiology and biochemistry of *T. ferrooxidans* is given by Nordstrom & Southam (1997). In higher pH (>4.5) the oxidation of Fe^{II} may be undertaken by bacteria such as *Gallionella ferruginea* and *Leptothrix sp.* (Emerson & Reusbech, 1994; Fenchel *et al.*, 1998). *G. ferruginea* is notable for consisting of "twisted stalks" morphology, which may become encrusted in Fe^{III} precipitates (Emerson &

Reusbech, 1994; Tyrrel & Howsam, 1997), and is found in poorly oxidising waters with dissolved oxygen <10% saturation (Emerson & Reusbech, 1994).

The Fe draining from coal mines frequently is dominated by Fe^{II}, this is because the reaction of Fe^{3+} with pyrite is so rapid that these cannot be found in co-existence (section 2.2.1) (Stumm & Morgan, 1996). In flowing streams the concentration of Fe^{II} can be affected by both the rate of oxidation of the Fe^{II} to Fe^{III} (Nordstrom, 1985) and the rate of photoreduction of Fe^{III} precipitates (section 2.2.5) as shown by the detailed studies of Kimball, McKnight and other researchers (McKnight *et al.*, 1988; Kimball *et al.*, 1992; Waite & Morel, 1984).

2.2.3a Chemical and electrode determination of Eh

The measurement of redox potential using a reference electrode is well established in natural water determinations. The Pt electrode compares the reading to a reference electrode to produce a measurement of Eh (for more details see Appelo & Postma, 1994; Hem, 1985; Nordstrom & Munoz, 1994). The Eh of waters can also be calculated from the measurement of a redox sensitive pair of ions; these can then be used to compute the aqueous Eh as demonstrated below (from Appelo & Postma, 1994). This calculated Eh is referred to as Nernstian Eh (Eh_N) (equation 2.13) to distinguish the value obtained from that measured using Pt-electrodes (Eh_m)

$$bB_{red} + cC_{ox} = dD_{ox} + gG_{red}$$

$$E = E^o + \frac{RT}{nF} \ln \frac{[D_{ox}]^d [G_{red}]^g}{[B_{red}]^b [C_{ox}]^c}$$

Where E = redox potential (volts); R = gas constant; T = absolute temperature (kelvin); n = number of electrons; F = Faraday constant.

Eq. 2.13 The Nernst Equation (Appelo & Postma, 1994)

This equation can be written for the Fe^{2+}/Fe^{3+} couple (of particular importance in mine water studies - see below) as shown in equation 2.14.

$$Fe^{2+} \leftrightarrow Fe^{3+} + e^-$$

$$Eh = 0.77 + 0.0059 \log \frac{[Fe^{3+}]}{[Fe^{2+}]}$$

Eq. 2.14 The Nernst Equation for the Fe^{2+}/Fe^{3+} couple (Appelo & Postma, 1994)

The E^o for Fe^{III}/Fe^{II} is 0.77V (Appelo & Postma, 1994); thus (from equation 2.14) the activity of the two ions is equal at 0.77V, $Fe^{III} > Fe^{II}$ when Eh > 0.77V and $Fe^{III} < Fe^{II}$

when Eh < 0.77V (Appelo & Postma, 1994). The Eh as measured or calculated for any redox pair then enables the redox distribution for all species in a homogenous aqueous system to be calculated, because if the system is in equilibrium the speciation of all redox sensitive elements is fixed for a given Eh (Appelo & Postma, 1994).

Hostettler (1984) reviews the chemical principles of Eh (and pH) in great detail. A problem is that for a Pt electrode to function, the redox couple must be electrically active, Hostettler (1984) shows that O_2, CH_4, HCO_3^-, N_2 and SO_4^{2-} are not electrically active, which means that redox couples involving those ions are not measured by an electrode (Hostettler, 1984; Appelo & Postma, 1994).

Comparative studies of the measurement of Eh_N and Eh_m have been carried out by several studies. Lindberg & Runnells (1984) compared Nernstian redox values with those measured using a Pt-electrode. That study found that internal disequilibrium was the norm where multiple redox couples were studied, and that these did not generally agree with the electrode determined Eh. These measurements are important input parameters into geochemical models as they are master variables in determining speciation of ions. Lindberg & Runnells (1984) recommend that several redox couples are measured and compared, to establish whether a water is in thermodynamic equilibrium or not. The study of Runnells & Lindberg (1990) reaches the same conclusion in a study of the Se^{VI}/Se^{IV} system.

Kempton *et al.* (1990) conducted a very detailed study of Eh_N and Eh_m comparisons in laboratory solutions to study electrode responses. The only redox couple which was found to give quantifiable responses was Fe^{III}/Fe^{II}. Macalady *et al.* (1990) reviewed the reasons for the lack of ideal response of electrodes in natural waters, factors such as electrode poisoning, O_2 absorption by electrode, system disequilibria and colloidal material. The exchange current between the species needs to be high enough to generate sufficient electrode response, which this study also found was most applicable to Fe^{III}/Fe^{II} (Macalady *et al.*, 1990).

Nordstrom *et al.* (1979a) suggest that homogeneous phase reactions may reach equilibrium more rapidly than heterogeneous phase reactions, and thus may be responsible for internal disequilibrium within a system. Mine drainage generally has very high concentrations of Fe (e.g. tables 2.1-2.3), of which the species Fe^{2+} and Fe^{3+} (equation 2.14) are electroactive, and this makes it an environment where there exists a greater possibility for Eh_m to be close to Eh_N. These workers found that O_2/H_2O was in

equilibrium with the atmosphere, but not the Fe redox couple (Nordstrom *et al.*, 1979a). The low exchange current of the O_2/H_2O couple means that it does not contribute to Eh_m. When Fe $<10^{-6}$ M l^{-1} the Eh_N is partially due to O_2/H_2O, rather than being dominated by Fe, and so the Eh_m becomes much less reliable (Nordstrom, 1996). Nordstrom & Munoz (1994) state that redox disequilibrium should be regarded as the rule rather than the exception. The requirement for an electrode to represent the Eh of system is electroactive species at least 10^{-5} M l^{-1} in solution, this often means in practice that S^{2-}, Fe^{II} and Fe^{III} are the species which are going to be detected, and analytical methods exist for all of these and are recommended by Nordstrom & Munoz (1994), and are reviewed briefly for Fe in section 4.3.1h. Nordstrom *et al.* (1992) found reasonable agreement with Eh_m and Eh_N in metalliferous mine waters (high Fe) in Brazil, whilst of Ball & Nordstrom (1985) show that the difference between Eh_m and Eh_N increases at higher pH and lower Fe concentrations, when plotted against each other. They found that where Fe >0.5 mg l^{-1}, there is reasonable agreement between Eh_m and Eh_N.

Alternative methods of assessing the redox status have been suggested. Scott & Morgan (1990) suggest the "oxidative capacity" of waters gives a more complete status of the waters, however this has the problem that it requires the analysis of multiple redox couples, which is expensive and time consuming. Berner (1981) proposed the division of oxygenating - reducing status based on the measurement of indicator species / dissolved gases, which was also recommended by the comparative study of Lindberg & Runnells (1984) where quantifiable data is not required. This classification is based on the presence or absence of mutually exclusive ions (e.g. dissolved O_2 and total dissolved sulphides) and defining a sediment / fluid as oxidising / reducing (which is then divided into sulphidic, methanogenic). This system works for general classification, but for the purposes of geochemical modelling a single quantifiable value needs to be input into the model input file, such that this does not readily enable (see recommendation of Lindberg & Runnells, above).

2.2.3b Determination of the dissolved component of aqueous samples

The sampling of natural waters necessarily involves the filtering of the waters upon collection to remove suspended material. The sampling of the "dissolved" phase is in fact sampling of an operationally defined fraction, with "dissolved" being that fraction <0.45μm and "suspended" being that >0.45μm (Hem, 1985). The size distribution is continuous from particles to solutes (Stumm, 1992), and thus this is a somewhat arbitrary cut-off point. In the UK, filtering at 0.45μm is used by the regulatory

authorities to define "dissolved", and thus, exceedance of any water quality guidelines (Gardiner & Mance, 1984).

There are several problems associated with filtering. Firstly the filter pore size, which Karlsson *et al.* (1994) showed should be regarded as a size distribution, rather than a single pore size. In their study it was found that a nominal filter size of 0.40μm removed particles down to 0.23μm in size from the water. Another sampling artefact arises from clogging of the filter by suspended material, which will lead to a reduction in the effective pore size of the filter (Horowitz *et al.*, 1996). Samples should also be filtered on collection to avoid agglomeration and precipitation taking place, which will change the filtered composition of the waters (Karlsson *et al.*, 1994). Studies of differing filter diameter sizes (Horowitz *et al.*, 1996) and different brands (Hall *et al.*, 1996) (of the same nominal pore size in both cases) have exhibited bias between the filtrate chemistry. Whilst the differences obtained are not thought to be excessive (Hall *et al.*, 1996), they would seem to suggest that conformity within a sampling study of brands and method of filtering would be a way of reducing any sampling bias. Jones *et al.* (1974) approached the problem from the inverse direction. Their study utilised measured concentrations of ions to derive saturation indices, and then use those results to suggest whether colloidal material has passed through the filter.

Ultrafiltration studies of the size distribution of colloids in natural waters have shown that colloids may be composed of ions of importance in aqueous systems, such as Fe (Marley *et al.*, 1991; Kimball *et al.*, 1992). These studies have reported the occurrence of elements such as Fe in the sub-0.1μm fraction and Wen *et al.* (1997) used ultrafiltration to show the agglomeration of colloids to form suspended particles takes place very rapidly (a large proportion within 4 hours), by the process of colloidal pumping.

In a study of filtering sizes McKnight & Bencala (1989) found most dissolved Fe occurred as Fe^{II}, and most of that was to predicted to occur as Fe^{2+}. Kimball *et al.* (1992) used Fe^{II} and Fe_t determinations to study iron photoreduction in field and laboratory experiments. The study by these authors measured unfiltered, <0.1μm and ~<0.01μm size fractions. The filtering at <0.01μm was done with an ultrafiltration unit, with a nominal pore size of 100000MW, and it was found that colloidal Fe was occurring in an acid mine drainage impacted stream (Kimball *et al.*, 1992). The different Fe

concentrations caused the modelled saturation index for ferrihydrite and the modelled Eh (using Fe^{II}/Fe^{III} - equation 2.14) to be different for the two size fractions.

The ultrafiltration work of Smith (1994a) on mine drainage in the Durham Coalfield suggests that little Fe is occurring at the <0.45μm size fraction in the deep mine drainage site of Stony Heap (section 3.4.1d).

The reports on the size of ferrihydrite (section 2.2.5b) suggest that this should pass through 0.1μm filter pores, and thus may be included in the measurement of Fe^{III} when speciation determinations are undertaken (section 2.2.3a).

The problems associated with filtering include trapping of particles < nominal pore size (due to the pore size distribution and attraction and agglomeration of particles whilst filtering) and the retention of solutes on the filter equipment (Stumm, 1992). However Stumm (1992), unusually, also states the advantages of filtering, which relate to the fact that if a natural water is filtered to <0.5μm this removes bacteria (i.e. filter sterilises) and that these sub-micron particles will move as solutes. The problem comes with thermodynamic calculations which are based on solutes (Stumm, 1992).

2.2.4 Fe^{III} hydrolysis

The pH of hydrolysis of Fe^{3+} is ~2 (Levinson, 1980) and above that value of pH Fe^{3+} rapidly hydrolyses at rates quoted by Broshears *et al.* (1996) as being of a T(1/2) < 1 second. Thus, this is not a rate limiting step in the pyrite oxidation series of reactions, and will result in very low concentrations of Fe^{3+} in solution, due to the low solubility of Fe^{III} at pH 6-8 (Cornell & Schwertmann, 1996). Because the precipitation of all of these phases (below) is due to a hydrolysis reaction (equation 2.3) it should be noted that their precipitation causes a release of H^+ into the aqueous system (equation 2.3). A decline in pH due to hydrolysis of Al and Fe in an intensive study of a natural acid mine drainage impacted system was shown by Broshears *et al.* (1996).

2.2.5 Fe^{III} precipitate mineralogy

As shown in figure 2.4, the stable phase of Fe^{III} expected to precipitate is goethite, however there are kinetic hindrances to the precipitation of goethite (section 2.2.5a). The oxidation of Fe^{II} may be bacterially catalysed, causing Fe^{III} to hydrolyse and rapidly precipitate, but this is a purely extracellular effect with the bacteria having no control over the mineral formed (Bigham *et al.*, 1992; Bigham, 1994). The association of bacteria with such precipitates has been shown by Ferris *et al.* (1989) who found

ferrihydrite associated with bacterial cells, and the subject reviewed more recently by Konhauser (1997) to which the reader is referred for more references. Clarke *et al.* (1997) showed that precipitation can occur within cells as well as externally. The work of Winland *et al.* (1991) suggested that up to 3g m^{-2} d^{-1} of ochre could precipitate from water draining abandoned mines in the Ohio coalfield.

The surface charge associated with Fe^{III} hydrous oxides (below) is generally at a minimum at pH 6-8, with a net positive charge below this value and a net negative charge when the pH is higher (Cornell & Schwertmann, 1996). However, it has been suggested that sorption of trace ions, e.g. SO_4 and organics, may predominate over the Fe mineral charge in natural samples and that the amount of organic material available for sorption may control the surface charge (Newton & Liss, 1987; Ranville *et al.*, 1988), and has been shown to cause near neutral surface charge in pH 3.5 water (Ranville *et al.*, 1988).

The properties of the Fe minerals dominating those found in ferruginous drainage environments are reviewed extensively in many studies (Cornell & Schwertmann, 1996; Murad *et al.*, 1994; Bigham, 1994 and references therein). These minerals are also reviewed by Schwertmann & Taylor (1989) in the context of soil forming minerals. The reader is referred to these publications for further detail to the brief review provided here.

2.2.5a Goethite

Goethite (α-FeOOH) is the mineral which is thermodynamically favourable in most acid and near-neutral mine drainage environments (Bigham *et al.*, 1992). Natural goethite has a surface area of 8-200 m^2 g^{-1} (Cornell & Schwertmann, 1996). Goethite is rarely detected as dominating mine drainage precipitates, which usually consist of metastable minerals (Bigham, 1994). The metastable minerals transform to goethite, the rate of which may be determined by trace ions or organic C present. The presence of 250 - 1000 mg l^{-1} SO_4 has been suggested by Brady *et al.* (1986) to increase the rate of transformation of ferrihydrite to goethite. The presence of organic matter or Si may delay the transformation to goethite (Schwertmann & Taylor, 1989; Bigham, 1994). Schwertmannite and ferrihydrite are metastable with respect to goethite on a temporal scale (Bigham *et al.*, 1992), and jarosites are metastable with respect to goethite in the event of increases in aqueous pH (section 2.2.5d). Goethite is only occasionally found as the major phase in mine drainage precipitates, those sites being of pH 6.5 - 7.5 in the

aqueous phase (Bigham *et al.*, 1992; Bigham, 1994). The goethite which does form was found to be different in its chemical behaviour to that of synthetic goethite (largely solubility data), which was attributed by Murad *et al.* (1994) to the small particle size and invariable occurrence in an admixture of ferrihydrite / schwertmannite. Goethite may form directly where Fe^{II} dominated waters are neutralised by HCO_3^- water (Bigham, 1994). An explanation proposed for the favouring of metastable phases (ferrihydrite and schwertmannite) over goethite in mine drainage environments, has been suggested by Cornell & Schwertmann (1996) to be the smaller size of the stable nucleus of ferrihydrite than goethite, causing ferrihydrite to be energetically favoured; further detail is contained in that reference. There is a possible kinetic effect too, in that the slow hydrolysis of Fe^{III} favours goethite precipitation, and the presence of "contaminants" commonly found in natural (mine drainage) systems, such as SO_4 (Brady *et al.*, 1986) and silicates (Carlson & Schwertmann, 1981; Cornell & Schwertmann, 1996), can hinder the rate of transformation of metastable minerals to goethite. It can take goethite >40 years to equilibrate with an aqueous phase, whilst ferrihydrite is very rapidly formed in mine drainage environments (Cornell & Schwertmann, 1996). The work of Brady *et al.* (1986) showed that a SO_4/Fe ratio <0.5 favoured goethite with respect to ferrihydrite, whilst a ratio of >1.5 showed a relationship to the formation of ferrihydrite. The increasing crystallinity of precipitates, which may be related to transformation to goethite has been shown by Ford *et al.* (1997) to result in the release of Pb and Cd from surface sorption sites, whilst Sperring (1995) showed that in an accumulation of ochre, the concentrations in the lower ochre of Pb, Ni and Co were at least an order of magnitude lower than those in the surface ochre (washed away in an erosional event).

2.2.5b Ferrihydrite

The mineralogy of mine drainage minerals formed were frequently regarded as "amorphous" ferric hydroxide, or given the generic name "limonite". More detailed studies of the ochrous material precipitating in such environments has shown that these are dominated by poorly crystalline materials, of which ferrihydrite is one (Bigham *et al.*, 1990) and schwertmannite another (Bigham *et al.*, 1994). Chemical and physical methods of analysis of such minerals are described by Bigham (1994) and Murad *et al.* (1994). The exact unit formula of ferrihydrite varies slightly between investigators. Here that of Bigham (1994) will be used: $Fe_5OH_8.4H_2O$. This mineral is found associated with the rapid oxidation of Fe^{II} by acidophillic bacteria in low pH environments (Bigham *et al.*, 1990). Ferrihydrite is always poorly crystalline, and can be found with 2-6 lines on X-ray diffraction spectra (Bigham *et al.*, 1992). The work of Murad *et al.* (1994) showed

that the peaks are very weak and broad and have very low counts. When the count rate is changed from 20 s/step to 40 s/step, those workers found that trace goethite and schwertmannite could be resolved (Murad *et al.*, 1994). The conversion of ferrihydrite to goethite in a core of ochre, the base of which was initiated 30 years previously and the depositing pH 6.8, was shown by Bigham *et al.* (1992). Ferrihydrite particles are typically highly aggregated spheroids (Bigham *et al.*, 1990), with observed sizes of 0.4-0.5 μm (Brady *et al.*, 1986) and 20-100 nm (Nordstrom *et al.*, 1992). Spheroidal ferrihydrite particles are shown in Ranville *et al.* (1988) and Schwertmann & Taylor (1989), using SEM, and are suggested to be aggregating around organic residues. The surface area recorded for ferrihydrite is 100-400 $m^2 g^{-1}$ (Cornell & Schwertmann, 1996). Additional information provided by Cornell & Schwertmann (1996) suggest that organic C promotes aggregation of spheroids, because surface area has been found to correlate with organic C.

2.2.5c Schwertmannite

Bigham *et al.* (1994) give a comprehensive summary of the details of the newly described mineral schwertmannite ($Fe_8O_8(OH)_6SO_4$). The surface area of this mineral is 125-300 $m^2 g^{-1}$ (Cornell & Schwertmann, 1996). It is suggested that this mineral forms largely in environments with a pH from 2.5 - 4.0 and SO_4 concentrations from 1000-3000 mg l^{-1} (Brady *et al.*, 1992). This mineral is metastable with respect to goethite (Bigham *et al.*, 1994; Bigham *et al.*, 1996a, b), which proceeds according to equation 2.15 (Murad *et al.*, 1994), liberating H^+ and SO_4^{2-} in the conversion. The laboratory experiments on this subject by Murad *et al.* (1994) showed that conversion was complete within 200 days, when the schwertmannite was dialysed with DIW. This modelled the effects of an amelioration in stream conditions where schwertmannite had formed. This mineral is also capable of occluding As and Se within the structure (Cornell & Schwertmann, 1996) and sorbing up to 6% (wt.) SO_4 (Bigham *et al.*, 1990). Further details can be found in the references cited in this section, and those given in section 2.2.5.

$$Fe_8O_8(OH)_6SO_4 + 2H_2O \Rightarrow 8FeOOH + H_2SO_4$$

Eq. 2.15: Ageing of schwertmannite to goethite (Murad et al., 1994)

Much as ferrihydrite is considered the dominant phase precipitating in circum-neutral pH environments, so it has been suggested that schwertmannite is the dominant phase occurring in acid, sulphate environments, which was previously described as amorphous (Bigham *et al.*, 1990).

2.2.5d Jarosite minerals

This group (as formed in mine drainage environments) can be represented by the following formula: $XFe_3(SO_4)_2(OH)_6$, where X can be K^+, H^+, NH_4^+ or H_3O^+ (Grishin *et al.*, 1988). The precipitation reaction is shown as equation 2.16.

$$3Fe^{3+} + X^+ + 2HSO_4^- + 6H_2O \Rightarrow XFe_3(SO_4)_2(OH_6) + 8H^+$$

Eq. 2.16: Precipitation of jarosite minerals (Grishin et al., 1988)

These minerals precipitate generally between pH 2.5 (hydrolysis of Fe^{III} (Grishin *et al.*, 1988)) and 3.5 (Bigham *et al.*, 1992). Bigham *et al.* (1992) observed that jarosite is rarely found in nature where SO_4 concentrations are <3000 mg l^{-1}. Below this concentration they suggest that schwertmannite is the most likely precipitate (Bigham *et al.*, 1992). Figure 4.3 shows that jarosite has a highly crystalline nature and very distinct XRD pattern to the other minerals discussed here, and is easily recognisable by XRD where it does form. Grishin *et al.* (1988) and references therein give more details on this mineral group, as do the general references at the beginning of section 2.2.5. Jarosites are observed to rapidly transform to ferric oxyhydroxides in environments where the concentrations of ions in solution decreases and the pH increases (Brady *et al.*, 1986).

2.3 Minor and trace ion geochemistry in mine and spoil drainage

The geochemistry of selected minor and trace ions are discussed here. This review focuses on those elements which are described and discussed in this study (chapters 5-8).

2.3.1 Sources of aqueous minor and trace ions

A large body of literature exists on the trace elements associated with coal, due to the importance of those ions in the power generation industry (end-users of coal); the reader is referred to Clarke & Sloss (1992) and, particularly, to Swaine (1990) and references therein. These publications, and other literature surveyed, do not contain details of the occurrence of trace element associations in the Durham Coalfield (section 3.2.1). However, a number of useful publications show that elements such as Zn, Cu, Pb, Ni and Co are associated in general with the sulphide phases (Helz *et al.*, 1987; Speight, 1994; Querel & Chenery, 1995; Kotsova *et al.*, 1996). The sources of these ions may be from dissolution of the sulphides (Nordstrom & Southam, 1997) such as sphalerite (ZnS), chalcopyrite ($CuFeS_2$), galena (PbS), vaesite (NiS) and cattierite (CoS_2), or as

isomorphic substitutions within the pyrite lattice (Deer *et al.*, 1966), which are released upon pyrite oxidation (section 2.2.1). In low pH conditions these ions would be expected to remain in solution (e.g. as Zn^{2+}). Increases in pH will result in the precipitation (or co-precipitation with other phases) of these ions. This will be discussed in section 2.3.3. The association of these ions may not be exclusively with the sulphide fraction. The occurrence of Zn in the carbonate phase has been noted by Helz *et al.* (1987), and the association of Cu and Zn with the organic phase in low rank coals has been noted by Swaine (1990) and Huggins & Huffman (1996). However, in an area such as the Durham Coalfield the sulphide phase may be expected to dominate as the coals are not low rank (e.g. NCB, 1959) and the area is in the outer part of the North Pennines orefield (Dunham, 1990) (section 3.2.1 gives more detail). Barium in the Durham Coalfield is specifically reviewed in section 3.3.4. It should be noted that Pb concentrations at discharge of SO_4 rich waters may be expected to be low, due to the poor solubility of anglesite ($PbSO_4$ - log K_{sp} = -7.8 (Appelo & Postma, 1994)) (Fuge *et al.*, 1994), this is described with reference to Ba in section 3.3.4.

The sources of two other ions which may be associated with acid mine waters, Al and Mn are not associated with a sulphide phase (Swaine, 1990). The source of Al to acid waters is the dissolution of silicates (section 2.2.2) and examples of the concentrations of Al which have been found in mine waters are shown in table 2.2, and these may be expected in low pH waters (section 2.3.2). Thus Al will not be discussed any further here.

Manganese can be very elevated in mine waters; Dryburgh *et al.* (1991) found 243 mg l^{-1} Mn in waters draining abandoned mines in the coalfield of Pennsylvania. This however, would appear to be exceptional in comparison with those values shown in tables 2.1 & 2.3. The source of Mn in the study of Dryburgh *et al.* (1991) was found to largely be siderite containing up to 2% Mn; siderite is also noted as a major source of Mn by Swaine (1990). Manganese may also be associated with the clay (illite) fraction (Huggins & Huffman, 1996; Swaine, 1990) and (especially in low rank coals) the organic fraction of coal (Swaine, 1990). The precipitation of Mn in mine drainage waters is described in section 2.3.3.

2.3.2 Aluminium precipitation

The geochemistry of Al in waters is generally controlled by a hydroxy phase above pH 4.5, where Al^{III} is stable, and is rarely controlled by adsorption, due to the high affinity for hydroxy ions (Paces, 1978). At pH <4.5, Al^{3+} is the stable dissolved species and is

highly soluble (Hem, 1985). Polymerisation of Al^{III} leading to gibbsite (or precursor phases) occurs between pH 4.5 and 6.5. At a pH>6.5 Al(V) dominates the speciation (Hem, 1985). Where dissolved Si occurs in appreciable concentrations, a Al-Si phase may be more stable than either oxide (Paces, 1978), and the presence of organic acids and F can lead to complexation in solution (Hem, 1985).

However, the speciation and stable phase of Al is changed in the presence of high SO_4, with Al-SO_4 phases being precipitated (Nordstrom, 1982b; Nordstrom & Ball, 1986). Aluminium can be undersaturated with respect to gibbsite or kaolinite in acid sulphate waters, and that this could be due to the control of Al concentrations by jurbanite, alunite or basaluminite (Nordstrom, 1982b). Winland *et al.* (1991) compared pOH, pH and pSO_4 and suggested that Al concentrations in the coal mine drainage water studied were controlled by jurbanite. Whilst Nordstrom (1982b) suggests that basaluminte ($Al(SO_4)(OH)_{10}.H_2O$) may be the stable phase initially for kinetic reasons similar to those described for the goethite - ferrihydrite system (section 2.2.5). These phases can also precipitate as minerals which are, at least initially, very poorly crystalline (Nordstrom, 1982b). The relationship proposed for the different Al-SO_4 phases by Nordstrom (1982b) is shown in figure 2.6. The Al precipitates forming in mine drainage impacted waters have been shown to be formed by rapidly reversible reactions, resulting in release of Al where pH declines (Smith *et al.*, 1988). It should be noted that because the precipitation of Al arises from hydrolysis reactions, a decrease in pH would be expected to accompany the precipitation.

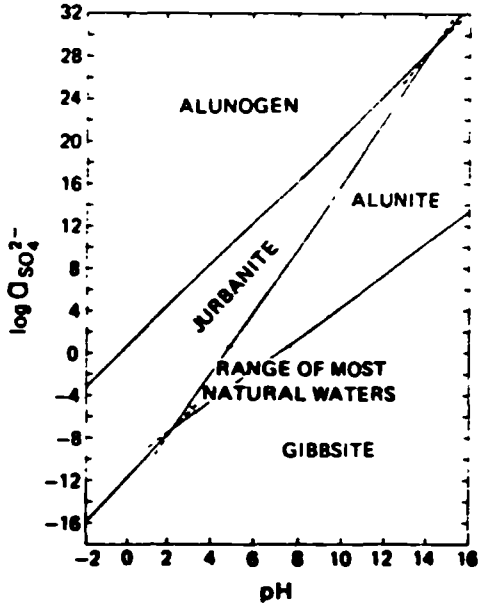


Figure 2.6: Stability fields of Al-SO_4 phases which may form from acid mine drainage (Nordstrom, 1982b).

2.3.3 Manganese precipitation

Manganese will be reduced, where occurring as MnO_2, in sediments by the development of Fe^{II} rich waters, and can be directly reduced by Fe^{II} to form Mn^{2+} in solution (Appelo & Postma, 1994). Thus high concentrations of Mn may be observed in mine drainage (table 2.2 & section 2.3.1). The pH of hydrolysis of Mn^{2+} is 8-8.5 (Levinson, 1980), and thus it is the oxidation of Mn^{II} to Mn^{IV} which may be expected to form MnO_2 (Krauskopf & Bird, 1995), although these precipitates may form as multivalent and / or amorphous phases, which remain amorphous over a period of years (Hem, 1985; Gramm-Osipov, 1990; Nicholson & Eley, 1997). As stated above, the redox potential required to oxidise Mn^{II} is greater than that required to oxidise Fe^{II}, and thus precipitation of Mn^{IV} may occur after the precipitation of Fe^{III} (Krauskopf & Bird, 1995). The stability fields for Mn species are shown in figure 2.7. Nordstrom *et al.* (1992) compared the Eh and Mn concentrations of mine drainage, but could find no relationship in the field data. Where Mn deposits form, the pH of zero charge is at ~ 1.5-2 (Nicholson & Eley, 1997) and thus the Mn oxides can sorb high concentrations of cations (Eley & Nicholson, 1993; Nicholson & Eley, 1997).

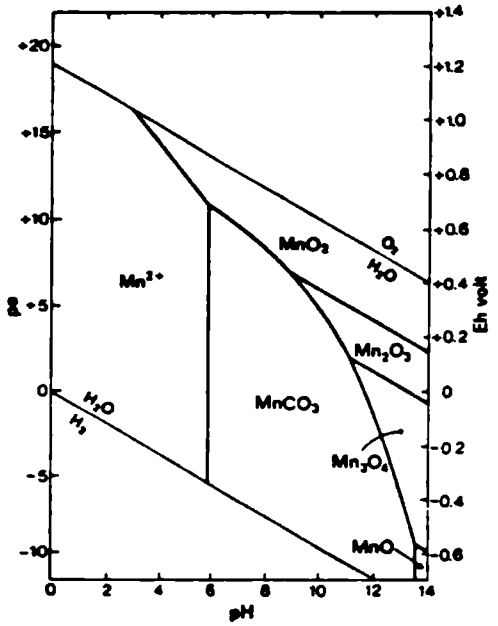


Figure 2.7: Stability fields of Mn species in natural waters (Appelo & Postma, 1994). Plotted for 25°C, $\Sigma S = 10^{-6}$ and $TIC = 10^{0}$ M.

2.3.4 Sorption of trace and minor ions on suspended material in stream waters

Concentrations of Zn and Cu downstream from the point of entry of acid mine drainage waters have been shown to decrease due to sorption to Fe^{III}-hydrous oxide phases in many studies (Boult, 1996; Boult *et al.*, 1994; Chapman *et al.*, 1983; Fuge *et al.*, 1994;

Johnson, 1986; Johnson & Thornton, 1987; Smith *et al.*, 1988; Webster *et al.*, 1994), of which these are only a few.

The maximum increase in sorption occurred at pH ~3.4-4.5 for Cu and ~5-6 for Zn in the study of Smith *et al.* (1988). The affinity has been suggested as Cu > Zn > Mn (Schwertmann & Taylor, 1989). The pH of hydrolysis of Cu^{2+} is 5.3 and that of Zn is 7.0 (Levinson, 1980), and it is the pH that has the strongest effect, because it is the hydrolysed species (MOH^{+}) which is sorbed to the ferric hydrous oxide (rather than the free ion) (Schwertmann & Taylor, 1989). This pH dependency for Cu and Zn sorption has also been noted by Johnson (1986) in extensive field sampling of an acid mine drainage impacted stream system. The sorption of ions to hydrous ferric oxides, particularly from studies with synthetic Fe^{III} precipitates, was extensively reviewed by Dzombak & Morel (1990) to which the reader is referred for more detail.

Where it is not possible to intensively study a stream (c.f. McKnight *et al.*, 1992; Broshears *et al.*, 1996) and use discharge and concentration measurements to determine loss from an aqueous system, the use of element ratios (where one element is presumed to be conservative in solution) can successfully show where reactive loss is taking place (Chapman *et al.*, 1983; Nordstrom, 1985).

2.4 Management of abandoned mine and spoil drainage in Britain

The effects of mine drainage are not small, with 200 km of surface waters affected in the UK (NRA, 1994b). All the regions of mining shown in figures 2.1 and 2.2 have observed some form of detrimental mine drainage (high metal concentrations / low pH / high salinity); selected hydrogeochemical analyses are summarised in tables 2.1 and 2.2. Such discharges are currently responsible for over 25% of water quality failures in Wales (NRA, 1994b). This section will briefly review the lack of legislation providing for the remediation of abandoned discharges, the effects of such discharges in relation to water quality guidelines and the natural and built environment, and finally will briefly review the currently favoured method of passive remediation of abandoned mine waters.

2.4.1 Legislative context

Abandoned mine drainage specifically has an exemption for the mine owners from prosecution under the Water Resources Act (WRA) 1991 s161(4) (Hughes, 1994; Lane & Peto, 1995) for "knowingly permitting" discharge from an abandoned mine; for which the exemption will only be removed by the Environment Act 1995 for any mine, or part

of mine, closed after 31 December 1999 (Lane & Peto, 1995 - who give the reasons behind this decision). This act has already improved the situation from that under the WRA 1991, by requiring 6 months notice of intention to cease groundwater pumping to be given to the EA (s58 & s59) and the powers for the EA to recover any remediation costs under s60(6) (Lane & Peto, 1995), although the recovery of costs from a mine which has closed due to financial problems may well be difficult (NRA, 1994b). This was introduced as a response to the criticisms of the Royal Commission on Environmental Pollution (RCEP) (RCEP, 1992) findings. The only successful prosecution for abandoned mine drainage has been at the Dalquharran mine (RCEP, 1992), with a case presented

against a discharge in the South Wales coalfield losing in court (ENDS, 1993). After the Wheal Jane discharge of mine water, which had a large impact on Restronguet Creek and the Fal estuary (Sperring, 1995; Younger *et al.*, 1997), the NRA was unable to bring a prosecution because the complex mining history and hydrogeology of the region would have made success unlikely (NRA, 1994b), however, £8M was provided for clean up and treatment operations, due to the national publicity arising from the incident (ENDS, 1991).

The early concerns raised about the closure of the deep coal mines in several areas of Britain are reflected in NRA (1994b), Hughes (1994) and Welsh Affairs Committee (1992) which devotes 36 pages to the evidence given in March 1992, in contrast to DoE *et al.* (1984) where water pollution from abandoned mines was dealt with in one short paragraph. NRA (1994b) and Dudeney & Monhemius (1992) provided early summaries of water pollution arising from coal mines and spoil heaps in the wave of concern which arose after it became obvious that many mines would close (Bailey, 1993; Robb, 1994; Robb & Robinson, 1995; Younger, 1993; Younger & Bradley, 1994; Younger & Sherwood, 1993) The present situation in the Durham Coalfield is summarised in section 3.5.

2.4.2 Effects of mine and spoil drainage

The environmental impacts of abandoned mine lands have been summarised in many publications (King, 1995; Förstner & Wittman, 1979; Kelly, 1988) and will not be reviewed here, except in the context of water quality guidelines. Smith (1981) mentions some of the mining related problems expected specific to County Durham and DoE (1994) reviews the impact of mine workings on water quality for metalliferous mines in Britain. The concentrations of metals in surface waters are largely compared to environmental quality standards (EQS) by the EA (now NRA) (1994b) and concern

exists wherever these are exceeded. Table 2.5 summarises the maximum concentrations of Cu and Zn allowed in rivers for the protection of two fish classes (NRA, 1994c). The pH of the waters for these fish should be 6-9 (Gardiner & Mance, 1984). The concentrations of other ions studied in this research are largely covered by ranges of concentrations allowable for intake to public water supply extraction, which sets Fe at a maximum of 2 mg l^{-1} and 1 mg l^{-1} (Gardiner & Mance, 1984). Copper and Zn are also regulated to maximums of 200 μg l^{-1} and 2.5 mg l^{-1} respectively, although it should be noted that this is an average annual value (Gardiner & Mance, 1984). Comparison of these data with tables 2.1 & 2.2 show that there is ample scope for these values to exceeded in coal and metalliferous mine waters in Britain. Davies *et al.* (1997), reporting the results published in NRA (1994a) classified sites on the area of stream bed affected by ochreous deposition, because Fe was found to be the major impact at the 90 discharges studied in the coal mines of north and south Wales. The EQS for Al (1 mg l^{-1} at pH 6-8) was never exceeded, but the Fe EQS of 2 mg l^{-1} was exceeded by many of the sites (figure 2.3). This was also found to be the biggest contributory factor to the impoverished benthic fauna found by Jarvis (1994) in a stream impacted by mine drainage in County Durham. The dominant cause of water quality failure being attributable to Fe is in contrast to the metalliferous mines of Wales, where Zn is the major concern (Richards, Morehead & Laing, 1992; Whitehead *et al.*, 1995).

Table 2.5: The maximum permissible concentrations of Zn and Cu in salmonoid rivers.

HARDNESS	Zn (mg l^{-1})		Cu (mg l^{-1})	
(mg l^{-1} CaCO3)	salmonoid	cyprinid	salmonoid	cyprinid
< 50	0.03	0.3	0.005	0.005
50 - 100	0.2	0.7	0.022	0.022
100 - 250	0.3	1.0	0.04	0.04
> 250	0.5	2.0	0.112	0.112

From NRA (1994c)

The effects of mine and spoil drainage are largely studied by investigation of the benthic invertebrate community of a stream, many studies have shown that a decrease in the population diversity and numbers are experienced due to these waters (Greenfield & Ireland, 1978; Letterman & Mitsch, 1978; Jarvis, 1994). The study of Jarvis (1994) showed that this was the case at a mine (Stony Heap) and spoil (Quaking Houses) drainage in the Durham Coalfield.

The drainage of abandoned mine workings may also be expected to have an impact on the use of river valleys for amenity purposes (Bailey, 1993; Younger & Harbourne, 1995), and a detrimental effect on engineering constructions, for instance where concrete which is not SO_4 resistant forms part of the fabric of a bridge (Henton & Young, 1993; DoE, 1994 and references therein).

2.4.3 Remedial options for abandoned coal mine and spoil heap drainage

The reclamation of colliery sites is described in Hartley & Wright (1988), including the various uses land could be restored to in a number of case studies; remediation of abandoned coal mines was not carried out (Glover, 1983). The use of passive treatment stems from the desire to provide a low cost, long term solution, and has been the subject of considerable research in the remediation of mine waters from the coalfields of the USA in both constructed (e.g. Faulkner & Richardson, 1990; Wieder, 1993; Tarutis & Unz, 1995) and natural (Wieder & Lang, 1984; Kwong & Van Stempvoort, 1994) wetlands impacted by acid mine drainage. The restoration of water quality has been attempted at a number of abandoned mine sites in Britain. One of the earliest is the limestone filter constructed in 1955 to ameliorate drainage from the abandoned metalliferous mine drainage at Cwmrheidol mine, Ceredigion (Fuge, 1972; Fuge *et al.*, 1994). More recent initiatives include the passive treatment systems at Wheal Jane, Cornwall (Payne, 1994; Younger *et al.*, 1997), Pelenna, Glamorgan (Younger, 1994) and Quaking Houses (Younger *et al.*, 1997) which were all initiated in the last 4 years. The publication of documents driven by the need to assess the effectiveness of wetlands in affecting mine drainage in Britain has drawn on the effects of natural wetlands at abandoned mining sites (Richards, Morehead & Laing, 1992). A more complete list of treatment methods can be found in Steffan, Robertson & Kirsten (1989). The biggest hindrance to the construction of treatment works in Britain is the lack of provision of central government funding to enable the EA to carry out the works, except in specific instances such as Wheal Jane (Younger *et al.*, 1997).

2.5 Summary

This chapter has reviewed the geochemical processes which lead to the formation of acid and / or ferruginous drainage as a result of pyrite oxidation, after the summary of typical concentrations of ions which may arise from coal mine drainage. The influences of processes affecting the aqueous and solid phase chemistry of both major and minor ions has been reviewed, along with the probable sources of those ions to mine and spoil drainage. Finally the chapter has briefly reviewed the legislative and management

options which are currently in place, these will be described specifically for the Durham Coalfield in chapter 3.

3.0 Regional and local context of study sites

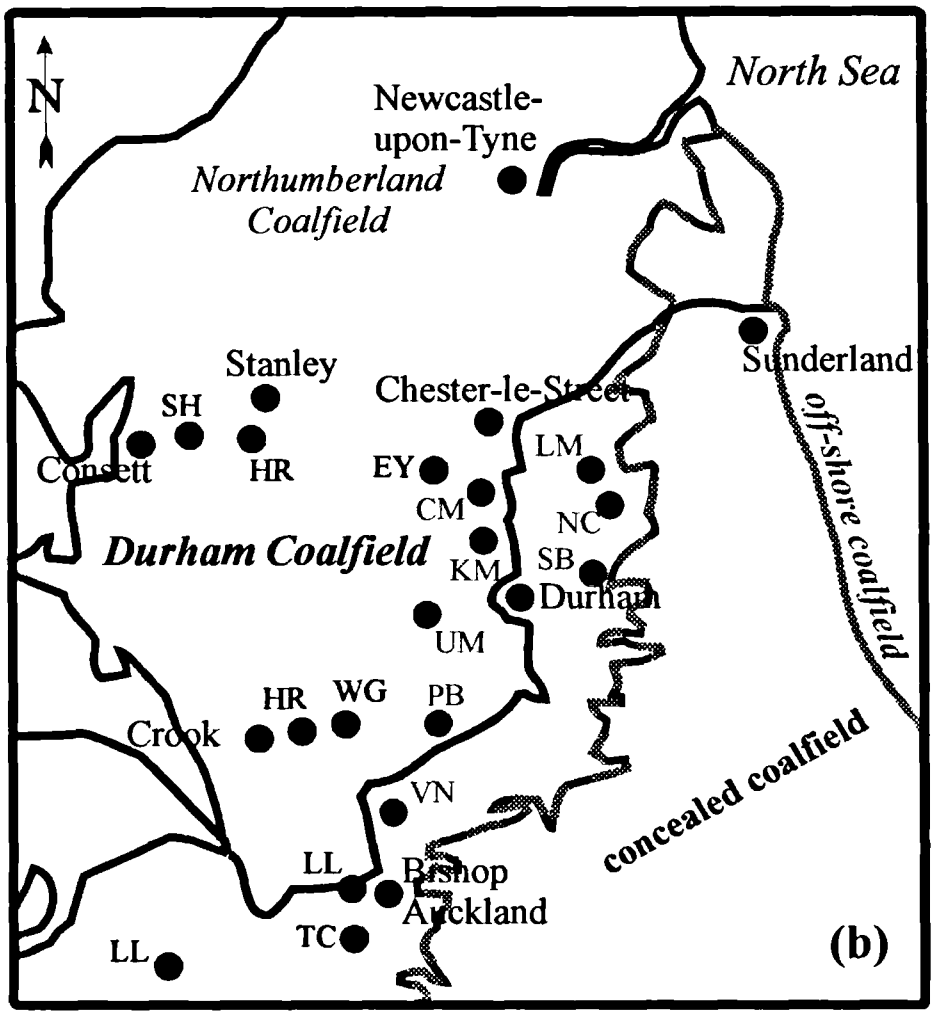
This chapter will discuss the regional geology and hydrology of the Durham Coalfield. As will be noted at several intervals below, the detail of information required for a study such as this was largely unavailable for the specific study sites. This review therefore refers in general to studies completed elsewhere, which may be applicable in a general sense to the Durham Coalfield. This information will be related to the interpretation of the chemistry of the waters observed at the discharge points in chapters 6 and 8. The description of sites is contained in section 3.2 below.

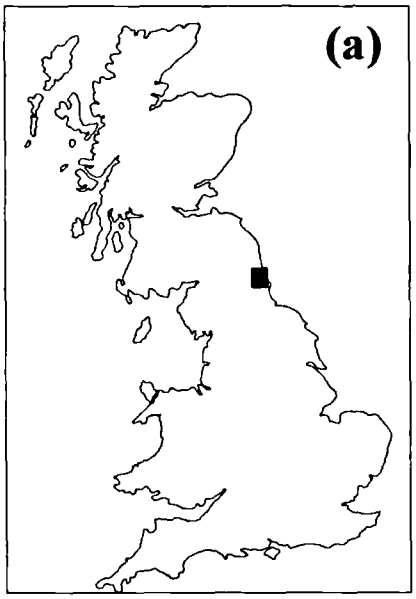
3.1 Location and physical setting of the Durham Coalfield

The Durham Coalfield is the part of the North East coalfield which lies within County Durham (National Coal Board / British Coal terminology (NCB, 1959)). The discharge sites studied for this thesis are all abandoned mine and spoil drainage's located in the catchment of the river Wear. The sites are all located in the western region of the Durham Coalfield. County Durham is highly urban in the region of the coalfield, due to its industrial history, and most sites lie close to roads and settlements (section 3.2). The location of the sites in specific detail is given in section 3.2. In figure 3.1 the location of the study sites in relation to the geography and geology of County Durham is shown. This coalfield is one of many in Britain which occur within Carboniferous age rocks, the location of this coalfield in relation to others is shown in figure 2.1.

The Durham Coalfield has a history of extraction stretching back to the Roman era (Smith, 1994b). The history of the coalfield is briefly reviewed by Smith (1994b; references therein). The age of the extractions affected the proportion of coal removed from the seam. Early workings were not as efficient at removing coal as the modern longwall methods, which take ~100% of the coal from the worked region (Smith, 1994b). The mining of the Durham Coalfield progressed from west (outcropping coal) to east (sub-Permian workings) down the dip of the Coal Measures sediments. The eastwards progression of mining, down the dip of the coal seams, was carried out as shallow surface workings became exhausted, and improvements took place in mine engineering capabilities (especially the ability to pump water to the surface from greater depths). Deep mining incorporating dewatering commenced in 1600-1700 (Younger & Sherwood, 1993). These advancements in engineering enabled mining to take place at a greater depth in the outcropping Coal Measures and enabled extraction from beneath the Permian strata (which extend beneath the North Sea from the east coast) both on- and off-shore to the east (figure 3.1).

Figure 3.1: The location of sites within the Durham Coalfield.
(a) the location of the main map within Britain
(b) the location of the field sites within the Durham Coalfield.





Carboniferous Coal Measures

Permian lithologies

River Wear

Towns

Pumping stations

Mine and spoil discharge sites studied

Pumping stations:
CM- Chester Moor; KM- Kimblesworth; LM- Lumley 6th; NS- Nicholsons; PB- Page Bank; SB- Sherburn Hill; UM- Ushaw Moor; VN- Vinovium.
From Harrison *et al.*, 1989 and Younger, 1993.

Sampling locations:
BB- Broken Banks; EY- Edmondsley Yard Drift; HR- Helmington Row; LL- Low Lands; QH- Quaking Houses; SH Stony Heap; TC- Tindale Coliery; WG0- Willington.
Grid references for all sites are given in appendix I.

At the time the coalfield closed the workings had extended 7km from the coast, beneath the North Sea, in the easterly extreme (Smith, 1994b). The cessation of deep coal mining in County Durham in 1993 led to fears for the river Wear, if the dewatering were to stop (Younger, 1993). These fears arose because, although deep mining was only taking place beneath the Permian outcrop on the east coast and offshore (figure 3.1), the dewatering was still covering a large part of County Durham to minimise pumping costs (section 3.3.2). This led to a number of studies of the Durham coalfield hydrogeology, which are summarised in section 3.3.2, and these showed that the river Wear could be expected to be severely impacted by the rebounding of the groundwater (Younger & Sherwood, 1993).

3.2 Geology of the Durham Coalfield

This section will review briefly the available information on the coal and associated sediments of the Durham Coalfield. The information included will be that which is pertinent to understanding the mineralogy and geochemistry of the sediments, which will be discussed in section 3.1.3.

3.2.1 Carboniferous Period

These are the oldest sediments encountered as interacting with deep or shallow water circulation in this study. The entire river Wear catchment lies within the Carboniferous sequence, with its headwaters in the Dinantian (carbonate and gritstone dominated) of the North Pennines. However, the Coal Measures sediments are the only lithologies of this sequence which are encountered by the mine waters, and thus the succeeding descriptions will be of these.

3.2.1a Coal Measures

The geology of the central coalfield area of Durham is not covered by a specific memoir of the BGS publications (sheet 26-Wolsingham), however, there is general information available on the surrounding areas in other sheet publications for Tynemouth (Land, 1974), Sunderland (Smith, 1994b), Durham to West Hartlepool (Smith & Francis, 1967) and Barnard Castle (partially covers the most southerly sites of this study (Mills & Hull, 1976)). The review of the mineralisation of the North Pennines by Dunham (1990) also contains an overview of the Durham Coalfield and the regional geology of North East England can be found in Taylor *et al.* (1971). The reader is pointed to those references and references therein for more detail on aspects not covered in this report. The local

solid and / or drift (1:50000) map for each site is given in appendix I. The sequence of lithologies in the Coal Measures is shown in figure 3.2.

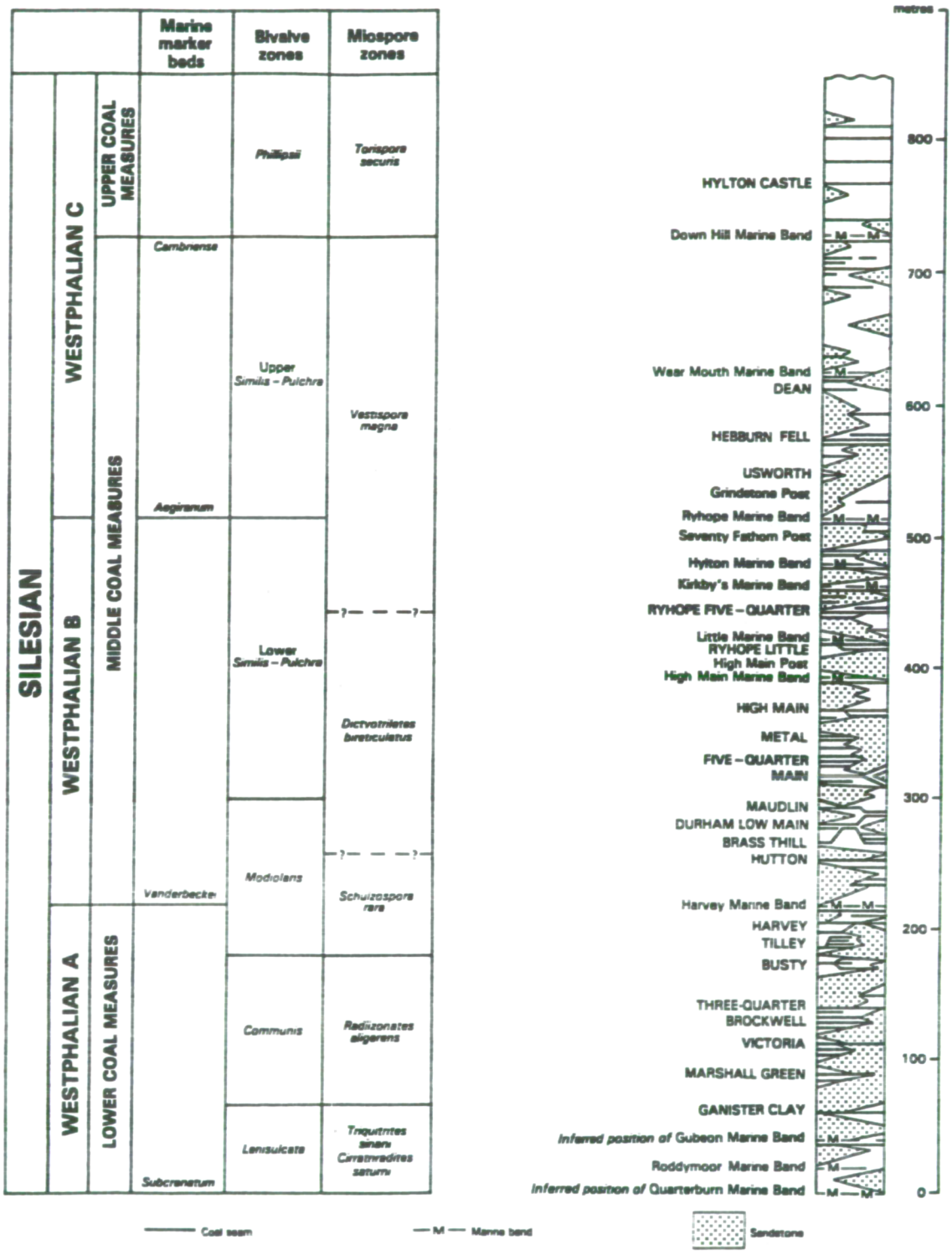
The productive Coal Measures are located within the lowest third of the Middle Coal Measures, which is the Westphalian B (Smith, 1994b). The older lithologies are generally arenaceous (60-90% sandstone) and the younger sequences argillaceous (Smith, 1994b) as shown on figure 3.2. The productive Coal Measures themselves are generally >50% sandstone occurring as intercalations with coals, marine sediments and other argillaceous strata (Smith, 1994b) and comprise a sequence ~370m thick in the Westphalian (Dunham, 1990). The sedimentology of the Coal Measures was subject to detailed study by Fielding (1984a; b; 1985; 1986), however these publications were largely concerned with environmental reconstructions and do not provide additional information on the mineralogy and geochemistry of the sediments, beyond confirmation of the general occurrence of marine or freshwater facies and argillaceous or arenaceous dominated sediments. This does not aid the understanding of the distribution of the most chemically reactive minerals within a sequence, such as pyrite and carbonates (section 2.2). A point of note is that marine bands (associated with increased pyritiferous and carbonate sediments (section 2.2.1a)) are fewer in the Durham Coalfield than in the more southerly coalfields of Britain, as a result of the depositional environment being less prone to marine incursions (Smith, 1994b). Thus, the productive Coal Measures are thought to have little marine influence, as determined by the scarcity of marine bands in the Durham Coalfield (Fielding, 1984).

3.2.1b Mineralisation in the Coal Measure sediments

The nature of coal mine drainage means that sulphide (and other) mineralisation is of interest as a source for the trace metals found associated with mine drainage; the mode of occurrence of these ions in other coalfields is reviewed in sections 2.2 and 2.3. The Durham Coalfield lies on the most easterly extremity of the North Pennines orefield, a region of major metalliferous mining (Dunham, 1990). The relationship of the Durham Coalfield to the centre of mineralisation in the North Pennines orefield is discussed by Dunham (1990; and references therein) extensively and the reader is referred to that publication for more information.

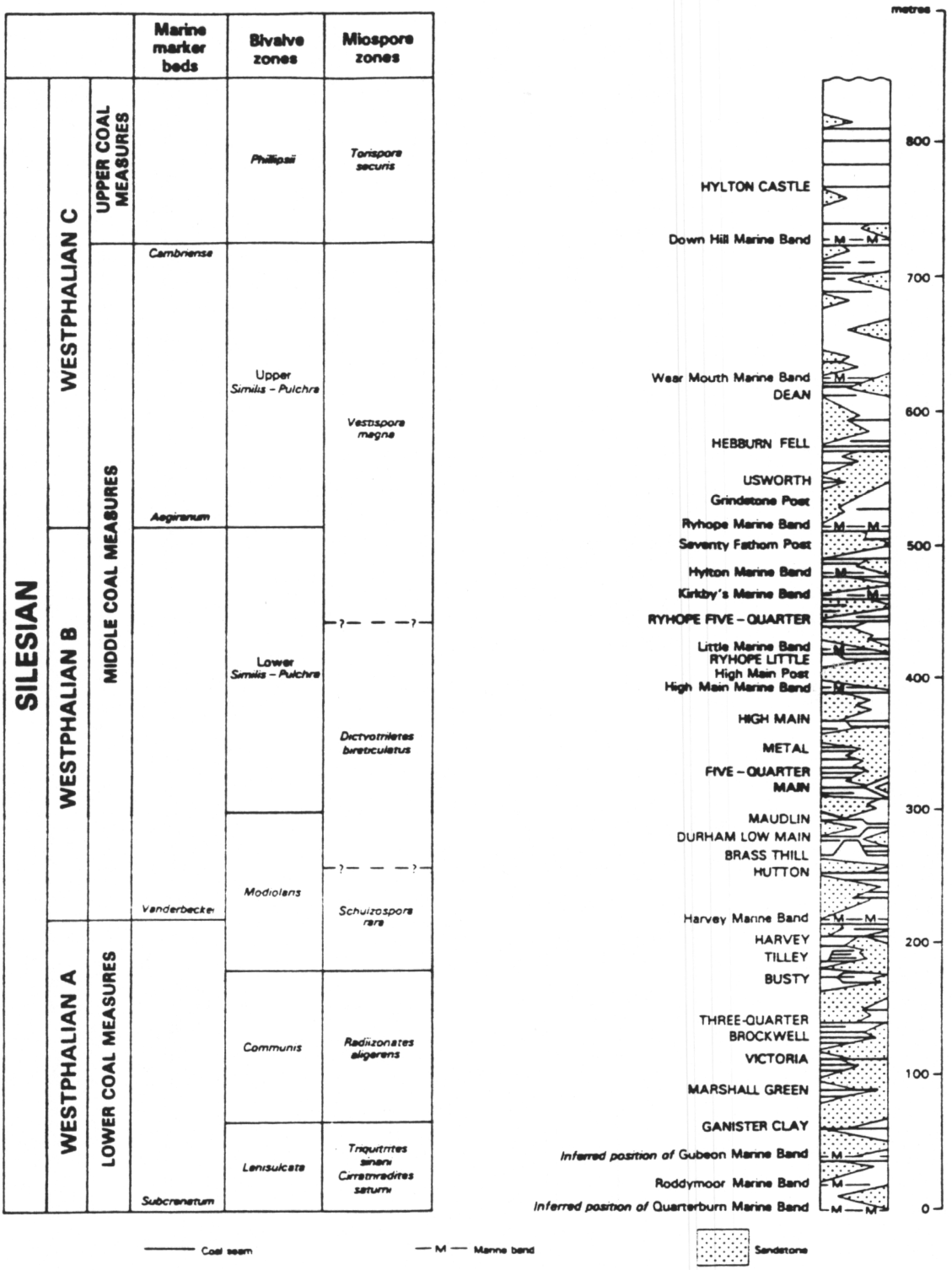
Up to the mid-1960's the NCB would measure both inorganic and organically associated S, however, after that time only total S in the coal was determined (Rippon, 1997). The quarterly coal analyses by British Coal report concentrations of selected elements as

Figure 3.2: The lithological sequence of the Durham Coalfield (Smith, 1994b).



The aranaceous strata are represented by the stippled areas and argillaceous strata by blank areas in the lithological column.

Figure 3.2: The lithological sequence of the Durham Coalfield (Smith, 1994b).



The aranaceous strata are represented by the stippled areas and argillaceous strata by blank areas in the lithological column.

oxides for operational mines and open-cast workings (e.g. British Coal, 1990). However, no reports were archived for reference after the disposal of the contents of the previous British Coal library in London and thus were unavailable to this study.

The two seams (Hutton & Busty) worked most extensively in the North East England coalfield are the only two for which seam maps of important chemical and physical parameters are available (NCB, 1959; 1961). Thus these are the only lithologies for which information is available on the inorganic S content (presumed to be dominated by sulphides in unweathered coal samples). The Hutton seam (NCB, 1961) is shown to have a composition of 1.5-2%, reaching 3% S locally, in the west of the coalfield. The concentrations in the most easterly (offshore) regions were 2.2-3% (Smith, 1994b). The Busty seam shows a concentration of 0.5-1% S in the west of the coalfield, with a general trend of increase to the east up to a regional average of 1.0-1.5% in coastal sections (NCB, 1959). This follows the general trend of an increase in rank with depth (Hutton is younger than Busty (figure 3.2)) and to the south west of the coalfield (Taylor *et al.*, 1971; Smith, 1994b). However, the lateral variations through the seams have been found to be greater than the extent of vertical differences (Smith, 1994b). High S coals are thought to often be associated with marine deposition (Thomas, 1992), and Land (1974) notes the occurrence of siderite and pyrite beneath the Harvey Marine Band (a laterally continuous marine band throughout the Durham Coalfield). Section 2.2.1a briefly reviews the problems associated with the correlation of marine sequences and S concentrations.

A problem is that the acquisition of information on the chemistry of coals was largely related to its end-purpose, so that parameters such as the percentage S in the coals is of importance in its use in power generation. In the prediction or understanding of water quality in a coal mined aquifer, the sediments remaining underground, exposed in the mining void, will be subject to most oxidation. The mining induced fracturing which will increase air and water permeability will be variable in extent around a mined area depending on the lithology of the surrounding facies (Neate, 1980). This means that with modern extraction techniques removing all the coal available, leaving the roof to fall behind the workings into the void whilst the extraction progresses, a large volume of the Coal Measures rock is exposed to an oxidising atmosphere (Frost, 1979). Thus the analysis of coal brought to surface is of considerably less use than information regarding the rock chemistry and thus that of the remaining aquifer. Unfortunately, no such information was available here, and the composition of the sediments and cements can only be inferred from references in other contexts and other regions of this and other

Carboniferous deposits in Britain. Attempts were made to track down data, and the following workers are acknowledged for kindly replying to my requests for information: John Aitken (Oxford Brookes University), Steve Dumpleton (BGS, Keyworth), Alan Spears (University of Sheffield), Dalway Swaine (CSIRO, Australia), Brian Turner (University of Durham) and Brian Young (BGS, Edinburgh).

Land (1974) briefly describes the cements found in the Westphalian sequences as including kaolinite, chlorite, micas, calcite, barytes and pyrite. However, there is no indication of the distribution and frequency of these minerals in the various sediments. Fielding (1982) also presents some information on the mineralogy of the sandstones, but this is largely concerned with the structural evolution of the Durham Coalfield, and details only those minerals showing conversion after metamorphism (e.g. the generation of kaolinite). Other papers which have discussed the mineralogy of Carboniferous Coal Measures in Britain, have been site specific studies for purposes other than acid generating and buffering potential and thus are not as able to provide data other than the frequent presence of carbonates (calcite, dolomite, ferroan calcite, ankerite and siderite) in the coal and associated sediments (Taylor & Spears, 1967; Hirst & Kaye, 1971; Hawkins, 1978; Spears & Sezgin, 1985; Rippon & Spears, 1989).

The Durham Coalfield contained one of the major centres for the extraction of barytes ($BaSO_4$) and witherite ($BaCO_3$) (and other minor Ba minerals) in Britain (Dunham, 1990). In addition to mining of Ba minerals, Ba was commercially extracted from the Coal Measure brines encountered in the mines (section 3.3.4a). The locations at which these deposits were mined are listed by Young (1985) and Dunham (1990). Sulphide minerals recorded in the Durham Coalfield mines are varied: galena, sphalerite, Ag-rich galena, arsenopyrite and chalcopyrite are specifically named (Dunham, 1990; Smith, 1981). Fluorspar is mined extensively in the North Pennines (Dunham, 1990) and its occurrence within the Durham Coalfield is noted by Taylor *et al.* (1971). Thus these minerals may be expected to be major sources of trace ions to drainage from abandoned coal mine workings in the Durham Coalfield.

A problem with interpretation of this data is that whilst it provides information on which minerals may be present, there was no incentive to specifically record the presence of minerals unless they were at or close to economic grade. The range of minerals encountered in the central North Pennines orefield are generally observed at lower concentrations throughout the Durham Coalfield, but rarely of economic grade and therefore not of note (Brian Young, BGS, Edinburgh, pers. comm.).

The history of mining, and more particularly, groundwater pumping at these sites was not elucidated in any detail during the period of study. No historical chemical data for the points of discharge was found. Whether any such data ever existed has become completely unclear, subsequent to the closure of most divisions of British Coal (previously National Coal Board). An attempt to find any historical data, or chemical and mineralogical data on the regions of interest was unsuccessful in locating where these records would be (if they did exist and still exist), due to a lack of cataloguing of material disposed of, donated and retained by the remnant of British Coal upon the closure of that company. This much information was gained from current and former employees of the companies mentioned, whose patient help I would like to acknowledge.

Due to the above problems, the information discussed below largely relies upon the relationships noted by other workers studying the mineralogy and chemistry of coal and associated sediments which are likely to be generally applicable to the Durham Coalfield.

3.2.2 Post-Carboniferous

3.2.2a Permian

The Coal Measures in the easterly extreme of County Durham, and offshore, were mined from beneath Permian cover (figure 3.1) until closure of the coalfield. The unconformable contact between the Carboniferous and Permian sediments is overlain by Yellow Permian Sands (maximum of 70m thick) for ~2/3 of the area (Smith, 1994b). These are generally poorly consolidated (Taylor *et al.*, 1971). The younger lithologies are carbonate dominated, calcite and dolomite, and intercalated with evaporites. These lithologies are described by Lee (1994) and Smith (1994b). This sequence is of little relevance to this study, other than in the context of the relation to the coalfield as a whole, and thus will not be discussed in any greater detail here.

3.2.2b Quaternary

Published information on the detailed nature of the Quaternary deposits of the area is scarce. The sediments which make up this period are a mixture of lithologies, which generally cover the area and may be from a thin veneer to over 60m thickness in some valleys (Smith, 1994b). Further information can be found in Smith (1994b), Smith &

Francis (1967) and Mills & Hull (1976), no detailed local information was available for the study sites.

3.2.2c Igneous

The only igneous lithology occurring in the study area is the Whin Sill and associated dykes. The geology of these rocks is covered in the general references given in section 3.2. These lithologies are not of significance in understanding the composition of coal mine drainage, as far as can be ascertained. The only recorded effect of the injection of the sills and dykes is locally anomalously high ranks of coals (Land, 1974; Creaney, 1980).

3.2.3 Structure

The Durham Coalfield lies on the Alston Block, which is bounded to the south by the Butterknowle (Lunedale) fault, and by the Ninety Fathom (Stublick) fault (Smith, 1994b). The general structure of the Carboniferous sediments is an overall 10° easterly dip, gentle folding and Hercynian fault structures (Land, 1974; Fielding, 1982). Faults occur throughout the region, the Butterknowle fault is the only fault specifically recorded as affecting groundwater flow (section 3.3.2)., but this is likely to be due to a lack of information on the other faults, rather than assuming that they have not had an effect. Chadwick *et al.* (1995) give a comprehensive review of the structure of NE England, to which the reader is referred.

3.3 Hydrology of the Durham Coalfield

3.3.1 Physical hydrology

The surface drainage of all the sites monitored in this study is in the river Wear catchment. The relation of the discharges to the streams in which they flow is shown in the figures referred to in section 3.4, as appropriate. These streams are not part of the stream discharge gauging network of the Environment Agency (EA), formerly the National Rivers Authority (NRA), and thus there is no flow volume data available for these sites.

3.3.2 Physical hydrogeology

The hydrogeology of an unmined Coal Measures aquifer is likely to be dominated by lateral flow along bedding, unless modified by preferential fracture flow. This is due to the high permeability contrast between the intercalated lithologies, such that the bedding of the sequences induces horizontal flow (Neate, 1980). Neate (1980) and Aldous (1986)

record low permeabilities for the seat earth clays, mudstones and coals, in relation to arenaceous lithologies, for the Carboniferous Coal Measures. This is supported by the large chemical variations found vertically in groundwaters of the Durham Coal Measures (section 3.3.3a).The rate of recharge to the aquifer will probably vary depending on the presence and nature of any overlying Quaternary deposits, as a result of their varying permeabilities (Cairney, 1972) and where the aquifer is overlain by Permian sequences, the basal Permian generally forms an aquiclude (Cairney, 1972). The groundwater resources associated with active coalfields were reviewed by Rae (1978), and Ineson (1967) also reviews similar material (largely for South Wales), neither of these reports provide specific local details for this study, other than [coal extracted]:[water pumped] ratios. Harrison *et al.* (1989) studied the groundwater distribution and temperatures in the Durham Coalfield, they found temperatures in the order of 11-16°C for the mines, which were still operating at that time. No other physical or chemical information was published in that study. The pumping regime at the time of complete colliery closure in the Durham Coalfield was 105 Ml d^{-1} (Younger, 1993), the surface area of pumping was much greater than was required for the safe operation of the coastal and sub-North Sea active mines, because it is much cheaper to pump from low groundwater head close to the recharge zone than to pump from above the Permian cover down to the active mines. The area of pumping at the time of mine closure is shown in figure 3.1; however, the coastal pumps were switched off in 1994, where all the rebounding water would enter the sea bed directly (Younger, 1995b) The region of the Wear catchment is, however, still being pumped to a depth greater than will allow infiltration into the river Wear. In the north of the coalfield the groundwater surface was up to 150m below land surface at the time of closure of the mines (Younger *et al.*, 1997).

The nature of mining in the Durham Coalfield is that multiple seams are mined from interconnected adits and shafts. This results in the aquifer changing to one with high vertical interconnectivity (Sherwood & Younger, 1994). Aldous (1987) and Aldous *et al.* (1986) showed that the post-closure mine permeability could be impeded by expansion of seat earth clay floors to mine roadways and that this could lead to "catastrophic" bursts.

In the case of the Durham Coalfield, the groundwater movement has been modelled as occurring in a series of "ponds" by Sherwood & Younger (1994). The Butterknowle Fault provides an impermeable southern boundary to the Durham Coalfield (Bradley, 1993; Younger, 1993). Predictive modelling of the groundwater flow paths has been

undertaken (Sherwood & Younger, 1994). This suggests that despite the high subsurface interconnectivity, the groundwater would not discharge into the North Sea, via the most easterly "pond", thus, Younger & Sherwood (1993) predict that the first surface discharge from a rebounding water table in the Durham Coalfield would occur in the Bishop Auckland area, within 15 years of ceasing to pump. The final discharge of groundwater to surface on complete abandonment of pumping would be expected to be of the order of 60-100 Ml d^{-1} (Younger, 1993). The conceptual model of groundwater flow during and post mining developed by Sherwood & Younger is shown in figure 3.3.

3.3.3 Hydrogeochemistry of surface water and stream sediments

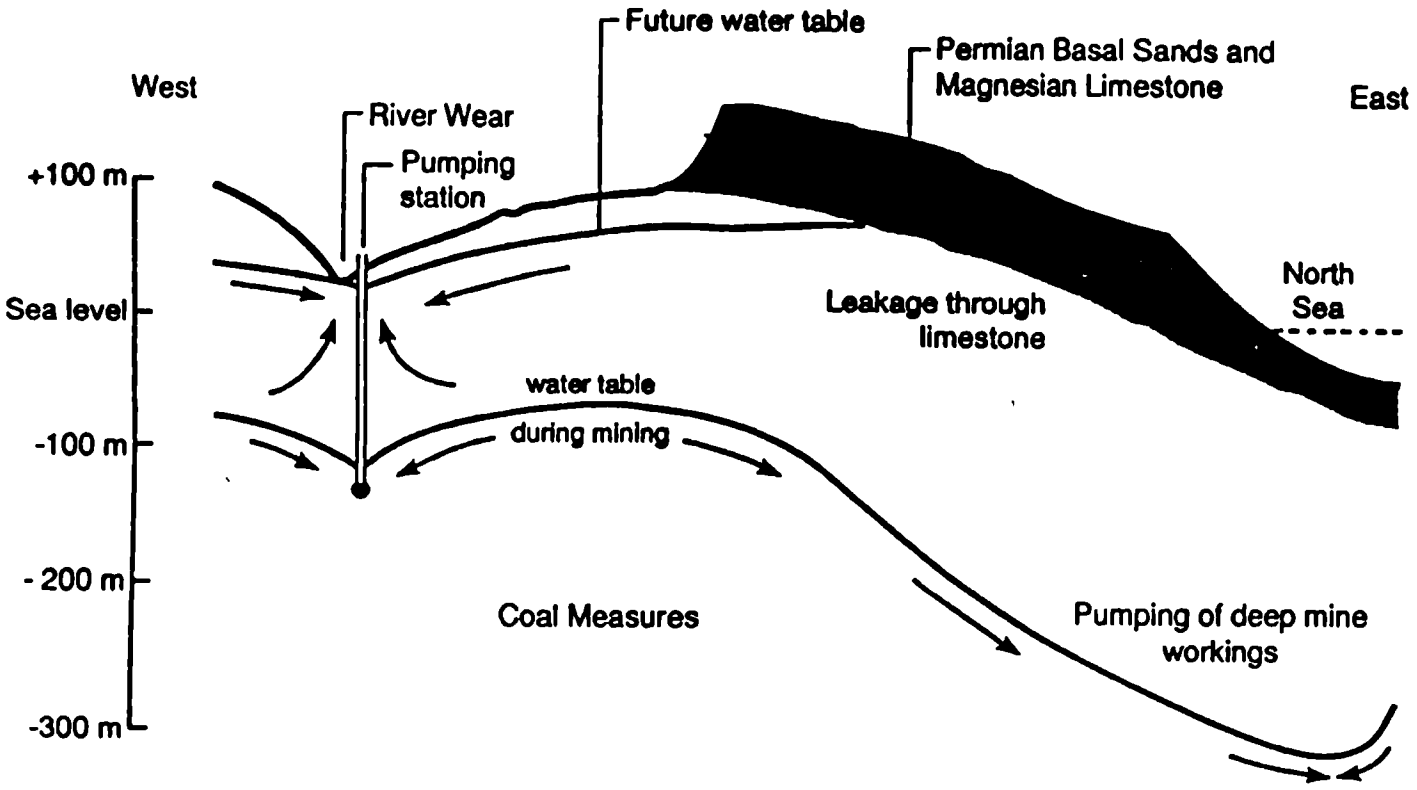
There is little specific data on the chemistry of the streams in the study area. BGS (1996b) provide comprehensive stream sediment coverage for Northern England and selected aqueous analyses. The concentration categories in which the elements are reported are broad, but show a regional pattern, with reference to the rest of Northern England. These data suggest that pH is generally 5.4-7.8 in the coalfield, and that HCO_3^- is 52-269 mg l^{-1}. In stream sediments Mn (0.25-2 %), Cu (47-900 mg kg^{-1}) and Zn (>360 mg kg^{-1}) are all elevated with respect to other lithologies, and is likely to be due to natural enhancement and industrial activities throughout the Durham Coalfield (BGS, 1996b).

3.3.4 Hydrogeochemistry of groundwater

3.3.4a Chemistry of waters in an undisturbed Coal Measures aquifer

The outcrop waters of Coal Measures are generally of a Ca-HCO_3 type, as the waters flow down gradient the hardness and SO_4 concentrations may increase, with the waters ultimately ending as a saline type (>10,000 mg l^{-1} TDS) (Rae, 1978), which has also been observed by Banks (1997) in Coal Measures groundwaters of Derbyshire and Yorkshire. Cairney & Frost (1975) found that the waters >300' (~100m) deep in the Coal Measures (unconfined and confined) show a 4x increase in mineralisation compared to recharge waters. The Coal Measures groundwaters encountered within mines showed a high degree of mineralisation in many instances, and a very varied chemical composition vertically (Anderson, 1945; Sheppard & Langley, 1984). Natural brine (Na-Cl or Ca-Cl type) springs, were observed to discharge into the river Wear prior to dewatering for coal mining (Anderson, 1945a). The location of these springs are recorded by Anderson (1945a; b) and Smith (1994b). Anderson (1945a) notes that these springs altered in composition temporally and were recorded to have a variation in concentration of the main ions from 100% Ca-Cl to 70% Na-Cl, 30% Ca-Cl (Smith,

Figure 3.3: Conceptual model of groundwater flow during- and post- mining in County Durham (Robins & Younger, 1996).



1994b). Barium was, in places, commercially extracted from the Ba-Cl brines (in addition to Ba mineral deposits (section 3.2.1b)). The Ba concentration in the brines could be sufficient (750-2700 mg l^{-1} Ba) to obtain 100 tons/week Ba from the groundwaters (Dunham, 1990). The source of these brines has been studied by Edmunds (1975) and Sheppard & Langley (1984). The study of Sheppard & Langley (1984) refutes the suggestion of Edmunds (1975) that the brines (up to 230 g l^{-1} TDS (Edmunds, 1975)) are largely of connate origin, and use isotopic evidence to show a meteoric origin, chemically altered by the dissolution of Permian evaporites (Sheppard & Langley, 1984). Durham Coalfield brine analyses have been given in Anderson (1945a), Edmunds (1975) and Burley *et al.* (1984). These analyses have all shown a highly mineralised composition, which can either be dominated by Cl or SO_4 as the major anion. Those which are Cl dominated often contain high concentrations of Ba, whilst SO_4 waters are lower in Ba due to the low solubility of $BaSO_4$ (log K_{sp} of $BaSO_4$ = -9.97 (Appelo & Postma, 1994)). The Durham coalfield has very saline waters in comparison with other coalfields in Britain, such as the South Wales coalfield (Ineson, 1967). The lower salinity of groundwaters found in the South Wales coalfield is attributed by Ineson (1967) to the absence of a post-Carboniferous cover, which allowed flushing of the connate waters.

The only specific information published on background shallow groundwater is by Dearlove (1994) who described them as Ca-SO_4 or Ca-Cl waters (no data published), which was attributed by Dearlove (1994) to agricultural land use of the soils overlying the aquifer measured. Iron was found to be "low" (0.02-0.16 mg l^{-1} Fe), with alkalinity 4-17 mg l^{-1} and 3-63 mg l^{-1} SO_4 (Dearlove, 1994).

3.3.4b Chemistry of waters in an actively mined Coal Measures aquifer

The chemistry and location of the modern pumping stations was reviewed by Younger (1993). Younger (1993) showed the chemical composition of the pumped waters to be temporally stable, with generally moderate pH values and lower Fe concentrations than the abandoned discharges, in general (Younger, 1995a, b, 1997a).

3.3.4c Chemistry of waters in an abandoned, mined Coal Measures aquifer

The expected processes of pyrite oxidation and subsequent potential for buffering of the chemistry are described in section 2.2.2. The studies by Frost (Frost, 1977; 1978a; b; Cairney & Frost, 1974), Jarvis (1994), Smith (1994a), Turner (1994) and Younger (Younger, 1993; 1994; 1995b; Younger & Sherwood, 1993; Younger & Bradley, 1994;

Sherwood & Younger, 1994) provide some background information on the chemistry of abandoned mine waters in the Durham Coalfield. These publications are complimented by additional publications on the chemistry of coal mine waters in Britain (section 2.1.1). This section will only review those studies of this coalfield, more general information can be found in section 2.1.

The chemical analyses for sites monitored as part of this study are shown in table 3.1 for selected ions. Younger (1995b) found that a high proportion of the discharges were not acid and have a high alkalinity. Using the calculation of mineral acidity it was found that some then became net acidic, although not all sites. The alkalinity of these discharge sites is attributed to microbial SO_4 reduction (Younger, 1997a) as reviewed in section 2.2.2.

The sampling of the ochre precipitated at the discharge sites found that at Broken Banks goethite was being precipitated, whilst "all" other sites were of an amorphous composition (Younger & Bradley, 1994; Younger, 1995b). The "yellow" ochres found in the summer are attributed to jarosite precipitation at Helmington Row (= "Crook" of Younger) and Quaking Houses from the work of Turner (1994). This net loss of SO_4 from the stream flow is thought to buffer the water acidity and results in SO_4 not being conservative as is normal . This jarosite will then dissolve when it rains (Younger, 1995b). Two sites having higher flows are expected to result in the persistence of anoxic conditions further downstream than the other sites studied (Younger, 1995b).

3.4 Description of the study sites

This section will provide a brief description of the sites selected for study in this thesis (more sites given in Younger & Bradley (1993)). The rationale behind their selection is included within the methods (section 4.1.2), and will not be reviewed here. The location of each sampling site and the occasions on which they were all sampled is shown in appendix I. The location of each point of discharge is shown in figure 3.1, with the downstream sites at Stony Heap, Helmington Row and Quaking Houses being shown in figures 3.4-3.6. The location of the sites only studied at their point of discharge are shown in figures 3.5 (Willington), 3.7 (Broken Banks and Edmondsley Yard Drift) and 3.8 (Low Lands and Tindale Colliery) for completeness.

3.4.1 Deep mine drainage

3.4.1a Broken Banks (BB)

This discharge emerges close to the bank of the river Wear (close to Bishop Auckland), and runs parallel for some 500m before entering the river Wear. Mining of the Busty seam ceased in 1955 (Younger & Sherwood, 1993; Younger, 1997a), the initial discharge data is not recorded. The volume of drainage of the stream is insignificant in comparison to the Wear, and the visible ochre along the length prior to the confluence, does not persist after the confluence. The location and sampling details are given in appendix I, and the site is marked on figure 3.1. The site is shown in plate 5.1. Previous chemical data determined by Turner (1994), Jarvis (1994), Smith (1994a) and Younger (1995b).

3.4.1b Edmondsley Yard Drift (EY)

This discharge (near the village of Edmondsley, Chester-le-Street) emerges from the bank of the Cong Burn, ~5m above the stream, before entering the stream. Mining and closure details are not known. The discharge is shown in plate 5.3a. The site and sampling details are given in appendix I. Sampling downstream from the discharge was not possible, due to the inaccessibility of the stream downstream from the point of discharge.

3.4.1c Low Lands (LL)

This site has a mine discharge overlain by a spoil heap, near the village of Low Lands. The discharge lies at the base of the spoil heap. However, the volume of discharge is small compared to the volume of the river Gaunless (plate 6.1). The overlying spoil heap is a very clear example of the practise of landscaping and stabilising, but not remediating a spoil heap. The land is used as sheep grazing. The spoil can clearly be seen at the surface, the grass coverage is poor, as is soil development (plate 6.1). The site location and sampling details are shown in appendix I.

3.4.1d Stony Heap (SH)

This deep mine drainage lies between Consett and Annfield Plain (location and sampling details appendix I). The length of stream sampled and the sampling locations are shown in figure 3.4. The discharge and stream length sampled is surrounding by pastoral farmland and minor roads. The point of discharge lies close to some derelict mine buildings. The discharge site is largely overgrown and in a collapsed (possibly) bell pit structure (Bradley, 1993), it is not possible to clearly photograph the discharge, but the

ochre accumulation at the discharge can be seen in plate 5.4b. The sites are either accessible from the road or with landowner's permission. Previous chemical data determined by Turner (1994), Jarvis (1994), Smith (1994a) and Younger (1995b).

3.4.1e Tindale Colliery (TC)

This site (in St Helen Auckland) lies on the edge of an industrial estate and derelict mine lands and flows into pastoral agricultural land (plate 3.1), and eventually drains into the river Gaunless. The site is shown in figure 3.1 and the location and sampling details are given in appendix I. The discharge is easily accessible, although somewhat awkward to sample.

3.4.2 Spoil heap drainage

3.4.2a Helmington Row (HR)

This spoil heap lies on the site of the Bowden Close colliery near Helmington Row. No deep mine drainage was observed at this site, where the Hutton seam was mined (Younger, 1997a). The spoil is landscaped and covered by a golf course in part, and the rest by shrub / tree plantings, which was completed in August 1970 (C.M. Hoult, Environment Dept., Durham County Council, pers. comm.). The flow through the spoil heap is channelled and controlled. The sides of the spoil heap are bare in places, and the golf course appeared to have a very thin soil covering on top of spoil. The main discharge of spoil water is from a pipe emerging from the spoil heap (plate 5.6), which then drains into the main channelled flow path. The stream then runs a natural course through arable land (with roads passing over) (figure 3.5). The sampling locations and details are given in appendix I. Previous chemical data determined by Turner (1994), Jarvis (1994), Smith (1994a) and Younger (1995b), where it is also sometimes referred to as "Crook".

3.4.2b Quaking Houses (QH)

This discharge emerges from the site of the Morrison Busty (initially South Moor Colliery) Colliery, which became the Chapman's Well opencast colliery before closure and reclamation (C.M. Hoult, Environment Dept., Durham County Council, pers. comm.). No deep mine drainage has been observed at this site. The spoil heap is cut through by a main road and a waste processing plant covers part of it. The spoil heap is landscaped and stabilising works have taken place, particularly on the road embankments. However, the remainder of the tip is covered by only sparse birch plantings, with the spoil at surface and no herbaceous coverage of the surface. The water

emerges from a pipe in the spoil heap (plate 5.5) and flows along the Stanley Burn. The discharge and downstream sampling occasions are shown in figure 3.6. The location and sampling details are given in appendix I.

3.4.2c Willington (WG)

The discharge at this site emerges from a pipe underground and flows down a concrete channel before entering the stream course (plate 3.2). The site was Brancepeth Colliery. Site location and sampling details are shown in appendix I.

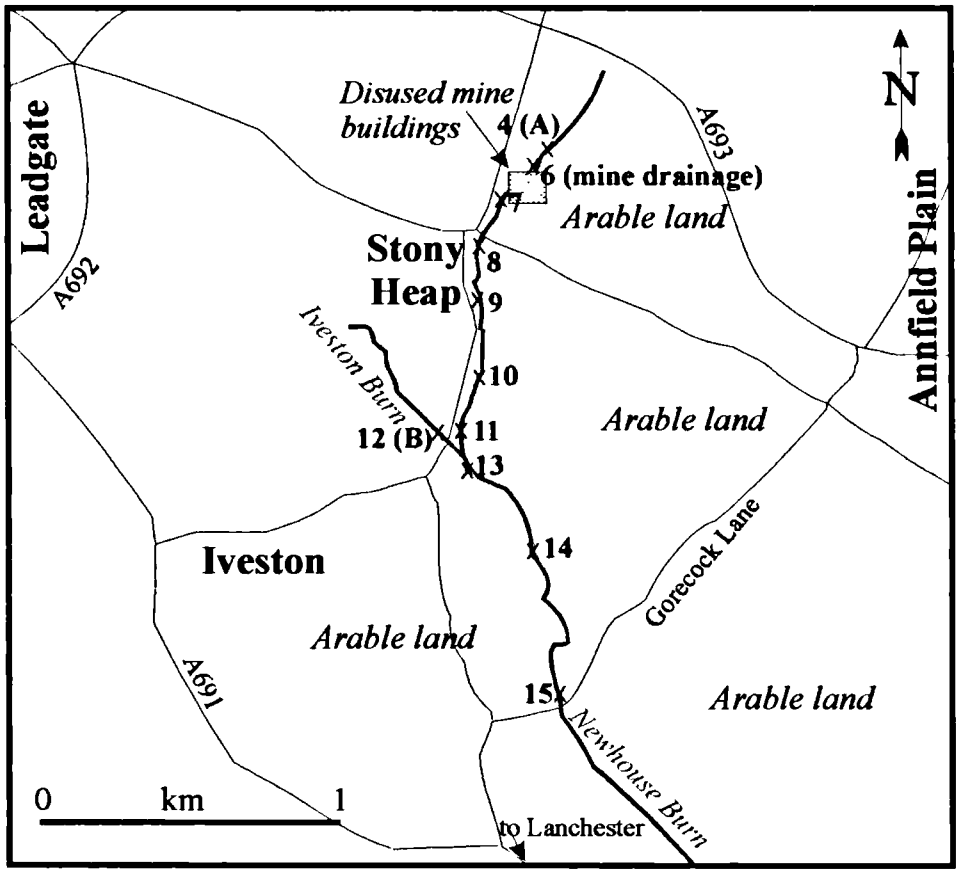
3.5 Historical and Present management of the Durham Coalfield

The cessation of deep mining in the Durham Coalfield, left no legal imperative or operational necessity to maintain groundwater pumping (section 2.4), which at the time was 105 Ml/day (Younger, 1993). The continued pumping of groundwater in the region has been assured until some (unspecified) method of remediation of the minewaters rebounding to surface has been developed (Schofield, 1995), although the pumping in the coastal region has now ceased, as those waters should rebound only to the floor of the North Sea (Keith Whitworth, IMC Ltd, pers. comm.). The only active management of the discharge sites studied here is the wetland development at Quaking Houses (Younger *et al.*, 1997), which treats a small volume of water draining from that discharge. This treatment did not affect the measurement of water chemistry at this site, and was constantly changing in design during this research, and so will not be discussed here.

3.6 Summary

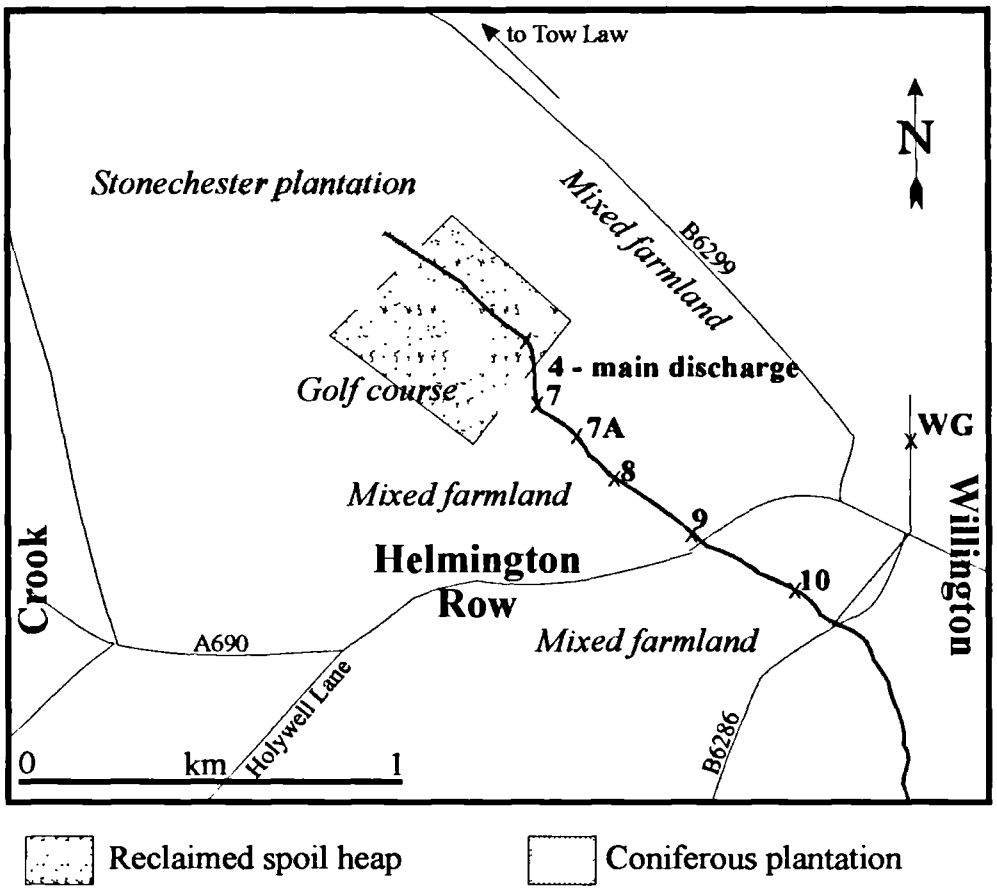
This chapter has described the local geological and hydrogeological conditions as far has been established during the course of this research, followed by location information for the discharge sites. The methods used to sample these sites will be described in chapter 4.

Figure 3.4: Map of Stony Heap stream system and sampling locations



5 - this is the sample site number as listed in appendix I. The national grid reference for each site is also provided in appendix I.

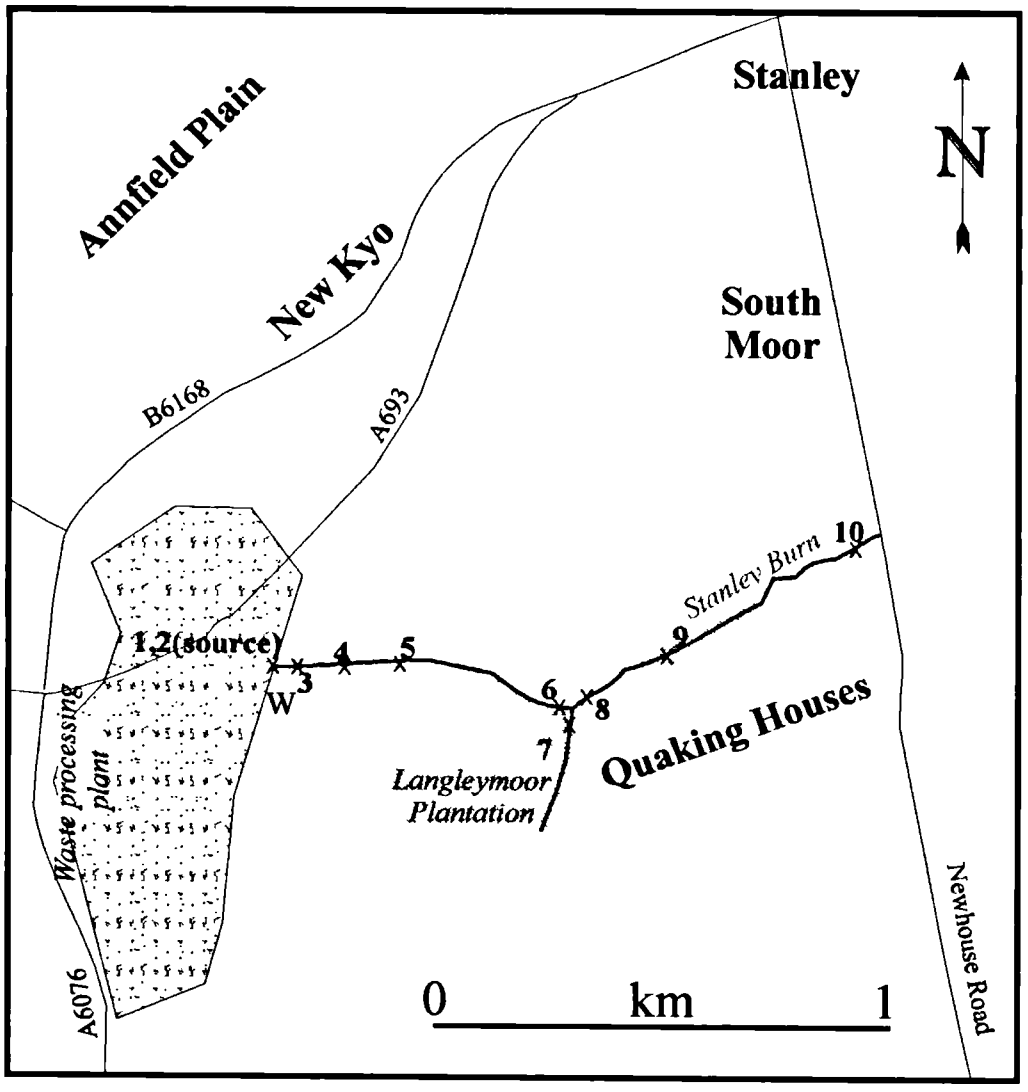
Figure 3.5: Map of Helmington Row stream system and sampling locations



5 - this is the sample site number as listed in appendix I. The national grid reference for each site is also provided in appendix I.

WG Willington discharge site. The national grid reference is provided in appendix I.

Figure 3.6: Map of Quaking Houses stream system and sampling locations



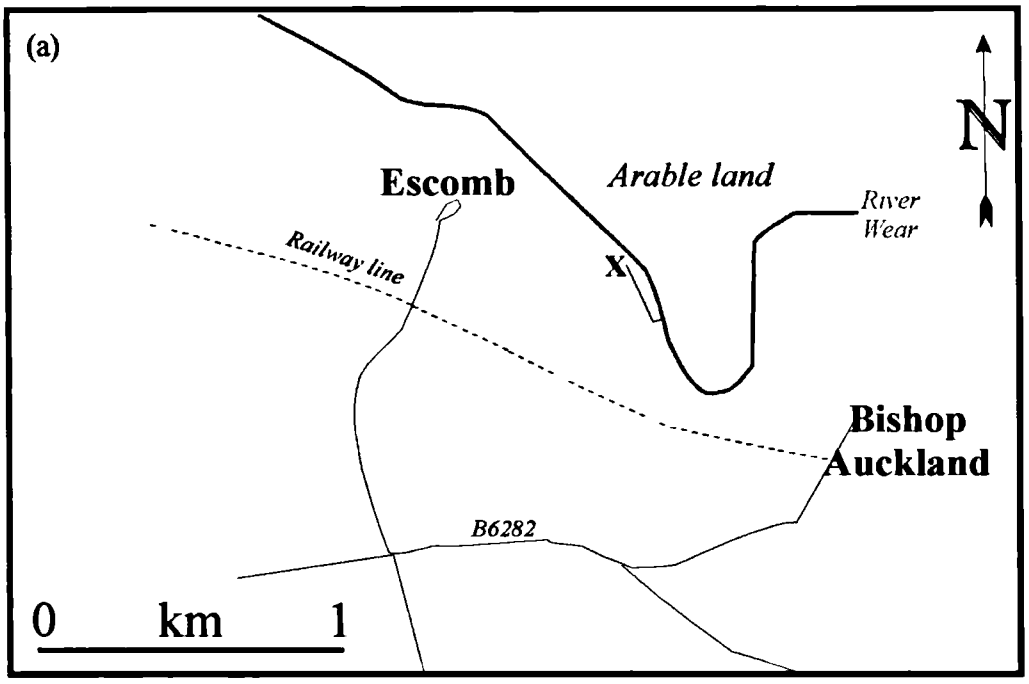
Coniferous plantation

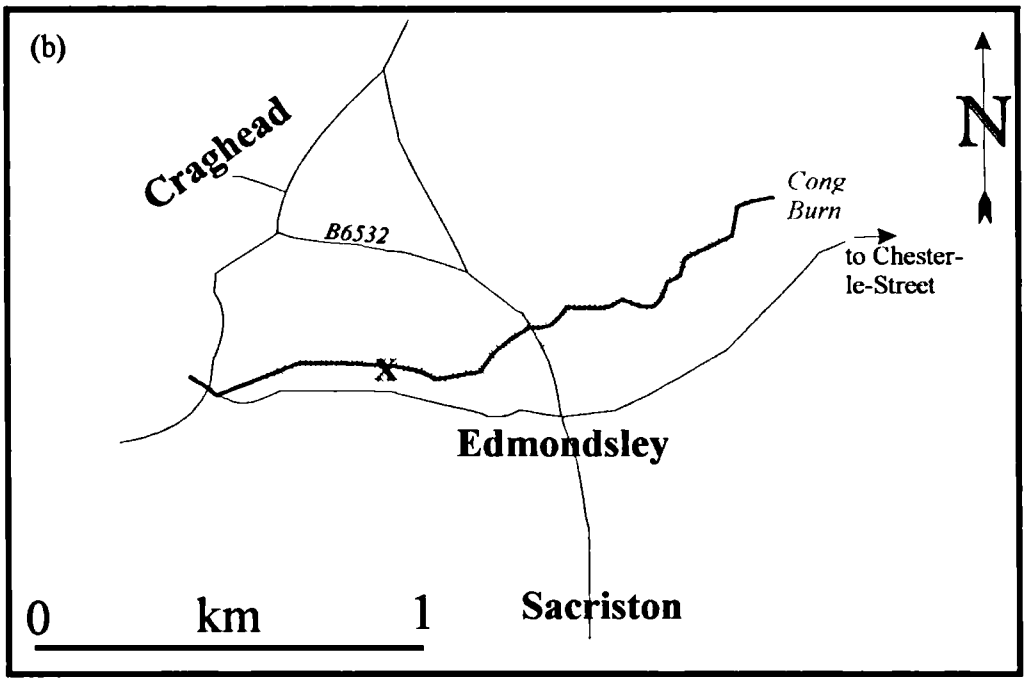
Landscaped spoil heap

5 - this is the sample site number as listed in appendix I. The national grid reference for each site is also provided in appendix I.

W - wetland spoil drainage treatment area (Younger *et al.*, 1997).

Figure 3.7: Maps of sites monitored only at the point of discharge
(a) Broken Banks (b) Edmondsley Yard Drift

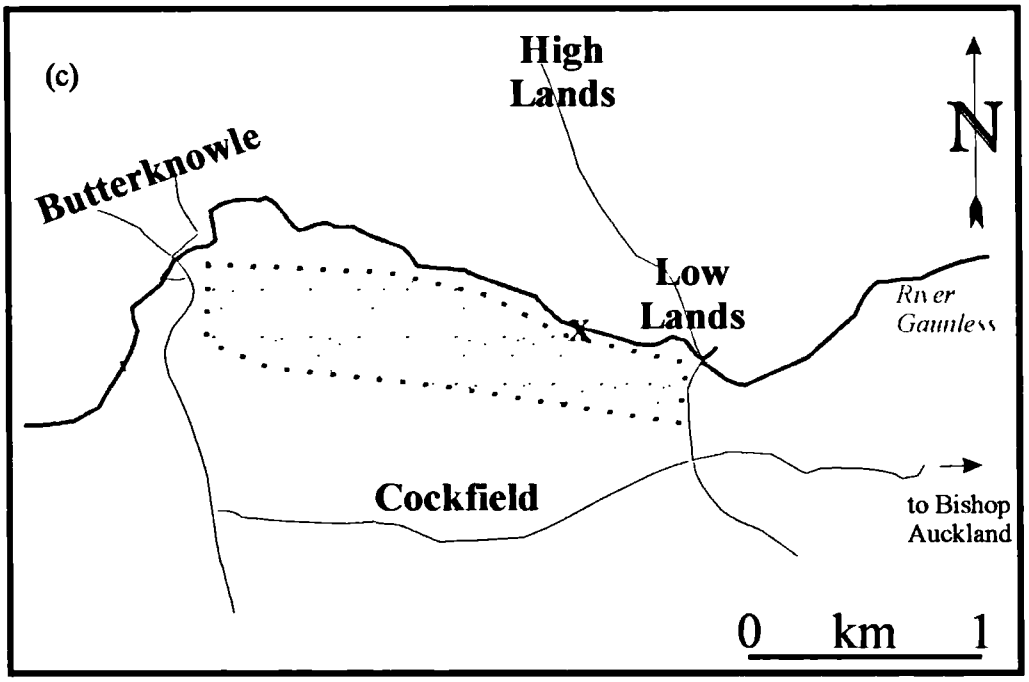


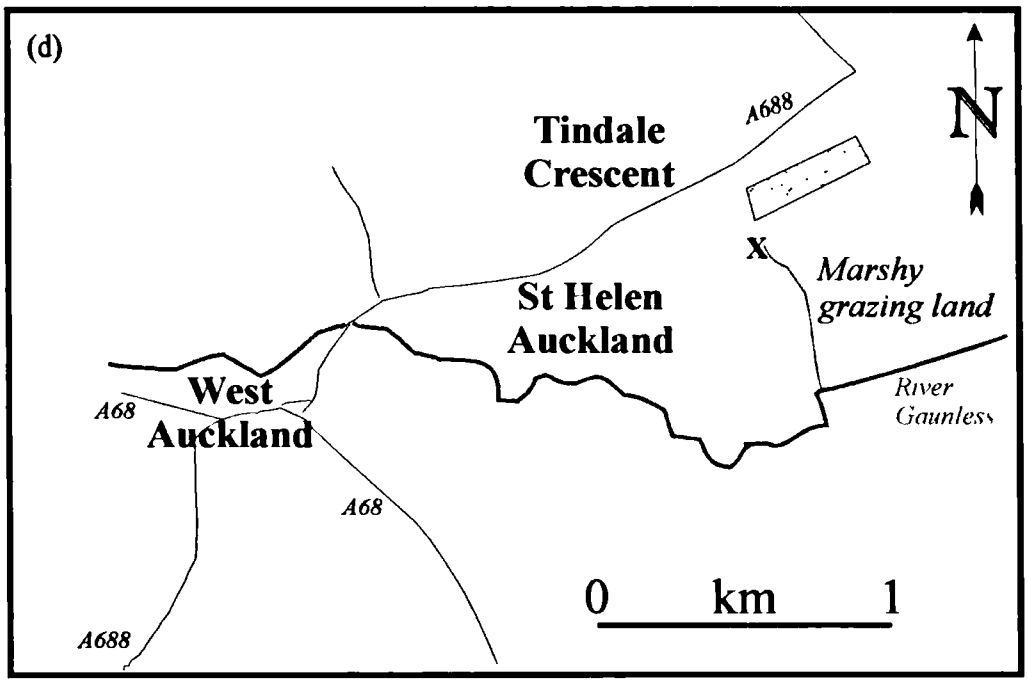


Woodland

X - the discharge site. The national grid reference for each site is provided in appendix I.

Figure 3.7: Maps of sites monitored only at the point of discharge
(c) Low Lands (d) Tindale Colliery





Landscaped spoil heap

X - the discharge site. The national grid reference for each site is provided in appendix I.

Plate 3.1: Tindale Colliery discharge. The point of emergence and view downstream.



Plate 3.2: Willington discharge



4.0 Sample collection and analytical methods

This chapter will describe the criteria (both scientific and logistical) by which field sampling localities were selected within the Durham Coalfield. Whilst the descriptions of the sites are in chapter 3, the reasoning behind their selection is discussed here in the context of practicality for sampling. The rationale behind the specific sampling sites at each locality is then described, followed by the sampling, analytical and interpretative techniques utilised. The methods described can be assumed to apply to all subsequent samples discussed unless otherwise specifically mentioned.

4.1 Field sampling protocol

4.1.1 Site Selection

The sites monitored during this study were selected from the work previously undertaken by Turner (1994) and Dr P.L. Younger (Department of Civil Engineering, University of Newcastle-upon-Tyne) (see descriptions of sites in chapter 3). A field observation visit was made to all the sites to assess their suitability for sampling, and whether investigations could be conducted downstream from the discharge location.

4.1.2 Sampling Location Selection

The sampling localities for each site were chosen firstly on the basis of expected usefulness in determining the downstream geochemical behaviour of the waters and sediments, and secondly on the basis of safe access. Thus, samples were collected at the point of discharge at all 8 sites selected; these sites were divided between coal spoil discharges and deep coal mines. For Helmington Row, Stony Heap and Quaking Houses it was possible to collect samples at downstream localities. These downstream localities were selected on the basis of field observations and an expected distance decline from the levels of ions at the point of discharge, as found in other studies (section 2.2). Where possible at these sites, a sample of water and sediment was collected upstream of the discharge to try and quantify the natural background chemistry of the catchment. The locations of Helmington Row, Stony Heap and Quaking Houses are shown in figure 3.1. Site location information is discussed in section 3.4 and summarised in Appendix I.

4.1.3 Sampling Frequency

Ideally sampling for a truly "seasonal" study would be undertaken at least monthly and preferably more frequently. This was precluded in this study due to the distances and cost involved. Thus as the objective was to monitor in varying hydrologic conditions, it

was decided to monitor at 3 monthly intervals for the first year, i.e. 4 sampling occasions. It was hoped that there would be significant differences in the discharges and that this would allow some estimation of the effect of seasonal variation on the geochemical behaviour of the coal working drainage. The sampling dates for all localities can be found in Appendix I. The number of sites visited and samples collected was adversely affected by bad weather and shorter daylight hours in November 1995 and March 1996.

4.2 Sample collection methods

Sites were sampled working upstream to avoid contamination and where possible all in-stream work was completed within as brief a time as possible to limit the chemical differences introduced by short term variations (such as storm events or diurnal fluctuations) in the streams. At approximately 10% of sites duplicate field samples were collected for each of the sampling media. This was to allow data quality analysis (section 4.4).

4.2.1 Waters

Samples were collected and stored according to the requirements specific to maintaining the sample integrity for the subsequent analytical technique to be used (section 4.3.1). Water samples (~200ml) were collected and stored in high density polyethylene bottles which had been through a rigorous washing process with a (phosphate free) soap solution, tap water rinse, nitric acid wash and finally a DIW rinse before being dried in an oven.

The waters were filtered at the field site using 0.45m cellulose acetate filters (Millipore Corporation). These parameters were kept the same for all field visits to minimise bias in results between sampling occasions (section 2.2.3b). Care was taken not to disturb bottom sediment in shallow streams, which would affect the suspended sediment loading (section 4.2.2). The waters required for ion chromatography (section 4.3.1.5) were kept out of the light at ~4°C to minimise reactivity and thus avoid changes in solution chemistry. Those which were to be analysed using ICP-AES (section 4.3.1.2&3) were acidified immediately upon collection using 1ml of concentrated ('Aristar') HCl. The acidity reduces the potential for chemisorption, hydrolysis and precipitation of elements (Thompson & Walsh, 1989). Waters for alkalinity determinations were kept in the same conditions as those for ion chromatography until analysis (performed at the end of sampling at site or on return to car, depending on conditions). On the sampling

occasions October 1996 and July 1997 filtering was undertaken at 0.2μm and 0.1μm respectively, in addition to the routine 0.45μm filtering. Samples were stored in identical fashion to the method described above. The assumptions associated with filtering and the potential problems were discussed in section 2.2.3b.

4.2.2 Suspended Sediment

The cellulose acetate filter papers used in filtering of the waters at each site were kept. Storage was in labelled boxes and sealed bags to prevent cross-contamination. The volume of water flushed through each filter paper was noted at the time of collection as it varied from site to site depending on water turbidity. The chemical analysis of these filters then was used to provide the suspended sediment loading in the stream.

4.2.3 Stream Sediment Samples

These were collected with a plastic scoop before being placed into a strong paper bag designed for wet sediment storage. These were kept in free draining ventilated conditions until returned to the laboratory. Special problems were encountered near the points of discharge because the stream bed was frequently composed of large boulder (>64mm), cobble size debris (>256mm) (Tucker, 1988) or were artificially concreted. At these sites the "stream sediment" consisted entirely of ochre coating on these stream bed materials. Problems exist in trying to collect sufficient of this ochre because fast running waters remove any disturbed material in suspension. This was also observed to be a problem at other sites in general since a very much more turbid water would occur after sediment sampling.

4.3 Analytical Methods

This section describes briefly the methods used to analyse samples chemically. The only method on which any developmental work was undertaken within the duration of these studies is that of the colorimetric Fe(II) method (section 4.3.1.8). A full, explicit method for all the techniques used can be found in Appendix II

All analyses undertaken included reagent blanks, analytical replicates and where possible reference materials in a randomised sequence with the samples to enable evaluation of the data quality using the techniques described in section 4.4. The analytical vessels used were all subjected to the same thorough washing process outlined in section 4.2 for the sampling vessels.

4.3.1 Stream Waters: Physico-chemical analyses

A number of different parameters were measured both in the field (pH, Eh, temperature, conductivity and alkalinity) and in the laboratory. Selected analyses are presented in section 6. A brief description of each method is given below. Acknowledgement is paid to Mr Barry Coles who ran all the analyses described below on ICP-AES.

4.3.1a Eh and pH

These parameters were measured directly in the field at the point of collection using a water test meter (Hanna Instruments). The pH meter was calibrated to pH 4 and pH 7 before analysis and found to be very stable during field work. These readings were also verified with pH paper (0.5 units) where possible, to ensure that the meter was functioning correctly. The Eh meter consisted of a platinum electrode which cannot be calibrated. The problems associated with Eh readings are discussed in section 2.3, and with reference to the chemical determination of Eh in section 4.3.1h. Each measurement was taken 3 times at each sampling location, with the mean result being presented in this work.

4.3.1b Dissolved oxygen

Dissolved oxygen (DO) was measured on the last 2 field visits (governed by availability of the instrument). The probe was calibrated using standard solution prior to fieldwork and found to be stable when carefully stored between analyses. Three measurements were made at each site, the mean of which is used in this thesis. Dr Giles Brown (University of Wales, Aberystwyth) and Dr Irena Tarasova (Imperial College) are thanked for the loan of their DO meters.

4.3.1c Major cations

These ions are well above the detection limit of the ICP-AES by direct nebulisation of the samples collected. For this method 5ml of sample was further acidified using concentrated HCl (Aristar) in the ratio 10:1 so that the standards and samples have the same acidity (Thompson & Walsh, 1989) and the solutions homogenised before analysis by ICP-AES.

4.3.1d Minor and trace ions

A non-selective evaporative pre-concentration technique with a La internal standard was used (Thompson *et al.*, 1982) (see Appendix II). This method is suitable for non-saline waters (Thompson & Walsh, 1989). 1.3ml of 5 $\mu g\ ml^{-1}$ La solution was added to 13ml of

sample. This was evaporated to ~1.3ml. The 10x concentration of the sample is to increase the concentration of trace elements in solution so that they are above the detection limit of the ICP-AES technique, as discussed by Thompson *et al.* (1982). The concentrated solution was then ready for direct analysis.

4.3.1e Arsenic, Sb and Bi

These elements were determined using an adaptation of the hydride generation technique of Thompson *et al.* (1981); the reasons for using hydride generation for these elements are given by Thompson & Walsh (1989). A 5ml sample was mixed in a 1:1 ratio with a 0.2% KI solution (Appendix II) which reduces all the elements enabling them to form hydrides more efficiently (Thompson & Walsh, 1989). Potassium iodide replaces the 5% KBr solution of Thompson *et al.* (1981) because it is a stronger reducing agent (B.J. Coles, pers. comm.). The solutions were then analysed by ICP-AES coupled to a hydride generation unit.

4.3.1f Sulphate and Cl^-

These analyses were undertaken using a Dionex 2003i/SP ion chromatograph (at Anamet Laboratories, Avonmouth, Bristol) with an AS450 column and electrical conductivity detection. All samples were initially determined at 100x dilution to avoid column saturation, dilution factors were then varied iteratively so that concentrations in solution fell within the calibration used. The analysis for F^-, NO_3^- and PO_4^{3-} proved impossible because the high dilution factor required for SO_4^{2-} and Cl^- left these ions below the detection limit. The field sampling for HS^- was undertaken using Pb-acetate paper, which rapidly shows a PbS (black) deposit where there is >0.5 mg l^{-1} HS^- in water, however, no positive result was obtained. The high concentrations of SO_4 measured (chapter 5), the absence of HS^- at concentrations >0.5 mg l^{-1}, and the rapid oxidation of S in pyrite weathering (section 2.2.1), is suggested as evidence that assuming all the S present to be SO_4 at the time of collection, is correct.

4.3.1g Alkalinity

The total alkalinity of the water was measured by titration of 20ml of sample with 0.01M HCl. BDH '4.5' indicator solution was used. The titration volume could then be used to calculate the alkalinity (Krauskopf, 1979). The titration was performed either at the site or on return to the car, depending on site access and conditions, because long term storage of alkalinity is not possible (Hem, 1985). This method was not used on the first field trip because the acid taken was of the wrong molarity.

4.3.1h Iron(II) and Fe^{III} by colorimetry

The Fe^{II}/Fe^{III} redox couple present the opportunity to determine the Eh of an aqueous system if both can be measured (section 2.2.3a and below). However, there was no method available at the start of this study. Thus a short investigation was initiated which was parallel to the thesis research, and enabled the determination of Fe^{II}/Fe^{III} on the final sampling visit of the thesis. All the work described here was undertaken in collaboration with Dr Ron Fuge (University of Wales, Aberystwyth) and shall briefly be reported here, and is in preparation for future publication.

The reason for measurement of Eh is that this can theoretically be used to determine the distribution of all other redox sensitive species, if thermodynamic equilibrium is assumed (section 2.2.3a). The errors associated with the measurement of Eh by Pt-electrodes (Eh_m) are reviewed in section 2.2.3a, and many researchers on the subject advocate the analysis of individual redox species to produce Eh (Eh_N) (section 2.2.3a). The reason to quantify the Eh, despite all the problems, is in the input data for geochemical modelling packages, where species distributions will be determined using the input data, or in the case of a model such as PHREEQ-C, using a default value if no data is input, because Eh is a master variable in such calculations (Parkhurst, 1995). The high concentrations of Fe in mine waters make Fe^{II}/Fe^{III} an ideal redox couple to use to calculate Eh from chemical information (e.g. Nordstrom & Munoz, 1994).

Methods have long existed for the determination of Fe^{II}/Fe^{III} in aqueous samples, and have recently been reviewed by Pehkonen (1995). However, that comprehensive review of methodology makes no mention of the problem of sample stability between collection and analysis, and most of the recent advances in that field require equipment which is expensive and / or not field portable at low cost. Thus the selection of a method for investigation was driven by the following points: field collection followed by laboratory analysis saves valuable time in the field and is easier than field determinations; if such field determinations are to be meaningful, samples should be stabilised in the field for storage until analysis; equipment and chemicals should be freely available and a pre-existing method is preferred.

A body of literature already exists on the measurement of Fe^{II} and total Fe (Fe_t) using Fe^{II}-dipyridyl complexes (Moss & Mellon, 1942) and methodology is established (e.g. Skougstad *et al.*, 1977a,b). This method determines Fe^{II} directly and uses a reducing agent to determine Fe_t, with Fe^{III} being calculated by difference. The detection method is

by colorimetry, which is standard laboratory equipment, however field portable colorimetry was not available in this work, so the need to transport stabilised solutions back to the laboratory was established. The work of Moss & Mellon (1942) showed the colour complex to be stable over long periods (months) of time in laboratory synthesised solutions, however for field determinations workers specifically highlight the need for instant, field analysis (Skougstad *et al.*, 1972a,b).

Thus work was undertaken with Dr Ron Fuge (University of Wales, Aberystwyth) on samples in the mid-Wales orefield region. This involved sampling of an acidic (pH~3.4) and Fe_t 10-30 mg l^{-1} and near neutral (pH~5.8) and Fe_t 0.1 - 1.0 mg l^{-1} location. The results showed that for filtering at 0.45 and 0.1μm the samples were stable for Fe^{II} and Fe_t over a period of at least 48 days. Thus, the long-term stability of the colour complex was established (Ander & Fuge, 1997). This enabled samples to be collected in County Durham and returned to the laboratory at Imperial College (analyses with the assistance of Mr Peter Watkins) or Aberystwyth (analyses by Dr Ron Fuge) without fear of the equilibria changing from that present at the time of sampling. These determinations were undertaken in March 1996 and July 1997 (October 1996 missed). The full method is supplied in Appendix II.

4.3.2 Stream Waters: Discharge measurements

The streams monitored in this investigation were too small to use a flowmeter effectively, because the water was too shallow to allow the complete covering of the impeller blades of the current flowmeter which was used. Discharge was measured at Quaking Houses by the capture of all the discharge within a 10*l* bucket and timing the filling of a bucket with a stopwatch. This was not possible at the other sites. At the other sites discharge was always estimated, to allow the assessment of "high", "normal" and "low" discharge volumes when comparing chemical results between sampling occasions. Operator experience (with previous work, measuring stream flows) in doing this suggests that estimation is probably a valid technique for order of magnitude estimations, enabling gross differences between sampling visits to be qualitatively recorded. Another line of evidence of stream discharge, is the visual observation of the height of the water surface in relation to the bank of the stream. This is particularly evident in streams precipitating ochre, because they leave an ochreous deposit.

4.3.3 Suspended Sediment

The cellulose acetate filter papers collected (section 4.2) were digested in a HNO_3 - $HClO_4$ (2:1 volume ratio) attack which was evaporated to dryness (Appendix II). Then

the remaining salts were leached with 1ml of 5M HCl and 4ml of DIW. The solutions were then analysed by ICP-AES.

4.3.4 Stream Sediments and minewater precipitates

These were dried at room temperature (~25°C) and then disaggregated using a pestle and mortar. The material was then sieved to <80mesh (~0.177mm). A smaller weight of sample was used for the ochres than stream sediments, to avoid saturation of the solution with Fe. Sample digestion was achieved by evaporating to dryness after the addition of HNO_3 (4ml) and $HClO_4$ (1ml). Subsequently, the dry residue was leached with 2ml of HCl and 8ml of DIW (Appendix II).

Coring was undertaken at EY and SH using a simple plastic tube, which had been cut in half lengthways and then sealed with tape. This enabled the core to be cut open on site and re-used by sealing again as necessary. The cores were opened and sub-sampled at ~5cm intervals immediately after collection. At BB discharge a brick surface was cleaned and place back into the discharge (plate 5.1) in October 96 and sampled in July 97, thus assuring the precipitate to be no older than 9 months. The brick had not noticeably been disturbed when it was collected.

4.4 Data Quality Control

Data quality analysis is undertaken prior to interpretation of the data to determine the limits to which the data can be realistically interpreted and utilised. The methods by which this has been done are briefly reviewed here.

4.4.1 Detection Limit

The detection limit can be defined as the concentration at which the instrument signal is significantly different from that obtained by running reagent blanks within the sample sequence (Miller & Miller, 1984). These "procedural blanks" are vital in detecting contamination from the digestion chemicals, vessels and airborne pollution (Thompson & Walsh, 1989). The reagent blanks are an integral part of the randomised sample sequence in every analysis (section 4.3)

It should be noted that the actual detection limit (ADL) can be somewhat different to the instrument detection limit (IDL), which is the theoretical minimum signal which the instrument in use can detect (Thompson & Walsh, 1989). Any values which fall within an order of magnitude of the ADL cannot be discriminated from instrumental "noise"

and so are not included in any interpretative evaluations. The reagent blanks in the sequence are automatically compared, in post-run analysis, to the instrument blanks and used to correct the results if they are significantly different from the instrument blanks (B.J. Coles, pers. comm.). The method of calculation for ADL and the results for IDL and ADL are given in Appendix III.

The results for selected elements are given in Appendix III. All the results for the ADL are at or close to the IDL; where they are above the IDL they are so far below the concentrations in the samples that they are irrelevant in the interpretation of the data.

4.4.2 Bias

It is necessary to monitor any bias present in the method used to ensure the comparability of the data to other measurements in the field of study, and separate batches within a single study such as this. It is also particularly important when relating results to any statutory requirements that the bias is acceptable and accounted for in the interpretation.

Bias is the systematic error of a method producing a variation from the true value and is different from accuracy which is the closeness of one result to the true value. Bias can be determined by three methods: 1. Data quality comparison with different techniques / laboratories (laborious and expensive). 2. Spike recovery (matrix matching problems). 3. Reference materials (used in this study and discussed below). The bias should be <10% for an acceptable level of data quality (Thompson & Walsh, 1989).

The reference materials were part of the randomised batch of samples whenever they were used (section 4.3). The reference materials in this study were house reference materials (HRM's) HRM1 (silicate matrix, low analyte concentrations) HRM2 (silicate matrix, high analyte concentrations) and HRM10 (aqueous solution). HRM1 and HRM2 are good matrix matches for stream sediment analysis, because they are closely matched to the composition of the sample (Thompson & Walsh, 1989) but for the ochres (predicted to be dominated by iron (oxy)hydroxides) CRM's were additionally used to attempt a closer matrix match than the HRM's would be predicted to achieve. All those used and their accepted or certified concentrations are summarised in Appendix III with the results of running them in each batch (where the method of calculating bias is also presented).

4.4.3 Precision

It is necessary to measure precision to enable assessment of the error on the data and thus the limits between which the sample value could actually fall. This is important both for interpretative work and application of results to statutory levels in various media.

It is possible to determine precision from either repetitive analyses of one sample or duplicate analysis of several samples. Duplicate analyses are the better method for the estimation of precision, because they cover a wider range of sample concentrations which can affect the error (Thompson & Walsh, 1989), than the re-analysis of smaller numbers of samples (such as HRM's or CRM's (section 4.4.2)) (Thompson, 1992). The duplicate analyses of reference materials as used to calculate bias, are not suitable for analytical precision calculations because they are likely to be more homogenous than the samples and as such will give an estimate of precision which is somewhat biased in itself from that obtained from the samples (Thompson & Walsh, 1989).

The method used here is that of robust ANOVA (analysis of variance). This is a calculation which can separate analytical, sampling and geochemical sources of variance in the data, to enable the precision to be estimated for the samples (Thompson & Ramsey *et al.*, 1995). Sampling error should be significantly less than the geochemical variation so that the geochemical variation is clearly observable (Thompson & Walsh, 1989).

At approximately 10% of field sites a duplicate set of samples were collected, with each then subject to replicate analysis. These 4 samples from one site are the minimum requirement to use robust ANOVA calculations (Ramsey, 1993). The program used was Robcoop4 (Analytical Methods Committee, 1989) because it automatically downweights the effects of results which are extreme in relation to the bulk of the data (Thompson & Ramsey *et al.*, 1995). Robust ANOVA is useful because the classical ANOVA is sensitive to the actual values entered when these vary by two or more orders of magnitude (Ramsey, 1993). However, robust ANOVA can incorporate data from beyond that range rather than discount the widely dispersed results and therefore is more applicable to the type of samples encountered in this study where both gross elevation and "background" values exist (section 2). The use of the robust analysis can result in the values for the different sources of variance falling within their recommended limits, whilst the classical analysis indicates the data to be far less reliable (Ramsey *et al.*,

1992). Ramsey (1993) points out the application of this method for environmental data in general.

Ramsey *et al.* (1992) showed the additive variances as summarised below:

$$s^2_{total} = s^2_{geochemical} + s^2_{analytical} + s^2_{sampling}$$

$$s^2_{technical} = s^2_{analytical} + s^2_{sampling}$$

The recommended limits for these various sources of error are summarised in figure 4.1a. If the $s^2_{technical} < 1\%$ of s^2_{total} there is no benefit in further reducing $s^2_{technical}$ because the minimal increased quality of data would not be justified (Ramsey *et al.*, 1992).

The results are given in Appendix III and show that all the results are within the precision limits suggested by Ramsey (1993) (figure 4.1a) and thus are suitable for further interpretation. An example of the output is shown in figure 4.1b.

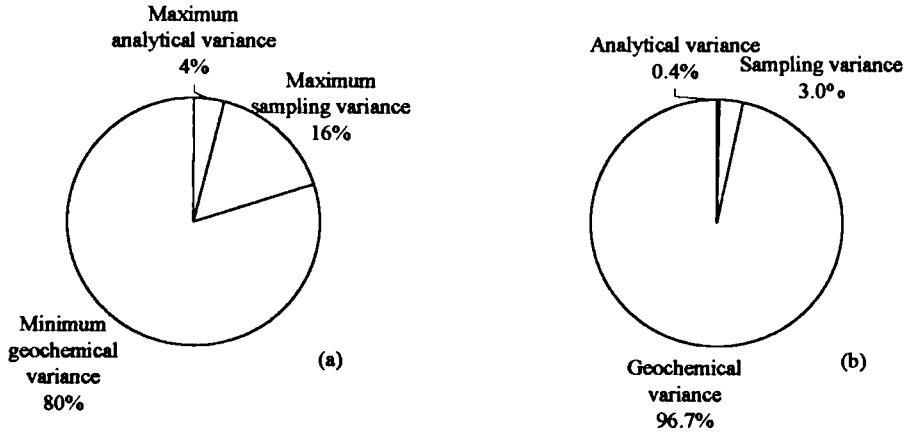


Figure 4.1: Robust ANOVA analysis (a) Maximum allowable variances in robust ANOVA analysis of results (Ramsey, 1993), (b) Distribution of variance of Fe in stream sediment samples from robust ANOVA analysis

4.5 Mineralogical analysis of sediments and iron rich precipitates

For all the analyses conducted below the samples used were ochreous materials sieved (with very gentle disaggregation where it was occasionally required) to a particle size <62μm. These were the same samples which were analysed chemically, which are reported in the succeeding chapters of this thesis.

4.5.1 X-ray powder diffraction

The theory behind XRD will not be discussed in detail here, as the instrument was simply used as a tool to study the materials collected in this study; reference will only be made to those factors pertinent to the interpretation of ochreous materials and the particular problems they may present. Acknowledgement must be paid to Mr Martin Gill, who operated the instrument and ran all the samples and gave instruction on the use of the interpretative software with which the processing of the XRD scans was undertaken. Background information on the X-ray diffraction analysis of Fe oxyhydroxides is provided by Brown (1980), Schwertmann & Taylor (1989) and Cornell & Schwertmann (1996).

The instrument used in this study was a Phillips P1830 diffractometer with a Cu-$K\alpha$ source; further information is supplied in Appendix II. A monochromator was used to remove the fluorescence which Fe generates; this otherwise hinders resolution of the diffraction pattern, by causing a high background (Schwertmann & Taylor, 1989). The initial instrument set-up was to scan from 1.600 - 70.000 °2θ with a step-size of 0.020 °2θ and step-time of 2s/step. This produced patterns typically like that shown in figure 4.2a, for the minerals from deep mine localities (section 5.1.5). However, because the background:signal was high, it was decided to reduce the width scanned (10 - 80 °2θ) but increase the time-step (10s/step and 20s/step) to produce a better resolved trace; the results of an experimental run are shown in figure 4.2b and c. It can be seen that the phase(s) present are considerably better resolved using 10s/step, than 2s/step. The time taken to run the samples shown in figure 4.2 was 2 hours 5mins, 3 hours 58mins and 7 hours 51mins for 2s/step, 10s/step and 20s/step respectively. It can therefore be seen that 10s/step was the optimum step-time for improved data quality without excess instrument time being needed. The samples were back-mounted into a Philips cavity powder mount, being careful to minimise any potential for alignment of the particles. The patterns were processed using a peak matching program Philips PC-APD (controlling, analysis and output software) containing the ICDD (International Centre for Diffraction Data) database; however, some minerals were not included in the program and were identified

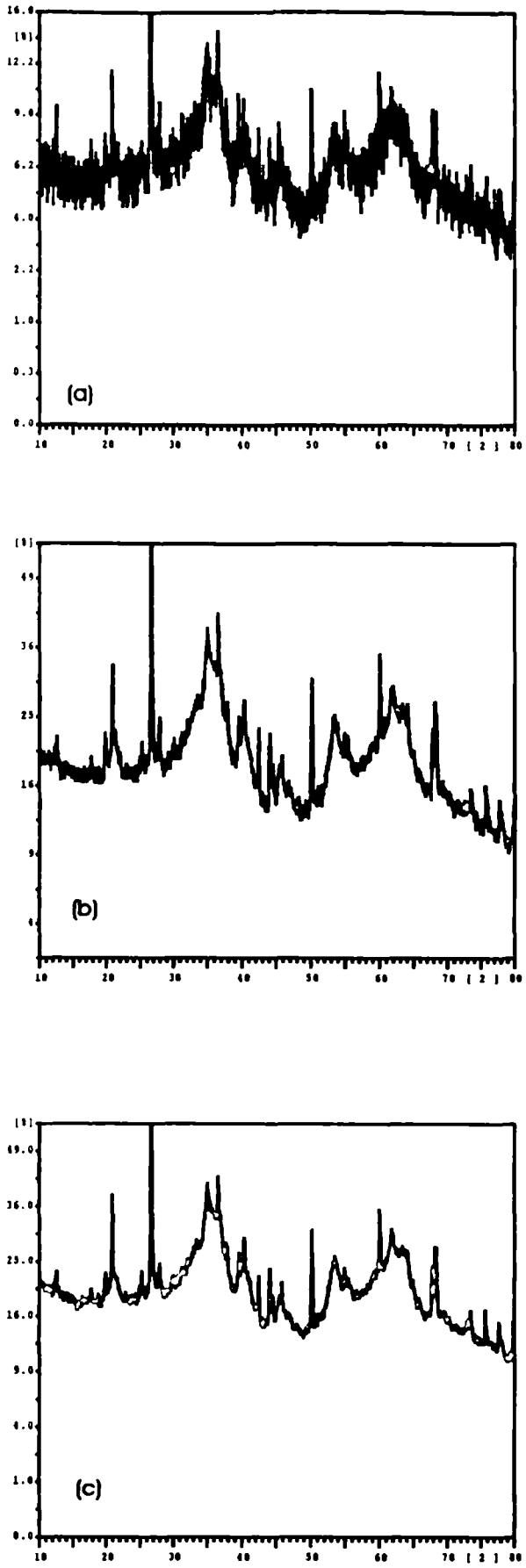


Figure 4.2: XRD plots for sample SH06 used to compare the benefit of different step-times (a) 2s/step (b) 10s/step (c) 20s/step. See section 5.1.5 & 5.2.5 for interpretation of XRD plots.

using other data sources (table 4.1). This step time chosen is less than that used by Murad *et al.* (1994) (40s/step (section 2.2.5b)), but the additional time needed on the instrument would not have been possible.

The minerals which may be expected exhibit differing characteristics. Jarosite (all types) is a high crystallinity phase, which is readily identifiable using XRD (figure 4.3). Goethite is generally well-ordered, but may vary somewhat more than jarosite (Schwertmann & Taylor, 1989); the other typical mine drainage minerals tend towards a very low degree of ordering. Typical plots for these minerals are shown in figure 4.3. Ferrihydrite is a common mineral which occurs in varying degrees of crystallinity, it can occur with from 2 - 6 XRD lines (table 4.1) (Cornell & Schwertmann, 1996). However, none of the minerals are completely X-ray amorphous (Bigham *et al.*, 1990) (section 2.2.5).

Additional complications to interpretation exist. The first is that with natural, rather than synthesised, precipitates there is frequently an admixture of minerals, albeit with one phase forming a dominant component. This leads to the possibility of either an amorphous background interfering with the clarity of the pattern or material such as crystalline quartz obscuring some peaks (Schwertmann & Taylor, 1989). Peak widening will result from both small particle size (<100nm) and low crystallinity (Cornell & Schwertmann, 1996).

4.5.2 Scanning electron microscopy

Scanning electron microscopy (SEM) can be operated in two different modes: backscattered electrons (BSE) or secondary electrons (SE) which allow compositional and topographical information respectively. These will briefly be described below. A comprehensive review of all methods of SEM analysis for earth surface materials is provided by Reed (1996) and references therein. Acknowledgement is paid to Mr Dick Giddens who operated the instrument for analyses.

4.5.2a Compositional analysis

The samples were prepared (by Ms Lizzie Morris), mounting the ochreous powder in resin and polished flat to prevent any spurious readings due to topography (Reed, 1996). The analyses were conducted in BSE mode using a JEOL733 instrument with energy dispersive spectrometer (EDS) X-ray detection. The BSE enable analysis because they vary with atomic number; a full explanation is given by Reed (1996) and references

Table 4.1: Diagnostic d-line spacings for commonly occurring minerals in mine drainage waters (Cornell & Schwertmann, 1996).

Goethite 29-713			Lepidocrocite 8-98			Akaganéite 13-157 (tetragonal cell)			Schwertmannite[1]			δ-FeOOH[2]			Feroxyhyte[3]			Ferrihydrite 29-712			HP FeOOH[4]	
d	I	hkl	d	I	hkl	d	I	hkl	d	I	hkl	d	I	hkl	d	I	hkl	d	I	hkl	d	I
0.498	12	020	0.626	100	020	0.740	100	110	0.486	37	200,111	0.461	1	001	0.256	100	100	0.250	100	110	0.333	200
0.4183	100	110	0.329	90	120	0.525	40	200	0.339	46	310	0.2545	10	100	0.223	85	101	0.221	80	112	0.256	50
0.3383	10	120	0.279	10R	011	0.370	10	220	0.255	100	212	0.2255	10B	101	0.170	65	102	0.196	80	113	0.2488	80
0.2693	35	130	0.247	80	031	0.3311	100	310	0.228	23	302	0.1685	10VB	102	0.147	50	110	0.172	50	114	0.222	50
0.2583	12	021	0.236	20	111	0.2616	40	400	0.195	12	412	0.1471	10	110				0.151	70	115	0.216	30
0.2527	4	101	0.209	20	131,060	0.2543	80	211	0.166	21	522	0.1271	2	200				0.148	80	300	0.175	70
0.2489	10	040	0.1937	70	051,200	0.2343	20	420	0.151	24	004	0.1223	2	112							0.168	80
0.2450	50	111	0.1848	20	220	0.2285	40	301	0.146	18	204,542	0.1104	2VB	202							0.165	50
0.2303	1	200	0.1732	40	151	0.2097	20	321				0.0965	2B	210							0.154	30
0.2253	14	121	0.1566	20	080	0.2064	20	510				0.0943	2B	211							0.150	30
0.2190	18	140	0.1535	20	002	0.1941	60	411													0.144	50
0.2089	1	220	0.1524	40	231	0.1854	10	440													0.136	50
0.2011	2	131	0.1496	10R	022	0.1746	40	600				B: broad										
0.1920	5	041	0.1449	10	180	0.1719	10	501,431				VB: very broad										
0.1802	6	211	0.1433	20	171	0.1635	100	521														
0.17728	1	141	0.1418	10	260	0.1515	40	002														
0.17192	20	221	0.1389	10	122	0.1497	20	611														
0.16906	6	240	0.1367	30	251	0.1480	20	112,710														
0.16593	3	060	0.1261	10	091,320	0.1459	10	610														
0.16037	4	231	0.1213	10	280	0.1438	80	541														
0.15637	10	151	0.1196	20	022,191	0.1374	40	730,312														
0.15614	8	160	0.1189	20	1,100																	
0.15091	8	002,250	0.110	20																		
0.14675	2	320	0.1075	40																		
0.14541	5	061																				
0.14207	2	112																				
0.13936	3	330																				
0.13694	2	301																				
0.13590	3	170																				
0.13459	1	260																				
0.13173	3	132																				
0.12921	<1	042																				
0.12654	1	331																				
0.12437	1	142																				
0.11994	1	341																				
0.11506	1	081																				
0.11445	1	410																				
0.11263	1	242																				

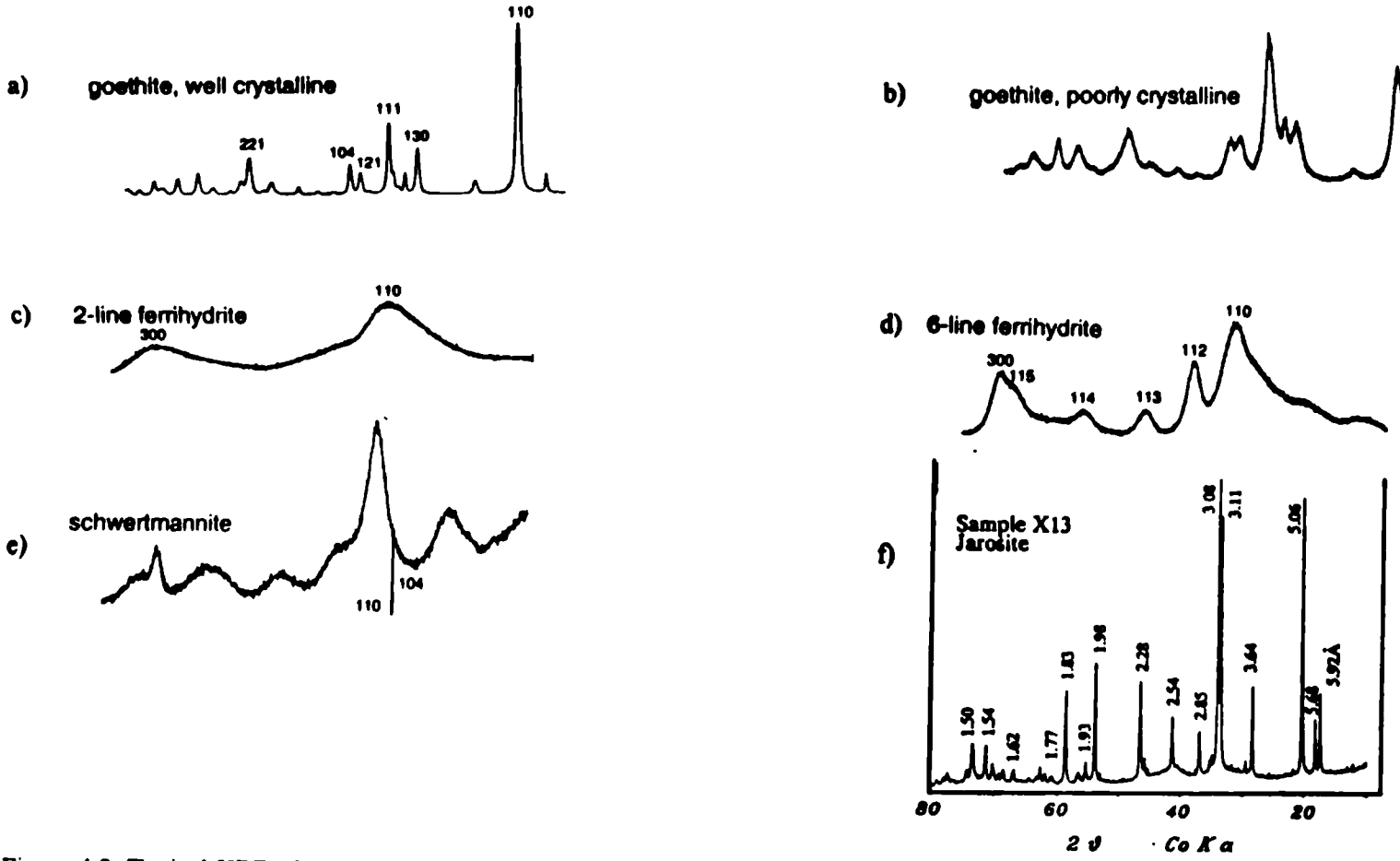


Figure 4.3: Typical XRD plots for the minerals commonly found in mine drainage waters (a) highly crystalline goethite (b) poorly crystalline goethite (c) 2-line ferrihydrite (d) 6-line ferrihydrite (e) schwertmannite (all Cornell & Schwertmann, 1996) (f) jarosite (Bigham *et al.*, 1992).

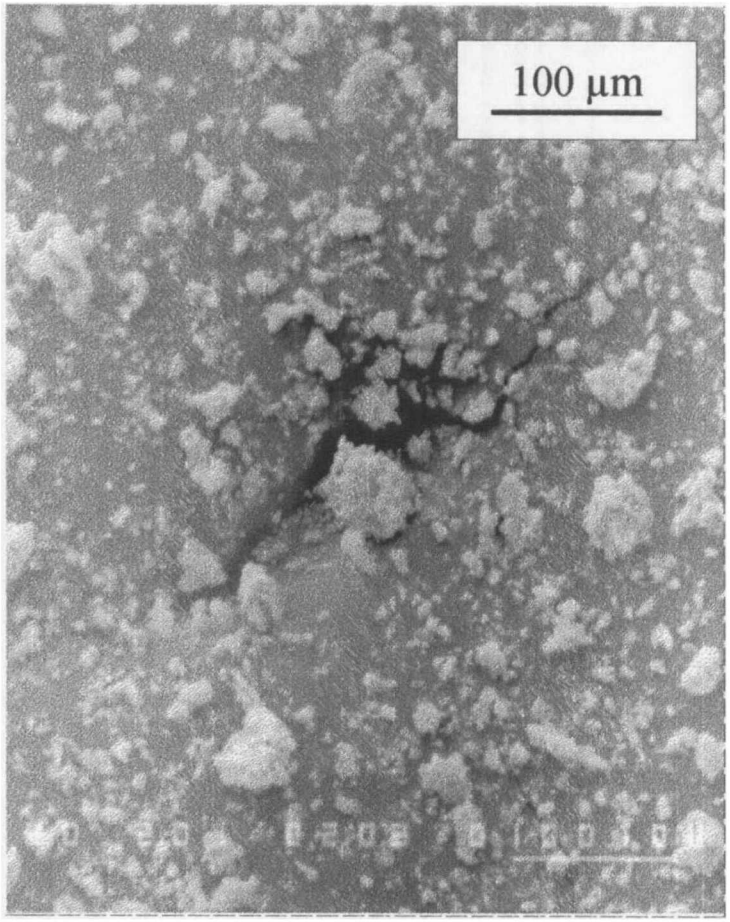
therein. The samples are given a conductive carbon coat because it has a minimum effect on the X-ray spectra (Reed, 1996). The whole spectrum is collected simultaneously by EDS (Reed, 1996). The instrument was calibrated at ~60 minute intervals, using a Co standard.

When conducting analyses, the processed data converts all analyses to a percent oxide composition. This is problematic because hydrated or carbonate (C, H & O not detected) materials show a total <100% (Reed, 1996) (typical mineral compositions given in section 2.2.5). This problem is shown in sections 5.1.5 & 5.2.5 for the samples in this study. The fact that most whole-rock analyses add up to 100% is a commonly used check on the quality of the analysis (Reed, 1996), but is not available to this work. Another problem is that when the analysis is being conducted, a very highly hydrated sample may decompose under the beam, leaving a crater in the sample. This renders the results useless, as the effect of the sputtered material on the emitted electrons cannot be assessed (Reed, 1996).

4.5.2b Topographical analysis

These samples were mounted onto filter paper by Buchner filtration of a small amount of sample disaggregated in pre-filtered (<0.45μm) absolute ethanol. The disaggregation was achieved using ultrasound for ~10s to avoid damage to the particle surfaces. This disaggregation was found to be essential after experimental comparison of samples (plate 4.1) mounted in different styles. Without ultrasound preparation the high density of particles (plate 4.1) caused a charge build-up, hindering the analysis; ultrasound causes much higher dispersion of particles on the filter paper surface (plate 5.2a). The filter paper was immediately placed on wet conductive carbon paint on a glass slide. This was repeated for up to 6 filter papers per slide. Duplicate slides were made to enable one to be Au coated and the other to be C coated. Coating with Au is used for topographical work as it has a higher electron yield than C. Carbon coated samples were made to enable specific particle types to be qualitatively analysed for the elements present. The SE analysis has a resolution of <10nm (compared with <100nm for compositional analysis) (Reed, 1996). Little effect on the generated SE is caused by the atomic number and only those generated near surface escape and the yield is related to the angle that the SE leave the specimen, causing a 3D effect discussed in full by Reed (1996) and references therein.

Plate 4.1: The ochre loading, without disaggregation, for SEM analysis. An example of the effect of disaggregation is shown in plate 5.2a.



4.6 Hydrogeochemical modelling of water data

Computer modelling is a potentially powerful technique in aqueous geochemistry. To assist in understanding the water chemistries observed in this work, one such model has been used (section 4.6.1). However, the data produced by any computer model should not be accepted at face value (section 4.6.2). This section briefly reviews the selection of the program used and some of the advantages and disadvantages in using hydrogeochemical modelling.

4.6.1 PHREEQ-C modelling package

The model selection for undertaking work in this project was based on several factors. Suitability for the system being studied was the primary criteria. PHREEQ-C (Parkhurst, 1995) is the latest version in a series of programs produced by the US Geological Survey (and is thus available free of charge) for the purpose of assessing low temperature-pressure-ionic strength systems. The intention had been to use WATEQ-4F (Ball *et al.*, 1987), which has been widely used in the published literature to study minewaters (e.g. Nordstrom *et al.*, 1992), however, investigation of available programs showed WATEQ-4F to have been superseded by PHREEQ-C. The program code is, however, accompanied by 3 databases (Parkhurst, 1995), of which the WATEQ-4F database is one (Ball & Nordstrom, 1991); this was used throughout the modelling work undertaken in this study. The user's manual (Parkhurst, 1995) contains extensive information on the program and will not be repeated here.

4.6.2 Advantages and limitations of using a hydrogeochemical modelling package

Hydrogeochemical modelling packages are a fast and effective way of simultaneously assessing the probable distribution of aqueous species, and the predicted precipitating mineral phases (using saturation indices) from a complex natural water body. The number of calculations performed far exceeds anything which could otherwise be achieved, and allows a rapid assessment of factors such as the common ion effect, which may be harder to discern with a series of individual calculations. Modelling packages are however prone to mis-use, by assuming that the derived information is wholly correct. The points below are given to show that caution must be exercised in the interpretation of such data, and, as always, corroboration of predictions using other techniques is desirable.

There are numerous assumptions implicit in the model and the way it functions which cannot be ignored in the interpretation of any results produced. One assumption which

has been made throughout this work is that the model code is without error. This model (Parkhurst, 1995) has been used as an "off-the-shelf" package, which has not had its code modified at all in use.

There are numerous assumptions implicit in modelling: use of the wrong type of model or database would probably invalidate drawing even the most tentative conclusions. The sources of uncertainty in modelling are reviewed by Nordstrom & Munoz (1994). Two major studies are by Broyd *et al.* (1985) and Nordstrom *et al.* (1979b) who compared 15 and 13 different models, respectively, and review the major sources of discrepancy in the results produced. The findings of those studies are still valid, despite the evolution of the actual computer programs since then, because the geochemical data is the largest source of errors.

A source of (largely) unquantified error is the thermodynamic data held in the database (Bethke, 1996; Bi & Yin, 1995; Broyd *et al.*, 1985; Nordstrom *et al.*, 1979b, 1985). These errors are variable depending on the fundamental studies which provided the data and there is also a relationship to the degree of understanding of a system. The Ca-H-C-O system was found to be reproducible between databases because it has been so extensively studied at low temperature and pressure, (Nordstrom *et al.* 1979b) compared with the Fe^{II}-Fe^{III}-SO_4-H_2O system which is poorly understood (Stipp, 1990). The uncertainties in the data associated with sampling and analyses (which can be assessed (section 4.4)) are low in comparison with the uncertainty in the database parameters (Bi & Yin, 1995).

Other factors affecting the data produced by the model are: the number of species included in the database (Nordstrom & Munoz, 1994), which affects the number of ions pairs and thus the free ion concentration (Nordstrom, 1985); the method used to calculate ion activities (Stipp, 1990; Nordstrom & Munoz, 1994); and the redox couple used to derive Eh (Nordstrom, 1985). The other source of error is in the interpretation of the model, which will depend upon how much corroborating information is available to the user, and how that information is used (Nordstrom & Munoz, 1994).

Another major assumption with a model as used in this project is that it assumes thermodynamic equilibrium. The system is assumed to have internal equilibrium and kinetic effects, on the rate of precipitation of super-saturated mineral phases for instance, are ignored. The likelihood of internal equilibrium being reached is low (section 2.2.3b) and the effects of kinetics on the results have been reviewed by Nordstrom & Munoz

(1994). However, these workers note that pyrite (and other sulphides), calcite, gypsum (and other sulphates) are minerals for which kinetics do not play too large a role, in comparison with silicates (Nordstrom & Munoz, 1994). A case of barytes existing in stable supersaturation due to its precipitation being slower than the release of SO_4 by pyrite oxidation was given by Nordstrom *et al.* (1992). As discussed in section 2.2.3b, colloidal transport, both as a transport mechanism and as a source of error in aqueous geochemical results, is an important factor in the measurement and understanding of the water chemistry. Bethke (1996) gives a case study of the effect of colloidal material being included in dissolved analyses on modelling results.

Although there has been a discussion of the possible errors associated with modelling, it still has a value as discussed above. The aim of this section has been to point out the limitations in the extent to which the data can be interpreted, so that there is no danger of "over-interpretation" of the data, pushing it beyond what can sensibly be deciphered.

4.7 Summary

This chapter has described the process by which sites have been selected and the way in which samples were collected. The methods used to acquire data (both geochemical and mineralogical) on the various sample media collected have been detailed. It can be assumed that the criteria by which samples were collected, and the methods by which they were analysed were unvarying from the descriptions contained here unless explicitly stated otherwise in this thesis.

Finally the data quality control on the samples has allowed some quantification of the errors associated with the samples. These will be shown in the form of error bars on data plots in subsequent chapters, but have been found to be minimal in comparison with the geochemical fluctuations described therein. As described in section 4.6.2, there are considerable uncertainties associated with geochemical modelling, some attempt to assess the effect of those errors is included in the subsequent sections (section 5.3 & chapter 7) where such work has been undertaken.

5.0 Characteristics of the discharge localities

This chapter presents the results of analyses performed on the samples collected from the sites which were described in chapter 3. The analytical methods used, unless otherwise explicitly stated, are as described in chapter 4. The major subdivision of this chapter is between spoil heap and deep mine drainage. Within each of these sections the following sequence is observed: water chemistry (measured and modelled) and suspended sediment results are presented first, followed by mineralogical and chemical analyses of the precipitates formed at the discharge points. In each section the water chemistry is divided according to the broad classification of Freeze & Cherry (1979), of the elements which are "major" (>5 mg l^{-1}), "minor" (0.01-10.0 mg l^{-1}) or "trace" (<0.1 mg l^{-1}).

5.1 Deep mine drainage

This section will discuss the chemistry of the mine drainage from the sites of study at Broken Banks (BB), Edmondsley Yard Drift (EY), Low Lands (LL), Stony Heap (SH) and Tindale Colliery (TC). The site locations were given in section 3.4.

5.1.1 Physical characteristics

As described in section 4.3.2 the discharge volumes could not be quantitatively assessed, and only qualitative assessment of the water flows using field observations was possible. For this reason the discharge volumes were considered to be essentially stable throughout the sampling visits.

5.1.2 Aqueous chemistry: Major ions

The Eh-pH status of the waters is shown in figure 5.1. It can be seen that for all sites the readings were very stable and were consistently of a poorly oxidising, circum-neutral pH type. Comparison with the spoil heap discharges shows these deep mine drainages to be much more stable in their composition over the period of study.

The water type according to the major ion provenance of the deep mine drainage is shown in figure 5.2. It can be seen that although the different localities have very consistent chemistries, there are spatial differences between sites. The waters are Ca=Mg types (figure 5.2a), with the exception of EY which is a Ca-Mg type with a greater proportion of Ca than the other localities. The anion results (figure 5.2b) show a greater divergence into specific localities. EY is dominated by SO_4, and thus is a Ca-Mg-SO_4 water. BB is a HCO_3^- water, and thus is classified as a Ca=Mg-HCO_3^- water. SH is

shown to have a closely consistent anion chemistry, with a dominance of SO_4 and is thus a Ca=Mg-SO_4 water. TC and LL are also SO_4 dominated waters (type is Ca=Mg-SO_4), although their Cl proportion contributes to the differing secondary ion position on figure 5.2b.

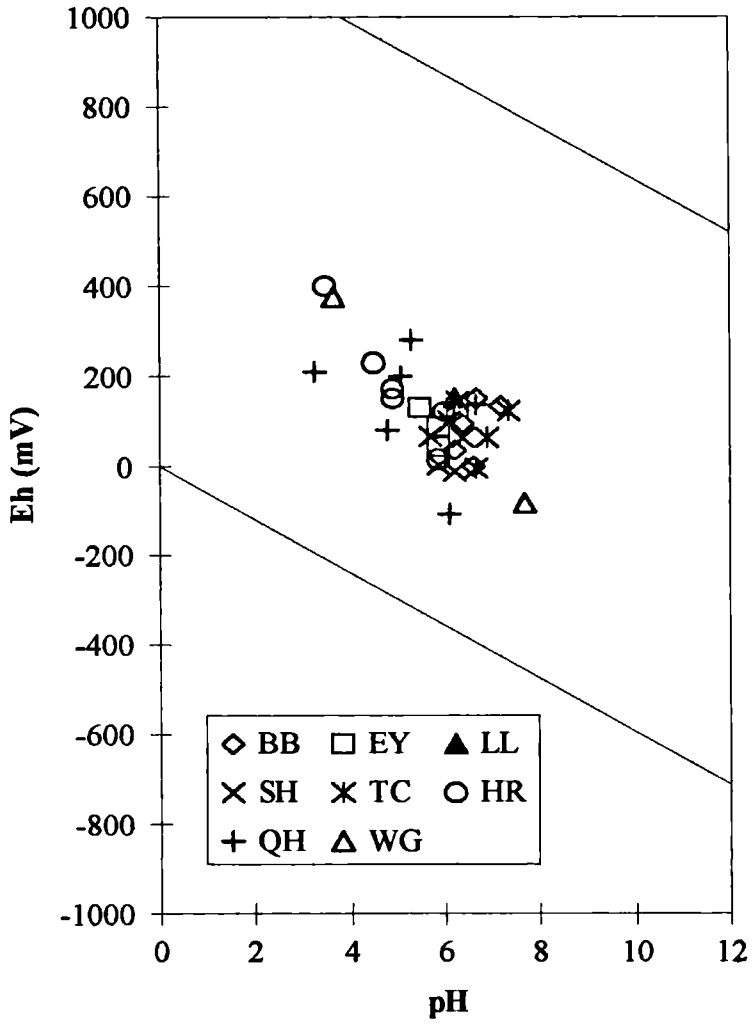


Figure 5.1: Eh - pH values recorded at mine and spoil discharge sites. All the Eh values were recorded using a Pt-electrode meter system. Deep mine discharge are green symbols; spoil heap discharge are orange symbols.

When Na is plotted against Cl (figure 5.3) it can be seen that Cl has an excess for all the deep mine drainage. When the data is examined site by site, BB has an average Na:Cl of 0.8, whilst EY and SH have averages of 0.4. This suggests that the Cl excess is 2.5x at the latter two sites, whilst the excess at BB is only 1.25x. It is known that Ba-Cl waters can exist in the Coal Measures of County Durham (section 3.3.4). The expected molar ratio for a simple mixture of these two compounds (which occur dissociated in solution) is (Ba+Na):Cl = 2:3, from equation 5.1.

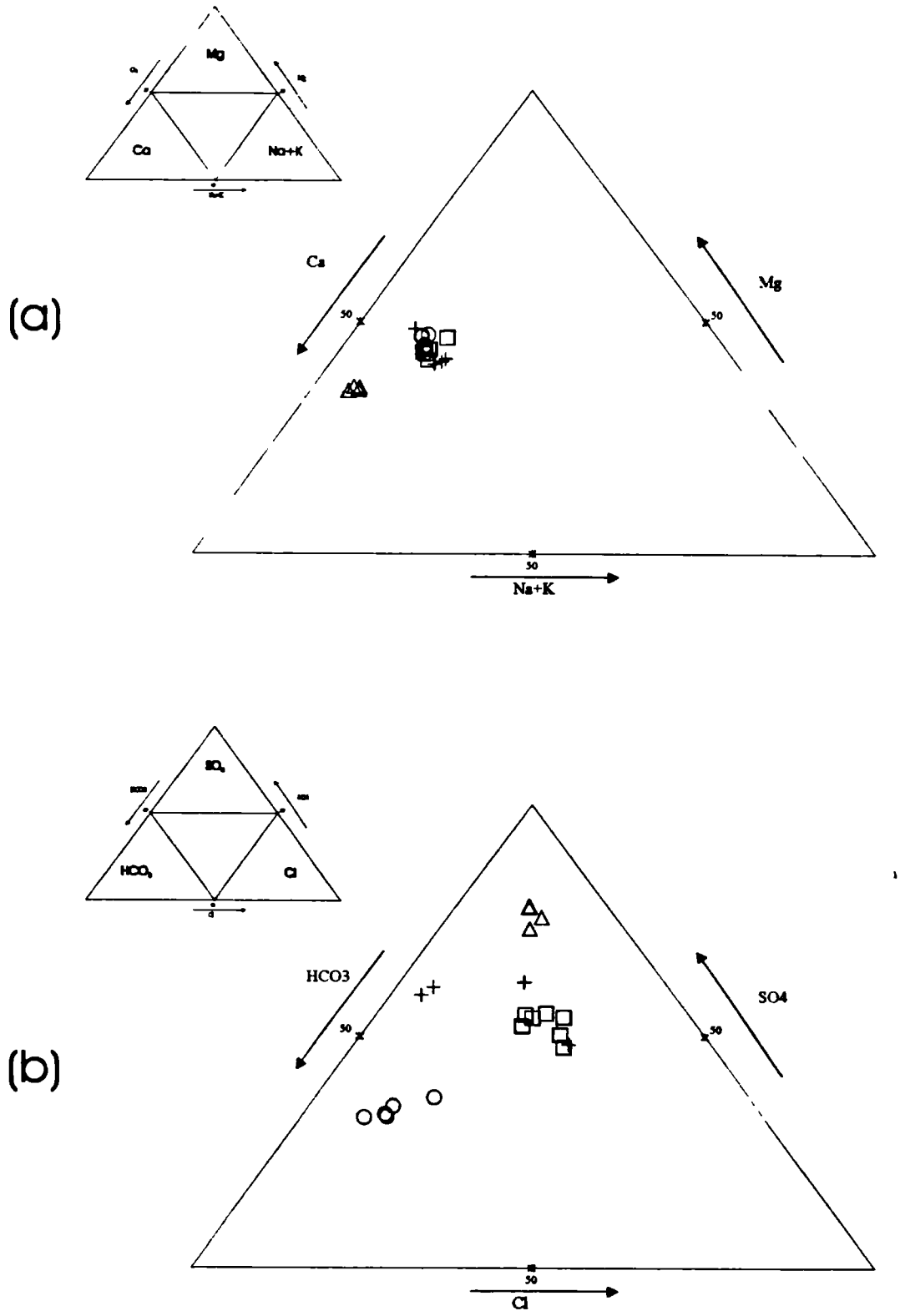


Figure 5.2: Triangular plots of major ion chemistry at deep mine discharge locations. (a) cations: Ca, Mg, Na & K (b) anions: HCO_3, SO_4 & Cl. Labelling as follows: BB = circles; EY = triangles; SH = square & TC & LL = cross. Units are %meq, with 50% marked on each axis. The occurrence of dominant ions on the diagram is described by the associated inset to each plot.

$$BaCl_2 + NaCl \Rightarrow Na^+ + Ba^{2+} + 3Cl^-$$

Eq. 5.1: The molar relation of Na, Ba and Cl mixing

However, the concentrations of Ba are low in comparison to Na (appendix IV), and they cause little difference in the results, and are thus not shown in figure 5.3. However, Ba^{2+} is not expected to be conservative in SO_4 waters due to the insolubility of $BaSO_4$ (log K_{sp} = -9.97 (Appelo & Postma, 1994)). This renders it difficult to establish whether the Cl has a Ba association as well as Na.

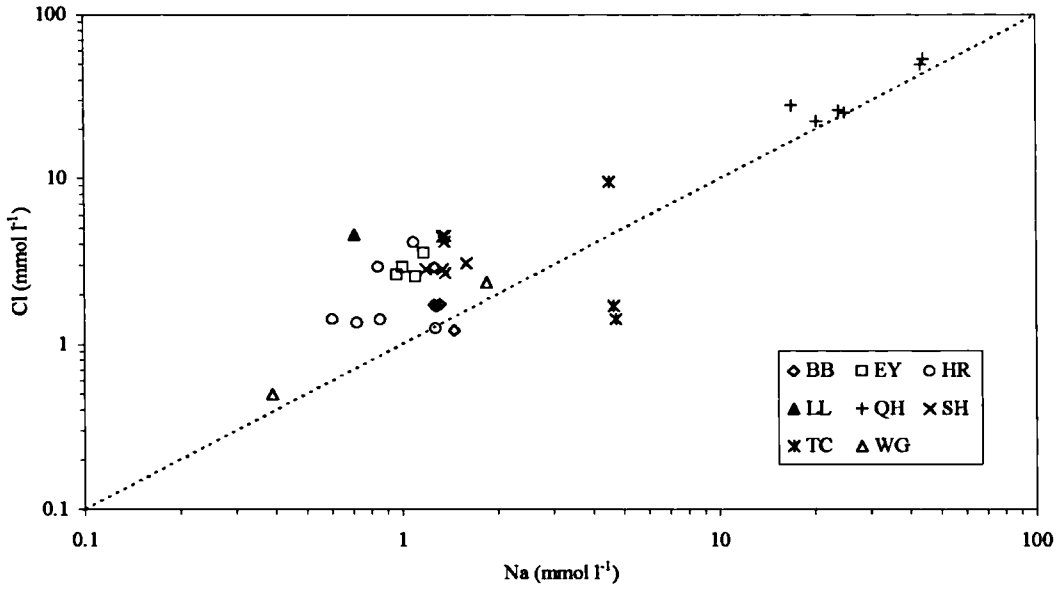


Figure 5.3: Sodium and Cl molar concentrations in mine and spoil drainage. Mine discharges - BB, EY, LL, SH & TC; spoil discharges - HR, QH & WG. The line shown represents a Na:Cl of one.

Whilst Fe is not generally considered a major ion in natural waters, in the situation of ferruginous drainage it becomes a major ion in almost all waters described, and is thus included here. However, figure 5.4 shows the triangular diagram of figure 5.2 redrawn to include Fe, with Mg and Ca being grouped together. This diagram shows that the waters can still be considered a Ca-Mg-SO_4 type, even whilst considering Fe. Temporal variations in pH and selected ions (Fe, SO_4 and Ca) at the deep mine discharge locations is shown in figure 5.5. In contrast to the spoil heap waters, abandoned deep mine discharge shows a highly consistent chemistry. As was noted above, the discharge volumes of these localities did not appear to appreciably differ between sampling visits.

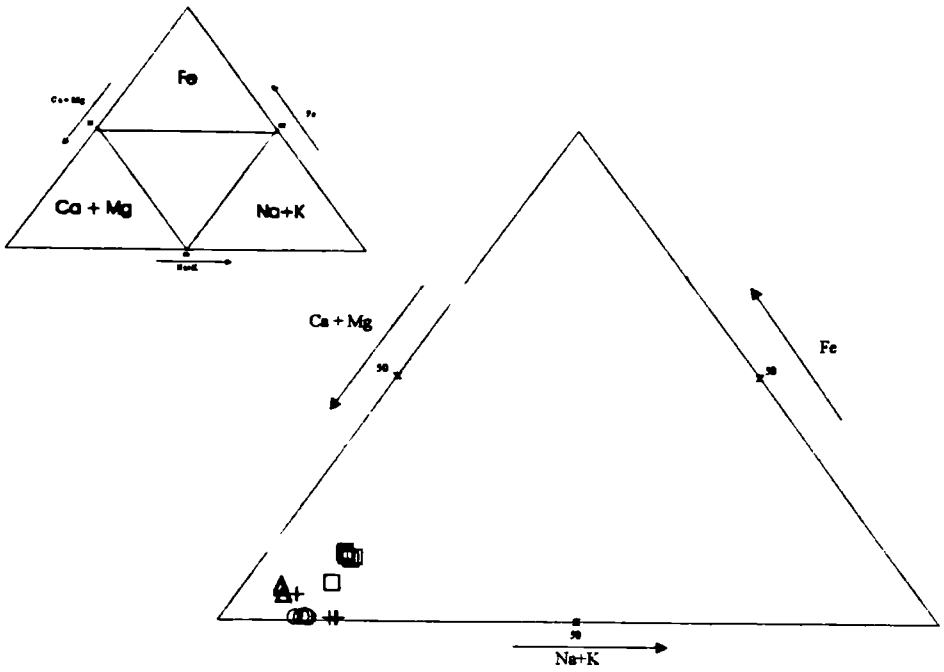


Figure 5.4: Triangular diagram of major cations in deep mine drainage, including Fe.

Figure 5.5a shows that there is a circum-neutral pH for all sites on all sampling occasions. There is small inter-site variation but little intra-site temporal variation. BB and TC show a pH~7, whilst EY, SH and LL have a pH~6 during the period of this study. Thus, there is some spatial variation between sites, but each site shows a very consistent value for pH on all sampling occasions. This pattern of temporal consistency is repeated for figures 5.4b-d, although the pattern of concentrations is different for some of the sites between elements. Figure 5.5b shows Fe concentrations, it can be seen that the concentrations are very consistent at the sites, but that the different sites group into different concentration ranges; BB (~2000 $\mu g\ l^{-1}$) and TC (~2700 $\mu g\ l^{-1}$) are one group with LL more variable and EY and SH being very similar (~30000 $\mu g\ l^{-1}$).

The concentrations of SO_4 and Ca (figure 5.5c & d) however, show EY and TC are similar and BB, LL and SH form another grouping. This is different to the distribution of localities shown in figure 5.2. There EY showed a difference in cations to the rest, including TC, and the anions showed a different distribution of chemistry between all the different sites. The reason for these differences is that EY has a much higher Ca:Mg molar ratio (~2.7) in comparison with the other sites (~1.5-1.7) The higher Ca concentration in TC being matched by an increase in Mg, TC is the site with highest concentrations of both elements.

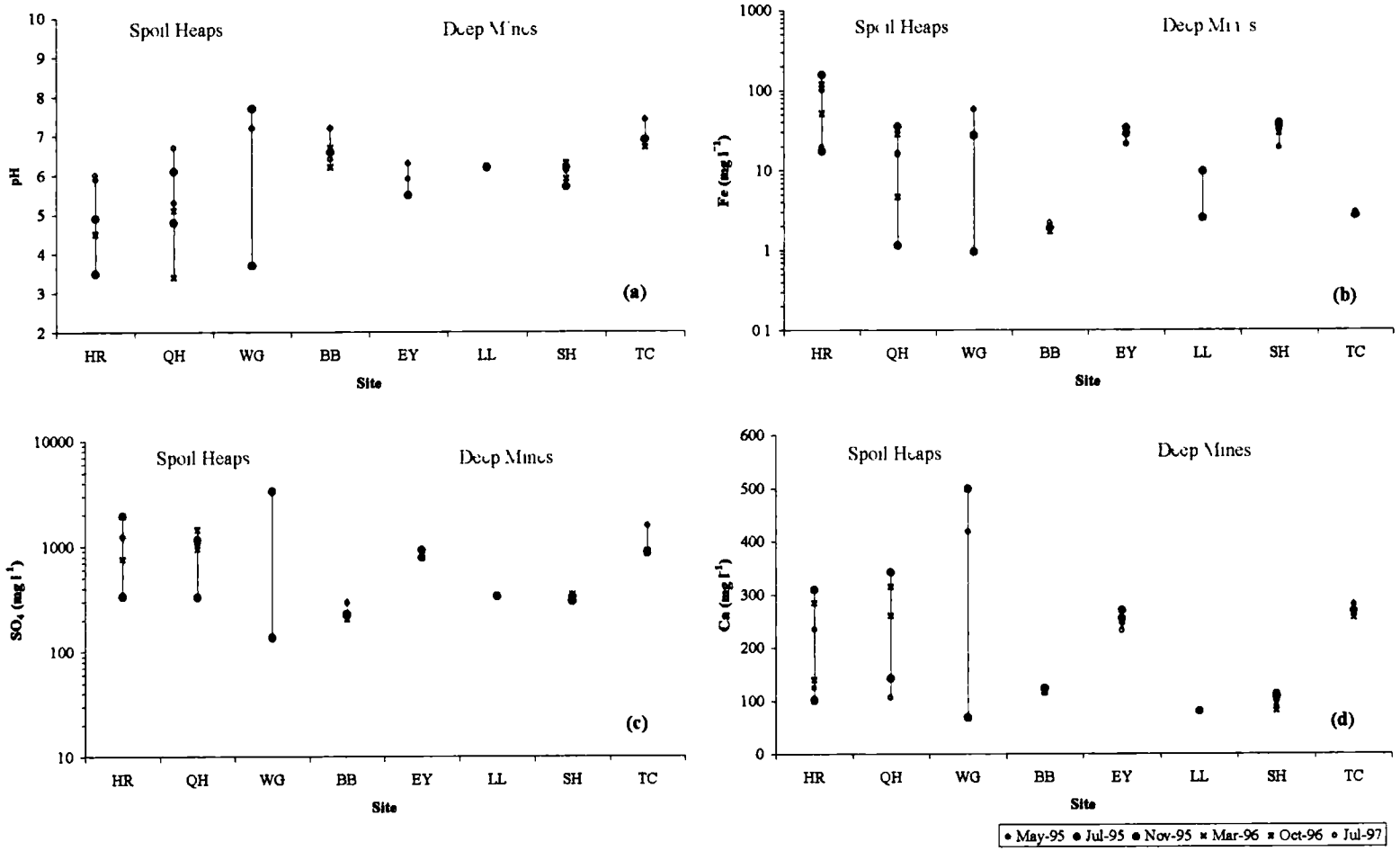


Figure 5.5: Temporal variability in pH and selected major ions measured in spoil heap and deep mine drainage. (a) pH, (b) Fe (c) SO_4 (d) Ca. The sites are labelled as follows: Helmington Row (HR), Quaking Houses (QH), Willington (WG), Broken Banks (BB), Edmondsley Yard Drift (EY), Low Lands (LL), Stony Heap (SH) and Tindale Colliery (TC).

Silicon was only determined for 3 sampling visits, but shows consistent chemical results, with an apparent systematic difference in the results. BB has a concentration of ~4.5 mg l^{-1}, EY of 10 mg l^{-1} and SH of 8-10 mg l^{-1}. Dissolved oxygen (DO) could only be measured in October 96 and July 97, but the results of the measurements show a value consistently <1 mg l^{-1} for BB, EY and SH. The only exception to this is SH in October 96 (2.6 mg l^{-1}), but that may be due to difficulty in reaching the immediate area of the point of emergence on that occasion. These results were substantiated by the Fe^{II} determinations which were undertaken in July 97. These showed that the proportion of the total Fe (Fe_t) occurring as Fe^{II} was >94% for BB and EY (DO of 0.3 mg l^{-1}) and 88% for SH (DO of 0.8 mg l^{-1}).

The calculations performed by PHREEQ-C (Parkhurst, 1995) allowed prediction of the aqueous speciation. For all speciation data described in this chapter and chapter 7, the database used was WATEQ-4F. The results are subject to sources of error, which were described in section 4.6. This means that the results are merely a prediction of the speciation or saturation of a mineral. That these are predictions should be read as implicit in the following descriptions; for brevity it will not be stated in every case.

Dissolved Fe is largely composed of Fe^{II} species (table 5.1). The dominant ion for these waters is Fe^{2+}, the secondary species being either $FeHCO_3^+$ (BB) or $FeSO_4^o$ (EY & SH). The speciation of total dissolved Fe in these waters is almost entirely accounted for by these three species (table 5.1). The importance of HCO_3 as a complex at BB is greater than at EY and SH due to its higher proportional concentration (figure 5.2b). Iron(III) is a very small fraction of the total Fe (table 5.1), and it can be seen that three species account for all the Fe^{III}. The major difference between the samples is that again BB shows a differing proportional distribution of the species to EY and SH. The uncharged complex $Fe(OH)_3^o$ has a higher concentration at BB than at the other two sites, reducing the amount of Fe^{III} complexed as $Fe(OH)_2^+$, although that species is dominant at all three sites.

Figure 5.6 shows that S^{VI} largely occurs as uncomplexed SO_4^{2-}, such as shown in figure 5.6a for BB and figure 5.6b for SH. The high concentrations of SO_4 can control the speciation of other ions; table 5.2 shows that the complex with SO_4 constitutes ~50% of the speciation of Ba, Ca and Mg. BB shows a marginally lower total percentage from the two ions given than does EY and SH (table 5.2), this is due to up to 1.5% of the Ca and Mg predicted to occur as $CaHCO_3^+$ and $MgHCO_3^+$.

Table 5.1: Iron concentrations and modelled speciation in deep mine water discharge.

	Fe(total) (mol l^{-1})	Fe^{II} (mol l^{-1})	Fe^{III} (mol l^{-1})	*% of* Fe^{II}			
				Fe^{2+}	$FeSO_4^o$	$FeHCO_3^+$	*total*
BB	$1.75*10^{-06}$	$1.75*10^{-06}$	$5.09*10^{-12}$	76.4	6.7	16.5	100
EY	$3.78*10^{-04}$	$3.78*10^{-04}$	$6.49*10^{-11}$	77.3	19.8	2.7	100
SH	$2.85*10^{-04}$	$2.85*10^{-04}$	$2.42*10^{-10}$	82.9	11.7	5.1	100

	Fe(total)	Fe^{II}	Fe^{III}	*% of* Fe^{III}			
				$Fe(OH)_2^+$	$Fe(OH)^{2+}$	$Fe(OH)_3^o$	*total*
BB	$1.75*10^{-06}$	$1.75*10^{-06}$	$5.09*10^{-12}$	87.1	0.3	12.6	100
EY	$3.78*10^{-04}$	$3.78*10^{-04}$	$6.49*10^{-11}$	94.8	1.1	4.1	100
SH	$2.85*10^{-04}$	$2.85*10^{-04}$	$2.42*10^{-10}$	92.6	0.6	6.8	100

Calculation using the PHREEQ-C model (WATEQ-4F database). The data cited here are for Fe concentrations sampled in July 97, but are similar to all results for each site, due to the consistent intra-site chemistry of the mine drainage. The total percentage of Fe^{II} and Fe^{III} concentrations that the species quoted here constitute are shown in the final column

Table 5.2: The speciation of Ca, Mg and Ba as affected by SO_4 in deep mine drainage.

	BB *July 97*	*EY* *July 97*	*SH* *July 97*
Ca (mol/l)	**$2.82*10^{-3}$**	**$5.80*10^{-3}$**	**$2.24*10^{-3}$**
% Ca^{2+}	88.0	74.4	83.9
% $CaSO_4^o$	*10.2*	*25.4*	*15.6*
% of total	98.2	99.8	99.5
Mg (mol/l)	**$2.96*10^{-3}$**	**$3.56*10^{-3}$**	**$2.194*10^{-3}$**
% Mg^{2+}	88.3	75.9	84.9
% $MgSO_4^o$	*9.4*	*23.8*	*14.5*
% of total	97.8	99.7	99.4
Ba (mol/l)	**$1.09*10^{-7}$**	**$5.87*10^{-8}$**	**$9.18*10^{-8}$**
% Ba^{2+}	74.5	50.8	65.3
% $BaSO_4^o$	*24.6*	*49.1*	*34.4*
% of total	99.0	99.9	99.8

The concentrations of Ca, Mg and Ba were measured on the occasion shown in the second column. The speciation of these ions was calculated using the PHREEQ-C model (WATEQ-4F database). The total percentage of the measured concentration of the ions that the species quoted here constitute are shown in the final column

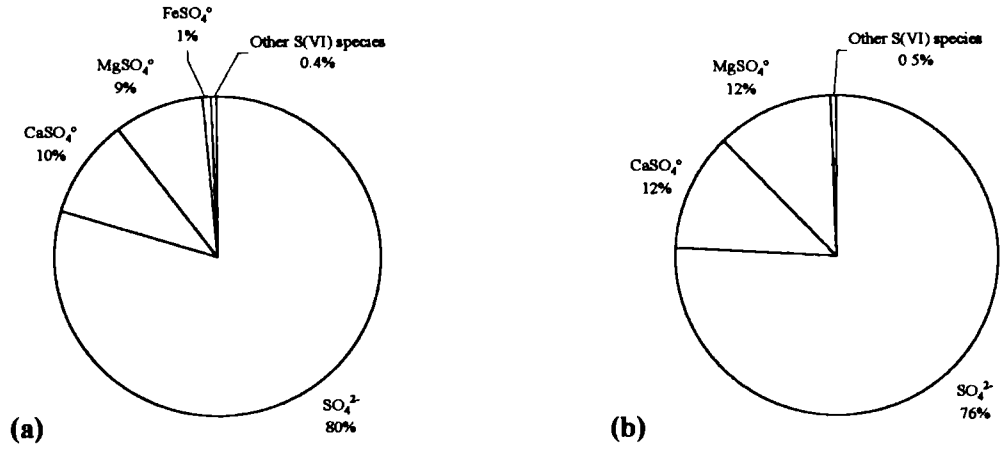


Figure 5.6: Deep mine drainage S speciation. (a) BB (July 97) (b) SH (July 97). Proportion of dissolved S(VI) predicted to be in the species shown by the program PHREEQ-C (WATEQ-4F database).

Chloride is predicted as being dominated by the uncomplexed ion, Cl^-, in all samples measured. Dissolved inorganic carbon (DIC) is dominated by HCO_3^- and CO_2, the distribution depending on the pH of the water (section 2.2.2). Sodium and K are also dominated by the free ion in deep mine waters, as is the case with spoil heap waters.

The calculation of the saturation index (SI where SI = log (ion activity product/solubility product) for the major Fe bearing minerals shows that $Fe(OH)_3$ is generally undersaturated (e.g. SI = -3.6 in July 95 at SH), but goethite (e.g. SI = 2.2 in July 95 at SH) is supersaturated in all instances. The jarosite minerals are not predicted by PHREEQ-C to precipitate from these waters, as would be expected from the conditions favouring their formation (section 2.2.5). Gypsum ($CaSO_4.2H_2O$) is close to equilibrium at EY (~-0.4) whilst being more undersaturated at the other localities, <-0.1. Anglesite ($PbSO_4$) is undersaturated at all localities by <-3.0. SI calculations suggest that the waters are in equilibrium with baryte, with SI values of 0.01-0.1. The modelled concentrations of Ba^{2+} and $BaSO_4°$ predicted are approximately equal, and are ~10^{-8} M l^{-1}. The concentration of Al in solution was 20-40 μg l^{-1} in most instances, yet the model suggests equilibrium or supersaturation with respect to Al bearing minerals in all cases determined, particularly the Al hydroxide species, such as gibbsite (e.g. SI = 0.9 in July

95 at SH), whilst amorphous $Al(OH)_3$ phases show approximate equilibrium (e.g. SI = -2.0 in July 95 at SH). The formation of Al-SO_4 phases is also predicted, with alunite $(KAl_3(SO_4)_2(OH)_2$ having a predicted SI of 2.5 in July 95 at SH.

5.1.3 Aqueous chemistry: Minor and trace ions

The deep mine waters are characterised by generally low concentrations of these ions in solution, compared to those concentrations found in spoil waters (figure 5.7). Manganese is an element which is generally elevated in mine drainage environments (section 2.1), and that is also the case here. Figure 5.7a shows that Mn in these waters is generally of the order 1-3 mg l^{-1}. Figure 5.7b shows that Al concentrations are low and generally too close to the detection limit of the method (<10x detection limit (section 4.4.1)) to produce discernible fluctuations. Trace element data for those elements frequently associated with acid mine drainage, such as Cd and As (section 2.1) are generally too close to detection limit to allow interpretation in these samples (see appendix IV). Those ions which are detectable will be described for spoil heap drainage in sections 5.2, 7.2 & 7.3 where concentrations are higher than in deep mine drainage. Other elements of interest are summarised as mean values in table 5.3. It can be seen that Sr, Ba and Li results show a pattern, in that TC and BB have the highest concentrations (by a considerable margin for Sr). The concentrations then decrease in the sequence EY, (LL) and SH for Sr, with Ba and Li concentrations showing a very similar pattern. Interestingly the pattern is reversed for Zn, with BB and TC effectively being at the limit of detection, but EY, (LL) and SH all being similar and significantly higher.

Table 5.3: Trace and minor ion mean concentrations for deep mine drainage sites.

Sample	Sr	Ba	Li	Zn	Mn
	$\mu g\ l^{-1}$	$\mu g\ l^{-1}$	$\mu g\ l^{-1}$	$\mu g\ l^{-1}$	$\mu g\ l^{-1}$
BB	1114	19	183	1	1871
EY	586	10	100	38	3315
LL	317	14	130	42	2550
SH	215	14	96	39	1981
TC	1613	26	363	1	2508

For LL it should be noted that only one sample was obtained. The other sites are as follows: BB n=5, EY n=4, SH n=7 and TC n=3.

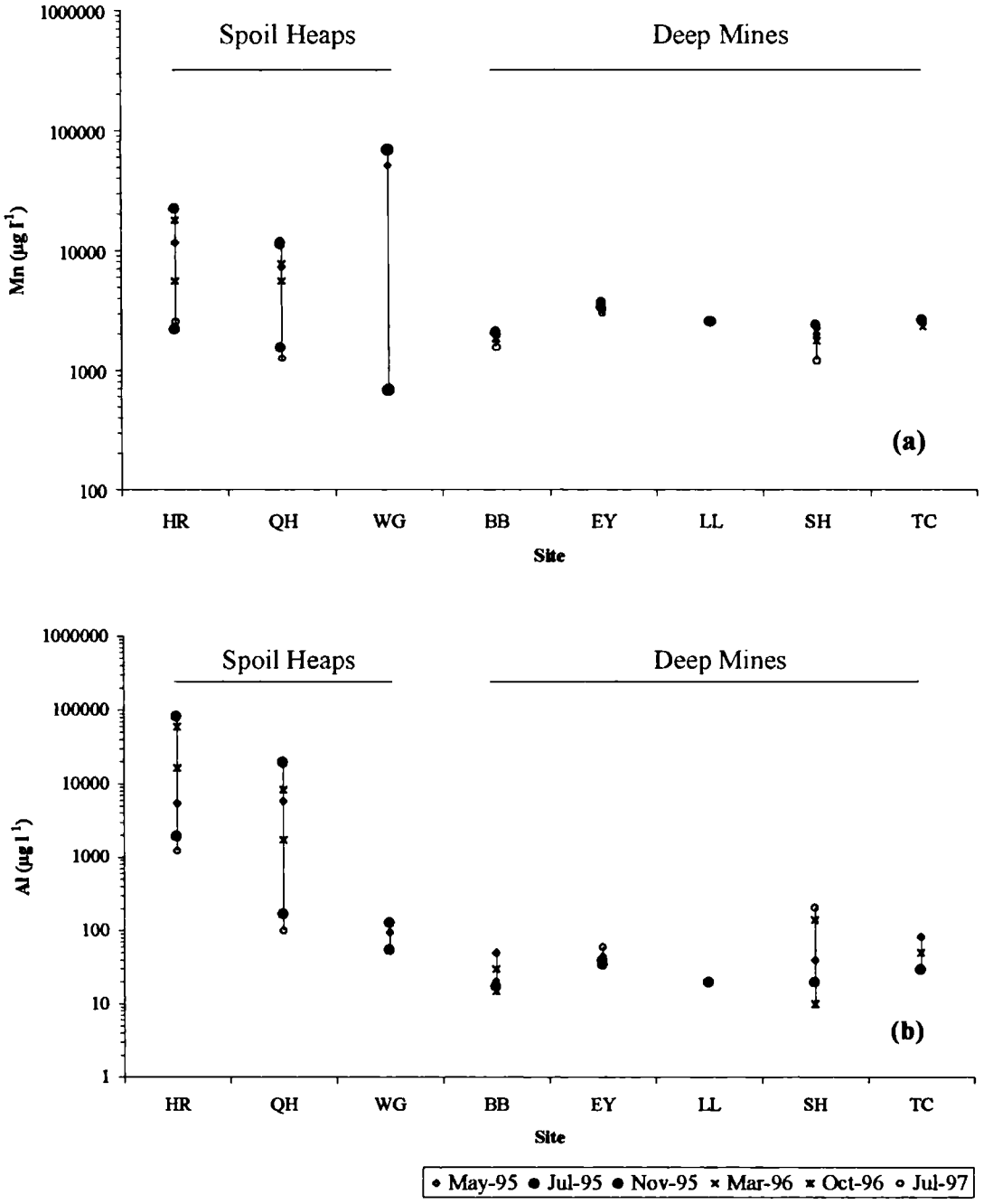


Figure 5.7: Temporal variability of Mn and Al concentrations in spoil heap and deep mine drainage at the study sites. (a) Mn (b) Al. The sites are labelled as follows: Helmington Row (HR), Quaking Houses (QH), Willington (WG), Broken Banks (BB), Edmondsley Yard Drift (EY), Low Lands (LL), Stony Heap (SH) and Tindale Colliery (TC).

5.1.4 Suspended sediment

Suspended sediment loading was low for mine drainage sites. The main constituent of such drainage was presumed to be silicate detrital matter, because Na, K, Mg, Ca and Al tend to occur simultaneously in the suspended sediment where measurable concentrations were observed. Iron concentrations were generally low (<1 mg l^{-1}) with the exception of EY, which had concentrations of ~1 mg l^{-1}. Suspended sediment is a more important constituent of spoil heap drainage (section 5.2) and downstream from points of discharge (chapter 7), and will thus be discussed in the appropriate sections.

5.1.5 Minewater precipitate mineralogy

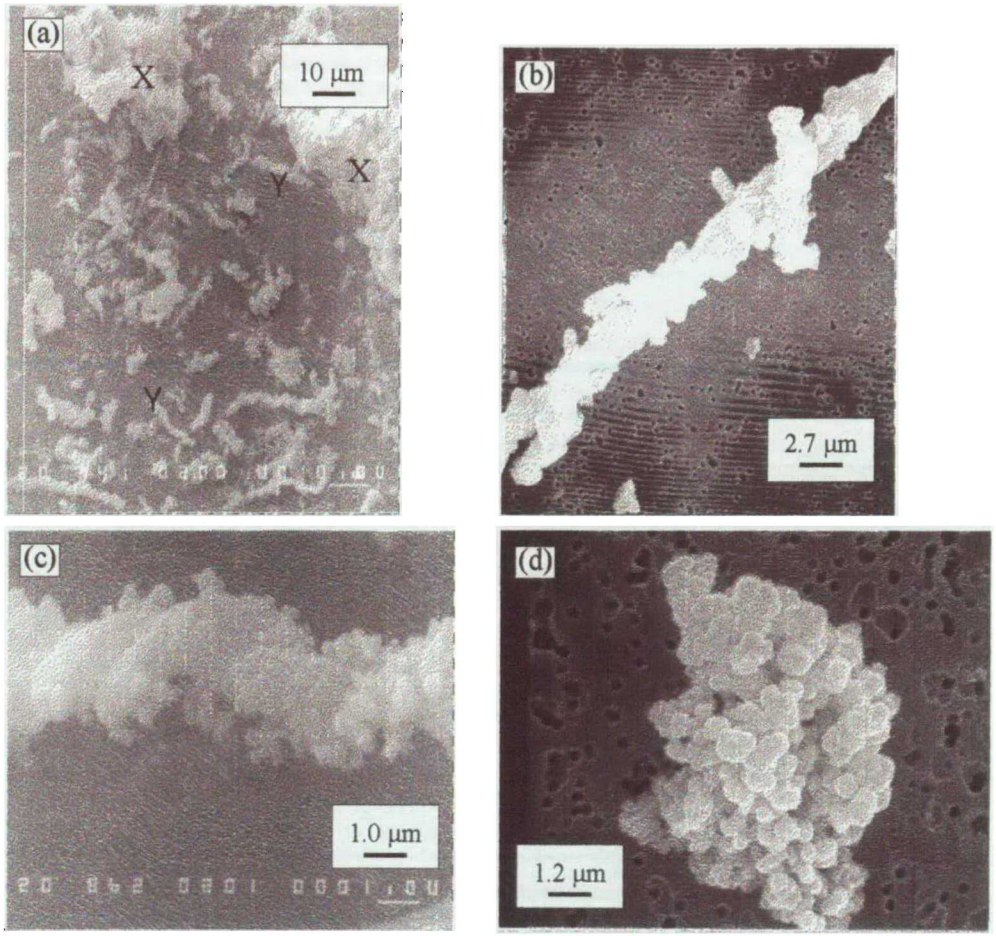
Figure 5.8 shows the XRD patterns acquired for a selected sample at BB collected in July 1997. This sample was collected from a brick surface (Plate 5.1) which was placed in the discharge in October 1996 (time of 9 months) (section 4.3.4), and is thus known to represent relatively fresh deposition as compared with the mixed age sample expected to be collected normally. The diffraction pattern would appear to be that of (possibly) goethite in an admixture with a more amorphous component. The diffraction patterns for EY01 and SH06 (July 97) are described in section 5.1.5, where they were part of cores collected. All the samples analysed showed a similar nature, of a poorly crystalline substance and a very large unresolved amorphous background (figure 5.8a & b). SEM analyses of the mine drainage generated ochres was unable to resolve fine details of the morphology of Fe minerals, however it did show some larger scale features (>~1μm) within the "matrix" of smaller particles. Plate 5.2a shows the loading of a mounted specimen from SH discharge point. It can be seen that the ochre is characterised by aggregated material and elongated "twisted rope" structures, which are tentatively identified as *Gallionella sp.* coated in ochre (section 2.2.3). These two types of particle were ubiquitous in all SH discharge samples studied. Plate 5.2 shows progressively larger scales of SEM images, which show some detail of the morphology of these particles. Morphological inspection was also made of the ochre from BB, which showed the *Gallionella sp.* structure and the spheroidal particles as observed at SH. The analyses of particles using the SEM in analytical mode (section 4.5.2a) enabled some determinations to be made of the major (percentage concentrations) composition of ochres. Analyses were made of several samples from SH and EY, and these showed similar compositions. These measurements showed the samples to contain 50% Fe (standard deviation of 3.6) and 3.2% Si (standard deviation of 0.45) in 39 analyses.

Plate 5.1: Broken Banks deep mine discharge. (a) discharge site with a view downstream (b) discharge and the brick cleaned and laid for the collection of "fresh" ochre on the subsequent sampling occasion.





Plate 5.2: SEM images of ochreous material at SH. (a) low magnification view of sample loading. two types of particle are apparent, one an aggregated "clump", the second a "twisted rope" structure. (b) a closer view of a "twisted rope" structure. (c) the highest magnification view possible whilst still maintaining a view of the twisted rope structure.



These determinations apply to both types of particle observed in plate 5.2 (spheroidal and bacterial). A typical spectra from one of these analyses is shown in figure 5.9, with a background "blank" signal included for assurance that no contamination occurred from the resin or otherwise in the sample (and thus cause a "false" Si measurement). Analyses of the samples by ICP-AES showed that the composition of the ochres was very stable (appendix IV), and can be summarised as being dominated by Fe, with average concentrations of 44% at BB, 47% at EY and 48% at SH. The only other ion occurring in concentrations over 1% was Ca at BB, where the concentrations found were up to 2% (Ca concentration at EY and SH <0.5%). The minerals predicted to precipitate, using PHREEQ-C saturation indices, are given in section 5.1.2.

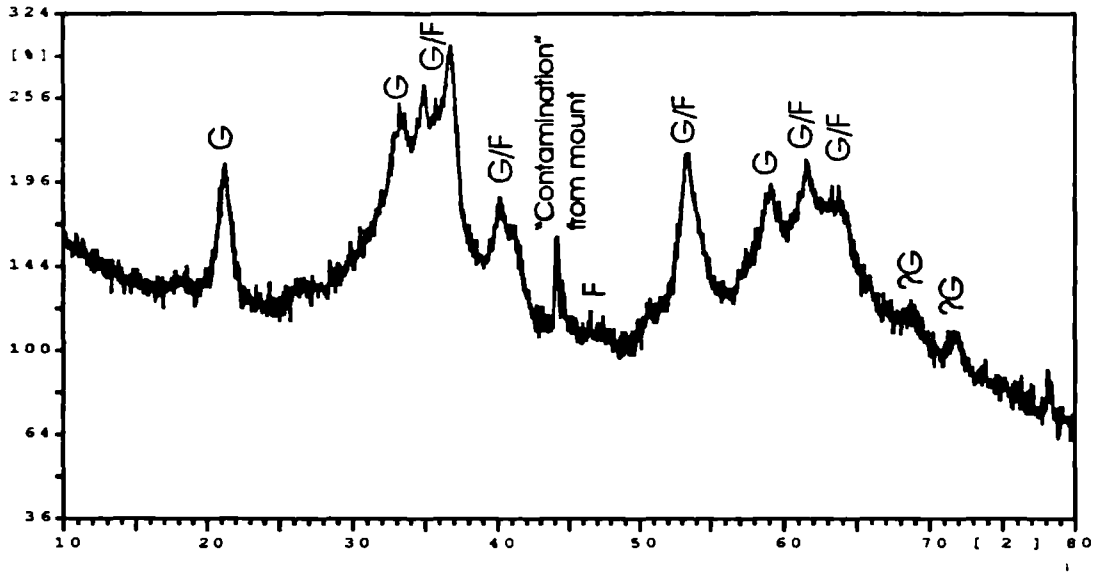


Figure 5.8: Diffraction pattern of ochreous material at BB01 (July 1997). Goethite peaks are marked "G" and ferrihydrite peaks are marked "F".

5.1.6 Ochre cores

The accumulation of ochreous material at two sites was so voluminous that a short core was collected from each (method described in section 4.3.4). The sites where this was possible were EY and SH. These cores were analysed chemically and selected samples were analysed by XRD. Figure 5.10 shows the changing chemistry downcore for EY and SH. In these figures, K is used to "fingerprint" the lithic component, and Fe is shown as the dominant ochre component. Plates 5.3 & 5.4 show that the bases of both cores were a pale grey material, which was very plastic in its properties. This is borne out chemically as a silicate layer by the high proportion of Li, K, Na, Mg, Ti and Al found (appendix IV) in the lowest section of both cores.

Figure 5.9: SEM-EDS spectra for deep mine ochres. (a) analysis of ochre showing Fe and Si detected (qualitative vertical scale) (b) analysis of background (i.e. the resin the sample is embedded in) showing no detectable Fe or Si resulting from the resin.

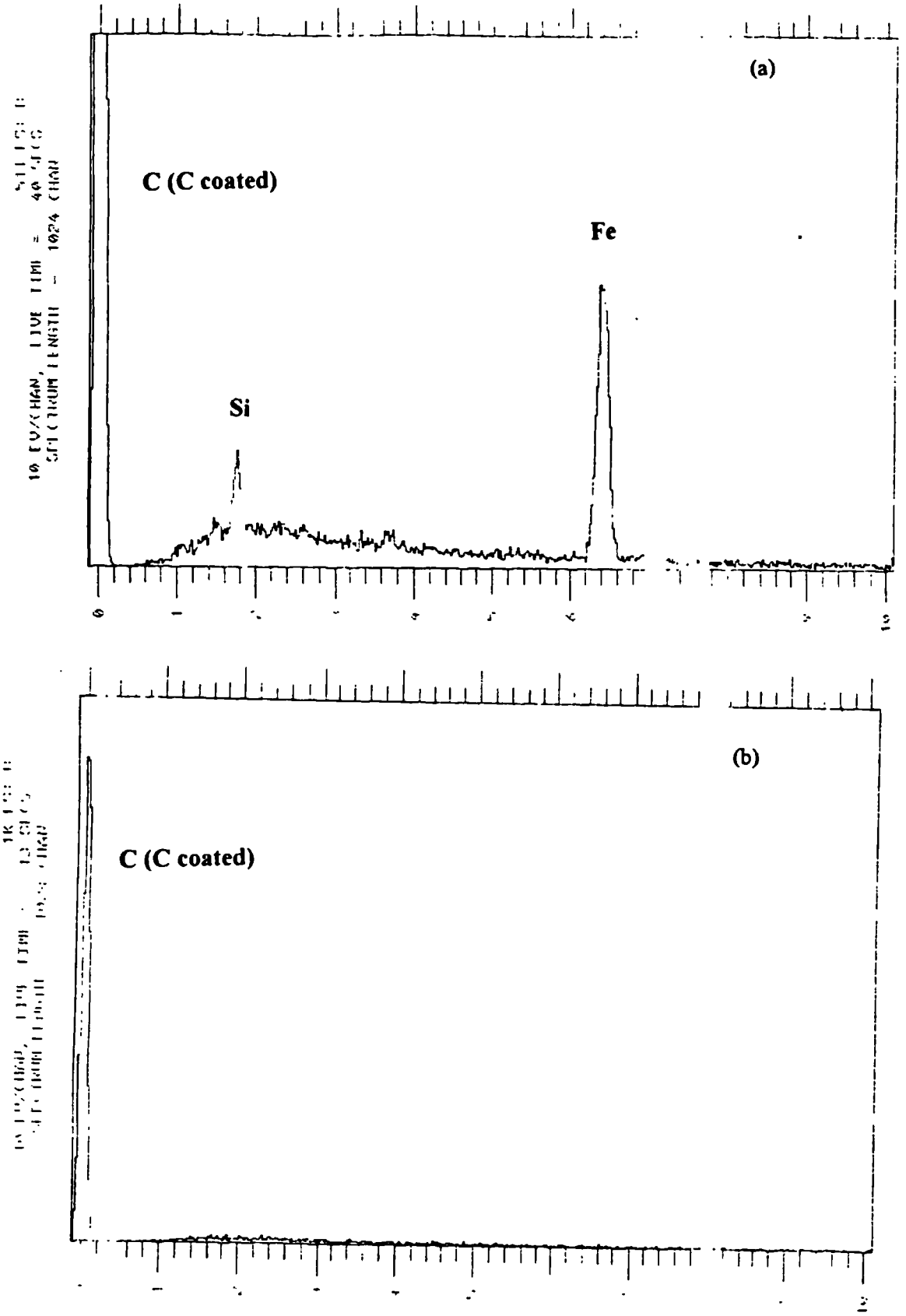


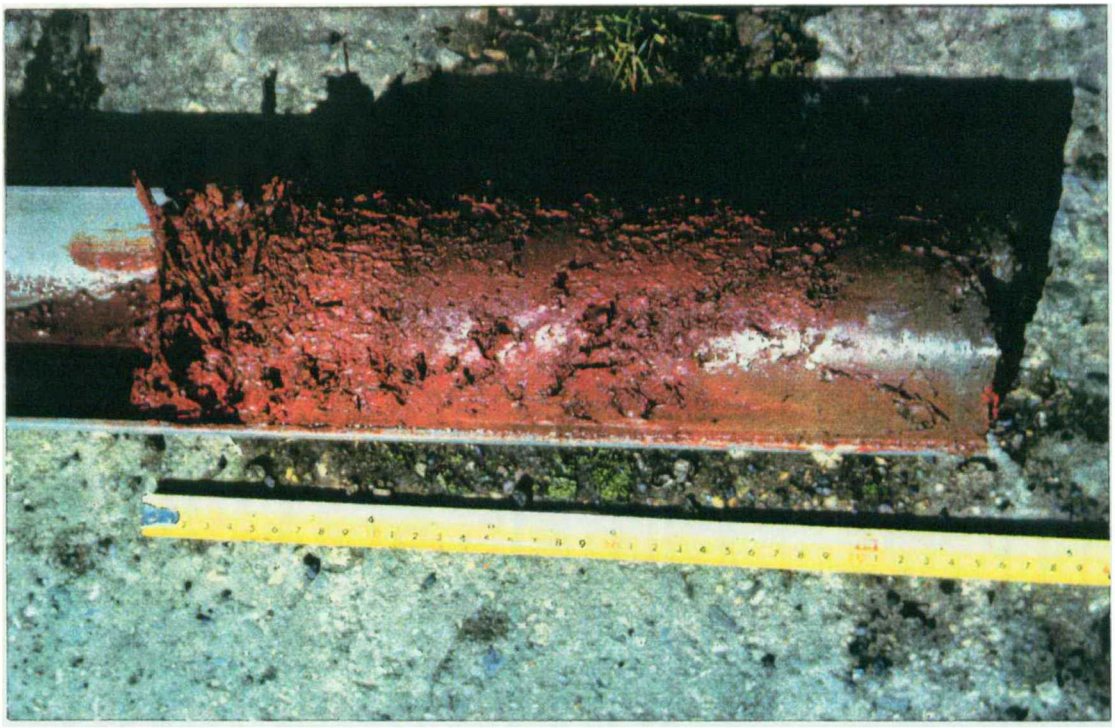
Plate 5.3: Edmondsley Yard Drift (EY) core sample. (a) the ochre accumulation from the discharge point (b) the core recovered from the ochre accumulation at the point of discharge





Plate 5.4: Stony Heap (SH) location and core collected. (a) the ochre accumulation close to SH (note that due to dense vegetation and the nature of the discharge point (section 3.4.1d) no better photo was possible) (b) the core recovered from the ochre accumulation.





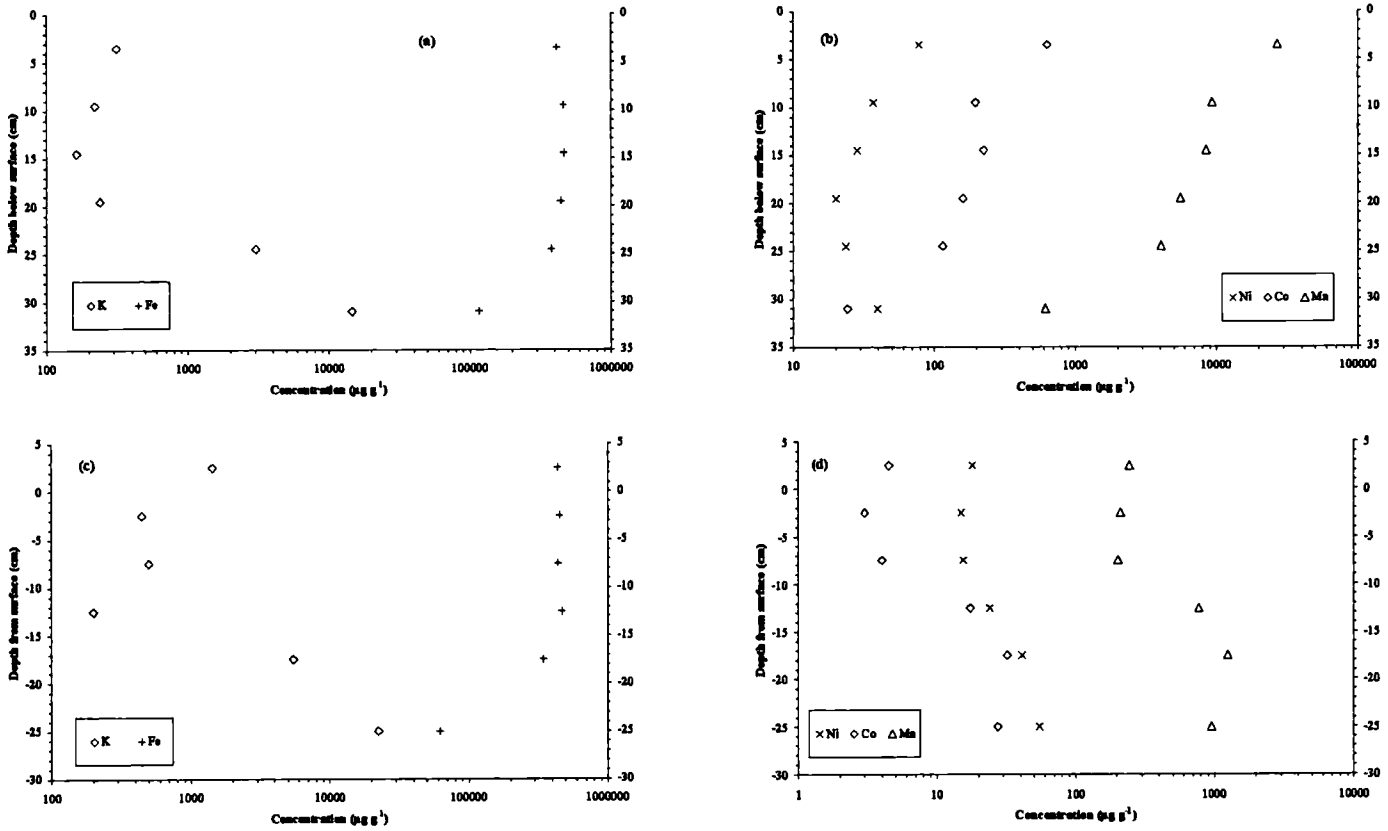


Figure 5.10: Downcore chemistry at EY and SH. (a) Downcore K and Fe concentrations at EY. (b) Downcore Mn, Ni & Co concentrations at EY. (c) Downcore K and Fe concentrations at SH. (d) Downcore Mn, Ni & Co concentrations at SH.

For other selected elements, the two cores show some differing behaviours than the simple dilution relationship between Fe and K, which suggests transition from an ochreous sample at the surface to a silicate sample at the lower end of the core. In the EY core Co and Mn follow the same pattern as Fe, decreasing with depth (figure 5.10b), Ni shows a decrease from the top sample, but then shows a stable concentration with depth. For Ni the biggest decrease occurs between the top two sampling intervals, whilst the other ions also exhibit a large proportional decrease at this point, their total concentration remains sufficiently elevated to observe the diluent effect in the lowest two samples, the latter one being wholly the plastic, grey clay described above, from observation. The concentrations of Fe are >40% for all the samples where ochre was the only "phase" observable. It can be seen from figure 5.10a & c that the concentration generally rises in the 10cm below the surface sample for both EY and SH. The SH core had much lower concentrations of Co and Ni, such that they are not shown here. It can be seen that these elements are primarily concentrated in the lithic fraction at the base of the cores at SH. The same is true for Mn (figure 5.10d), Co and Ni at SH. Calcium and Zn have very consistent concentrations of ~0.3% in the ochre at EY, ~0.2% in the other samples being 150-200 $\mu g\ g^{-1}$ respectively.

XRD analysis has been undertaken of selected samples in these two cores, the results of these are shown in figure 5.11. The top samples (figure 5.11a & c) have been compared to the lowest ochreous samples (figure 5.11b & c). It can be seen that there is an apparent increase in the proportion of goethite in the deepest samples, as evidenced by the more distinct peaks in figure 5.11b & d.

5.1.7 Deep mine summary

This section has described the results obtained for deep mine drainage locations in the Durham Coalfield. The aqueous, suspended sediment and precipitate chemical compositions have been presented and described, with the mineralogical information gained on the precipitates. These show a temporally consistent chemistry with a precipitate dominated by ferrihydrite. Modelling with PHREEQ-C has shown complexation with SO_4 to be important in the speciation of cations in solution and that SO_4 minerals are at equilibrium with the discharge chemistry. This information will be discussed in section 6.1.

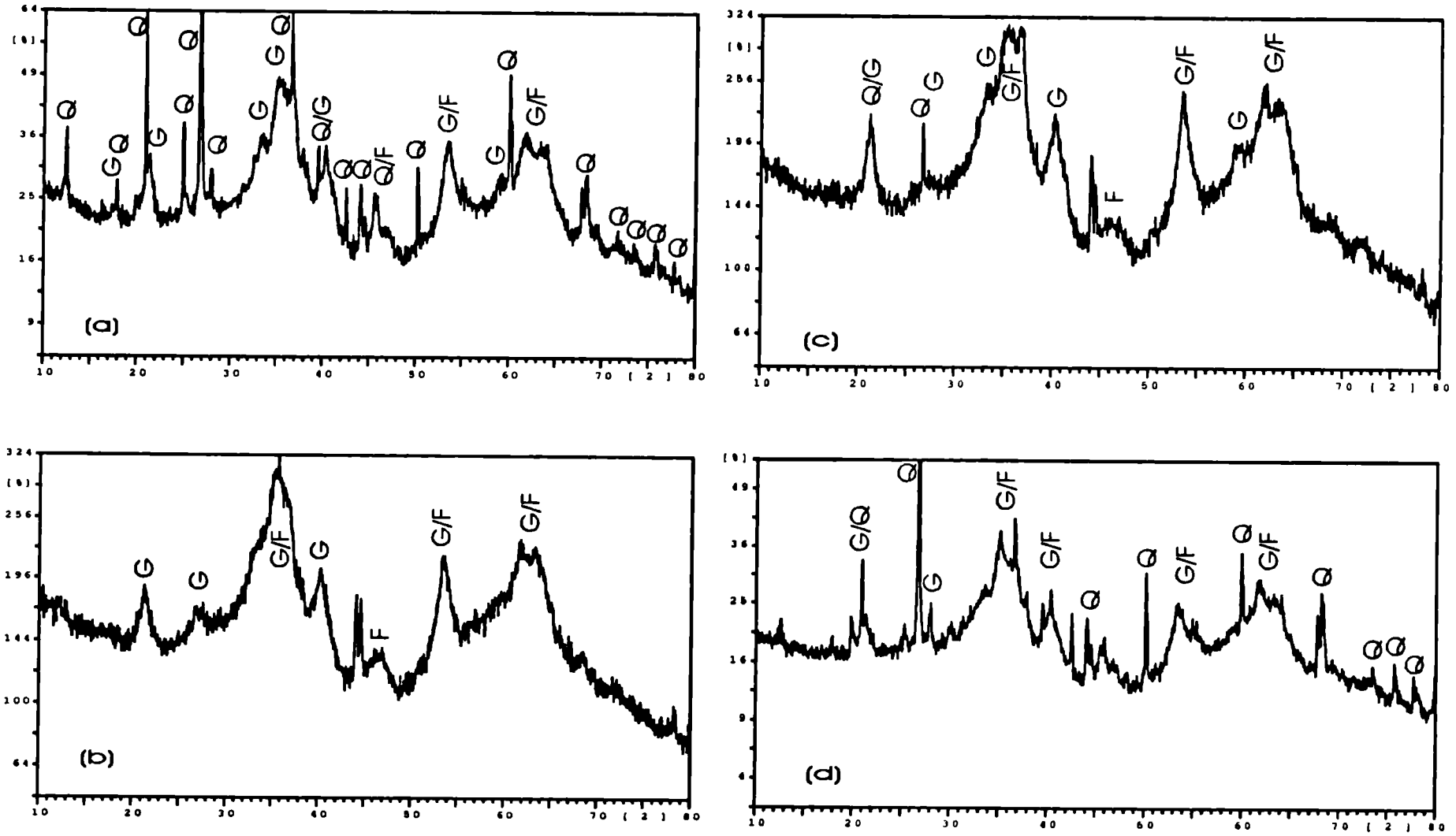


Figure 5.11: X-ray diffraction of ochre cores at EY and SH. (a) core top at EY (b) base of ochre in core at EY (c) core top at SH (d) base of ochre in core at SH. Goethite peaks are marked "G" and ferrihydrite peaks are marked "F" and detrital quartz is marked "Q".

5.2 Spoil heap drainage

This section will describe the observed chemical variations at each of the spoil heap discharge localities visited, Helmington Row (HR), Quaking Houses (QH) and Willington (WG). Preceding this will be a review of the hydrological regime at the sampling times, using data provided by the EA.

5.2.1 Physical characteristics

The spoil heap drainage shows extreme variability on the different sampling occasions, which would appear to be related to the short-term hydrological fluctuations. It was not possible to quantify the discharge rates for any site (except QH on some occasions) as described in section 4.2. Thus "high", "low" and "intermediate" or "normal" flows relate only to the qualitative records made of the discharges and cannot be used to compare different localities. An example of the variation in flow volumes can be seen for QH in plate 5.5, where a high and low flow can be observed at the discharge.

5.2.2 Aqueous chemistry: Major ions

The physico-chemical nature of the waters measured is summarised in figure 5.1. The spoil heap discharges are shown in orange, with the sites being distinguished as shown in the key. The spoil heap discharges have a larger variation in results than do the deep mine discharges (described in section 5.1). It can be seen that pH varies with sampling occasion over a range of ~3 - ~7. Eh also varies from an oxidising environment through a transitional zone into a poorly oxidising environment. The variability of the seasonal visits is reflected further in the series of diagrams in figure 5.5, and in both these figures shows a large contrast with the deep mines, where the sites show a temporal consistency.

The major ions are plotted on triangular diagrams, with the cations (Ca, Mg, Na+K) shown in figure 5.12a and the anions (HCO_3, SO_4, Cl) in figure 5.12b, with inset diagrams showing the dominant ion divisions. Spoil heap waters can be seen to be different types both between localities and on a temporal scale. HR is a Ca-Mg-SO_4 type water on all sampling occasions, despite the changes in actual concentration which are described below (figure 5.5). The site would appear to show a slight change in chemistry on different occasions, with a change from ~50% Ca and Mg (November 95 sample) to a slightly higher proportion of Ca (July 95 sample). Sulphate is in all cases the dominant anion, the only major compositional difference occurs with an increase to ~10% of HCO_3 in the November 95 sample. WG (Ca-Mg-SO_4 type) shows a very similar nature to HR, but the two samples have greater variation than that of HR. QH is a Na-K-Cl

Plate 5.5: Quaking Houses (QH) spoil heap drainage, showing the variation in discharge between low flow and high flow conditions. (a) low flow (b) high flow





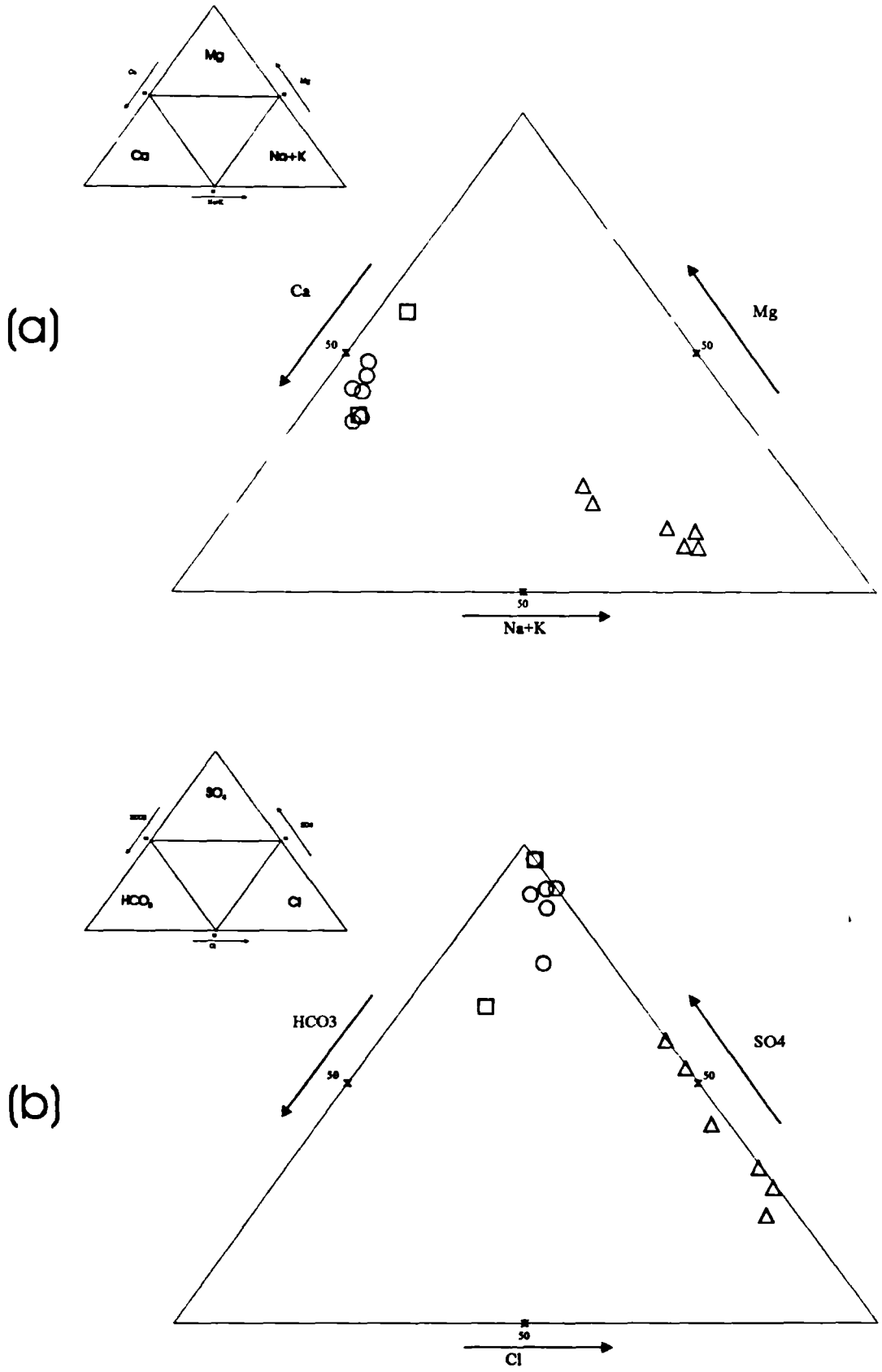


Figure 5.12: Triangular plots of major ion chemistry at spoil heap discharge locations. (a) cations: Ca, Mg, Na & K (b) anions: HCO_3, SO_4 & Cl. Labelling as follows: HR = circle; QH = triangle & WG = square. Units are %meq, with 50% marked on each axis. The occurrence of dominant ions on the diagram is described by the associated inset to each plot.

water type (figure 5.12), but the Cl component is lower in July 95 and October 96, when it is a Na-K-SO_4-Cl type water. The QH samples would appear to move along a mixing line for Na+K and Cl in figure 5.12.

The concentrations of Na and Cl have been plotted in figure 5.3, to compare with the stoichiometry of the concentrations expected by dilution of a NaCl solution. It can be seen that QH plots along the line suggesting a mixing line of a Na-Cl end-member with a water of comparatively negligible Na and Cl concentrations. Another discharge which shows the same slope of line is WG, but this water would appear to have excess Cl. HR shows a more complex pattern of increases in Na with no concomitant Cl increase.

Figure 5.5 shows the results of the measurement of the pH and selected major ions (Fe, SO_4 and Ca). Figure 5.5 shows that there is a considerable difference between the nature of the spoil heap and deep mine drainage, the full results of all analyses are given in appendix 4. The spoil heap waters exhibit a temporal variability of more than an order of magnitude for the concentrations of Fe and SO_4 and variations of 3-5 pH units. The data points are labelled according to the time when they were collected. Whilst it was not possible to quantitatively assess the discharge volumes (section 4.3.2), the samples could be broadly classified on whether the flows were "high", "low" or "intermediate" for each site (the terms used implying no specific discharge volume, simply a comparative measure specific to each site), supported by the data presented in section 5.2.1. The highest flows recorded at all sites were during November 1995 after a period of heavy rainfall, these are marked in blue throughout figure 5.5. The lowest flows recorded at all sites were in July 1995 during a dry period of very low rainfall, these are marked in red throughout figure 5.5. All other flows are marked in black symbols and were intermediate to the two visits described above, whilst not sufficiently different to each other to be distinguished on the qualitative scale.

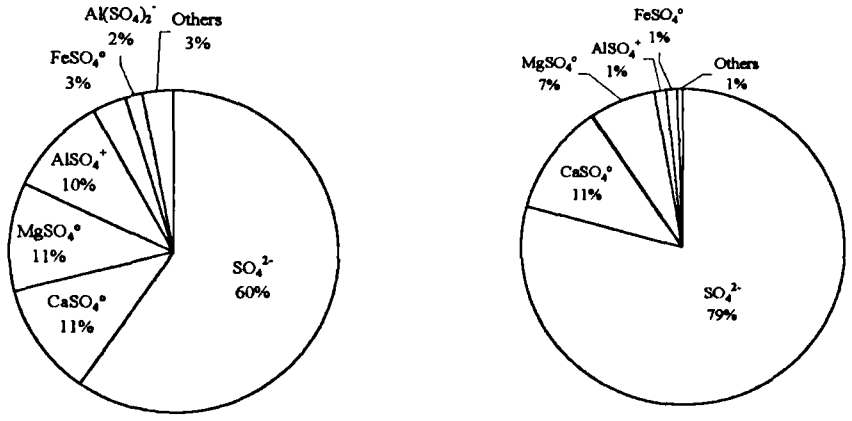
The pH values presented in figure 5.5a show a general trend of higher pH at the time of highest (flood) discharge and low pH at the time of lowest discharge. An inverse trend can be seen for the selected elements (Fe, SO_4 & Ca) presented (figure 5.5b-d) with that shown by the pH. At lowest flows they tend to higher concentrations, at highest flows they tend to lowest concentrations. Iron (figure 5.5b) is one of the major products of pyrite oxidation (section 2.2), and can be seen to vary by several orders of magnitude on a temporal scale. There is also some difference between sites, with QH and WG showing a wider range of values than does HR, with HR having consistently higher concentrations on each sampling occasion. Sulphate (figure 5.5c) is one of the other

products of pyrite oxidation, values can be seen to be comparable at all the sites, but vary temporally by over an order of magnitude. Calcium (figure 5.5d) concentrations at all sites vary widely on a temporal scale, but are comparable between sites, although the proportion of the cation balance of the waters which they constitute was shown in figure 5.12 to vary between sites, particularly between HR and QH, due largely to the high concentration of Na and Cl at QH.

Analysis for Si was made on three sets of samples, however, given the variability observed and the small number of samples, these results will not be presented in isolation here. Dissolved oxygen (DO) was measured only in October 96 and July 97, and thus there are also only a small number of values available. The speciation of Fe was only measured on a limited number of samples in July 97. The work including DO, Fe^{II} and Fe^{III} is described in section 5.3.

The use of PHREEQ-C (Parkhurst, 1995) enabled some assessment of the degree to which complex formation affects the activity of ions in solution (reviewed in section 2.2.3c). A large output dataset is created by PHREEQ-C (WATEQ-4F database used), there is room to review only selected aspects of the model output here. A comparison of the effect of complex formation on individual ions is shown in figure 5.13. The two sample results presented here show that for the HR discharge point, SO_4^{2-} is the dominant S^{VI} species on both occasions (as on all others not presented here), but that the proportion is higher in figure 5.13a when the concentrations of ions are all higher (figure 5.5c) than when the discharge was in flood (figure 5.13b) and concentrations of all ions were lower, (figure 5.5c). Table 5.4 shows that the presence of such high concentrations of SO_4 measured in solution, has a large influence on the speciation of some cations in solution.

It can be seen that whilst SO_4^{2-} is predicted to dominate the distribution of S species, SO_4 complexes themselves can dominate the speciation of other ions, particularly divalent ions and Al^{III}. The species shown in table 5.4 account for ~100% of the total speciation for each cation, excepting Al in QH (November 95). Table 5.4 shows that Ca^{2+} accounts for some 70-85% of the predicted speciation of Ca, with $CaSO_4^o$ increasing in proportion as the actual concentration of Ca increases. Barium speciation is dominated by $BaSO_4^o$ when the Ba concentration is highest (July 95); the proportion then decreases as the concentration of Ba decreases, as was observed with Ca. Aluminium speciation in these waters is dominated by the SO_4 complexes shown in table 5.4. The only sample where the percentage of the total recorded is not ~100% is QH (November 95), this is because



(a) (b)

Figure 5.13: Proportion of dissolved S(VI) predicted to be in the species shown by the program PHREEQ-C. Refer to figure 5.5c (& appendix IV) for concentrations of SO_4 in solution. (a) HR (July 95) (low flow conditions) (b) HR (November 95) (high flow conditions).

Table 5.4: The speciation of Ca, Ba and Al^{III} as affected by SO_4 in spoil heap drainage.

	HR			*QH*		
	July 95	*November 95*	*March 96*	*July 95*	*November 95*	*March 96*
Ca (mol/l)	**$7.76*10^{-3}$**	**$2.55*10^{-3}$**	**$3.50*10^{-3}$**	**$8.59*10^{-3}$**	**$3.57*10^{-3}$**	**$6.51*10^{-3}$**
% Ca^{2+}	69.97	84.27	76.58	71.81	89.05	82.94
% $CaSO_4^o$	*29.97*	*15.72*	*23.41*	*28.19*	*10.77*	*17.00*
% of total	99.94	99.99	100	100	99.82	99.95
Ba (mol/l)	**$1.50*10^{-7}$**	**$3.06*10^{-7}$**	**$2.05*10^{-7}$**	**$1.91*10^{-7}$**	**$6.54*10^{-7}$**	**$4.38*10^{-7}$**
% Ba^{2+}	45.52	64.71	52.69	48.12	74.03	63.12
% $BaSO_4^o$	*54.48*	*35.28*	*47.31*	*51.88*	*25.88*	*36.88*
% of total	100	99.99	100	100	99.91	100
Al (mol/l)	**$3.1*10^{-3}$**	**$7.23*10^{-5}$**	**$6.09*10^{-4}$**	**$7.44*10^{-4}$**	**$6.31*10^{-6}$**	**$6.40*10^{-5}$**
% Al^{3+}	23.76	34.01	26.33	26.15	17.92	43.44
% $AlSO_4^+$	*65.56*	*57.93*	*64.51*	*61.78*	*15.76*	*52.02*
% $Al(SO_4)_2^-$	*10.57*	*2.95*	*6.08*	*9.75*	*0.64*	*4.45*
% $AlOH^{2+}$	0.10	4.72	2.89	2.16	29.36	0.09
% $Al(OH)_2^+$	0	0.40	0.20	0.15	32.20	0
% of total	100	100	100	100	95.89	100

July 95 represents the low flow extreme observed, the November 95 samples represent the highest flow volumes observed at the discharge points. March 96 samples are presented as an intermediate flow condition. The total ion concentrations quoted were measured on the occasions given. The speciation of those ions was modelled using the PHREEQ-C model (WATEQ-4F database).

some Al^{V} species are predicted to occur in addition to Al^{III}. The SO_4 complexes are of a higher concentration than Al^{3+} and hydroxy-complexes, which is in agreement with the prediction by PHREEQ-C that Al-SO_4 phases would be expected to precipitate. The predicted speciation of trace metals will be presented further in section 5.2.3 for spoil heaps.

Of the other major ions, Mg speciation is similar to Ca, for which Ca^{2+} and $CaSO_4^{o}$ dominate. Sodium and K are predicted to be present as Na^{+} and K^{+} (>95%) in all cases. However, Na may form up to 5% of the total S speciation (as $NaSO_4^{+}$) at QH in the conditions of highest concentration. Chloride speciation is also expected to be dominated by its monovalent anion. Dissolved inorganic carbon is controlled by HCO_3^{-} or CO_2 (H_2CO_3) depending upon the pH of the solution (section 2.2.2).

5.2.3 Aqueous chemistry: Minor and trace ions

Interest in minor and trace ions stems from their potential as indicators of the mechanisms operating and their compliance with statuary limits, which are themselves a manifestation of concern over toxicity to various organisms and amenity value of streams (section 8.3)

The concentrations of Mn and Al are shown in figure 5.7. It can be seen that the concentrations of Mn vary by >10x (figure 5.7a). The concentrations are highest in July 95 (lowest flow conditions), with the high flow conditions being at, or near, the lowest concentration observed. The concentrations observed in November 95 are close to background (see sections 7.2 and 7.3 for further confirmation of this). Figure 5.7b shows Al concentrations at the spoil heap locations. The same pattern of highest concentrations in July 95 and those of Nov 95 being among the lowest in high flow conditions. What is very noticeable is the elevated concentrations of Al even in Nov 95 when the pH is >5 for all sites (figure 5.5a). This is particularly evident for HR where the concentration is >1000 $\mu g\ l^{-1}$ in Nov 95.

Figure 5.14a shows the variations in Al concentration with pH. The deep mine drainage data is also plotted to provide more information about any relationship between the two, but was not of sufficiently elevated concentrations to study variations. The diagram shows that the lower concentrations of Al are generally associated with the higher pH values at the sites, and conversely that higher concentrations are associated with lower pH values. Figure 5.14b shows that a similar relationship can be seen with the concentrations of Cu and Zn at HR and QH discharges. The concentration of Cu and Zn

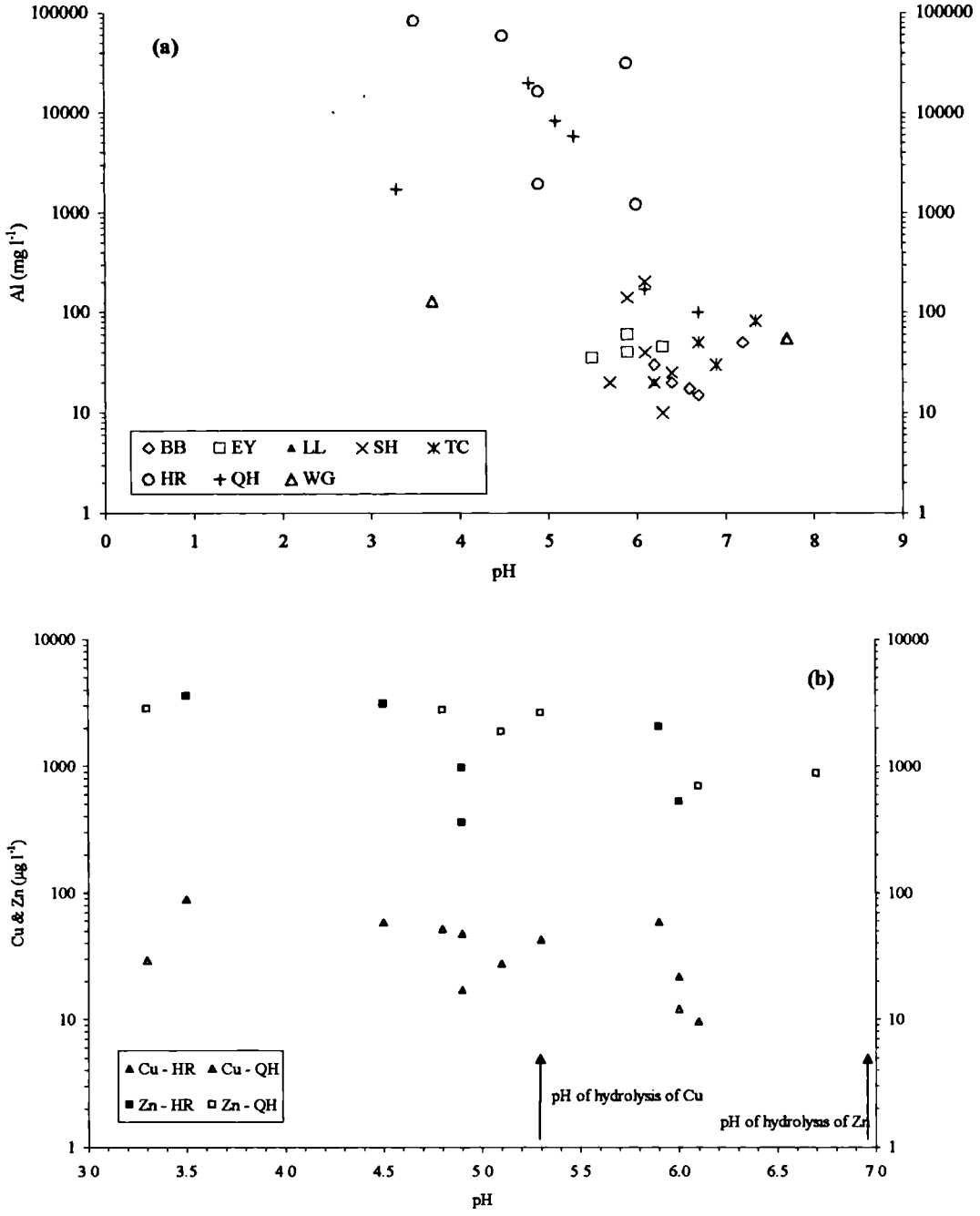


Figure 5.14: Comparison of pH and dissolved Al, Cu and Zn concentrations at the point of discharge. (a) pH and Al concentrations in spoil drainage, with deep mine drainage included for comparison. Deep mine discharge are green symbols; spoil heap discharge are orange symbols (b) pH relationship to Cu and Zn in drainage from HR and QH spoil discharge. pH of hydrolysis taken from Levinson (1980).

can be seen to generally decline with increasing pH at both sites. The pH variations are shown on a temporal basis in figure 5.5. The concentrations of Cu and Zn can each be seen to be comparable at the two sites, with Zn concentrations being higher at both than Cu. The pH of hydrolysis of each is also marked on the diagram (figure 5.14b), and many of the samples can be seen to fall above the pH of hydrolysis of Cu, whilst none are greater than that for Zn.

5.2.4 Suspended sediment

As part of the assessment of the loading of the aqueous phase, the suspended (>0.45μm) phase was measured as described in section 4.3.3. The concentrations of elements can be seen to show a difference between sampling occasions and also to be greater for spoil heap discharges than deep mines (figure 5.15).

Figure 5.15 shows the results of analyses of suspended sediment for three selected elements. Figure 5.15a shows that Fe concentrations in all sites are very low in comparison with their dissolved concentrations (figure 5.5b). The spoil sites show a much greater fluctuation in concentrations than the deep sites (with the exception of EY), and whilst QH and WG follow the patterns observed in dissolved concentrations with the July 95 and Nov 95 samples being at the two extremes of the range, HR shows a different trend with the other samples having a higher concentration than those two sampling occasions. It is largely true that the suspended phase concentrations form a minimal proportion of the total stream load of a given element, this is something which is described further within chapter 7. Figure 5.15b shows K concentrations, which have been used as a proxy for the transport of silicate matter from the aquifer. This diagram shows that whilst all the spoil heaps have higher K concentrations than the deep mines, especially for the Nov 95 samples, QH is particularly enriched in K, showing a consistently high concentration, the concentrations being highest in May 95 and March 96. The latter sample being during snowmelt and therefore associated with a relatively high flow volume.

Figure 5.15c shows the concentrations of Al in the suspended phase. This is a more complex figure, because Al transport can be physical, in the transport of silicates, or reactive in the transport of Al weathered within the aquifer in low pH conditions. It is suggested that that the concentrations observed at QH are the result of silicate clay transport, whilst that at HR is due to reactive transport. These deductions are supported by the chemistry of the associated waters, and the colour of the filter papers after sampling (brown clay colours observed in turbid flow from QH, red ochreous colours

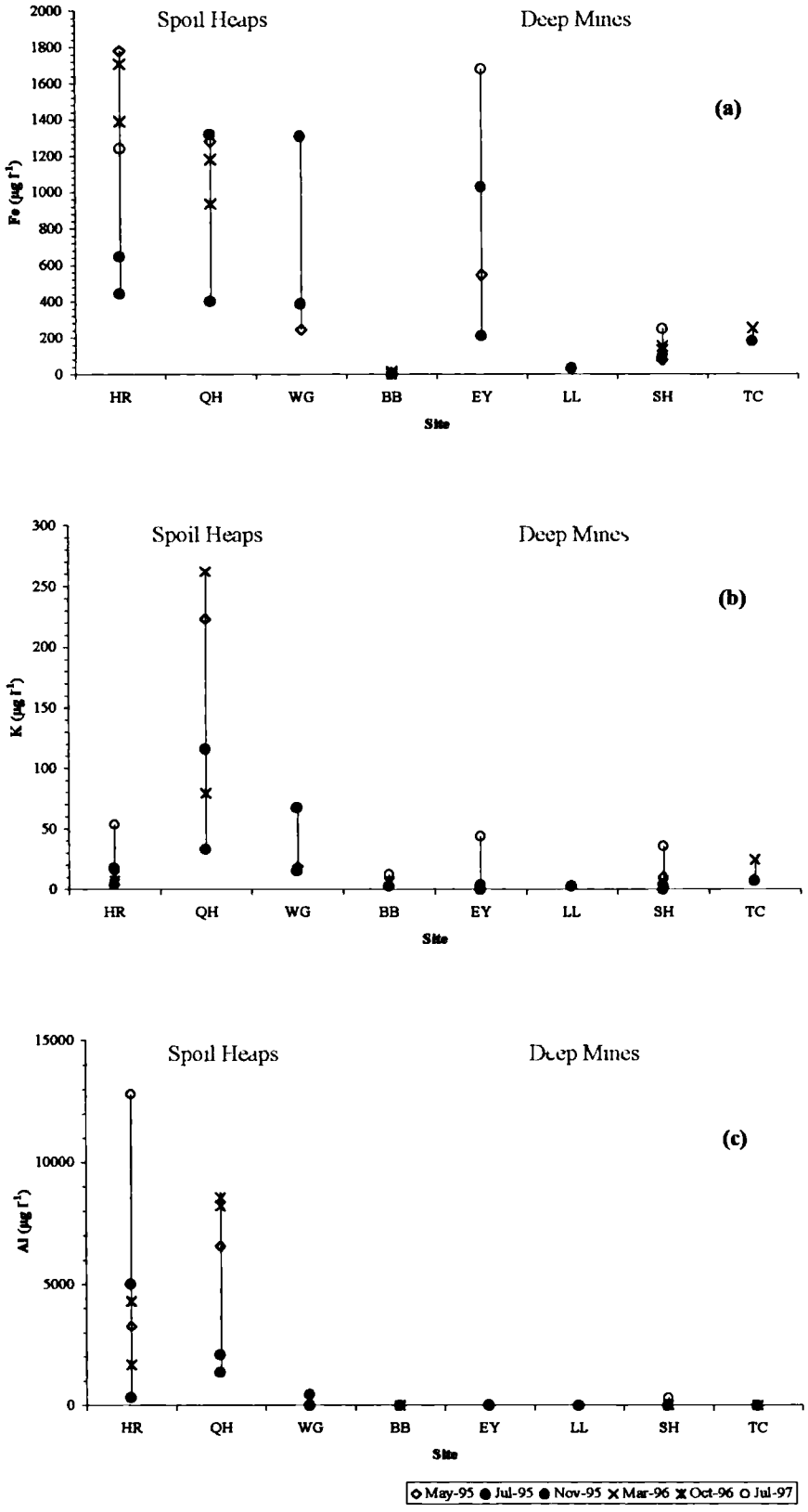


Figure 5.15: Concentrations of selected ions in suspended sediment from spoil heap and deep mine drainage. (a) Fe (b) K (c) Al.

from circum-neutral flows at both sites, and pale yellow colours from low flow at HR, associated with high Al in precipitates (section 5.2.5)). The occurrence of other trace elements in the suspended phase as compared to their dissolved phase is described further in chapter 7.

5.2.5 Spoil heap discharge precipitate mineralogy

As may be expected the nature of the minerals precipitated from the spoil heaps varies as the chemistry of the waters changes temporally. The precipitates have been subjected to chemical analysis at HR and QH. However, the volumes of precipitate forming at QH were very small, and it was not possible to collect wholly precipitate samples, so these will not be discussed here. Discussion of the changes in stream sediment chemistry can be found in section 7.3.4. The chemical composition of precipitates at the discharge point of HR have been determined, as has the mineralogical composition of selected precipitates.

The chemical composition of precipitate at HR is shown in table 5.5 and can be seen in plate 5.6 (a & b show the discharge; c & d show the changing precipitate colour). It can be seen from this that the precipitate is no longer a pure Fe hydrous oxide phase, as high concentrations of Al, S and Ca were also detected (table 5.5).

Table 5.5: Concentration of selected elements in precipitate at HR spoil heap drainage discharge site

Date	Fe	S	Al	Ca
		wt. %		
May 95	30	3.5	5.1	0.4
July 95	29	3.6	4.2	1.1
November 95	32	2.7	3.8	0.1
March 96	34	3.3	3.6	0.1
October 96	30	3.3	2.7	0.1
July 97	16	2.6	8.9	3.6

additional results are shown in appendix IV.

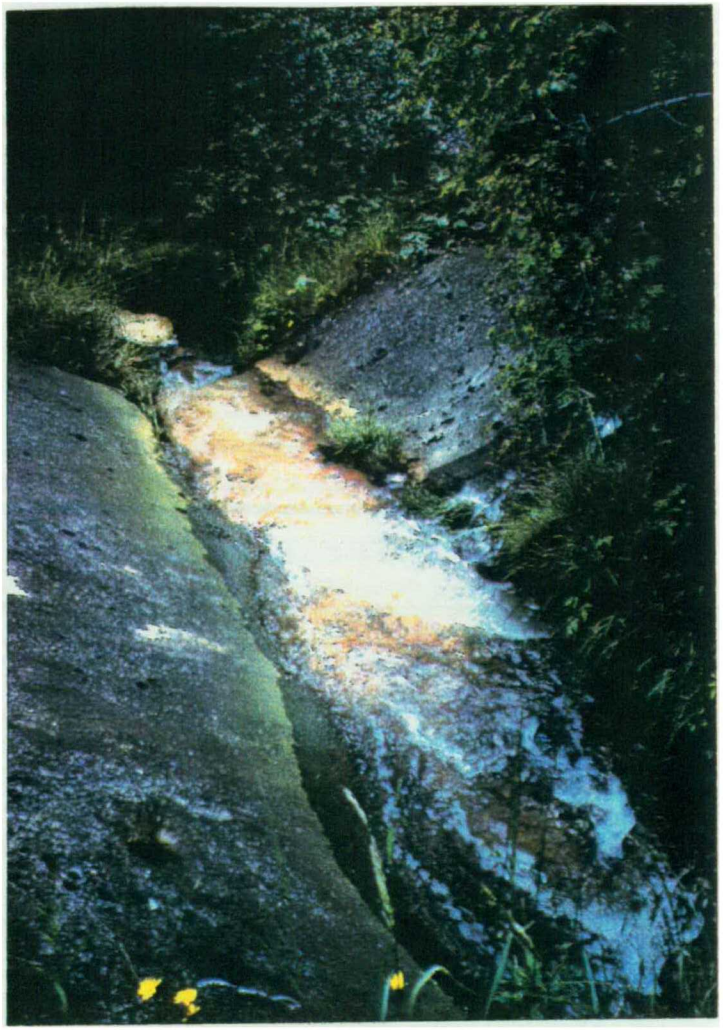
A comparative set of results using SEM analysis (section 4.5.2a) are shown in table 5.6, using SEM analysis Si was not detectable and neither was Ca, which suggests that Si did not form an intrinsic part of these precipitates as it does in the deep mine drainage (section 5.1.5). These results suggest that either a Fe-S-Al phase is precipitating or that there is an admixture of minerals, which are composed of these elements. The SEM analyses did not allow the determination of individual particles, because these samples were agglomerates of small particles (as shown for SH in plate 5.2d). No *Gallionella sp.*

Plate 5.6: Helmington Row (HR) spoil heap discharge. (a) the point of discharge of the main drainage of the spoil heap. (b) the pale and ochreous precipitate accumulating in the discharge pipe. (continued on next page)





Plate 5.6: Helmington Row (HR) spoil heap discharge. (c) the discharge during higher pH and ochreous precipitate discharge (d) the discharge during low pH and pale precipitate discharge (continued from previous page)





morphologies (as found in the deep mine ochres (section 5.1.5)) were observed at this site, in topographical analysis mode. The XRD study of samples from this site is shown in figure 5.16. These show a largely amorphous background, with quartz providing the only sharp peaks. The sample appears to contain ferrihydrite, possibly gypsum, and other poorly crystalline phases.

Table 5.6: Chemical results for HR discharge site using SEM analysis

Fe	S	Al
	wt. %	
50	n.d.	n.d.
46	3.46	3.54
41	3.99	5.67
46	3.15	3.10
32	2.17	2.97
40	3.25	5.20
42	2.69	4.52
38	3.69	6.43

All results are for analyses on HR04 (March 1996) precipitate sample.

The predicted precipitate mineralogy can be assessed by studying saturation indices (section 2.2.2b). Selected results of modelling predicted saturation indices are shown in tables 5.7 & 5.8. These results are those which are thought probably to affect the major ion chemistry. Iron is included as a major ion, but Al is also quoted because it affects the speciation of SO_4 in solution (section 2.2.3c). Iron minerals would appear to dominate the mineralogy of the stream precipitates and thus the prediction of their form is of interest in a study such as this. It can be seen that the "amorphous" $Fe(OH)_3$ phase is not predicted to precipitate at all, which is true of all the samples of spoil heap drainage. Goethite is predicted to precipitate as shown in table 5.7. Jarosite is included for reference, as it has frequently been identified as a product of acidic, ferruginous drainage (section 2.2.5d), but it can be seen that it is not predicted to precipitate at all in the samples listed, which was true for all spoil heap drainage. As table 5.8 shows, SO_4 would not be expected to be conservative in solution because the SI of Al-SO_4 minerals shows supersaturation for several phases, such as alunite, basaluminite and jurbanite. If these minerals precipitate a net loss of SO_4 from the aqueous phase will result.

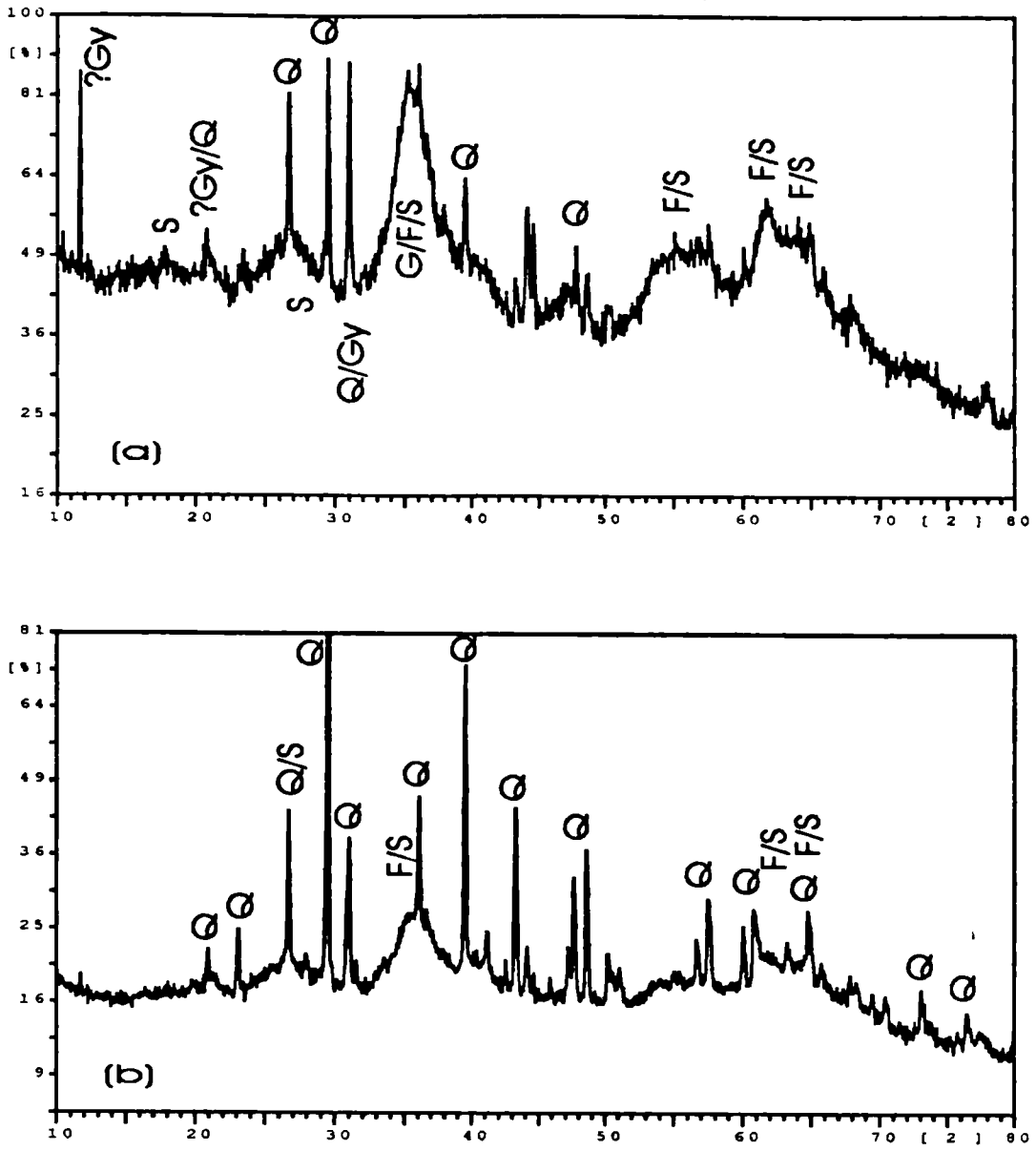


Figure 5.16: X-ray diffraction results for ochre at Helmington Row (HR) discharge site, associated with contrasting aqueous chemical conditions. (a) July 95 (low flow) (b) July 97 (moderate flow). Goethite peaks are marked "G", ferrihydrite peaks are marked "F", quartz peaks as "Q", schwertmannite as "S" and gypsum as "Gy".

Table 5.7: Selected saturation indices (SI) for Fe in solution.

		$Fe(OH)_{3(a)}$	*Goethite*	*Jarosite-K*	*Jarosite-Na*
HR	*July 95*	-4.0	1.7	-8.2	-11.7
	Nov 95	-4.5	1.2	-15.2	-18.6
	March 96	-4.5	1.2	-14.8	-18.2
QH	*July 95*	-6.2	-0.4	-17.6	-20.5
	Nov 95	-6.9	-1.1	-25.0	-28.1
	March 96	-9.4	-3.7	-23.4	-26.4

These were calculated from the measured concentrations by the PHREEQ-C model (using the WATEQ-4F database). The results are quoted as log SI calculated according to equation 2.12.

Table 5.8: Selected saturation indices (SI) for Al in solution

		Alunite	*Basaluminite*	*Jurbanite*	*$Al(OH)_{3(a)}$*	*Gibbsite*
HR	*July 95*	0.4	-5.7	0.5	-5.3	-2.4
	Nov 95	3.9	3.3	0.3	-2.3	0.5
	March 96	6.4	6.3	1.3	-1.7	1.1
QH	*July 95*	7.3	4.7	1.2	-1.9	0.9
	Nov 95	7.3	9.0	-0.1	-0.3	2.5
	March 96	-5.0	-14.0	-1.4	-7.5	-4.7

These were calculated from the measured concentrations by the PHREEQ-C model (using the WATEQ-4F database). The results are quoted as log SI calculated according to equation 2.12.

Although concentrations of Na^+ and K^+ are generally high, they are conservative in solution, unless a jarosite mineral (section 2.2.5d) is precipitating, which is not predicted to happen here (table 5.7). High concentrations of Cl^- are recorded at QH in particular, but are expected to be conservative in solution. The SI_{gypsum} is <-1.0 for all the waters analysed here, apart from the November 95 samples, which were very high flows and lower elemental concentrations (figure 5.5). In July 95, SI_{gypsum} is -0.27 and -0.26 for HR and QH respectively, implying that neither Ca or SO_4 may be stable in solution.

5.2.6 Spoil heap summary

This section of work has demonstrated the large scale variations occurring in the spoil heap discharge chemistry. These variations have also been shown to be reflected in the suspended sediment concentrations and compositions, and the precipitate chemistry and mineralogy. Identification of the precipitating phases of Al-SO_4 minerals could not be achieved, due to the complex chemical mixture, high amorphous background signal (XRD) and high hydration state (SEM). These results will be discussed in section 6.2.

5.3 Measurement of Fe^{II} and Fe^{III} in different filter fractions

This section will briefly describe the small dataset acquired, when sites were sampled in October 96 and July 97 and where analysed for DO and (in July 97) Fe speciation. This sampling was augmented by a number of the sites sampled in October 96 and July 97 being filtered at 0.2μm and 0.1μm, respectively, for comparison with the normal sampling protocol of 0.45μm filtering.

5.3.1 Filter size comparison results

In October 96 samples had been collected at 0.2μm and 0.45μm filter sizes, but the data had largely only shown a difference in the Fe concentrations, which led to the sampling of waters at 0.1μm as well as 0.45μm nominal pore size on the final sampling occasion, July 97. Thus the data presented here is largely of the 0.1μm filtered fraction, because if there is a difference to be observed, then it would be expected at this size more than 0.2μm, as more colloids would be expected to be trapped.

The comparison of analytical data for different pore filtering sizes is shown in table 5.9 for two sites sampled in July 97 (full results for all sites in appendix IV). This shows that the Fe^{II} concentrations are the same, whether measured in the 0.1μm or 0.45μm filter fraction. Iron(III) however, shows a small difference, higher concentration in the 0.45μm filtered sample, at HR, but little difference at SH. This is however, a very tentative suggestion, with so few analyses. Figure 5.17 shows the comparison of the Fe concentrations in the different pore filtered fractions. It can be seen that in comparison to the range of concentrations observed the deviation from the line showing a one:one ratio is small.

Table 5.9: Comparison of aqueous chemistry arising from filtering a different nominal pore sizes.

Site	Pore size	pH	Eh	Fe^{II}	Fe^{III}	SO_4	Mn	Al	Si	Cu	Zn
	μm		V	mg l^{-1}	mg l^{-1}	mg l^{-1}	μg l^{-1}	μg l^{-1}	mg l^{-1}	μg l^{-1}	μg l^{-1}
HR	*0.1*	6.0	0.39	15.5	1.3	482	2540	760	9.4	20.3	522
HR	*0.45*	6.0	0.40	15.7	2.4	471	2570	1220	9.59	21.6	524
SH	*0.1*	6.1	0.39	16.1	2.5	242	1200	135	7.85	6.45	49
SH	*0.45*	6.1	0.38	16.8	2.1	240	1220	205	7.93	6.85	52

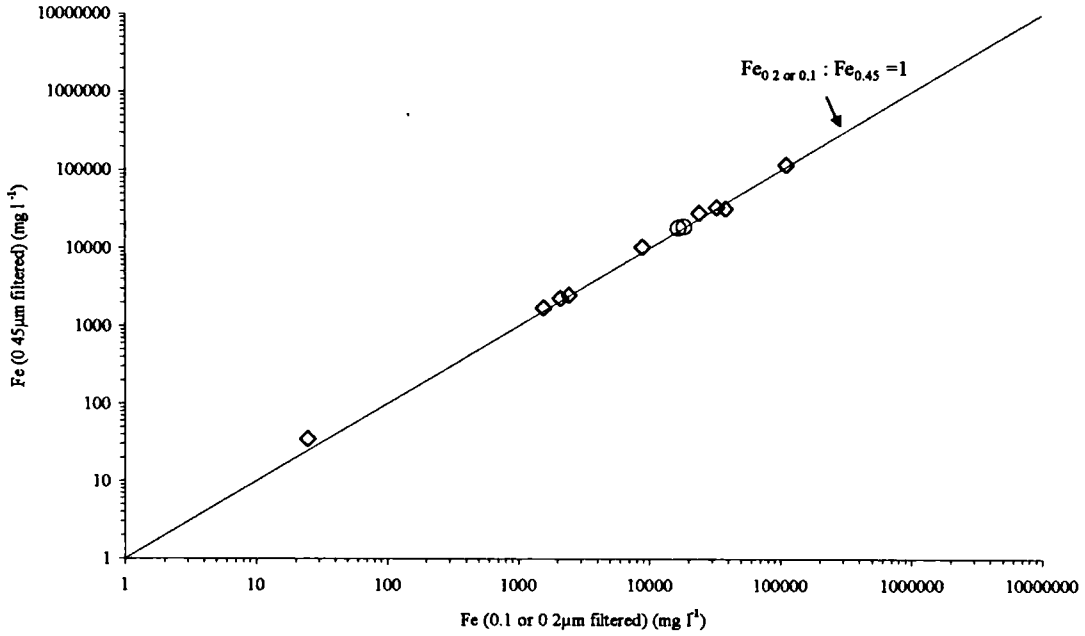


Figure 5.17: Comparison of Fe concentrations in waters filtered at 0.2µm or 0.1µm with filtering at 0.45µm. The data is from October 96 0.2 and 0.45µm filtering (diamonds) and July 97 0.1 and 0.45µm filtering (circles) for all samples collected.

The SO_4, Mn, Si, Cu and Zn all appear to show no difference in the two filter fractions, however Al shows a considerable difference at HR, with the concentration 1220 µg l^{-1} in the 0.45µm filtered sample, compared with 760 µg l^{-1} in the 0.1µm filtered fraction.

5.3.2 Eh measurement, comparison of results by different methods

The measurement of Eh is necessary where geochemical modelling is to be undertaken, because it is a master variable in the input data file. Not entering a value into the file will cause a default value to be used in the case of PHRREQ-C. The effects of differing measurement techniques and factors such as thermodynamic disequilibrium on the Eh value obtained were reviewed in section 2.2.3a. This study incorporated the measurement of Eh using 3 different methods on a limited number of samples. Thus these were used to test the effect of the input Eh value on predicted aqueous and solid phase species.

The methods of Eh measurement used were Pt-electrode (Eh_m), the O_2/H_2O couple (Eh_{DO}) and the Fe^{II}/Fe^{III} couple ($Eh_{FeII/III}$). This modelling was undertaken using PHREEQ-C with the WATEQ-4F database (Parkhurst, 1995) (section 4.6). The same input data files of each site were modelled three times, changing only the Eh values used, thus allowing a direct comparison of the effect of changing the Eh. The samples

used for this modelling were collected in October 96 (Eh_m and Eh_{DO}) and July 97 (Eh_m, Eh_{DO} and $Eh_{FeII/III}$). The more complete dataset was thus obtained for July 97, and selected results from that sampling exercise are reviewed here. The modelling results described below for the July 97 samples are also shown by the October 96 samples.

Table 5.10 shows the results for three selected sites sampled in July 1997. The pH value measured in the field is shown in the third column and the Eh value shown in column 4 is that measured in the case of Eh_m, or that modelled in the case of Eh_{DO} and $Eh_{FeII/III}$. The Fe^{2+} and Fe^{3+} concentrations shown compare the results which were measured for $Eh_{FeII/III}$ and predicted by modelling for Eh_{DO} and Eh_m. Note that because the $Eh_{FeII/III}$ embodies the measurement of these species it can be considered the most accurate results for the Fe speciation, and used to compare with the results modelled using Eh_m and Eh_{DO}. The modelled goethite and amorphous $Fe(OH)_3$ SI results are shown in the second column.

It can be seen in table 5.10 that the aqueous speciation of Fe is predicted more closely by the Pt-electrode results than Eh_{DO}, for $Fe^{2+}_{(aq)}$, but that the concentration of $Fe^{3+}_{(aq)}$ appears to be predicted better using the Eh_{DO} than the Eh_m values. As a result of the closer agreement of Eh_{DO} with $Eh_{FeII/III}$ in the prediction of Fe^{3+} concentrations, the saturation indices of Fe^{III}-hydrous oxide phases which are then calculated by PHREEQ-C also are also closest for these two methods of measurement of Eh, because they rely on the calculated activity of Fe^{3+} (e.g. Appelo & Postma, 1994).

Table 5.10: Comparison of different Eh measurement methods on predicted saturation indices.

Site	Eh method	pH	Eh	Fe^{2+}	Fe^{3+}	SI $Fe(OH)_{3(a)}$	SI Goethite
			V	mol l^{-1}	mol l^{-1}		
BB	*Pt-electrode*	6.4	0.09	$1.35*10^{-6}$	$4.04*10^{-18}$	-3.6	2.2
BB	*$Fe^{II}/^{III}$*	6.4	0.33	$1.26*10^{-6}$	$8.65*10^{-14}$	0.8	6.5
BB	*O_2/H_2O*	6.4	0.85	$1.29*10^{-14}$	$1.37*10^{-12}$	2.0	7.7
SH	*Pt-electrode*	6.1	0.10	$2.44*10^{-4}$	$7.89*10^{-16}$	-2.2	3.6
SH	*$Fe^{II}/^{III}$*	6.1	0.38	$2.17*10^{-4}$	$9.82*10^{-11}$	2.9	8.7
SH	*O_2/H_2O*	6.1	0.87	$3.41*10^{-12}$	$8.76*10^{-10}$	3.9	9.7
HR	*Pt-electrode*	6.0	0.12	$2.91*10^{-4}$	$2.18*10^{-15}$	-2.1	3.7
HR	*$Fe^{II}/^{III}$*	6.0	0.40	2.25*10-4	$2.70*10^{-10}$	3.0	8.8
HR	*O_2/H_2O*	6.0	0.89	$3.81*10^{-12}$	$2.02*10^{-9}$	3.9	9.7

All samples filtered at 0.45μm at site listed (July 97 samples).

5.3.3 Sensitivity analyses of modelling, with respect to filter pore size and Eh measurement method

In order to assess the relative importance of the two processes described above, which alter the input data to a geochemical modelling program, a simple sensitivity analysis was undertaken. The samples at the different filter pore sizes used (0.2 and 0.45μm in October 96 and 0.1 and 0.45μm in July 97) were modelled using the available redox species to model the Eh (October 96 used Eh_m and Eh_{DO}, and July 97 used Eh_m, Eh_{DO} and $Eh_{FeII/III}$). These results were then compared to see if the filter fraction or the Eh measurement method caused a larger variation in the output results from the model.

Figure 5.18 shows the comparison of saturation indices obtained at HR and SH using three different Eh measurement methods for each site (July 97 data). This figure shows that the data points lie very close to the one:one ratio line plotted, indicating that the difference between modelling the data obtained by filtering at 0.1μm is very similar to the data obtained by modelling at 0.45μm pore size. The scatter of points along the line, shows that for both sites, the method of measuring the Eh, and thus the model program input, causes a much larger difference in results than does the filter pore size through which the sample was obtained. This figure shows, as was observed in table 5.10, that the Eh_m data gives a far lower predicted SI than does the $Eh_{FeII/III}$, and that the Eh_{DO} method predicts a greater SI value than $Eh_{FeII/III}$, but is closer numerically to the $Eh_{FeII/III}$ results than the Eh_m values are.

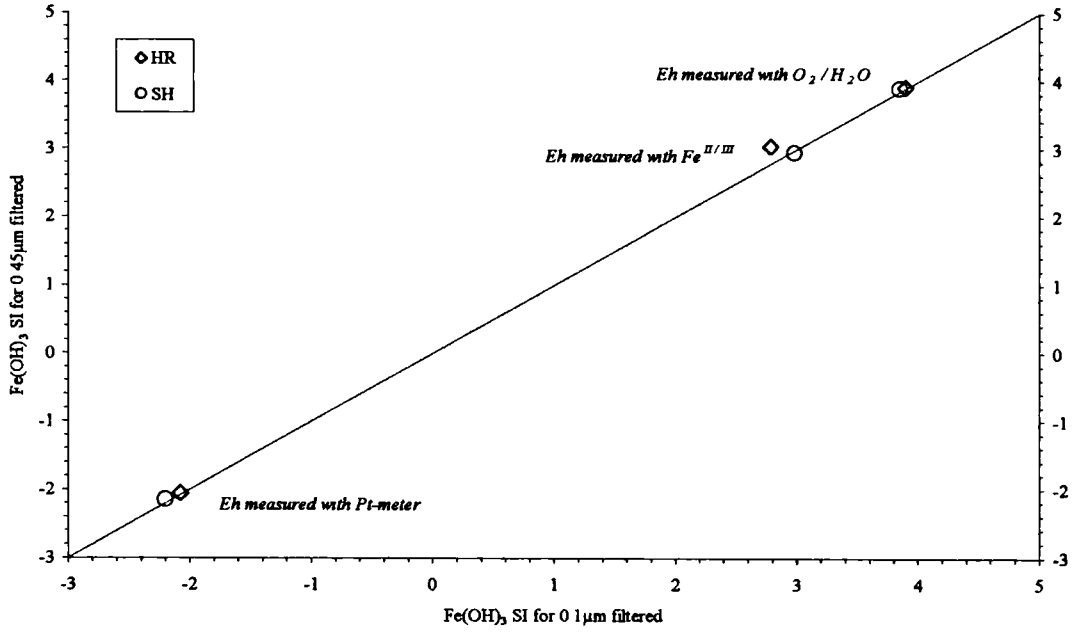


Figure 5.18: Comparison of the effect of filtering at different pore sizes and measuring Eh by different methods on the predicted SI of amorphous $Fe(OH)_3$. The data is shown for all samples collected in July 97.

5.3.4 Summary of filtering and modelling results

This section has briefly discussed the small number of results obtained in October 96 and July 97 comparing different filter sizes, and the use of different redox indicator species to measure ion concentrations in solution, and subsequently use the data for modelling. The results for filtering at different pore fractions shows, for the ions determined, that Fe is the ion mainly affected. The samples for July 97 show that it may largely be Fe^{III} which is causing the discrepancy in results. The modelling of speciation and, hence, saturation indices was shown to be influenced by the method of determining the Eh input to the model (which is a master variable). A simple sensitivity analysis showed that greater differences were obtained from modelling using different Eh measurement methods, than by the use of smaller filter fractions than 0.45μm.

5.4 Summary

It has been shown in this chapter that the localities studied are divisible into two types, based on the chemical and mineralogical results acquired over 6 sampling visits. The spoil heaps waters have a highly variable chemistry on the sampling visits, in contrast to the deep mine waters which show a high consistency of hydrogeochemistry. As may be expected from this both the predicted mineralogy of precipitates (sections 5.2.4 and 5.1.4) and the mineral phases observed (sections 5.2.5 and 5.1.5) are variable for the spoil heaps and consistent for the deep mine discharges. The reasons for, and importance of, the variation found in the spoil heap discharges will be discussed in chapter 6, using all the information described in this chapter. The factors deduced to be controlling the consistency of the deep mine waters will also be described in chapter 6.

The effect of the chemistry of the discharge localities will also be one of the dominant controlling factors in any consideration of the behaviour of such waters, as will be described in chapter 7 and discussed in chapter 8.

Comparison of data obtained by filtering of waters at different pore sizes and subsequently modelling that data has been presented in this section, and will be discussed in section 6.4.

6.0 Hydrogeochemistry of ferruginous drainage from abandoned coal mines and spoil heaps

This chapter will discuss the results presented and described in chapter 5. Firstly the processes responsible for controlling the water chemistry in deep mines will be discussed, with reference to pyrite oxidation and acidity buffering controls on the major ion chemistry. The chemical variations of major ions observed in the of spoil heap waters, with comparison to deep mine waters, will be discussed in section 6.2. Trace and minor ion chemistry will be discussed in the context of both types of discharge in section 6.3 to explain the factors controlling the concentrations of these ions at the points of discharge. The mineralogy of the precipitates will be discussed in section 6.1 and 6.2 as appropriate. Section 6.4 will review the hydrogeochemical modelling, and particularly relate this to the different filter pore sizes and methods of attributing an Eh value to the aqueous chemistry, that were described in section 5.3. This chapter concludes with a summary of the findings of the work in this and the preceding chapter.

6.1 Controls on major ion chemistry of deep mine drainage

The purpose of the discussion below is to establish the controls dominating the chemistry of waters in deep mines, as measured at their point of surface emergence. This work initially records the presence of pyrite oxidation, followed by an assessment of acidity buffering to produce the circum-neutral values observed at all the deep mine discharge locations.

6.1.1 Conceptual model of local hydrogeological conditions in the aquifers of the mines studied

An overall conceptual model of the physical hydrogeology of the Durham Coalfield published in Robins & Younger (1996) is shown in figure 3.3. This section describes the local conditions of the aquifers being drained by the sites studied in this research, as a guide to understanding their composition. As is described in section 5.1 the chemical composition of individual abandoned coal mine discharges is found to be very consistent on a maximum of 6 sampling occasions during the 2 years of study, in contrast to spoil heaps (section 6.2). No long term trend in the data is observed and short term meteorological fluctuations (such as affected the spoil discharge composition) were not reflected in the mine drainage chemistry. The other line of evidence in qualitative observations of discharge volumes is that there was no obvious variation in the height to which the flows extended, which would be expected to be evidenced in low flows by a residual coating of Fe-hydroxides on the stream bank.

There is no hydrogeological information available to this study which enables a hypothesis to be tested, however, it is suggested here that the stable chemical composition is reflecting a very stable water table (Frost, 1977). A stable water table implies that the water-rock interactions taking place do not vary due to seasonal oxidation and flushing of pyrite oxidation products when the aquifer recharges (Frost, 1977). Thus, it is suggested that the water table in the vicinity of these discharges has rebounded to a height in equilibrium with the net recharge and discharge volumes of the aquifer. The age of these discharges are not known, but they are generally thought to be at least 20 years old (P.L. Younger, University of Newcastle-Upon-Tyne, pers. comm.).

This presents a major dichotomy: if the water table is stable there should be only very minimal pyrite oxidation products emerging in the mine drainage, the degree of pyrite oxidation related to the continual supply of Fe^{3+} or O_2 into the groundwater. The drainages could be assumed to be reasonably stable in terms of their water table and chemical composition. Aldous (1987) and Frost (1977) have both shown that an exponential decline (T(1/2) = 2-5.5 years) of the Fe and SO_4 concentrations occurs in abandoned coal mines (section 2.1). If this can be assumed to be the same in the study area, the drainage may be reaching a chemical composition which will improve only very slowly, or may have reached a stable rate, governed by the aquifer properties. The aqueous concentrations of Fe and SO_4 observed and the voluminous precipitates formed at the discharge points suggest that pyrite oxidation is taking place within the aquifers, and there is no suggestion that pyrite oxidation has totally ceased due to the resumption of reducing conditions, as suggested by Frost (1977) (section 2.2.2).

6.1.2 Major ion chemistry

The major ion chemistry, pH and Eh of the waters was described in section 5.2. The major ion composition of the waters leads to them being broadly classified as Ca-Mg-SO_4 types (with or without the inclusion of Fe in the calculation (figures 5.2 and 5.4)). The anion composition shows a wider scatter than that of the cations (figure 5.2); the drainage at EY being most SO_4 dominated, that at BB being most HCO_3 dominated (figure 5.2b). The drainage at SH shows the highest Cl component of all the deep mine discharge concentrations (figure 5.2), which may be attributable to the nearby roads (figure 3.4) causing recharge to be high in Na and Cl from rock salt applied on roads in freezing conditions. The concentration of Na and Cl is moderate in comparison with that found at QH (figure 5.3).

The chemical composition of waters predicted from simple pyrite oxidation would suggest Fe and SO_4 in high concentrations, and a low pH (section 5.1). The data for the deep mine sites shows (figure 5.5) that BB has a low concentration of Fe, Ca and SO_4 relative to the other sites, whilst that at EY is highest. SH, however, has a different compositional pattern. It can be seen that the concentration of Fe is close to that of EY, whilst the concentrations of SO_4 and Ca were close to those of BB. Figure 5.5 shows the high degree of temporal consistency of the aqueous chemistry throughout the period of study and that there is a variation in chemistry between sites, which is greater than that within a site, but that even the inter-site variation for the deep mines is less than the intra-site variation at the spoil heaps. These data are summarised (from data used in figure 5.5, table 5.3 and data in appendix IV) as mean values in table 6.1 for convenience for BB, EY and SH. These sites have been selected for further discussion. The reasons for this are: the greater frequency of analyses obtained than at LL and TC, the possibility of dilution of the deep drainage at LL by spoil heap drainage, and at TC dilution by run-off from surrounding industrial works (section 3.4).

Table 6.1: Summary of mean chemical composition of discharge at BB, EY and SH.

Site	*SO_4* mg l^{-1}	*Ca* mg l^{-1}	*HCO_3* mg l^{-1}	*pH*	*Li* µg l^{-1}	*Sr* µg l^{-1}	*Ba* µg l^{-1}	*Al* µg l^{-1}
BB	227	121	459	6.6	183	1114	19	27
EY	889	251	174	5.9	100	586	10	45
SH	326	100	178	6.1	96	215	14	66

Site	*Mn* µg l^{-1}	*Fe* µg l^{-1}	*Co* µg l^{-1}	*Ni* µg l^{-1}	*Cu* µg l^{-1}	*Zn* µg l^{-1}	*Si* mg l^{-1}
BB	1871	1945	8.0	9.4	0.55	0.62	4.5
EY	3315	26350	30.0	47.6	2.22	38.23	10.3
SH	1981	31243	18.7	35.7	1.64	38.70	9.3

This data is a summary of that shown in figures 5.4 & 5.6 and table 5.3. The equivalent molar concentrations for selected ions can be found in table 6.2 (Fe & SO_4) and 6.3 (Ca & HCO_3).

The data in table 6.1 shows that the sites exhibit a differing chemistry relative to each other. The composition of BB has the highest pH and concentrations of Ba, Sr, Li and HCO_3, EY and SH tend to have the highest concentrations of Fe, Co, Ni, Cu, Zn and SO_4, which are all ions associated with pyrite oxidation (section 2.3.1). The concentration of these ions is higher at EY than SH, but both show a distinct difference to BB; they also have a higher Si concentration than BB. The lower concentrations of ions associated with products of pyrite oxidation and the higher pH value of BB suggests that the concentration of pyrite may be lower in the aquifer of BB than EY and SH. The other possibility is that the fluctuations in the water table which do occur are greater at

EY than SH and that those two sites have a much greater (in relative terms) fluctuation than BB. The other noticeable feature of the chemistry of BB is that the concentration of ions such as Ba and Sr are relatively much higher than at EY and SH, this may suggest a Coal Measure brine component in the discharge as these ions are frequently elevated in the older coal measure waters (section 3.3.4). Another factor which may relate to the reactive processes taking place in the respective aquifers of BB, EY and SH is the Si concentration. The concentration at BB (4.5 mg l^{-1}) is suggested by Haines & Lloyd (1985) to be typical of reasonably young waters, but that the increasing concentrations of Si can be related to reactions taking place. The maximum concentration recorded in UK aquifers by those workers was 30 mg l^{-1} Si (Haines & Lloyd, 1985), suggesting that a concentration of ~10 mg l^{-1} at EY and SH represents a significant increase with respect to the value at BB. This may support the evidence from the pyrite associated ions (above) that there is more pyrite oxidation taking place at EY and SH. The concentration of Si being 1 mg l^{-1} higher at EY than SH (table 6.1) could be diagnostic of more pyrite oxidation in the aquifer at EY than at SH, as is implied by the pyrite associated ions in the mine drainage (above). The concentrations of ions at LL and TC (table 5.3 and appendix IV), would suggest that TC is closest in behaviour to BB, and that LL is closer to SH and EY in its chemical characteristics.

The DO concentrations at BB, EY and SH show that they contain <1 mg l^{-1} DO at the point of discharge, which classes them as poorly oxidising (at the boundary of the oxic (>10^{-6} M l^{-1}) and anoxic (<10^{-6} M l^{-1}) classification of Berner (1981)). These waters are also not SO_4 reducing because <5 mg l^{-1} HS^- was present at any site (section 4.4.3.1f), and total SO_4 was high (table 6.1). This redox status is confirmed by the presence of Fe, almost entirely as Fe^{II} (>90%) where measured. The use of Eh values to quantify the redox status for the purposes of hydrogeochemical modelling is given in section 6.4.

The nature of waters arising from pyrite oxidation was reviewed in section 2.1. From that review it could be seen that the major chemical disturbance to the waters could be expected to be a lowering of pH and increased Fe and SO_4, but that this is not necessarily the case for coal mine drainage in Britain (table 2.1). The data here is summarised in figure 6.1 as a comparison with the data published by the NRA (1994a) for the South Wales coalfield. It can be seen that the Fe and SO_4 concentrations fall exactly into the field observed in South Wales. This suggests that whatever processes are controlling the chemistry of mine water in the Durham Coalfield may be the same as those occurring in other British Coalfields. The data obtained in this study (e.g. table 6.1) also correlates very well with that obtained for the Durham Coalfield by Younger

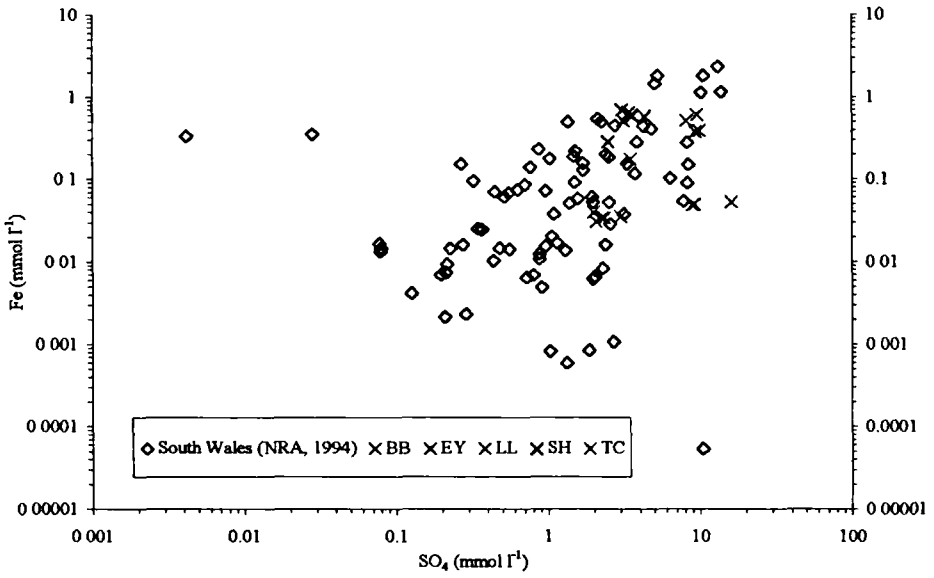


Figure 6.1: Comparison of Fe and SO_4 concentrations measured in this study with abandoned mine drainage in the South Wales coalfield. The discharge sites in this study are shown as crosses, compared to the diamonds representing the data of NRA (1994a).

and co-workers and summarised in Younger (1995b). In a wider context, the degree of hydrological and geological variations between coalfields will affect interpretations. The mineralogy of the aquifer, particularly in terms of the most reactive components such as sulphides and carbonates (Nordstrom & Munoz, 1994), is likely to be the controlling influence, as well as time from initial discharge (section 2.1).

The data discussed above, will be used in a series of simple inverse modelling exercises, to study the reactions taking place in the aquifer, as well as can be achieved in the absence of aquifer mineralogical information. The sites BB, EY and SH have been subject to the greatest study, and are thus most appropriate for interpretation, as there is more confidence in their consistency than there is for LL (overlain by a spoil heap) and TC (adjacent to an industrial estate, and a drainage site in which diesel has been observed).

6.1.3 Pyrite oxidation

The process of pyrite oxidation is reviewed in section 2.2, the stoichiometry of the reactions is well established. These reactions are shown in equations 2.1 and 2.4, below.

$$FeS_{2(s)} + \frac{7}{2}O_{2(aq)} + H_2O_{(l)} \longrightarrow Fe^{2+}_{(aq)} + 2SO^{2-}_{4(aq)} + 2H^{+}_{(aq)}$$

Eq. 2.1: Oxidation of pyrite by O_2

$$FeS_{2(s)} + 14Fe^{3+}_{(aq)} + 8H_2O \longrightarrow 15Fe^{2+}_{(aq)}\ 2SO^{2}_{4(aq)} + 16H^{+}_{(aq)}$$

Eq. 2.4: Oxidation of pyrite by Fe^{3+}

Equations 2.1 & 2.4 from Stumm & Morgan (1996)

These reactions show that whilst the overall reaction is incongruent, if the reactions do not proceed to Fe^{II} oxidation, then they should be congruent. Thus it may be reasonable to investigate the molar ratios of the ions generated, to see if they conform to the stoichiometric relationships shown by equations 2.1 and 2.4. This process is used here as a very simple inverse modelling approach to understanding which processes may have been taking place.

It can be seen that the oxidation of pyrite by oxygen (equation 2.1) yields a ratio of Fe^{2+}:SO_4^{2-}:H^+ of 1:2:2, and that the oxidation of pyrite by Fe^{3+} (equation 2.4) yields a ratio of Fe^{2+}:SO_4^{2-}:H^+ of 1:0.13:1.07. These are the ratios of these ions which would be expected in solution after the oxidation of pyrite by each reaction, assuming no Fe^{II} oxidation and Fe^{III} hydrolysis are taking place. Thus the ratios of these ions can be used to study whether the observed concentrations correspond to their expected relative yields. This calculation assumes that the concentration of one ion (at least) has been conservative in solution since pyrite oxidation took place. Due to the high solubility of Fe sulphates (section 2.2.1) the concentration of Fe^{II} was chosen as the conservative ion for initial calculation. This very simplistic approach assumes that the concentrations are related only to the process of pyrite oxidation, that no addition or removal of the ions studied takes place and that pyrite oxidation is the dominant source of Fe, SO_4 and H^+. Evidently these are very broad and simplistic assumptions. An assumption which is harder realistically to assess is that the processes affecting the reactants at the different localities are the same. This cannot be assessed by any mechanism other than the chemical data as there is no information on the local hydrogeology or aquifer mineralogy (section 3.2), which can lead to circular arguments about the processes occurring. It is thus taken as an assumption here that the processes affecting each discharge are identical. The concentration of Fe at the discharge point was assumed to be entirely Fe^{II} and measurements of the Fe redox couple at EY and SH in July 97 would suggest that this is not an unreasonable assumption, and is an insignificant source of error in comparison with the other assumptions.

The results of this initial simple modelling are summarised in table 6.2. The table shows the concentrations of Fe and SO_4 and the pH values recorded in the field. These figures are the mean of the data acquired for each site. The modelling of SO_4 and pH marked "a" assumed that the measured Fe represented a conservative concentration at discharge originating entirely from pyrite oxidation, and the reaction path was by $O_{2(aq)}$ oxidation of pyrite (stoichiometry as equation 2.1), the concentrations marked "b" assumed the reaction path was by Fe^{3+} pyrite oxidation alone (stoichiometry as equation 2.4) to model SO_4 and pH.

A comparison of the measured and predicted SO_4 concentrations and pH values (table 6.2) shows that the modelling results are lower than those actually measured for all sites using either model scenario (in the case of pH). The lower concentration of SO_4 predicted reflects that the Fe:SO_4 molar ratio is <1 when measured, showing a SO_4 excess in solution in relation to pyrite oxidation. If the circumstance of Fe^{II} being conservative in solution is true, this suggests a SO_4 source other than pyrite oxidation is needed and it should contribute at least 10x the SO_4 from pyrite oxidation in all cases. Whilst brines may contribute (section 3.3.4) this does not appear the case at SH and EY and not a major source at BB (section 6.1.2). SH lies at the western edge of the coalfield, which suggests it would be in the recharge (rather than discharge) zone of the aquifer, and other brine associated ions would also be expected to be elevated (section 3.3.4). The trace elements show (table 6.1) that EY and SH have higher concentrations than BB of the elements associated with pyrite oxidation (section 2.3). The pH which would be predicted from such pyrite oxidation is consistently shown to be lower than that recorded in the field. This suggests that buffering reactions must be taking place, if the assumptions given above are correct.

The large "excess" of SO_4, using the molar ratio Fe:SO_4, suggests that it may be incorrect to assume that Fe is conservative and that Fe^{II} loss from solution should be considered. The next calculation assumed the conservative behaviour of SO_4 instead of Fe^{II}. The Fe^{II} concentrations and pH values marked "c" and "d" were modelled assuming conservative SO_4 with Fe^{II} and H^+ being generated solely by pyrite oxidation via $O_{2(aq)}$ and Fe^{3+} respectively (equations 2.1 and 2.4). These concentrations, as would be expected from the information already provided, suggest that Fe^{II} is lost from solution and that the pH has been buffered from the modelled values of ~1.0 - 2.5 up to the measured pH of ~6.0. This represents the loss of sufficient H^+ to reduce its concentration in solution from 10^{-1} M l^{-1} H^+, down to the measured concentration of ~10^{-6} M l^{-1} H^+.

Table 6.2: Modelling of pyrite oxidation using measured deep mine drainage data.

Site	Fe	SO_4	pH	SO_4^a	pH^a	SO_4^b	pH^b	$Fe(II)^c$	pH^c	$Fe(II)^d$	pH^d	$Fe:SO_4$
	meas. ($mM\ l^{-1}$)	meas. ($mM\ l^{-1}$)	meas.	*C* ($mM\ l^{-1}$)	*C*	*C* ($mM\ l^{-1}$)	*C*	*C* ($mM\ l^{-1}$)	*C*	*C* ($mM\ l^{-1}$)	*C*	meas. Molar ratio
BB	0.03	2.4	6.6	0.06	4.2	0.004	4.5	1.2	2.6	18	1.7	0.02
EY	0.47	9.3	5.9	0.94	3.0	0.063	4.2	4.7	2.0	70	1.1	0.05
SH	0.56	3.4	6.1	1.12	3.0	0.075	4.1	1.7	2.5	43	1.6	0.16

Calculated parameters are denoted by "*C*", measured values / concentrations are denoted by "meas.". Measured data are the mean values of parameters for BB (n=5), EY (n=4) & SH (n=7). Sulphate and pH are calculated using the concentration of Fe for values "a" and "b"; the Fe(II) and pH are calculated using the concentration of SO_4 for values "c" and "d". The calculated values "a" & "c" are using equation 2.1; the values "b" & "d" utilise equation 2.4. The stoichiometric molar ratio's for $Fe:SO_4$ are 0.5 for equation 2.1 and 0.13 for equation 2.4. Full descriptions in text.

Table 6.3: Modelling of acidity buffering reactions in deep mine drainage.

Site	Ca	$H^{+\,(1)}$	$H^{+\,d}$	Ca^d	$Ca:SO_4$	Siderite SI	Gypsum SI	Ca:Fe	Alkalinity
	meas. ($mM\ l^{-1}$)	*C* ($mM\ l^{-1}$)	*C* ($mM\ l^{-1}$)	*C* ($mM\ l^{-1}$)	meas.	*C*	*C*	meas. Molar ratio	meas. ($mM\ l^{-1}$)
BB	3.01	3.01	19.2	19.2	1.29	-0.6	-1.2	87	7.53
EY	6.27	6.27	74.4	74.4	0.68	-0.8	-0.5	14	2.83
SH	2.49	2.49	27	27	0.75	-0.3	-1.1	5	2.93

The reaction is assumed to be calcite dissolution according to reaction 2.5 Calculated parameters are denoted by "*C*", measured values / concentrations are denoted by "meas.". Measured data are the mean values of parameters for BB (n=5), EY (n=4) & SH (n=7). The calculated $H^{+\,(1)}$ is generated by the measured Ca concentration. The calculated Ca^d concentration uses the predicted H^+ of condition "d" in table 6.2. Gypsum and siderite saturation indices (SI) are calculated by PHREEQ-C (WATEQ-4F database). Full descriptions in text.

In assessing the feasibility of these reactions assessing which is the more likely pyrite oxidation pathway is important. The reaction below pH of 4 is dominated by the Fe^{3+} oxidation pathway for kinetic reasons (Nordstrom, 1982a; section 2.2). The pH in the local environment of the pyrite cannot be determined within this study, which may have an effect on the chemical composition not reflected in the overall aqueous composition (Nordstrom & Southam, 1997). However, it will be assumed that the generation of H^+ by pyrite oxidation is sufficient to elevate H^+ to concentrations $>10^{-4}$ M l^{-1} in the local environment, suggesting that Fe^{3+} oxidation will be prevalent, although work by Moses *et al.* (1987) has suggested that Fe^{3+} can be the dominant oxidation pathway, even at circum-neutral pH, when Fe^{III} activity is lowest (Cornell & Schwertmann, 1996) (section 2.2.1). The H^+ generated by these reactions, is assumed to undergo buffering, as indicated by the modelling results. However, conservative behaviour has been assumed for Fe and SO_4 in these models. The Fe^{II}-SO_4 salts are very soluble and generally form as efflorescence on surfaces (Alpers *et al.*, 1994a; section 2.2.1b), which would not be predicted as a sink for these ions in the stable water table environment invoked for these localities. The other point of note is that the $Fe^{II}SO_4$ salts are generally found with an Fe:SO_4 molar ratio of 1, the hydration state being the variable between compounds (Alpers *et al.*, 1994a) (section 2.2.1b). Thus precipitation of these minerals would not affect the Fe:SO_4 measured were it the only reactive loss. This leaves the possibility that either one or both ions are being affected by precipitation of other mineral phase(s). This suggests that the Fe and / or SO_4 could be lost from solution due to reaction with ions, which may be the products of dissolution or buffering reactions. One such reaction is the buffering of H^+ by $CaCO_3$ (referred to henceforth as calcite, ignoring polymorphs for these purposes). This reaction is shown in equation 2.5, and can be seen to generate Ca^{2+} and HCO_3^- in solution. This argument will be developed further below.

6.1.4 Buffering of water chemistry

Pyrite oxidation in this aquifer is not generating the acidity at the point of discharge which may be expected (section 6.1.1), from the comparison of either Fe or SO_4 (SO_4 > Fe) concentrations and H^+ concentrations. This suggests that there is a buffering of the aqueous pH by interaction with aquifer minerals. To achieve a pH 6-7, a probable buffering mineral would appear to be calcite (section 2.2.2). Thus the potential for calcite to be the source of buffering will be assessed using a very simplistic approach, similar to that used above for pyrite oxidation (above).

The saturation indices (SI) of gypsum ($CaSO_4.2H_2O$) and siderite ($FeCO_3$) have been studied, due to their potential to precipitate SO_4 and Fe^{II} from the aqueous phase in acid

mine drainage environments (section 2.2.2). It can be seen from the values given in table 6.3 (mean SI values quoted) that the waters are all in equilibrium with siderite and are marginally undersaturated with respect to gypsum, apart from EY which is in equilibrium with gypsum. The concentrations of Ca and SO_4 are highest at EY (figure 5.5 & tables 6.2 & 6.3), accounting for the equilibrium with gypsum. The SI for both BB and EY shows an ion activity product (IAP - section 2.2.2b) which is 10x lower than the solubility product (K_{sp}) and thus are assumed to be slightly undersaturated. The accuracy of this prediction will depend upon the measurement errors and the errors in the thermodynamic data used for modelling (section 4.6), this is acknowledged as a source of uncertainty in this work. If the solutions are saturated with siderite and / or gypsum this implies a source of Ca^{2+} and CO_3^{2-} in the waters. The dissolution of calcite would provide both these ions (equation 2.5), and would affect pH in the aquifer (section 2.2.2). The precipitation of gypsum will drive more of the calcite into solution, due to the principles of equilibrium and cause an increase in pH. This reaction removes Ca^{2+} from solution, which would cause the pH to increase as more HCO_3^- is formed from calcite dissolution (equation 2.5). The dissolution of siderite is, however, a reaction which provides no net buffering if it goes to completion, precipitating Fe^{III} hydrous oxide (equation 2.8), but will consume acidity until Fe^{II} is oxidised (equation 2.9), and is thus thought to contribute to acid neutralisation (Morrison *et al.*, 1990; section 2.2.2). It should be noted though, that a buffering reaction by calcite, possibly with siderite, does not explain the SO_4 excess found in these waters.

To investigate whether the Ca in solution could be derived from calcite dissolution simple inverse modelling of the reactions has been undertaken, using the measured concentration of one ion as was done above for simple pyrite oxidation modelling. Table 6.3 shows the moles of H^+ which would be consumed by the dissolution of calcite, were all the Ca in solution the result of this process. This shows that up to 3 mM l^{-1} of H^+ could have been consumed to generate the Ca measured in solution. However, as has already been discussed, the Ca concentrations could be limited in the waters by the SO_4 concentrations, subsequent to calcite dissolution. Thus, taking the modelling of pH using SO_4 as the conservative ion and Fe^{3+} as the pyrite oxidant, the concentration of Ca which this would have generated in solution is shown in table 6.3. It can be seen that this concentration is considerably higher than that measured, and would certainly lead to the net precipitation of gypsum (if the phase is not already in dynamic equilibrium), given the SI already calculated for these waters is just undersaturated (table 6.3). It is also of interest to note that at BB the low concentrations of Fe and SO_4 (relative to EY and SH), mean that the $Ca:SO_4$ molar ratio is >1 (table 6.3), this suggests that if gypsum

precipitation is taking place in the aquifer, the Ca is limiting the SO_4 solubility, rather than vice versa as would be the case at the other sites. The Ca:Fe molar ratio is much greater at BB than observed at the other sites, and this site has a much higher alkalinity that the other two sites (table 6.3), which are of comparable concentrations. However, if siderite is precipitating in the mine, with gypsum this becomes more complex.

The composition of the deep mine waters is dominated by Ca and Mg as the cations (section 6.1.2), which suggests that buffering of the acid generated by pyrite oxidation could be taking place (e.g. Bethke, 1996), but the simple reactive processes used above, cannot explain all of the variations. The dissolution of calcite by H^+ (generated from pyrite oxidation) will lead to the increased concentration of Ca^{2+} and HCO_3^- in the aquifer, and could account for the high concentrations of other carbonate associated ions, such as Mg (appendix IV). Where the pH is <~4, the alkalinity would be expected to occur as $H_2CO_{2(aq)}$, rather than as HCO_3^- (section 2.2.2). The precipitation of siderite will, however, lead to the regeneration of H^+ from the HCO_3^- ion, if the pH is sufficiently high. The precipitation of minerals in the aquifer, nor the concentration of calcite, have been determined as part of this study, and thus it is not known whether there is some other factor, which has not been accounted for. Certainly, the reaction paths discussed above would not seem to be able to generate sufficient buffering of pH to produce the circum-neutral pH observed for the concentration of either Fe^{II} or SO_4 measured in solution. Whether this is due to a large Fe^{II} source from siderite buffering of acidity (equation 2.9) or some other mechanism, cannot be assessed here. The absence of detectable sulphide in the mine drainage waters (section 4.3.1f), and the high concentrations of SO_4 measured (table 6.1) suggest that SO_4 reduction (Younger,1997a; equation 2.10) as an acidity removal mechanism is not influential.

6.1.5 Precipitation of ochre from mine drainage

The chemistry and mineralogy of the precipitates at the mine discharge sites was described in section 5.15. The composition of the precipitates are dominated by Fe, with concentrations of 45% (BB, LL), 47% (EY) and 48% (SH) Fe (see appendix IV for data). The only exception is TC where there is an average concentration of 36% Fe. Whilst these values dominate the chemistry of the precipitate, they are not as high as the Fe percentage in the formula composition of ferrihydrite (58% Fe) and goethite (63% Fe). The concentrations of these phases represent an increasing Fe percentage as crystallinity increases and goethite is de-hydrated relative to ferrihydrite. Thus the explanation given here for the lower percentage Fe found in the samples at the deep mine sites than in the theoretical mineral composition, is that there is higher hydration of

the freshly precipitated phases, than in the accepted pure phase formula. An additional decrease in the concentration of Fe may be caused by dilution with detrital matter, such as plant debris (see discussion of ochre core material, below) and silicates washed into the ochre from the surrounding soil profile. Detrital silicates in the ochres are suggested by the presence of K (0.02 - 0.07%) in the precipitate (see also figure 5.10). It would be impossible to collect natural material without the presence of detrital material.

Mineralogical analysis of selected samples from these discharge sites has shown a reasonably uniform nature. The samples from BB (figure 5.8), EY and SH (figure 5.11) show an admixture of goethite and ferrihydrite (figures 5.7, 5.11 & 5.12 respectively). There is a large amorphous background which may be due to amorphous Fe precipitate and / or microcrystalline precipitate, which is expected from the rapid oxidation of Fe^{II} at circum-neutral pH (section 2.2.5b). Whilst aqueous Fe^{II} may be expected to be dominated by Fe^{2+}, the higher concentration of $FeHCO_3^+$ at BB (table 5.1) may help to control the precipitated phase, as this species is thought to promote the precipitation of goethite (Cornell & Schwertmann, 1996). The concentration of $FeSO_4^o$ was equally high for EY and SH (table 5.1), but any effect on the precipitation kinetics of ions other than $FeHCO_3^+$ has not been recorded in the literature surveyed for this thesis. Table 5.1 also shows that the speciation of Fe^{III} is dominated by hydroxy- species, which may be expected to polymerise to form ferrihydrite precipitates. The presence of *Gallionella sp.* (tentative identification) at EY and SH (plate 5.2) may also provide some small enhancement in the rate of precipitation of ochre (section 2.2.3), thus favouring ferrihydrite over goethite further still (section 2.2.5b) because the catalytic effect of bacteria does not control the mineral precipitated (Nordstrom & Southam, 1997). The spheroids found in association with the *Gallionella sp.* (plate 5.2) are very similar to those published by Ranville *et al.* (1988) and Schwertmann & Taylor (1989), where ferrihydrite was observed precipitating.

Sufficient depth of ochre had accumulated at EY and SH to allow short cores to be collected (section 5.1.5 & plates 5.3 & 5.4). The reason for the thick accumulation of material at these sites must be due to, firstly the higher concentration of dissolved Fe at these sites than at BB (table 6.1); secondly, the fact that both drainages occur in the hillslope above the main stream course (e.g. plate 5.3 for EY) means that they flow as a shallow stream over the top of the river bank for some 10m before entering the stream. This appears to aid the accumulation of the ochre. It is not known whether the ochre is still accumulating at these sites, or whether an equilibrium height has been obtained between the erosional capacity of the water draining from the mine, and the rate of ochre

precipitation. This facet was not quantified in this study. These cores (plate 5.3 & 5.4) show a chemistry dominated by Fe as would be expected (figure 5.10a & c). The analyses of these cores showed the Fe concentrations in both to be >40% until the lowest 10cm of both, where a grey clay was encountered, forming the base of the deposit. The occurrence of this is also picked out by the increasing concentration of K (figure 5.10a & c). The fact that none of the deposits is pure ochre is shown by the vegetation debris throughout the length of the core (plates 5.3b & 5.4b) (shown most clearly in plate 5.4b, but present in both) and the presence of silicate matter, demonstrated by the occurrence of K throughout the length of the core.

The downcore mineralogy at the two sites (figure 5.11) does not show a transition to a completely crystalline material within the total depth of material (~30cm for both cores at the points of sampling). The transition of poorly crystalline and micro-crystalline Fe-oxyhydroxides to a more crystalline phase with ageing is well recorded (section 2.2.5a), and would be expected downcore. The reason why the core precipitates have not become more crystalline is not known. It may be that the rotting vegetation increases the dissolved organic matter which hinders greater crystallinity, or the presence of inorganic ions which may perform the same function (Cornell & Schwertmann, 1996). The age of these precipitates is not known, but presumed to be as old (and undisturbed) as the discharge, i.e. estimated as ~15 years (section 3.4). Thus differing chemical composition of trace elements downcore could suggest either a change in the discharge chemistry or remobilisation due to crystal ageing (which would be expected to release sorbed materials as the crystal structure becomes more ordered). Which of these is the cause could not be delineated in this study.

Figure 5.10b shows the concentrations of 3 selected minor ions in the core from EY, the same ions are shown for the SH core in figure 5.10d. The concentrations of Ni, Co and Mn can be seen to decrease through the ochreous part of the core at EY, with only Ni showing an increase in concentration in the basal (clay) sample. The converse is true at SH, with all the ions showing an increase in concentration ~10cm downcore. This concentration is then maintained into the clay fraction. The decrease in concentrations at EY may be explained either by crystallisation of the Fe precipitate (which expelled the ions into the pore fluid from sorption surface sites) or that the concentration of these ions has increased through the time of deposition of the core. The large decrease in concentration of Co and Mn in the clay fraction, compared with the ochre fraction suggests that these ions are largely associated with the precipitated minerals rather than a transported detrital fraction. There is little evidence of a large percentage of the

precipitated matter ageing to a more crystalline form, however, if the initial crystallisation is micro-crystalline this would tend to show with a large amorphous background. The differing behaviour of the two cores would suggest that at least one of them may have been being affected by changes in discharge chemistry. The abrupt change in the concentration of Mn and Co (and Ni to a lesser extent) suggests that a change in water composition may have taken place. In the absence of corroborating evidence, this cannot be taken any further. This work is not easy to interpret, and does not show the simple depth decline in concentration which was found by Sperring (1995) and predicted by Ford *et al.* (1997) for ageing ochre deposits.

6.1.6 Deep mine drainage summary

The chemistry of deep mine drainage has been shown to be consistent in varying hydrological conditions. This has been attributed to the stability of the water table on a local scale; however, this cannot be substantiated in the absence of borehole measurements. It is taken as the most likely scenario in the light of published data of a similar nature, and has been used as a working conceptual model of hydrogeological conditions in these uncontrolled, abandoned deep mine drainages.

The composition of the waters is compared with that predicted from simplistic stoichiometric modelling of pyrite oxidation. This has shown that the observed Fe and SO_4 concentrations cannot be accounted for by conservative transport of pyrite oxidation products to the point of discharge. The data for all three sites (BB, EY and SH) where this modelling was undertaken, shows an excess of SO_4, relative to Fe^{II}. This implies that either there is a source of SO_4 which has a great enough concentration to dominate the chemical composition over the inputs due to pyrite oxidation, or that there is reactive loss of Fe^{II}. Study of the SI of siderite and gypsum suggests that the waters are at equilibrium with siderite, and marginally undersaturated with respect to gypsum. Thus, siderite precipitation is invoked as the removal mechanism of Fe^{II} most likely to be occurring, with the possibility that some SO_4 is lost via gypsum precipitation. The source of Ca^{2+} and CO_3^{2-} for the gypsum and siderite formation, respectively, could be calcite dissolution as a response to H^+ generation from pyrite oxidation. Both calcite and siderite are suggested to contribute to the acidity buffering mechanism, because Fe^{II} is not oxidised (section 2.2.2), and thus the siderite dissolution is acid consuming (equation 2.9). The plausibility of these mechanisms cannot be assessed without confirmation by textural analysis of (saturated zone) aquifer material or experimental study of the aquifer material. Thus it is accepted that calcite, and possibly siderite, buffering of the acidity produced is probably taking place, but the simple modelling undertaken here could not

account for all the reactions taking place, and would have benefited from corroborating evidence from the aquifer mineralogy. The similarity of the composition of the waters here to other coal mine drainage in Britain, suggests that Carboniferous Coal Measures of Britain may contain sufficient carbonate, in relation to pyrite, to neutralise the acid production of pyrite oxidation.

6.2 Spoil heap discharge geochemistry

The aim of this section is to discuss the chemistry of the spoil heap discharge water in the context of the reactions controlling the chemistry, up to the point of emergence. The discussion will highlight those processes which lead to the differing composition with respect to the deep mine drainage.

6.2.1 Pyrite oxidation & buffering of pH

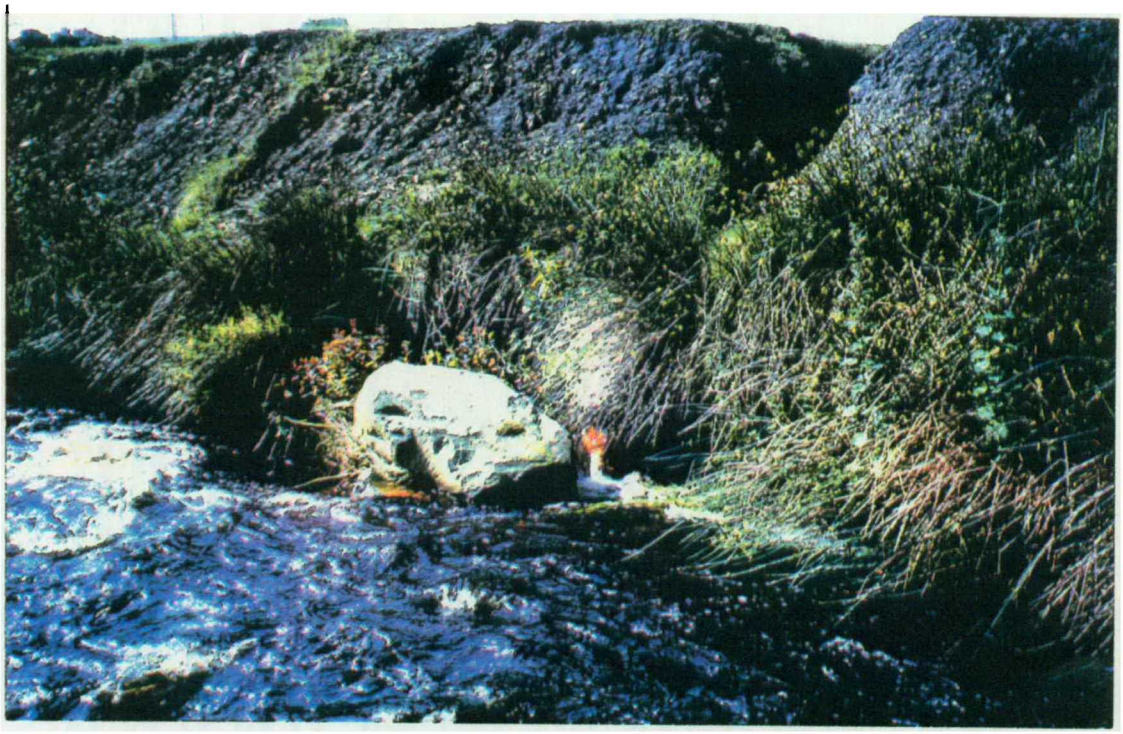
Spoil heap drainage is characterised by a wide temporal variations in chemistry, demonstrated when the sites were repeatedly sampled on 6 occasions over 2 years. This discussion will focus largely on the chemistry of Helmington Row (HR) and Quaking Houses (QH), because there is far more information for these sites than Willington (WG), which was not characterised as well as the others.

The discharge volumes were briefly reviewed in a qualitative sense in section 6.2.1, and it was noted that each site had the lowest discharge recorded in July 95 and the highest recorded in November 95, and that these affected the points of discharge (plate 5.5). The reason for these rapidly changing discharge volumes is suggested here to be due to the high permeability and porosity of the spoil heap as an aquifer (suggested not quantified). This is aided by the poor soil covering found on all of the spoil heaps, an example of which is shown clearly in plate 6.1.This demonstrates the poor soil coverage, typical of that which was also observed at HR and QH.

The major ions plotted on figure 5.2 show a mixing trend at QH, from high to low Na+K and Cl, the highest concentrations of these ions being found in November 95 and the lowest in July 95. These are thought to be controlled by recharge to the aquifer by runoff from roads, containing road salt used in sub-zero temperatures to keep roads ice free (Younger *et al.*, 1997). Helmington Row and WG show a similar mixing trend of major ion composition, but at those sites it is more controlled by changing SO_4 concentrations, with the lowest concentrations being found in November 95 (figure 5.5). As stated above, November 95 drainage was associated with the highest discharge volumes at all

Plate 6.1: Low Lands spoil heap and mine drainage. (a) view of the sparsely vegetated landscaped abandoned spoil heap. The land in the plate is used for sheep and cattle grazing. The spoil lies to the south bank of the river Gaunless (b) the mine discharge into the river Gaunless, the volumes of the discharge is too small in relation to the river to have a noticeable effect. The erosion of the banks of the river (spoil material) should also noted.





spoil heap sites (e.g. plate 5.5b) and it is suggested that discharge chemistry at this time was influenced by dilution of waters which have reacted with pyrite. It is not possible to assess the degree of dilution, because neither the relative volumes nor end-member compositions are known in this study. The effects of dilution have previously been observed in studies of mine drainage to affect the downstream dispersion of elements (Chapman *et al.*, 1983; Nordstrom, 1985).

The concentrations of selected majors ions (Fe, SO_4 and Ca) and pH shown in figure 5.5 demonstrate that the variations in spoil heap drainages are greater for HR and QH than they are between the different mine drainage sites. The concentrations of Fe and SO_4 can be seen to vary by ~10x in figure 5.5. As discussed above, the triangular diagrams (figure 5.12) suggest that this may be due to dilution of water containing the products of pyrite oxidation by unmodified recharge water in times of high precipitation, as evidenced by the changing proportion of SO_4 observed. Other evidence is the proportion of suspended material which has been observed draining from QH during periods of relatively high flow after heavy rainfall. This is not clear on figure 5.6b, but is supported by the data shown in figure 5.15 for the concentrations of K and Al carried out as particulate matter from the spoil heaps, which are used as a proxy for silicate minerals. The samples collected at HR for the determination of Fe^{II} and Fe_t would appear to suggest that more Fe is in the form Fe^{III} (2.4 mg l^{-1}) than was the case for the deep mine drainage, and that the recharge of the aquifer by precipitation brings oxidising water into the water table, however, more data is required for confirmation of this.

The pH of the system will be also be affected by the degree of pyrite oxidation, as this is the process expected to dominate H^+ generation in a pyritiferous aquifer. The reason for the November 95 sites having a generally higher pH is postulated here to be due to dilution, by rainfall, of aquifer water affected by pyrite oxidation. This is suggested as the dominant reason for the low pH being found in July 95 at HR and QH (figure 5.5). The reasons behind this may be more complicated though, because on all other occasions dilution was recorded yet a low (<5) pH was observed. The other factor which may affect the pH is whether the aquifer is being recharged or in recession. This is suggested because a low pH has been observed as a result of the flushing of pyrite oxidation products by a rising water table through an oxidised zone (section 2.1). The information which would delineate this was not available to this study, and thus this discussion cannot be developed any further here.

The variations in concentration of the major ions was described in section 5.2.2, and has been introduced in relation to figure 5.5 above. Figure 6.2 shows a comparison of the measured molar concentrations at HR and QH of Fe and SO_4 with the expected ratios from pyrite oxidation due to $O_{2(aq)}$ and Fe^{3+} oxidation pathways (equations 2.1 & 2.4). These data are plotted individually, because a mean value (as used in table 6.1 for mine drainage), would not be representative of a dataset with an unknown frequency distribution and a maximum of only 6 data points over 2 years. What the data do consistently show is that there is an excess of SO_4, as compared to Fe, which would be expected from pyrite oxidation (as was shown for deep mine drainage in this study and NRA (1994a) data (figure 6.1)).

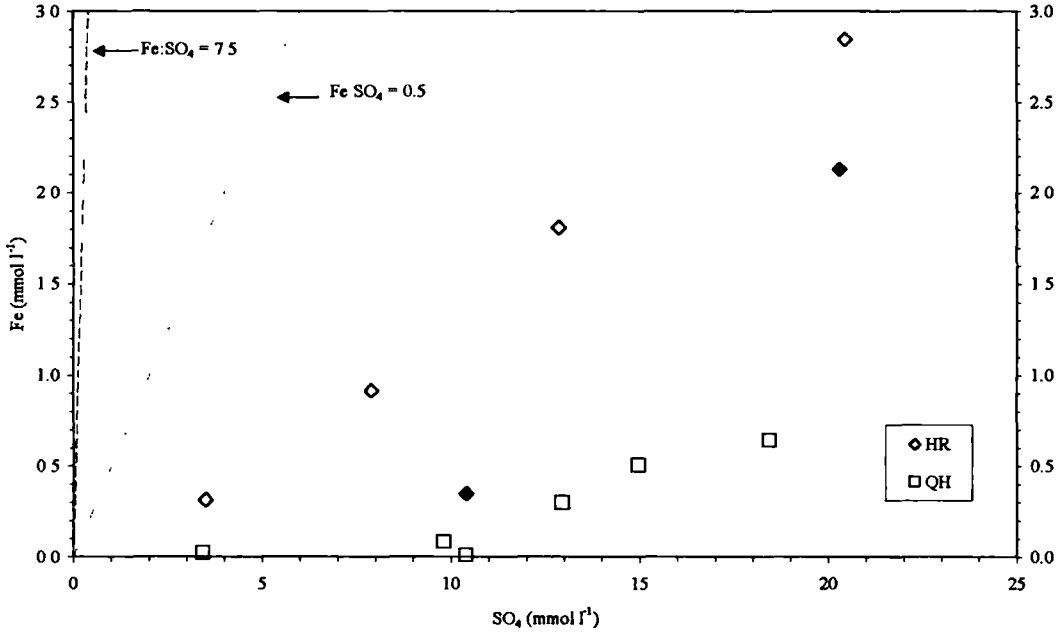


Figure 6.2: Comparison of spoil heap Fe and SO_4 with theoretical ratios from pyrite oxidation reactions. The dark points for HR represent one trend discussed in text; the open points the alternative trend discussed. See text for explanation of $Fe:SO_4$ ratios.

However, the distribution of data does not appear to be a random scatter. Whilst there is very little data (thus enabling limited conclusions only) the data for HR would tentatively suggest that there are two lines with the same slope as the theoretical lines (figure 6.2). The slope of these lines is similar at 0.15 and 0.18 respectively. These data are largely separated by the predicted axis intersection position. Whether these represent two waters with an initially different SO_4 concentration cannot be deduced from such

limited data; a larger dataset may show these to be scatter, rather than having two different trends. However, what is of interest from this data-set is the suggestion that the Fe:SO_4 ratio actually lies along a line fitted by a ratio of ~0.15-0.18, rather than 0.5 (O_2 oxidation) or 7.5 (Fe^{III} oxidation pathway). The data for QH show an even lower ratio of ~0.07 (figure 6.2). The reason for this is not known.

The reason for the data falling along lines of high - low Fe and SO_4 concentrations is attributed to dilution of waters which contain pyrite oxidation products with those rapidly flowing through the aquifer after precipitation events. The diluting water will contain lower concentrations of Fe, SO_4 and H^+. It can be seen on figure 6.2 that the line extends from the highest concentrations (low flow) via intermediate flow conditions to the lowest concentrations (high flow). As stated above, the trend of changing concentrations of ions in the differing hydrological conditions, is repeated for H^+ as observed for Fe and SO_4, but there is not a simple relationship between the H^+ and Fe concentrations, as was observed for SO_4 and Fe.

Simple inverse modelling of the Fe, SO_4 and H^+ concentrations of the water predicted by Fe and SO_4 measured concentrations (analogous to that of deep mine waters in section 6.1.2) also shows that the pH predicted, by both mechanisms and measured ion concentrations, is lower than that measured (see section 6.1.3 for assumptions). Selected data from this exercise is shown in table 6.3. The concentrations of Fe and SO_4 predicted obviously relate to the measured concentration used and the reaction pathway, as described in section 6.1.2. Thus buffering of the pH is taking place within this aquifer. Using the data generated by PHREEQ-C, the solutions are again shown to be close to equilibrium with gypsum (as was shown for mine waters (table 6.3)). This would suggest a control on the concentration of Ca by SO_4 (the molar concentrations of SO_4 are always Ca.

Thus it is shown that pH buffering is taking place in this aquifer. The low pH reached by the aquifer, in July 95 (pH 3.5) suggests that buffering by $CaCO_3$ is not taking place (circum-neutral pH expected). The higher pH values recorded for these sites (high flow conditions) have been attributed to the process of simple dilution of waters, which have been modified by the presence of oxidising pyrite, by rapid infiltration of precipitation. Thus the calcite buffering exercise used in section 6.1.4 has not been undertaken here, and it is tentatively suggested that the $CaCO_3$ buffering capacity of the aquifer which may have existed previously has been exhausted. Buffering of pH to a value of ~3-4 suggests that silicate minerals may be responsible. However, these reaction are more

complex kinetically (Nordstrom & Munoz, 1994) and with respect to knowing the products of incongruent dissolution (e.g. equation 2.11), as well as a lack of knowledge of the minerals present. The occurrence of alumino-silicate buffering of aqueous pH in the aquifer, when the pH is ~4, is supported by the elevated Al concentrations at these sites (e.g. ~100 mg l^{-1} at HR (figure 5.7)) in July 95), and the high concentrations of Si (with respect to mine drainage), when dilution by recent rainfall was zero within the aquifer. The concentrations of Si were not measured very frequently (appendix IV) but the results for May 95 and October 96 are 16-20 mg l^{-1} for HR and QH, with only HR in July 97 showing a lower value of 9.6. Whilst insufficient data exists to test this hypothesis, it would seem reasonable that if Al is being weathered from silicates by acid dissolution, then Si concentrations may also be expected to be higher (Haines & Lloyd, 1985), indicating more intense weathering of silicates by more acid waters within spoil heaps in County Durham than occurs in the abandoned coal mines.

6.2.2 Mineralogy of precipitates

At the spoil heap discharge sites studied the precipitation of ochre in the stream bed at the discharge site was observed, but never with an accumulation of a large volume of ochreous precipitate, such as was observed at some deep mine drainage sites (e.g. at EY and SH (plates 5.3 & 5.4)). The discharge site at QH can be seen not to precipitate a large volume of ochre, even in moderate flow conditions (plate 5.5a) and thus was not described in section 5.2.5. However, sufficient precipitate formed in the discharge pipe of HR (plate 5.6b) to allow sampling and analysis.

The changing water chemistry at HR (sections 5.2.2 and 5.2.3) suggests that the composition of the precipitate also would be expected to change. Visual inspection of the precipitates forming (plates 5.6c & d) shows that this is the case.

The precipitate formed in July 97 (figure 5.16b) shows a composition with a large proportion of ferrihydrite, with detrital quartz and some goethite. The chemistry of the waters, pH~6, and SO_4 < 500 mg l^{-1}, would predict the precipitation of ferrihydrite, followed by ageing to goethite. The chemical composition of this precipitate was shown in table 5.5, and was of low concentrations of Fe (16%), S (2.6%), Al (9%) and Ca of 3.6%. It is possible that the Ca and S are associated in the precipitate as gypsum, but the concentration of this would be too low to be detectable using XRD (<~2-5%). The phase of the Al is not known, Al-SO_4 phases are not predicted in such low SO_4 concentrations, the Al may be substituted into the Fe precipitate, as a hydroxide phase precursor

(Nordstrom, 1982a) or as detrital silicate minerals (Si was not determined in these samples).

The precipitate sampled in July 95 shows a ferrihydrite dominated sample, with a large amorphous background. The sharply defined peaks on the pattern are tentatively identified as gypsum (section 5.2.5). The chemical composition of that sample is shown in table 5.5, and contains >1% Ca by weight. This sample is also elevated in Fe, Al and S. Conversion of the composition shown in table 5.5 to molar units shows that there is 272 mmol kg^{-1} Ca and 1110 mmol kg^{-1} S in the precipitate. If all the Ca is assumed to exist as gypsum ($CaSO_4.2H_2O$), this suggests that there is ~270 mmol kg^{-1} of gypsum, and that there is an excess of 840 mmol kg^{-1} of S. When this "excess" S is compared to the Al concentration (1560 mmol kg^{-1}), this gives a molar ratio of Al:S = 1.9. This ratio does not correspond exactly to any of the Al-SO_4 phases which may form in such environments (Nordstrom, 1982a); alunite has a ratio of 1.5 and basaluminite a ratio of 4. The precipitation of basaluminite has been found to produce a very poorly crystalline phase initially, and is kinetically favoured over the thermodynamically predicted alunite (Nordstrom, 1982a; section 2.3.2). It is thus suggested here that basaluminte is the more likely phase in which the Al-SO_4 is precipitating, and that the low ratio found, with respect to that of basaluminte, can be reasonably explained by the assumption that all S is precipitated as SO_4, when it may also be sorbed.

Schwertmannite has not been positively identified at this site, although the aqueous chemistry (pH ~3.5 and SO_4 > 1000 mg l^{-1}) is within the range of chemical conditions conducive to the precipitation of this metastable phase (Bigham, 1994). Study of the Fe:S ratio in this precipitate shows that there is insufficient SO_4 to form both an Al-SO_4 phase and schwertmannite, to the exclusion of ferrihydrite, particularly given the tentative identification of gypsum on figure 5.16. This mineral is described by Bigham (1994) as being a "bright yellow colour", and the precipitate at HR was certainly a more yellow colour on this occasion than other sampling occasions. What is not noted by Bigham (1994), or the other publications in this suite of research (section 2.2.5c), is the relative importance of ferrihydrite and schwertmannite on the colour of the precipitate (c.f.. the importance of trace haematite on the colour of a goethite dominated Fe phase in soils (Schwertmann & Taylor, 1989)). It is possible that the two phases (ferrihydrite and schwertmannite) are existing in an admixture (Bigham *et al.*, 1996a), caused either by the simultaneous precipitation of both phases, or by changes in the water chemistry causing schwertmannite to be actively precipitating from the water, but the ferrihydrite to be a "remnant" of precipitation from a less acid and lower SO_4 concentration water. It

is not stated by any of the research on schwertmannite, whether a decrease in pH and increase in SO_4 inputs to a system precipitating ferrihydrite, cause the ferrihydrite to convert to schwertmannite or remains stable. Although Turner (1994) states that jarosite may be precipitating at this site, and is subsequently quoted by Younger (1995b), there has been no evidence of jarosite precipitation found by XRD analysis, and the chemical composition of the waters was never noted to be extreme enough to precipitate a mineral of this group (section 2.2.5d). This is not to preclude the possibility, because jarosite is metastable with respect to goethite if SO_4 concentrations decrease and pH increases and thus would not remain in changing aqueous conditions, but this study appeared to sample the spoil heap drainage approaching the most extreme low flow and high flow which could be expected. Younger (1995b) also suggests that the more white-yellow precipitates observed in high acidity and metal ion concentrations at HR and QH may contain gibbsite ($Al(OH)_3$), however, there is no evidence to suggest that this phase is occurring given the high SO_4 concentrations and the stability relationships described by Nordstrom (1982b) and Nordstrom & Ball (1986) (section 2.3.2). Observation of this sample using SEM did not show any evidence of *Gallionella sp.*, which are not expected under the conditions of sampling on these occasions (reference), but would find the right environment when the discharge chemistry is that of July 97 (above). However, Nordstrom & Southam (1997) note that a drainage environment which alternates on a variable basis, does not provide the ideal conditions for a stable microbiological community. The low pH oxidation of Fe^{II} is probably facilitated by *T. ferrooxidans* (section 2.2.3) in the low pH (3.5) found in July 95, but this aspect was not studied here.

6.2.3 Spoil heap discharge summary

Spoil heap drainage has been shown here to be highly variable in composition, from circum-neutral pH to pH ~3.5, which appears to vary with hydrological conditions as reflected in the drainage discharge volumes at HR and QH. This variation has been attributed to the dilution of waters chemically modified (low pH, high SO_4 and metal ion concentration) by prolonged contact with oxidising pyrite, with that of the rapidly recharging precipitation. The aquifer is postulated to buffer the pyrite oxidation products by silicate dissolution (high Al and Si concentrations observed); when there is no recharge diluting these waters a pH of 3.5 was recorded at HR, whilst a pH of 4.8 was recorded at QH. These data and the chemical composition of the waters suggest any calcite which was buffering reactions in these aquifers has been consumed and is no longer effective.

The variable discharge chemistry results in a very variable precipitate mineralogy and chemistry, which in low pH conditions at HR was found to constitute an Fe-Al-SO_4-Ca phase, thought to be an admixture of ferrihydrite-(schwertmannite)-gypsum-(basaluminte).The identifications were very tentative for schwertmannite and basaluminite, because the XRD patterns showed a large amorphous background and the samples are so highly hydrated that they decompose under the SEM beam, leaving little corroborating evidence for the conclusions drawn from the chemical data.

6.3 Minor and trace element hydrogeochemistry from mine and spoil workings

6.3.1 Effect of Eh and pH

The effect of Eh and pH on the solubility of minor and trace ions was reviewed in section 2.3, and it was shown that the solubility of Al, Mn, Zn and Cu are markedly affected by the pH and (especially for Mn) the Eh of the solution.

The concentration of Mn in deep and spoil heap drainage is shown in figure 5.7a. The concentrations can be seen to be lowest in the high discharge (November 95) waters from spoil heaps, and of a similar concentration consistently in the deep mines, of ~1 mg l^{-1}. The source of Mn in coal mine drainage waters is thought largely to be Mn containing carbonates (section 2.3.1). The concentration of Mn in mine drainage would be expected to relate to the Eh of the waters (section 2.3.3). To investigate this figure 6.3 shows the concentrations of Mn at the discharge points, on the occasions when DO was

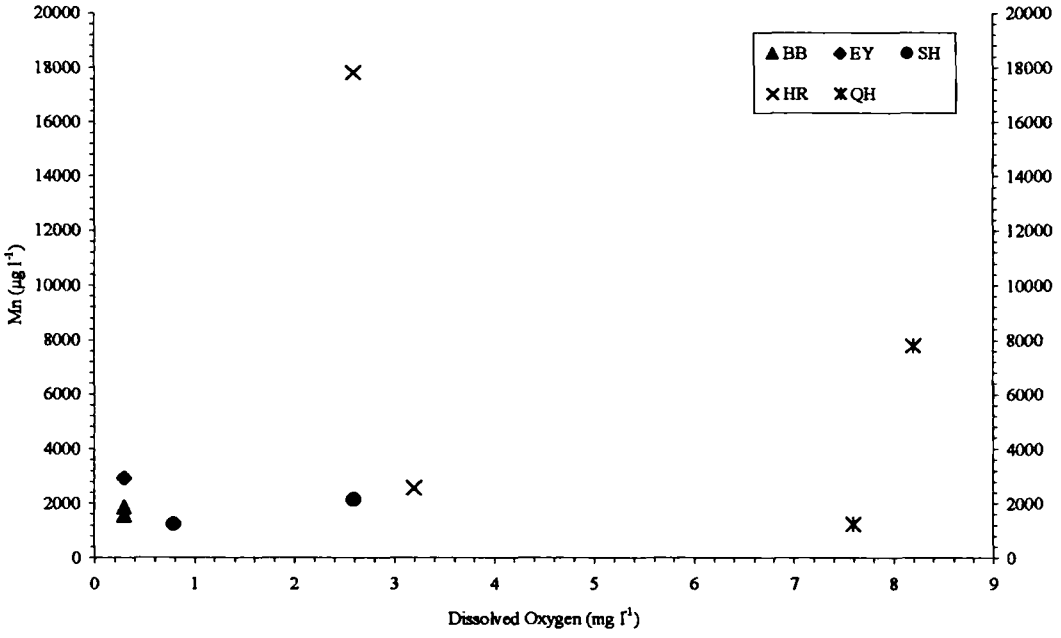


Figure 6.3: Comparison of Mn concentrations and DO concentrations in discharge from abandoned spoil heaps and coal mines

measured; it can be seen that there is no clear relationship between these two parameters, based on the limited information here, which is in accordance with the findings of Nordstrom *et al.* (1992a) (section 2.3). It is not known what the limiting factor on Mn concentrations is without more Eh_N determinations.

To study the effects of pH on the concentrations of ions, figure 5.14a compares the dissolved Al concentrations found in all the discharge samples collected with the pH recorded at those sites. It can be seen that the deep mine drainage has a consistently low concentration of Al in comparison to the spoil heaps (figure 5.7b). The concentrations of Al in the spoil heap drainages are very variable (~2 orders of magnitude) and high (generally >1 mg l^{-1}) at the discharge points. Figure 5.7b shows that in July 95 the highest concentration of Al was recorded at both HR and QH spoil discharges, and was ~100 mg l^{-1} Al in the water at HR. As had been noted in section 5.2.2, the pH recorded at these sites was lowest (3.5) at HR on this occasion. Comparison of all the concentrations in figure 5.14a, suggests that these are due to the low pH. Aluminium is much more soluble in low pH than circum-neutral pH waters, and hydrolyses to a hydroxy phase at pH~4.5 in most (low SO_4) natural waters (section 2.3.2). The source of Al in these waters is presumed to be the dissolution of silicates in the aquifer (Nordstrom & Ball, 1986), which buffer the pH to the recorded value of 3.5 on this occasion.

Determination of the chemistry and mineralogy of the solid phases precipitating at this site (section 6.2.3), suggest that an Al-SO_4 phase is precipitating, which is most likely to be basaluminite from the work of Nordstrom (1982b). The geochemical modelling of SI for the aqueous chemistry at this site also supports the idea that a Al-SO_4 phase is in equilibrium with the water (table 5.8), and thus controlling the Al as described by Nordstrom (1982b). Amorphous $Al(OH)_3$ is shown to be undersaturated, because the Al concentrations in the waters are controlled by a SO_4 phase (Nordstrom, 1982b). Whilst basaluminite is shown to have a lower saturation index than alunite (the predicted stable phase in the pH, Al and SO_4 concentrations at this site), basaluminite may occur as a kinetically favoured precursor to alunite in such waters (Nordstrom, 1982b); because the mineralogical analysis undertaken here could not determine the phase present, this cannot be developed any further. The probable occurrence of these phases will also be discussed in section 8.2.1, with respect to the downstream controls on Al concentrations at HR.

The chemistry of Cu and Zn is also strongly affected by pH, as shown on figure 5.14 the concentrations of these ions decrease with increasing pH at HR and QH spoil drainage sites. The pH of hydrolysis of Cu (~5.3) and Zn (~7) is shown in this figure. Thus the pH would be expected to play a control in the dissolution of Cu from the aquifer material, the concentration of Cu in the deep mines (table 6.1) being so low in comparison to the spoil heaps because the pH of the water is so high in comparison to the pH of hydrolysis. The high concentration of Cu (relative to the deep mines) in the spoil heaps shown in figure 5.14 is attributed to the lower pH within the spoil when the pyrite oxidises, the oxidation products being flushed out by the drainage waters. The reason for the concentrations remaining high when there is a higher pH than the pH of hydrolysis may be due to lack of equilibrium, with the rate of transport of the Cu being faster than any precipitation and sorption reactions which may take place (Broshears *et al.*, 1996). The source of Cu in these drainages is attributed to its occurrence as solid solutions within pyrite, and the presence of chalcopyrite within the aquifers (section 2.3.1). This is also the source attributed to the concentrations of Ni and Co shown in table 6.1, because these ions are strongly associated with pyrite (section 2.3.1).

The concentrations of Zn at the discharge from spoil heaps (figure 5.14b), can be seen to be between 1-10 mg l^{-1} on most sampling occasions; this is considerably higher than the concentrations of <1 μg l^{-1} (BB) and ~40 μg l^{-1} (EY and SH) found at deep mine sites (table 6.1). The source of the Zn in the aqueous phase at all of these sites is attributed both to pyrite and sphalerite (ZnS) oxidation and there may be an association with a $ZnCO_3$ phase, which has been reported for coal and associated sediments previously (section 2.3.1). The concentrations of Zn should not be affected by hydrolysis, because the pH of hydrolysis is ~7 (Levinson, 1980). It is not thought that Zn is mobilised by sulphide weathering and then re-precipitated because Zn forms extremely soluble SO_4 phases (Alpers *et al.*, 1994) and $ZnCO_3$ (smithsonite) is not predicted by modelling with PHREEQ-C (Parkhurst, 1995) to precipitate and control the Zn concentrations in the deep mine drainage. The lower concentrations are thus attributed to less pyrite oxidation taking place in the coal mines than the spoil heaps, or the concentration of Zn in sulphide phases available for weathering is lower in the deep mines. The first explanation is preferred, for reasons discussed in the preceding sections of this thesis, but neither can be proved without more information, not available here. The high concentrations in the spoil heap drainage are explained by the oxidation of Zn containing sulphides, particularly sphalerite, and the slightly lower concentrations at the higher pH values shown in figure 5.14b, may be due to the dilution of the pyrite oxidation products by precipitation recharge as described in section 6.2.1.

6.3.2 Effect of SO_4 on trace and minor ions

The activity of many ions in solution was shown to be affected by the high concentrations of SO_4 in the waters from coal mines and spoil heaps. Speciation data are shown in tables 5.1, 5.2 & 5.4 and shown in figures 5.5 & 5.11.The high concentrations of neutral species formed by divalent cations (Fe^{II}, Ca, Mg and Ba) is shown in tables 5.1, 5.2 and 5.4 for mine and spoil drainage. These can account for ~50% of the cation speciation predicted in solution by PHREEQ-C, and suggest that they may be important with regard to the mobility of these cations. Consideration of the concentration of these ions is particularly important with regard to the activity of the free cation (e.g. Ca^{2+}) in solution, which will be lower in the presence of SO_4, which will affect the degree of saturation with respect to any Ca phases modelled, because it is the free ion on which such calculations are based (e.g. Stumm, 1992). Such complexation could also affect toxicity predictions of natural waters (section 8.3).

6.4 Hydrogeochemical modelling

A brief study of the effects of two measurement variables is described in section 5.3. This work examined, firstly, the comparison of different filter pore sizes in the sampling of aqueous chemistry. Secondly, the different methods of Eh measurement on their subsequent use as quantitative, master variable inputs to hydrogeochemical modelling programs were studied.

Work carried out on both filtering effects (section 2.2.3b) and Eh measurement methods (section 2.2.3a) have already been reviewed. The filtering of waters is frequently carried out at 0.45μm for both practical reasons (the filters cost less than those of 0.1μm nominal pore size and filtering time is reduced) and because this may be the statutory definition of "dissolved" (section 2.4). This study showed little benefit was discernible, using the analytical methods employed here, between filtering at 0.1 or 0.2μm or at 0.45μm pore size (figure 5.17 and table 5.9). The element which showed the largest difference was Fe, in general (table 5.9), but in the range of concentrations studied, and taking consideration of the variability of the spoil heap discharges with hydrological conditions, this was found to be negligible. The concentration differences are suggested by a small dataset to be due entirely to Fe^{III} differences (table 5.9), which was also supported by the work undertaken on the mid-Wales orefield on the Fe^{II}/Fe^{III} method development (section 4.3.1h) (Ander & Fuge, 1997; Ander & Fuge, unpublished data). The unpublished data from this study also suggests that a higher precision method (ICP-

MS) of analysis for trace ions may show differences in concentration between 0.1 and 0.45μm filtering (Ander & Fuge, unpublished data) which has been shown in other studies (section 2.2.3b). The differences occurring in Fe^{III} concentrations would suggest that this is a source of error which would be larger in the spoil heap drainages, because these are generally more oxidising at the point of emergence than the deep mine drainage.

Eh is a master variable in geochemical modelling, and thus a value must be entered into each input file. The effect of different methods of measurement of Eh, and disequilibrium problems, have been shown previously (section 2.2.3a). A comparison was carried out in this study looking at the change in the Eh value using 3 different methods of determination, the results of which were shown in section 5.3.2. This -shows that there is a large difference between Eh measured with a Pt-electrode (Eh_m) and modelled using the O_2/H_2O couple (Eh_{DO}) and the Fe^{II}/Fe^{III} couple ($Eh_{FeII/III}$), but that the deviation from the Fe couple (which was measured chemically and therefore taken as the "correct" value benchmark) was dependant on the aqueous species of Fe under investigation. The results would certainly seem to imply an internal disequilibrium between the O_2/H_2O couple and the Fe^{II}/Fe^{III} couple, which has been shown in other studies (sections 2.2.3a and 4.6). The closer agreement of Fe^{II} predicted from Eh_m than from Eh_{DO} is shown in table 5.10, and this table also shows the closer agreement of Eh_{DO} with Fe^{III} than does the Eh_m. This results in Eh_{DO} being a better predictor of the saturation indices of Fe^{III} phases, because the calculation depends on the activity of Fe^{3+}. This is caused by the Eh of Eh_m being closer to that of $Eh_{FeII/III}$ than is Eh_{DO}, but would seem to be an anomalous situation. The cause of the deviations observed here between values, must be attributable to the overestimation of Eh by Eh_{DO} and the underestimation of Eh by Eh_m, compared to $Eh_{FeII/III}$. The difference in Eh and a calculated saturation index (for ferrihydrite) for different filtering sizes was reported by Kimball *et al.* (1992) in their study of a mine drainage impacted stream.

The results of this small study are in agreement with the body of literature which suggests that Eh should be measured directly in all appropriate cases, and that system equilibrium should never be assumed to occur, because it generally does not in pyrite oxidation systems in particular (sections 2.2.3a and 4.6).

The simple sensitivity analysis presented in section 5.3.3 shows that the method chosen to input Eh to model the data acquired in this study is far more important a variable than the filter pore size used in collecting aqueous samples. This may be a general application

but whether that is the case cannot be answered here. This study has also ignored the errors in the thermodynamic database and effects of kinetics (section 4.6), and thus the relative importance of Eh cannot be assessed, although direct measurement is generally recommended as the preferred method (section 2.2.3a).

6.5 Summary

This chapter has discussed the data acquired in the sampling of both abandoned coal mine drainage and coal spoil drainage at selected sites in County Durham. The water chemistry of deep mine drainage is thought to be controlled by the oxidation of pyrite and neutralisation of acidity by carbonate buffering reactions. The consistent chemical composition of these waters over the period of study is attributed to the stable water table of the aquifers causing a stable equilibrium of buffering and acid generating reactions to take place, which do not vary on a short term temporal scale. These waters are poorly oxidising at surface emergence with S occurring as S^{VI} and Fe occurring as Fe^{II}. The precipitation of ochre at surface due to oxidation of Fe^{II} and hydrolysis of Fe^{III} has been observed to produce a solid phase dominated by poorly crystalline ferrihydrite, which is kinetically favoured over goethite.

The water chemistry of spoil heap drainage is thought to be controlled by the processes of pyrite oxidation with subsequent buffering due to silicate dissolution. This is prevalent in low flow when the aquifer is not recharged by precipitation for a period of time. These conditions are associated with low pH and high SO_4 and metal ion concentrations. The precipitates forming from these phases are a complex mixture of minerals, which were only tentatively identified, due to their largely poorly crystalline nature. The high pH, low SO_4 and metal ion concentration in the aqueous phase were always associated with high discharge volumes, which also carried much suspended material out of the spoil heap. The recharge to the aquifer is thought to be very rapid, as the spoil heaps studied are landscaped but not remediated by clay capping or other procedure. The rapid recharge is thought to raise the pH and lower the concentration of ions in solution (derived from pyrite oxidation) by the simple mechanism of dilution of the water which has evolved chemically due to its longer residence time in the aquifer and contact with pyrite which oxidises.

The pH conditions and general degree of water-rock interaction taking place in the aquifers of mines and spoil heaps are found to strongly influence the trace element concentrations of the discharges, with ions associated with sulphides, carbonates and

silicates. The concentrations of these ions is lower in the deep mines than spoil heaps due to less pyrite oxidation taking place, and can be used to distinguish the degree of reaction taking place in deep mine drainage. The measurement of such parameters using comparative filtering sizes and Eh measurement techniques on a small number of samples supports the findings of other studies that Eh is best measured chemically rather than using a Pt-electrode meter, and a sensitivity analysis showed this parameter to be more important in determining modelling results for aqueous speciation and saturation indices than alternative filtering sizes for field sampling of natural waters.

7.0 Results of geochemistry downstream from discharge points

In this chapter the changes in chemistry observed downstream from the effluent discharges described in chapter 5 will be discussed. This chapter will focus on those variations occurring downstream from the points of emergence, the discharge location chemistries have already been described (chapter 5) and discussed (chapter 6). Three points of emergence were selected for study due to their differing characteristics and suitability. Firstly a deep mine location, Stony Heap (SH), will be discussed, where the mine water is diluted after discharge by varying volumes of receiving waters. Secondly two spoil drainage sites, Helmington Row (HR) and Quaking Houses (QH), will be discussed. These sites have a high loading of minor ions and occasionally low pH, and minimal dilution at the point of emergence.

7.1 Stony Heap

As discussed in section 5.1 this location is of an uncontrolled, abandoned deep mine discharge. The discharge can be summarised as both being of a consistent flow volume and chemical composition; circum-neutral pH, high Fe and SO_4 concentrations, with few minor / trace ions being of elevated concentrations (section 5.1). The consistent chemical composition is attributed to a stable water table, with possible carbonate buffering (section 6.1).

7.1.1 Physical characteristics

The sites selected for study are described in section 3.4. It can be seen that the mine drainage flows into a receiving stream, close to the source of the stream (figure 3.4). The flow of the receiving stream was observed to vary on a seasonal basis (much as described for the spoil heaps in section 5.2), in July 95 it was dry up to the vicinity of the mine drainage emergence. Flood conditions were observed, in the receiving stream, in November 95 as described in section 5.2. Otherwise conditions were of an "intermediate", if unquantified (section 4.3.2) nature to those extremes. In all the figures in this chapter demonstrating seasonal variations, low flow (July 95) will be shown in red, and high flow volumes (November 95) in blue.

7.1.2 Aqueous chemistry: major ions

Neither dissolved oxygen (DO) nor Fe speciation were recorded on the downstream sampling visits at SH, but Eh was routinely recorded, and not withstanding the limitations of this measurement (section 2.2.3a), the results are shown in figure 7.1. Whilst quantitative interpretation of these results is not valid, there do appear to be some

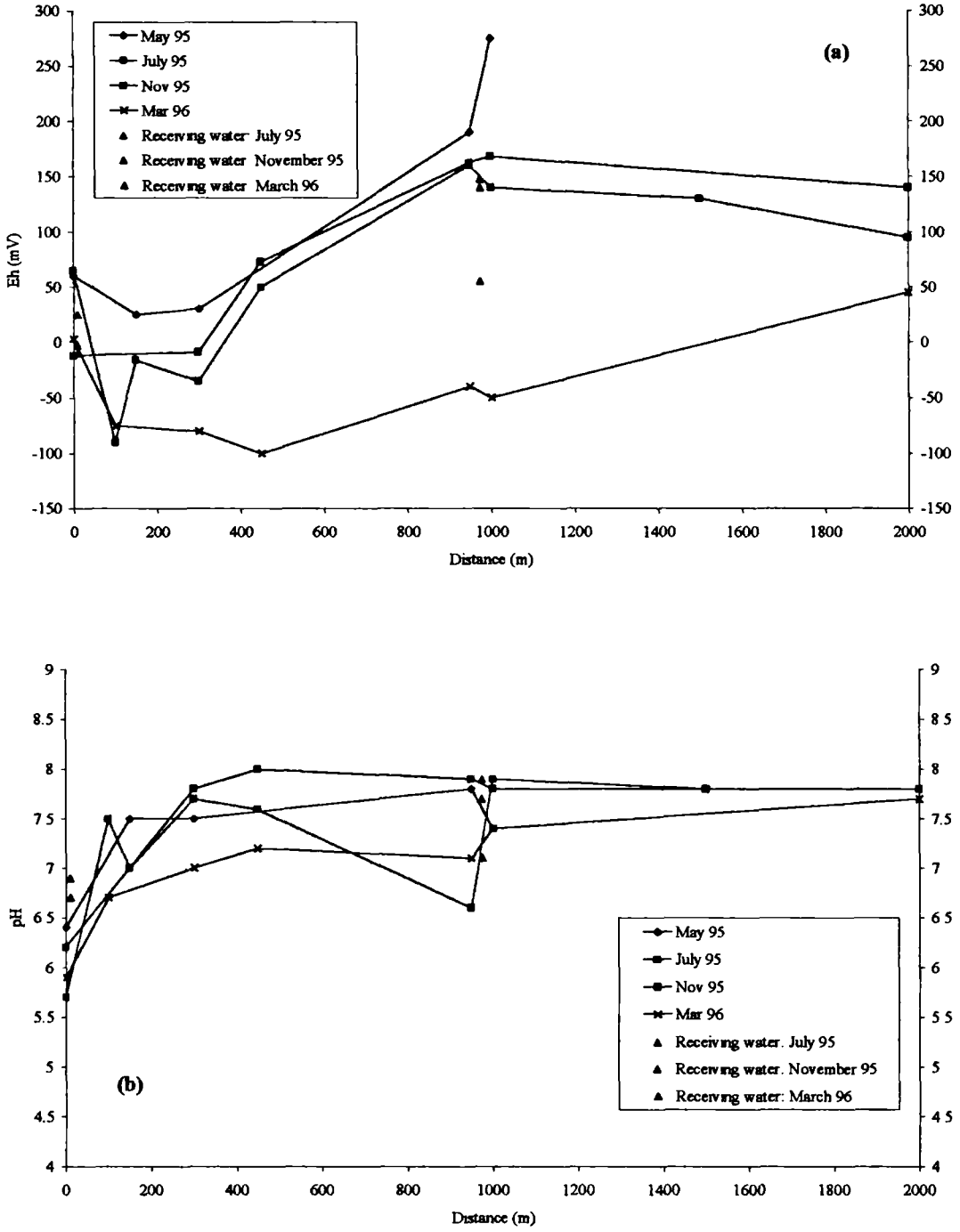


Figure 7.1: Downstream variations of selected parameters at SH. (a) Eh (b) pH. The highlighted flows are July 96 = low stream flow (red) and November 95 = highest stream flow (blue), intermediate flow conditions are shown in black. The receiving water is shown as an inflow at 10m for convenience, and a further inflow is shown at 975m.

trends which are consistent. An initial decrease in the Eh after emergence and mixing of the mine drainage with the receiving stream is evident. The readings are then characterised by an increase downstream, with March 96 appearing to take longer to rise from the more negative readings maintained after mixing. Figure 7.1a shows pH increases from 6.0 - 6.5 to ~7.0 within 150m of the point of discharge. This pH is then generally maintained, the only exception to this being the site at 950m in July 95, where the pH can be seen to decrease from 7.6 - 6.6.

The major ions are plotted on triangular diagrams on figure 7.2. It can be seen that the waters behave differently on the sampling occasions illustrated. July 95 samples can be seen to vary little downstream from their initial Ca-Mg-SO_4 type, and there is no dilution of the discharge at 10m on this occasion (figure 7.3). The receiving stream and inflow at 975m downstream can be seen to be of a very similar chemistry to each other, and with a higher proportion of HCO_3 than the mine water impacted localities. The November 95 samples (highest flow) show the effects of mixing of waters of different types downstream from the discharge. Both the receiving stream and inflow water contain a higher proportion of Cl, thus causing the water type to change from Ca-Mg-SO_4 at the point of discharge, to a Na-K-Cl water (as is the receiving stream) downstream of the discharge. A similar pattern is seen for the March 96 samples, however, the proportions of HCO_3 as well as Cl are higher than they were in November 96, and the inflowing stream at 975m is a Ca-Mg-HCO_3 water (figure 7.2). It should also be noted that on both these sampling occasions the proportion of Na+K and Cl can be seen to be higher than the receiving water after mixing than it is in either the mine drainage or receiving water.

Figure 7.3 shows the variation in concentration of selected ions downstream from the discharge. Calcium is shown in figure 7.3a. This diagram would appear to show that Ca is conservative and affected only by dilution at the initial confluence; the larger decrease in concentration in November 95 being accounted for by the larger dilution of the receiving water. On all the occasions shown here, except July 95, the concentration would appear to be relatively stable until mixing after the confluence at 975m is reached. There is little difference between the inflowing and coal mine drainage impacted stream concentrations, but in July 95 the stream shows a drop to a lower, and subsequently consistent, concentration of ~85 mg l^{-1}, this is however, only ~10 mg l^{-1} lower than upstream of the confluence. Magnesium also shows a consistency of concentration instream, like that of Ca and thus, is not shown here. Sodium has a more complicated downstream pattern than Ca. Figure 7.3b shows Na to be consistent and apparently conservative in waters at 10m and May and July 95, with only minor fluctuations caused

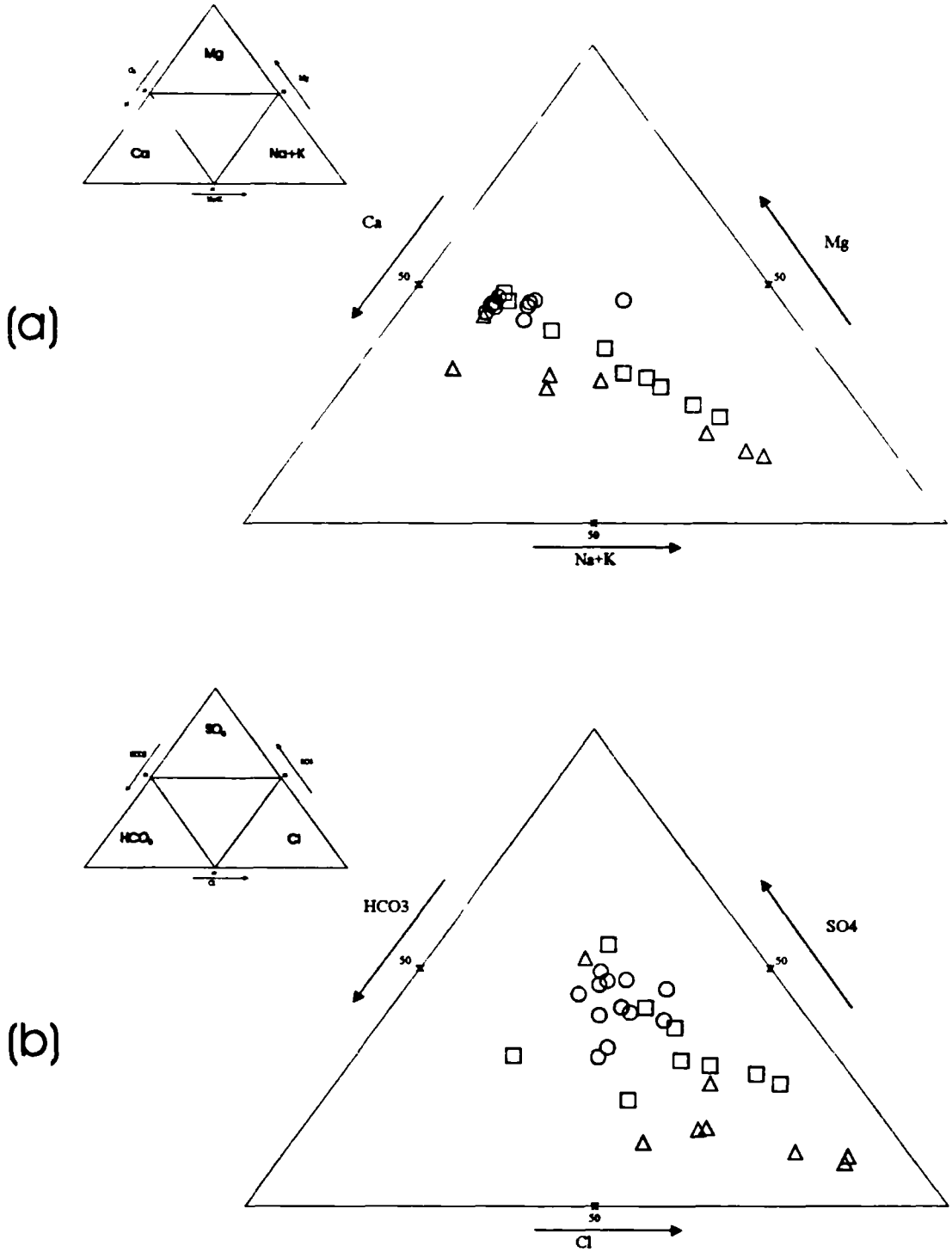


Figure 7.2: Triangular plot of major ion chemistry at SH (a) cations: Ca, Mg, Na & K (b) anions: HCO_3, SO_4 & Cl. Labelling as follows: July 95 = circles, Nov 95 = triangles & March 96 = squares. Units are %meq, with 50% marked on each axis. The occurrence of dominant ions on the diagram is described by the associated inset to each plot.

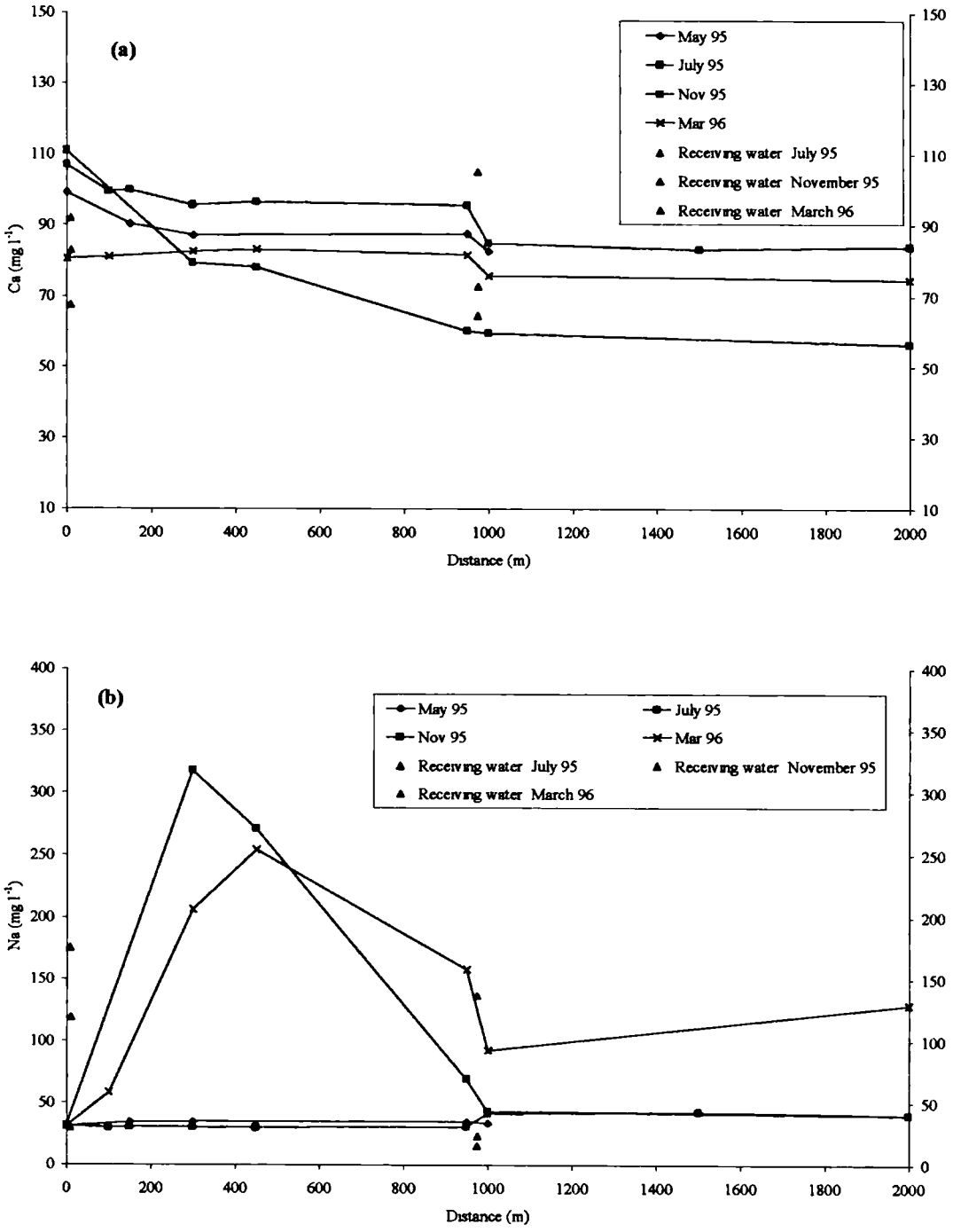


Figure 7.3: Downstream variations in selected ions. (a) Ca (b) Na (c) HCO_3 (d) Cl (e) SO_4. The highlighted flows are July 95 = low stream flow (red) and November 95 = highest stream flow (blue), intermediate flow conditions are shown in black. The receiving water is shown as an inflow at 10m for convenience, and a further inflow is shown at 975m.

(continued on next page)

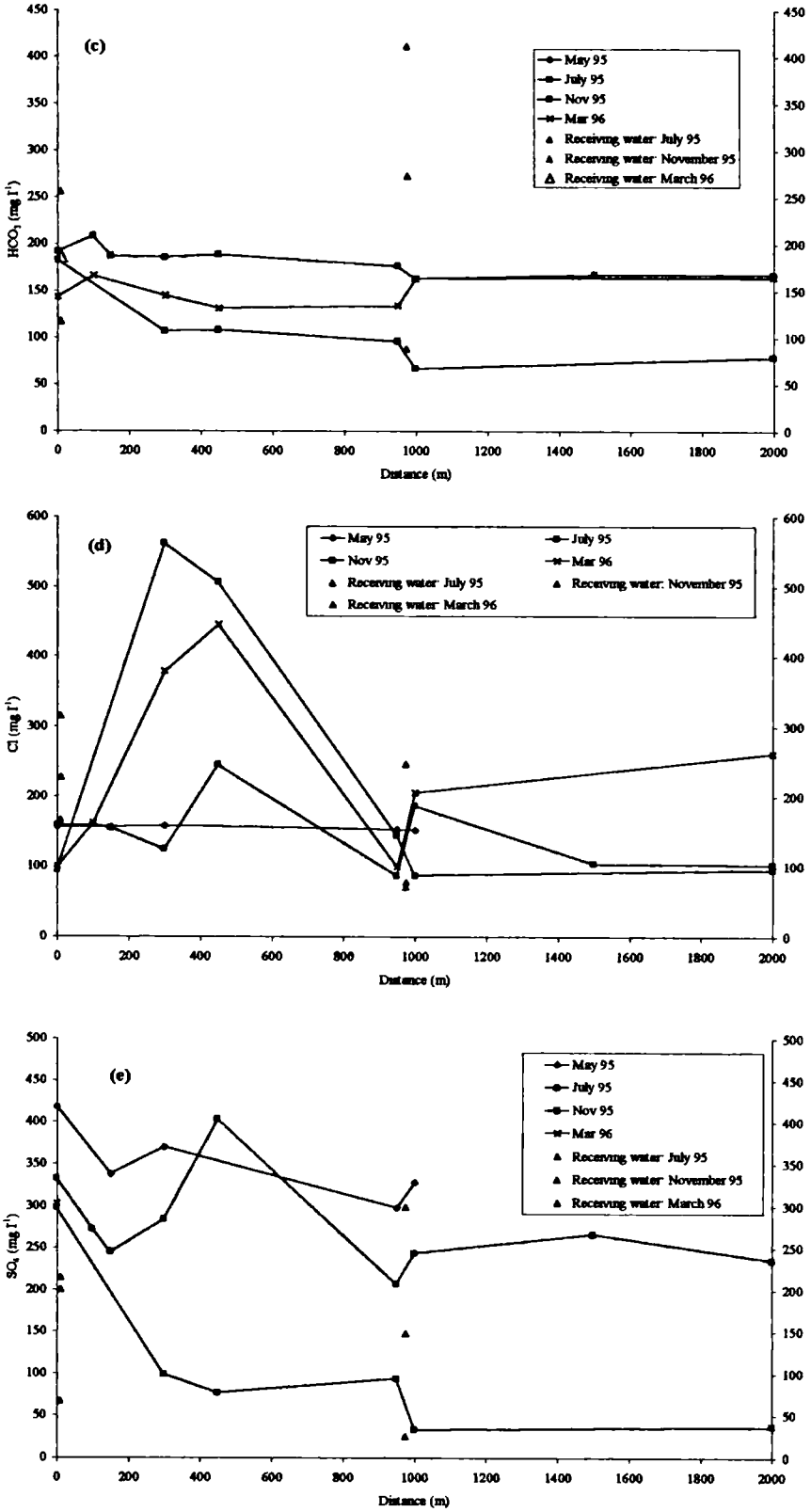


Figure 7.3: (continued from previous page)

by dilution, and little difference between the concentration in the mine drainage effluent and the receiving stream. In November 95 and March 96 it can be seen that there is a large influx of Na to the receiving water system and again further downstream, at ~300-450m, before the confluence at 975m. These peaks in concentration disappear by the confluence and upon mixing with the confluence the November 95 waters reduce to those values seen on other occasions, whilst March 96 remains at a higher concentration. The inflow at 975m can be seen to have a much higher concentration in July 95 than the main stream, but the effect was negligible as dilution by the receiving stream was large. In November 95 and March 96 the reverse was true, with the lower concentration, but higher volume, of the inflowing water being sufficient to further dilute the main stream. Potassium concentrations follow a similar pattern, and thus are not displayed here.

Figure 7.3c shows HCO_3 concentrations downstream from the deep mine drainage. It can be seen that the concentrations are stable, apart from mixing with receiving / influent 975m. The November 95 samples show this effect most, due to the larger volumes of water the main stream was mixed with at the confluence, and these samples are the only ones where the final concentration is measurably different, at <100 mg l^{-1}, in comparison to ~160 - 190 mg l^{-1} for the other sampling occasions. This figure should be compared with figure 7.3a, due to the similar behaviour of Ca and HCO_3. Figure 7.3d shows the variations in Cl downstream from the mine drainage source. May 95 samples show a very constant concentration downstream, whilst July 95 samples are somewhat more variable, although not in a systematic fashion (figure 7.3d), which is presumed to be due to the worse detection limit of the analytical method when SO_4 is high, because a greater sample dilution is required (section 4.3.1f). The November 95 and March 96 samples can be seen to follow a very similar pattern, with a much higher concentration in the receiving water than the mine discharge causing an initial rise in concentration, followed by a further rise at ~300-450m downstream, which then falls away before the confluence at 975m is reached. The water then falls close to the values for the influent stream at 975m. This figure should be compared to figure 7.3b, to highlight the similarity of this behaviour with Na. Figure 7.3e shows the variations in SO_4 downstream from the mine drainage source. All these data show an overall decrease in concentration from source downstream. May 95 samples show a consistently higher concentration than the other sampling occasions. The much higher concentrations in the mine drainage than the receiving water result in a dilution immediately upon mixing, the rate of decline of concentration from 150m until 950m is then variable for the different sampling occasions. In July the concentration increases, in November 95 and in March 96 it decreases, but in March 96 all the decrease is accommodated in the length 450-950m,

unlike November 95 when most of the decrease takes place between the initial mixing and 300m. The concentration after the confluence is largely governed by the relative volume of influent water to the stream, and the concentration of SO_4 in that water. There would appear to be some correlation between the variations observed for SO_4 with those noted for Na and Cl above.

To further examine the similarities in results described above, Na and Cl are shown in figure 7.4a. It can be seen that there appears to be consistent excess of Cl in comparison with the line of unity with Na. However, the slope of the line for concentrations >~5 mmol l^{-1} would appear to parallel the theoretical NaCl dilution line, but with a Cl intercept of ~2. The comparison of SO_4 and Cl and Na is shown in figure 7.4b & c. It can be seen that they appear to co-vary apart from in November 95 and March 96, when the increases in Cl described above are not matched by an increase in SO_4.

The variations in Fe_t downstream from the discharge point (figure 7.5a) show that the dissolved constituent decreases from ~30,000 μg l^{-1} at the point of discharge to ~1000 μg l^{-1} at 300m downstream in July 96 and November 95, whilst in March 96 it took a further 700m of stream flow for the concentration to reduce this far. The data for October 96 is less conclusive because a sample was not collected at 450m downstream. This pattern would appear to be contradictory to that intuitively predicted by the high stream flow causing rapid dilution of inflowing coal mine drainage and low dilution causing the lowest rate of loss of Fe_{aq} from the aqueous system. This can be examined further with reference to figure 7.5b. This diagram shows the behaviour of the Fe in the stream system on three contrasting field visits. The data for low flow (red) shows that there is a rapid transfer of the Fe from the dissolved to suspended phase within the first 300m, with concentrations being approximately equal in the two phases at the 150m sampling point. From this point the Fe_{aq} decreases very rapidly to an almost constant concentration of ~30-50 μg l^{-1}, and the suspended sediment load dominates as far downstream as samples were collected. In November 95 (high stream flow), it can be seen that a longer reach of stream was required before the Fe_{aq} ceased to dominate the stream Fe loading, and that the receiving stream had a lower Fe concentration, and (something which cannot be incorporated into this figure) a much higher rate of flow than July 95. It can be seen that the Fe_{ss} dominated the Fe loading from 450m downstream and continues to do so for the length of stream measured, it also has a very consistent concentration in contrast to July 95, when the concentration of Fe_{ss} fell markedly between 450m and 950m downstream. The Fe_{aq} concentration drops to a lower value than that of July 95, but the suspended, and therefore Fe_t, remains higher than

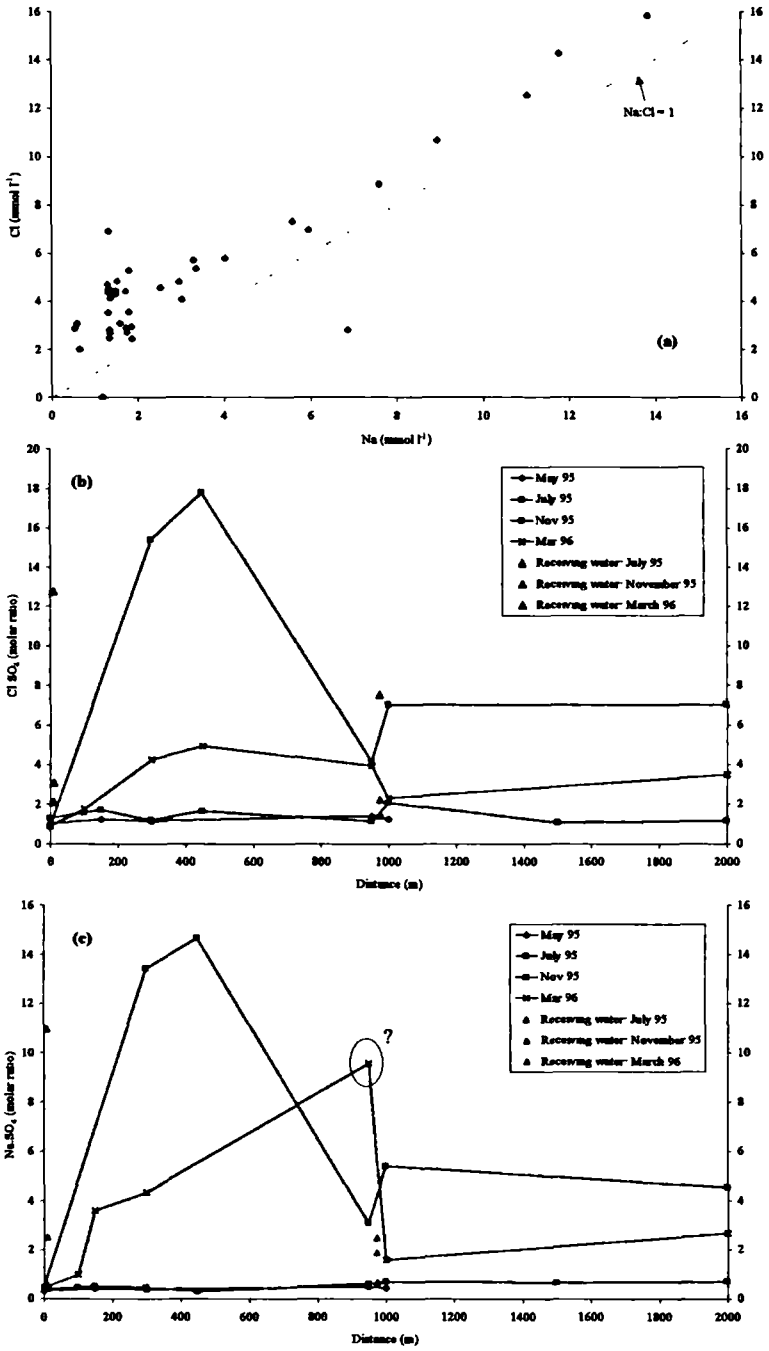


Figure 7.4: Comparison of molar concentrations or ratios at SH. (a) Na and Cl (molar values) to compare with a theoretical NaCl dilution line (shown); (b) downstream $Cl:SO_4$ (molar ratio) for different sampling occasions; (c) downstream $Na:SO_4$ (molar ratio) for different sampling occasions. Labelling for b & c as follows: highlighted flows are July 95 = low stream flow (red) and November 95 = highest stream flow (blue), intermediate flow conditions are shown in black. The receiving water is shown as an inflow at 10m for convenience, and a further inflow is shown at 975m.

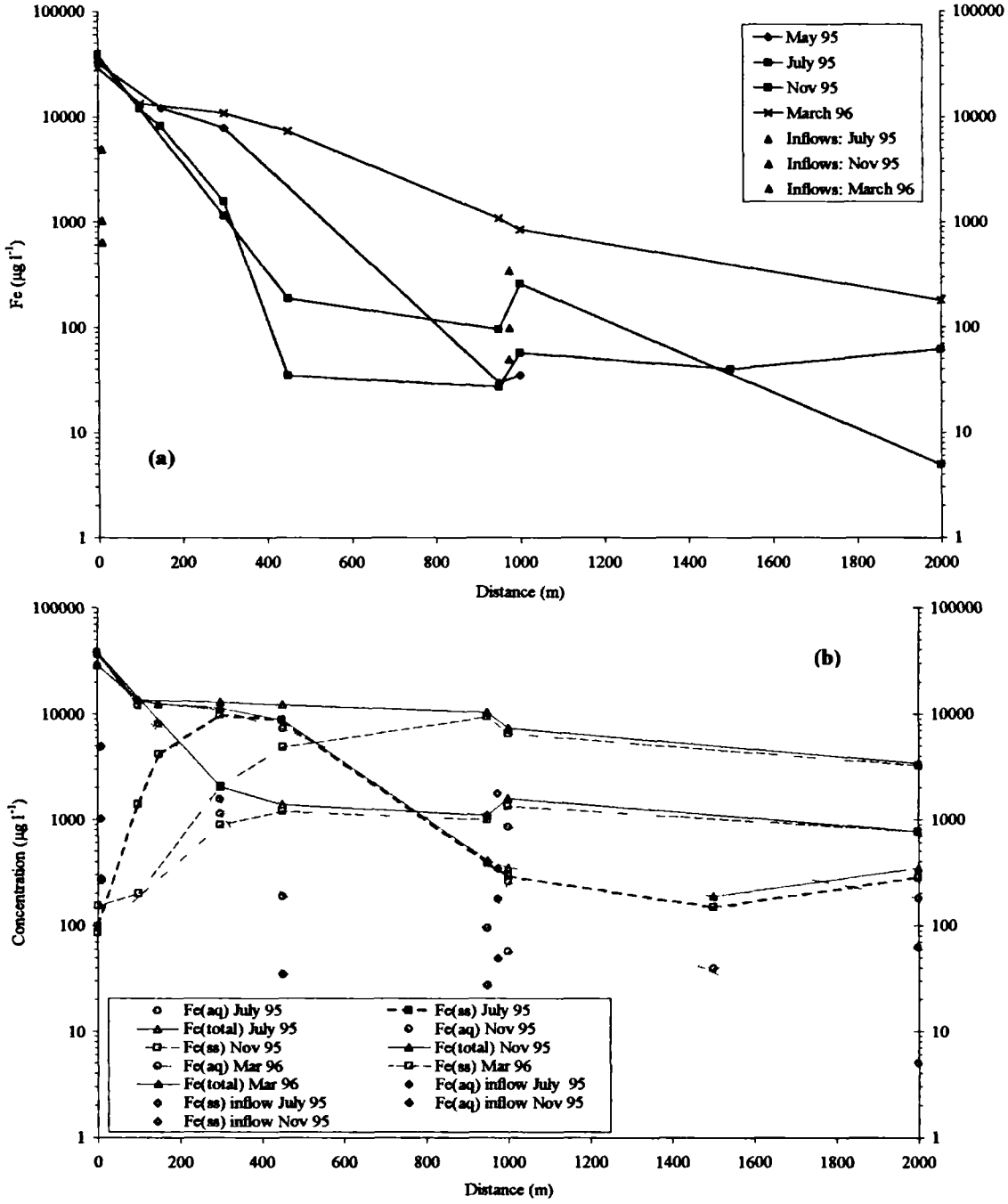


Figure 7.5: Downstream variations in Fe loading in the stream system at SH. (a) dissolved Fe variations downstream from source. The highlighted flows are July 95 = low stream flow (red) and November 95 = highest stream flow (blue), intermediate flow conditions are shown in black. (b) Comparison of Fe loading in dissolved and suspended phases. Solid lines = Fet, dotted lines = Fe_{aq} & dashed lines = Fe_{ss}. Low stream flow = July 95 (red), highest stream flow (blue), and intermediate stream flow = March 96 (grey). The receiving water is shown as an inflow at 10m for convenience, and a further inflow is shown at 975m in both figures.

July 95. In both July and November 95 it can be seen that the influent water at 975m had a minimal short term effect on the chemistry of the main stream. In March 96 (intermediate stream flow), it can be seen that the Fe_{aq} phase dominates the Fe_t for a longer length of stream than it did in the two extreme flow conditions, with Fe_{ss} not becoming the dominant control on Fe_t until 950m downstream. There was, however, little change in the Fe_t during this transition from Fe_{aq} to Fe_{ss}, this is very different to July and November 95.

7.1.3 Aqueous chemistry: minor & trace ions

Figure 7.6a shows the changes in Mn concentrations downstream from the deep mine discharge. The distance downstream at which the Mn concentrations start to decline, is noticeably further than that observed for Fe (figure 7.5). November 95 samples are the most rapid to decline, with July 95 samples having a higher rate of decrease after 450m than May 95 and March 96. On the latter sampling occasions the Mn concentration did not appreciably decrease in the length of stream studied. It can also be seen that the concentrations arising from the mine drainage are higher than those occurring in either diluting stream. Figure 7.6b shows a complete summary of the Mn loading in the aqueous system for 3 sampling occasions of contrasting hydrological conditions. Most noticeable is that, in contrast with Fe (figure 7.5b) the Mn_t is dominated by Mn_{ss} along the entire length of sampling, with the sole exception of the site 2km downstream in November 95. The Mn_{ss} increase from the point of emergence in all cases, to level off after ~300m in the case of November 95 and March 96. The Mn_{ss} in July 95, however, increases until ~450m, after which it then decreases to a value lower than the other sampling occasions It can also be seen that Mn_{aq} dominates over Mn_{ss} in the convergent streams.

The concentrations of most trace ions are not notable in comparison with the spoil heap drainage observed in this study (section 5.1), many being close to detection limit at the point of discharge, so little information is discernible on their controls in waters downstream from the discharge point. Zinc is an element which can be observed to decline from source, as shown in figure 7.7a. It can be seen that although the concentrations do not differ over an order of magnitude as is the case for Fe, the concentration does follow a decline from source to values <10 $\mu g\ l^{-1}$ (*i.e.* approximately 10x detection limit and thus the lower limit of measurable fluctuation). It can be seen that the decline in concentration would appear to be most rapid in July 95. Since it is not

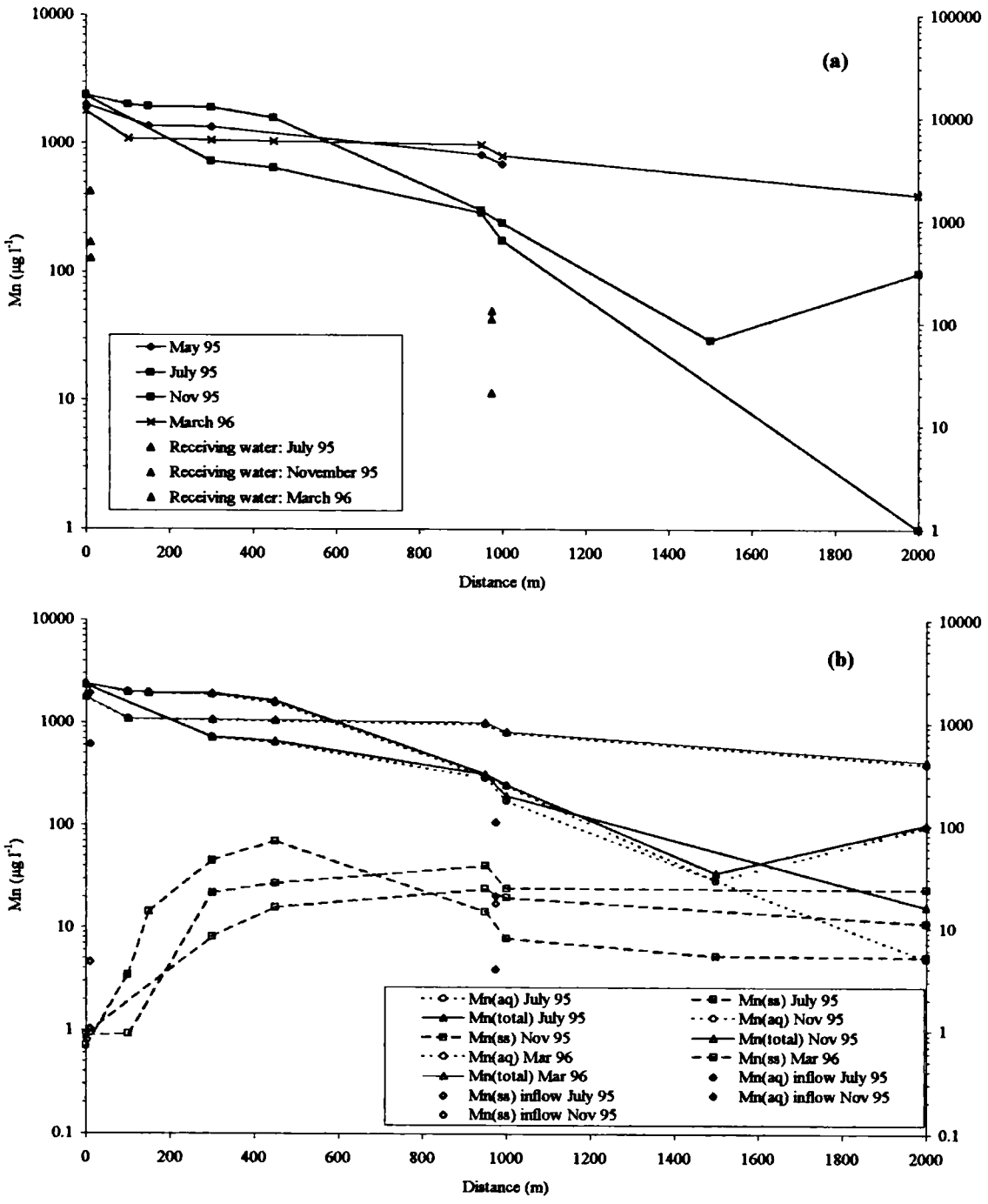


Figure 7.6: Downstream variations in Mn loading in the stream system at SH. (a) dissolved Mn variations downstream from source. The highlighted flows are July 95 = low stream flow (red) and November 95 = highest stream flow (blue), intermediate flow conditions are shown in black. (b) Comparison of Mn loading in dissolved and suspended phases. Solid lines = Mn_t, dotted lines = Mn_{aq} & dashed lines = Mn_{ss}. Low stream flow = July 95 (red), highest stream flow (blue), and intermediate stream flow = March 96 (grey). The receiving water is shown as an inflow at 10m for convenience, and a further inflow is shown at 975m in both figures.

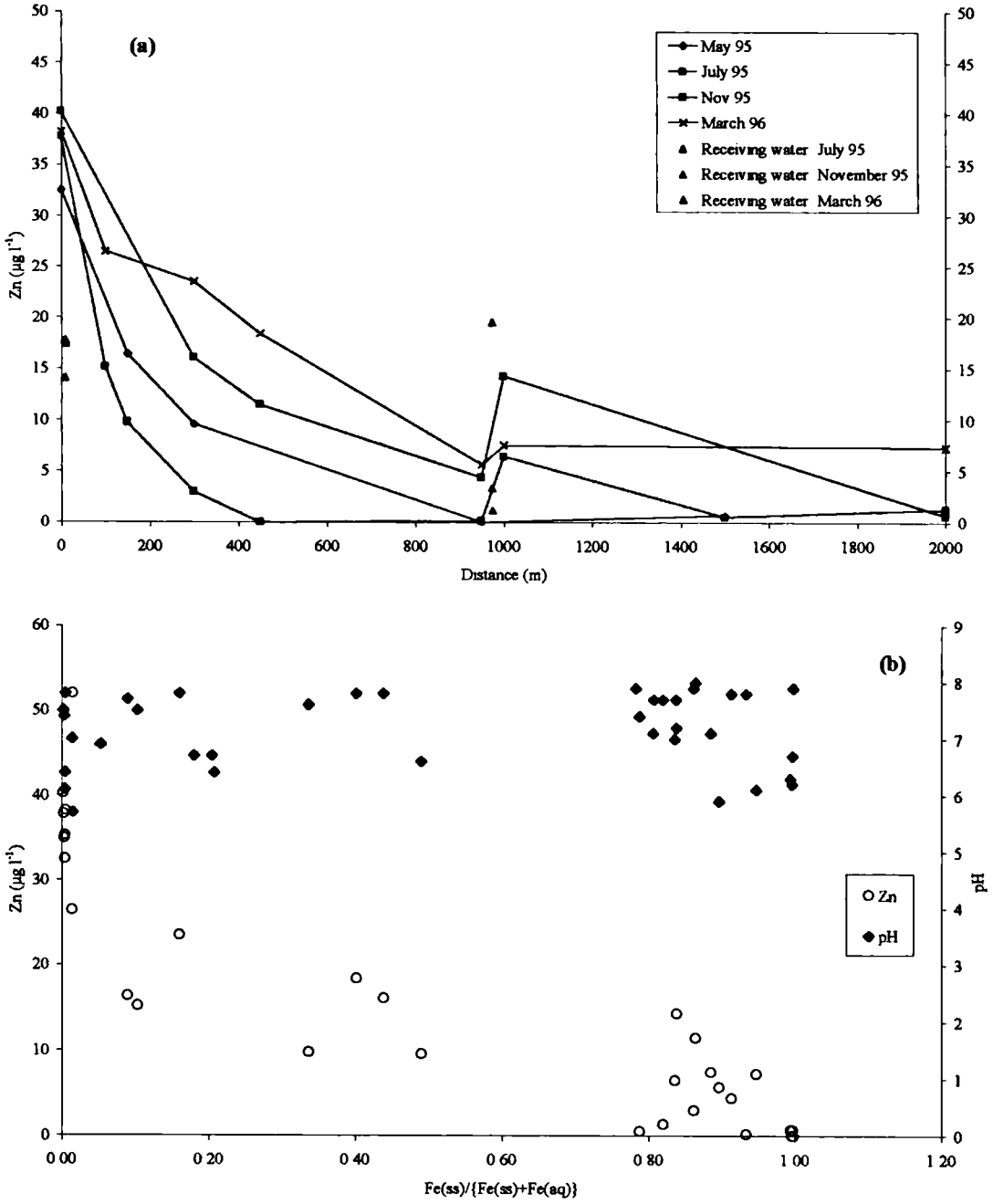


Figure 7.7: Downstream variations in Zn loading in the stream system at SH. (a) dissolved Zn variations downstream from source. The highlighted flows are July 95 = low stream flow (red) and November 95 = highest stream flow (blue), intermediate flow conditions are shown in black. The receiving water is shown as an inflow at 10m for convenience, and a further inflow is shown at 975m. (b) Zn concentrations compared with the proportion of Fe occurring as Fe_{ss}, with pH plotted on the second axis.

predicted from such low concentrations that precipitation of Zn minerals would be responsible for such a decline, Zn_{aq} was plotted against the proportion of Fe as Fe_{ss} to establish whether that could be a potential control on the concentration. Figure 7.7b shows that the Zn concentration diminishes as the Fe_{ss} proportion increases, with all data points being plotted. pH is a factor which can affect sorption of ions to suspended or colloidal surfaces, and figure 7.7b shows that the pH is approximately constant for all samples plotted, at a circum-neutral value. However, it should be noted that the pH of hydrolysis of Zn is ~7 (Levinson, 1980). The variation in the cluster of figures where Zn <10 $\mu g\ l^{-1}$ is probably due to proximity to the detection limit of the method.

The behaviour of additional minor and trace ions in-stream will be described further in sections 7.2 and 7.3, where concentrations are higher.

7.1.4 Stream sediment chemistry

Figure 7.8 shows the concentrations of Fe and Mn in the stream sediments, downstream from the source. It can be seen (figure 7.8a) that the initial concentration is ~50% Fe initially, which then decreases downstream. The decrease in November 1995 is most rapid, which is related to dilution of the mine drainage waters being greater than was the case in July 95. Figure 7.8a also shows that the inflowing stream at ~950m is sufficient to return the stream bed chemistry to a stable value of 2-5% Fe on all occasions. Figure 7.8b shows a more complex pattern for Mn, with an increase in concentration from the point of discharge (~0.01%), on all occasions, with a decrease at the confluence as was observed for Fe. The intermediate concentrations can be related to dilution, with November 95 (high flow) showing the lowest concentrations and July 95 showing the highest.

In calculations of the predicted minerals precipitating using PHREEQ-C, it was found that goethite was predicted to be supersaturated in all solutions, with the degree of supersaturation increasing downstream. The same pattern was observed for amorphous $Fe(OH)_3$, but with the degree of saturation being less due to the respective K_{sp} of amorphous $Fe(OH)_3$ and goethite (section 2.2.5). XRD analysis of samples downstream from source (shown in figure 5.11c & d) were not undertaken in the SH stream system.

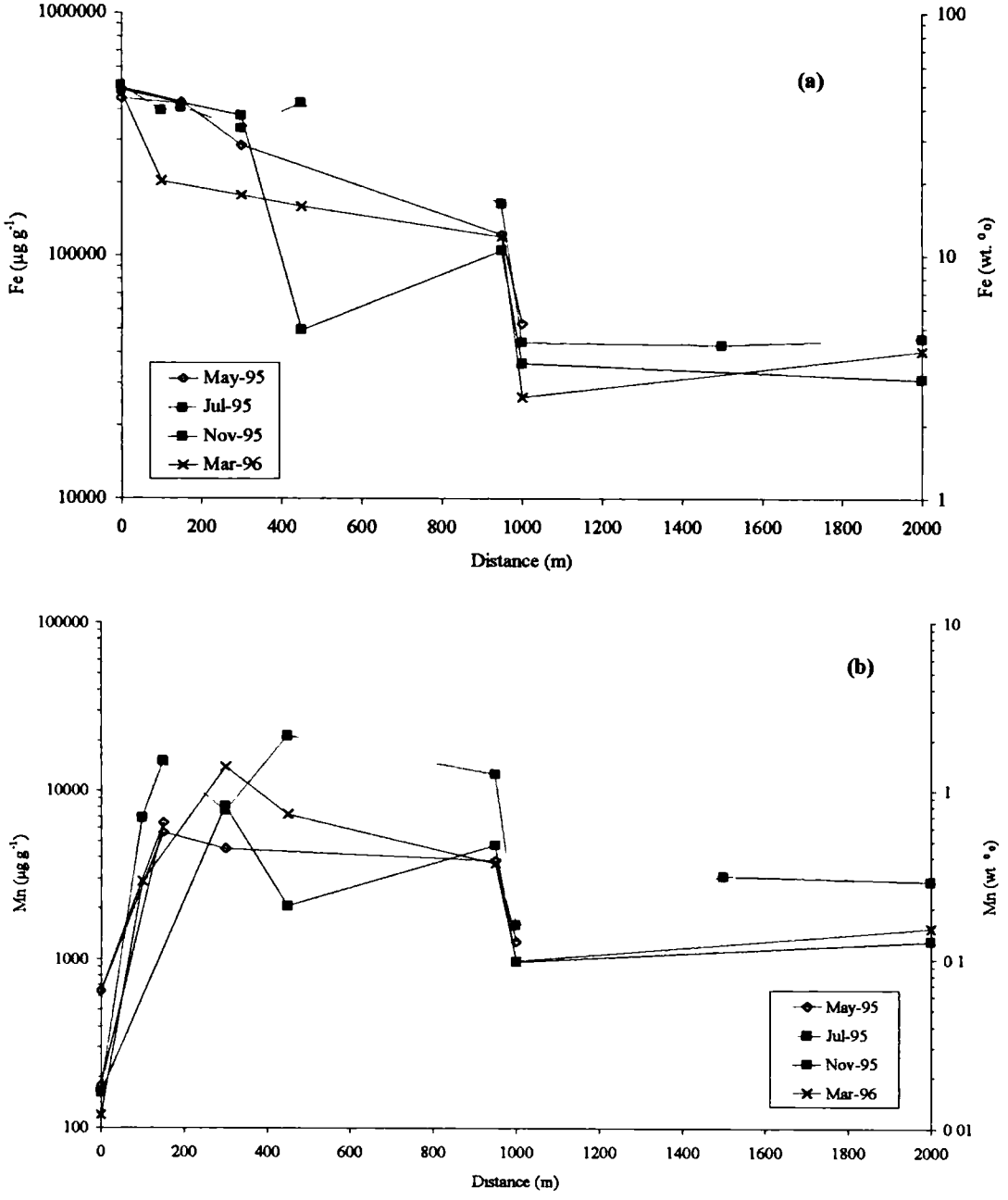


Figure 7.8: Variations in the concentration of Fe and Mn in stream sediments downstream from SH discharge. The highlighted flows are July 95 = low stream flow (red) and November 95 = highest stream flow (blue), intermediate flow conditions are shown in black. The receiving water is shown as an inflow at 10m for convenience, and a further inflow is shown at 975m.

7.2 Helmington Row

This location is a spoil heap discharge, the chemistry and nature of which was discussed in section 5.2. The drainage exhibits highly variable chemistry in differing hydrological conditions. The water contains not only high Fe and SO_4 concentrations, but also minor ions such as Cu and Zn in relatively high concentrations, at the point of discharge. The control on the chemistry was considered to be the physical fluid flow characteristics of the spoil heap aquifer (section 6.2).

7.2.1 Physical characteristics

As described in section 5.1, the discharge varied from extreme low flow in July 95 to flood in November 95. The other sampling occasions occurred in intermediate flow conditions. Also pertinent to these descriptions is that in both March and October 96 there was several days of cold weather / snowfall before and during the sampling visit, causing rock salt to be applied to roads.

7.2.2 Aqueous chemistry: major ions

The Eh and pH measured in the HR stream system are presented in figure 7.9. Figure 7.9a shows the Eh measured on the different sampling occasions. A general trend of decrease from source, with a subsequent increase from 800m can be seen (similar to SH (figure 7.1a)). The July 95 samples are also have generally higher values than the other sampling occasions. Figure 7.9b shows the pH of the waters. It can be seen that in July 95, from an initial pH of 3.5 the stream increased to a pH of >7.5 in 800m from the discharge point. The steepest rate of increase in pH is between 550-800m in July 95. On all other sampling occasions a pH of ~6 was found in a shorter stream length from the source, but the initial pH was lower. The rate of increase in pH is similar for all visits between 0-800m, with the exception of July 95.

The major ion chemistry is plotted in figure 7.10 on a triangular diagram. Cation chemistry is shown on figure 7.10a. The distribution of species can be seen to vary very little in the localities, the Ca proportion is approximately constant at 50%, with all the waters being either a Ca type or a Ca-Mg type. These small fluctuations are attributable to changing proportions of Mg and Na+K. Anion chemistry is shown in figure 7.10b. It can be seen that whilst the discharge is generally a SO_4 type (November 95 excepted), the water moves towards a higher HCO_3 component as it moves downstream. Individual fluctuations are shown by 100m (July 95) where the HCO_3 proportion appears to drop before rising, this is due to a pH drop from the point of discharge, before rising again.

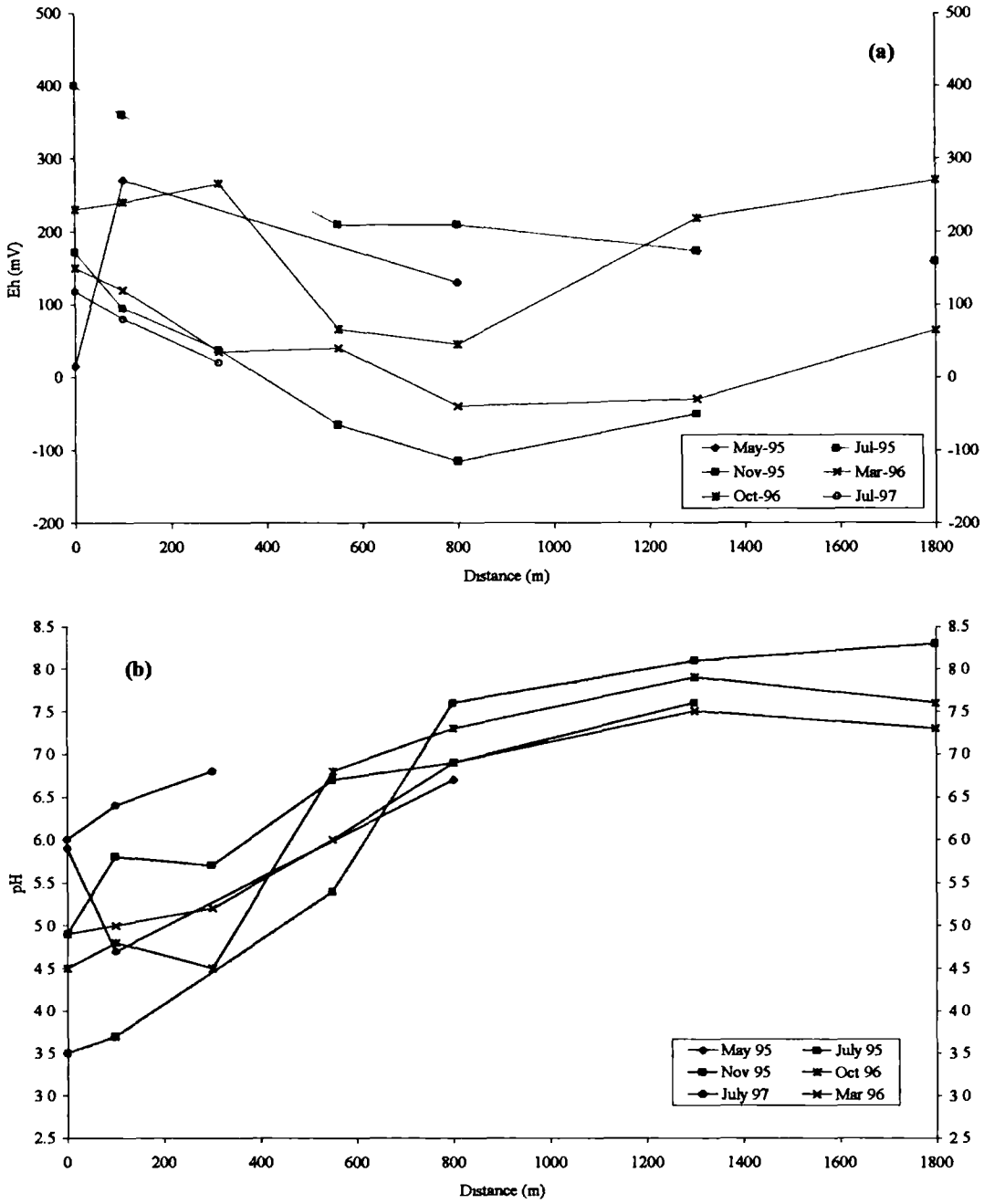


Figure 7.9: Downstream variations of selected parameters at HR. (a) Eh (b) pH. The highlighted flows are July 96 = low stream flow (red) and November 95 = highest stream flow (blue), intermediate flow conditions are shown in black.

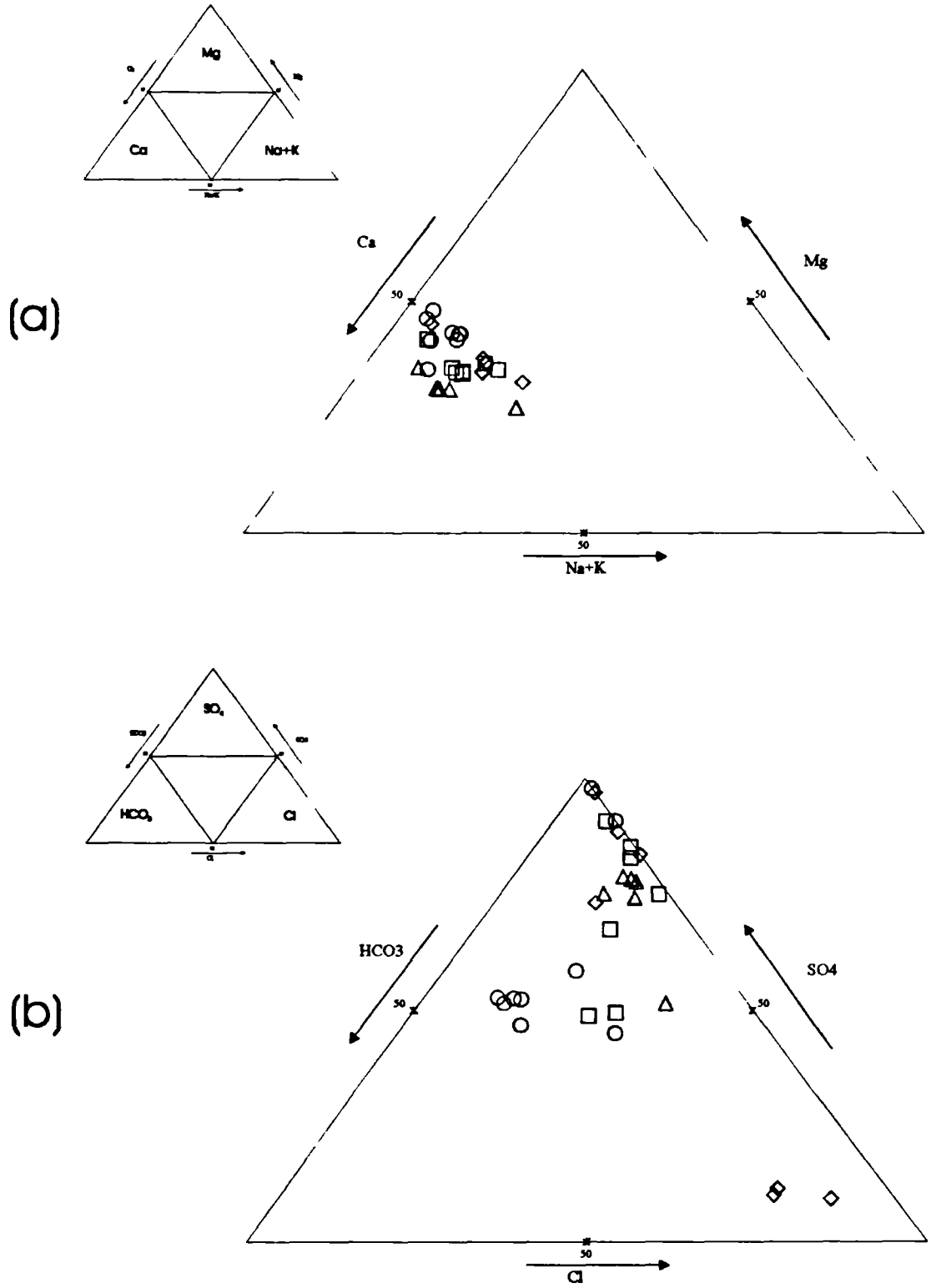


Figure 7.10: Triangular diagram of major ion chemistry at HR (a) cations: Ca, Mg, Na & K (b) anions: HCO_3, SO_4 & Cl. Labelling as follows: July 95 = circles, Nov 95 = triangles, March 96 = squares & October 96 = diamonds. Units are %meq, with 50% marked on each axis. The occurrence of dominant ions on the diagram is described by the associated inset to each plot.

The proportion of Cl making up the anion balance of the samples can be seen to increase generally on all occasions, with the higher proportion of Cl occuring at the dicharge and proximal sites. This is due to the proximity of the site at 800m to a road, and the highway drainage incorporating melting snow / ice and also "road salt". This can be seen to have an impact most significantly in October 96, but is also evident in the increasing Cl proportion in at 1300 and 1800m downstream in March 96.

Figure 7.11a shows the Ca variation downstream from the spoil heap discharge. It can be seen (in contrast to SH (figure 7.3a)) that in May and July 95 decreases in concentration are found, which cannot be attributed to surface water dilution, after 100m downstream. On the other sampling occasions Ca can be seen to be of a more consistent (temporal and spatial) concentration along the length of stream sampled, after the initial decrease at 0-100m. This initial decrease may be a result of both dilution and net loss from the stream system, due to precipitation/sorption reactions. Magnesium shows a very similar trend to Ca, and thus is not plotted here. The only samples which deviate from a linear relationship are those of July 95, (discharge and 100m) and October 96 (source). What is noticeable is that the molar ratio changes between 100-300m in July 95 to fit the linear pattern of all samples (n=32). The change in molar ratio for October 96 may be accounted for by dilution by surface waters, but this is not the case for July 95. The Ca_{ss} (the suspended sediment component) is invariably <100x the concentration of Ca_{aq} (the dissolved component), however, an increase in Ca_{ss} between 100-800m is noticeable. This is the only measurable change in the concentration downstream from source of Ca_{ss} during all sampling occasions, and concentrations are (other than July 95) <400 $\mu g\ l^{-1}$, whilst those of July 95 rise to ~700 $\mu g\ l^{-1}$ at 800m downstream. When Ca_{aq} speciation was predicted using PHREEQ-C, these same samples were the only ones to show a significant change in the Ca speciation downstream from the point of discharge. The dominant species are Ca^{2+} and $CaSO_4^o$ (figure 7.11), which increase from ~70% to ~88%, and decrease from ~30% to 12% of total dissolved Ca downstream from source, respectively. The ion $CaHCO_3^+$ is the third most abundant, but is <0.5% of the total in all cases, apart from HR 800-1800m in July 95.

Figure 7.12a shows the concentration of Na downstream from source. It can be seen that the only changes in concentration are caused by dilution immediately after the point of discharge. The exception to this is July 95 when there were no diluting waters. It can be seen that there is a higher concentration of Na after mixing in November 95, March 96 and October 96. Potassium follows a very similar series of trends, albeit at lower concentrations, and is not shown here. Figure 7.12b shows Cl concentrations on the

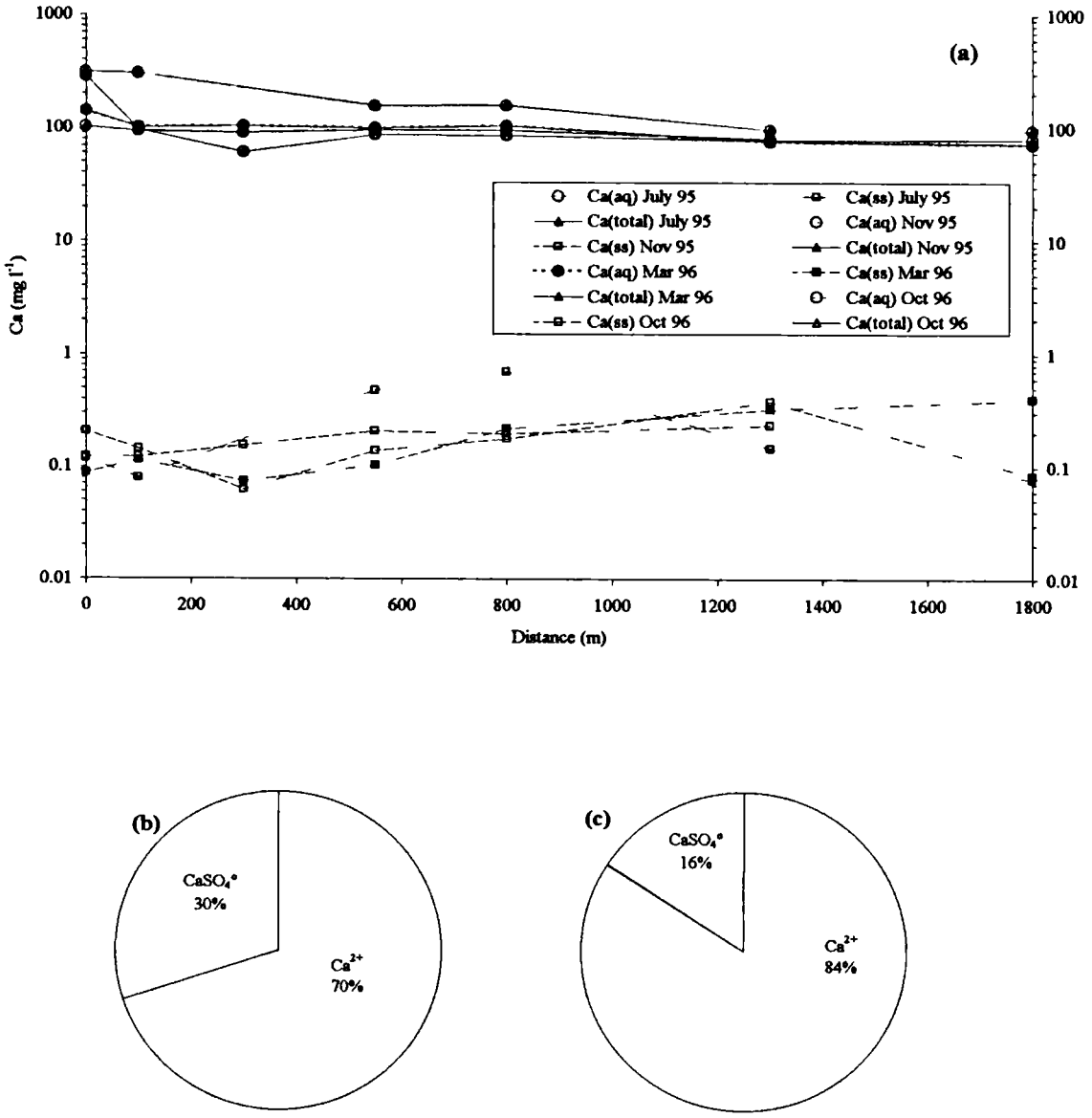


Figure 7.11: Physical and chemical partitioning of Ca in the HR stream system. (a) Concentration of Ca in the aqueous and suspended sediment phases. The highlighted flows are July 95 = low stream flow (red) and November 95 = highest stream flow (blue), intermediate flow conditions are shown in black. (b) Ca speciation at discharge point (0m) in July 95 (c) Ca speciation at 800m downstream in July 95. The subsript $_{ss}$ represents the suspended sediment component, $_{aq}$ the dissolved and $_{t}$ the sum of $_{ss}$ and $_{aq}$.

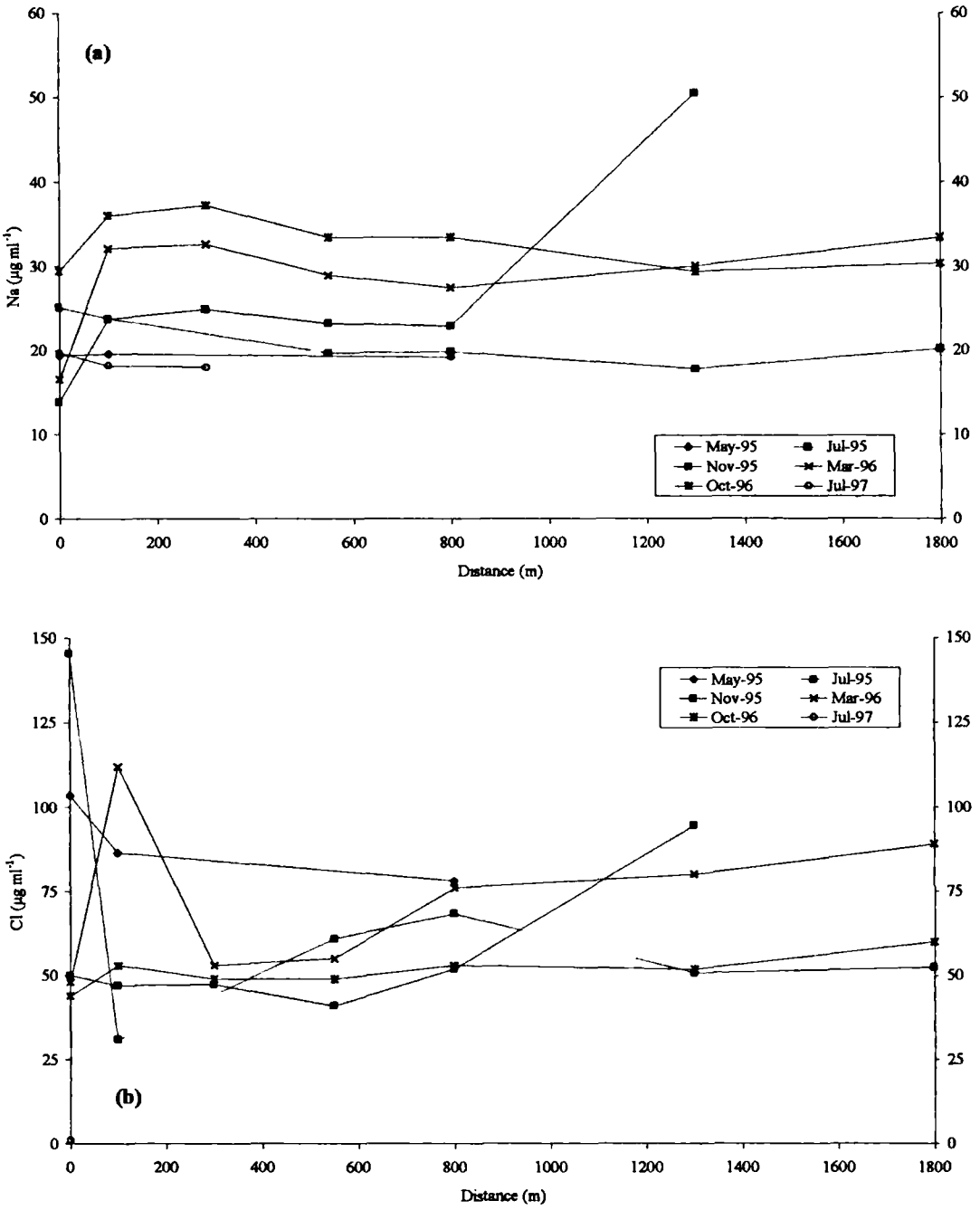


Figure 7.12: Downstream variations in selected ions at HR. (a) Na (b) Cl (c) SO_4 (d) HCO_3^-.The highlighted flows are July 95 = low stream flow (red) and November 95 = highest stream flow (blue), intermediate flow conditions are shown in black. The receiving water is shown as an inflow at 10m for convenience, and a further inflow is shown at 975m.
(continued on next page)

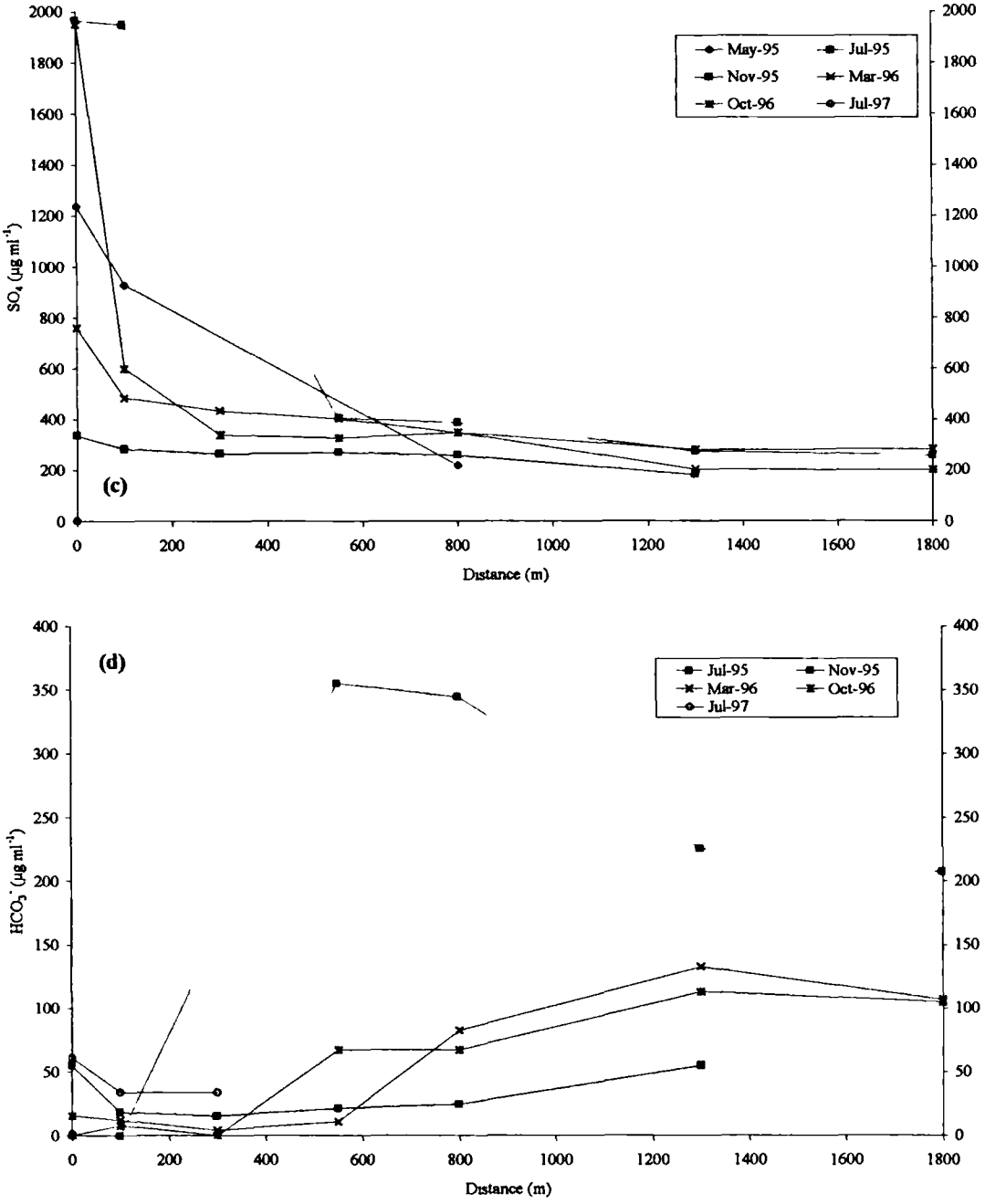


Figure 7.12: continued from previous page.

different sampling occasions, downstream from source. It can be seen that the patterns followed are similar to those for Na, the exceptions to this are the source chemistry in July 95 and at 300m in March 96. Sulphate concentrations are shown in figure 7.12c. This ion appears to be conservative in November 95 and March 96 (after dilution at 100m). In May 95, July 95 and October 96 SO_4 concentrations appear to decrease after mixing with surface waters (no mixing in July 95). The largest decrease is in July 95, from ~2000 mg l^{-1} at 100m to ~400mg l^{-1} at 550m (no sample at 300m). At more than 50m downstream the SO_4 appears to be conservative in all cases. Alkalinity (figure 7.12d) shows a general increase with distance downstream, largely related to the increase in pH (figure 7.9b and section 2.2.2). The stream seems to reach a steady state of ~100 mg l^{-1} HCO_3^- at 1300m. The exception to this is July 95, with the concentration reaching a peak of ~350 mg l^{-1} from 550-800m downstream from source (this corresponds to the region of maximum decrease of concentration in most other ions discussed in this section). The concentration then decreases to ~200 mg l^{-1}, by 1800m downstream.

Study of the molar ratios of selected major ions (figure 7.13) can be used to elucidate relations potentially caused by dilution and / or loss from the system due to precipitation / sorption. Figure 7.13a shows the changes in Ca:SO_4 downstream from the point of discharge on all sampling occasions. It can be seen that the July 95 samples move towards a molar ratio of 1 from <0.4 by ~550m downstream, after which the molar ratio maintains a value of 0.9-1.0. The period of changing molar ratio is marked by changes in the concentrations of both Ca and SO_4, but the increase in ratio shows that there is a greater loss of SO_4 from the stream system, on a molar basis. March and October 96 samples also show an increase in the molar ratio, but it is not as marked as that observed in July 95, which owes more to SO_4 decrease than changes in Ca. As may be predicted from the changing SO_4 concentrations, but stable Cl concentrations, the ratios of these ions decrease from a molar ratio of 4-6 at the point of discharge, down to ~2 further along the stream course. Sodium appears to be conservative in solution, and has been compared to SO_4 in figure 7.13b. It can be seen that the decrease in SO_4 between 100-550m & 100-800m for July 95 and May 95 cannot be attributed to dilution, and are representative of a net loss of SO_4 from solution.

The variations in Fe_{aq} downstream from the discharge point (figure 7.14a) show that the dissolved constituent decreases in concentration most rapidly in July 95 (low flow). The greatest rate of decrease in July 95 and 97 can be seen between 100-550m downstream, after which the concentration returns to "background". The distance at which the

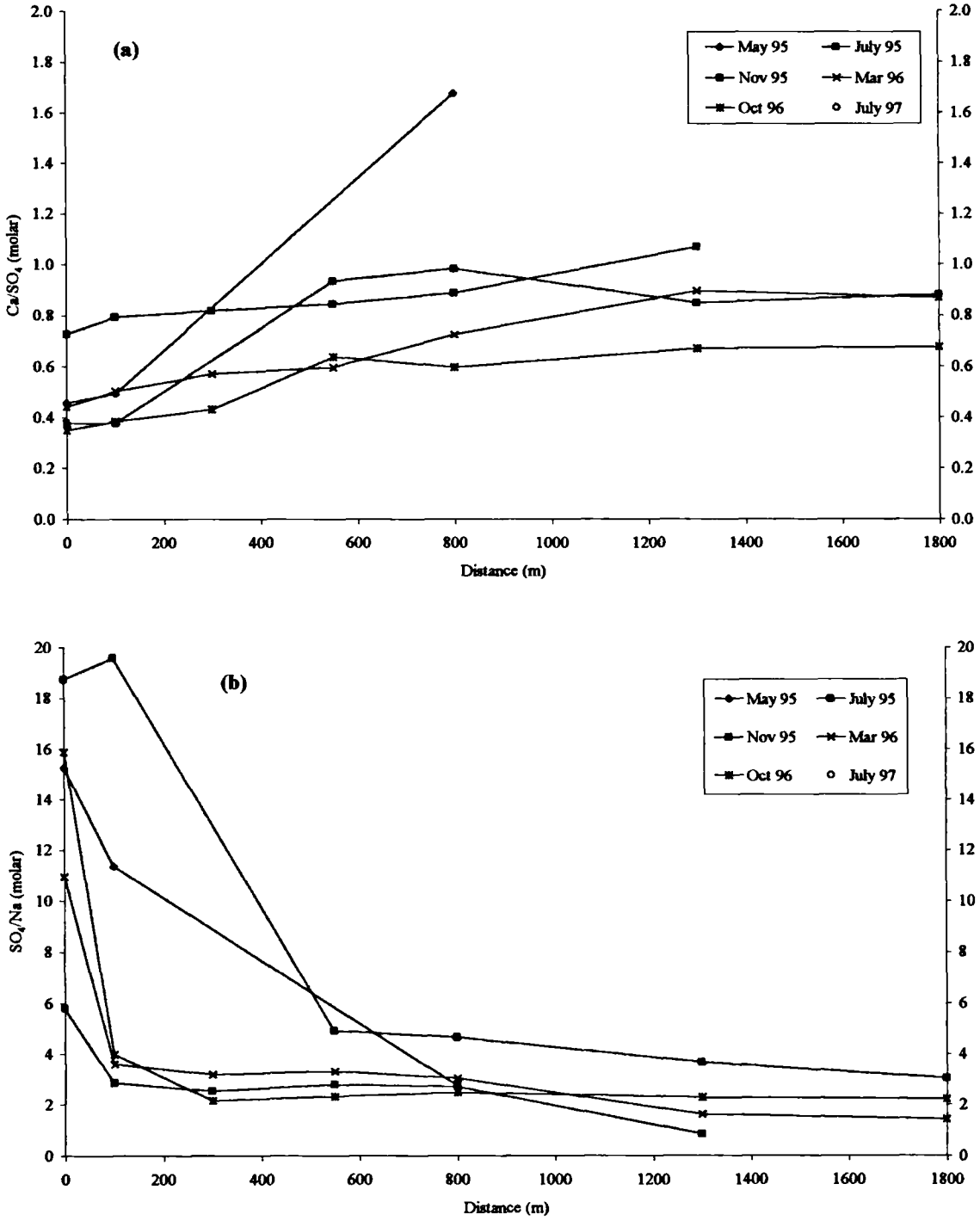


Figure 7.13: Molar ratios of conservative and reactive elements downstream from source at HR. (a) Ca:SO_4 (b) SO_4:Na.

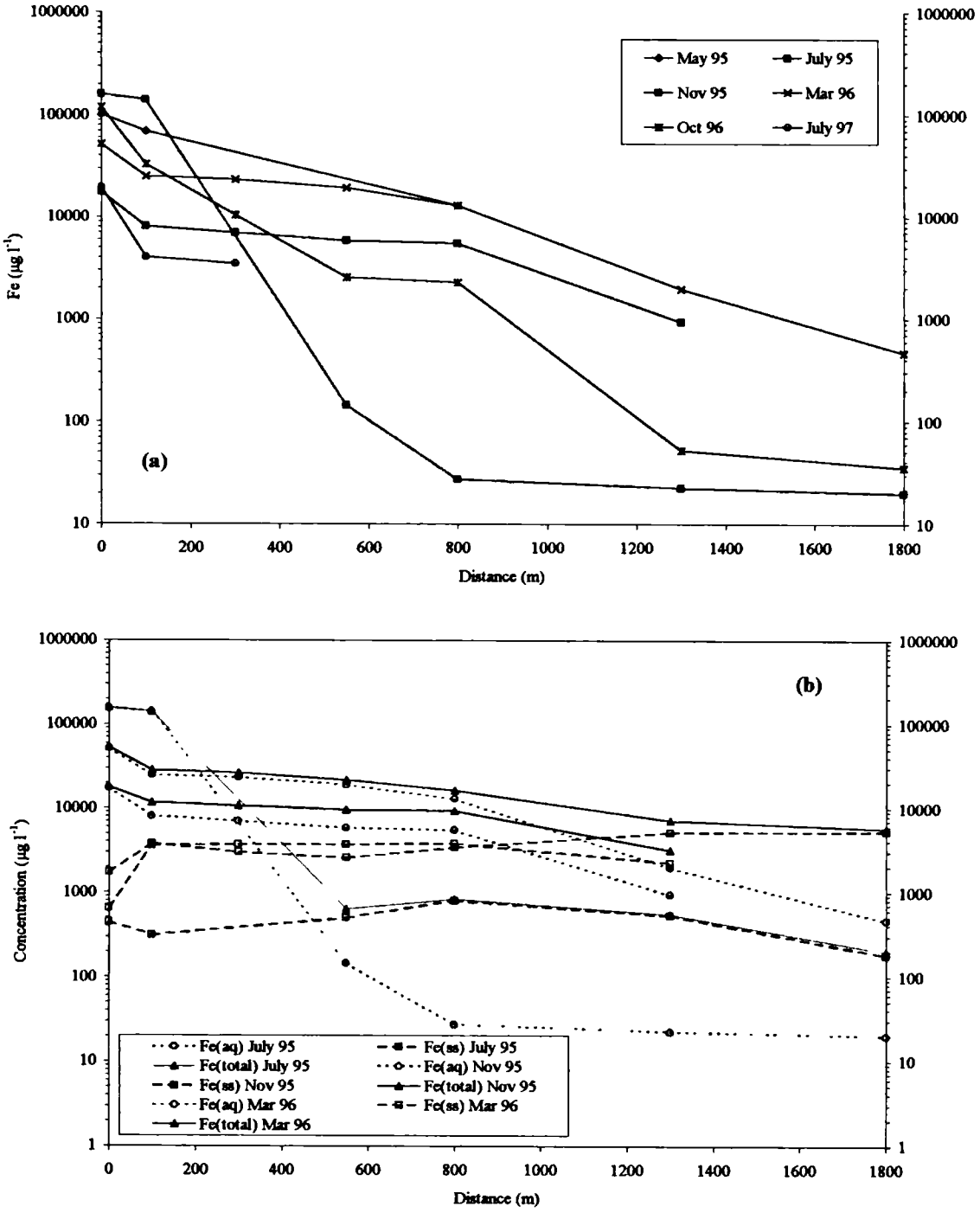


Figure 7.14: Downstream variations in Fe loading in the stream system at HR. (a) dissolved Fe variations downstream from source. The highlighted flows are July 95 = low stream flow (red) and November 95 = highest stream flow (blue), intermediate flow conditions are shown in black. (b) Comparison of Fe loading in dissolved and suspended phases. Solid lines = Fe_{aq}, dotted lines = Fe_t & dashed lines = Fe_{ss}. Low stream flow = July 95 (red), highest stream flow (blue), and intermediate stream flow = March 96 (grey). The receiving water is shown as an inflow at 10m for convenience, and a further inflow is shown at 975m in both figures.

maximum rate of decrease in concentration occurs in October 96 is divided into two regions, 100-550m and 800-1300m. On the remaining sampling occasions, a more constant rate of decline is found. It should be noted that this distribution is very similar to that observed at SH, with the July 95 concentrations reduced to a lower value than all other sampling occasions at the final sampling locations, ~2km downstream. Figure 7.14b shows the changes in dissolved Fe in relation to the variations in Fe_{ss} and Fe_{aq}. It can be seen that the rapid decrease in Fe_t in July 95 results in Fe_{ss} becoming the dominant component of Fe_{aq} before 550m downstream (no sample at 300m), however the concentration of Fe_{ss} varies little along the length of stream sampled. In November 95, it can be seen that the point at which Fe_{ss} becomes dominant is displaced ~400m downstream and that March 96 is a further ~200m downstream, with the Fe_{aq} taking a similar distance to decline in concentration. It is also notable that the Fe_{ss} concentration for all the sampling occasions shown here is very constant when compared to the magnitude of decline in Fe_t concentrations.

7.2.3 Aqueous chemistry: minor and trace ions

Figure 7.15 shows the downstream behaviour of Mn, Al, Zn & Cu. It can be seen that all these elements follow the same pattern, with the July 95 sample being of highest concentration initially (section 5.2), and then decreasing more rapidly than the concentrations observed on the other sampling occasions. November 95 samples can be seen to have the lowest concentration, which does not vary largely downstream. It can be seen that Mn and Al (figure 7.15a,b) decrease very rapidly instream in July 95. Manganese shows a two step decrease, firstly between 100-550m (no sample at 300m), and secondly between 1300-1800m (last sample collected), on other sampling occasions there is a decrease in concentration associated with mixing of water flowing from further up the spoil heap (section 3.4.2). Aluminium shows the greatest decrease from 100-550m in July 95, with no dilution by surface waters. October 96 samples show a very similar pattern, but that of March 96 does not decline for a further 250m to a similar concentration.

Figure 7.16a shows that Mn aqueous loading is dominated by dissolved Mn for the length of stream studied on these occasions, with the influence of Mn_{ss} appearing to increase in the region where sampling ceased. It is thus suggested that this is a trend which would have continued had sampling continued further downstream. This is the same general trend as was observed for SH. Figure 7.16b shows the Al distribution downstream from the spoil drainage source. This has quite a different series of trends to those of Mn. In the July 95 samples the Al_t is dominated by Al_{ss} after 550m downstream

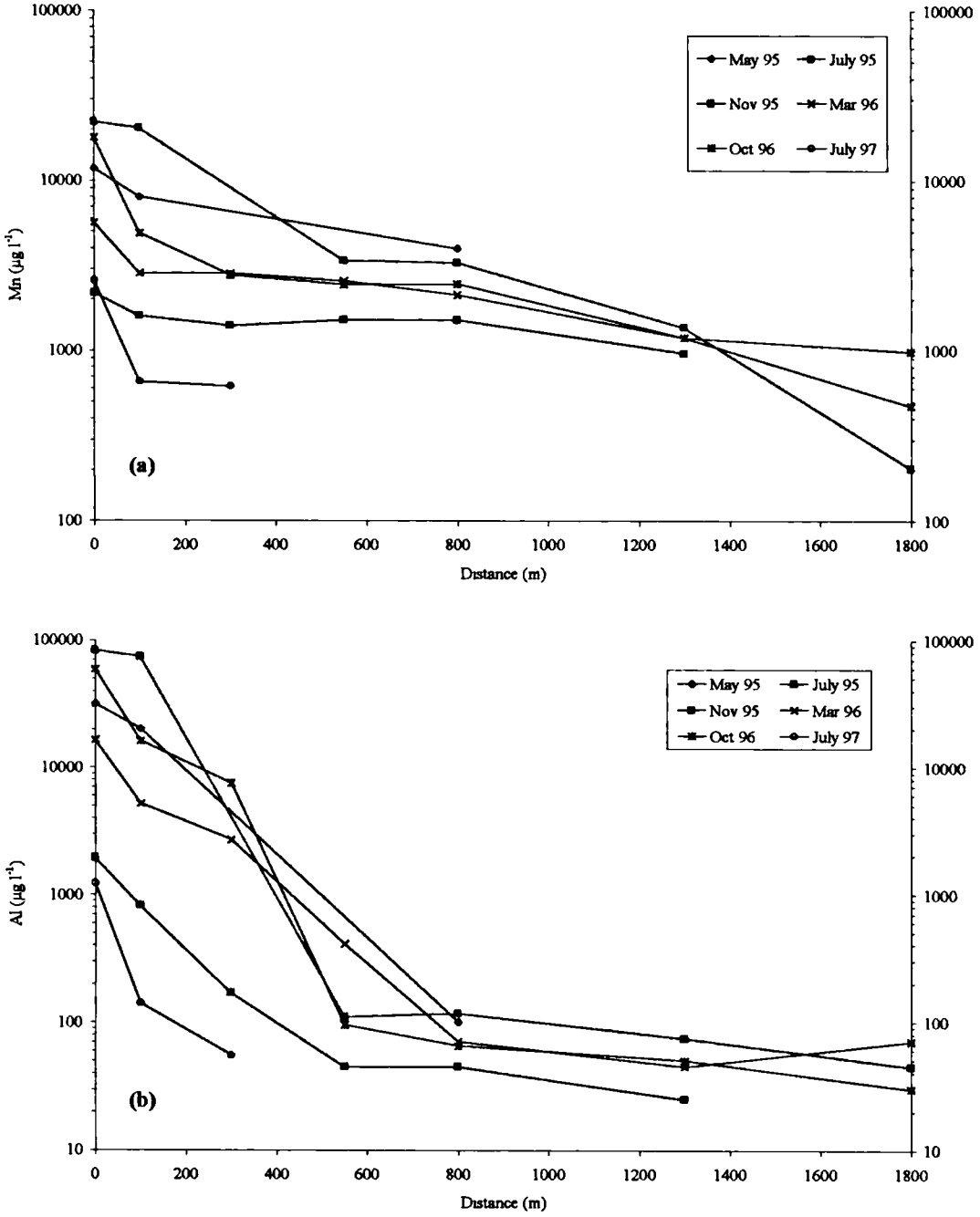


Figure 7.15: Downstream variations in selected ions. (a) Mn (b) Al (c) Cu (d) Zn. The highlighted flows are July 95 = low stream flow (red) and November 95 = highest stream flow (blue), intermediate flow conditions are shown in black. The receiving water is shown as an inflow at 10m for convenience, and a further inflow is shown at 975m.
(continued on next page)

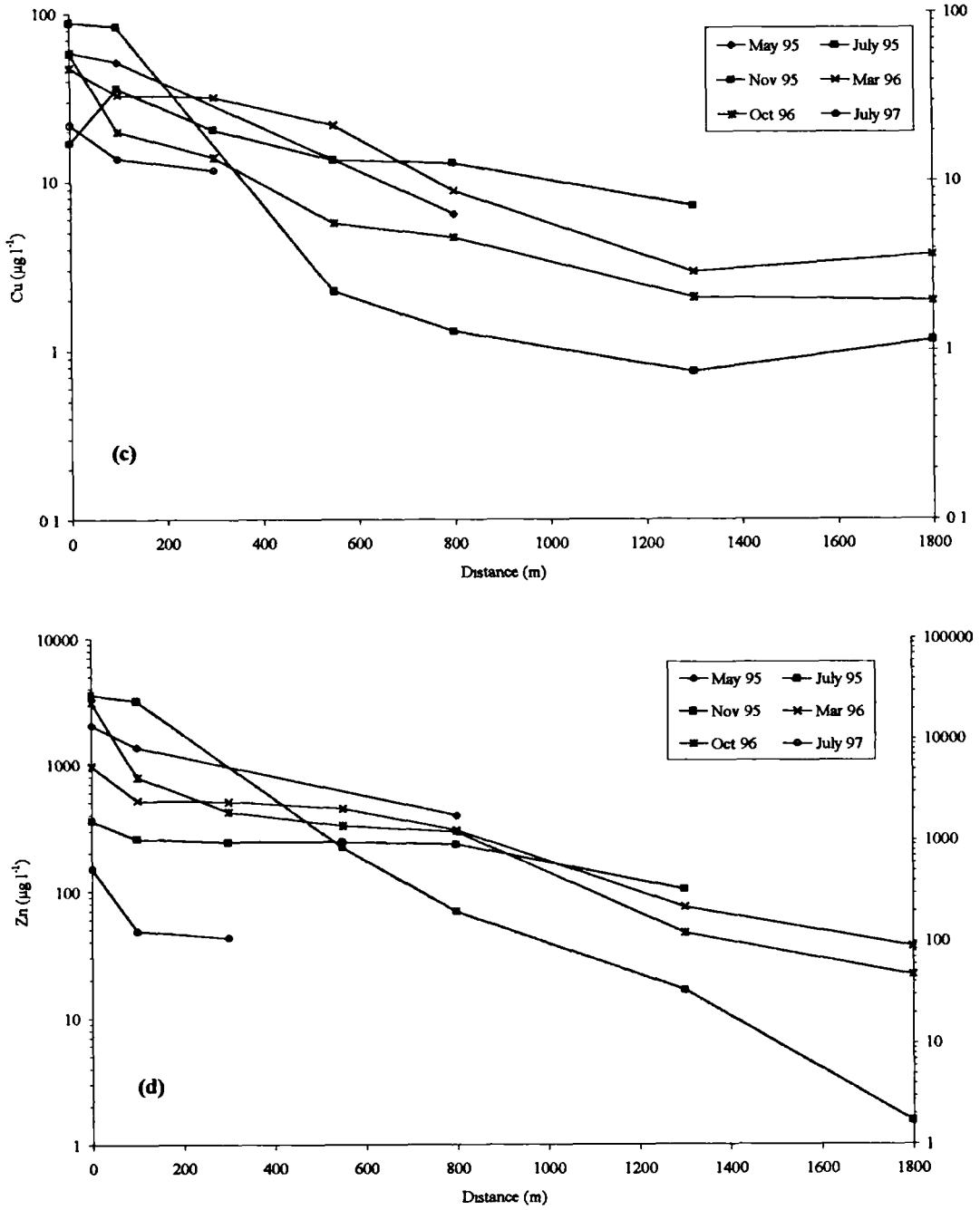


Figure 7.15: continued from previous page

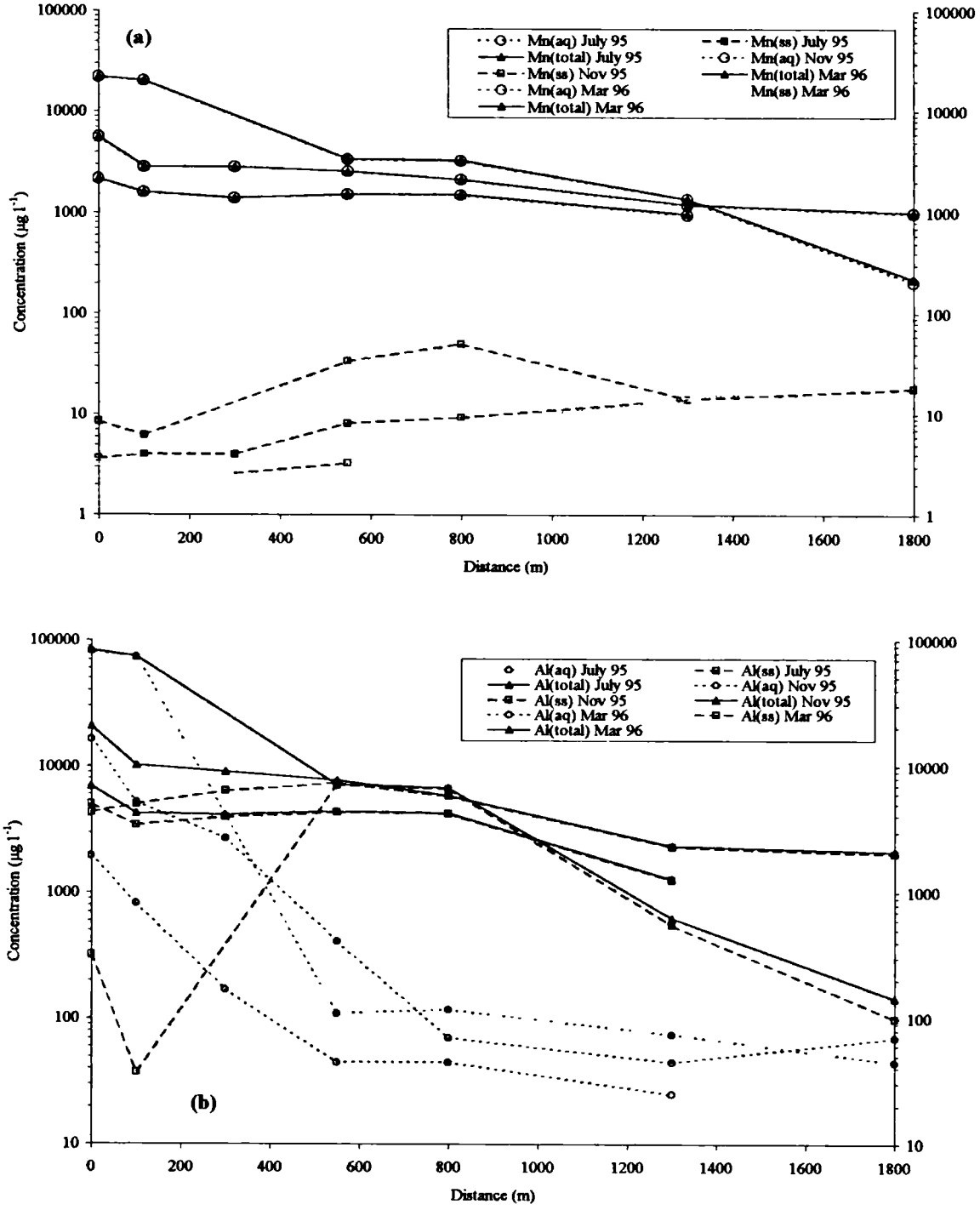


Figure 7.16: Downstream variations in Mn and Al loading in the stream system at HR. (a) Comparison of Mn loading in dissolved and suspended phases. (b) Comparison of Al loading in dissolved and suspended phases. Solid lines = Mn_t / Al_t, dotted lines = Mn_{aq} / Al_{aq} & dashed lines = Mn_{ss} / Al_{ss}. Low stream flow = July 95 (red), highest stream flow (blue), and intermediate stream flow = March 96 (grey). The receiving water is shown as an inflow at 10m for convenience, and a further inflow is shown at 975m in both figures.

(no sample at 300m), and the subsequent decrease in Al_t concentrations is caused by a decrease in Al_{ss} after 800m. In November 95 it can be seen that $Al_{ss} > Al_{aq}$ from the point of discharge, and that whilst Al_{aq} decreases downstream, Al_{ss} remains constant until 800m, and is subsequently characterised by a minimal further decrease in concentration to 1300m downstream. In March 96 the concentration of Al_{ss} remains constant from the point of discharge, but Al_{aq} can be seen to decrease to an equal concentration at 100m downstream. The speciation of Al_{aq} can be seen to change from a SO_4 dominated association ($Al(SO_4)_2^-$ and $AlSO_4^+$) and Al^{3+}, to Al-hydroxy species, in particular $Al(OH)_4^-$ at 550m downstream in July 95. The importance of SO_4 in affecting speciation (observed at the points of discharge (section 5.2)) can be seen in these samples too, especially for Zn, Ba, Ca, Mg, Sr -SO_4 neutral complexes. Figure 7.17 shows a net loss of Al from the stream system, when compared with Na (Na used as a conservative ion to ratio against).

Copper concentrations (figure 7.15c) can be seen to decrease very rapidly from 100-550m in July 95, to values close to the detection limit of the method (accounting for the fluctuations observable from 100m downstream). There is little decrease from source in November 95, to such an extent that the final concentration measured at 1300m is higher than any other visit at that point. The intermediate flow conditions show patterns of a more gentle decline than July 95, from lower initial concentrations, and maintain a higher concentration than July 95 after 550m downstream. Figure 7.15d shows that Zn concentrations show a similar pattern to Cu, with the exception that the concentration in the July 95 samples appears to decrease at a greater rate than that observed for Cu in the same samples. To examine the potential controls on Cu and Zn transfer from the dissolved phase, figure 7.18a shows the effect of Fe_{ss} on the concentration of Cu and Zn. It can be seen that there is a general trend of both decreasing as the proportion of Fe_{aq} occurring as Fe_{ss} increases. However, it should be noted that as these ions decrease in concentration, the pH and the proportion of Fe_{ss} (figure 7.18). Figure 7.18a shows that the concentrations of Cu and Zn decrease with increasing pH, and that Cu concentrations are lower than those of Zn. The relationship of dissolved Cu and Zn to the fraction of the Fe_t occurring as Fe_{ss} is shown in figure 7.18b, and again the concentrations of the two ions can be seen to decrease as the proportion of Fe_{ss} increases. Finally, the proportions of Cu and Zn occurring in the suspended phase are shown with aqueous pH plotted against the proportion of Fe_{ss} (figure 7.18c), and it can be seen that the highest proportions of Cu and Zn in the suspended phase are associated with the highest pH values and the highest Fe_{ss} proportions.

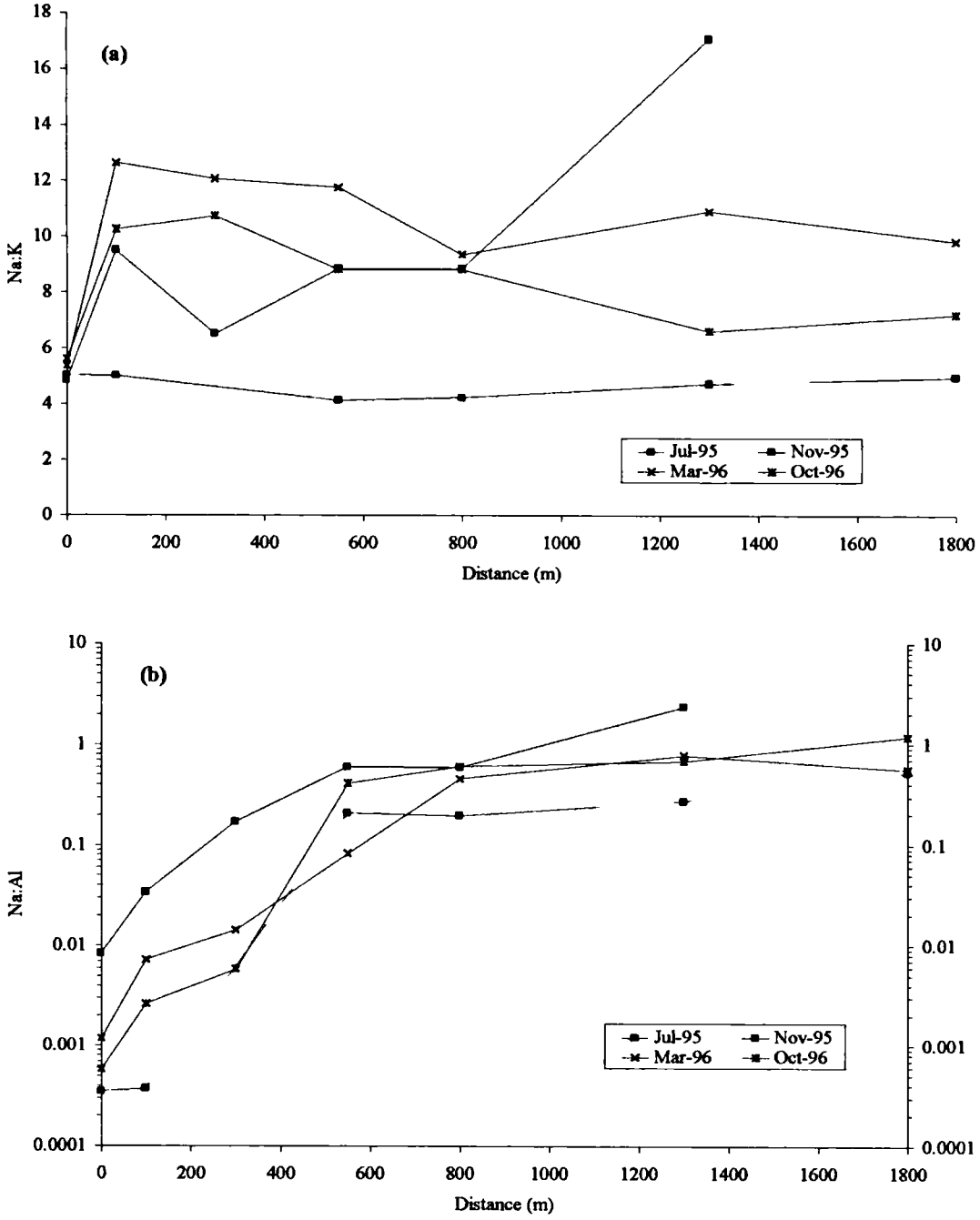


Figure 7.17: Molar ratios of selected ions at HR to study reactive loss and dilution from source (a) molar ratio of Na and K to show dilution of the discharge by the receiving water (b) molar ratio of Al (reactive) and Na (conservative) downstream from source at HR

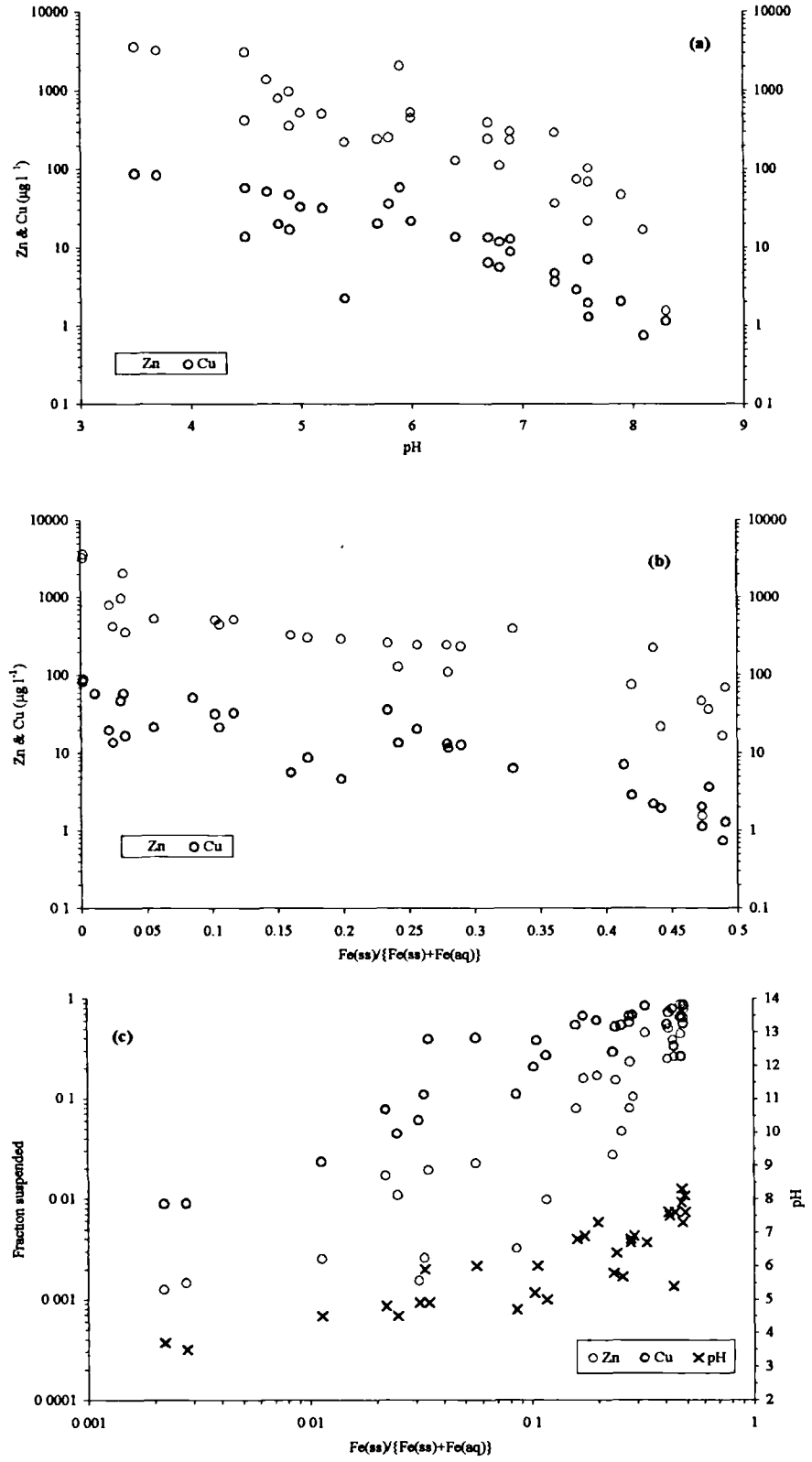


Figure 7.18: Relationship between aqueous and suspended sediment Cu and Zn with Fe_{ss} and pH at HR. (a) Comparison of dissolved Cu and Zn with pH (b) Comparison of dissolved Cu and Zn with the proportion of Fe_t occurring as Fe_{ss} (c) Comparison of the proportion of total Fe, Cu & Zn occurring in the suspended phases, with the water pH.

7.2.4 Stream sediments

The concentrations of selected ions (Fe, Ca and Al) are shown downstream from source in figure 7.19. The Fe concentration can be seen to decrease from source, in a similar pattern to that observed for SH (section 7.1.4), with November 95 (high flow) decreasing most rapidly. When the stream has flowed for 1km the Fe concentrations had decreased to <10% on all the sampling occasions. Manganese concentrations can be seen to increase from source, before levelling off to an approximate concentration of 1%, along the length of stream studied here. Calcium concentrations decrease from source before increasing after 150m downstream, also showing a concentration plateaux, although with July 95 samples showing a considerably higher concentrations.

The XRD pattern of the source and one downstream precipitate is shown in figure 7.20 for two sampling occasions, with very differing aqueous chemistry (section 7.2.2). The July 95 (low flow) ochre at 550m downstream shows an almost completely amorphous background, with only detrital quartz showing any peaks. This is in contrast to the discharge where there some suggestion of a more crystalline component, although still with a high amorphous background signal. The chemical composition of these samples (and one at 800m downstream in July 95) is shown in table 7.1. It can be seen that the concentration of Fe has decreased to 2 mol g^{-1} of Fe after the discharge site, but that the concentration of Al has increased. The concentration of S in the precipitate can be seen to be lower from the point of discharge, but Ca does not change markedly. It was not possible to analyses individual particles using the SEM as these samples tended to disintegrate under the beam (section 4.5.2). The chemical composition is reversed for July 95 samples, which were of a lower ion concentration and higher pH (section 7.2.2), and the XRD pattern derived for these two samples (figure 7.20c & d) can be seen to suggest a ferrihydrite dominated precipitate at 300m downstream.

Table 7.1: Concentrations of selected ions in precipitates at the discharge and downstream from HR

Date	Distance	Fe	Al	Ca	S	Mn
	m			mmol g^{-1}		
July 95	0	5193	1564	272	1110	2.5
July 95	550	2292	5189	240	259	39.3
July 95	800	2543	3743	377	161	30.4
July 97	0	2847	3306	891	814	10.7
July 97	300	6822	704	7	1054	0.8

the concentrations of these and other ions are in appendix IV, in the measurement units of μg g^{-1}.

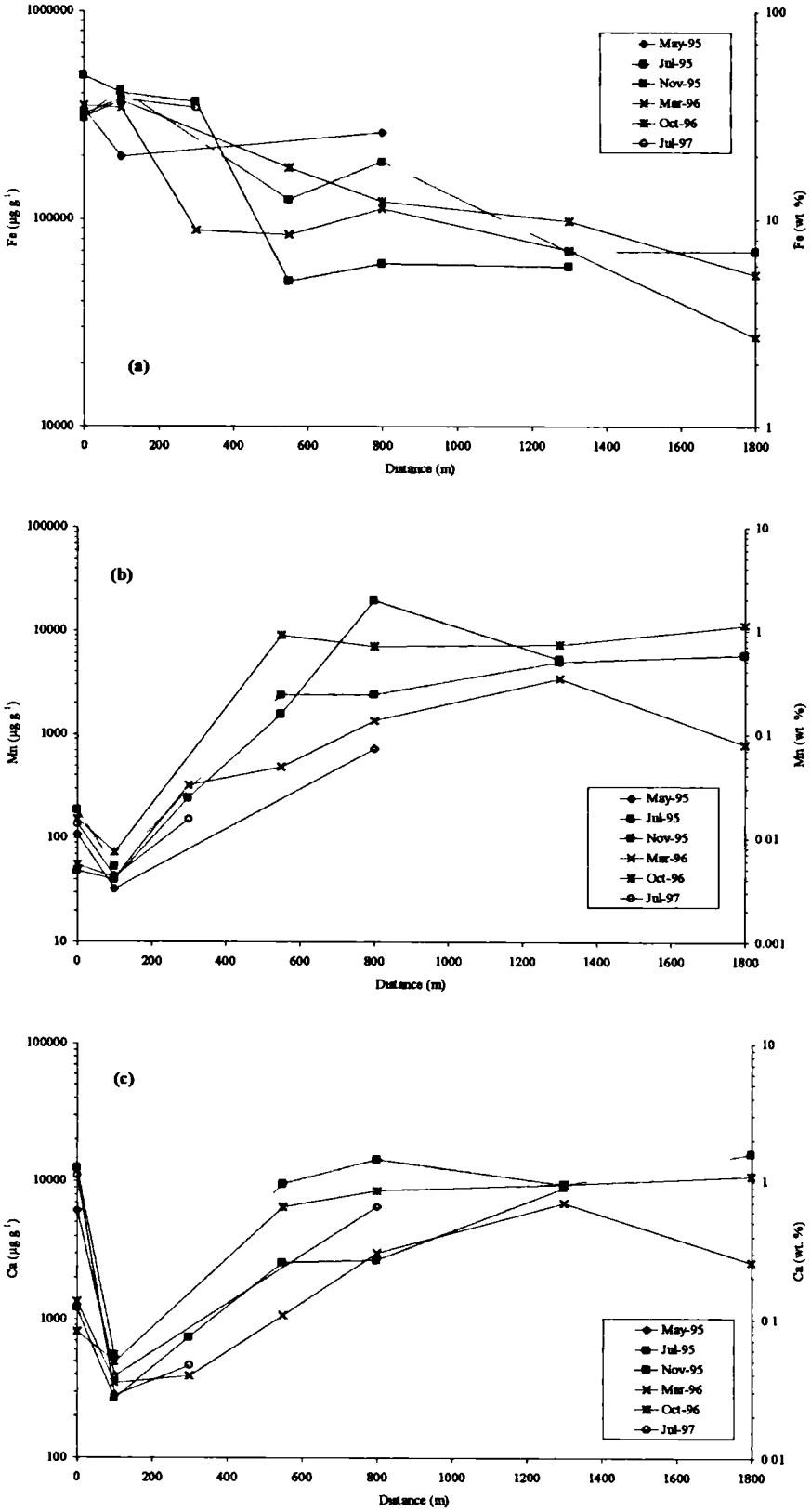


Figure 7.19: Concentrations of selected elements in stream sediments downstream from source at HR. (a) Fe (b) Mn (c) Ca.

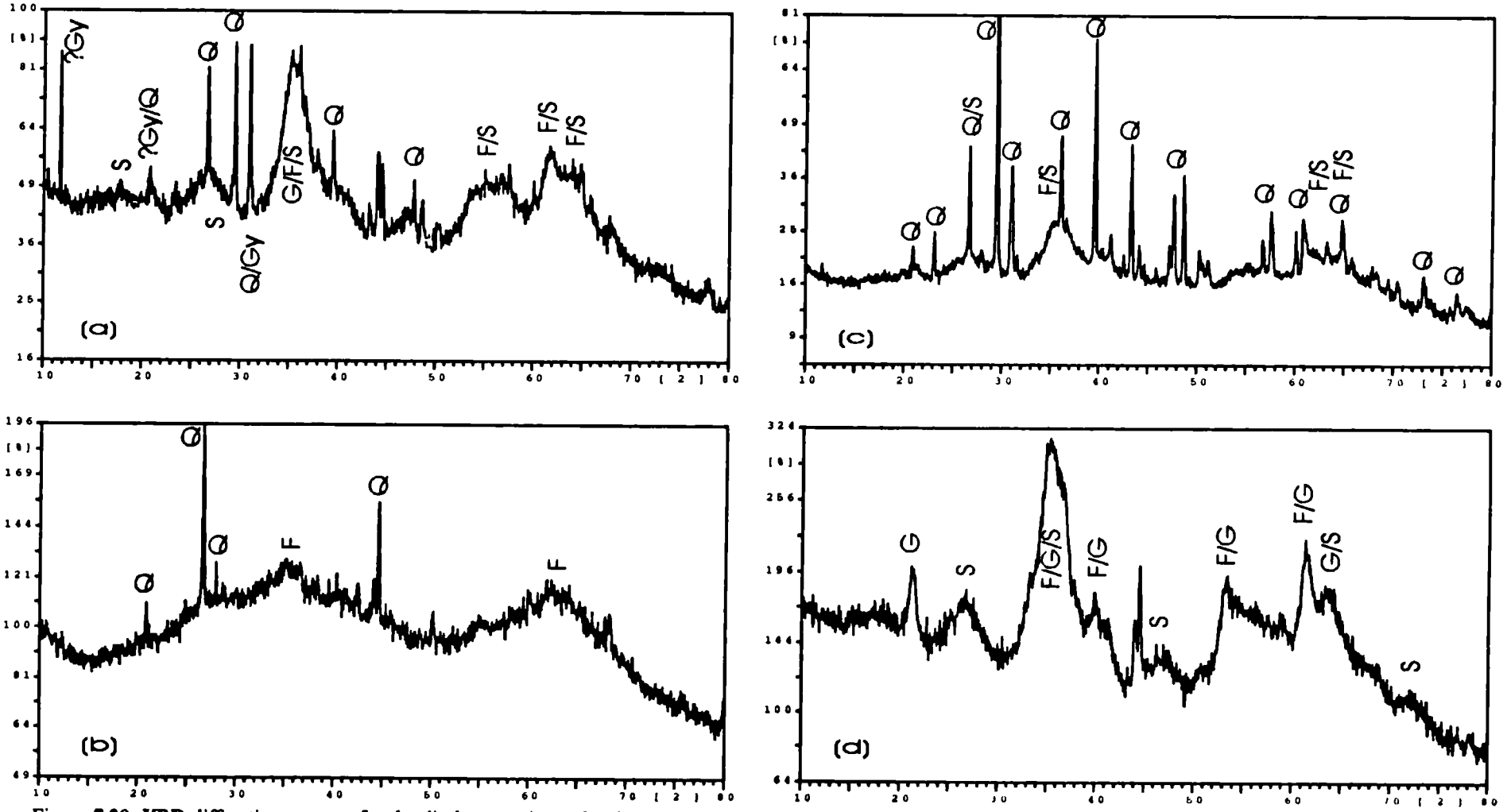


Figure 7.20: XRD diffraction patterns for the discharge point and a downstream location on two sampling occasions. (a) HR discharge (July 95); (b) HR 550m downstream from source (July 95); (c) HR discharge (July 97); HR 300m downstream from source (July 97). Goethite peaks labelled as "G", ferrihydrite peaks labelled as "F", quartz peaks as "Q" schwertmannite peaks as "S" and gypsum peaks as "Gy".

The modelling of the aqueous chemistry predicted jurbanite and alunite supersaturation at the point of discharge, moving to their undersaturation and basaluminite supersaturation downstream from the source. Gypsum has SI~0 along stream length 0-550m (July 95), 0-800m (March 96) and 0-300m (October 96) respectively. November 95 samples do not show saturation at all. The Fe^{III} minerals all show supersaturation (by several orders of magnitude) at all sites, with the exception of $Fe(OH)_{3(a)}$, which only shows supersaturation in July 95 at >550m downstream.

The concentrations of trace ions in solution are highest at this site (section 7.2.3), and thus the changes in concentration of Al and Zn in stream sediments have been shown for the length of stream sampled (figure 7.21). Aluminium concentrations can be seen to decrease from source on all occasions except March 96 and July 97, with subsequent increases, as is suggested by table 7.1. The concentration of Zn can be seen to behave in a different manner, with the highest concentrations generally occurring ~800m downstream from the source (figure 7.21b), then decreasing again for the remainder of the stream length studied.

7.3 Quaking Houses

This site is the second spoil heap discharge surveyed downstream from source (see HR above). The chemical and physical nature of this site was discussed in section 5.2. The concentration of Fe and SO_4 at the point of discharge vary from elevated to low concentrations (figure 5.5). Like HR, the dominant condition controlling the chemistry of discharge was thought to be the physical hydrology of the spoil heap "aquifer". However, this site also showed indications of a highway runoff component (section 6.2).

7.3.1 Physical characteristics

The physical characteristics of this site, relevant to the interpretation of analyses, are largely those given for HR (section 7.2). Extreme low flow occurred in July 95 with the most elevated discharge in November 95. The other sampling occasions occurred in intermediate flow conditions. As mentioned previously, March and October 96 saw cold weather / snowfall before and during the sampling visit, causing roads to be blocked and rock salt to be applied to roads.

7.3.2 Aqueous chemistry: major ions

Eh values (figure 7.22a) show a general increase along the stream length. Only the readings for November 95 do not show a decrease before the increase in Eh downstream

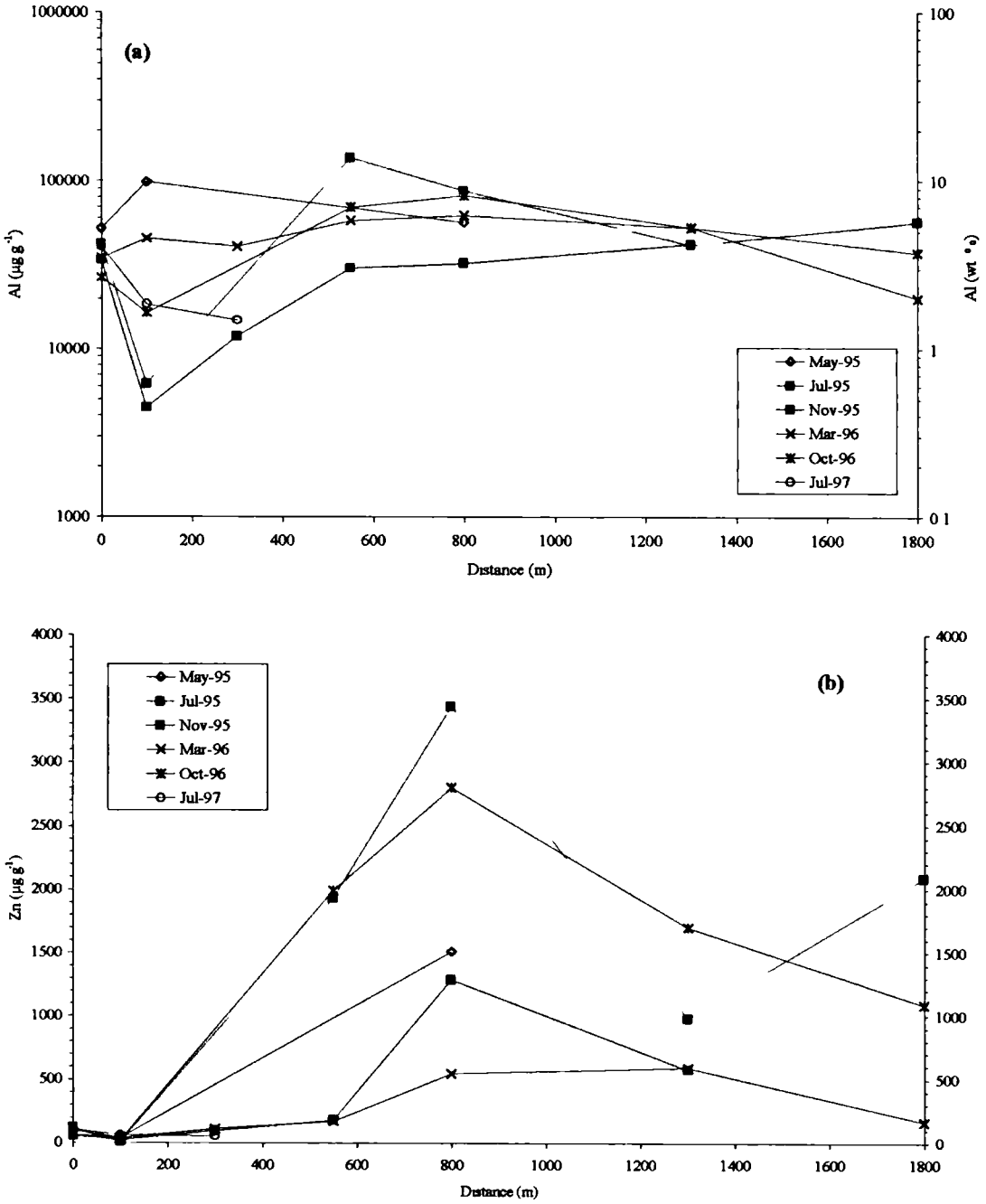


Figure 7.21: Concentrations of Al and Zn in stream sediments downstream from HR (a) Al (b) Zn

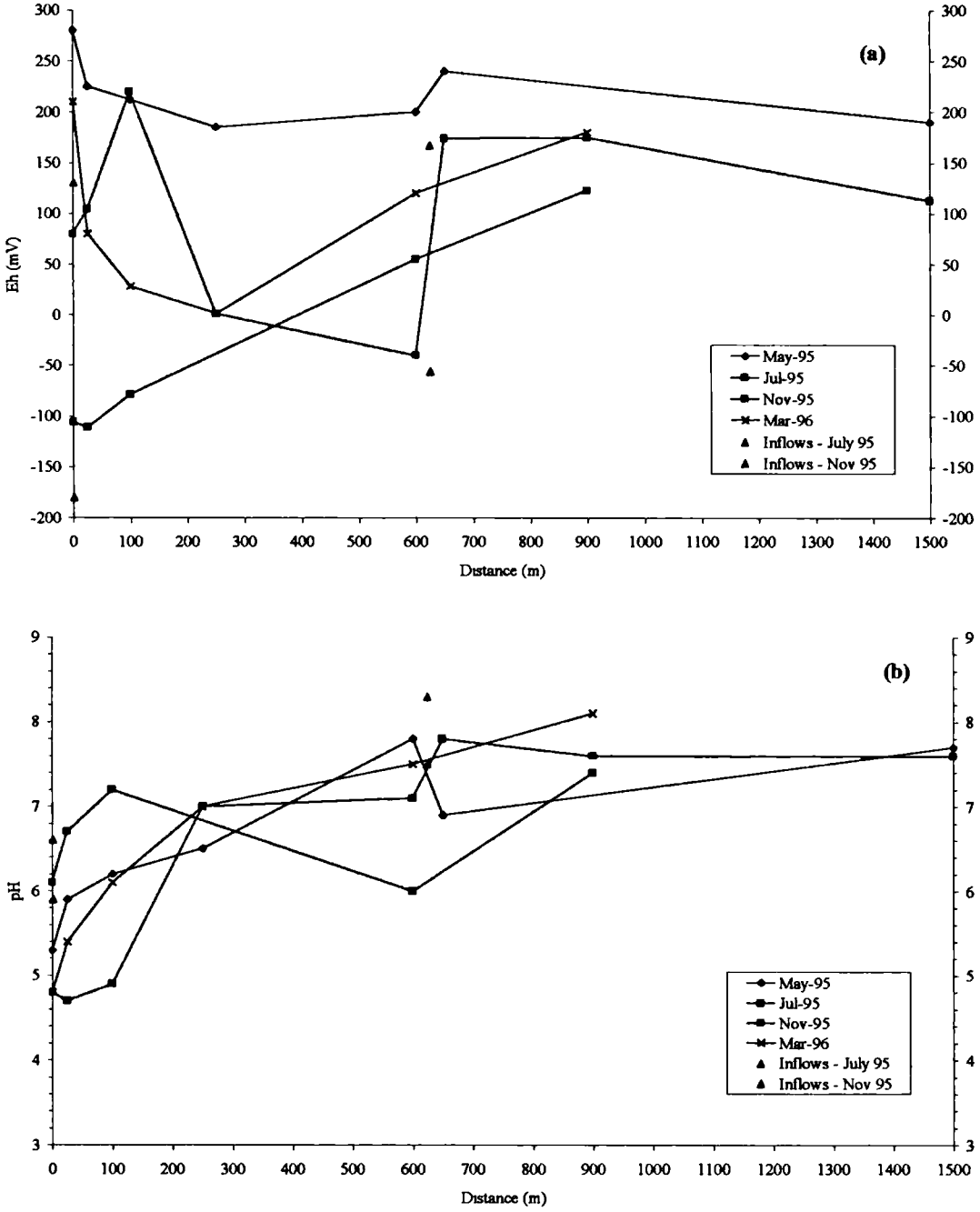


Figure 7.22: Downstream variations of selected parameters at QH. (a) Eh (b) pH. The highlighted flows are July 96 = low stream flow (red) and November 95 = highest stream flow (blue), intermediate flow conditions are shown in black.

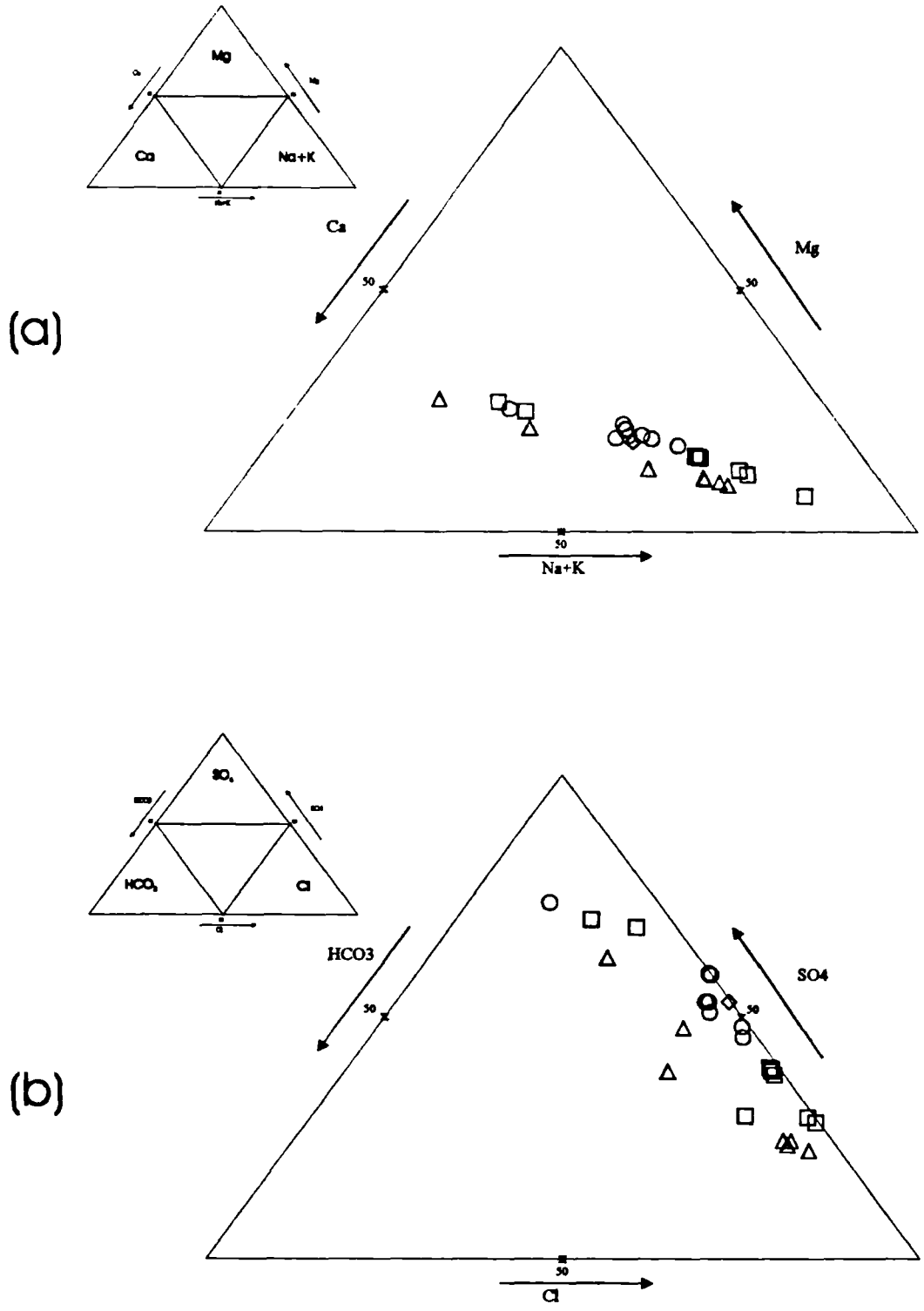


Figure 7.23: Triangular diagram of major ion chemistry at QH (a) cations: Ca, Mg, Na & K (b) anions: HCO_3, SO_4 & Cl. Labelling as follows: July 95 = circles, Nov 95 = triangles, March 96 = squares & October 96 = diamonds. Units are %meq, with 50% marked on each axis. The occurrence of dominant ions on the diagram is described by the associated inset to each plot.

from the point of discharge (figure 7.22b). The pH can be seen to increase downstream from the source. July 95 shows the most rapid rate of recovery (between 100-250m), to reach a circum-neutral pH at a similar distance downstream to that observed on other occasions (excepting November 95).

Figure 7.23 shows triangular plots of the major cation (figure 7.23a) and anion (figure 7.23b) chemistry. It can be seen that the sites are dominated by Na+K and Cl when compared with SH and HR. When Na and Cl are plotted in molar concentrations (figure 7.24) it can be seen that the concentrations correspond to a dilution of a Na-Cl solution, which explains the linearity of the triangular plots. The waters also appear to be Mg depleted in relation to Ca from that observed at other locations. The July 95 samples show the most consistent chemistry of all discharges.

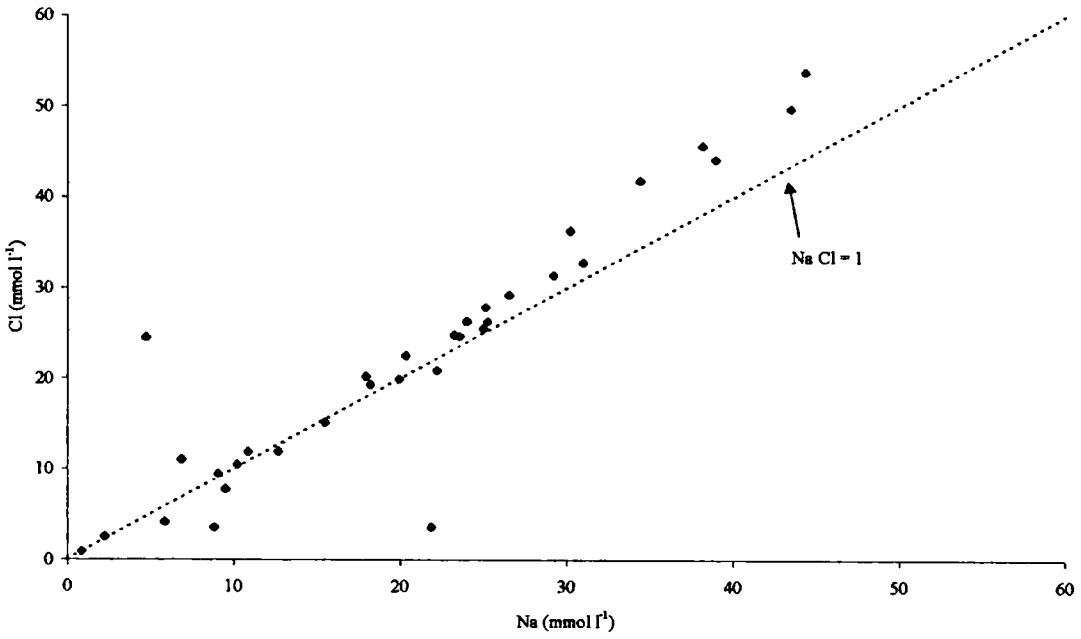


Figure 7.24: Composition of waters compared to a NaCl mixing line.

When studying the major ion concentrations downstream, Na can be seen (figure 7.25a) to have extremely high concentrations in March and October 96 at the point of discharge. The concentration shows an immediate decrease after dilution with the receiving waters. A more constant decline is then noticed until the confluence at 625m when another sharp decline in concentration caused by dilution with water of a lower Na

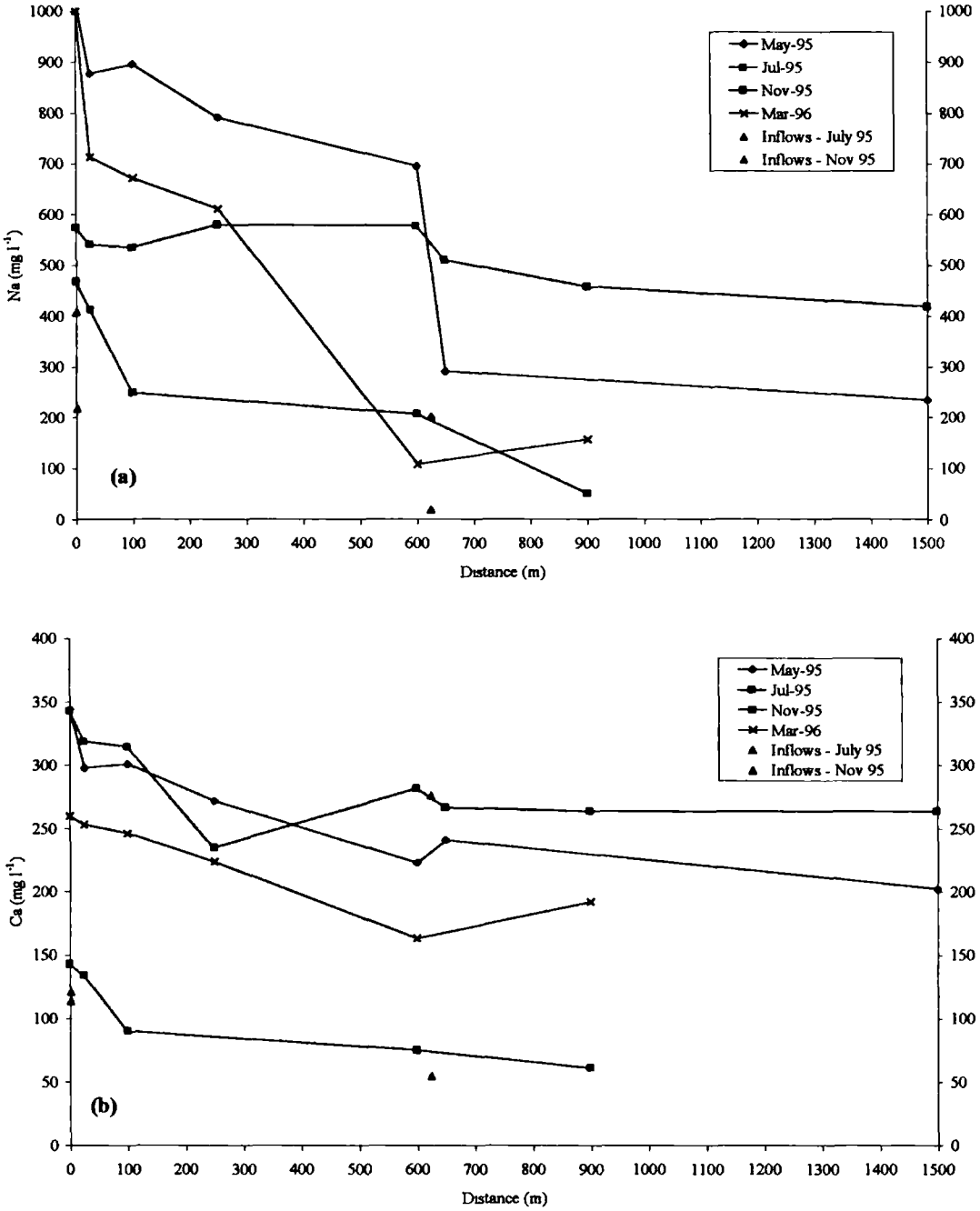


Figure 7.25: Downstream variations in selected ions. (a) Na (b) Ca (c) SO_4 (d) Cl^-.The highlighted flows are July 95 = low stream flow (red) and November 95 = highest stream flow (blue), intermediate flow conditions are shown in black. The receiving water is shown as an inflow at 10m for convenience, and a further inflow is shown at 975m.
(continued on the next page)

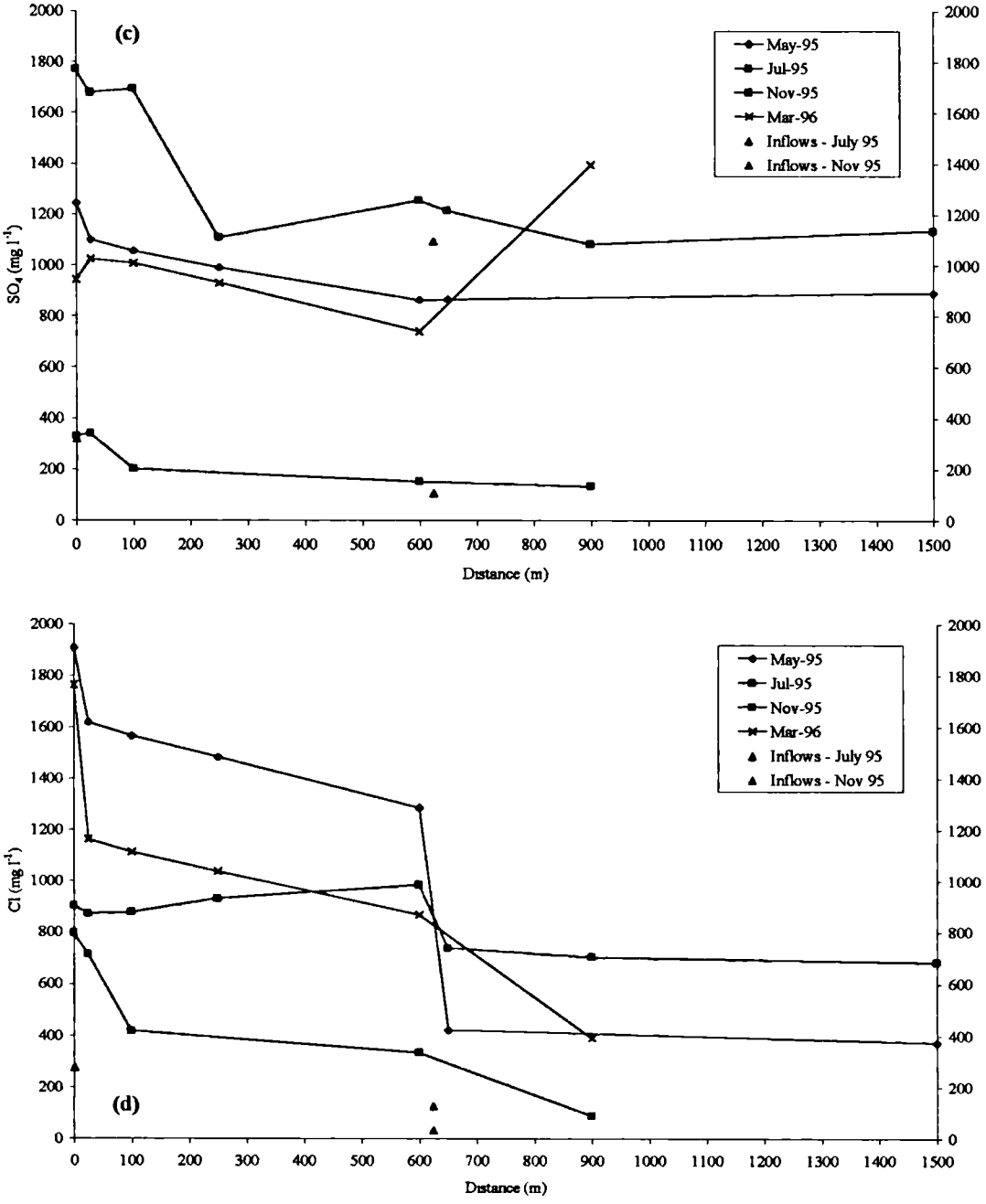


Figure 7.25: continued from previous page

concentration. In July 95 the Na concentration is higher than the November 95 sampling occasion. The concentration can be seen to be stable, with the exception of dilution by the inflowing water at 625m downstream. The dilution caused by mixing at the point of discharge was also minimal due to the very low flow of that location. In November 95 the dilution can be seen to be large from 0-100m downstream, there is then another sharp decline after 625m, due to the lower concentration and high flow volumes of the influent water. The immediate dilution at the point of discharge is minimal on this occasion, due to the high discharge volume of the main spoil effluent. It should also be noted that the Na concentration was lowest on this occasion for much of the length of stream studied on all occasions. The concentration variations observed for K were of an identical pattern to those for Na, so they are not repeated here. The Ca concentrations observed from the point of discharge are shown in figure 7.25b. It can be seen that the November 95 samples follow the pattern shown by Na, in so far that they are of consistently lower concentration along the stream length. The concentration along the stream length in July 95 (highest initial concentration with May 95) shows a sharp decline in concentration between 100-250m downstream, after mixing with the receiving waters (which were of low volume) with a subsequent increase before mixing at the confluence at 625m. The May 95 and March 96 samples show a steady decline in concentration between 100-600m downstream. Magnesium shows the same pattern of behaviour as Ca, and so is not shown here. Both these ions have a predicted aqueous speciation as that found for SH and HR, with M^{2+} and $M^{II}SO_4^{o}$ dominating, in approximately equal concentrations.

Sulphate concentrations are shown in figure 7.25c. It can be seen that the concentrations of SO_4 vary hugely between sampling visits not only at the point of discharge, but continued downstream. The samples generally show a very similar pattern of behaviour to Ca and Mg. In July 95 a decrease of >600 mg l^{-1} between 100-250m downstream was observed, after which the SO_4 appeared to be conservative. In November 95 the lowest concentrations were observed at the point of discharge (~300 mg l^{-1}), and were conservative downstream. Aqueous speciation modelling showed the influence of SO_4 species for Ca, Mg (see above), Ba, Pb, Mn, Zn and Fe (see below for Fe). However, the S^{VI} speciation is dominated by SO_4^{2-} (as for SH and HR). Chloride concentrations (figure 7.25d) show a very similar pattern of concentrations to Na (figure 7.25a) and K. May 95 and March 96 show identical patterns to Na, with a gradual dilution between the inflows at source and 625m. The July 95 sampling occasions showed very little change downstream, other than dilution at 625m. The November 95 samples halve in concentration from 800 mg l^{-1} at source by 100m downstream, a further gradual decline

to the confluence at 625m can be seen to occur. Chloride is dominated by the Cl^- ion, but Cl^- complexes are predicted to be of percentage concentrations for minor ions, see Fe below. Alkalinity is generally low from the discharge point.

Iron concentrations are shown in figure 7.26a. It can be seen that the November 95 samples show a more constant, and finally higher, concentration than the other sampling occasions. The July 95 samples showed a constant rate of decrease between source and 600m downstream. The rate of decline in May 95 is lower than that of July 95 from 0-600m and March 96 0-250m, although that rate increases from 250-600m. Figure 7.26b shows that this rapid decline is caused by the transfer of Fe_{aq} to Fe_{ss}, although after 300m both decline rapidly, and only after 600m does $Fe_{ss}>Fe_{aq}$. November 95 samples show a similar pattern to those exhibited for this sampling occasion at SH and HR. The March 96 samples show an intermediate behaviour to the extreme flow conditions, with $Fe_{aq}<Fe_{ss}$ further downstream than November 95, but not as far as July 95, and the Fe_t at 900m downstream being greater than that in November 95. Speciation modelling shows that complexes are important to the understanding of the water chemistry. The neutral SO_4 complex (table 7.2) is the second most dominant ion behind Fe^{2+}, which accounts for 75% of the predicted Fe^{II} speciation (using PHREEQ-C (Parkhurst, 1995)) throughout the stream length on this occasion. The concentration of Cl in these waters is shown to be important by the $FeCl^+$ ion accounting for ~1% through the stream length. The ion $FeHCO_3^+$ increases as the alkalinity increases downstream from source, this is associated with a concomitant decrease in Fe^{2+} and $FeSO_4^o$. This pattern of concentrations is repeated on the other sampling occasions, with the exception that $FeSO_4^o$ is of a lower proportion, and Fe^{2+} is of a higher (~80-90%) proportion.

Table 7.2: Iron(II) speciation predicted by PHREEQ-C for QH downstream from the discharge in July 1995.

Distance (m)	*% Fe^{2+}*	*% $FeSO_4^o$*	*% $FeHCO_3^+$*	*% $FeCl^+$*	*Fe^{II} (mmol l^{-1})*
0	77	23	0.01	1.1	**0.65**
100	75	24	0.006	1.1	**0.30**
600	77	20	1.5	1.3	**0.007**
900	74	18	5.5	0.9	**0.002**

The Fe^{II} concentrations and the speciation shown are predicted by PHREEQ-C model (using the WATEQ-4F database) from measured ion concentrations.

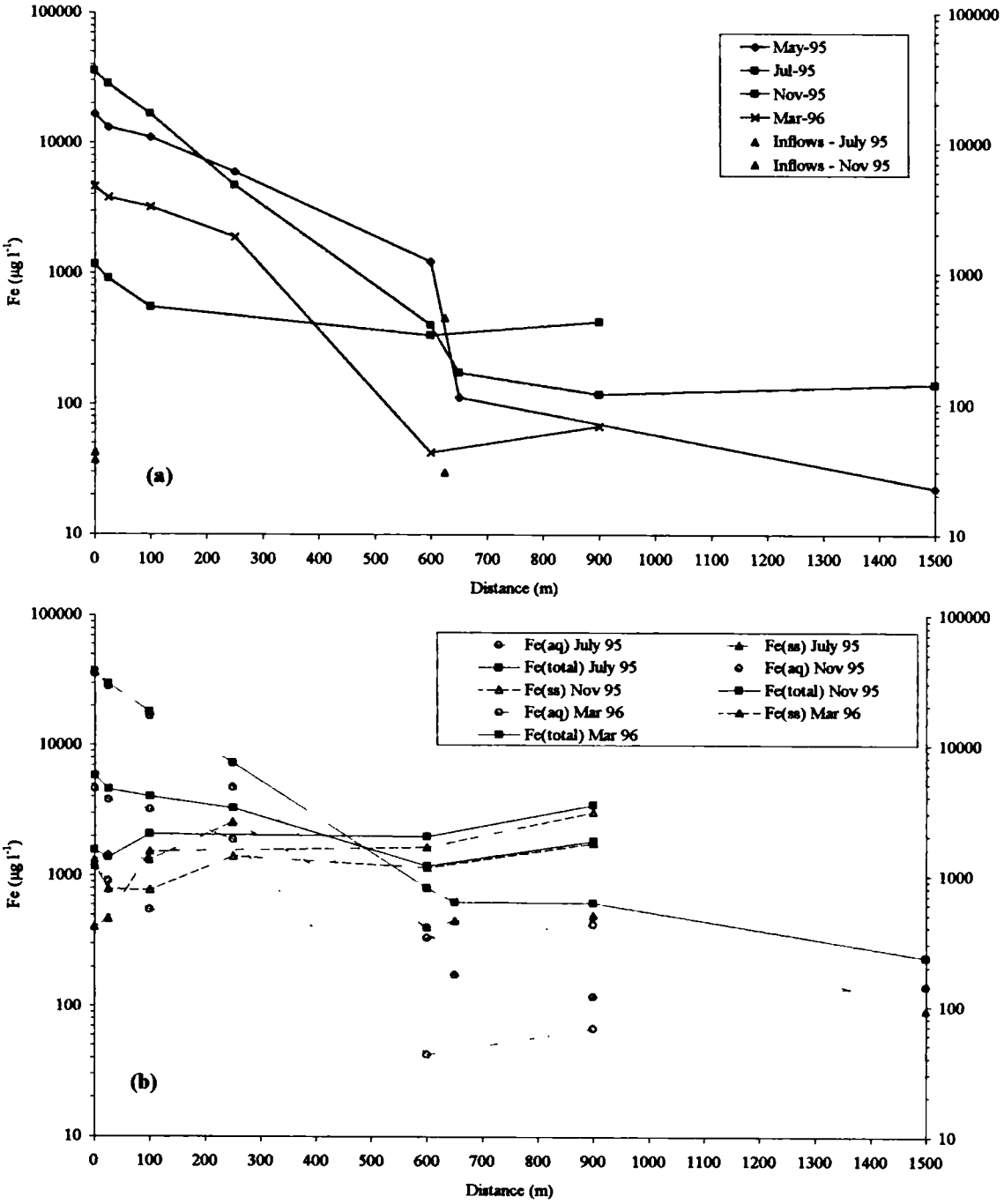


Figure 7.26: Downstream variations in Fe loading in the stream system at QH. (a) dissolved Fe variations downstream from source. The highlighted flows are July 95 = low stream flow (red) and November 95 = highest stream flow (blue), intermediate flow conditions are shown in black. (b) Comparison of Fe loading in dissolved and suspended phases. Solid lines = Fe_t, dotted lines = Fe_{aq} & dashed lines = Fe_{ss}. Low stream flow = July 95 (red), highest stream flow (blue), and intermediate stream flow = March 96 (grey). The receiving water is shown as an inflow at 10m for convenience, and a further inflow is shown at 975m in both figures.

7.3.3 Aqueous chemistry: minor and trace ions

Figure 7.27a demonstrates the downstream changes in chemistry of Mn. It can be seen that the highest concentrations along the stream length occur in low flow conditions (July 95), in highest flow conditions the concentration of the main stream is actually increased by the influent water at 625m. The concentrations of May 95 and March 96 samples decrease gradually along the length of stream until 600m, May 95 then decreases by a large amount due to the confluence. In the July 95 samples, the largest decrease is at the 625m confluence, with the concentration decreasing from ~10000 μg l^{-1} to <100 μg l^{-1} at 1500m.These concentration changes dominate the Mn_{aq} stream loading for the length of stream observed, as was found for SH and HR.

Dissolved Al varies from 20000 μg l^{-1} (July 95) in low flow to ~200 μg l^{-1} in high flow (November 95) at the point of discharge (section 5.4). This elevated concentration in July 95 rapidly drops to <300 μg l^{-1} between 0-250m, with the concentration falling from 10000 μg l^{-1} at 100m to 270 μg l^{-1} at 250m (figure 7.27b). On all other occasions, the Al_{aq} is dominated by Al_{ss}, this occurs after 250m in July 95. Figure 7.27c shows the variations in Zn concentrations downstream from source. This shows that the concentrations on all occasions, except November 95, were ~2700 μg l^{-1}, which subsequently declined after dilution at the source, then continued to decrease downstream. The scale of decrease due to dilution at 625m was greater for May 95 than July 95 due to the larger volume of water in the influent stream on the first of those occasions. Copper shows a very similar trend to Zn (figure 7.27d). The November 95 initial concentrations do not vary downstream, and those of the other sampling occasions reach this terminal concentration range at 600m downstream. The July 95 samples show the greatest rate of decline between 100-250m downstream.

7.3.4 Stream precipitate chemistry

There was never a large amount of precipitation observed at this site, as demonstrated by plate 5.5 (e.g. compare with plate 5.4). Thus only Fe concentrations in stream sediments are shown in figure 7.28 and insufficient sample could be collected to make XRD analysis of precipitate possible. Figure 7.28 shows that the concentration of Fe is never much more than 10% in the stream sediment, and that after peaking at a value of 30-40% at 100m downstream, the concentration rapidly declines to <10%, and invariably decreases to 1-2% after the confluence at ~625m downstream.

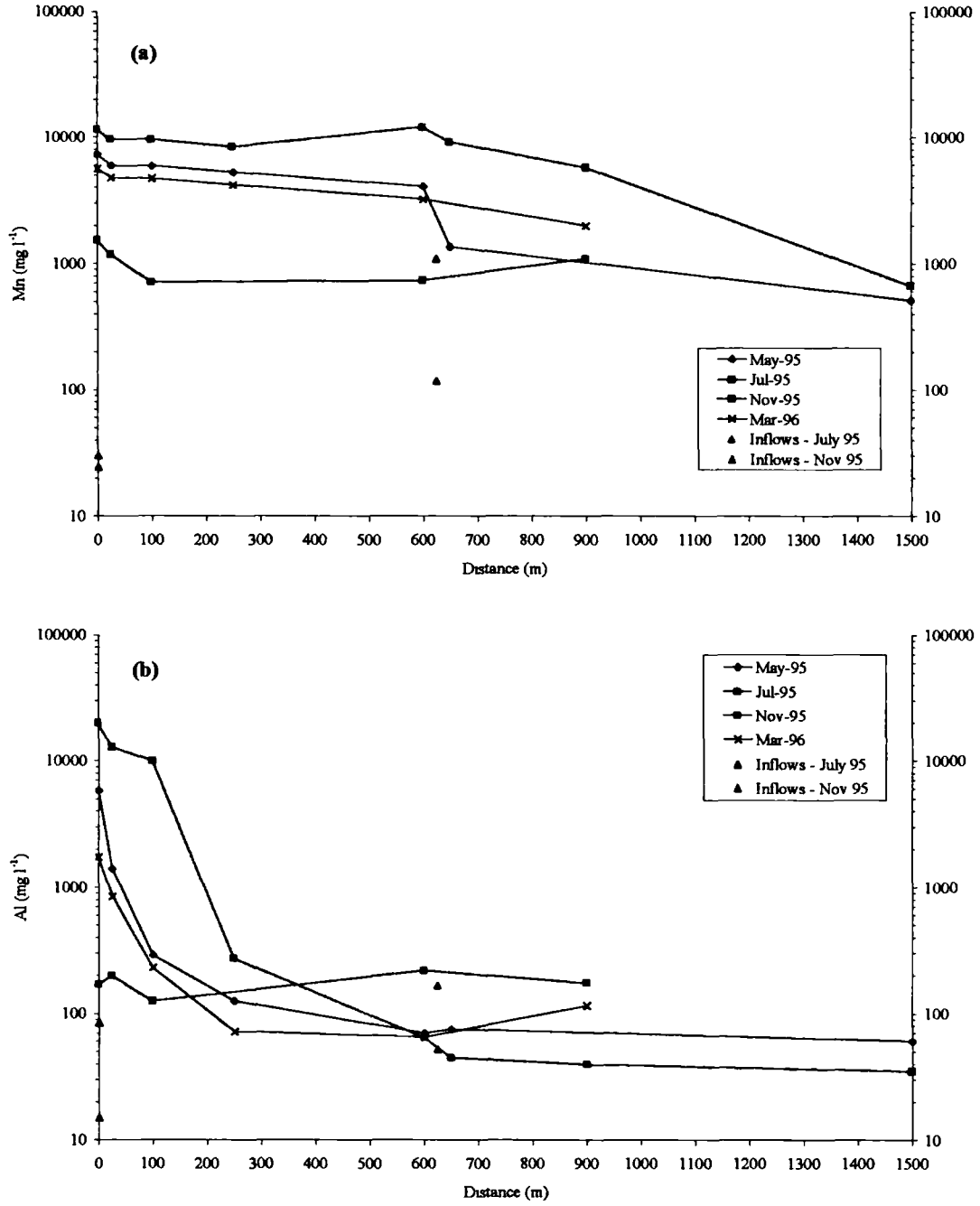


Figure 7.27: Downstream variations in selected ions. (a) Mn (b) Al (c) Zn (d) Cu. The highlighted flows are July 95 = low stream flow (red) and November 95 = highest stream flow (blue), intermediate flow conditions are shown in black. The receiving water is shown as an inflow at 10m for convenience, and a further inflow is shown at 975m.

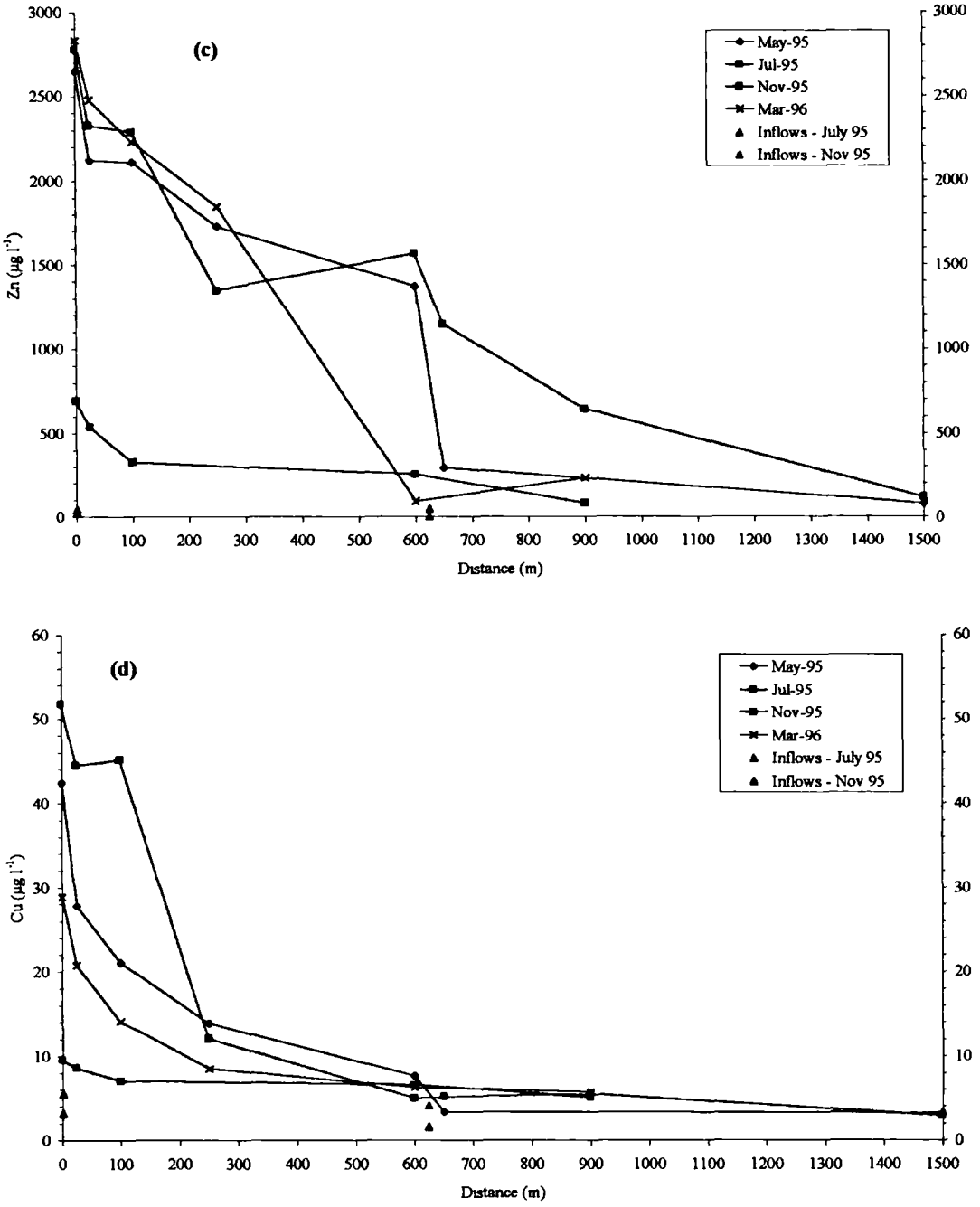


Figure 7.27: continued from previous page

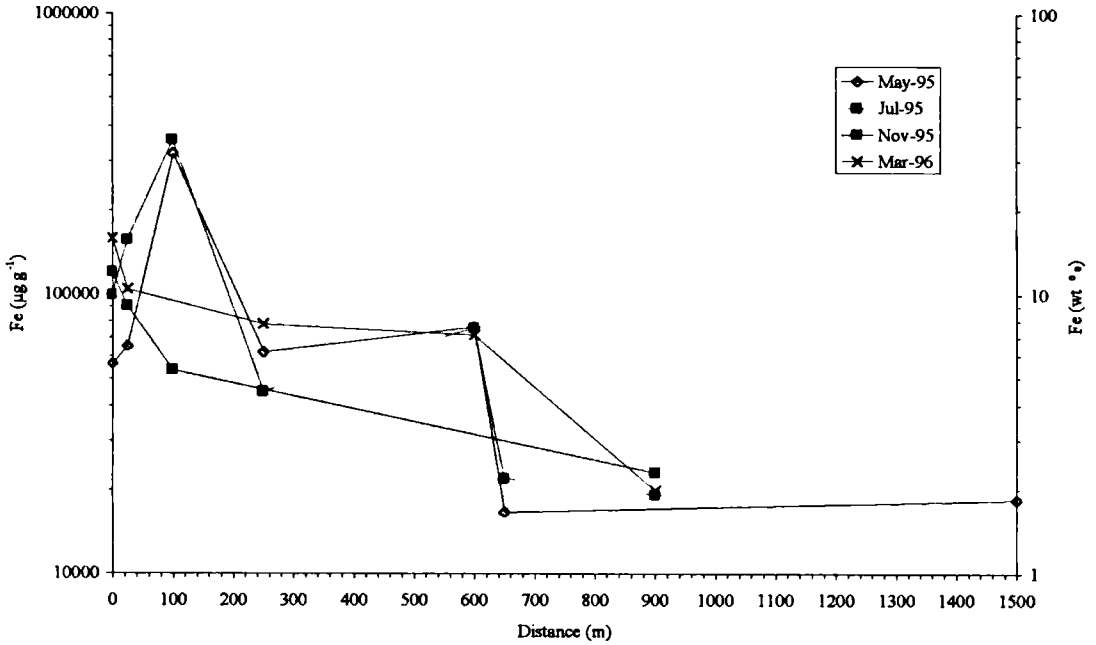


Figure 7.28: Concentrations of Fe in stream sediments downstream from source at QH.

7.4 Summary

This chapter has described the variations in chemistry of the three phases (dissolved, suspended and precipitate), and mineralogy of selected precipitates, measured during this study downstream from three points of discharge. The downstream declines of selected elements have been shown for Stony Heap (SH), a deep mine drainage, and Helmington Row (HR) and Quaking Houses (QH), spoil heap discharges. The processes controlling the chemical and mineralogical variations observed here will be discussed in chapter 8.

8.0 Processes controlling chemistry downstream from coal mine and spoil water discharge

This chapter will discuss the chemical, mineralogical and hydrogeochemical modelling results presented in chapter 7. The results will be drawn together to produce a discussion of those processes causing the observed changes in aqueous chemistry downstream from one mine and two spoil heap discharges being studied. The discussion will be focused on those factors which control the major ion chemistry, namely Eh and pH in section 8.1. Section 8.2 will assess the behaviour of the trace ions downstream in order to elucidate the factors controlling their behaviour. Section 8.3 will briefly highlight the examples of chemical disequilibria found in this study. Section 8.4 will discuss the data acquired in this study with respect to the potential water toxicity variations in differing conditions and from differing sites.

8.1 Controls on major ion chemistry downstream from mine and spoil discharge

This section will show which major ions in solution are controlled by dilution or reactive loss downstream from the point of mine / spoil water emergence. The potential reactive processes which can affect the concentration of ions in solution are precipitation and sorption. Precipitation is delineated by the observation (here using XRD) of mineral phases in ochreous precipitates. Sorption is studied by comparison of minor ion concentrations with controlling factors such as pH and suspended sediment concentrations. The usefulness of hydrogeochemical modelling (with specific reference to PHREEQ-C, used here) in the context of predicting mineral phases precipitating is also discussed in section 8.1.3. As has been the case throughout this thesis, Fe is included in the discussion as a major ion, however, because ochreous material is evident on the stream bed of all the sites, discussion of this ion is deferred until section 8.1.2. Aluminium is discussed in the context of its potential effect on the behaviour of S in solution. This section then discusses the sinks for the major ions lost from solution due to precipitation. This information will be used in assessing the behaviour of selected trace and minor ions in section 8.2.

8.1.1 Dilution

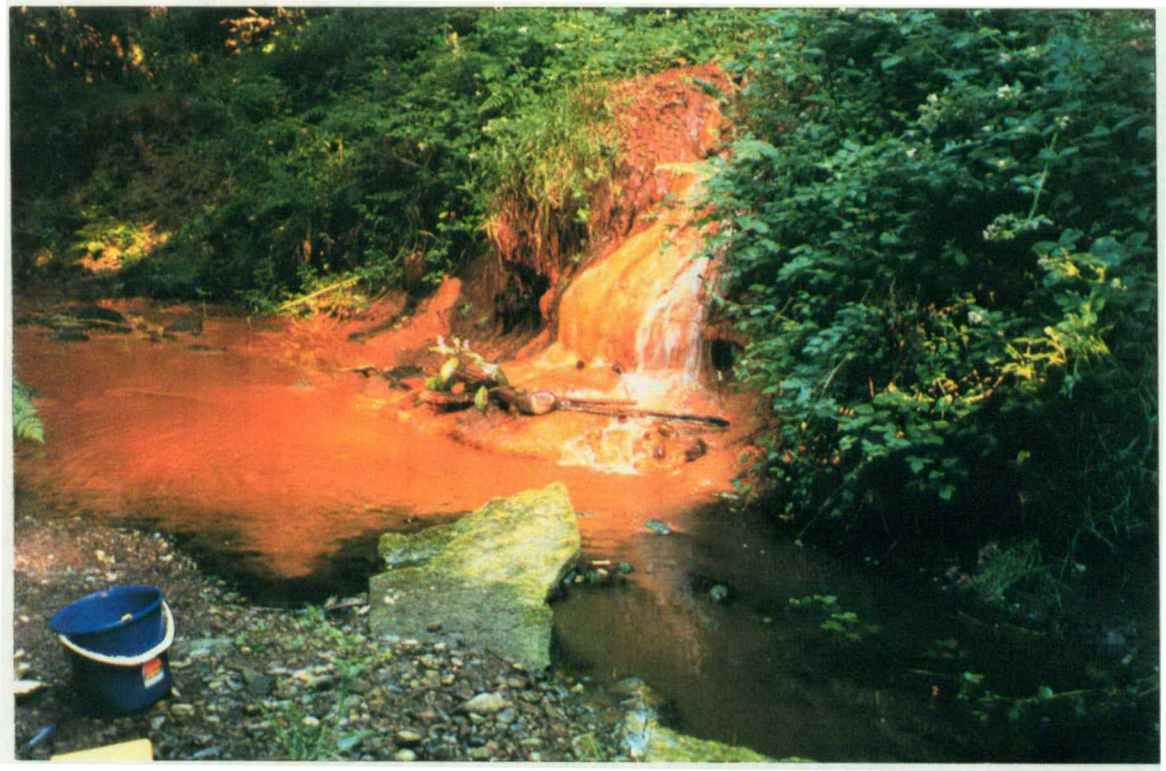
Dilution is a process which will act to change concentrations of conservative ions in proportion to the ratio of mixing of two or more water compositions. Conservative ions are those not generally subject to reaction in a (near)-surface environment, and thus their concentrations are affected by changes in the water mass, caused by addition (dilution) or loss (evaporation) of water. Delineation of this depends on differing concentrations of

at least one conservative ion (where there are two waters) in each mixing water. Reactive loss of ions from solution can be discriminated by the fact that the decrease in their concentration will exceed that observed for conservative ions. In addition to simple dilution, the mixing waters can induce reactive loss due to their chemical properties being different to those of (in this instance) the mine drainage, having for instance a greater buffering capacity. A visual example of the effect of dilution by high and low flow volumes in the receiving water at EY is shown in plate 8.1. It can be seen that the impact of the discharge (constant volume and consistent chemical composition) is much greater in low flow of the receiving water than in high stream flows.

Sodium, K and Cl are frequently quoted as conservative tracers used in their naturally occurring concentrations or as injected tracers into a hydrologic system (Appelo & Postma, 1994). The only mineral precipitation which could affect the concentrations of Na, K and Cl are of the jarosite group (Na and K), none of which occur in the variety of geochemical environments found in this study (sections 7.1.4, 7.2.4 & 7.3.4). Simple concentration plots downstream from a point source in a stream can give an indication of whether dilution and / or reaction can be causing variations in the chemistry observed, assuming that surface water inflows are marked (e.g. figure 7.1). A further test of reactive loss from the stream system is to plot the ratio of the element of interest to a conservative element. Sodium and Cl are two ions which readily lend themselves to the assumption of conservative behaviour, and occur in detectable concentrations in all samples, because they are major ions. However, in mine drainage studies other ions, such as SO_4 have been assumed to be stable in solution and thus used as tracers of mine drainage waters, although generally in a qualitative sense only (Nordstrom & Ball, 1986).

The results for the deep mine discharge Stony Heap (SH) were presented in section 7.1. The triangular diagram of the major ion chemistry facies at SH (figure 7.2) shows that the downstream dilution of waters appears to take place in November 95 and March 96. Figure 7.3 suggests that the major ions (except Fe) are conservative at SH downstream from the point of discharge. When there is no dilution close to the point of discharge in July 95 there was no change (beyond the measurement uncertainty fluctuations) in the concentrations of Ca (and Mg), Na (and K), Cl, HCO_3 and SO_4 from the point of discharge to the last point of sampling, apart from dilution effects at the confluence at 975m, where the chemistry of the inflows are also shown (figure 7.3). On the sampling occasions other than July 95 dilution did occur immediately below the point of discharge, and this dilution as well as that at 975m were responsible for controlling the

Plate 8.1: Edmondsley Yard Drift discharge in high and low flow of receiving water. (a) The discharge entering the Cong Burn in when the river was in low flow (July 1995). The stream sediment after mixing of the two waters contained 41% (wt.) Fe (b) The discharge entering the Cong Burn when the river was in high flow (November 1995). The stream sediment after mixing of the waters contained 2.5% (wt.) Fe





concentration of the 7 ions mentioned (Ca, Na, Cl, HCO_3 and SO_4 shown in figure 7.3), as confirmed by figure 7.4b & c (SO_4 dilution shown). As described in section 7.1.2, the Na and Cl can be seen to follow a Na:Cl mixing line (figure 7.4a) between a water type with negligible Na and Cl and one which contains a high concentration of Na-Cl relative to the first water type. The source of the high Na-Cl water is postulated to be local road runoff which, when rock salt is applied in periods of cold weather, drains into local water courses and ground waters as has previously been recorded in other studies (section 3.3). These high Na and Cl concentrations thus "fingerprint" some of the inflow to the stream as being from road drainage. Figures 7.4b & c also show the dilution effect of two water masses. Sodium and Cl could both therefore be used to study dilution effects, however, the better precision of the Na measurements (section 4.4) means that Na is the preferred ion for studying molar ratios of a conservative element with another element, and shall be used as such henceforth.

As cited above and in section 2.1, SO_4 has been used as a conservative tracer in mine water studies, which would appear to generally be valid in this stream system. The conservative behaviour of Ca and SO_4 is explained by their behaviour in waters of the chemistry found at this locality. The circum-neutral pH conditions found downstream from this discharge means that both this ions are expected to be conservative in solution, unless the solubility of gypsum is exceeded (section 2.3.2). Gypsum was not detected using XRD analysis and modelling using PHREEQ-C did not predict gypsum precipitation (section 7.1.4). When there is no dilution (July 95 until 975m) the ratio of $Cl:SO_4$ and $Na:SO_4$ does not change downstream, whilst an input of a Na:Cl water (November 95) within the first 300m of the stream and minewater confluence, causes the ratio to change considerably as the mixing water is depleted in SO_4 (figure 7.3d & e) and elevated in Cl with respect to the mine water. The reason for the ratio falling off again after 450m is not clear, however it is postulated that this is as a result of overland flow from adjoining arable land, which causes the concentration of both ions to drop (figure 7.3d & e), and that the effect on Cl is larger because the initial concentration was larger. Sulphate concentrations can be decreased in the presence of high concentrations of Al, due the precipitation of Al-SO_4 minerals (section 2.3.2). However, concentrations of Al are too low (<70 $\mu g\ l^{-1}$) here for that to be considered possible. Aluminium will be discussed further in section 8.2.1 as a minor ion.

Bicarbonate would be expected to vary as a result of changes in pH (section 2.2.2), thus the lack of any major fluctuations at this site are explained by the consistently circum-neutral pH of the discharge and stream waters.

Helmington Row (HR) differs from SH because it is a spoil heap drainage and the spoil heap itself is the sole source of water to the length of stream along which samples were collected. A highly variable discharge chemistry for this site was shown in section 5.2, and this is reflected in the downstream chemistry presented in section 7.2. Recharge including runoff from roads was not found at this site (Na-Cl in lower concentrations than at QH). Sodium, K and Cl are assumed to be conservative, and Na is used to study reactive loss in the stream system. The drainage from higher up the spoil heap than the discharge can be distinguished from the spoil heap drainage by a different Na:K and figure 7.17b confirms that no dilution took place in July 95 (low flow), which is important in assessing reactive loss from the stream system.

It was shown in section 7.2.2 that Ca is not invariably conservative in this stream system. In July 95 (low flow) the concentration could be seen to decrease downstream from the point of discharge, with no dilution affecting the concentration. This will be discussed further in section 8.1.2. There is a decrease in some other months, however, where dilution is a component of that decline on mixing from the point of discharge (figure 8.a1). It should be noted that Mg follows the behaviour of Ca and thus is not shown here. Sulphate is not conservative in all conditions either, as shown by figure 7.13b. The normalisation of SO_4 to Na downstream from the point of discharge shows those parts of the stream where in May and July 95 there is a net loss of SO_4 from the stream. This too will be discussed further in section 8.1.2. However, it should be noted that when concentrations of Ca and SO_4 are low (figure 7.11a & 7.12c), these ions are conservative (as discussed for SH above) and either do not vary in concentration or are affected solely by dilution (e.g. figure 7.23b for November 95). Alkalinity was also not conservative in solution at this site (figure 7.24d) in July 95. Minor fluctuations occur on the other occasions, but would be expected from the pH variations downstream (figure 7.9b), irrespective of any other processes which may be taking place (section 8.1.2).

Quaking Houses (QH) is a spoil heap drainage. At QH the concentrations of Na and Cl dominate the water type (figure 7.23) and would appear to follow a Na-Cl mixing line (figure 7.24), as described for SH, which is attributed to road drainage, resulting from run-off in cold weather (March 96 and October 96) when rock salt had been applied (Younger *et al.*, 1997). Downstream (0 - 100m) from the point of discharge a sharp decline in Na, K and Cl concentrations is found on all occasions, except July 95 (figure 7.25), due to dilution by the receiving stream. The chemistry of the inflows in July and November 95 are shown, and would appear to confirm this supposition. These values enable the dilution caused by the inflows to be calculated as a ratio. However,

particularly in high rainfall, this can be confounded by further decline due either to influent groundwater flow or overland flow in addition to mixing by streams.

Calcium and SO_4 show a similar pattern to Na and Cl (figures 7.25b & c), which is also attributed to dilution in all cases with the exception of 100-250m downstream of the discharge in both cases. This will be discussed in more detail in section 8.1.2 with the data for HR which showed a similar trend. The occasions when Ca and SO_4 are affected purely by dilution are when the stream has lower concentrations of the major ions and lower pH, as observed for HR.

This section has used the conservative behaviour of Na, K and Cl in stream systems to examine the behaviour of the other major ions. It has been shown that when there is low pH (<~5) and high Ca and SO_4 concentrations the latter two ions cannot be presumed to be conservative. This will be discussed more in the next section. However, in most situations Ca and SO_4 have been affected by dilution alone. The sources of high Na, K and Cl downstream from SH and QH "fingerprint" the inflow of road drainage, and are not linked to mine / spoil water evolution. The behaviour of Ca and SO4 in these conditions will be discussed in the next section with Fe for which ochre precipitation demonstrates reactive loss.

8.1.2 Reactive loss from the aqueous phase

This section will discuss the behaviour of those major ions present in concentrations too elevated to be stable in solution. Iron is known to be reacting to form a solid phase, as evidenced by the actively precipitating ochreous material in the stream systems studied. The pH and redox behaviour of the waters are also discussed herein, for reasons explained below. The behaviour of Ca and SO_4 when subject to reactive loss in streams impacted by spoil heap waters are discussed at the end of this section.

Iron is the element most obviously undergoing reaction in the stream course, as seen by the voluminous ochreous deposits at some of the discharge locations (Plates 5.3 & 5.4) sampled throughout this research. Iron is the dominant ion in the (upper reaches of the) stream systems studied (sections 5.1 & 5.2) and it largely occurs as Fe^{II} at the point of emergence (section 5.3). Both the oxidation of Fe^{II} and hydrolysis of Fe^{III} (equations 2.2 - 2.3) affect the pH-Eh status of the stream water, suggesting that these parameters will not be stable in the presence of precipitating Fe, irrespective of any other reactive processes which may be taking place. This section will briefly discuss these parameters individually, prior to entering into a unified treatment for selected samples.

The oxidation and hydrolysis reactions of Fe^{II} and Fe^{III} are shown in section 2.2. The Fe^{III} produced in solution due to the oxidation of Fe^{II} is then hydrolysed to form an amorphous ferric hydroxide mineral (equation 2.3). $Fe^{III}_{(aq)}$ has a very low solubility and the rate of reaction to form a solid phase is rapid where pH is circum-neutral (Cornell & Schwertmann, 1996) (section 2.2.3), precipitating at the point of discharge and downstream from the point of discharge (such as shown in plate 5.1). This discussion will be resumed below, following an introductory discussion of pH and Fe variations downstream from the point of emergence, which equations 2.2 - 2.3 show to be the other parameters affected directly by the oxidation of Fe^{II}.

The controlling process on the concentration of dissolved Fe is evidently reactive loss, as observed from the precipitation of ochre at the point of discharge and along the initial part of the stream length in all cases studied here. Validation of this will be presented, the method of which is extended to other elements affected by reaction in section 8.2.1. The concentrations of Fe downstream from the points of discharge are shown in figures 7.5, 7.14 and 7.25 for SH, HR and QH respectively. It can be seen that there are decreases in concentration, confirmation that these are due to reactive loss is shown by the precipitation of ochreous minerals in the stream (section 8.1.3).

The mechanism of decline of total Fe from the stream column is shown in figures 7.5b, 7.14b and 7.25b as a transfer from the dissolved phase to the suspended phase, which could cause a visible opacity in the stream water. This suspended material will then settle out to form part of the stream sediment, the causes of the differential rate in this process are discussed in section 8.1.3.

Sulphate is not suitable for the investigation of dilution along stream system at HR, because it is not invariably conservative in solution (figure 7.13). However, dilution is shown immediately after the point of emergence on all occasions except July 95 (figure 7.17a), with November 95 showing the greatest dilution of the spoil heap discharge for SO_4 at HR.

The Eh and pH changes downstream from the point of discharge are shown in figures 7.1, 7.9 & 7.21 for SH, HR and QH, respectively. The SH discharge shows a decrease in Eh from the initial value (which was generally the lowest value recorded), with a subsequent increase (figure 7.1). The initial decrease is most pronounced in July 95 (low flow conditions), and least pronounced in November 95. The general pattern is followed

on all occasions, with March 96 standing out as the sampling occasion on which Eh maintained a low value along the whole length of stream sampled. At HR the decrease is also most pronounced in July 95 (figure 7.9a), but the Eh does not show an increase within the length of stream studied. The other sampling occasions at HR show a general decline, either immediately after the point of discharge, or after mixing with surface water from the spoil heap (May 95). The QH stream system also generally shows a decrease in Eh downstream of the point of emergence (figure 7.22a). The only exception to this being July 95 (low flow), where there is an increase in the measured Eh prior to a decrease. On this occasion the dilution by an inflow at ~600m seems to dominate the Eh downstream from that point. In November 95 (high flow), the opposite occurred with the inflow showing little influence. A more major impact was observed for this site than that shown for SH.

An important factor in explaining these changes in the oxidation potential of the streams (as measured with Pt-electrode meter) is the reactions of Fe^{II} downstream from the discharge. As described in section 2.2.3, Fe^{II} is unstable in water in equilibrium with an oxidising atmosphere, which it encounters upon entering a surface stream system. Equation 2.2 shows that Fe^{II} is oxidised by $O_{2(aq)}$ to form Fe^{III}, consuming $0.5O_{2(aq)}$ for every mole of Fe^{II} oxidised (equation 2.2). The electron donor is thus depleted in the stream system, but is constantly replenished from the atmosphere in this open system. Thus the Eh of the stream may be expected to reduce further than its initial value, in the situation where the $O_{2(aq)}$ is replenished more slowly than it is consumed. The other assumption in predicting a reduction in Eh is that the Fe^{II} concentration is sufficiently high to control the stream system Eh in a quasi-equilibrium (sections 2.2.3a & 4.6).

pH tends to show an increase along the length of stream until circum-neutrality has been reached from the initial value (figures 7.1b, 7.9b & 7.21b). SH has a very consistent initial pH because it is a deep mine drainage (section 5.1.2), these similarities continue along the stream course independent of the degree of dilution of the mine water by the receiving stream (figure 7.1b). The increase in pH is thus reasonably uniform between sampling occasions, despite differing dilution factors (high in November 95 and negligible / zero in July 95). The pH values shown in figure 7.1b are all clustered around 7, so the fluctuations which can be seen on figure 7.1b are not likely to represent a significant changes in pH, and the discharge can be viewed as not perturbing the pH of a circum-neutral drainage system.

The pH from the point of discharge at HR and QH are more variable due to their being spoil heap drainages (section 5.2). The pH in July 95 at HR (figure 7.9b) shows the greatest rate of increase from 3.5 at the discharge to 7.6 at 800m downstream (figure 7.9b). The pH has reached circum-neutrality by 800m downstream on all sampling occasions at HR, despite the differing initial values, this shows that the rate of increase is greater when the initial pH is lowest. The pH is not as low at QH as it is at HR, however the same generalisation can be made for this locality. The rate (with respect to distance downstream) of increase of pH is greatest in low flow conditions in July 95 from 4.8 at discharge to 7.0 by 250m downstream; on this occasion the stream had flowed some 100m from the point of emergence before the pH began to increase.

Thus there is a general rule that the rate of increase of pH is greater when the initial pH from the point source into the stream is lowest. This is not related to dilution, because the three sites discussed in this chapter underwent zero or minimal dilution when the pH was lowest (July 95) at the two spoil heap discharges (HR and QH). The amelioration of pH was more rapid at QH than at HR (figures 7.21b & 7.9b), this is thought to be due to the greater elevation of ion concentrations from the point of discharge at HR than was measured at QH (section 5.2). There are only 3 occasions on which a decrease of pH was observed between sites downstream from source. The decreases at 100m at SH (July 95) is from 7.5 to 7.0, however it should be born in mind that this represents a difference in concentration of H^+ of only $0.5*10^{-7}$ mol l^{-1}. More significant is the change in pH from 7.6 (450m) to 6.6 (950m), in July 95 which represents a 10 fold increase in H^+. The other pH decrease is in November 95 (from 950 to 1000m downstream), but once again represents a change which is small in terms of the H^+.

A point of major interest in relation to the measured pH values is that, with reference to equations 2.2 & 2.3, it can be seen that a decrease in pH would be expected from the generation and hydrolysis of Fe^{III}. This feature was not observed at any point during this study, even when the pH was circum-neutral and generation of $>10^{-5}$ mol l^{-1} of H^+ would dominate the existing pH. This will be discussed in further detail, with Eh and Fe, after an introductory discussion of the controls on aqueous Fe chemistry.

Thus it has been shown qualitatively that the oxidation of Fe^{II} and subsequent precipitation of amorphous Fe oxides has not resulted in the changes to the pH status of a stream receiving an influx of water with elevated Fe^{II} concentrations. There has been an apparent effect on the Eh status, with the decrease in Eh after emergence being due to the high Fe^{II} concentrations and depletion of $O_{2(aq)}$ received from atmospheric exchange.

The high concentration of Fe at the point of discharge in the stream studied here may be expected to control the Eh-pH status of the water. Thus a more quantitative approach is now used to assess the perturbations in pH and Eh which may be expected from the reactions of Fe^{II} and Fe^{III} using the measured Fe concentrations.

A very simple inverse modelling approach has been used for the processes of Fe^{II} oxidation and Fe^{III} hydrolysis. Namely, that the stoichiometric relationships shown in equations 2.2 and 2.3 are used and no buffering of H^+ generated in these reactions is allowed for. Thus using equation 2.2 it can be seen that the oxidation of Fe^{II} consumes $0.25O_2$ and one H^+, thus there is a net transfer of one electron and one proton. In the subsequent (for this purpose assumed to be instant) hydrolysis of Fe^{III} there is a production of $3H^+$. Thus the net reaction yields $2H^+$ and consumes $0.25O_2$ per mole $Fe^{II}_{(aq)}$ converted to $Fe^{III}_{(s)}$.

The method used was to calculate the change in Fe (mol l^{-1}) between two adjacent sampling locations, and assume that the whole change was caused by Fe^{II} oxidation and subsequent Fe^{III} hydrolysis, according to the stoichiometry of reactions 2.2 and 2.3. The moles of H^+ released as a result of this reaction are then calculated. The pH which they would generate is then plotted in conjunction with the pH measured along the downstream reaction path. The predicted pH values are not plotted cumulatively, i.e. the pH displayed is the one resulting from the ΔFe between the two sites and not summed with the calculated pH of the previous site. The major assumption of the calculation is that the dissolved Fe is all Fe^{II}.

This calculation has been performed for selected samples at SH and HR, using the simple approach outlined above. If a coincidence is obtained between the predicted and measured pH, this would suggest the controlling process has been identified. Where a discrepancy is observed between the predicted and measured pH (larger than can be accounted for by measurement errors in the pH and / or the Fe concentrations used), this suggests that this simple assumption of Fe controlling the stream chemistry is not wholly correct.

The acidity potential at the points of discharge due to Fe^{II} can be calculated by assuming that all the dissolved Fe is Fe^{II}. This is shown on selected sampling occasions for SH and HR in table 8.1, it can be seen that the potential exists for a H^+ concentration of $10^{-2.2}$ - $10^{-3.2}$ mol l^{-1}, were the Fe to oxidise and hydrolyse instantaneously. The acid generation

is presented below as controlled by the rate of Fe reaction downstream from the point of discharge.

Selected samples recorded for HR are shown in figure 8.1a, where the pH measured is compared to that calculated from the simple reactions as described above. It can be seen that the pH predicted is consistently lower, showing a difference in H^+ concentration between that measured and predicted of several orders of magnitude. Despite the lack of coincidence between the pH values, the downstream profiles shown in figure 8.1a display a similarity in their trends. The two occasions for which this is most noticeable are July 95 and July 97. The July 95 (low flow) samples show that a pH 2 units lower than the initial concentration is expected by 550m downstream, prior to the loss of Fe from solution decreasing to such an extent that the pH is predicted to be higher again after 550m. In terms of H^+ concentration differences, the discrepancy at 550m between a predicted pH of 2.3 and a measured pH of 5.4 is one of the largest observed. In July 97 the loss of Fe between 0-100m predicts a pH drop from the initial value of 6 to 3.5, however the pH then increases as the Fe lost from solution is lower. The sampling occasions on which the stream was affected by dilution due to melting snow / rainfall are represented by November 95 (highest flow) and March 96 in figure 8.1b. These are noticeable for maintaining a larger discrepancy downstream between the predicted and measured pH.

The difference between the sampling occasions in July 95 (low flow) and November 95 (high flow) is the stream flow conditions, with dilution being a major factor in November 95 as compared to July 95 when there was no dilution (section 8.1.1). This is reflected in the suspended sediment concentrations of Fe and K (figure 5.13 for the discharge) on these respective occasions. The higher concentration of Fe in July 95 showed a suspended sediment almost entirely consisting of precipitating / aggregating $Fe(OH)_3$, however, the concentrations of Fe in November 95 were lower, and those of elements such as K (representing detrital silicate material) were higher than they were in July 95. This higher concentration of suspended material may be responsible in part for the deviation from the predicted pH observed in November 95 being greater down the length of the stream than that for July 95. In concert with the higher buffering capacity of the influent waters (surface runoff and throughflow), the suspended material will provided a larger surface area for buffering reactions to take place.

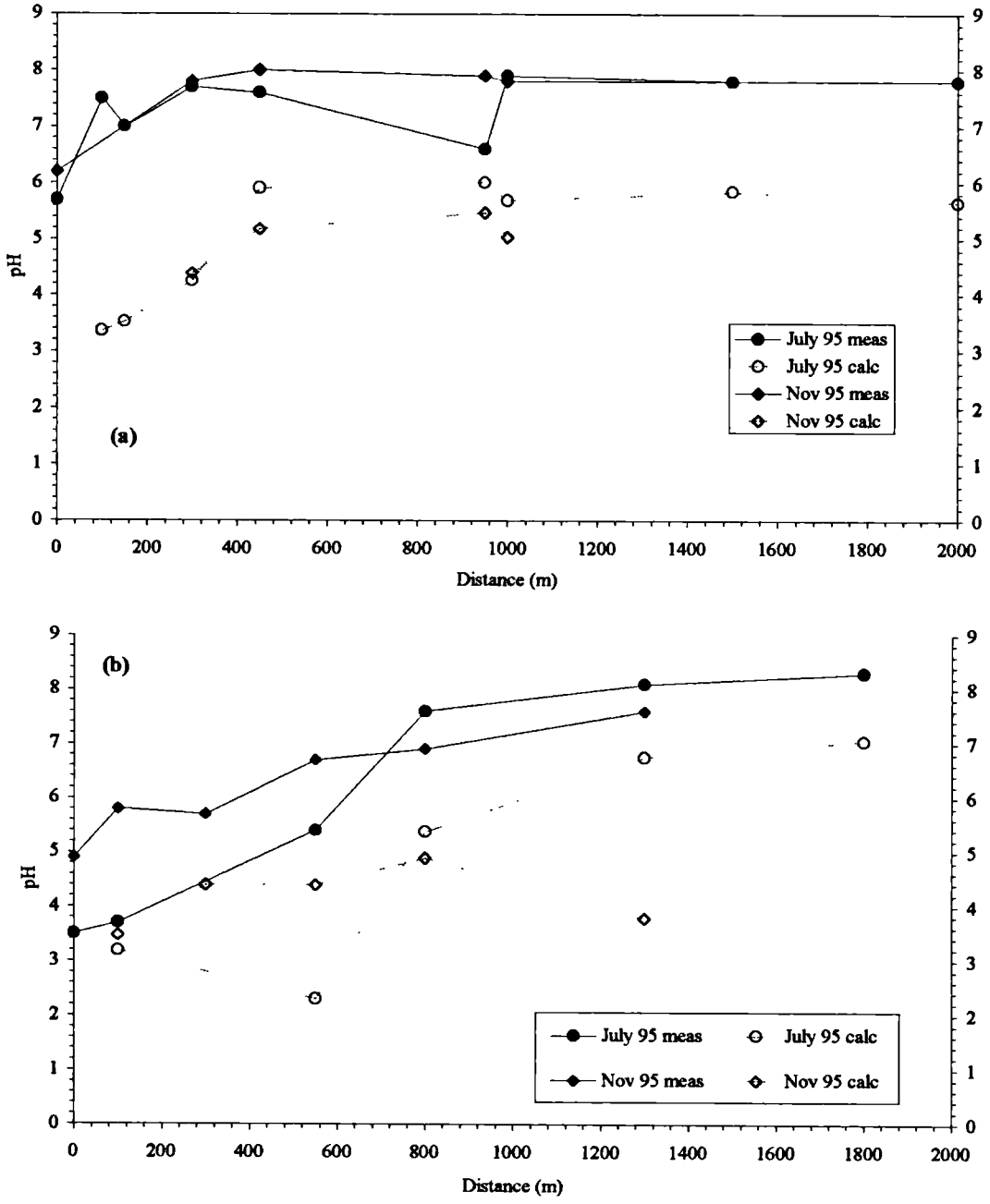


Figure 8.1: Simple inverse modelling results for pH using measured Fe at SH and HR.
(a) measured and modelled pH at SH (b) measured and modelled pH at HR

Selected results of modelling pH using the loss of Fe from solution are shown for SH in figure 8.1b. These show a large discrepancy between the field measured pH and that predicted from the reactions of Fe in the stream. July 95 (low flow) shows a predicted pH of 6 by 450m downstream, this is due to the rate of decrease of Fe being greatest on this occasion at SH. The measured pH is 7.6 for at 450m downstream in July 95, this represents a difference of $\sim 10^{-6}$ mol l^{-1} H^{+}. November 95 (high flow) shows a consistently lower pH predicted than for July 95, and this is due to the relative rate of removal of Fe from solution being less than in July 95. As was observed at HR, the pH values appear to have a similar curve shape downstream, however, the oxidation and hydrolysis cannot be seen to have any effect on the pH (by lowering the value) at this site.

Figure 8.2 shows that the rate of change of pH and Fe, Al and Mn concentrations downstream from source in July 95 is different for the different sites. This figure shows a consistency in that all sites appear to reach a more stable value at a similar distance downstream (~750m for Fe), irrespective of the initial variations in concentrations. This suggests that the processes operating on all the streams are the same, and are increased in rate when the concentration or pH deviates most from the quasi-stable value reached.

8.1.3 Sinks of major ions from the aqueous phase

In this section the receptor for major ions which undergo reactive loss (section 8.1.2) in the aqueous system will be discussed. This receptor is a solid phase precipitate, which may be found as suspended matter in the stream loading, or as sediment, forming part of the stream bed material. Sorption to the precipitate in either of these occurrences is also a pathway by which ions are transferred from the aqueous phase to the solid phase. The net transfer of ions could not be calculated as part of this study, because information on the stream discharge rates and the volume of stream bed material would be required in the calculation of element fluxes. However, a brief discussion of the mechanism of transfers will be presented here using the data described chapter 7.

In the case of the major ions it has been shown above that Fe is invariably reactive on emission from mine or spoil drainages in this study, and that in some instances Ca and S may be reactive. Observation of the ochreous deposits show that Fe is a major stream bed forming precipitate close to the point of discharge in many cases. The proportion which forms directly onto the stream bed, and the proportion which is carried as suspended material is not known, because stream flow measurements were not

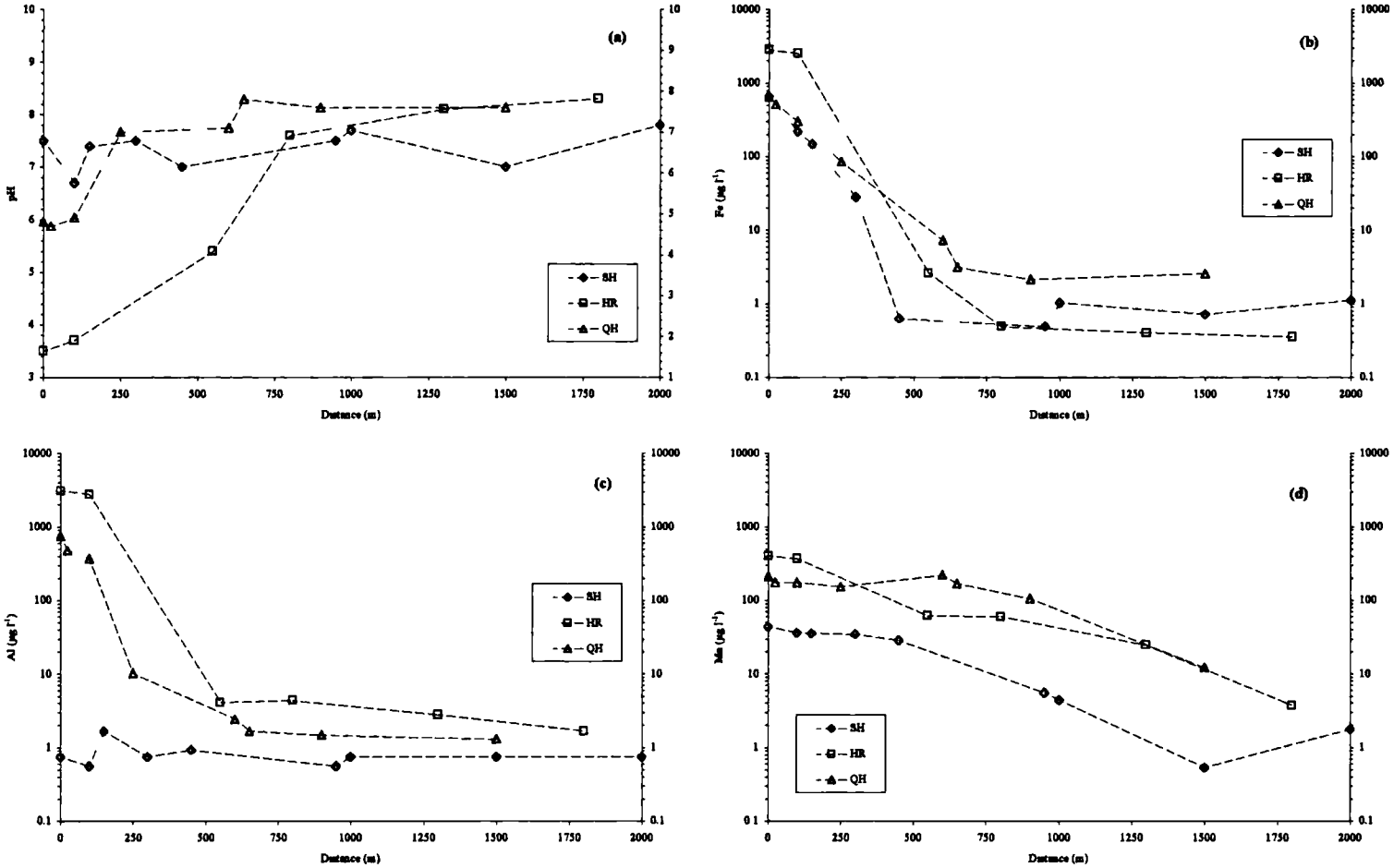


Figure 8.2: Comparison of the concentrations of pH and selected ions downstream from the points of discharge. (a) pH (b) Fe (c) Al (d) Mn

conducted as part of this study. The minerals forming from these ions, either as observed (Fe) and / or as predicted / modelled (Fe, Ca and S), will be discussed below.

The concentrations of Fe in the stream dissolved and suspended loads were compared in section 7.5 for SH, 7.14 for HR and 7.25 for QH. The increase in suspended phase in comparison to the proportion of the dissolved phase making up the total stream load of Fe can be seen to be more rapid for SH and HR in July 95 (low flow). The cause of this has not been elucidated quantitatively, however, a combination of factors may be seen to be the likely cause. Firstly, the stream temperature was in general some 10°C greater than it was measured to be in November 95 or March 96. Temperature may be expected as a general rule to increase the rate of reactions taking place (Krauskopf & Bird, 1995), in the case the oxidation of Fe^{II}, the hydrolysis of Fe^{III} and the polymerisation of complexes to form $Fe(OH)_{3(am)}$. Another factor is that a high temperature and long daylight hours would suggest that biological activity would be at its greatest for the year, and whilst biogenic reactions have not been studied in this research, they may be expected to play a fundamental role in the in-stream reactions, such as Fe^{II} oxidation (Nordstrom & Southam, 1997). Nordstrom (1985) demonstrated that the dilution of bacteria populations, by rainfall or other inflow, will reduce the rate of Fe^{II} oxidation. These could also have an effect in supplying organic matter to which may coat the Fe phases and lower the pH of zero charge (Newton & Liss, 1987), which will affect the rate of coagulation (Cornell & Schwertmann, 1996). Finally, the stream competence will be lower in times of low flow than it is in times of high flow, and thus settling may be expected to occur closer to the source of discharge.

On sampling occasions other than July 95 the following patterns in the transfer of Fe from the aqueous to suspended phase were observed. At SH the largest dilution (qualitatively assessed) occurred in November 95 (high flow) between the point of discharge (0m) and sampling at 300m downstream, (figure 7.4c), and there was also a dilution in March 96 (figure 7.4c). In these conditions it took a greater distance downstream for the suspended Fe to become higher than the dissolved load than in July 95 (low flow, no dilution). The length of stream required for this to happen was greater in March 96 than November 95. HR shows the same pattern in the transfer of Fe from the aqueous phase to suspended sediment as SH. The stream in July 95 (low flow) requiring the shortest distance downstream for this transfer, followed by November 95 (high flow) and March 96 in the stream length required. It is postulated that the reciprocal of the reasons hypothesised to control the rate of reaction in July 95 (lower temperature, shorter daylight hours, higher stream velocity and thus stream competence,

and lower ion concentrations) are the cause of the longer distances taken for the reaction and settling of Fe particles in the streams on these occasions.

At QH the pattern shown by the transfer of Fe from the aqueous to suspended phase is different to SH and HR. In July 95 the stream length required for the transfer of Fe from the aqueous phase to the suspended sediment phase is greater than for the other sampling occasions. The most rapid transfer occurred in November 95, occurring within the length of stream between the discharge and the first sample of mixed water (100m). March 96 was intermediate to these two conditions. The aqueous concentrations of Fe are lower from discharge at QH, than HR and (generally) lower than SH (figure 5.5), but what is also notable is the high proportion of the total stream loading of Fe that Fe_{ss} constitutes in November 95 and March 96. This is quite different to SH and HR, and to QH in July 95, and the reasons put forward (above) for the greater rate of transfer of Fe to the solid phase in hotter, lower flow conditions would seem valid, thus this result is hard to explain.

The dominant mineralogy of Fe precipitates at SH was an admixture of ferrihydrite and goethite (section 7.1.4). This mineralogy was controlled by the aqueous circum-neutral pH (figure 7.1b) and the high (~20-30 mg l^{-1}) Fe^{II} concentrations which are rapidly oxidised to Fe^{III} (Nordstrom, 1985) (section 2.2.3), conditions which are favourable to the precipitation of ferrihydrite (section 2.2.5b). Iron(III) has a low solubility where the pH is circum-neutral and its activity is controlled by hydrous oxide precipitation (section 2.2.5b). Ferrihydrite has a higher solubility (log K_{sp} = -39 to -37 (Cornell & Schwertmann, 1996)) than goethite (log K_{sp} = -40 (Cornell & Schwertmann, 1996)), causing modelling of the discharge and downstream chemistry to show a large supersaturation of goethite (SI = 4 at 150m downstream in July 95). The cause for the precipitation of ferrihydrite initially is that it is kinetically favoured over goethite, as reviewed by Cornell & Schwertmann (1996) and described for the discharges in section 6.1.5. The effect of kinetics on the pathways of precipitating / sorbing ions is an aspect which is not incorporated into most modelling programs (section 4.6), and these results show one limitation of their application. The precipitation of the metastable product ferrihydrite is thus thought to control the stream chemistry at SH, as far downstream as the concentrations of Fe remain high enough for Fe^{III} precipitation. The formation of goethite has been shown by Murad *et al.* (1994) to be due to the transformation of the metastable ferrihydrite to goethite (the stable phase) as an ageing process. This process has been shown by Bigham (1994) to be rapid enough that an admixture of ferrihydrite and goethite may be expected in stream formed precipitates, such as found at SH in this

study. The nature of the stream precipitates is temporally stable, reflecting the consistent chemical composition of the stream waters at this discharge point.

The pathway of transfer from the aqueous phase to a stream bed precipitate could not be assessed quantitatively in this study. Thus it could not be assessed whether the forming minerals precipitated directly onto the stream bed, or were sedimented out from the suspended phase. Considerable transfer of Fe to the stream bed loading via the suspended state was observed (section 7.1.4) and this suspended sediment was visibly a (red-brown) ochreous colour and chemically was dominated by Fe (figure 7.8). This suggests that the Fe aggregated in suspension, prior to settling to form the precipitate on the stream bed.

It has been shown here that whilst SH precipitates are characterised by a mixture of ferrihydrite and goethite. It is likely that goethite forms *in-situ* post ferrihydrite precipitation and thus it may be hypothesised that the stream chemistry, controlled by precipitation of Fe, is a response to the precipitation of a mono-minerallic ferrihydrite phase (Bigham, 1994; section 2.2.5a). The use of hydrogeochemical modelling in predicting this occurrence would be of limited applicability, since the program used considers only thermodynamic processes, not accounting for (in this instance) the kinetic favourability of ferrihydrite over goethite.

The aqueous geochemistry of Helmington Row (HR) is characterised by large variations in the major ion composition and pH recorded, depending on hydrological conditions (section 5.2). Iron is the dominant cation in the system at the point of discharge (figure 5.5) and undergoes reactive loss along the stream length. The conditions recorded on the field visits do not reach those required for the precipitation of a jarosite phase (which is widely found in low pH, high Fe and SO_4 environments (section 6.2.2)), thus ferrihydrite is the dominant Fe containing phase expected from considering both the thermodynamic predictions and kinetic constraints. Figure 7.20 shows the XRD patterns acquired for 4 selected precipitates from HR. It can be seen that ferrihydrite and (possibly) goethite phases may be present. Whilst the diffraction patterns for all these naturally precipitated minerals are characterised by a high background (section 4.5.1), it can be seen that the large amorphous signal for HR makes identification of the Fe phases more problematic than for SH. The cause for this will now be examined.

The concentration of several major ions in selected precipitates from HR is shown in table 7.1. It should be noted that the digestion method for these particular samples was a

5M HCl leach, and thus the concentrations are taken to represent those of a precipitate dominated fraction. It can be seen from this that, in addition to high Fe concentrations, Ca, Al and S are also found in high concentrations. Aluminium is therefore discussed here, due to its effect on the behaviour of S, despite its general occurrence in minor concentrations in the aqueous and precipitate phases. These are the ions which were found in section 8.1.2 to be non-conservative in the low pH environment found in this stream system on occasions, with July 95 being the most extreme example. Hydrogeochemical thermodynamic modelling also predicts that Al-SO_4 phases should be found to precipitate from waters of such a composition. However, because study of these precipitates by XRD has confirmed only the presence of ferrihydrite and (possibly) goethite, this suggests that whatever mineral is occurring is dominated by a poorly crystalline nature, and is the cause of the high amorphous background observed in the XRD plots (figure 7.20). The use of SEM-EDS was not possible either, because the samples were too hydrous to be examined for particle specific element ratios without disintegrating under the beam current (section 4.5.2). Thus in trying to assess the mineralogy of these precipitates, use must be made of the modelling results, and also published studies of such systems.

The mineralogy of Al-SO_4 phases which may occur in mine / spoil drainage environments was reviewed by Nordstrom (1982a). Whilst alunite may be expected to be the most stable precipitate, basaluminite may occur as an amorphous metastable phase (analogous to the occurrence of ferrihydrite rather than goethite), and jurbanite may be stable should be the pH be low and the SO_4 activity be high enough (section 2.3.2). These phases all have specific Al:S ratios which could be used as diagnostic from the chemical results obtained. However, such a use is limited in poly-mineralic systems, where the Al and S may be associated with each other (in more than one phase), or with Fe minerals (section 6.2.2), or the S could be associated with Ca as gypsum. The Ca in its turn cannot be predicted to be wholly associated with S, since sorption / substitution of Ca in the Fe precipitating minerals cannot be discounted either. The molar ratios of the measured concentrations of the ions are shown in table 7.1, but can be seen to display a more complex situation than can be resolved by utilisation of the ratios alone. In analysing the results of modelling of the aqueous chemistry, it can be seen from table 7.1, that several of the possible phases are expected to precipitate given that they are supersaturated in solution. However, the potential for basaluminite to be kinetically favoured reduces the effectiveness of modelling in accurately predicting the precipitating phase. Thus it is tentatively suggested, largely using the extensive review

of Nordstrom (1982a), that basaluminite may be the precipitated form of Al and S in this system, but that this may be metastable with respect to alunite.

However, a further complication exists to the interpretation of this data. A change in hydrological conditions at this site, has been shown to effect a change in the physico-chemical parameters of the discharge (section 6.2). The occurrence of higher discharge volumes at the source may also be accompanied by greater dilution effects of the waters. It may be expected that this change in composition would take place rapidly following a rainfall event. This will result in a change in the composition of the precipitates actively forming equally quickly. For instance, higher pH results in the precipitate being dominated by ferrihydrite / (possibly) goethite (plate 5.6c). However, that material already precipitated on the stream bed may not respond as rapidly. This can cause a disequilibrium between the aqueous composition and the mineralogy and chemistry of the precipitates collected. The effect of this disequilibrium will be reviewed further in section 8.3. Two sampling instances at HR particularly show this effect, and will be discussed below.

Firstly, two samples were collected at the sampling location 800m downstream from the source at HR; one from the stream thalweg and one from a pool upstream of a large boulder. The thalweg sample showed a chemical composition dominated by Fe (Al = 9 wt.%; Fe = 19 wt.%), the pool sample a concentration dominated by Al in addition to Fe (Al = 15 wt.%; Fe = 6 wt.%). These samples were collected from within 2m of each other and thus are expected to be influenced by the same water composition. This suggests that physical translocation of the material found in the still water may have occurred from the thalweg, where an Fe precipitate was dominant in the stream bed sediment. It also shows that the precipitate found in the still water did not become chemically unstable, or metastability could occur due to the kinetics of dissolution being slow. Analysis of the water chemistry and reliance upon modelling to understand the predicted mineral compositions cannot incorporate such disquilibria between the composition of the waters and the stream sediment. Thus sampling of the stream sediment cannot be replaced by hydrogeochemical modelling, nor should the potential for disequilibria between the stream solid and dissolved phases be neglected when sampling. Another demonstration of disequilibrium is found in the discharge pipe at HR (plate 5.6b) where the main drainage discharge occurs from the spoil heap. The interior of this pipe was sampled and found to be a pale precipitate (plate 5.6b) with little evidence of ochreous material.

Thus the work undertaken at HR has shown that both Fe and Al, S and Ca phases have been found to precipitate. However, the mineralogy of their occurrence has not been delineated within this study, due to the difficulty in attributing the measured chemistry to specific phases in the absence of conclusive mineralogical information. These ions may all sorb onto Fe precipitates, such as ferrihydrite, or they may form precipitates. It is more probable that these ions are part of the precipitate structure, due to their high concentrations (table 7.1). The changing chemistry of the stream water at this locality has also highlighted the difficulty in assessing the relationship between mineral phases and the simultaneously sampled water body. This is particularly so where metastable phases may be expected to age to more crystalline compounds; this process then being interrupted by the changing chemical conditions to which the mineral is exposed. As was noted above for SH, the use of hydrogeochemical modelling in assessing the probable mineral phase expected to precipitate cannot be used in the absence of mineralogical data in systems such as these where metastable phases are commonly found as the mineral precipitating and controlling the water chemistry. The minerals found here, and those not positively identified, such as schwertmannite, are discussed in section 6.2.2; the reasoning behind which is also valid for this section.

8.1.4 Major ion summary

The processes controlling the major ion chemistry of the stream systems studied here have been discussed in this section. It has been shown that Na, K and Cl are stable ions, and at SH and QH form "fingerprints" for inflowing road drainage, when sampling took place in cold weather conditions. At HR, Na and K occur in different concentrations in the water emanating from the main source of spoil heap drainage and that of dominantly overland flow from higher on the spoil heap. Calcium and S, as SO_4, were shown to not be stable in solution under all sampling conditions. On the occasions where pH was low (<~5) and ion concentrations high (particularly in July 95) these ions could be seen to undergo reactive loss from solution.

Simple inverse modelling has shown considerable pH buffering to be taking place in the stream, whether this is due to aqueous-gas (atmosphere) interactions or aqueous-solid (stream sediment minerals) reactions is not known.

Mineral phases precipitating in the stream could not be determined completely, largely due to the poorly crystalline nature of these minerals (XRD amorphous for instrument conditions used here) and poly-mineralic, which meant that simple chemical ratios of the elements determined could not attribute the Fe, S, Al and Ca to clearly defined phases.

8.2 Factors affecting minor and trace element chemistry

Trace and minor ions are frequently found in elevated concentrations in ferruginous mine and spoil heap drainage as a result of the extreme chemical conditions resulting from pyrite oxidation (section 2.1). Thus it is reasonable to assume that reactive loss from the aqueous phase is going to be prevalent amongst these ions once the higher pH and Eh values are encountered downstream from the point of discharge (section 8.1.2). This reactive loss can be due to precipitation or sorption reactions (section 2.3). This section will discuss the data presented on selected trace ions in chapter 7. The ease of analysis of a wide range of elements using ICP-AES means that more data has been generated than discussion of which can be accommodated within this work. Thus, the following ions have been selected for discussion here: Al, Zn, Cu and Mn. Aluminium, Zn and Cu are notable for their potential toxicity to aquatic biota, and thus the controls on their behaviour in solution when they occur in elevated concentrations (as at the sites of study here) are of interest. The relationship of these data to statuary levels is reviewed in section 8.4 and will not be included here. Manganese is discussed here to study the controls on the aqueous phase concentration, downstream from the point of discharge.

8.2.1 Mechanisms controlling Al, Zn and Cu

The potential mechanisms causing decreases in the concentrations of these ions have been the subject of extensive investigation, as reviewed in section 2.3. The processes include precipitation and sorption. The literature available on this subject generally records the formation of Cu and Zn minerals only in the extreme environment of efflorescences (section 2.2.1). Sorption onto colloidal (Fe) surfaces is generally recognised as a controlling influence on Cu and Zn in mine / spoil drainage waters. Aluminium is also subject to sorption processes, however, in low pH environments where SO_4 is the dominant anionic species an Al-SO_4 phase may be the most stable phase for Al (Nordstrom, 1982a). The most stable phase otherwise expected (in the absence of SO_4) is gibbsite, although this may form via amorphous pre-cursor stages (section 2.3.2).

The concentrations of Al at HR and QH were high, in the order of 10-100 mg l^{-1} at HR and 1-10 mg l^{-1} at QH on sampling occasions other than November 95 (high flow) and July 95 (at HR). In November 95 the concentration at both the points of discharge was low and controlled by the circum-neutral pH of the discharge points. Confirmation that the reductions in concentration at HR (figure 7.17b) is due to reactive loss from solution

is provided by the changing molar ratio of Al and Na in July 95 (which figure 7.17a shows was unaffected by dilution because the Na:K ratio did not vary). This also suggests that reactive loss may be occurring on other occasions, particularly as the stream is not crossed by a road until 650m downstream and thus Na inputs from road drainage before that point would not be expected. The reactive loss of Al from the HR stream system has also been confirmed using mineralogical techniques (section 8.1.3). The probable sink for Al in the solid phase has already been established as an Al-SO_4 precipitate, the nature of which has not been able to be identified (section 8.1.3). The Al from QH is similarity expected to precipitate as a SO_4 phase when concentrations are elevated, with saturation index calculations by PHREEQ-C showing supersaturation for alunite in July 95. Figure 7.16b shows that the total stream loading of Al is dominated by the suspended phase in November 95 at HR. This is further evidence of the transport of silicate material by the high flow waters as suggested in figure 5.15. In July 95 at HR the loading of Al in the stream can be seen to be dominated by the suspended phase after 500m, however, the rate of decline from suspension of the Al is not as great as that observed for dissolved Al and the concentrations are higher than those of Fe in suspension (figure 7.14) until 1300m downstream. This continued high concentration in suspension was not investigated via particle size measurement or any other physical property of the suspension, but it would seem probable that the cause is the continued competence to hold the Al phase in suspension. Whether this is caused by the physical competence of the stream (Fe_{ss} concentrations do not decrease over this distance) or due to the chemical characteristics of the aqueous system (pH below pzc) has not been established here.

The decreasing concentration of Zn downstream from the point of discharge at SH is shown in figure 7.7a. It can be seen that, as recorded for Fe (section 8.1.2), the decrease in concentration of Zn is most rapid in July 95, with the rate of decline being slower on subsequent occasions, despite an initial dilution occurring. The decline in Zn concentrations was not accompanied by Zn mineral phases being identified in the stream precipitate and the Zn concentrations are too low to suggest a major mineral forming phase. This suggests that the sink for Zn may be dominated sorption rather than precipitation. The colloidal and suspended phases available for sorption would be expected to be Fe in this stream environment, because the Fe concentrations are high in the dissolved and suspended phases downstream from the point of discharge (figure 7.5b). To investigate whether the occurrence of Fe in a suspended fraction could affect the behaviour of Zn in this stream system, figure 7.7b shows that as the fraction of Fe occurring in the suspended phase increases, so the dissolved Zn decreases. The pH

change associated with the increased Fe_{ss} proportion is not very great, as discussed in section 8.1.2 the pH is circum-neutral from the point of discharge downstream, suggesting that pH may not be an important variable in the loss of Zn from solution by sorption, but that the availability of Fe surfaces to sorb to may be the dominant factor. These findings are in agreement with those cited in section 2.3.4, particularly the study of Johnson (1986).

The Zn concentrations at HR are also subject to the most rapid decline in concentration in July 95. It should be noted that the initial concentrations of Zn at this site are invariably between 10 and 100 times greater than those at SH. The changes in dissolved Zn concentration with the proportion of Fe occurring as Fe_{ss} are shown in figure 7.14b. This shows that the concentrations decrease as the proportion of Fe_{ss} increases, however, an association with increasing pH is also shown by figure 7.14a. Thus, the sink for Zn from these data is postulated to be sorption to the suspended Fe phase, though whether the controlling influence is the concentration of Fe_{ss} in solution, or the change in pH of the stream is not determinable.

At QH the concentration of Zn in solution can be seen to be >2.5 mg l^{-1} on all sampling occasions, except November 95 (high flow), this is comparable with the concentrations observed from HR at the point of discharge. The greatest concentration of Fe_{ss} at this site in July 95 (low flow) can be seen on figure 7.26b to be 100 - 300m downstream from the point of discharge, this is associated with the greatest decrease in Zn concentrations, subsequent to this site the concentrations show a gradual decline along the length of stream and would appear to follow the behaviour in stream of dissolved Fe. The stream length 100 - 300 m is also associated with the most rapid rise in pH along the length of stream, from 4.8 (100m) to 7 (300m). This is also reinforced by comparison of the behaviour of Zn in May 95 and March 96, which shows a more rapid decrease in concentration than in July 95 over the length of stream sampled. The control on the changes in concentration is thus thought to be the transfer of Fe to the suspended phase from the dissolved phase. The low concentration of Zn along the entire length of stream in November 95 (high flow) is controlled by the large throughflow of water (section 6.3).

The concentrations of Cu in solution at HR are illustrated in figure 7.15c, and show that the concentrations of Cu are lower than those recorded for Zn (figure 7.15d). However a similar pattern of declining concentrations downstream from the point of discharge can be observed, with the concentration in July 95 decreasing from 88 to ~2 μg l^{-1} between

200 and 550 m downstream respectively. The pattern on the other occasions also follows the pattern observed for Zn and Fe as described above. When Cu concentrations in solution are plotted against the pH (figure 7.18a) and the proportion of Fe occurring as Fe_{ss} both show the same relationship as observed for Zn (above). This is as the pH increases, so the Cu concentration decreases, and as the proportion of Fe_{ss} increases, so the dissolved Cu concentration decreases. Whilst the dissolved Zn concentrations are greater than the concentrations of Cu (figure 7.18a), the Cu shows a greater affinity for the suspended phase than does Zn (figure 7.18c). The behaviour of Cu in solution at QH cannot be elucidated as is possible at HR. Figure 7.15c shows that the highest concentration of Cu at the point of discharge occurs in July 95 (low flow), but that the concentration rapidly decreases from ~50 to ~15 $\mu g\ l^{-1}$ by 250m downstream from the point of discharge. The subsequent concentrations and those of the other sampling occasions are too low to be able to discern information about the controls on the behaviour of Cu.

From the results discussed above it can be seen that Zn and Cu show a strong tendency to move into the suspended phase and are unstable in solution. It is suggested here that the Zn and Cu occurring in suspended sediment are sorbed to the surfaces of amorphous Fe hydroxides in suspension in the stream as found previously by Johnson (1986) (section 2.3.4). The effect of pH on the behaviour of colloidal and suspended Fe in the stream were discussed in section 8.1.3. The suspended sediment surfaces will be subject to decreasing positive charge as the pH increases (Cornell & Schwertmann, 1996), and this, along with the pH of hydrolysis of Cu being ~5.3 (Levinson, 1980) forming the hydroxyl complex which can be sorbed (Schwertmann & Taylor, 1989), increases the attraction to the surface for the dissolved Zn and Cu species. This would suggest that the increasing concentration of Fe_{ss} downstream from the source and the increase of pH (often occurring the greatest rates simultaneously) would be enhancing the sorption of Cu and Zn from solution onto the suspended Fe phase. These data are plotted only for HR, because the variations in pH are marked at this site, and the concentrations of these two ions elevated enough to be able to discern trends in the data. The same controls are thought to occur at QH, however, the behaviour of Fe in solution and suspension at this site shows a different pattern of behaviour to that found at HR, and thus Zn and Cu concentrations show a different pattern.

8.2.2 Mechanisms controlling Mn concentrations

Figure 7.6 shows the behaviour of Mn in the aqueous and suspended phases downstream from the discharge at SH. The initial concentration was ~2 $mg\ l^{-1}$ on all occasions (figure

7.6a). It can be seen that the two occasions on which the concentration of Mn decreased most rapidly from the point of discharge were July 95 and November 95 (figure 7.6a), whilst higher concentrations were maintained in May 95 and March 96. This shows the same pattern for different sampling occasions as Fe at this location (figures 7.5 & 7.6), however it can be seen that a greater length of stream was required before the sharpest decrease in concentration in comparison to Fe. The process controlling the decrease of Mn in July 95 (low flow) would appear to be similar to the control on Fe, in that the rate of reaction from the stream is much more rapid on this occasion. A point of interest is the comparison of the location along the stream length for the decrease in concentration of Mn with that of Fe. Figure 7.6b shows that in July 95 the concentration of Mn in suspension did not exceed that of the dissolved phase along the length of stream studied. This will be discussed further below. The cause for the November 95 (high flow) sampling occasion reaching the lowest concentration recorded at this site at 1800m downstream can be elucidated in part from figure 7.6b. The concentration of Mn_{ss} can be seen to exceed that of Mn_{aq} at this location, and this is the only occasion that this occurs, this shows that Mn is being removed from solution to a greater degree than recorded on other occasions at this site.

The chemistry of Mn at HR is shown in figures 7.15a. It can be seen that the concentrations of dissolved Mn are generally higher (~2 - 20 mg l^{-1}) than those recorded at SH. Figure 7.15a shows that the concentration of Mn is very variable from the point of discharge depending on hydrological conditions and has a similar pattern of concentration downstream from the discharge, on the different sampling occasions, to that shown for Fe (figure 7.14a). The concentration of Mn is initially highest in July 95 (low flow) which falls off to the lowest concentration (at 1800m downstream) recorded in the stream length studied. This pattern follows that of Fe (figure 7.14b) as was observed for Mn at SH. At HR the suspended sediment loading of Mn was always less than the dissolved fraction along the length of stream studied here (figure 7.16a), although an increase in the suspended sediment concentration can be seen from 100 - 800m downstream in July 95 (low flow), and a more gradual increase from ~3 to ~11 mg l^{-1} from the discharge to 1800m downstream on the other occasions shown.

At QH the concentrations of Mn in solution (figure 7.27a) can be seen to decrease by the most in July 95, when the concentration changed from ~10 (source) down to ~0.7 mg l^{-1} (1500m) along the length of the stream studied. Some part of this decline is attributable to the lower concentration of Mn in the influent stream at 650m downstream. The concentration in November 95 varied little, and increased after the confluence at 650m

downstream, when the influent stream had a higher Mn concentration. On the other sampling occasions the initial concentration and decline in concentration were intermediate to the two extreme conditions.

A major difference in the chemistry of Mn compared to Fe is the higher redox potential required for Mn^{2+} oxidation to Mn^{4+} (Eh^{o} = 1.23), than that of Fe (Eh^{o} = 0.77) (Krauskopf & Bird, 1995) (section 2.3). Thus it would be anticipated that in a stream system containing Fe^{II} and Mn^{II}, sufficient Fe^{II} oxidation would need to take place to enable the Eh to rise to a value where Mn^{II} oxidation can take place on a large scale. To assess whether this is recognisable as an influence on Fe and Mn concentrations in the stream systems studied, the molar ratios of Fe and Mn and Al (to compare the effect of pH) to Na for all three sites are shown in figure 8.3a-c. July 95 has been selected to demonstrate these data, because there is minimal dilution by influent waters downstream from the points of discharge on this occasion. It can be seen that in all three systems there is a net decline in the concentration of Mn which is subsequent to the length of stream in which most reactive loss of Fe occurs. These patterns can be explained in the following ways. Aluminium is controlled by pH rather than redox changes. Because the pH of hydrolysis of Al^{3+} is lower than that of Fe^{2+} (section 2.3), this reaction would be expected to predominate earlier in the stream length, where (in the situations studied here) the pH is lower than those recorded further downstream. The control on Fe is the oxidation of Fe^{II} and subsequent hydrolysis of Fe^{III}, both of which may delay the removal of Fe from solution (section 8.1.2). The process of most relevance to understanding the behaviour of Mn in solution is the consumption of $O_{2(aq)}$ in the oxidation of Fe^{II}. It was shown in section 5.3 that the dominant form of the dissolved Fe downstream from source is Fe^{II}, and it is possible that the control on the rate of reaction is the assimilation of dissolved oxygen from the atmosphere, as well as water temperature and bacterial concentration (section 8.1.3). The oxidation potential required for Mn^{II} oxidation is greater than that for Fe^{II}, so that the removal of Mn from solution is retarded until the rate of consumption of $O_{2(aq)}$ by Fe^{II} has diminished sufficiently for the oxidation of Mn^{II} to proceed.

The hydrolysis reaction of Mn is acid generating and is simplistically represented (section 2.3.3), by equation 8.1.

$$Mn^{2+} + 2H_2O \leftrightarrow MnO_2 + 4H^+ + 2e^-$$

Eq. 8.1: Oxidation and hydrolysis of Mn^{II} (Krauskopf & Bird, 1995)

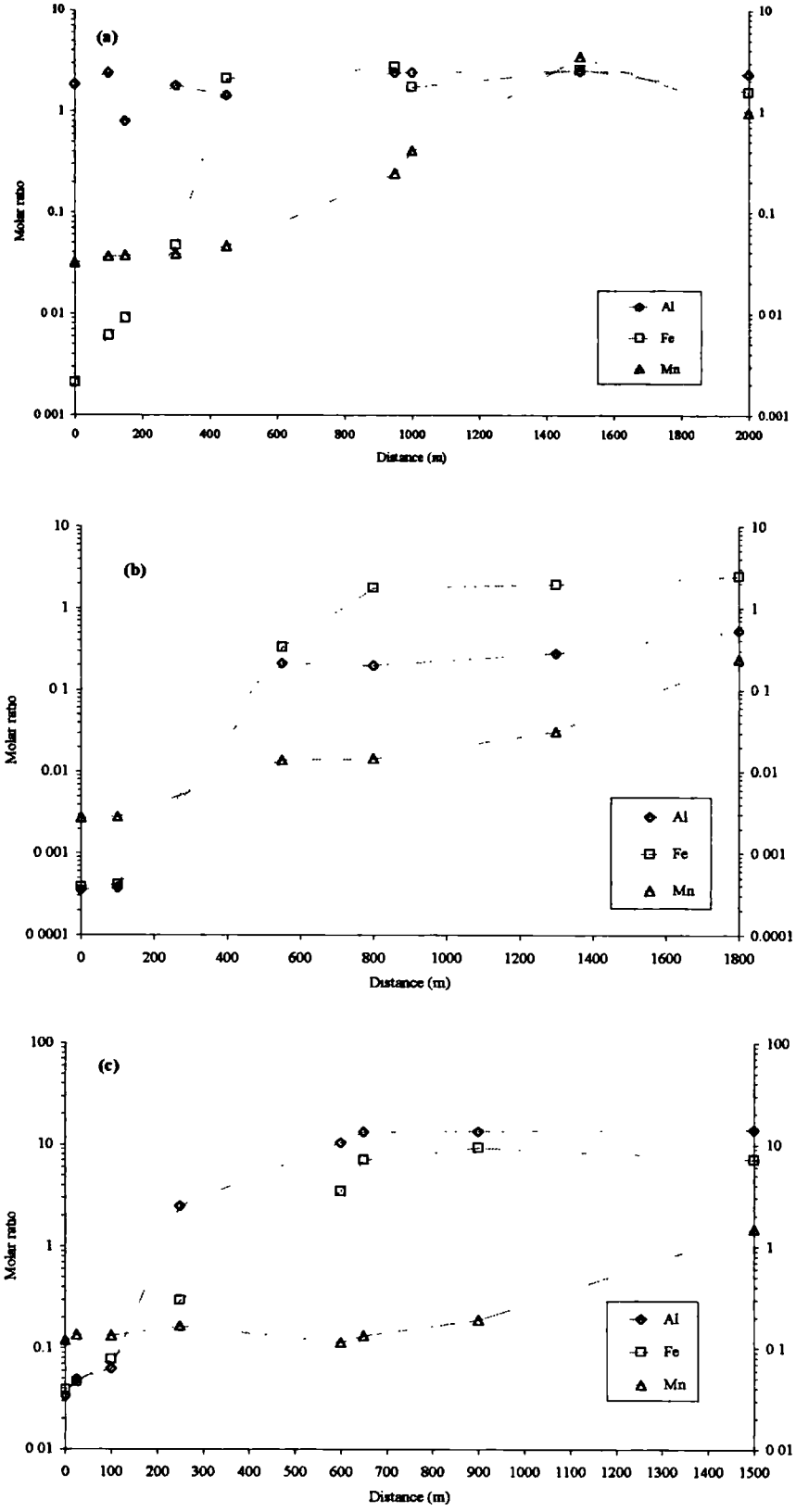


Figure 8.3: Reactive loss of Al, Fe and Mn along the stream length of the discharge sites. (a) Stony Heap (b) Helmington Row (c) Quaking Houses. The ratio plotted is that of Na to Al, Fe and Mn, respectively. Sodium is taken as a conservative tracer of reactive loss from the aqueous phase.

In conjunction with the hydrolysis of Al^{III} and Fe^{III}, it can be seen that the acid potential at the point of discharge for a locality such as HR and SH is larger than that calculated in table 8.1 for Fe^{II} alone. However, the stream had sufficient buffering capacity to absorb the H^+ generated by Al and Fe hydrolysis (section 8.1.2), such that the occurrence of Mn hydrolysis further downstream would not be expected to result in a measurable difference in the pH, as the buffering capacity of the stream should be adequate to absorb the generated H^+.

Table 8.1: The potential acidity due to Fe^{II} at SH and HR discharge localities.

Site	Date	Fe ($mg\ l^{-1}$)	Fe ($mmol\ l^{-1}$)	H^+ ($mmol\ l^{-1}$)	*pH	pH
SH	July 95	36500	654	0.0013	2.9	5.7
SH	November 95	38700	693	0.0014	2.9	6.2
SH	March 96	28800	516	0.0010	3.0	5.9
HR	July 95	159000	2847	0.0057	2.2	3.5
HR	November 95	17500	313	0.0006	3.2	4.9
HR	October 96	119000	2131	0.0043	2.4	4.9
HR	July 97	19500	349	0.0007	3.2	6.0

* - this pH is that due to the generation of H^+ by the oxidation and hydrolysis of Fe alone, and is not summed with the existing H^+ in the system. The pH measured in the field is recorded in the final column.

8.2.3 Minor and trace ion summary

This section has shown that concentrations of Cu and Zn in solution downstream from the point of discharge are controlled by the concentration of suspended Fe and the pH of the water. Aluminium concentrations were shown to be controlled by pH and can be seen to decrease rapidly from the point of discharge. Manganese concentrations appear to be controlled by the changes in Fe concentration downstream; the redox potential being insufficient to precipitate Mn until the much of the Fe^{II} has been oxidised.

8.3 Factors controlling the toxicity of the waters

The toxicity assessment of waters such as these is an important part of the practical assessment of the impacts of waters emanating from mines and spoil heaps. In the discussion here, the concentrations observed will be related to the regulatory limits imposed by legislation, and those limits appropriate for agricultural usage of water. The problems associated with making these assessments and mapping stream sediment chemistry, relating to observations from this study will also be discussed.

8.3.1 Consideration of results obtained in this study in a statuary water quality context

The deep mine drainage observed in this study generally has a concentration of Fe (table 6.1) at the discharge point which is greater than that permitted, 2 mg l^{-1}, (Davies *et al.*, 1997), which was the main source of water quality detriment observed by Davies *et al.* (1997) in the Welsh Coalfields. The spoil heap discharge sites showed a highly variable composition (section 5.2), with Fe concentrations at HR and QH only <2 mg l^{-1} in flood conditions. Figures 7.8, 7.14 and 7.26 show the decrease in Fe concentrations downstream from SH, HR and QH on different sampling occasions, and it was demonstrated that dilution of the stream as well as the input chemistry of the discharge play an important role in determining the length of stream which will have a dissolved Fe concentration of >2 mg l^{-1} (section 8.1). A similar argument can be constructed for Al (regulatory limit 1 mg l^{-1}), Cu and Zn (table 2.5 - varies with alkalinity), concentrations in the spoil heap discharges (figures 7.7, 7.15 & 7.27). These show that the required concentration limits are exceeded, but that the length of stream impacted is variable. This would have implications for fisheries, invertebrates and the calculation of livestock intakes (section 2.4.2). The concentrations of dissolved Al, Zn and Cu from spoil heaps can be considered harmful to the stream using the EQS values presented in section 2.4.2, but any assessment of the impact on a length of stream would have to consider the degree of impact in relation to hydrological variations as well as the discharge chemical variations. This would also apply to the construction of treatment facilities for such discharges (Younger *et al.*, 1997). Another factor which should be noted is the widely acknowledged major problem of mine drainage is the high Fe concentrations (above) which will also lead to the smothering of benthic fauna by ochreous deposits (Davies *et al.*, 1997; Jarvis, 1994). The precipitation of Fe also uses $O_{2(aq)}$ in the oxidation of Fe^{II}, which may continue for a considerable (but variable) distance, which will also be to the detriment of the biota of a stream system.

8.3.2 Comparison of the water and stream sediment quality in relation to background concentrations

The concentrations of ions such as Fe at all sites, and Al, S and Ca at the spoil discharges, are evidently above any background concentration which could be defined for the Durham Coalfield, because the precipitation of Fe dominated ochre was generally seen to take place for a considerable length of the stream. The concentrations of elements in streams sediments of the region has been the subject of part of the ongoing investigation of the UK by BGS (BGS, 1996b; section 3.3.3b). The regional Mn (0.25-2%), Cu (470900 mg kg^{-1}) and Zn (>360 mg kg^{-1}) concentrations are all elevated above the rest of NE England described in BGS (1996b). These concentrations are comparable

to those reached in the downstream region of the stream systems studied here (e.g. figure 7.21b; appendix IV). The variation in concentrations of Mn (figure 7.19b) and Zn (figure 7.21b) downstream from source were shown to vary in maximum concentration and the distance at which maximum concentration was reached. These results and those of the aqueous sampling study suggest that any use of the mapping results on a small (catchment) scale should be treated with caution where inputs of differing types of water may vary volumetrically seasonally.

8.4 Disequilibria observed in this study

This section is intended to give a brief synopsis of the different types of disequilibria observed in this study. The assumption of equilibrium within a system is an essential component of modelling systems, such as undertaken here. This is not an assumption which can be proven and, indeed, has been shown to be false in some studies. The disequilibria can be caused by a lack of thermodynamic equilibrium between different components within the aqueous system, e.g. redox couples. There is also the potential for disequilibrium between the different phases of the stream system, if the response time to changes imposed on the system is different between those phases. Finally, the chosen sampling protocol can produce results which are operationally defined, rather than a based on chemical principles. A body of literature exists on these subjects, some of which is reviewed in sections 2.2.3a, b and 4.6 and the aim of this section is to briefly review their occurrence within this study. The importance of these factors is that realisation of the potential for these to occur is essential in the interpretation of data obtained from manipulation of the measured data.

8.4.1 Chemical disequilibria

This section refers to the situation where thermodynamic equilibrium is not achieved in a system (here the aqueous phase) due to kinetic effects. These situations are known to arise, and have been particularly studied in mine drainage situations in the measurement of the oxidation potential of a stream system (sections 2.2.3a & 4.6). It has been shown that using different redox couples to measure Eh may produce different Eh values. Where this occurs it is due to kinetic effects causing the system to be out of equilibrium.

The comparison of the Eh derived from DO readings and the Fe^{II}/Fe^{III} couple are shown in section 6.4. It can be seen that the data collected in this study also suggest that there is a disequilibrium between the DO and Fe redox couples. The errors bars are not plotted on these data, because the uncertainties on the thermodynamic data cannot be assessed,

and may well be larger than the analytical uncertainties, particularly where a system is poorly characterised experimentally (Nordstrom & Munoz, 1994; Stipp, 1990) or where highly variable minerals exist (such as ferrihydrite) which have calculated solubility products varying by some 2 or more orders of magnitude (Cornell & Schwertmann, 1996). Whilst there may be no significant difference in the numerical value of the calculated saturation indices, the consistent trend is an indication that there is a systematic difference between using DO or Fe as the redox determinant.

8.4.2 Aqueous - solid phase disequilibria

A temporal disequilibrium between different phases in a system can occur where the response of one phase is slower than that of another phase. Here the changes in water chemistry may exceed the rate of changes in precipitate chemistry. The situation which is observed here (section 8.1.3) was a precipitate containing Al, S and Ca as well as Fe to one side of the thalweg, where the precipitate was an Fe dominated mineral (undetermined mineralogy). The main course of the stream had changed in composition in response to the change in water chemistry, but the water-sediment out of the main flow had yet to respond.

8.4.3 Aqueous disequilibria as a result of sampling artefacts

This lack of equilibria results from the sampling protocol used. Sampling of the dissolved component of a stream requires the use of an operationally definition of "dissolved". The most frequent nominal pore size used is 0.45μm in water quality studies, but investigations into the chemistry of mine waters have highlighted the difference in chemistry of waters sampled at 0.45μm and lower pore sizes (0.2 or 0.1μm are the most common alternatives) or the use of ultrafiltration techniques (section 2.2.3b). The use of lower pore sizes generally leads to the conclusion that Fe is carried as colloidal material through 0.45μm, however, ultrafiltration studies have also shown that Fe is carried as colloidal material through 0.1μm filters.

A comparison of filtering at 0.45 and 0.1μm was carried out as an addition to this study (section 5.3), and it was shown that the smaller filter pore size had a lower concentration of ions passing through than did the 0.45μm filtered sample (section 5.3). The investigation also established that of the Fe species, it is exclusively Fe^{III} which is shown to be affected by the filter pore size (section 6.4), which would be predicted from the relative solubilitys of Fe^{II} salts as compared to Fe^{III} salts (section 2.2). These results are in accordance with those obtained in studies such as Kimball *et al.* (1992).

8.5 Summary

This chapter has shown that downstream dispersion of ions from coal mine and spoil heap drainage is controlled by the initial chemistry of the discharge, the degree of dilution received by the discharge, and may well also relate to other environmental factors such as temperature and flow rate. The streams are capable of not only neutralising the H^+ emerging from the discharge, but also that arising from the oxidation and hydrolysis of Fe and Mn and hydrolysis of Al (as evidenced by the increasing pH downstream from discharge). It is not known whether the source of this acid neutralising capacity is from atmospheric exchange of CO_2, or due to interaction with stream sediment minerals. The distance decline in ion concentrations downstream from the discharge point of the three sites studied has been shown to be similar when the sites are not affected by dilution due to rainfall. Aluminium concentrations decrease most rapidly due to the lower pH of hydrolysis of Al^{3+} than that of Fe^{II}. The decrease in concentration of dissolved Mn has been postulated to be controlled by the rate of Fe^{II} oxidation. The concentration of Zn and Cu are also shown to be controlled by the rate of reaction of Fe^{II} due to the concentration of suspended Fe and the pH of the stream. Precipitates forming from solutions with low pH and high Al and SO_4 were shown to be of undetermined polymineralic phases containing Fe, Al, S and Ca.

This chapter has also shown that the comparison of single point data to study the toxicity of mine and spoil heap drainage needs to treated with extreme caution. The deep mines are subject to differential dilution, which affects the rate of amelioration of the stream, spoil heaps are complicated by a highly variable discharge chemistry, in addition to any further dilution. The deep mines are probably only severely detrimental to aquatic life in terms of $O_{2(aq)}$ consumption (in Fe^{II} oxidation) and blanketing ochreous precipitates. Whilst these factors are going to affect spoil heap discharges, they may also contain high concentrations of trace ions such as Zn and Cu which are considered detrimental to aquatic flora and fauna.

The chapter concludes with a brief summary of the sources of disequilibria observed in this study, which may be due to system disequilibrium within a phase or between phases, and that apparently occurring as a result of sampling and analytical procedures.

9.0 Summary, conclusions and future research

This chapter will summarise briefly the findings from chapters 6 (mine and spoil drainage) and 8 (downstream chemistry). The findings will then be listed as conclusions, related back to the aims and objectives (repeated below) given in chapter 1. The thesis will then conclude with the areas of potential future work, arising from this research, but not covered by the research described herein.

9.1 Summary

This thesis has reported the results and conclusions from the investigation of two aspects of abandoned coal mine and spoil heap drainage. Firstly the chemistry of the waters at the point of discharge were described in chapter 5 and then discussed in more detail in chapter 6. The geochemistry of the mine / spoil waters in the surface hydrological system were described in chapter 7, with a discussion following in chapter 8. These were undertaken with the aim of understanding the processes controlling the chemistry in each situation.

The processes controlling both deep mine and spoil heap water chemistry were shown in chapter 6 to be pyrite oxidation, which generates H, Fe^{II} and SO_4, and subsequent buffering ameliorating the pH. The systematic difference between the two types of discharge is ascribed to the relative stability of the water table within the two types of aquifer. The deep mines are postulated to have a stable water table, which leads to the consistent discharge volume observed and chemical composition. The Fe and SO_4 in the discharge are generated by pyrite oxidation, whilst pH is buffered, by carbonate dissolution, to circum-neutral values. The spoil heaps are characterised by a more rapid response to precipitation events, with a high run-off volume after precipitation, and much lower flow volumes during dry periods. This results in large chemical variations due to the hydrological changes, e.g. at Helmington Row concentration ranges recorded were from 2000 mg l^{-1} SO_4 in low pH (3.5) to 300 mg l^{-1} in higher pH (5.0) conditions, which were associated with low and high flow respectively. It is suggested that dilution by rainfall is largely responsible for the higher pH values observed in high flow conditions. The lower pH (<4.5) waters emanating from spoil heaps have high Al, Cu and Zn concentrations in addition to Fe and SO_4. The main mineral phase precipitating from the higher pH and lower ion concentration is ferrihydrite, the polymineralic phases from low pH waters could not be elucidated, due to their poorly crystalline nature. These low crystallinity precipitates had a chemistry dominated by Al, Ca, S and Fe. The Cu and Zn are transferred to the solid phase via sorption onto hydrous Fe oxides.

The monitoring of the chemical variations downstream from three points of discharge showed varying results in differing hydrological conditions. Dilution by receiving waters and at confluences downstream is responsible for the decrease of the concentration of ions in solution. Reactive loss of ions from solution was also observed, and was delineated by ratios to conservative ions. These suggest that at times of highest ion concentration, the rate of loss from the dissolved phase is greatest, at two sites of differing initial composition. The study of Fe transfer, from dissolved to the solid phase, showed that the rate of transfer of Fe to the solid phase, from the dissolved phase was greater when the concentrations of Fe were highest in the stream courses. The H^+ expected to be generated by the oxidation and hydrolysis of Fe was found to be consumed by an unresolved buffering reaction taking place in the stream. The SO_4 in the stream was generally shown to be conservative in solution, with the exception of low pH, high SO_4 concentrations at Helmington Row, where a net loss of SO_4 could be seen from ratios with conservative ions. Calcium was also found to behave in a non-conservative fashion in some situations, which coincided with the reactive loss of SO_4 from the aqueous phase. The loss of these could not be wholly accounted for by gypsum precipitation, however, because the ratio of $Ca:SO_4$ removed did not equal one. The loss of Mn from solution was observed to be related to distance downstream and decline in the concentration of Fe. This has been attributed to the requirement of a higher system Eh for the precipitation of Mn, the Eh is controlled by the oxidation of Fe^{II} until such point as most of the Fe^{II} has been oxidised. Only then can the bulk stream Eh rise sufficiently to oxidise the aqueous Mn^{II} causing it to precipitate as a MnO_2 phase (precipitate composition presumed, not observed). The removal of Cu and Zn from solution was found to closely coincide with the increase in Fe_{ss} concentrations. This leads to the proposed mechanism being sorption to the Fe minerals in suspension, however, the pH of hydrolysis of Cu (~5.3) is sufficiently low that precipitation as hydroxide may be responsible for some loss, and this may occur to a lesser extent for Zn. The precipitates formed downstream from the point of discharge were found to be dominated by ferrihydrite for the few samples analysed from circum-neutral pH conditions. Where the concentrations of Al, SO_4 and Ca were also higher in the streams, the large amorphous component made it impossible to tell which minerals are present, it is surmised from published work that a hydrous $Al\text{-}SO_4$ phase is most probable.

During the course of this research, the direct measurement of Fe^{II} and Fe^{III} was identified as an important variable and this led to development of an existing Fe speciation analytical method. Testing of the 2,2-dipyridyl method for the determination of Fe^{II} and

Fe_t in natural samples showed that storage of filtered, complexed solutions in cool (~4°C) and dark conditions for a month produced no degradation in the Fe^{II}-dipyridyl complex (a parallel study, with Dr Ron Fuge, University of Wales, Aberystwyth). This was an aspect of the method which had not been demonstrated in the literature surveyed. Thus, the determination of Fe^{II} and Fe_t in samples from County Durham on the July 97 field sampling trip. The combination of dissolved oxygen and Fe redox couple data allowed Nernstian Eh to be compared with field meter measured Eh readings for these samples. This was achieved using equilibrium modelling with PHREEQ-C (WATEQ-4F database). These showed that whilst there was a difference in the Eh produced by all three methods, $O_{2(aq)}$ and the Fe redox couple were closer to each other than they were to the field meter measured Eh, and a sensitivity analysis showed the Eh method to be more important in determining the modelled speciation and saturation results, than is filtering at different pore sizes. These findings are in line with previous studies of this subject.

9.2 Conclusions

The conclusions are summarised below, in relation to the aims and objectives of the project.

Aim 1:

To understand the processes controlling the chemistry of deep mine and spoil heap drainage

Specific objectives:

I.a) Describe the chemistry of deep mine drainage, highlighting any characteristics specific to this type of discharge.

Uncontrolled, abandoned deep coal mine drainage in a mined Carboniferous Coal Measure aquifer produces water of circum-neutral pH and high Fe^{2+} (~30 mg l^{-1} at Stony Heap) and SO_4 (~300 mg l^{-1} at Stony Heap) concentrations. The other mine drainage sites have similar compositions.

The hydrogeochemistry varies spatially but is consistent temporally at individual sites.

I.b) Describe the controls on the observed fluctuations

The stable water table of these aquifers is postulated as the reason for the consistent chemical nature of the discharge waters over a 2 year timescale of study.

The presence of Fe and SO_4 is controlled by the processes of pyrite oxidation; although subsequent siderite and / or gypsum precipitation may control the discharge concentrations.

The circum-neutral pH is due to acidity buffering subsequent to the pyrite oxidation H^+ generation. This buffering has been attributed to carbonate dissolution.

The variations between sites are attributed to different concentrations of pyrite in the aquifer and / or different water table fluctuations (relative to each other), distinguished using concentrations of trace elements associated with pyrite, as well as major ions.

The presence of high concentrations of Sr, Ba and HCO_3 at Broken Banks is attributed to older Coal Measures water, mixing with the younger (pyrite oxidation product) water.

The concentrations of Cl and Na+K observed at Stony Heap are attributed to recharge of the aquifer from road run-off containing rock salt.

Ferrihydrite is found to precipitate at the points of discharge. The large accumulations at Edmondsley Yard Drift and Stony Heap are attributed to the rapid oxidation of Fe^{II}, which may be catalysed by the Gallionella sp. observed in these deposits.

The ochreous precipitates all contained evidence of goethite, which is due to the ageing of ferrihydrite, and was observed to be higher in the lower part of cores from Edmondsley Yard Drift and Stony Heap.

II.a) Describe the chemistry of spoil heap drainage, highlighting any characteristics specific to this type of discharge.

Uncontrolled, abandoned spoil heap drainage produces water of highly variable compositions at any one site. At Helmington Row (HR) high ranges of pH (~3.5-6.0) and ion concentrations were observed e.g. Fe (17-160 mg l^{-1}), Al (2-83 mg l^{-1}) and SO_4 (300-2000 mg l^{-1}). Similar results were obtained for other ions at this site, and for the compositions of Quaking Houses (QH) and Willington (WG) drainage sites.

The precipitates forming from these waters were found to vary chemically with the water composition; mineralogical analyses were largely unsuccessful due to the complex admixture of phases found when aqueous pH was low.

II.b) Describe the controls on the observed fluctuations

Spoil heap drainage chemistry is highly variable on a short temporal scale. The sampling took place on a temporal scale of months, over a period of 2 years. The fluctuations observed are postulated to be responses to short term (days - weeks) precipitation events, rather than a discernible long term trend.

The presence of Fe and SO_4 in solution is due to the process of pyrite oxidation.

The elevated concentrations of ions, associated with low pH (<5) values, are controlled by the buffering of H^+ by the spoil heap aquifer mineralogy (e.g. Ca, Al) or solubilisation from sulphide mineral oxidation (e.g. Cu, Zn).

When circum-neutral pH occurs this thought to largely be due the diluting effects of precipitation.

Recharge from road runoff is evidenced by the high concentrations of Na, K and Cl at Quaking Houses, and the correspondence to a Na:Cl mixing line.

Aim 2:

To understand the controls on the chemical fluctuations observed downstream from coal mine or spoil drainage into receiving water courses

Specific objectives:

I.a) Study the chemical variations observed on a temporal basis at each site

The rate of removal of Fe and other ions are variable downstream from discharge points.

As the concentrations of dissolved Fe, Al, Mn, Zn and Cu decreases, so their concentration in the suspended phase increases.

I.b) Compare those fluctuations between different sites

The comparison of the decline in concentrations of Al, Fe and Mn downstream shows that the decline to a lower plateau concentration takes place over a similar length of stream for all the sites, despite differing initial chemistry.

I.c) Describe the controls on the observed fluctuations

Downstream variations in chemical composition from points of discharge have been found to vary due to dilution and reactive loss.

Simplistic modelling of Fe precipitation downstream from source shows that whilst pH is affected by ferrihydrite precipitation, the stream system has adequate buffering capacity to remove the H^+ predicted by the stoichiometric reactions.

Whilst Ca and S are generally conservative in solution, in low pH conditions Ca and S have been shown to undergo reactive loss downstream from the point discharge.

The transfer of Mn from the aqueous phase to the solid phase was found to be largely controlled by the prior transfer of much of the Fe, due to the higher redox potential required for the oxidation of Mn^{II} than Fe^{II}.

Copper and Zn are transferred from the aqueous phase to the solid phase (suspended) downstream from source. This is attributed to sorption onto suspended hydrous Fe oxide phases, which is enhanced by the increases in pH observed..

Ferrihydrite precipitation is found to control the aqueous chemistry of moderate pH, high Fe concentration waters.

A more complex heterogeneous mineral assemblage was found to form from low (<5) pH, high Fe, Al, SO_4 and Ca concentration waters. The minerals present, other than ferrihydrite / ?goethite, could not be determined with the techniques available to this study, due to the large amorphous component.

Notwithstanding the above point, the chemistry of Al in solution is thought to be controlled by the precipitation of hydrous Al-SO_4 phases where pH is low (<5) and Al concentrations are high.

II.a) Describe the implications of the fluctuations observed, with respect to toxicity assessment and geochemical monitoring of such streams.

The discharge waters are in exceedance of water standards for Al, Cu and Zn at spoil heap discharges in low flow, and Fe on all occasions from deep mine discharges, and all except the highest discharges from spoil heaps.

The precipitation of ochre occurs in a variable length of stream, and has a toxic effect via the blanketing of the stream bed.

Deep mine drainage which is low in ions other than SO_4 and Fe, and has a circum-neutral pH is found to have a toxic effect. This is due to the chemical oxygen demand of Fe^{II} oxidation, which is rapid and consumes much of the dissolved O_2 downstream from the point of discharge.

The effects of deep mine and spoil heap drainage cannot fully be assessed for a site without cognisance of the receiving waters chemistry and volume, relative to the discharge, and repeated geochemical sampling over a period of time, specifically under differing hydrological regimes.

Aim 3:

To utilise appropriate techniques for assessing the chemical composition of the aqueous and solid phases studied

Specific objectives:

I.a) Increase the range of protocols used as methods are developed and equipment becomes available during the study

The determinants increased as the project progressed. Access was gained to dissolved oxygen meters enabling field measurements. Method testing was undertaken to ascertain that Fe^{II} and Fe_t samples could be field stabilised and returned for laboratory analysis within a month.

I.b) Analyse the mineralogical and chemical composition of solid phases

It was not possible to identify chemically heterogeneous hydrous phases of Fe and Al using XRD (poorly crystalline and excessive instrument time required) and SEM (samples disintegrate).

Care needs to be exercised assuming that there is chemical equilibrium between the aqueous and solid phases, particularly where recent changes in the chemical composition of the waters has taken place.

I.c) Use geochemical modelling to assess the aqueous speciation and saturation indices of the aqueous phase samples

Hydrogeochemical modelling proved useful for aqueous speciation prediction, however, no independent verification of the predictions was possible and thus, given the well established limitations of modelling, they should be treated with due caution.

Modelling of saturation indices modelling was undertaken, but proved of limited success applied to the systems studied, due metastable phases being kinetically favoured over the most thermodynamically stable phase. Thus metastable phases control the water chemistry. This control was confirmed on all occasions by the relationship between the occurrences of ferrihydrite and goethite.

9.3 General considerations

This research has showed that deep mine drainage is characterised by high Fe and SO_4 loading in the dissolved phase. The moderate pH has been attributed to carbonate buffering. These chemical compositions may not be relevant to a newly emerging water table (which are known to generally by of a lower pH and higher Fe and SO_4 concentrations - section 2.1), but they do suggest that if pumping of groundwater ceases in the Durham Coalfield, then where the groundwater discharges to surface water courses (Sherwood & Younger, 1994), without any remediation, they would be expected to provide a large loading of Fe and SO_4 to the river Wear catchment for decades, at least. These findings are also believed to be applicable on a broad scale in Britain, due to the similarities of the chemical composition of the waters found in other studies, with those observed here.

The spoil heap discharges have been shown to be a have a more deleterious effect on the recipient streams, and are thought to have been draining for an equally long time. It is suggested that this is due to the pyrite (and other sulphides) concentrations being greater than the carbonate buffering capacity of the spoil heap. These discharges have shown difference in behaviour between sites, and this is likely to be due to variations in the composition of the spoil heaps. This suggests that spoil heaps require a more specific site investigation, and knowledge of the composition of material laid down would be invaluable in determining the controlling influences on their discharge chemistry.

9.4 Recommendations for further work

Deep mine drainage:

Mineralogical analysis of the coal and associated sediments of the study area would confirm whether the buffering of pH by carbonates is feasible.

Water table and discharge volume monitoring could assess the role of a stable water table in maintaining lower concentrations of the Fe and SO_4 than is found in spoil heaps.

Spoil Heap drainage:

The monitoring of the discharges through a storm event would enable assessment of the composition of the aqueous phase when any Fe^{II}-sulphates are flushed out.
The toxicity assessments of the streams impacted by these discharges would appear to be important due to their increased trace element burden on the stream in low flow conditions.

Downstream behaviour of ions:

The relative contribution of temperature, water flow velocity and chemistry could be studied to see how they interact in maintaining suspended phases in suspension.
The phases controlling the precipitation of Al from solution could be studied in greater detail, particularly with reference to their behaviour in a stream where the pH subsequently increases.

References

Ahonen, L. & Tuovinen, O.H. 1989 Microbiological oxidation of ferrous iron at low temperatures. *Applied and Environmental Microbiology* **55** 312-316

Aldous, P.J. 1987 *The Groundwater Hydrology of an Abandoned Coal Mined Aquifer. A Case Study of the Forest of Dean Coalfield.* Unpublished PhD Thesis, University of Bristol, pp271

Aldous, P.J., Smart, P.L. & Black, J.A. 1986 Groundwater Management Problems in a Coal Mined Aquifer System: A Case Study from the Forest of Dean Coalfield, England. *Quarterly Journal of Engineering Geology* **19** 375-388

Alpers, C.N., Blowes, D.W., Nordstrom, D.K. & Jambor, J.L. 1994a Secondary minerals and acid mine-water chemistry. **In:** Jambor, J.L. & Blowes, D.W. (eds) *The environmental geochemistry of sulfide-mine wastes.* Short course handbook, Mineralogical Association of Canada, Waterloo, Ontario. Chapter 9 247-270

Alpers, C.N., Nordstrom, D.K. & Thompson, J.M. 1994b Seasonal variations of Zn/Cu ratios in acid mine water from Iron Mountain, California. **In:** Alpers, N. & Blowes, D.W. (eds) 1994 *Environmental Geochemistry of Sulfide Oxidation.* ACS Symposium Series **550**. American Chemical Society, Washington, D.C., USA. Chapter 22 325-344

Alpers, C.N. & Blowes, D.W. (eds) 1994 *Environmental Geochemistry of Sulfide Oxidation.* ACS Symposium Series **550**. American Chemical Society, Washington, D.C., USA.

Analytical Methods Committee 1989 Robust statistics - how not to reject outliers. Part 2 interlaboratory trials. *Analyst* **114** 1699-1705

Ander, E.L. & Fuge, R. 1997 Iron(II) and iron(III) determinations in ferruginous mine drainage: testing a colorimetric method. *Geological Society of America abstracts with programs*, **29(6)**, 154, October 1997.

Anderson, W. 1945a On the Chloride Waters of Great Britain. *Geological Magazine* **82** 267-273

Anderson, W. 1945b *Water Supply from Underground Sources of North-East England.* Wartime Pamphlet No. 19, Geological Survey of Great Britain: England and Wales, London, pp20

Appelo, C.A.J. & Postma, D. 1993 *Geochemistry, Groundwater and Pollution.* AA Balkema Publishers, Rotterdam, pp536

Bailey, R.A. 1993 Proceedings of IWEM Symposium on Environmental Effects of Coal Mine Closures. *Journal of the Institution of Water and Environmental Management* 7 436-437

Ball, J.W. & Nordstrom, D.K. 1989 Final revised analyses of major and trace elements from acid mine waters in the Leviathan mine drainage basin, California and Nevada - October 1981 to October 1982. *US Geological Survey Water-Resources Investigations Report* **89-4138**

Ball, J.W. & Nordstrom, D.K. 1991 User's manual for WATEQ4F; with revised thermodynamic database and test cases for calculating speiciation of major, trace and redox elements in natural waters. *USGS Open-File report* **91-183**

Banks, D. 1997 Hydrogeochemistry of Millstone Grit and Coal Measures groundwaters, south Yorkshire and north Derbyshire, UK. *Quarterly Journal of Engineering Geology* **30** 237-256

Berner, R.A. 1981 A new geochemical classification of sedimentary environments. *Journal of Sedimentary Petrology* **51(2)** 359-365

Berner, R.A. & Raiswell, R. 1984 C/S method for distinguishing freshwater from marine sedimentary rocks. *Geology* **12** 365-368

Bethke, C.M. 1996 *Geochemical reaction modeling. Concepts and applications*. Oxford University Press, Oxford, UK.

BGS 1996a *Metallogenic map of Britain and Ireland* 1:1500000 series. BGS, Keyworth, UK.

BGS 1996b *Regional geochemistry of North-East England*. BGS, Keyworth, UK

Bhatti, T.M., Bigham, J.M., Carlson, L. & Tuovinen, O.H. 1993 Mineral products of pyrrhotite oxidation by Thiobacillus ferrooxidans. *Applied and Environmental Microbiology* **59(6)** 1984-1990

Bi, S. & Yin, W. 1995 Chemical equilibrium calculation for evaluating the buffering capacity of acidic natural water equilibria with the mineral phase gibbsite. *Analyst* **120** 2805-2811

Bierens de Haan, S. 1991 A review of the rate of pyrite oxidation in aqueous systesm at low temperature. *Earth-Science Reviews* **31** 1-10

Bigham, J.M. 1994 Mineralogy of ochre deposits formed by sulfide oxidation. **In**: Jambor, J.L. & Blowes, D.W. (eds) *Environmental geochemistry of sulfide mine-wastes*. Short course handbook, Mineralogical Association of Canada, Waterloo, Ontario. Volume 22, Chapter 4, 103-132

Bigham, J.M., Carlson, L. & Murad, E. 1994 Schwertmannite, a new iron oxyhydroxysulphate from Pyhäsalmi, Finland, and other localities. *Mineralogical Magazine* **58** 641-648

Bigham, J.M., Schwertmann, U. & Carlson, L. 1992 Mineralogy of precipitates formed by the biogeochemical oxidation of Fe(II) in mine drainage. **In:** Skinner, H.C.W. & Fitzpatrick, R.W. (eds) *Biomineralization processes of iron and managenese*. Catena supplement **21**, 219-232

Bigham, J.M., Schwertmann, U., Carlson, L. & Murad, E. 1990 A poorly crystallized oxyhydroxysulfate of iron formed by bacterial oxidation of Fe(II) im acid mine waters. *Geochimica et Cosmochimica Acta* **54** 2743-2758

Bigham, J.M., Schwertmann, U. & Pfab, G. 1996b Influence of pH on mineral speciation in a bioreactor simulating acid mine drainage. *Applied Geochemistry* **11** 845-849

Bigham, J., Schwertmann, U., Traina, S.J., Winland, R.L. & Wolf, M. 1996a Schwertmannite and the chemical modelling of iron in acid sulfate waters. *Geochimica et Cosmochimica Acta* **60** 2111-2121

Boult, S. 1996 Fluvial metal transport near sources of acid mine-drainage: relationships of soluble, suspended and deposited metal. *Mineralogical Magazine* **60** 325-335

Boult, S., Collins, D.N., White, K.N. & Curtis, C.D. 1994 Metal transport in a stream polluted by acid mine drainage - the Afon Goch, Anglesey, UK. *Environmental Pollution* **84** 279-284

Bradley, K.F. 1993 *A Study of Water Quality Deterioration as a Result of Coal Mine Drainage in Northumberland and Durham.* Unpublished MSc Thesis, Department of Civil Engineering, University of Newcastle-Upon-Tyne, pp60

Brady, K.S. Bigham, J.M., Jaynes, W.F. & Logan, T.J. 1986 Influence of sulfate on Fe-oxide formation: comparisons with a stream receiving acid mine drainage. *Clays and Clay Minerals* **34(3)** 266-274

British Coal 1990 *Coal analysis report for North East Group.* Scientific Services, Bretby, quarter ending 31 March 1990.

Broshears, R.E., Runkel, R.L., Kimball, B.A., McKnight, D.M & Bencala, K.E. 1996 Reactive solute transport in an acidic stream: experimental pH increase and simulation of controls on pH, aluminum, and iron. *Environmental Science and Technology* **30** 3016-3024

Brown, G. 1980 Associated minerals. **In:** Brindley, G.W. & Brown, G. (eds*) Crystal structures of clay minerals and their X-ray identification.* Mineralogical Society Monograph No. 5, London, UK. Chapter 6 361-410

Broyd, T.W., Grant, M.M. & Cross, J.E. 1985 *A report on the intercomparison studies of computer programs which respectively model: i) radionuclide migration ii) equilibrium chemistry of groundwater.* EUR 10231EN, Commission of the European Communities, Luxembourg.

Bullock, S.E.T. & Bell, F.G. 1997 Some problems associated with past mining at a mine in the Witbank coalfield, South Africa. *Environmental Geology* **33** 61-71

Burley, A.J., Edmunds, W.M. & Gale, I.N. 1984 *Investigation of the Geothermal Potential of the UK.* Catalogue of Geothermal Data for the Land Area of the United Kingdom. (Second Revision). BGS, Keyworth, pp26

Cairney, T. 1972 Hydrological investigation of the Magnesian Limestone of South-East Durham, England. *Journal of Hydrology* **16(4)** 323-340

Cairney, T. & Frost, R.C. 1974 A case study of mine water quality deterioration, Mainsforth Colliery, County Durham. *Journal of Hydrology* **25** 275-293

Carlson, L. & Schwertmann, U. 1981 Natural ferrihydrites in surface deposits from Finland and their association with silica. *Geochimica et Cosmochimica Acta* **45** 421-429

Carpenter, K.E. 1924 A study of the fauna of rivers polluted by lead mining in the Aberystwyth district of Cardiganshire. *Annals of Applied Biology* **11** 1-23

Carrucio, F.T., Ferm, J.C., Horne, J., Geidel, G. & Baganz, B. 1977 Paleoenvironment of coal and its relation to drainage quality. Report to US EPA, Industrial Environmental Research Laboratory, Cincinnati, Ohio, Interagency Energy-Environment Research and Development Program Report, EPA-600/7-77-067, pp118

Casagrande, D.J., Finkelman, R.B. & Caruccio, F.T. 1989 The non-participation of organic sulphur in acid mine drainage generation. *Environmental Geochemistry and Health* **11(3/4)** 187-192

Chadwick, R.A., Holliday, D.W., Holloway, S. & Hulbert, A.G. 1995 *The structure and evolution of the Northumberland-Solway Basin and adjacent areas*. British Geological Survey Subsurface Memoir, HMSO, London, UK.

Chapman, B.M., Jones, D.R. & Jung, R.F. 1983 Processes controlling metal ion attenuation in acid mine drainage streams. *Geochimica et Cosmochimica Acta* **47** 1957-1973

Clarke, L.B. & Sloss, L.L. 1992 *Trace Elements - Emissions from Coal Combustion and Gasification*. IEA Coal Research, London, pp111

Clarke, W.A., Konhauser, K.O., Thomas, J.C. & Bottrell, S.H. 1997 Ferric hydroxide and ferric hydroxysulfate precipitation by bacteria in an acid mine drainage lagoon. *FEMS Microbiology Reviews* **20** 351-361

Cornell, R.M. & Schwertmann, U. 1996 *The iron oxides*. VCH, Germany. ISBN: 3-527-28576-8

Creaney, S. 1980 Petrographic texture and vitrinite reflectance variation on the Alston Block, North-East England. *Proceedings of the Yorkshire Geological Society* **42(4)** 553-580

Davidson, W.H., Ashby, W.C. & Vogel, W.G. 1988 Progressive changes in minespoil pH over 3 decades. Mine Drainage and Surface Mine Reclamation. Volume II: Mine reclamation, abandoned mine lands and policy issues. *USBM IC* **9184** 89-92.

Davies, G., Butler, D., Mills, M. & Williams, D. 1997 A survey of ferruginous minewater impacts in the Welsh Coalfields. *Journal of the Chartered Institution of Water and Environmental Management* **11** 140-146

Dearlove, J.P.L. 1994 Baseline Hydrogeochemical Study of Shallow Groundwaters in NE England. (Extended Abstract) *Mineralogical Magazine* **58A** 217-218

Deer, W.A., Howie, R.A. & Zussman, J. 1966 *An introduction to the rock-forming minerals*. Longman, Harlow, UK.

Department of the Environment 1994. *The Reclamation and Management of Metalliferous Mining Sites*. HMSO, London, pp168

Department of the Environment, Department of Energy, Scottish Office & Welsh Office 1984 *Coal and the Environment. The Government's response to the Commission on Energy and the Environment's Report on 'Coal and the Environment'.* HMSO, London.

Dryburgh, P.A., Norton, P.J. & Scott, W.B. 1991 A source of manganese pollution in Appalachian coal shales. Proceedings *4th International Mineral Water Association Congress*, Ljubljana, Slovenia - Pörtschach, Austria, September 1991

Dudeney, A.W.L. & Monhemius, A.J. 1992 *Ferruginous discharges from disused coal workings in the United Kingdom.* Interim Report, R&D Project 339. NRA, Bristol, UK.

Dunham, K.C. 1990 *Geology of the Northern Pennine Orefield, Volume 1 Tyne to Stainmore (2nd Edition).* Economic Memoir of the British Geological Survey. HMSO, London, pp299

Dzombak, D.A. & Morel, F.M.M. 1990 *Surface complexation modeling: hydrous ferric oxides.* Wiley, New York.

Edmunds, W.M. 1975 Geochemistry of brines in the Coal Measures of Northeast England. *Transactions of the Institution of Mining and Metallurgy: Section B Applied Earth Sciences* **(84)** 39-51

Eley, M. & Nicholson, K. 1993 Chemistry and adsorption-desorption properties of manganese oxides deposited in Forehill Water Treatment Plant, Grampian, Scotland. *Environmental Geochemistry and Health* **15(2/3)** 85-91

Emerson, D. & Reusbech, N.P. 1994 Investigation of an iron-oxidising microbial mat community located near Aarhus, Denmark: field studies. *Applied and Environmental Microbiology* **60** 4022-4031

ENDS 1991 Mine Pollution "Time-Bomb" Highlights Weaknesses in Clean-up Liability. *ENDS Report* **195** 8

ENDS 1993 Failure of Test Case on Abandoned Mines. *ENDS Report* **227** 44-45

Faulkner, S.P. & Richardson, C.J. 1990 Iron and manganese fractionation in constructed wetlands receiving acid mine drainage. **In**: Cooper, P.F. & Findlatter, B.C. 1990 *Constructed Wetlands in Water Pollution Control.* Pergamon Press, Oxford.

Fenchel, T., King, G.M. & Blackburn, T.H. 1998 *Bacterial biogeochemistry: the ecophysiology of mineral cycling.* (2nd ed.) Academic Press, California, USA.

Ferris, F.G., Tazaki, K., & Fyfe, W.S. 1989 Iron oxides in acid mine drainage environments and their association with bacteria. *Chemical Geology* **74** 321-330

Fielding, C.R. *1982 Sedimentology and stratigraphy of the Durham Coal Measures and comparison with other British coalfields.* Unpublished PhD thesis, University of Durham.

Fielding, C.R. 1984a Upper delta plain lacustrine and fluviolacustrine facies from the Westphalian of the Durham Coalfield, NE England. *Sedimentology* **31(4)** 547-567

Fielding, C.R. 1984b 'S' or 'Z' shaped coal seam splits in the Coal Measures of County Durham. *Proceedings of the Yorkshire Geological Society* **45(1/2)** 85-89

Fielding, C.R. 1985 Coal depositional models and the distinction between alluvial and delta plain environments. *Sedimentary Geology* **42(1/2)** 41-48

Fielding, C.R. 1986 Fluvial channels and overbank deposits from the Westphalian of the Durham Coalfield, NE England. *Sedimentology* **33(1)** 119-140

Ford. R.G., Bertsch, P.M. & Farley, K.J. 1997 Changes in transition and heavy metal partitioning during hydrous iron oxide aging. *Environmental Science and Technology* **31** 2028-2033

Förstner, U. & Wittman, G.W. 1979 *Metal Pollution in the Aquatic Environment.* Springer, Berlin, pp486

Freeze, R.A. & Cherry, J.A. 1979 *Groundwater.* Prentice Hall, New Jersey, USA

Frost, R.C. 1977 *The nature of coal mine drainage in the South Durham Area.* PhD Thesis, Teesside Polytechnic. 328pp

Frost, R.C. 1978a Variations in the iron content of some outcrop waters in South Durham. *Colliery Guardian* **226(5)** 233-234

Frost, R.C. 1978b The variable iron content of mine flood water: implications for sampling and pollution control. *Colliery Guardian International* **226(10)** 36-38

Frost, R.C. 1979a Evaluation of the rate of decrease in the iron content of water pumped from a flooded shaft mine in County Durham, England. *Journal of Hydrology* **40(1/2)** 101-111

Frost, R.C. 1979b Pumping rates and the iron content of shaft mine water. *Effluent and Water Treatment Journal* **19(2)** 77-80

Fuge, R. 1972 The chemistry of some mine waters from Cardiganshire. Mineral Exploitation and Economic Geology. *Papers given at the University of Wales Inter-Collegiate Colloquim* Gregynog September 22-24 1972.

Fuge, R. Laidlaw, I.M.S., Perkins, W.T. & Rodgers, K.P. 1991 The influence of acidic mine and spoil drainage on water quality in the mid-Wales area. *Environmental Geochemistry and Health* **13(2)** 70-75

Fuge, R., Pearce, F.M., Pearce, N.J.G. & Perkins, W.T. 1994 Acid mine drainage in Wales and influence of ochre precipitation on water chemistry. **In:** Alpers, C.N. & Blowes, D.W. (eds) 1994 *Environmental Geochemistry of Sulfide Oxidation.* ACS Symposium Series **550**. American Chemical Society, Washington, D.C., USA. Chapter 18 261-274

Gardiner, J. & Mance, G. 1984 *UK water quality standards arising from European Community Directives.* Water Research Centre Technical Report TR204

Glover, H.G. 1983 Mine water pollution - an overview of problems and control strategies in the UK. *Water Science and Technology* **15(2)** 59-70

Gramm-Osipov, L. 1997 Formation of solid phases of manganese in oxygenated aquatic environments. **In**: Nicholson, K., Hein, J.R., Bühn, B. & Dasgupta, S. (eds) *Manganese mineralization: geochemistry and mineralogy of terrestrial and marine deposits.* Geological Society Special Publication **119** 301-308

Greenfield, J.P. & Ireland, M.P. 1978 A survey of the macrofauna of a coal-waste polluted Lancashire fluvial system. *Environmental Pollution* **16** 105-122

Grishin, S.I., Bigham, J.M. & Tuovinen, O.H. 1988 Characterization of jarosite formed upon bacterial oxidation of ferrous sulfate in a packed-bed reactor. *Applied and Environmental Microbiology* **54(12)** 3101-3106

Haines, T.S. & Lloyd, J.W. 1985 Controls on silica in groundwater environments in the United Kingdom. *Journal of Hydrology* **81** 277-295

Hall, G.E.M., Bonham-Carter, G.F., Horowitz, A.J., Lum, K., Lemieux, C., Quemerais, B. & Garbarino, J.R. 1996 The effect of using different 0.45μm filter membranes on "dissolved" element concentrations in natural waters. *Applied Geochemistry* **11** 243-249

Harrison, R., Scott, W.B. & Smith, T. 1989 A Note on the Distribution Levels and Temperatures of Minewaters in the Durham Coalfield. (Technical Note). *Quarterly Journal of Engineering Geology* **22** 355-358

Hartley, D. & Wright, P. 1988 Derelict land reclamation in the United Kingdom. Mine Drainage and Surface Mine Reclamation. Volume II: Mine reclamation, abandoned mine lands and policy issues. *USBM IC* **9184** 200-205

Hawkins, P.J. 1978 Relationship between diagenesis, porosity reduction, and oil emplacement in late Carboniferous sandstone resevoirs, Bothamsall Oilfield, E. Midlands. *Journal of the Geological Society of London*, **135** 7-24

Headworth, H.G., Puri, S. & Rampling, B.H. 1980 Contamination of a Chalk Aquifer by Mine Drainage at Tilmanstone, East Kent, UK. *Quarterly Journal of Engineering Geology* **13** 105-117

Helz, G.R., Dai, J.H., Kijak, P.J., Fendinger, N.J. & Radwa, J.C. 1987 Processes controlling the composition of acid sulfate solutions evolved from coal. *Applied Geochemistry* **2** 427-436

Hem, J.D. 1985 Study and Interpretation of the chemical characteristics of natural water. *USGS Water-Supply Paper* **2254** (3rd Edition).

Henton, M.P. 1976 Predicting the quality of mine water discharges. *Effluent and Water Treatment Journal* **16(11)** 568, 572

Henton, M.P. & Young, P.J. 1993 Contaminated land and aquifer protection. *Journal of the Institution of Water and Environmental Management* **7** 539-547

Hirst, D.M. & Kaye, M.J. 1971 Factors controlling the mineralogy and chemistry of an Upper Visean sedimentary sequence from Rookhope, County Durham. *Chemical Geology* **8** 37-59

Horowitz, A.J., Lum, K.R., Gabbarino, J.R., Hall, G.E.M., Lemieux, C. & Demas, C.R. 1996 The effect of membrane filtration on dissolved trace element concentrations. *Water, Air and Soil Pollution* **90** 281-294

Hostettler, J.D. 1984 Electrode electrons, aqueous electrons and redox potentials in natural waters. *American Journal of Science* **284** 734-759

Huggins, F.E. & Huffman, G.P. 1996 Modes of occurrence of trace elements in coal from XAFS spectroscopy. *International Journal of Coal Geology* **32** 31-56

Hughes, P. 1994 *Water Pollution from Abandoned Coal Mines.* Research Paper 94/43 (11 March 1994), Science and Environment Section, House of Commons Library, pp22

Ineson, J. 1967 *Groundwater conditions in the Coal Measures of South Wales Coalfield.* Institute of Geological Sciences Water Supply Paper, Hydrogeological Report No 3, pp69

Jambor, J.L. & Blowes, D.W. (eds) *The environmental geochemistry of sulfide-mine wastes*. Short course handbook, Mineralogical Association of Canada, Waterloo, Ontario. Volume 22.

Jarvis, A.P. 1994 *Impacts of acid mine drainage on the chemistry and invertebrate fauna of two streams in the Durham Coalfield.* Unpublished MSc Thesis, Department of Civil Engineering, University of Newcastle-Upon-Tyne, pp74

Johnson, C.A. 1986 The regulation of trace element concentrations in river and estuarine waters contaminated with acid mine drainage: the adsorption of Cu and Zn on amorphous Fe oxyyhydroxides. *Geochimica et Cosmochimica Acta* **50** 2433-2438

Johnson, C.A. & Thornton, I. 1987 Hydrological and Chemical Factors Controlling the Concentrations of Fe, Cu, Zn and As in a River System Contaminated by Acid Mine Drainage. *Water Research* **21(3)** 359-365

Jones, B.F., Kennedy, V.C. & Zellweger, G.W. 1974 Comparison of Observed and Calculated Concentrations of Dissolved Al and Fe in Stream Waters. *Water Resources Research* **10(4)** 791-793

Karlsson, S., Peterson, A., Häkansson, K. & Ledin, A. 1994 Fractionation of trace metals in surface waters with screen filters. *The Science of the Total Environment* **149** 215-223

Kelly, M. 1988 *Mining and the Freshwater Environment.* Elsevier Applied Science, London, pp231

Kempton, J.H., Lindberg, R.D. & Runnells, D.D. 1990 Numerical modeling of platinum Eh measurements using heterogenous electron-transfer kinetics. **In:** Melchoir, D.C. & Basset R.L. (eds) *Chemical modeling in aqueous systems II.* ACS Symposium Series 416 American Chemical Society, Washington, USA. Chapter 27, 339-349.

Kimball, B.A., McKnight, D.M., Wetherbee, G.A. & Harnish, R.A. 1992 Mechanisms of iron photoreduction in a metal-rich, acidic stream (St. Kevin Gulch, Colarado, USA). *Chemical Geology* **96** 227-239

King, T.V.V. (ed) 1995 Environmental considerations of active and abandoned mine lands. *US Geological Survey Bulletin* **2220** pp38

Kirby, C.S. & Brady, J.A.E. 1998 Field determination of Fe^{2+} oxidation rates in acid mine drainage using a continuously-stirred tank reactor. *Applied Geochemistry* **13(4)** 509-520

Konhauser, K.O. 1997 Bacterial iron biomineralization in nature. *FEMS Microbiology Reviews* **20** 315-326

Kostova, I., Petrov, O. & Kortenski, J. 1996 Mineralogy, geochemistry and pyrite content of Bulgarian subbituminous coals, Perik Basin. **In:** Gayer, R. & Harris, I. (eds) *Coalbed methane and coal geology.* Geological Society Special Publication **109** 301-314.

Krauskopf, K.B. & Bird, D.K. 1995 *Introduction to Geochemistry* (Third Edition). McGraw-Hill Inc., New York, USA.

Kwong, Y.T.J. & Van Stempvoort, D.R. 1994 Attenuation of acid rock drainage in a natural wetland system. **In:** Alpers, N. & Blowes, D.W. (eds) 1994 *Environmental Geochemistry of Sulfide Oxidation.* ACS Symposium Series **550**. American Chemical Society, Washington, D.C., USA. Chapter 25 382-392

Land, D.H. 1974 *Geology of the Tynemouth District.* Memoir of the Geological Survey of Great Britain. Institute of Geological Sciences, HMSO, London, pp176

Lane, P. & Peto, M. 1995 *Blackstone's guide to the Environment Act 1995.* Blackstone Press Ltd, London.

Lee, M.R. 1994 Emplacement and Diagenesis of Gypsum and Anhydrite in the Late Permian Raisby Formation, North-East England. *Proceedings of the Yorkshire Geological Society* **50(2)** 143-155

Letterman, R.D. & Mitsch, W.J. 1978 Impact of mine drainage on a mountain stream in Pennsylvannia. *Environmental Pollution* **17** 53-73

Levinson, A.A. 1980 *Introduction to Exploration Geochemistry.* Applied Publishing Limited, Wilmette, Illinois, USA. pp924

Lindberg, R.D. & Runnells, D.D. 1984 Ground Water Redox Reactions: An analysis of equilibrium state applied to Eh measurements and geochemical modeling. *Science* **225** 925-927

Lowson, R.T. 1982 Aqueous oxidation of pyrite by molecular oxygen. *Chemical Reviews* **82** 461-497

Macalady, D.L., Langmuir, D., Grundl, T. & Elzerman, A. 1990 Use of model-generated Fe^{3+} ion activities to compute Eh and ferric oxyhydroxide solubilities in anaerobic systems. **In:** Melchoir, D.C. & Basset R.L. (eds) *Chemical modeling in aqueous systems II.* ACS Symposium Series **416** American Chemical Society, Washington, USA. Chapter 28, 350-367.

Marley, N.A., Gaffney, J.S., Orlandini, K.A. & Dugue, C.P. 1991 An evaluation of an automated hollow-fibre ultrafiltration apparatus for the isolation of colloidal materials in natural waters. *Hydrological Processes* **5** 291-299

McKnight, D.M. & Bencala, K.E. 1989 Reactive iron transport in an acidic mountain stream in Summit County, Colorado: A hydrologic perspective. *Geochimica et Cosmochimica Acta* **53** 2225-2234

McKnight, D.M., Kimball, B.A. & Bencala, K.E. 1988 Iron photoreduction and oxidation in an acidic mountain stream. *Science* **240** 637-640

Miller, J.C. & Miller, J.N. 1984 *Statistics for analytical chemistry.* Ellis Horwood Ltd., Chichester.

Mills, D.A.C. & Hull, J.H. 1976 *Geology of the Country around Barnard Castle.* Institute of Geological Sciences, London. HMSO, pp385

Morrison, J.L., Sheetz, B.E., Strickler, D.W., Williams, E.G., Rose, A.W., Davis, A. & Parizek, R.R. 1990 Predicting the occurrence of acid mine drainage in the Alleghenian coal-bearing strata of western Pennsylvania; An assessment by simulated weathering (leaching) experiments and overburden characterization. **In:** Chyi, L.L. & Chou, C.-L. (eds) Recent advances in coal geochemistry. *Geological Society of America Special Paper* **248** 87-99.

Moses, C.O., Nordstrom, D.K., Herman, J.S. & Mills, A.L. 1987 Aqueous pyrite oxidation by dissolved oxygen and by ferric iron. *Geochimica et Cosmochimica Acta* **51** 1561-1571

Moss, M.L. & Mellon, M.G. 1942 Colorimetric Determination of Iron with 2,2'-Bipyridyl and with 2,2',2"-Terpyridyl. *Industrial and Engineering Chemistry, Analytical Edition* **14(11)** 862-865

Murad, E., Schwertmann, U., Bigham, J.M. & Carlson, L. 1994 Mineralogical characteristics of poorly crystallized precipitates formed by oxidation of Fe^{2+} in acid sulfate waters. **In:** Alpers, C.N. & Blowes, D.W. (eds) *Environmental geochemistry of sulfide oxidation.* ACS Symposium Series **550**, American Chemical Society, Washington DC, USA. Chapter 14 190-200

National Rivers Authority 1994a. *A Survey of Ferruginous Minewater Impacts in the Welsh Coalfields.* NRA Welsh Region (Welsh Office Contract WEP 100/138/11). pp40

National Rivers Authority 1994b *Abandoned Mines and the Water Environment.* Report of the NRA, Water Quality Series No 14 (March 1994), London, HMSO, pp45

National Rivers Authority 1994c *Implementation of the EC Freshwater Directives.* Water Quality Series No. 20. HMSO

NCB 1959 *Durham Coalfield. Seam maps - Busty.* Scientific Department, Coal Survey.

NCB 1961 *Durham Coalfield. Seam maps - Hutton.* Scientific Department, Coal Survey.

Neate, C.J. 1980 *Effects of mining subsidence on the permeability of Coal Measures rocks.* Unpublished PhD thesis, University of Nottingham.

Newton, P.P. & Liss, P.S. 1987 Positively charged suspended particles: studies in an iron-rich river and iis estuary. *Limnology Oceanography* **32** 1267-1276

Nicholson, K. & Eley, M. 1997 Geochemistry of manganese oxides: metal adsorption in freshwater and marine environments. **In**: Nicholson, K., Hein, J.R., Bühn, B. & Dasgupta, S. (eds) *Manganese mineralization: geochemistry and mineralogy of terrestrial and marine deposits.* Geological Society Special Publication **119** 309-326

Nordstrom, D.K. 1982a Aqueous pyrite oxidation and the consequent formation of secondary iron minerals. **In:** Kittrick, J.A., Fanning, D.S. & Hossner, L.R. *Acid Sulfate Weathering.* Soil Science Society of America Special Publication **10**, Madison, Wis., USA. Chapter 3 37-56

Nordstrom, D.K. 1982b The effect of sulfate on aluminium concentrations in natural waters: some stability relations in the system Al_2O_3-SO-H_2O at 298K. *Geochimica et Cosmochimica Acta* **46** 681-692

Nordstrom, D.K. 1985 The rate of ferrous iron oxidation in a stream receiving acid mine effluent. **In:** Subitzky, S. (ed) Selected Papers in the Hydrologic Sciences 1985. *USGS Water-Supply Paper* **2270** 113-119

Nordstrom, D.K. 1996 Trace metal speciation in natural waters: computational vs. analytical. *Water, Air and Soil Pollution* **90** 257-267

Nordstrom, D.K. & Alpers, C.N. 1997 Geochemistry of acid mine waters. **In:** Plumlee, G.S. & Logsdon, M.J. (eds) *The environmental geochemistry of mineral deposits*. Part A: Processes, techniques, and health issues. Reviews in economic geology **7A**. Chapter 6 (in press)

Nordstrom, D.K. & Ball, J.W. 1986 The geochemical behavior of aluminium in acidified surface waters. *Science* **232** 54-56

Nordstrom, D.K. & Munoz, J.L. 1994 *Geochemical thermodynamics* (2nd edition). Blackwell Scientific Press, Boston, Massachusetts, USA. ISBN: 0-86542-274-5

Nordstrom, D.K. & Southam, G. 1997 Geomicrobiology of sulfide mineral oxidation. **In:** Banfield, J.F. & Nealson, K.H. (eds) *Geomicrobiology: interactions between microbes and minerals*. Reviews in mineralogy **35** Mineralogical Society of America, Washington, D.C., USA.

Nordstrom, D.K. McNutt, R.H., Puigdomènech, I., Smellie, J.A.T. & Wolf, M. 1992 Ground water chemistry and geochemical modeling of water-rock interactions at the Osamu Utsumi mine and the Morro do Ferro analogue study sites, Poços de Caldas, Minas Gerais, Brazil. *Journal of Geochemical Exploration* **45** 249-287

Nordstrom, D.K., Jenne, E.A. & Ball, J.W. 1979a Redox equilibria of iron in acid mine waters. **In:** Jenne, E.A. (ed) *Chemical modeling in aqueous systems*. ACS Symposium Series **93**, American Chemical Society, Washington D.C., USA. Chapter 3, 51-79.

Nordstrom, D.K., Plummer, L.N., Wigley, T.M.L., Wolery, T.J., Ball, J.W., Jenne, E.A., Bassett, R.L., Crerar, D.A., Florence, T.M., Fritz, B., Hoffman, M., Holdren, C.R., Lafon, G.M., Mattigod,S.V., McDuff, R.E., Morel, F., Reddy, M.M., Sposito, G. & Thraikill, J. 1979b A comparison of computerized chemical models for equilibrium calculations in aqueous systems. **In:** Jenne, E.A. (ed) *Chemical modeling in aqueous systems*. ACS Symposium Series **93**, American Chemical Society, Washington D.C., USA. Chapter 38, 857-892.

Ordnance Survey, 1945 Coal and Iron, Great Britain (Map) Scale 1:625000, Sheet 1. Ordnance Survey, Southampton, UK.

Ordnance Survey, 1945 Coal and Iron, Great Britain (Map) Scale 1:625000, Sheet 2. Ordnance Survey, Southampton, UK.

Ott, A.N. 1987 Dual-acidity titration curves-fingerprint, indicator of redox state, and estimator of iron and aluminium content of acid mine drainage and related waters. **In:** Subitzky. S. Selected Papers in the Hydrologic Sciences 1987. *USGS Water-Supply Paper* **2330** 19-33

Paces, T. 1978 Reversible control of aqueous aluminium and silica during the irreversible evolution of natural waters. *Geochimica et Cosmochimica Acta* **42** 1487-1493

Parkhurst, D.L. 1995 User's guide to PHREEQC - a computer program for speciation, reaction-path, advective-transport, and inverse geochemical calculations. *US Geological Survey Water-Resources Investigations Report* **95-4227**

Payne, C.A. 1994 *A Study of the Effects of Metal Rich Mine Drainage on Reed Beds in Cornwall.* Unpublished MSc Thesis, Imperial College (University of London), pp105

Pehkonen, S. 1995 Determination of the oxidation states of iron in natural waters. A review. *Analyst* **120** 2655-2663

Querol, X. & Chenery, S. 1995 Determination of trace element affinities in coal by laser ablation microprobe-inductively coupled plasma mass spectrometry. **In**: Whateley, M.K.G. & Spears, D.A. (eds) *European Coal Geology*. Geological Society Special Publication **82** 147-155

Rae, G. 1978 *Mine Drainage from Coalfields in England and Wales. A Summary of its Distribution and Relationship to Water Resources.* Technical Note No 24, Central Water Planning Unit, Reading, pp22

Ramsey, M.H. 1993 Sampling and Analytical Data Quality Control (SAX) for improved error estimation in the measurement of Pb in the environment using robust analysis of variance. *Applied Geochemistry* **Supplimentary Issue 2** 149-153

Ramsey, M.H., Argyraki, A. & Thompson, M. 1995 Estimation of sampling bias between different sampling protocols on contaminated land. *Analyst* **120(5)** 1353-1356

Ramsey, M.H., Thompson, M. & Hale, M. 1992 Objective evaluation of precision requirements for geochemical analysis using robust analysis of variance. *Journal of Geochemical Exploration* **44** 23-36

Ranville, J.F., Smith, K.S., Macalady, D.L. & Rees, T.F. 1988 Colloidal properties of flocculated bed material in a stream contaminedate by acid mine drainage, St. Kevin Gulch, Colorado. **In:** Mallard, G.E. & Ragone, S.E. (eds) Proceeding of the technical meeting, USGS toxic substances hydrology program. *Water-Resources Investigation Report* **88-4220** 111-118

Reed, S.J.B. 1996 *Electron microprobe analysis and scanning electron microscopy in geology.* Cambridge University Press, Cambridge.

Richards, Morehead & Laing 1992 *Constructed wetlands to ameliorate metal-rich minewater. Study of natural wetlands.* NRA R&D note 103, NRA, Bristol, UK

Rippon, J.H. 1997 *Variation in tectonic style setting in British coalfields.* Unpublished PhD thesis, University of Keele.

Rippon, J.H. & Spears, D.A. 1989 The sedimentology and geochemistry of the sub-Clowne (Westphalian B) of north-east Derbyshire, UK. *Proceedings of the Yorkshire Geological Society,* **47(3)** 181-198

Robb, G.A. & Robinson, J.D.F. 1995 Acid drainage from mines. *The Geographical Journal* **161(1)** 47-54

Robb, G.A. 1994 Environmental consequences of coal mine closure. *Geographical Journal* **160** 33-40

Robins, N.S. 1990 *Hydrogeology of Scotland.* BGS, HMSO, London, pp90

Robins, N.S. & Younger, P.L. 1996 Coal abandonment-mine water and near-surface environment: some historical evidence from the United Kingdom. *Minerals, metals and the environment II.* IMM, London, UK p253-262

Royal Commission on Environmental Pollution 1992. *Freshwater Quality.* 16th report of the royal commission on Environmental Pollution, HMSO, London.

Runnells, D.D. & Lindberg, R.D. 1990 Selenium in aqueous solutions: the impossibility of obtaining a meaningful Eh using a platinum electrode, with implications for modeling of natural waters. *Geology* **18** 212-215

Sadler, P.J.K. 1998 Minewater remediation at a French zinc mine: sources of acid mine drainage and contaminant flushing characteristics. **In:** Mather, J., Banks, D., Dumpleton, S. & Fermor, M. (eds) *Groundwater contaminants and their migration.* Geological Society Special Publication **128** 101-120

Schofield, A. 1995 Oral presentation at "A poisoned legacy: water pollution from Britain's closed mines" Coalfield Communities Campaign, 21 February 1995.

Schwertmann, U. & Taylor, R.M.M. 1989 Iron oxides. **In:** Dixon, J.B. & Weed, S.B. (eds) *Minerals in soil environments.* (2nd edn) Soil Science Society of America, Book Series 1. Madison, Wisconsin, USA. Chapter 8 379-438

Scott, M.J. & Morgan, J.J. 1990 Energetics and conservative properties of redox systems. **In:** Melchoir, D.C. & Basset R.L. (eds) *Chemical modeling in aqueous systems II.* ACS Symposium Series 416 American Chemical Society, Washington, USA. Chapter 29, 368-378.

Sheppard, S.M.F. & Langley, K.M. 1984 Origin of Saline Formation Waters in Northeast England: Application of Stable Isotopes. *Transactions of the Institution of Mining and Metallurgy: Section B Applied Earth Sciences* **93** B195-B201

Sherwood, J.M. & Younger, P.L. 1994 Modelling Groundwater Rebound after Coalfield Closure: An Example from County Durham, UK. *Proceedings of the 5th International Mine Water Congress* (Vol 2), University of Nottingham & IMWA, 769-777

Singer, P.C. & Stumm, W. 1970 Acidic mine drainage: the rate-determining step. *Science* **167** 1121-1123

Skougstad, M.W., Fishman, M.J., Friedman, L.C., Erdman, D.E. & Duncan, S.S. 1979a Iron, ferrous, dissolved, colorimetric, bipyridine (I-1388-78) *Methods for the Determination of Inorganic Substances in Water and Fluvial Sediments*. Techniques of Water-Resources Investigations of the United States Geological Survey. Book 5, Chapter A1, 387-388

Skougstad, M.W., Fishman, M.J., Friedman, L.C., Erdman, D.E. & Duncan, S.S. 1979b Iron, dissolved, colorimetric, bipyridine (I-1379-78) *Methods for the Determination of Inorganic Substances in Water and Fluvial Sediments*. Techniques of Water-Resources Investigations of the United States Geological Survey. Book 5, Chapter A1, 373-374

Smith, D.B. 1994b *Geology of the country around Sunderland.* Memoir of the British Geological Survey Sheet 21. HMSO, London.

Smith, D.B. & Francis, E.A. 1967 *Geology of the country between Durham and West Hartlepool*. Institute of Geological Sciences, HMSO, London, UK.

Smith, D.J. 1994a *Distribution of metals between particulate, colloidal and dissolved phases in acid minewaters from North East England*. Unpublished MSc Thesis, Department of Fossil Fuels and Environmental Geochemistry, University of Newcastle-Upon-Tyne.

Smith, F.W. 1981 Some environmental aspects of geology and mining in Coal Measures and younger rocks in North-East England. **In:** Say, P.J. & Whitton, B.A. *Heavy Metals in Northern England: Environmental and Biological Aspects*. University of Durham, Durham, 19-28

Smith, K.S., Macalady, D.L. & Briggs, P.H. 1988 Partitioning of metals between water and flocculated bed materialin a stream contaminated by acid mine drainage near Leadville, Coloraodo. **In:** Mallard, G.E. & Ragone, S.E. (eds) Proceeding of the technical meeting, USGS toxic substances hydrology program. *Water-Resources Investigation Report* **88-4220** 101-109

Spears, D.A. 1997 Environmental impact of minerals in UK coals. **In:** Gayer, R. & Pesek, J. (eds) *European coal geology and technology*. Geological Society Special Publication **125** 287-295

Spears, D.A. & Sezgin, H.I. 1985 Mineralogy and geochemistry of the subcrenatum marine band and associated coal-bearing sediments, Langsett, South Yorkshire. *Journal of Sedimentary Petrology* **55(4)** 570-578

Speight, J.G. 1994 *The chemistry and technology of coal* (2nd edn). Marcel Dekker, New York, USA.

Sperring, T.M. 1995 *The relationship of water quality and ochre chemistry in mine waters from Cornwall and Wales*. Unpublished PhD thesis, University of Wales, Aberystwyth.

Steffan, Robertson & Kirsten 1989 *Draft Acid Rock Drainage Technical Guide Volume 1*. British Columbia Acid Mine Drainage Task Force Report August 1989, Vancouver

Stipp, S.L. 1990 Speciation in the Fe(II)-Fe(III)-SO_4-H_2O system at 25°C and low pH: sensitivity of an equilibrium model to uncertainities. *Environmental Science and Technology* **24(5)** 699-706

Stumm, W. 1992 *Chemistry of the solid-water interface*. John Wiley & Sons, Inc., New York, USA.

Stumm, W. & Morgan, J.J. 1996 *Aquatic Chemistry. An Introduction Emphasizing Chemical Equilibria in Natural Waters* (3rd Edition). Wiley Interscience, New York.

Swaine, D.J. 1990 *Trace Elements in Coal.* Butterworths, London, pp278

Tarutis, W.J. & Unz, R.F. 1995 Iron and manganese release in coal mine drainage wetland microcosms. *Water Science and Technology* **32(3)** 187-192

Taylor, B.E., Wheeler, M.C. & Nordstrom, D.K. 1984a Stable isotope geochemistry of acid mine drainage: experimental oxidation of pyrite. *Geochimica et Cosmochimica Acta* **48** 2669-2678

Taylor, B.E., Wheeler, M.C. & Nordstrom, D.K. 1984b Isotope composition of sulphate in acid mine Drainage as measure of bacterial oxidation. *Nature* **308** 338-341

Taylor, B.J., Burgess, I.C., Land, D.H., Mills, D.A.C., Smith, D.B. & Warren, P.T. 1971 *British Regional Geology: Northern England (4th Ed).* HMSO, London, pp121

Taylor, R.K. & Spears, D.A. 1967 An unusual carbonate band in the east Pennine coalfield (Engand). *Sedimentology* 9 55-73

Thomas, L. 1992 *Handbook of Practical Coal Geology.* J Wiley & Sons, Chichester, pp338

Thompson, M. 1992 Data quality requirements in geochemistry: the requirements and how to achieve them. *Journal of Geochemical Exploration* **44** 3-22

Thompson, M. & Ramsey, M.H. 1995 Quality concepts and practises applied to sampling - an exploratory study. *Analyst* **120** 261-270

Thompson, M. & Walsh, J.N. 1988 *A Handbook of Inductively Coupled Plasma.* 2nd edition. Blackie, London, UK

Thompson, M., Pahlavanpour, B. & Thorne, L.T. 1981 The simultaneous determination of arsenic, antimony, bismuth, selenium and tellurium in waters by inductively coupled plasma/volatile hydride method. *Water Research* **15** 407-411

Thompson, M., Ramsey, M.H. & Pahlavanpour, B. 1982 Water analysis by inductively coupled plasma atomic-emission spectrometry after a rapid pre-concentration. *Analyst* **107** 1330-1334

Tucker, M.E. (ed) 1988 *Techniques in Sedimentology.* Blackwell Scientific Publications, Oxford, pp394.

Tuovinen, O.H., Bhatti, T.M., Bigham, J.M., Hallberg, K.B., Garcia, O. & Lindström, E.B. 1994 Oxidative dissolution of arsenopyrite by mesophilic and moderately thermophilic acidophiles. *Applied and Environmental Microbiology* **60(9)** 3268-3278

Turner, S.J. 1994 A *Hydrogeochemical Investigation of Mine Water Drainage Contamination of Surface Waters in County Durham.* Unpublished MSc Thesis, Imperial College of Science, Technology and Medicine (University of London). pp95

Tyrrel, S.F. & Howsam, P. 1997 Aspects of the occurrence and behaviour of iron bacteria in boreholes and aquifers. *Quarterly Journal of Engineering Geology* **30** 161-169

Waite, T.D. & Morel, F.M.M. 1984 Photoreductive dissolution of colloidal iron oxides in natural waters. *Environmental Science and Technology* **18** 860-868

Walton, K.C. & Johnson, D.B. 1992 Microbiological and chemical characteristics of an acidic stream draining a disused copper mine. *Environmental Pollution* **76(2)** 169-175

Wandless, A.M. 1954 The occurrence of sulphur in British coals. *The Colliery Guardian* **October 28 1954** 557-560

Wandless, A.M. 1959 The occurence of sulphur in British coals. *Journal of the Institute of Fuel* **32** 258-266

Webster, J.G., Nordstrom, D.K. & Smith, K.S. 1994 Transport and natural attenuation of Cu, Zn, As, and Fe in the acid mine drainage of Leviathan and Bryant Creeks. **In:** Alpers, C.N. & Blowes, D.W. (eds) 1994 *Environmental Geochemistry of Sulfide Oxidation.* ACS Symposium Series **550**. American Chemical Society, Washington, D.C., USA. Chapter 17 244-260

Wen, L.-S., Santschi, P.H. & Tang, D. 1997 Interactions between radioactively labeled colloids and natural particles: evidence for colloidal pumping. *Geochimica et Cosmochimica Acta* **61(14)** 2867-2878

Whateley, M.K.G. & Tuncali, E. 1995 Origin and distribution of sulphur in the Neogene Beypazari Lignite Basin, Central Anatolia, Turkey. **In**: Whateley, M.K.G. & Spears, D.A. (eds) *European Coal Geology.* Geological Society Special Publication **82** 307-323

Whitehead, P.G., McCartney, M.P., Williams, R.J., Ishemo, C.A.L. & Thomas, R. 1995 A method to simulate the impact of acid mine drainage on river systems. *Journal of the Chartered Institution of Water and Environmental Management* **9** 119-131

Wieder, R.K. & Lang, G.E. 1984 Influence of wetlands and coal mining on stream chemistry. *Water, Air and Soil Pollution* **23** 381-396

Wieder, R.K. 1993 Ion input/output budgets for five wetlands constructed for acid coal mine drainage treatment. *Water, Air and Soil Pollution* **71** 231-270

Wiersma, C.L. & Rimstidt, J.D. 1984 Rate of oxidation of pyrite and marcasite with ferric iron at pH 2. *Geochimica et Cosmochimica Acta* **48** 85-92

Williams, E.G. & Keith, M.L. 1963 Relationship between sulphur in coals and the occurrence of marine roof beds. *Economic Geology* **58** 720-729

Winland, R.L., Traina, S.J. & Bigham, J.M. 1991 Chemical composition of ochreous precipitates from Ohio coal mine drainage. *Journal of Environmental Quality* **20(2)** 452-460

Young, B. 1985 The distribution of barytocalcite and alstonite in the Northern Pennine Orefield. *Proceedings of the Yorkshire Geological Society* **45(3)** 199-206

Younger, P.L. 1993 Possible environmental impacts of the closure of two collieries in County Durham. *Journal of the Institution of Water and Environmental Management* **7(5)** 521- 531

Younger, P.L. 1994 Minewater Pollution: The Revenge of Old King Coal. *Geoscientist* **4(5)** 6-8

Younger, P.L. 1995a Minewater pollution in Britain: past, present and future. *Mineral Planning* **65** 38-41

Younger, P.L. 1995b Hydrogeochemistry of Minewaters Flowing from Abandoned Coal Workings in County Durham. *Quarterly Journal of Engineering Geology* **28 supplement 2** s101-113

Younger, P.L. 1997a Coalfield abandonment: geochemical processes and hydrochemical products. **In:** Nicholson, K. (ed) *The environmental geochemistry of energy resources*. Society for Environmental Geochemistry and Health (in press)

Younger, P.L. 1997b The longevity of minewater pollution: a basis for decision-making. *The Science of the Total Environment* **194/195** 457-466

Younger, P.L & Harbourne, K.J. 1995 "To Pump or Not to Pump?" Cost-Benefit Analysis of Future Environmental Management Options for the Abandoned Durham Coalfield, UK. *Journal of the Institution of Water and Environmental Management* **9** 405-416

Younger, P.L. & Bradley, K.F. 1994 Application of Geochemical Mineral Exploration Techniques to the Cataloguing of Problematic Discharges from Abandoned Mines in North-East England. *Proceedings of the 5th International Mine Water* Congress (Volume 2), University of Nottingham & IMWA, pp857-871

Younger, P.L. & Sherwood, J.A. 1993 The Cost of Decommissioning a Coalfield: Potential Environmental Problems in County Durham. *Mineral Planning* **57** 26-29

Younger, P.L., Curtis, T.P., Jarvis, A. & Pennell, R. 1997 Effective passive treatment of aluminium-rich, acidic colliery spoil using a compost wetland at Quaking Houses, County Durham. *Journal of the Institution of Water and Environmental Management* **11** 200-208

Appendices

Appendix I: Summary information on sampling locations **264**

II.i Analytical Techniques - Water **265**
II.i.i HCl Acidification **265**
II.i.ii Lanthanum Evaporative Preconcentration Technique **266**
II.i.iii Hydride Generation **267**
II.i.iv Total Alkalinity **268**
II.i.v Iron(II) and Fe_t **269**

II.ii Analytical Techniques - Suspended sediment **270**
II.ii Cellulose Acetate Filter Paper Analysis **270**

II.iii Analytical Techniques - Sediments and Soils **272**
II.iii.i Stream Sediments, Soils and Spoil Heap materials **272**
II.iii.ii Ochres **273**

III Data quality analysis results **274**
III.i Water **274**
III.ii Suspended sediment **274**
III.iii Stream sediment **274**

IV Analytical results **275**
IV.i Water chemistry **275**
IV.ii Suspended sediment chemistry **285**
IV.iii Stream sediment chemistry **290**

Table I.i: Summary information

LOCALITY	SITE	NGR (NZ)	DATE OF VISIT 5/95	7/95	11/95	3 96	10 96	7/97
Broken Banks	1	1960 2948	✓	✓*		✓	✓	✓
	2	1980 2946		✓		✓		
Edmondsley	1	2330 4950	✓	✓	✓			✓
Yard Drift	2	2330 4950		✓				
	3	2330 4950		✓				
Helmington	1	1825 3610	✓				✓	
Row	2	1830 3680	✓	✓				
	3	1850 3675	✓	✓				
	4	1850 3580	✓	✓	✓	✓		✓
	4A	1850 3573		✓	✓			
	5	1850 3578	✓	✓				
	6	1850 3572	✓	✓				
	7	1852 3570	✓	✓			✓	✓
	7A	1860 3560		✓	✓	✓	✓	✓
	8	1875 3550			✓	✓	✓	
	9	1890 3540		✓	✓	✓	✓	
	10	1915 3525	✓	✓*	✓	✓	✓	
	11	1935 3510		✓	✓*	✓	✓	
	12	1935 3510		✓		✓		
	13	1945 3460		✓				
	14	1995 3410		✓				
	15	1935 3510		✓				
	W	1935 3510		✓				
Low Lands	1	1325 2580	✓	✓*				
	2	1328 2575	✓	✓				
	3	1330 2580						
	4	1335 2580						
	4B	1345 2505	✓	✓				
	5	1350 2495	✓	✓				
Quaking	1	1775 5095	✓	✓	✓			
Houses	2	1775 5095	✓	✓	✓	✓	✓	✓
	3	1780 5095	✓	✓	✓	✓		
	4	1785 5095	✓	✓				
	4A	1795 5100			✓			
	5	1803 5103	✓	✓		✓*		
	5A	1803 5103						
	6	1835 5092	✓	✓	✓	✓		
		1835 5092	✓			✓		

LOCALITY	SITE	NGR (NZ)	DATE OF VISIT 5/95	7/95	11/95	3 96	10 96	7 97
Quaking	8	1840 5090	✓	✓				
Houses	9	1855 5095		✓	✓	✓		
	10	1910 5130			✓			
Stony Heap	1	1500 5180	✓					
	2	1490 5175	✓					
	3	1485 5160	✓					
	5	1475 5160	✓					
	6	1475 5155	✓	✓	✓	✓	✓	✓
	7	1470 5145	✓	✓	✓	✓		
	8	1462 5135		✓		✓*		
	9	1460 5130	✓	✓				
	9A	1463 5125	✓	✓		✓		
	10	1465 5120			✓			
	10A	1465 5115		✓*		✓		
	11	1455 5070			✓			
	13	1455 5070	✓	✓	✓	✓		
	14	1485 5020	✓	✓	✓	✓		
	15	1490 4975	✓	✓	✓	✓		
	16	1545 4920		✓				
	A(4)	1485 5160		✓	✓	✓		
	B(12)	1455 5070		✓				
Tindale Colliery								
Colliery	1	1965 2685	✓	✓		✓		
Willington	1	1943 3560	✓	✓	✓			
	2	1942 3562		✓				
	3	1943 3558		✓*				
	4	1948 3540		✓				
	5	1935 3510		✓				

* - this records the collection of field duplicate samples at the site on the occasion where it is marked (see Chapter 4 and Appendix II for an explanation and the results of the field duplicate sampling).
For a complete list of results of analyses for each sample media at each site Appendix IV should be consulted.

II.i Analytical Techniques - Water

II.i.i HCl Acidification

Elements determined 24; elemental data used - 4:
Na, Mg, K & Ca

Equipment:

Polythene tubes
Tube caps
Autopipette (1-5ml and 0.5ml)
Pipette tubes

Reagents:

DIW
Aristar conc HCl
HRM10

Preparation:

Prepare a run sheet

Time:

Only the time it takes to pipette (allow 0.5 days per 100 samples)
Analysis on ICP-AES for 100 samples allow 0.5 days

Batch Organisation:

Singletons
Replicates (10%)
Duplicates - all replicated
DIW (10%) (RBLK)
Reference Material (HRM10) (10%)

Sample Codes for ICP-AES:

5 - Reference Material
6 - Replicates
7 - Singletons
8 - RBLK

Procedure:

1. Label tubes
2. 5ml of sample into tubes
3. + 0.5ml of Conc Aristar HCl
4. Cap tubes
5. Thoroughly mix

II.i.ii Lanthanum Evaporative Preconcentration Technique

Elements determined 24; elements used - 19:

Li, Be, Al, P, Ti, V, Mn, Fe, Co, Ni, Cu, Zn, Sr, Mo, Ag, Cd, Ba, La & Pb

Equipment:

Plastic centrifuge tubes
Plastic tube caps
Auto-pipette (1-5ml & <1ml)
Pipette tips
Heating block

Reagents:

DIW
Lanthanum solution (5μg ml^{-1} La in 1M Aristar HCl)
HRM10

Preparation:

Prepare a run sheet
None needed for samples

Time:

2 days for ~100 samples (limitation is the number which can be contained on the block at once)
Analysis on ICP-AES is 0.5 days

Batch Organisation:

Maximum of 120 tubes in the hotplate (*i.e.* maximum of 80 - 85 singletons)
Singletons
Replicates (10%)
Duplicates (replicate all)
Blank (10%) (RBLK)
Reference Material (HRM10) (10%)

Sample Codes for ICP-AES:

5 - Reference Material
6 - Replicates
7 - Singletons
8 - RBLK

Procedure:

1. Switch on block
2. 13ml of sample (3 x 4.33ml) pipetted into tubes
3. + 1.3ml (2 x 0.65ml) of La solution pipetted into tubes
4. Samples placed onto block and left for 12 hours
5. From (12) hours samples checked frequently and removed as they reach 1.3ml
6. Samples capped as soon as cool
7. Analysis performed from the same tubes

Reference:

Thompson *et al.* (1982)

II.i.iii Hydride Generation

Elements Determined:
As, Sb & Bi

Equipment:

Polythene tubes
Tube caps
Autopipette (5ml)
Pipette tips

Reagents:

DIW
0.2% KI in conc. A* HCl

Preparation:

Prepare a run sheet
No equipment or lab space needs to be booked

Time:

Allow 0.5 days preparation per 100 samples
ICP-AES manual injection - allow 0.5 days per batch

Batch Organisation:

No limit to the number of samples prepared
Singletons
Replicates (10%)
Duplicates - all replicated
Reagent Blanks (10%)

Sample Codes for ICP-AES:

6 - Replicates
7 - Singletons
8 - RBLK

Procedure:

1. Label tubes
2. +5ml of sample / DIW into tubes
3. +5ml of KI solution into tubes
4. Cap tubes
5. Thoroughly mix

References:

Thompson *et al.* (1981)

II.i.iv Total Alkalinity

Ions determined:
CO_3^{2-} & HCO_3^-

Equipment:

Plastic burette
Burette stand and clamp
60ml screw-top plastic conical flasks (for safety reasons)
Pasteur pipette
25ml measuring cylinder

Reagents:

0.01M (AR) HCl
BDH '4.5' indicator solution
DIW

Preparation:

HCl solution needs to be made up before travelling

Time:

Quick titration. Best undertaken from car boot.

Procedure: Measurement

1. Fill burette with HCl and record the level
2. Measure 20ml of water sample and put into a conical flask
3. + 5 drops of indicator solution
4. Titrate with HCl to a grey end point and record final volume of burette.

Procedure: Alkalinity calculation:

1. Alkalinity = $\frac{\text{vol of acid consumed x meq of acid used}}{\text{vol of sample}}$

II.i.v Iron(II) and Fe_t

Ions determined:
Fe^{2+} & Fe_t

Reagent preparation (adapted from Skougstad et al., *1977a,b)*
Dipyridyl reagent: dissolve 140g of sodium acetate in ~500ml DIW.
Separately dissolve 0.4g 2,2-dipyridyl in ~250ml DIW. Mix the solutions and make up to 1L (CAUTION: 2,2-dipyridyl is toxic by inhalation and skin contact)
Hydroxylamine hydrochloride reagent: dissolve 40g of hydroxlyamine hydrochloride in DIW and make up to 500ml

Laboratory preparation of sampling vessels
add 10ml of dipyridyl reagent to each bottle
add 8ml of hydroxylamine (Fe_t) or DIW (Fe^{II}) as required

Field collection of samples
add 10ml of water sample to necessary reagents

Analyses
analyses performed by automated colorimetry using a *Technicon AutoAnalyser*

Procedure: Calculation of concentrations

1. Plot calibration points and plot best fit line
2. Find the equation of the line ($y = mx + c$ because the calibration is linear at this wavelength)
3. Calculate the measured concentration
4. Multliply by the field dilution factor and the laboratory dilution factor
5. Final actual concentration derived.

II.ii Analytical Techniques - Suspended sediment

II.ii Cellulose Acetate Filter Paper Analysis

Elements determined (23):

Li, Be, Na, Mg, Al, P, K, Ca, Ti, V, Mn, Fe, Co, Ni, Cu, Zn, Sr, Mo, Ag, Cd, Ba, La & Pb

Equipment:

50ml beakers
Watchglasses
Polythene tubes
Tube caps
Tweezers
Hot plate from FC #3 (NB no foil)
Autopipette - 1ml fixed
Autopipette - 0.1ml fixed
Autopipette - 5ml adjustable
Large beaker for DIW / A* HCl
100ml beaker for HNO3

Preparation:

Prepare a run sheet
Wash beakers and watchglasses

Reagents:

DIW
HRM10
Blank filters
Conc Aristar HNO_3 (70%)
Conc Analar $HClO_4$ (60%) (in an oxford dispenser)
5M Aristar HCl

Time:

Two days for analytical preparation
0.5 days for ICP-AES analysis

Batch Organisation:

Maximum of 80 beakers
Singletons
Duplicates
0.1ml HRM10 spike blanks (10%)
Blank filters (10%)
Blank filters + 0.1ml HRM10 spike blanks (10%)
Acid blanks (10%)

Sample Codes for ICP-AES

5 - 0.1ml HRM10
6 - Blank filters
6 - Blank filters + 0.1ml HRM10
7 - Singletons & field duplicates (because impossible to replicate)
8 - Acid blanks (RBLK)

Procedure:

1. Place filter papers into beakers as required
2. Add 0.1ml HRM10 to beakers as required
3. + 2ml conc (63%) Aristar HNO_3 (2 x 1ml autopipette)
4. + 1ml $HClO_4$ (in oxford dispenser)
5. Leave at 70°C overnight covered with watchglass
6. Raise temperature to 130°C for 2 hours
7. Raise temperature to 150°C (~220 on dial)
8. Evaporate to dryness.
9. Leave to cool
10. + 1ml 5M Aristar HCl
11. Leach @ 50°C for 10 minutes with watchglasses on
12. + 4ml DIW
13. homogenise
14. Transfer solutions to polythene tubes and cap

II.iii Analytical Techniques - Sediments and Soils

II.iii.i Stream Sediments, Soils and Spoil Heap materials - Standard Attack #2

Equipment:

Glass attack
Plastic centrifuge tubes & caps

Reagents:

HNO_3 AR conc (70%) (oxford dispenser)
$HClO_4$ AR conc (60%) (oxford dispenser)
HCl 5M AR (oxford dispenser)
DIW (oxford dispenser)
HRM1
HRM2

Preparation:

Prepare a run sheet
Book fume cupboards
Book time on ICP

Time:

Wash tubes allow at least 2 nights
ICP allow a day if large batch

Batch Organisation:

Maximum of 252 solutions
Singletons
Replicates - 10%
Duplicates - all replicated
RBLK - 10%
Reference materials - 10%

Samples Codes for ICP-AES:

5 - Reference Material
6 - Replicates
7 - Singletons
8 - RBLK

Procedure:

1. Weigh out sediments 0.25g
2. + 4.0ml HNO_3
3. + 1.0ml $HClO_4$
4. Place on aluminium heating block. Switch control box to 'Manual' and set up as shown below:

Rise Rate sec/deg	Dwell Time hours	Dwell Temperature oC
1	3.0	50
1	3.0	150
1	22.0	190
1	0.1	195

5. Switch on fume cupboard and switch on programmer press 'reset' and then turn to 'auto'.
6. After 24 hours check if tubes all dry. Remove only those which dry and give rest more time to dry.
7. Tubes transfered to stainless steel racks and allowed to cool to room temperature.
8. + 2.0ml HCl
9. Put into heating block and leach at 60°C for an hour.
10. Place into wire racks and vortex.
11. + 8.0ml of DIW
12. Vortex
13. Decant into centrifuge tubes
14. Centrifuge at 2000 rpm for 2 minutes.

II.iii.ii Ochres - Standard Attack #2

as for II.iii.i, except

Procedure:

1. Weigh out sediments 0.1g

continue as above

III Data quality analysis results

III.*i Water*

Element	IDL ($\mu g\ l^{-1}$)	**ADL ($\mu g\ l^{-1}$)	Bias(%)	Precision(%)
Fe	5.0	15	2.9	8.0
Mn	0.5	6	2.4	3.3
Al	10	31	3.6	5.5
Cu	0.1	2.0	4.3	4.5
Zn	0.1	2.0	4.2	9.4

III.ii Suspended sediment

Element	IDL ($\mu g\ l^{-1}$)	**ADL ($\mu g\ l^{-1}$)	Bias(%)
Fe	0.5	5.6	7.4
Mn	0.05	0.2	11.4
Al	1.0	4.6	2.2
Cu	0.01	0.4	3.9
Zn	0.01	1.8	2.6

III.iii Stream sediment

Element	IDL ($\mu g\ l^{-1}$)	**ADL ($\mu g\ l^{-1}$)	Bias (%)	Precision(%)*
Fe	2	38	2.6	31
Mn	0.2	2.0	28	13
Al	4.0	34	1.6	22
Cu	0.04	0.4	4.1	22
Zn	0.04	1.1	2.4	48

* - it is thought that these have been adversely affected by the inclusion of some samples which should not have been included.

** - ADL is calculated as given by Miller & Miller (1984):

$$ADL = 3\delta + x$$

Where: δ = standard deviation of blank results
and x = mean of the blank analysis results.

IV Analytical results

IV.i Water chemistry

Date	Sample	Na	K	Mg	Ca	SO_4	Cl	HCO_3	pH	Eh	pe	Temp	Cond	Q	DO	Fe^{2+}	Fe^{3+}	Li	Be	Sr	Ba	Al
		µg ml^{-1}	µg ml^{-1}	µg ml^{-1}	µg ml^{-1}	µg ml^{-1}	µg ml^{-1}	µg ml^{-1}		mV		°C	µS	l s^{-1}	µg ml^{-1}	µg ml^{-1}	µg ml^{-1}	ng ml^{-1}	ng ml^{-1}	ng ml^{-1}	ng ml^{-1}	ng ml^{-1}
06 05/95	BB01	29	12	84	126	293	103	n.a.	7	131	2	10	230		n.a.	n.a.	n.a.	196	0.1	1170	20	50
04/05/95	EY01	27	13	94	246	950	125	n.a.	6	130	2	10	700		n.a.	n.a.	n.a.	98	0.5	585	10	45
03 05/95	HR01	12	5	18	48	163	112	n.a.	8	252	4	17	240		n.a.	n.a.	n.a.	24	0.0	191	61	90
03/05 95	HR02	16	4	33	112	483	92	n.a.	5	236	4	11	404		n.a.	n.a.	n.a.	155	3.5	267	12	5430
03/05/95	HR03	22	4	32	101	404	94	n.a.	5	275	5	15	420		n.a.	n.a.	n.a.	127	2.8	248	20	4060
03/05/95	HR04	19	7	115	235	1240	103	n.a.	6	15	0	10	255		n.a.	n.a.	n.a.	625	8.4	371	28	31700
03/05/95	HR05	20	6	84	185	956	113	n.a.	5	265	4	13	350		n.a.	n.a.	n.a.	465	6.4	327	25	20900
03/05/95	HR06	20	6	82	189	883	97	n.a.	5	260	4	13	750		n.a.	n.a.	n.a.	496	6.1	330	24	20800
03/05/95	HR07	20	6	84	191	929	86	n.a.	5	270	5	12	720		n.a.	n.a.	n.a.	463	6.2	332	68	20100
03 05/95	HR09	19	6	68	153	219	78	n.a.	7	130	2	14	575		n.a.	n.a.	n.a.	285	0.3	413	32	100
01/05/95	LL01	18	5	29	48	147	108	n.a.	9	193	3	12	220		n.a.	n.a.	n.a.	56	0.2	202	71	40
06 05/95	LL01	20	5	31	51	140	120	n.a.	n.a.	n.a.		n.a.	n.a.		n.a.	n.a.	n.a.	61	0.0	212	160	150
01/05/95	LL02	20	6	64	100	489	107	n.a.	n.a.	n.a.		11	n.a.		n.a.	n.a.	n.a.	94	0.4	292	11	830
06 05/95	LL02	19	6	63	99	435	102	n.a.	6	165	3	10	425		n.a.	n.a.	n.a.	95	0.4	290	10	470
01 05/95	LL03	22	6	64	104	454	106	n.a.	6	200	3	10	430		n.a.	n.a.	n.a.	88	0.5	300	41	745
01/05/95	LL04	19	5	70	124	534	114	n.a.	6	154	3	11	509		n.a.	n.a.	n.a.	124	0.4	353	40	180
06/05/95	LL04	18	6	57	86	157	77	n.a.	n.a.	n.a.		n.a.	n.a.		n.a.	n.a.	n.a.	111	0.2	305	48	45
01/05/95	LL05	17	5	34	55	178	105	n.a.	8	173	3	15	300		n.a.	n.a.	n.a.	61	0.2	211	59	185
06/05/95	LL05	19	5	35	57	n.a.	n.a.	n.a.	n.a.	n.a.		n.a.	n.a.		n.a.	n.a.	n.a.	67	0.1	221	55	60
04 05/95	QH01	356	23	33	145	463	536	n.a.	7	280	5	11	1110		n.a.	n.a.	n.a.	123	0.3	751	21	40
04 05/95	QH02	1020	167	124	344	1240	1900	n.a.	5	280	5	10	1740	1	n.a.	n.a.	n.a.	440	3.4	1330	47	5810
04/05/95	QH03	878	137	105	298	1100	1620	n.a.	6	225	4	12	1700		n.a.	n.a.	n.a.	382	1.9	1210	43	1390
04/05/95	QH04	896	137	105	301	1050	1570	n.a.	6	212	4	13	1660		n.a.	n.a.	n.a.	343	1.3	1190	87	290
04/05/95	QH05	792	122	95	272	989	1480	n.a.	7	185	3	13	1670		n.a.	n.a.	n.a.	331	0.4	1120	89	125
04 05/95	QH06	695	103	80	223	862	1290	n.a.	8	200	3	15	900		n.a.	n.a.	n.a.	272	0.4	940	43	70
04 05/95	QH07	135	16	79	247	1140	148	n.a.	7	202	3	15	1250		n.a.	n.a.	n.a.	517	0.3	1320	103	175
04 05/95	QH08	292	40	78	241	865	422	n.a.	7	240	4	13	1590		n.a.	n.a.	n.a.	462	0.3	1220	37	75
04 05/95	QH10	235	33	63	202	891	372	n.a.	8	190	3	14	1060		n.a.	n.a.	n.a.	353	0.3	983	47	60
02/05/95	SH01	76	4	26	65	395	203	n.a.	8	255	4	16	440		n.a.	n.a.	n.a.	42	0.3	153	49	130
02 05/95	SH02	77	4	26	65	276	190	n.a.	8	260	4	16	455		n.a.	n.a.	n.a.	42	0.2	154	42	135
02 05/95	SH03	68	4	31	62	234	171	n.a.	8	155	3	14	160		n.a.	n.a.	n.a.	41	0.2	155	43	25
02 05/95	SH04	14	6	67	85	280	109	n.a.	7	260	4	9	200		n.a.	n.a.	n.a.	65	0.1	163	27	70
02/05/95	SH05	40	6	56	80	265	157	n.a.	6	130	2	11	445		n.a.	n.a.	n.a.	54	0.2	183	33	30
02/05/95	SH06	31	7	62	99	344	147	n.a.	6	100	2	10	495		n.a.	n.a.	n.a.	90	0.3	210	14	40
05 05 95	SH06	31	7	62	99	418	157	n.a.	6	60	1	11	485		n.a.	n.a.	n.a.	93	0.3	210	14	25
02 05/95	SH08	35	6	59	88	311	172	n.a.	7	20	0	11	455		n.a.	n.a.	n.a.	70	0.2	195	37	35

n.a. - not analysed

Date	Sample	La	Ti	V	Cr	Mo	Mn	Fe	Co	Ni	Cu	Ag	Zn	Cd	Pb	P	S	B	As	Si
		µg ml^{-1}	ng ml^{-1}	ng ml^{-1}	ng ml^{-1}	ng ml^{-1}	ng ml^{-1}	ng ml^{-1}	ng ml^{-1}	ng ml^{-1}	ng ml^{-1}	ng ml^{-1}	ng ml^{-1}	ng ml^{-1}	ng ml^{-1}	ng ml^{-1}	ng ml^{-1}	ng ml^{-1}	ng ml^{-1}	ng ml^{-1}
06/05/95	BB01	0.02	1.9	2.5	<1.0	<1.0	1990	1970	8	9	<0.1	0.7	<0.1	<0.5	<3.0	4	77	0.16	<0.01	4.6
04/05/95	EY01	0.03	5.1	9.8	14.0	3.0	3210	21600	30	63	2	3.1	40	4	8	18	>110	0.12	0.04	10.5
03/05/95	HR01	0.01	0.9	<0.5	5.0	<1.0	61	140	<0.5	4	4	<0.2	19	3	<3.0	17	28	0.03	<0.01	4.5
03/05/95	HR02	0.02	3.6	9.5	15.5	2.5	2080	38500	55	126	45	2.2	504	9	9	34	>110	0.08	0.03	12.4
03 05/95	HR03	0.02	3.1	7.5	16.0	2.0	1760	15000	38	100	39	1.8	397	5	9	24	>110	0.06	0.03	10.0
03/05/95	HR04	0.06	7.8	12.5	2.5	5.5	11800	101000	206	435	58	3.8	2050	12	18	43	>110	0.17	0.09	16.4
03/05/95	HR05	0.04	6.4	11.5	15.5	4.0	8110	69500	146	320	53	3.2	1430	10	15	27	>110	0.13	0.06	14.2
03 05/95	HR06	0.06	5.5	7.3	<1.0	2.5	8060	69900	138	307	52	2.6	1360	7	9	24	>110	0.12	0.05	13.7
03/05/95	HR07	0.04	6.4	11.5	15.5	5.0	7990	69400	143	312	51	3.3	1370	9	14	28	>110	0.13	0.07	14.1
03 05/95	HR09	0.03	3.2	5.3	7.0	1.5	3970	13000	61	138	6	1.8	393	5	5	15	>110	0.14	0.02	9.3
01/05/95	LL01	0.01	1.4	4.3	13.5	1.5	152	393	2	5	3	0.7	8	1	3	281	25	0.07	<0.01	1.0
06/05/95	LL01	0.01	1.4	1.0	7.5	<1.0	112	130	1	3	1	<0.2	3	<0.5	<3.0	283	>110	0.07	0.03	6.2
01/05/95	LL02	0.02	3.1	6.5	16.5	2.0	5250	9220	33	42	4	2.0	226	4	6	12	25	0.09	<0.01	0.2
06/05/95	LL02	0.02	2.9	6.8	16.5	2.5	5230	8030	33	41	2	1.9	213	4	5	17	>110	0.07	0.03	6.2
01/05/95	LL03	0.02	3.3	8.8	21.0	2.5	4550	11000	32	47	5	2.4	310	5	8	12	>110	0.07	0.02	7.2
01 05/95	LL04	0.02	3.6	8.8	19.0	2.0	6890	33500	80	100	2	2.5	651	4	9	18	>110	0.08	0.04	11.2
06 05/95	LL04	0.01	1.7	3.0	6.0	1.5	2430	7000	21	31	0.5	0.9	41	1	<3.0	7	94	0.08	<0.01	6.4
01/05/95	LL05	0.01	1.6	4.8	15.0	1.5	609	1540	6	10	3	0.9	41	2	5	105	37	0.04	<0.01	1.3
06/05/95	LL05	0.01	1.1	3.3	9.5	1.5	605	245	6	10	2	0.6	17	1	<3.0	98	39	0.08	0.01	0.9
04 05 95	QH01	0.04	3.0	8.0	19.5	4.0	21	85	3	15	4	2.3	19	4	9	25	>110	0.20	0.03	4.9
04/05/95	QH02	0.09	6.7	6.0	<1.0	2.5	7320	16600	105	299	42	3.0	2650	11	35	32	>110	0.37	0.07	19.7
04/05/95	QH03	0.09	5.5	5.8	<1.0	2.0	5930	13100	84	247	28	2.7	2120	8	20	28	>110	0.34	0.06	15.9
04/05/95	QH04	0.08	6.3	11.5	20.5	4.5	5860	11000	87	248	21	4.0	2110	11	21	28	>110	0.34	0.06	15.4
04/05/95	QH05	0.08	4.9	5.8	4.0	2.5	5250	5990	71	215	14	2.8	1730	8	8	25	>110	0.31	0.06	13.2
04 05/95	QH06	0.06	4.7	6.0	10.5	2.5	4060	1230	49	165	8	2.7	1370	6	9	24	>110	0.27	0.06	10.2
04 05/95	QH07	0.04	4.7	7.3	18.0	3.0	248	35	3	19	3	2.5	7	2	5	24	>110	0.32	0.03	5.2
04/05/95	QH08	0.06	3.7	5.3	6.0	2.0	1350	113	16	59	3	1.9	294	3	5	22	>110	0.30	0.03	6.3
04 05/95	QH10	0.05	3.3	5.8	12.0	2.5	511	23	6	29	3	1.9	79	3	5	19	>110	0.25	0.03	5.5
02 05/95	SH01	0.01	3.3	6.8	16.0	2.0	79	485	3	11	8	1.3	34	30	8	40	73	0.04	0.02	5.1
02 05/95	SH02	0.01	2.6	5.0	15.0	1.5	96	355	2	9	4	1.2	14	3	8	12	74	0.04	0.02	5.0
02 05/95	SH03	0.01	2.0	5.8	16.0	2.0	506	558	3	8	3	1.4	9	2	5	11	63	0.04	0.02	4.5
02 05 95	SH04	0.01	4.1	3.5	10.5	<1.0	555	285	1	4	2	0.5	3	1	<3.0	11	71	0.04	<0.01	5.1
02/05/95	SH05	<0.006	2.3	5.3	16.0	1.5	880	1990	5	9	2	1.3	11	2	3	10	66	0.05	0.02	4.7
02/05 95	SH06	0.02	2.4	5.5	5.5	1.0	2030	32600	17	34	1	1.4	35	2	<3.0	8	110	0.06	0.03	10.2
05/05/95	SH06	0.02	2.3	5.5	6.0	1.5	2000	32400	17	33	1	1.3	33	2	<3.0	7	>110	0.06	0.02	9.9
02/05/95	SH08	0.01	2.4	5.3	13.5	1.5	1360	12900	10	19	1	1.4	19	4	3	8	85	0.05	0.02	6.9

n.a. - not analysed

Date	Sample	Na	K	Mg	Ca	SO_4	Cl	HCO_3	pH	Eh	pe	Temp	Cond	Q	DO	Fe^{2+}	Fe^{3+}	Li	Be	Sr	Ba	Al
		µg ml^{-1}	µg ml^{-1}	µg ml^{-1}	µg ml^{-1}	µg ml^{-1}	µg ml^{-1}	µg ml^{-1}		mV		°C	µS	l s^{-1}	µg ml^{-1}	µg ml^{-1}	µg ml^{-1}	ng ml^{-1}	ng ml^{-1}	ng ml^{-1}	ng ml^{-1}	ng ml^{-1}
05/05 95	SH08	34	6	59	90	338	156	n.a.	8	25	0	12	435		n.a.	n.a.	n.a.	71	0.2	195	64	65
05/05/95	SH09	35	6	58	87	370	158	n.a.	8	30	1	12	440		n.a.	n.a.	n.a.	73	0.1	194	21	40
05/05/95	SH11	35	7	57	88	298	153	n.a.	8	190	3	13	450		n.a.	n.a.	n.a.	73	0.1	191	19	25
05/05 95	SH12	12	5	89	89	253	102	n.a.	8	175	3	13	460		n.a.	n.a.	n.a.	24	0.1	187	45	35
05 05/95	SH13	34	7	59	83	329	152	n.a.	7	275	5	12	390		n.a.	n.a.	n.a.	70	0.0	183	20	20
06 05/95	TC01	104	17	160	281	1560	338	n.a.	7	123	2	12	1010		n.a.	n.a.	n.a.	339	0.4	1580	51	83
03/05/95	WG01	37	33	391	419	n.a.	n.a.	n.a.	7	65	1	12	1400		n.a.	n.a.	n.a.	2890	0.6	595	31	95
24/07/95	BB01	29	11	84	125	228	61	476	7	-3	0	11	800		n.a.	n.a.	n.a.	200	0.1	1190	20	18
24/07/95	BB02	29	11	83	124	240	159	n.a.	7	-5	0	12	792		n.a.	n.a.	n.a.	193	0.2	1180	20	20
29 07/95	EY01	23	13	96	256	781	103	185	6	130	2	10	960		n.a.	n.a.	n.a.	116	0.3	632	11	35
29/07 95	EY02	37	8	49	126	337	131	168	8	45	1	17	763		n.a.	n.a.	n.a.	55	0.1	367	57	25
29/07/95	EY03	28	11	81	212	688	118	177	7	45	1	13	917		n.a.	n.a.	n.a.	107	0.3	611	30	40
27 07/95	HR02	18	5	43	173	775	31	0	3	510	9	14	1000		n.a.	n.a.	n.a.	246	10.1	321	10	15900
27/07/95	HR03	26	4	46	201	549	119	58	6	200	3	18	950		n.a.	n.a.	n.a.	139	0.2	578	21	60
27/07/95	HR04	25	8	189	310	1970	146	0	4	400	7	10	1600		n.a.	n.a.	n.a.	1480	16.2	406	21	83400
27/07 95	HR05	25	8	183	303	2210	32	0	4	340	6	12	1620		n.a.	n.a.	n.a.	1410	15.6	400	20	78100
27/07/95	HR06	24	8	175	310	5560	48	0	4	352	6	12	1600		n.a.	n.a.	n.a.	1370	14.9	415	20	74300
26 07/95	HR07	24	8	174	307	1950	31	0	4	360	6	12	1640		n.a.	n.a.	n.a.	1390	15.0	415	20	74400
26/07/95	HR08	20	8	78	158	406	61	355	5	210	4	12	830		n.a.	n.a.	n.a.	256	0.2	559	35	110
26/07/95	HR09	20	8	78	159	388	68	345	8	210	4	14	845		n.a.	n.a.	n.a.	251	0.1	536	35	118
26 07/95	HR10	18	6	54	97	274	51	226	8	174	3	15	625		n.a.	n.a.	n.a.	149	0.1	322	27	75
26 07/95	HR11	20	7	53	95	259	53	207	8	160	3	16	640		n.a.	n.a.	n.a.	167	0.1	307	28	45
26 07/95	HR12	20	7	53	94	315	164	204	8	138	2	16	630		n.a.	n.a.	n.a.	177	0.1	302	30	125
26 07/95	HR14	20	7	49	92	215	58	209	8	144	2	16	600		n.a.	n.a.	n.a.	130	0.1	288	30	40
26/07/95	HR15	25	10	60	154	440	107	211	8	112	2	14	820		n.a.	n.a.	n.a.	255	0.2	383	32	60
27/07/95	LL01	25	7	35	59	141	47	229	9	135	2	22	520		n.a.	n.a.	n.a.	94	0.1	309	67	40
27 07 95	LL02	19	7	62	95	458	70	21	6	235	4	17	710		n.a.	n.a.	n.a.	104	0.3	284	11	250
27/07/95	LL04B	16	5	56	81	338	162	183	6	150	3	10	525		n.a.	n.a.	n.a.	130	0.1	317	14	20
27 07/95	LL05	22	6	40	65	213	161	204	7	-50	-1	19	570		n.a.	n.a.	n.a.	98	0.1	289	45	25
28 07/95	QH01	408	24	31	121	n.a.	n.a.	189	6	130	2	13	1600		n.a.	n.a.	n.a.	144	0.2	678	24	85
28 07/95	QH02	575	66	152	343	1770	904	9	5	80	1	11	>2000		n.a.	n.a.	n.a.	722	6.6	1510	26	20000
28 07/95	QH03	542	59	134	319	1680	873	5	5	104	2	12	>2000		n.a.	n.a.	n.a.	632	5.1	1370	26	12900
28 07/95	QH04	535	59	131	315	1690	880	3	5	220	4	14	>2000		n.a.	n.a.	n.a.	613	5.0	1360	26	10000
28 07 95	QH05	581	61	101	235	1110	932	61	7	1	0	14	1970		n.a.	n.a.	n.a.	390	0.4	930	44	275
28 07/95	QH06	578	58	117	282	1260	987	34	7	-40	-1	15	>2000		n.a.	n.a.	n.a.	426	0.3	1070	42	65
28/07/95	QH07	204	20	95	277	1090	126	282	8	167	3	16	1550		n.a.	n.a.	n.a.	726	0.2	1800	37	53

n.a. - not analysed

Date	Sample	La	Ti	V	Cr	Mo	Mn	Fe	Co	Ni	Cu	Ag	Zn	Cd	Pb	P	S	B	As	Si
		µg ml^{-1}	ng ml^{-1}	ng ml^{-1}	ng ml^{-1}	ng ml^{-1}	ng ml^{-1}	ng ml^{-1}	ng ml^{-1}	ng ml^{-1}	ng ml^{-1}	ng ml^{-1}	ng ml^{-1}	ng ml^{-1}	ng ml^{-1}	ng ml^{-1}	ng ml^{-1}	ng ml^{-1}	ng ml^{-1}	ng ml^{-1}
05 05/95	SH08	0.01	2.1	4.5	9.5	1.0	1360	12100	10	19	0.4	1.0	16	1	<3.0	5	85	0.05	0.02	6.9
05/05/95	SH09	0.01	2.4	3.5	9.5	1.5	1340	7870	9	17	1	0.8	10	1	<3.0	8	85	0.05	0.02	6.7
05 05/95	SH11	0.02	2.2	3.3	14.0	<1.0	811	30	5	10	1	0.9	<0.1	<0.5	<3.0	9	84	0.05	0.02	6.0
05/05 95	SH12	0.02	1.7	1.3	<1.0	<1.0	162	300	1	3	1	0.5	<0.1	<0.5	<3.0	9	72	0.05	<0.01	2.2
05/05/95	SH13	0.01	1.6	1.5	8.0	<1.0	685	35	3	10	0.4	0.6	1	<0.5	<3.0	183	84	0.07	0.01	5.6
06/05/95	TC01	0.05	5.9	7.5	<1.0	2.8	2530	2930	23	31	2	3.4	3	3	6	26	>110	0.27	0.05	4.8
03/05/95	WG01	0.05	7.3	11.5	<1.0	3.0	51700	58600	298	349	1	4.6	86	5	<3.0	45	>110	0.35	0.08	10.7
24/07/95	BB01	0.01	1.9	1.9	6.3	1.0	2100	1900	8	8	<0.1	0.7	<0.1	1	<3.0	7	n.a.	n.a.	n.a.	n.a.
24/07/95	BB02	0.01	2.6	2.8	6.5	1.5	2110	1600	8	9	<0.1	1.2	<0.1	2	<3.0	7	n.a.	n.a.	n.a.	n.a.
29/07/95	EY01	0.02	3.1	3.5	6.5	<1.0	3410	28600	27	37	<0.1	1.0	37	3	<3.0	16	n.a.	n.a.	n.a.	n.a.
29/07/95	EY02	0.01	2.4	2.8	6.0	1.5	101	58	1	5	1	1.0	2	1	<3.0	210	n.a.	n.a.	n.a.	n.a.
29/07/95	EY03	0.02	3.8	4.0	9.0	<1.0	2540	17800	21	30	1	1.4	28	3	<3.0	58	n.a.	n.a.	n.a.	n.a.
27/07/95	HR02	0.02	3.8	4.3	9.0	2.0	3860	19900	71	167	68	1.1	629	5	17	22	n.a.	n.a.	n.a.	n.a.
27/07/95	HR03	0.02	2.0	2.3	5.5	1.0	2650	473	18	50	2	0.8	72	2	<3.0	16	n.a.	n.a.	n.a.	n.a.
27/07/95	HR04	0.06	8.4	7.0	8.5	3.5	22100	159000	316	695	88	0.6	3570	19	<3.0	51	n.a.	n.a.	n.a.	n.a.
27/07/95	HR05	0.06	8.7	7.8	10.5	3.5	21200	153000	305	680	87	0.9	3420	20	5	46	n.a.	n.a.	n.a.	n.a.
27/07/95	HR06	0.07	8.0	7.0	10.5	3.5	20700	148000	297	661	83	0.6	3280	20	<3.0	40	n.a.	n.a.	n.a.	n.a.
26 07/95	HR07	0.06	7.7	6.5	10.0	2.5	20300	141000	292	649	84	0.5	3220	19	<3.0	39	n.a.	n.a.	n.a.	n.a.
26/07/95	HR08	0.02	2.2	2.5	7.0	<1.0	3390	145	36	79	2	0.9	223	3	<3.0	8	n.a.	n.a.	n.a.	n.a.
26 07/95	HR09	0.02	2.2	2.6	6.0	<1.0	3290	28	32	71	1	1.0	69	2	<3.0	10	n.a.	n.a.	n.a.	n.a.
26 07/95	HR10	0.01	1.6	2.3	5.5	1.0	1370	23	9	23	1	0.8	17	1	<3.0	11	n.a.	n.a.	n.a.	n.a.
26 07/95	HR11	0.01	1.9	2.0	5.0	1.0	204	20	1	8	1	0.7	2	1	<3.0	24	n.a.	n.a.	n.a.	n.a.
26/07/95	HR12	0.01	1.5	2.0	5.5	1.5	191	25	1	7	1	0.7	1	1	<3.0	24	n.a.	n.a.	n.a.	n.a.
26/07/95	HR14	0.01	1.9	2.5	5.5	1.0	83	33	1	3	2	1.1	1	2	<3.0	26	n.a.	n.a.	n.a.	n.a.
26/07/95	HR15	0.02	2.4	3.3	6.5	1.5	71	20	1	13	1	1.3	14	2	<3.0	44	n.a.	n.a.	n.a.	n.a.
27/07/95	LL01	<0.006	1.4	2.0	4.8	<1.0	84	95	1	4	2	0.8	3	1	<3.0	545	n.a.	n.a.	n.a.	n.a.
27/07/95	LL02	0.01	2.4	3.0	7.5	1.0	5190	3240	28	37	2	1.2	263	3	<3.0	13	n.a.	n.a.	n.a.	n.a.
27/07/95	LL04B	0.01	1.7	2.5	5.5	<1.0	2550	9790	23	33	<0.1	0.8	42	2	<3.0	8	n.a.	n.a.	n.a.	n.a.
27/07/95	LL05	<0.006	1.5	2.0	5.0	1.0	888	1390	8	13	1	0.8	27	1	<3.0	110	n.a.	n.a.	n.a.	n.a.
28/07/95	QH01	0.02	2.5	4.3	6.0	2.5	30	38	2	14	3	1.7	26	2	5	19	n.a.	n.a.	n.a.	n.a.
28 07 95	QH02	0.05	6.2	4.0	9.0	2.0	11600	35900	138	373	52	1.0	2780	11	5	36	n.a.	n.a.	n.a.	n.a.
28/07/95	QH03	0.05	5.5	3.8	7.5	2.0	9660	28700	115	312	45	0.9	2330	9	5	34	n.a.	n.a.	n.a.	n.a.
28/07/95	QH04	0.05	5.3	3.3	8.5	2.0	9620	16800	113	305	45	1.1	2290	9	6	33	n.a.	n.a.	n.a.	n.a.
28/07/95	QH05	0.02	3.4	3.3	7.5	2.5	8400	4760	87	236	12	1.0	1350	6	<3.0	126	n.a.	n.a.	n.a.	n.a.
28/07/95	QH06	0.04	3.6	3.3	8.5	2.0	12100	403	102	294	5	1.3	1570	5	<3.0	28	n.a.	n.a.	n.a.	n.a.
28/07/95	QH07	0.02	3.2	2.4	7.0	1.8	118	30	<0.5	8	2	1.1	1	1	<3.0	34	n.a.	n.a.	n.a.	n.a.

n.a. - not analysed

Date	Sample	Na	K	Mg	Ca	SO_4	Cl	HCO_3	pH	Eh	pe	Temp	Cond	Q	DO	Fe^{2+}	Fe^{3+}	Li	Be	Sr	Ba	Al
		µg ml^{-1}	µg ml^{-1}	µg ml^{-1}	µg ml^{-1}	µg ml^{-1}	µg ml^{-1}	µg ml^{-1}		mV		°C	µS	l s^{-1}	µg ml^{-1}	µg ml^{-1}	µg ml^{-1}	ng ml^{-1}	ng ml^{-1}	ng ml^{-1}	ng ml^{-1}	ng ml^{-1}
28/07/95	QH08	511	51	111	267	1220	740	90	8	174	3	15	>2000		n.a.	n.a.	n.a.	477	0.3	1200	40	45
28/07/95	QH09	459	47	103	264	1080	706	110	8	175	3	15	1980		n.a.	n.a.	n.a.	461	0.2	1210	41	40
28 07/95	QH10	419	40	95	264	1140	685	98	8	113	2	16	1850		n.a.	n.a.	n.a.	387	0.2	1180	50	35
29 07/95	SH05	30	6	66	92	214	167	256	7	25	0	10	636		n.a.	n.a.	n.a.	69	0.1	202	29	15
29/07/95	SH06	32	7	66	107	333	159	192	6	65	1	10	709		n.a.	n.a.	n.a.	103	0.2	234	14	20
29/07/95	SH07	30	7	67	100	273	160	209	8	-90	-2	11	680		n.a.	n.a.	n.a.	83	0.1	213	20	15
29/07/95	SH08	31	7	66	100	246	155	188	7	-16	0	12	690		n.a.	n.a.	n.a.	86	0.1	215	19	45
29/07/95	SH09	31	7	66	96	285	125	186	8	-35	-1	13	680		n.a.	n.a.	n.a.	89	0.1	216	17	20
29/07/95	SH10	30	7	66	97	404	245	189	8	50	1	16	725		n.a.	n.a.	n.a.	89	0.1	216	16	25
29/07/95	SH11	31	7	63	96	207	87	177	7	160	3	15	740		n.a.	n.a.	n.a.	85	0.1	218	18	15
29/07/95	SH12	137	54	134	105	299	247	412	8	140	2	17	1420		n.a.	n.a.	n.a.	101	0.1	465	139	40
29/07/95	SH13	41	12	66	85	245	187	163	8	140	2	16	767		n.a.	n.a.	n.a.	78	0.1	216	28	20
29/07/95	SH14	43	12	67	83	267	105	168	8	130	2	15	740		n.a.	n.a.	n.a.	75	0.1	225	36	20
29/07/95	SH15	40	12	63	84	236	103	168	8	95	2	16	750		n.a.	n.a.	n.a.	77	0.1	258	47	20
29/07/95	SH16	41	10	57	85	223	126	206	7	70	1	16	700		n.a.	n.a.	n.a.	60	0.1	261	83	30
24/07/95	TC01	109	18	160	269	863	50	679	7	60	1	13	1420		n.a.	n.a.	n.a.	405	0.2	1650	13	30
25/07/95	WG01	43	43	479	500	3370	83	0	4	375	6	12	>2000		n.a.	n.a.	n.a.	3440	0.6	625	22	130
25/07/95	WG02	16	4	22	38	162	157	119	7	170	3	15	290		n.a.	n.a.	n.a.	21	0.1	130	35	<10
25/07/95	WG03	18	8	67	80	414	101	99	8	50	1	16	665		n.a.	n.a.	n.a.	439	0.1	194	35	30
25/07/95	WG04	19	8	62	81	401	166	84	8	145	2	14	615		n.a.	n.a.	n.a.	362	0.1	196	28	25
25/07/95	WG05	9	2	18	55	12	33	168	8	106	2	15	335		n.a.	n.a.	n.a.	7	0.0	208	67	25
22/11/95	EY01	22	13	97	271	927	93	172	{3.9}	40	1	7	346		n.a.	n.a.	n.a.	108	0.4	627	9	40
21/11/95	HR03	n.a.	n.a.	n.a.	n.a.	n.a.	n.a.	n.a.	5	205	3	7	405		n.a.	n.a.	n.a.					
21/11/95	HR04 pipe	7	2	34	159	460	20	n.a.	4	270	5	7	469		n.a.	n.a.	n.a.	128	2.9	278	35	4920
21/11/95	HR04	14	5	39	102	337	50	55	5	172	3	8	462		n.a.	n.a.	n.a.	165	1.3	238	42	1950
21/11/95	HR07	24	4	32	94	284	47	18	6	95	2	7	441		n.a.	n.a.	n.a.	117	0.9	237	37	820
21/11/95	HR07A	25	6	32	91	266	47	15	6	38	1	7	443		n.a.	n.a.	n.a.	110	0.5	234	39	170
21/11/95	HR08	23	4	33	95	271	41	21	7	-65	-1	7	450		n.a.	n.a.	n.a.	117	0.3	253	40	45
21/11/95	HR09	23	4	33	96	260	52	24	7	-115	-2	7	444		n.a.	n.a.	n.a.	116	0.3	258	41	45
21/11/95	HR10	51	5	29	81	182	95	55	8	-50	-1	7	485		n.a.	n.a.	n.a.	83	0.1	240	45	25
19/11/95	QH01	219	19	28	114	320	276	169	7	-180	-3	9	1000		n.a.	n.a.	n.a.	129	0.1	681	34	15
19/11/95	QH02	468	67	38	143	330	799	81	6	-106	-2	8	1600		n.a.	n.a.	n.a.	114	0.4	587	90	170
19 11/95	QH03	413	58	36	134	341	717	104	7	-111	-2	8	1470		n.a.	n.a.	n.a.	121	0.3	599	81	200
19/11/95	QH04A	250	33	24	90	203	420	73	7	-79	-1	8	1040		n.a.	n.a.	n.a.	78	0.2	390	61	125
19 11/95	QH06	208	26	20	75	153	335	56	6	55	1	7	510		n.a.	n.a.	n.a.	67	0.3	328	67	220
19/11/95	QH07	20	4	17	55	106	32	28	8	-56	-1	4	276		n.a.	n.a.	n.a.	71	0.1	246	57	168

n.a. - not analysed

Date	Sample	La	Ti	V	Cr	Mo	Mn	Fe	Co	Ni	Cu	Ag	Zn	Cd	Pb	P	S	B	As	Si
		µg ml^{-1}	ng ml^{-1}	ng ml^{-1}	ng ml^{-1}	ng ml^{-1}	ng ml^{-1}	ng ml^{-1}	ng ml^{-1}	ng ml^{-1}	ng ml^{-1}	ng ml^{-1}	ng ml^{-1}	ng ml^{-1}	ng ml^{-1}	ng ml^{-1}	ng ml^{-1}	ng ml^{-1}	ng ml^{-1}	ng ml^{-1}
28 07 95	QH08	0.02	4.2	3.3	8.0	2.5	9220	175	78	226	5	1.2	1150	4	<3.0	33	n.a.	n.a.	n.a.	n.a.
28/07/95	QH09	0.02	3.2	2.8	6.5	2.0	5780	120	40	173	6	1.1	646	3	<3.0	28	n.a.	n.a.	n.a.	n.a.
28 07/95	QH10	0.02	3.1	2.3	6.5	1.5	671	143	2	67	3	1.3	119	2	<3.0	30	n.a.	n.a.	n.a.	n.a.
29/07/95	SH05	0.01	2.1	2.5	6.5	<1.0	1930	4940	7	12	0.3	1.1	14	2	<3.0	9	n.a.	n.a.	n.a.	n.a.
29/07/95	SH06	0.01	2.1	3.8	6.5	<1.0	2390	36500	20	36	<0.1	0.9	38	3	<3.0	8	n.a.	n.a.	n.a.	n.a.
29/07/95	SH07	0.01	2.1	3.3	6.5	<1.0	1990	12200	12	22	0	1.1	15	2	<3.0	7	n.a.	n.a.	n.a.	n.a.
29/07/95	SH08	0.01	1.9	2.5	6.5	<1.0	1950	8270	11	20	<0.1	1.0	10	2	<3.0	8	n.a.	n.a.	n.a.	n.a.
29 07/95	SH09	0.01	1.8	2.3	5.5	1.0	1900	1580	11	18	<0.1	0.8	3	1	<3.0	6	n.a.	n.a.	n.a.	n.a.
29/07/95	SH10	0.01	2.0	2.4	6.0	<1.0	1570	35	8	15	<0.1	1.0	<0.1	1	<3.0	7	n.a.	n.a.	n.a.	n.a.
29 07 95	SH11	0.01	1.8	2.0	5.5	<1.0	304	28	1	5	0	0.7	0	5	<3.0	12	n.a.	n.a.	n.a.	n.a.
29 07/95	SH12	0.01	2.2	1.8	7.0	1.0	21	50	2	11	2	0.7	3	1	<3.0	213	n.a.	n.a.	n.a.	n.a.
29 07/95	SH13	0.01	1.8	2.5	6.5	<1.0	243	58	1	9	1	0.9	7	1	<3.0	390	n.a.	n.a.	n.a.	n.a.
29 07/95	SH14	<0.006	1.5	2.0	5.5	1.5	29	40	<0.5	5	1	0.7	1	1	<3.0	257	n.a.	n.a.	n.a.	n.a.
29/07/95	SH15	0.01	2.1	2.8	7.5	1.5	98	63	2	5	2	1.3	1	2	<3.0	174	n.a.	n.a.	n.a.	n.a.
29 07/95	SH16	0.01	2.0	2.3	6.0	<1.0	1080	230	2	6	2	1.1	5	2	<3.0	38	n.a.	n.a.	n.a.	n.a.
24/07/95	TC01	0.02	3.2	1.8	5.5	1.0	2660	2710	20	26	<0.1	1.1	<0.1	2	<3.0	21	n.a.	n.a.	n.a.	n.a.
25/07/95	WG01	0.05	7.4	6.3	14.5	2.5	70700	27600	383	349	5	1.7	60	6	<3.0	41	n.a.	n.a.	n.a.	n.a.
25/07/95	WG02	<0.006	0.9	1.8	3.0	<1.0	18	18	<0.5	2	1	0.5	2	1	<3.0	18	n.a.	n.a.	n.a.	n.a.
25/07/95	WG03	<0.006	2.0	2.6	6.0	<1.0	6010	272	29	32	1	0.8	14	1	<3.0	22	n.a.	n.a.	n.a.	n.a.
25 07 95	WG04	0.01	1.5	2.3	5.0	<1.0	24	40	<0.5	3	1	0.8	0	1	<3.0	46	n.a.	n.a.	n.a.	n.a.
25 07/95	WG05	<0.006	1.1	1.3	3.0	<1.0	4	18	<0.5	<1.0	1	0.5	2	1	<3.0	11	n.a.	n.a.	n.a.	n.a.
22/11/95	EY01	0.02	4.0	4.0	81.5	1.0	3720	34100	33	47	2	1.7	42	<0.5	5	13	n.a.	n.a.	n.a.	n.a.
21 11/95	HR03																			
21/11/95	HR04 pipe	0.03	2.3	2.5	33.5	1.0	798	128	29	100	399	0.9	430	4	8	9	n.a.	n.a.	n.a.	n.a.
21 11/95	HR04	0.02	1.4	2.0	41.5	<1.0	2180	17500	34	79	17	0.4	357	2	9	7	n.a.	n.a.	n.a.	n.a.
21/11 95	HR07	0.02	1.1	1.8	32.5	<1.0	1600	8110	25	61	36	0.3	258	2	12	4	n.a.	n.a.	n.a.	n.a.
21/11/95	HR07A	<0.006	1.0	1.8	32.0	<1.0	1400	6990	23	58	20	0.4	243	2	<3.0	4	n.a.	n.a.	n.a.	n.a.
21 11/95	HR08	0.02	1.1	1.8	33.0	<1.0	1520	5860	24	60	13	0.5	243	2	<3.0	4	n.a.	n.a.	n.a.	n.a.
21/11/95	HR09	0.02	1.1	2.0	34.0	<1.0	1510	5500	23	60	13	0.5	234	2	<3.0	7	n.a.	n.a.	n.a.	n.a.
21/11/95	HR10	0.01	0.7	1.5	28.3	<1.0	964	936	12	32	7	<0.2	104	1	<3.0	3	n.a.	n.a.	n.a.	n.a.
19/11/95	QH01	0.02	1.3	2.5	29.0	2.0	25	43	1	19	6	0.6	44	1	3	8	n.a.	n.a.	n.a.	n.a.
19/11/95	QH02	0.02	2.0	4.5	38.5	2.5	1530	1160	20	68	10	0.9	695	4	8	12	n.a.	n.a.	n.a.	n.a.
19/11/95	QH03	<0.006	1.8	3.8	34.5	2.0	1180	913	15	55	9	0.7	539	3	8	13	n.a.	n.a.	n.a.	n.a.
19 11/95	QH04A	0.01	2.0	3.0	25.0	1.5	712	548	10	36	7	0.8	327	2	6	17	n.a.	n.a.	n.a.	n.a.
19 11 95	QH06	0.01	2.1	3.3	23.5	1.5	738	335	9	32	7	0.7	255	2	5	13	n.a.	n.a.	n.a.	n.a.
19 11 95	QH07	<0.006	2.5	1.6	18.8	<1.0	1090	454	5	16	4	0.2	48	<0.5	<3.0	20	n.a.	n.a.	n.a.	n.a.

n.a. - not analysed

Date	Sample	Na	K	Mg	Ca	SO_4	Cl	HCO_3	pH	Eh	pe	Temp	Cond	Q	DO	Fe^{2+}	Fe^{3+}	Li	Be	Sr	Ba	Al
		µg ml^{-1}	µg ml^{-1}	µg ml^{-1}	µg ml^{-1}	µg ml^{-1}	µg ml^{-1}	µg ml^{-1}		mV		°C	µS	l s^{-1}	µg ml^{-1}	µg ml^{-1}	µg ml^{-1}	ng ml^{-1}	ng ml^{-1}	ng ml^{-1}	ng ml^{-1}	ng ml^{-1}
19/11 95	QH09	52	7	18	62	135	89	34	7	123	2	5	395		n.a.	n.a.	n.a.	74	0.1	276	62	175
18 11 95	SH05	175	7	31	68	67	315	117	7	-3	0	6	779		n.a.	n.a.	n.a.	33	0.1	183	58	20
18/11/95	SH06	32	8	66	111	298	95	183	6	-12	0	9	655		n.a.	n.a.	n.a.	108	0.1	251	14	20
18/11/95	SH09A	318	12	36	79	99	562	107	8	-9	0	6	1130		n.a.	n.a.	n.a.	42	0.1	228	66	25
18/11/95	SH10A	271	9	34	78	77	507	108	8	73	1	5	986		n.a.	n.a.	n.a.	41	0.1	216	54	10
18/11/95	SH11	70	7	32	60	94	144	96	8	162	3	5	485		n.a.	n.a.	n.a.	41	0.1	162	30	15
18/11/95	SH12	15	6	24	65	26	71	89	8	147	2	4	323		n.a.	n.a.	n.a.	8	0.1	199	97	105
18/11/95	SH13	43	7	27	60	34	87	67	8	168	3	4	402		n.a.	n.a.	n.a.	23	0.1	181	67	60
18/11/95	SH15	40	7	23	57	37	96	79	8	140	2	4	367		n.a.	n.a.	n.a.	1	<0.01	0	1	<10
20 11/95	WG01	9	5	28	69	137	18	60	8	-83	-1	8	334		n.a.	n.a.	n.a.	126	0.0	189	40	55
20 11/95	WG02	n.a.	n.a.	n.a.	n.a.	n.a.	n.a.	n.a.	8	-7	0	6	259									
20/11 95	WG03	n.a.	n.a.	n.a.	n.a.	n.a.	n.a.	n.a.	8	-1	0	6	280									
10/03/96	BB01	30	11	80	116	219	62	464	6	32	1	10	722		n.a.	n.a.	n.a.	188	0.2	1140	20	30
10 03/96	BB02	30	11	79	115	218	90	441	7	30	1	10	n.a.		n.a.	n.a.	n.a.	210	0.0	1170	19	15
14 03/96	HR04	17	5	69	140	759	48	15	5	150	3	7	690		n.a.	n.a.	n.a.	440	4.9	270	28	16400
14 03 96	HR07	32	4	42	101	484	112	12	5	120	2	4	525		n.a.	n.a.	n.a.	226	2.4	237	32	5170
14/03/96	HR07A	33	5	42	103	434	53	4	5	35	1	4	510		n.a.	n.a.	n.a.	207	2.1	238	33	2680
14/03/96	HR08	29	4	41	100	402	55	11	6	40	1	3	475		n.a.	n.a.	n.a.	205	1.0	249	34	410
14 03/96	HR09	27	5	44	105	348	76	82	7	-40	-1	4	485		n.a.	n.a.	n.a.	164	0.3	299	37	70
14 03/96	HR10	30	5	37	76	203	80	133	8	-30	-1	5	410		n.a.	n.a.	n.a.	114	<0.01	247	35	45
14/03/96	HR11	33	6	35	72	200	89	107	7	65	1	4	385		n.a.	n.a.	n.a.	93	0.1	225	35	70
11/03/96	QH02	1000	130	105	260	943	1760	21	{3.3}	210	4	8	>2000		n.a.	n.a.	n.a.	349	2.0	1090	60	1720
15/03 96	QH02	964	115	102	257	n.a.	n.a.	40	6	150	3	7	>2000		n.a.	n.a.	n.a.	327	1.7	1090	78	1110
11 03/96	QH03	713	103	101	253	1020	1160	47	5	80	1	7	1990		n.a.	n.a.	n.a.	316	1.7	1100	41	840
11 03 96	QH04	672	98	100	246	1000	1110	46	6	28	0	7	1990		n.a.	n.a.	n.a.	383	0.9	1130	39	230
11/03/96	QH05	611	86	89	224	929	1040	37	7	1	0	5	1900		n.a.	n.a.	n.a.	295	0.4	986	38	72
11 03/96	QH06	109	11	58	163	739	868	35	8	120	2	4	1670		n.a.	n.a.	n.a.	243	0.3	835	26	65
11/03/96	QH07	503	70	72	180	635	127	126	8	180	3	3	780		n.a.	n.a.	n.a.	227	0.4	805	40	80
11 03/96	QH09	158	19	68	192	1400	391	142	8	180	3	3	920		n.a.	n.a.	n.a.	301	0.4	1010	27	115
15/03/96	QHW-1	1010	112	95	244	960	1690	44	6	120	2	6	n.a.		n.a.	n.a.	n.a.	311	1.4	1060	88	785
15 03/96	QHW-4	1830	119	91	252	102	154	43	6	120	2	2	n.a.		n.a.	n.a.	n.a.	302	1.0	1020	110	365
13/03/96	SH05	119	7	53	83	200	227	186	7	-10	0	5	720		n.a.	n.a.	n.a.	45	0.2	214	48	25
13 03 96	SH06	31	6	58	81	303	100	143	6	3	0	9	575		n.a.	n.a.	n.a.	98	0.4	181	16	140
13 03/96	SH07	58	6	55	81	251	162	166	7	-75	-1	7	600		n.a.	n.a.	n.a.	77	0.2	193	29	63
13 03 96	SH09	206	7	53	83	240	378	145	7	-80	-1	6	910		n.a.	n.a.	n.a.	68	0.3	201	34	40
13 03/96	SH10	254	7	53	83	244	445	131	7	-100	-2	6	1010		n.a.	n.a.	n.a.	66	0.2	202	34	35

n.a. - not analysed

Date	Sample	La µg ml^{-1}	Ti ng ml^{-1}	V ng ml^{-1}	Cr ng ml^{-1}	Mo ng ml^{-1}	Mn ng ml^{-1}	Fe ng ml^{-1}	Co ng ml^{-1}	Ni ng ml^{-1}	Cu ng ml^{-1}	Ag ng ml^{-1}	Zn ng ml^{-1}	Cd ng ml^{-1}	Pb ng ml^{-1}	P ng ml^{-1}	S ng ml^{-1}	B ng ml^{-1}	As ng ml^{-1}	Si ng ml^{-1}
19/11/95	QH09	0.01	2.1	1.8	20.0	<1.0	1090	425	6	19	5	<0.2	83	1	<3.0	17	n.a.	n.a.	n.a.	n.a.
18/11/95	SH05	0.01	1.1	1.8	30.5	<1.0	616	1030	2	7	3	0.5	18	1	3	6	n.a.	n.a.	n.a.	n.a.
18/11/95	SH06	0.01	1.6	2.3	63.5	<1.0	2330	38700	20	36	1	0.3	40	<0.5	<3.0	4	n.a.	n.a.	n.a.	n.a.
18/11/95	SH09A	<0.006	1.3	2.0	33.5	<1.0	720	1150	3	9	3	0.6	16	1	<3.0	11	n.a.	n.a.	n.a.	n.a.
18 11/95	SH10A	0.02	1.0	1.8	33.0	<1.0	642	188	3	8	3	0.5	12	1	<3.0	3	n.a.	n.a.	n.a.	n.a.
18/11/95	SH11	0.01	0.9	1.3	30.5	<1.0	290	95	1	5	3	0.4	4	<0.5	<3.0	13	n.a.	n.a.	n.a.	n.a.
18/11/95	SH12	<0.006	2.0	1.3	23.5	<1.0	109	343	1	3	4	0.2	20	<0.5	<3.0	31	n.a.	n.a.	n.a.	n.a.
18/11/95	SH13	<0.006	1.3	1.5	27.0	<1.0	176	258	1	5	4	0.2	14	<0.5	<3.0	74	n.a.	n.a.	n.a.	n.a.
18/11/95	SH15	<0.006	<0.2	<0.5	<1.0	<1.0	<0.5	<5.0	<0.5	<1.0	1	<0.2	1	<0.5	<3.0	<3.0	n.a.	n.a.	n.a.	n.a.
20/11/95	WG01	0.01	0.7	0.8	27.0	<1.0	694	970	3	8	6	<0.2	11	<0.5	<3.0	64	n.a.	n.a.	n.a.	n.a.
20/11/95	WG02																			
20/11/95	WG03																			
10/03/96	BB01	<0.006	3.3	4.3	8.0	1.5	1840	1930	9	10	1	1.3	<0.1	3	<3.0	10	n.a.	n.a.	n.a.	n.a.
10 03/96	BB02	<0.006	0.3	<0.5	2.0	<1.0	1790	1570	6	6	<0.1	<0.2	<0.1	<0.5	<3.0	<2.0	n.a.	n.a.	n.a.	n.a.
14/03/96	HR04	0.02	5.3	6.0	9.0	<1.0	5620	51200	99	220	47	1.8	973	4	11	17	n.a.	n.a.	n.a.	n.a.
14/03/96	HR07	0.01	3.8	5.5	7.5	1.5	2840	24600	53	125	33	1.6	519	5	8	13	n.a.	n.a.	n.a.	n.a.
14 03/96	HR07A	0.01	3.7	6.3	8.0	2.0	2830	23100	52	123	32	1.9	508	5	8	13	n.a.	n.a.	n.a.	n.a.
14/03/96	HR08	0.01	2.3	3.8	5.0	<1.0	2560	19000	45	107	22	0.8	449	3	<3.0	<2.0	n.a.	n.a.	n.a.	n.a.
14 03 96	HR09	0.01	2.8	4.5	7.0	1.5	2120	12900	37	87	9	1.4	302	4	6	9	n.a.	n.a.	n.a.	n.a.
14/03/96	HR10	<0.006	<0.2	<0.5	2.0	<1.0	1190	1960	13	34	3	<0.2	75	<0.5	<3.0	<2.0	n.a.	n.a.	n.a.	n.a.
14/03/96	HR11	0.01	1.8	2.8	4.0	<1.0	988	458	12	30	4	1.1	37	2	<3.0	11	n.a.	n.a.	n.a.	n.a.
11/03/96	QH02	0.03	6.0	7.8	10.5	3.0	5600	4610	90	297	29	2.9	2830	12	30	20	n.a.	n.a.	n.a.	n.a.
15 03/96	QH02	0.03	5.9	7.8	11.5	3.5	5360	5110	87	278	24	3.1	2510	11	23	22	n.a.	n.a.	n.a.	n.a.
11/03/96	QH03	0.03	5.7	9.3	10.0	4.5	4770	3790	80	278	21	2.9	2480	12	21	20	n.a.	n.a.	n.a.	n.a.
11/03/96	QH04	0.02	2.7	2.0	5.0	<1.0	4700	3220	70	253	14	0.7	2230	6	<3.0	<2.0	n.a.	n.a.	n.a.	n.a.
11 03 96	QH05	0.02	4.1	6.2	8.7	2.8	4160	1880	66	231	9	2.1	1850	9	6	14	n.a.	n.a.	n.a.	n.a.
11/03 96	QH06	0.01	3.8	5.8	8.5	1.5	3200	43	23	62	6	2.2	92	3	5	13	n.a.	n.a.	n.a.	n.a.
11 03/96	QH07	0.01	4.3	6.5	10.0	2.5	3580	600	53	187	7	2.5	1470	8	8	16	n.a.	n.a.	n.a.	n.a.
11 03/96	QH09	0.01	4.3	7.3	8.0	3.0	1990	68	19	69	6	2.3	233	5	8	17	n.a.	n.a.	n.a.	n.a.
15/03/96	QHW-1	0.02	5.5	7.3	11.0	3.0	4990	4540	81	255	20	2.7	2320	10	20	22	n.a.	n.a.	n.a.	n.a.
15/03/96	QHW-4	0.04	5.5	6.8	10.5	3.5	4790	2320	72	232	16	3.0	2070	9	15	22	n.a.	n.a.	n.a.	n.a.
13/03/96	SH05	0.01	2.6	5.3	6.5	2.0	428	640	3	10	2	1.8	17	3	6	7	n.a.	n.a.	n.a.	n.a.
13 03/96	SH06	<0.006	3.1	4.8	7.5	<1.0	1770	28800	20	38	1	1.7	38	1	5	5	n.a.	n.a.	n.a.	n.a.
13 03/96	SH07	0.01	2.0	3.3	5.3	<1.0	1080	13400	11	23	1	0.9	26	1	<3.0	3	n.a.	n.a.	n.a.	n.a.
13 03/96	SH09	0.01	3.2	6.3	9.0	1.5	1050	10900	12	24	3	2.1	24	3	6	8	n.a.	n.a.	n.a.	n.a.
13 03/96	SH10	0.01	2.8	5.3	7.0	2.0	1030	7290	11	22	2	1.9	18	3	5	7	n.a.	n.a.	n.a.	n.a.

n.a. - not analysed

Date	Sample	Na	K	Mg	Ca	SO_4	Cl	HCO_3	pH	Eh	pe	Temp	Cond	Q	DO	Fe^{2+}	Fe^{3+}	Li	Be	Sr	Ba	Al
		µg ml^{-1}	µg ml^{-1}	µg ml^{-1}	µg ml^{-1}	µg ml^{-1}	µg ml^{-1}	µg ml^{-1}		mV		°C	µS	l s^{-1}	µg ml^{-1}	µg ml^{-1}	µg ml^{-1}	ng ml^{-1}	ng ml^{-1}	ng ml^{-1}	ng ml^{-1}	ng ml^{-1}
13 03/96	SH11	158	8	54	82	69	100	134	7	-40	-1	6	885		n.a.	n.a.	n.a.	70	0.3	197	28	40
13 03/96	SH12	24	8	55	73	148	78	273	7	55	1	2	450		n.a.	n.a.	n.a.	27	0.1	218	59	20
13 03/96	SH13	93	8	56	76	242	205	163	7	-50	-1	5	700		n.a.	n.a.	n.a.	63	0.1	193	30	25
13 03/96	SH15	129	9	51	75	202	261	165	8	45	1	3	680		n.a.	n.a.	n.a.	51	0.2	208	47	55
10/03/96	TC01	107	18	157	256	891	60	631	7	-6	0	11	1360		n.a.	n.a.	n.a.	346	0.4	1610	14	50
09/10 96	BB01	34	12	77	123	202	43	458	7	150	3	10	682		0	n.a.	n.a.	182	0.1	1130	19	15
09/10/96	HR04	29	9	157	284	1950	44	0	5	230	4	10	1240		3	n.a.	n.a.	1120	13.3	377	24	59000
08/10/96	HR07	36	6	48	96	600	53	8	5	240	4	10	630		11	n.a.	n.a.	372	4.1	181	23	16100
08/10/96	HR07A	37	6	28	61	338	49	0	5	265	4	11	500		10	n.a.	n.a.	176	2.5	129	22	7460
08/10/96	HR08	33	6	39	87	326	49	67	7	66	1	11	535		10	n.a.	n.a.	170	0.6	243	30	95
08/10/96	HR09	33	6	38	86	347	53	67	7	45	1	11	540		11	n.a.	n.a.	168	0.3	241	25	65
08/10/96	HR10	29	8	38	78	280	52	113	8	218	4	10	500		10	n.a.	n.a.	124	0.1	234	27	50
08/10/96	HR11	30	7	38	79	281	60	105	8	270	5	10	500		11	n.a.	n.a.	121	0.1	236	26	30
09/10/96	QH01	553	69	115	315	1440	932	9	5	199	3	11	1830		8	n.a.	n.a.	544	4.4	1310	47	8340
09/10/96	SH06	37	7	64	112	345	109	186	6	143	2	10	673		3	n.a.	n.a.	98	0.2	244	13	10
09 10/96	BB01 0.2	34	12	76	122	202	43	458	7	150	3	10	682		0	n.a.	n.a.	231	<0.01	1180	19	<10
09/10/96	HR04 0.2	29	9	154	288	1950	44	0	5	230	4	10	1240		3	n.a.	n.a.	1310	12.6	392	24	62300
08 10 96	HR07 0.2	36	6	49	99	600	53	8	5	240	4	10	630		11	n.a.	n.a.	429	4.7	210	27	18700
08 10/96	HR07A 0.2	37	6	28	61	338	49	0	5	265	4	11	500		10	n.a.	n.a.	245	2.0	135	22	8220
08 10 96	HR08 0.2	33	6	39	86	326	49	67	7	66	1	11	535		10	n.a.	n.a.	166	0.5	243	25	50
08 10/96	HR09 0.2	34	7	39	86	53	347	67	7	45	1	11	540		11	n.a.	n.a.	173	0.3	244	25	30
08/10/96	HR11 0.2	30	7	39	80	60	281	105	8	270	5	10	500		11	n.a.	n.a.	129	0.1	237	26	55
09/10/96	QH01 0.2*	551	69	114	314	1440	932	9	5	199	3	11	1830		8	n.a.	n.a.	469	3.9	1080	39	7350
09 10/96	SH06 0.2	37	7	63	110	345	109	186	6	143	2	10	673		3	n.a.	n.a.	100	0.2	240	13	20
04 07/97	BB01	30	11	72	113	193	46	439	6	94	2	10	666		0	2	0	148	0.1	934	15	20
05 07 97	EY01	26	12	86	232	900	41	165	6	87	1	10	864		0	29	0	80	0.5	501	8	60
04/07/97	HR04	20	6	51	125	471	22	61	6	118	2	10	593		3	16	2	215	1.2	230	28	1220
04 07/97	HR07	18	4	20	55	161	32	34	6	80	1	12	362		9	5	0	66	0.3	132	32	140
04 07/97	HR07A	18	4	19	53	154	32	34	7	20	0	12	353		9	4	0	62	0.2	129	33	55
04/07/97	QH01	391	55	29	106	287	710	76	7	136	2	12	1460		8	1	0	84	0.4	385	126	100
05/07/97	SH06	28	6	53	90	240	61	186	6	97	2	10	566		1	17	2	82	0.4	173	13	205
04 07/97	HR04 0.1	20	6	51	124	482	23	61	6	118	2	10	593		3	16	1	208	1.1	224	27	760
05 07 97	SH06 0.1	27	6	53	90	242	59	186	6	97	2	10	566		1	16	3	78	0.3	168	12	135

n.a. - not analysed

Date	Sample	La µg ml^{-1}	Ti ng ml^{-1}	V ng ml^{-1}	Cr ng ml^{-1}	Mo ng ml^{-1}	Mn ng ml^{-1}	Fe ng ml^{-1}	Co ng ml^{-1}	Ni ng ml^{-1}	Cu ng ml^{-1}	Ag ng ml^{-1}	Zn ng ml^{-1}	Cd ng ml^{-1}	Pb ng ml^{-1}	P ng ml^{-1}	S ng ml^{-1}	B ng ml^{-1}	As ng ml^{-1}	Si ng ml^{-1}
13/03/96	SH11	0.01	4.1	5.8	9.0	2.5	971	1080	10	21	2	1.8	6	3	5	16	n.a.	n.a.	n.a.	n.a.
13/03/96	SH12	0.01	1.2	2.0	5.0	<1.0	131	98	1	4	2	0.7	1	1	<3.0	15	n.a.	n.a.	n.a.	n.a.
13/03/96	SH13	<0.006	2.6	3.8	7.0	<1.0	795	848	8	17	2	1.5	8	2	<3.0	46	n.a.	n.a.	n.a.	n.a.
13/03/96	SH15	0.01	3.3	4.3	7.5	1.5	396	180	4	12	3	1.5	7	2	3	31	n.a.	n.a.	n.a.	n.a.
10/03/96	TC01	0.02	5.7	8.0	9.5	3.0	2330	2760	22	31	3	2.8	1	6	5	20	n.a.	n.a.	n.a.	n.a.
09/10/96	BB01	0.02	2.4	2.8	9.0	1.0	1850	1710	9	11	<0.1	<0.2	<0.1	2	<3.0	8	74	0.15	0.02	4.5
09/10 96	HR04	0.09	8.1	4.5	17.5	2.5	17800	119000	280	619	58	<0.2	3100	12	23	68	613	0.21	0.11	20.0
08/10/96	HR07	0.02	3.1	2.8	10.0	<1.0	4870	32500	74	167	20	<0.2	796	5	6	23	192	0.08	0.03	8.1
08/10/96	HR07A	0.01	2.6	3.5	7.5	1.5	2760	10300	40	90	14	<0.2	422	3	8	17	112	0.05	0.01	6.1
08 10 96	HR08	0.02	2.9	4.3	9.0	2.0	2440	2530	34	76	6	<0.2	327	3	5	15	105	0.08	<0.01	6.7
08/10/96	HR09	0.02	2.4	3.8	8.0	1.0	2450	2260	33	75	5	<0.2	292	3	5	14	105	0.08	0.01	6.4
08/10/96	HR10	0.01	2.1	3.0	7.0	1.5	1190	53	11	29	2	0.4	47	2	5	66	83	0.07	<0.01	5.0
08/10/96	HR11	0.02	2.5	4.0	8.0	1.5	473	35	5	19	2	2.0	22	2	5	24	82	0.08	<0.01	4.8
09/10/96	QH01	0.10	5.3	3.8	12.5	2.0	7790	28200	101	274	28	<0.2	1860	6	8	39	484	0.33	0.06	19.7
09/10/96	SH06	0.03	2.5	3.8	10.0	<1.0	2130	33800	21	39	<0.1	3.2	35	1	5	11	111	0.06	0.02	9.3
09/10/96	BB01 0.2	0.03	<0.2	<0.5	1.5	<1.0	1660	1570	4	5	<0.1	<0.2	<0.1	<0.5	<3.0	<2.0	74	0.16	0.02	4.5
09/10/96	HR04 0.2	0.10	5.7	<0.5	10.0	<1.0	16600	112000	259	579	60	<0.2	2830	10	<3.0	57	613	0.20	0.12	19.9
08/10/96	HR07 0.2	0.03	3.5	3.3	11.5	2.0	5720	38200	87	199	23	<0.2	942	5	6	28	197	0.08	0.03	8.3
08/10/96	HR07A 0.2	0.02	<0.2	<0.5	<1.0	<1.0	2360	8890	30	74	12	<0.2	347	6	<3.0	5	110	0.05	0.02	6.0
08/10/96	HR08 0.2	0.02	2.2	3.5	8.5	1.0	2490	2460	34	77	5	<0.2	338	3	5	12	105	0.08	0.02	6.7
08/10/96	HR09 0.2	0.01	1.9	2.8	7.0	1.5	2380	2110	32	73	4	<0.2	281	3	<3.0	13	107	0.08	<0.01	6.4
08/10/96	HR11 0.2	0.01	2.0	3.0	7.5	1.0	452	25	4	18	2	<0.2	22	2	3	23	83	0.08	<0.01	4.9
09/10/96	QH01 0.2*	0.10	5.6	5.0	8.5	2.0	6710	24200	88	239	26	3.7	1600	4	17	26	476	0.33	0.06	19.6
09/10/96	SH06 0.2	0.03	2.5	3.3	10.0	<1.0	2080	32700	20	37	<0.1	<0.2	37	2	<3.0	12	110	0.06	0.02	9.2
04/07/97	BB01	0.01	2.2	2.8	5.5	<1.0	1570	98	7	9	1	1.9	3	1	3	5	72	0.14	0.02	4.5
05/07/97	EY01	0.01	6.9	9.3	13.0	3.5	2920	21100	31	44	5	6.1	33	3	23	18	280	0.08	0.02	10.0
04/07/97	HR04	0.01	3.8	5.0	8.0	2.0	2570	19500	58	133	22	3.2	524	3	15	12	171	0.08	0.02	9.6
04 07/97	HR07	0.01	1.4	2.8	4.5	1.0	655	4000	15	38	14	1.5	128	1	5	8	60	0.03	<0.01	5.9
04/07/97	HR07A	<0.006	1.5	2.0	4.0	<1.0	616	3430	13	34	12	1.2	110	1	5	6	57	0.03	<0.01	5.8
04/07/97	QH01	0.01	3.9	13.8	8.5	4.0	1240	575	20	78	12	3.8	881	5	17	16	111	0.13	<0.01	6.7
05/07/97	SH06	0.01	2.3	3.3	6.5	1.0	1220	15900	16	37	7	2.2	52	4	6	7	91	0.05	0.02	7.9
04/07/97	HR04 0.1	0.01	3.9	5.3	8.5	2.0	2540	18900	58	132	20	503	522	3	17	11	172	0.08	<0.01	9.4
05/07/97	SH06 0.1	0.01	2.4	3.5	6.5	1.0	1200	14500	16	36	6	2.2	49	2	8	5	90	0.03	<0.01	7.9

n.a. - not analysed

IV.ii Suspended sediment chemistry

Date	Sample	Li ng ml^{-1}	Na ng ml^{-1}	K ng ml^{-1}	Be ng ml^{-1}	Mg ng ml^{-1}	Ca ng ml^{-1}	Sr ng ml^{-1}	Ba ng ml^{-1}	Al ng ml^{-1}	La ng ml^{-1}	Ti ng ml^{-1}	V ng ml^{-1}	Cr ng ml^{-1}	Mo ng ml^{-1}	Mn ng ml^{-1}	Fe ng ml^{-1}	Co ng ml^{-1}	Ni ng ml^{-1}	Cu ng ml^{-1}	Ag ng ml^{-1}	Zn ng ml^{-1}	Cd ng ml^{-1}	Pb ng ml^{-1}	P ng ml^{-1}
06/05/95	BB01	0.1	25	3	<0.5	44	66	0.6	0.4	3	<0.05	0.0	<0.05	0.4	<0.1	1	17	<0.05	<0.1	0.4	<0.02	1	<0.05	<0.3	<0.2
04/05/95	EY01	<0.02	25	4	0.0	53	143	0.5	0.8	17	<0.05	0.2	<0.05	0.4	<0.1	2	1090	<0.05	<0.1	0.5	<0.02	1	<0.05	<0.3	1
03 05/95	HR04	1.4	51	16	1.4	173	349	0.9	2.5	6540	0.5	1.8	1.2	1.5	0.5	17	3570	0.3	0.5	7.2	<0.02	5	<0.05	<0.3	12
03/05/95	HR05	0.7	44	7	1.0	133	285	0.8	1.8	5590	0.3	1.4	1.0	1.8	<0.1	12	5130	<0.05	0.5	6.0	<0.02	4	<0.05	2	15
03/05/95	HR06	0.8	50	17	0.9	105	227	0.6	1.6	5530	0.3	0.7	0.9	2.0	<0.1	10	4700	<0.05	<0.1	5.5	<0.02	4	<0.05	<0.3	14
03/05/95	HR07	1.1	46	32	1.1	121	256	0.7	1.7	7290	0.3	2.4	1.2	1.9	0.5	12	7200	<0.05	0.5	6.4	<0.02	4	<0.05	1	18
03/05/95	HR09	0.4	47	6	5.2	153	1030	4.3	3.1	17700	7.3	2.7	0.4	1.8	0.9	44	12600	1.9	5.0	36.2	<0.02	333	0.89	5	12
06/05/95	LL01	0.2	69	92	0.0	113	285	1.7	7.8	223	<0.05	4.8	<0.05	<0.05	<0.1	60	748	0.4	0.9	1.5	<0.02	11	<0.05	2	156
06/05/95	LL02	<0.02	21	<0.5	0.0	37	58	0.2	0.3	74	<0.05	0.2	<0.05	0.3	<0.1	3	69	<0.05	<0.1	0.8	<0.02	1	<0.05	<0.3	2
06/05/95	LL04	<0.02	14	<0.5	<0.5	31	54	0.2	0.2	3	<0.05	<0.02	<0.05	1.1	<0.1	1	495	<0.05	<0.1	0.6	<0.02	1	<0.05	<0.3	3
06/05/95	LL05	0.1	29	22	0.0	46	148	0.9	2.8	63	<0.05	1.2	<0.05	0.4	<0.1	17	807	0.3	0.5	0.7	<0.02	13	<0.05	1	93
04/05/95	QH01	0.8	258	86	0.0	95	232	1.4	9.5	313	0.2	8.4	0.9	0.4	<0.1	4	292	0.2	0.5	2.1	<0.02	4	<0.05	1	14
04/05/95	QH02	0.5	1400	223	2.4	169	450	2.5	2.3	13100	1.2	2.3	0.5	1.4	0.9	11	2550	<0.05	0.6	21.1	0.20	27	0.26	30	12
04/05/95	QH03	0.8	1260	208	3.7	177	476	2.9	4.2	16300	1.6	5.0	0.7	2.8	1.1	11	2170	<0.05	0.6	22.5	0.15	35	<0.05	32	15
04/05/95	QH04	1.1	1520	263	5.3	199	574	3.4	4.0	18300	2.9	5.3	0.9	2.5	1.5	13	3270	0.2	1.2	31.6	0.24	66	0.36	41	17
04/05/95	QH05	0.5	1230	186	4.3	168	549	3.3	8.1	11800	6.1	4.1	0.5	1.7	0.7	16	5000	0.4	1.7	26.6	0.10	180	0.33	34	12
04/05/95	QH06	0.4	867	143	1.4	113	356	2.2	3.1	3550	3.6	1.5	<0.05	1.9	<0.1	11	3640	0.3	1.6	11.0	<0.02	108	<0.05	10	7
04/05/95	QH07	0.5	85	21	0.0	59	203	1.6	1.2	121	<0.05	1.9	0.2	0.3	<0.1	6	488	0.1	0.6	0.7	<0.02	8	<0.05	<0.3	6
04/05/95	QH08	0.7	261	66	0.5	91	390	2.9	2.6	1140	1.7	3.3	0.2	0.8	<0.1	14	1930	0.6	2.5	3.9	<0.02	209	0.25	3	8
04/05/95	QH10	0.6	136	56	0.1	54	143	1.2	7.2	310	0.3	6.0	0.3	0.3	<0.1	6	376	0.2	0.6	1.0	<0.02	22	<0.05	1	7
02/05/95	SH02	0.5	65	49	0.0	56	100	0.6	2.0	220	0.2	2.7	0.3	1.1	<0.1	10	295	0.1	0.7	1.2	<0.02	6	<0.05	1	12
02/05/95	SH03	0.3	59	35	0.0	52	74	0.5	2.0	212	<0.05	2.9	0.3	1.0	<0.1	7	501	<0.05	0.3	1.1	<0.02	3	<0.05	1	11
02/05/95	SH05	0.1	39	26	0.0	54	76	0.4	1.5	136	<0.05	2.1	0.2	0.6	<0.1	11	524	<0.05	<0.1	0.9	<0.02	2	<0.05	<0.3	4
02/05/95	SH06	0.1	34	10	<0.5	43	68	0.2	0.2	4	<0.05	0.1	<0.05	1.2	<0.1	1	145	<0.05	<0.1	0.5	<0.02	1	<0.05	<0.3	1
05/05/95	SH06	0.1	31	10	<0.5	42	66	0.2	0.2	<1.0	<0.05	<0.02	<0.05	0.7	<0.1	1	157	<0.05	<0.1	0.5	<0.02	0	<0.05	<0.3	1
05 05/95	SH08	<0.02	55	<0.5	0.0	72	149	0.5	0.8	28	<0.05	0.4	<0.05	1.0	<0.1	3	1200	<0.05	<0.1	1.1	<0.02	3	<0.05	<0.3	3
05/05/95	SH09	<0.02	69	4	0.1	107	453	2.0	3.2	31	<0.05	0.5	0.2	1.3	<0.1	17	7570	0.4	0.9	1.1	<0.02	14	<0.05	<0.3	3
05/05/95	SH11	0.8	82	128	0.1	228	955	5.3	11.8	648	0.5	13.8	1.1	1.9	<0.1	153	14700	2.3	5.1	1.9	<0.02	25	<0.05	<0.3	47
05/05/95	SH12	<0.02	28	22	0.0	131	231	1.0	2.4	159	<0.05	3.5	0.3	0.9	<0.1	3	1260	<0.05	<0.1	1.0	<0.02	3	<0.05	<0.3	18
05/05/95	SH13	0.8	81	92	0.1	197	720	3.9	9.3	502	0.3	9.7	0.7	1.6	<0.1	88	9780	1.2	3.5	2.0	<0.02	20	<0.05	1	104
03/05/95	WG01	0.4	88	19	0.0	113	213	1.7	0.3	3	<0.05	0.2	<0.05	0.8	<0.1	2	489	<0.05	<0.1	1.0	<0.02	1	<0.05	<0.3	8
24/07/95	BB01	0.1	18	3	<0.5	22	31	0.3	0.1	<1.0	<0.05	<0.02	<0.05	0.4	<0.1	1	2	<0.05	<0.1	0.0	0.08	4	<0.05	<0.3	<0.2
24/07/95	BB02	0.1	28	8	<0.5	35	69	0.7	0.2	<1.0	<0.05	<0.02	<0.05	0.8	<0.1	3	214	<0.05	0.9	0.2	0.07	11	<0.05	<0.3	2
29/07/95	EY01	0.1	20	4	0.0	29	82	0.3	0.6	10	<0.05	0.1	<0.05	0.6	<0.1	1	1030	<0.05	0.5	0.1	0.07	4	<0.05	<0.3	1
29/07/95	EY02	0.1	38	15	<0.5	32	97	0.4	1.4	22	<0.05	0.3	<0.05	0.8	<0.1	17	84	<0.05	0.8	0.4	0.14	5	<0.05	<0.3	19
29/07/95	EY03	0.1	35	13	0.0	44	170	0.7	1.8	22	<0.05	0.3	<0.05	1.0	<0.1	9	1690	<0.05	1.4	0.7	0.14	23	<0.05	<0.3	38
27/07/95	HR02	0.2	23	3	0.0	13	49	0.1	0.2	12	0.1	0.2	0.1	0.3	<0.1	2	210	0.1	1.5	0.2	0.13	4	<0.05	<0.3	2
27/07/95	HR03	0.1	33	9	0.0	23	109	0.4	0.3	83	<0.05	0.1	<0.05	1.9	<0.1	2	1120	<0.05	1.8	0.8	0.14	10	<0.05	<0.3	8

Date	Sample	Li ng ml^{-1}	Na ng ml^{-1}	K ng ml^{-1}	Be ng ml^{-1}	Mg ng ml^{-1}	Ca ng ml^{-1}	Sr ng ml^{-1}	Ba ng ml^{-1}	Al ng ml^{-1}	La ng ml^{-1}	Ti ng ml^{-1}	V ng ml^{-1}	Cr ng ml^{-1}	Mo ng ml^{-1}	Mn ng ml^{-1}	Fe ng ml^{-1}	Co ng ml^{-1}	Ni ng ml^{-1}	Cu ng ml^{-1}	Ag ng ml^{-1}	Zn ng ml^{-1}	Cd ng ml^{-1}	Pb ng ml^{-1}	P ng ml^{-1}
27/07 95	HR04	0.7	29	4	0.1	81	118	0.2	0.1	324	<0.05	0.1	0.1	0.2	<0.1	9	446	0.2	0.7	0.8	0.08	5	<0.05	<0.3	2
27/07/95	HR05	0.9	36	15	0.0	88	131	0.3	0.7	150	0.2	0.7	0.5	1.0	<0.1	11	1570	0.4	<0.1	1.9	0.18	28	0.19	1	5
27/07/95	HR06	0.4	22	<0.5	0.0	51	82	0.1	0.1	43	<0.05	0.1	0.2	0.3	<0.1	5	407	<0.05	0.6	0.3	0.08	4	<0.05	<0.3	3
26 07/95	HR07	0.5	29	3	0.0	48	80	0.2	0.2	38	<0.05	0.2	0.2	0.6	<0.1	6	314	0.1	0.6	0.8	0.10	4	<0.05	<0.3	3
26/07/95	HR08	0.3	56	10	1.8	84	483	2.1	1.1	7060	3.2	1.1	<0.05	1.0	<0.1	34	499	0.7	2.3	8.8	0.21	142	<0.05	3	5
26 07/95	HR09	0.3	24	10	1.6	96	707	3.2	1.7	6660	3.0	0.9	<0.05	0.5	<0.1	50	807	2.6	6.5	8.6	<0.02	258	0.42	3	6
26/07/95	HR10	0.1	16	6	0.1	36	148	0.7	0.8	555	0.3	0.1	<0.05	0.5	<0.1	14	532	0.4	1.7	1.0	0.08	31	<0.05	<0.3	10
26/07/95	HR11	0.1	19	9	0.0	31	79	0.4	1.2	100	<0.05	0.1	<0.05	0.8	<0.1	18	181	<0.05	0.8	0.4	<0.02	11	<0.05	<0.3	8
26/07/95	HR12	0.3	22	15	0.0	38	93	0.5	1.3	167	<0.05	0.9	<0.05	<0.05	<0.1	32	304	0.3	1.0	0.8	0.10	13	<0.05	<0.3	10
26/07/95	HR14	0.4	33	19	0.0	45	108	0.5	1.4	102	0.2	1.0	0.3	0.8	<0.1	16	350	0.3	1.5	0.5	0.21	13	<0.05	1	10
26/07/95	HR15	0.1	16	9	0.0	23	63	0.2	0.5	58	<0.05	0.5	<0.05	0.2	<0.1	10	91	<0.05	0.6	0.3	0.07	6	<0.05	<0.3	10
27/07/95	LL01	0.1	29	22	<0.5	49	127	0.8	1.7	23	<0.05	<0.02	<0.05	<0.05	<0.1	13	246	<0.05	<0.1	0.3	<0.02	5	<0.05	<0.3	47
27/07/95	LL02	0.2	14	11	0.1	24	40	0.2	0.7	670	0.2	0.6	0.3	0.3	<0.1	3	4220	0.1	<0.1	0.5	<0.02	5	0.25	1	4
27/07/95	LL04B	0.1	14	3	<0.5	16	23	0.1	0.0	<1.0	<0.05	<0.02	<0.05	0.3	<0.1	1	35	<0.05	<0.1	<0.1	<0.02	0	<0.05	<0.3	1
27/07/95	LL05	0.2	58	23	0.0	84	250	1.8	4.0	50	<0.05	<0.02	<0.05	1.7	<0.1	19	1350	0.4	0.8	0.5	<0.02	17	<0.05	<0.3	209
28/07/95	QH01	0.2	145	16	<0.5	29	68	0.4	1.5	49	<0.05	1.1	0.2	0.5	<0.1	4	67	<0.05	0.5	0.5	0.10	4	<0.05	<0.3	4
28/07/95	QH02	0.4	291	33	0.2	75	173	0.9	0.3	1380	<0.05	<0.02	<0.05	0.7	<0.1	6	1320	<0.05	0.8	6.1	0.06	17	<0.05	5	2
28/07/95	QH03	0.5	446	45	0.8	111	253	1.2	0.8	5340	0.2	0.9	<0.05	1.3	<0.1	8	1450	<0.05	1.3	5.7	0.21	19	<0.05	6	4
28/07/95	QH04	0.5	272	35	0.4	68	145	0.8	5.6	4100	<0.05	1.3	<0.05	0.8	<0.1	6	1320	<0.05	0.7	2.2	0.08	7	<0.05	2	5
28/07/95	QH05	1.7	1660	263	1.3	423	1300	6.8	13.9	3080	2.9	11.3	2.5	6.7	<0.1	59	2570	<0.05	9.2	26.3	1.00	176	<0.05	15	952
28/07/95	QH06	0.3	323	36	0.0	66	151	0.8	10.8	51	0.3	0.2	0.1	1.0	<0.1	9	406	0.1	<0.1	1.3	0.19	22	<0.05	2	16
28/07/95	QH07	0.4	93	15	<0.5	42	134	0.9	0.4	21	<0.05	0.5	<0.05	0.4	<0.1	5	137	<0.05	0.5	0.2	0.09	5	<0.05	<0.3	4
28 07 95	QH08	0.3	260	32	0.0	58	149	0.8	1.1	29	<0.05	<0.02	<0.05	0.4	<0.1	10	454	0.1	1.0	1.1	<0.02	29	<0.05	<0.3	14
28/07/95	QH09	0.6	538	70	0.0	127	330	1.7	3.4	43	<0.05	0.6	<0.05	1.0	<0.1	14	506	<0.05	2.5	1.1	0.25	35	<0.05	<0.3	12
28/07/95	QH10	0.2	146	20	0.0	35	98	0.5	1.0	20	<0.05	0.4	0.1	0.2	<0.1	5	93	<0.05	0.6	1.1	0.12	9	0.33	<0.3	5
28/07/95	QHW-1	0.8	528	68	0.3	272	513	1.9	18.7	1820	<0.05	2.1	<0.05	1.0	<0.1	11	2000	<0.05	1.3	7.4	<0.02	41	<0.05	7	6
28/07/95	QHW-4	0.7	601	76	0.0	150	314	1.5	1.7	655	<0.05	0.6	<0.05	0.8	<0.1	10	1800	0.4	1.0	5.4	0.15	62	0.63	<0.3	30
29/07/95	SH05	0.0	16	4	<0.5	16	26	0.1	0.2	7	<0.05	<0.02	<0.05	<0.05	<0.1	1	278	<0.05	<0.1	0.1	<0.02	1	<0.05	<0.3	2
29/07/95	SH06	0.1	15	4	<0.5	20	32	0.1	0.0	<1.0	0.1	<0.02	<0.05	0.3	<0.1	1	98	0.1	<0.1	0.0	<0.02	1	<0.05	<0.3	1
29/07/95	SH07	0.0	18	5	0.0	23	85	0.4	0.5	5	0.1	0.3	0.1	<0.05	<0.1	3	1410	0.1	<0.1	0.1	<0.02	3	<0.05	<0.3	1
29/07/95	SH08	0.1	18	6	0.0	40	218	1.1	1.6	9	0.1	0.1	0.3	0.4	<0.1	14	4190	0.3	0.5	0.1	<0.02	7	0.16	<0.3	2
29/07/95	SH09	0.2	23	21	0.0	64	478	2.5	4.0	75	0.3	0.7	0.5	0.6	<0.1	46	9850	0.6	1.6	0.3	<0.02	14	0.36	<0.3	5
29/07/95	SH10	0.1	23	10	0.0	66	496	2.6	4.0	25	0.2	0.4	0.4	<0.05	<0.1	70	8870	1.1	2.1	0.1	<0.02	13	0.34	<0.3	4
29 07 95	SH11	0.1	16	8	0.0	21	48	0.2	0.5	25	0.1	0.2	<0.05	0.2	<0.1	15	386	<0.05	0.4	0.2	<0.02	2	<0.05	<0.3	4
29/07/95	SH12	0.5	136	77	0.0	132	105	0.7	1.4	167	0.3	1.8	0.3	0.8	<0.1	4	180	0.2	<0.1	0.2	<0.02	4	<0.05	<0.3	12
29/07/95	SH13	0.2	53	28	0.0	67	96	0.4	1.1	92	0.2	1.2	0.2	<0.05	<0.1	8	293	0.2	<0.1	0.3	<0.02	4	<0.05	<0.3	21
29 07/95	SH14	0.2	47	19	<0.5	56	83	0.3	0.7	29	<0.05	0.2	<0.05	0.6	<0.1	5	149	<0.05	<0.1	0.2	<0.02	3	<0.05	<0.3	20
29 07/95	SH15	0.2	42	23	<0.5	53	98	0.4	1.2	54	0.2	0.5	0.3	1.0	<0.1	5	284	<0.05	0.8	0.4	<0.02	5	<0.05	<0.3	38

Date	Sample	Li ng ml^{-1}	Na ng ml^{-1}	K ng ml^{-1}	Be ng ml^{-1}	Mg ng ml^{-1}	Ca ng ml^{-1}	Sr ng ml^{-1}	Ba ng ml^{-1}	Al ng ml^{-1}	La ng ml^{-1}	Ti ng ml^{-1}	V ng ml^{-1}	Cr ng ml^{-1}	Mo ng ml^{-1}	Mn ng ml^{-1}	Fe ng ml^{-1}	Co ng ml^{-1}	Ni ng ml^{-1}	Cu ng ml^{-1}	Ag ng ml^{-1}	Zn ng ml^{-1}	Cd ng ml^{-1}	Pb ng ml^{-1}	P ng ml^{-1}
29/07/95	SH16	0.2	63	40	<0.5	61	143	0.7	3.0	96	0.3	1.5	0.4	<0.05	<0.1	23	877	<0.05	0.8	1.1	<0.02	6	<0.05	<0.3	54
24/07/95	TC01	0.2	40	8	0.0	46	87	0.7	0.1	<1.0	0.2	<0.02	0.2	0.3	<0.1	1	182	0.1	<0.1	0.3	<0.02	0	<0.05	<0.3	2
25/07/95	WG01	1.2	18	15	<0.5	138	124	0.2	0.1	8	<0.05	0.2	0.1	0.3	<0.1	18	1310	0.2	<0.1	0.0	<0.02	1	<0.05	<0.3	3
25/07/95	WG02	0.2	11	21	0.0	34	48	0.2	1.4	99	0.2	1.2	0.3	0.4	<0.1	21	143	0.1	<0.1	0.2	<0.02	2	<0.05	1	6
25/07/95	WG03	0.2	10	9	<0.5	27	43	0.1	0.3	29	0.1	0.3	0.1	0.5	<0.1	10	300	0.2	0.4	0.1	<0.02	2	<0.05	<0.3	6
25/07/95	WG04	0.1	11	6	<0.5	18	30	0.1	0.2	15	0.1	0.2	<0.05	<0.05	<0.1	5	154	<0.05	<0.1	0.1	<0.02	1	<0.05	<0.3	4
25 07/95	WG05	0.1	10	8	<0.5	12	27	0.1	0.6	38	0.1	0.5	0.1	0.3	<0.1	2	39	0.1	<0.1	0.1	<0.02	1	<0.05	<0.3	2
22/11/95	EY01	<0.02	28	<0.5	<0.5	72	180	0.4	<0.001	<1.0	<0.05	<0.02	<0.05	2.9	<0.1	3	213	<0.05	<0.1	<0.1	<0.02	3	<0.05	<0.3	<0.2
21/11/95	HR04PIPI	0.2	50	12	1.0	53	223	0.5	0.9	5890	0.3	0.9	<0.05	13.3	<0.1	2	1850	<0.05	0.7	26.7	0.40	7	0.33	<0.3	7
21/11/95	HR04	0.3	38	18	0.7	44	123	0.4	0.8	5010	0.3	1.4	0.3	6.3	<0.1	4	650	<0.05	0.5	10.9	0.30	7	0.38	12	12
21/11/95	HR07	<0.02	88	8	0.6	44	122	0.4	0.7	3450	<0.05	1.3	<0.05	14.3	<0.1	4	3580	<0.05	<0.1	15.1	<0.02	7	<0.05	7	32
21/11/95	HR07A	0.0	1	0	0.0	1	2	0.0	0.0	42	0.0	0.0	0.0	0.2	<0.1	0	39	<0.05	<0.1	0.3	0.00	0	<0.05	0	0
21/11/95	HR08	0.1	62	<0.5	1.1	68	207	0.7	1.0	4340	<0.05	0.8	<0.05	15.0	<0.1	8	3710	<0.05	<0.1	27.8	<0.02	21	<0.05	7	29
21/11/95	HR09	0.1	85	12	1.1	62	197	0.7	1.1	4230	<0.05	1.2	<0.05	15.3	<0.1	9	3800	<0.05	<0.1	28.0	<0.02	27	<0.05	7	32
21/11/95	HR10	0.7	105	63	0.3	130	236	1.1	3.3	1260	0.7	3.9	0.7	13.3	<0.1	14	2260	0.4	1.2	9.1	0.40	35	0.42	7	29
19/11/95	QH01	0.3	269	39	0.0	64	181	1.0	1.8	75	<0.05	1.8	0.5	4.1	<0.1	3	97	<0.05	<0.1	1.0	0.44	6	0.47	<0.3	4
19/11/95	QH02	<0.02	1030	116	0.4	118	481	2.3	12.8	2090	<0.05	2.5	<0.05	6.9	<0.1	7	403	<0.05	<0.1	5.3	<0.02	43	<0.05	15	100
19/11/95	QH03	<0.02	928	100	0.4	133	528	2.8	20.4	2110	<0.05	3.3	<0.05	7.5	<0.1	8	469	<0.05	<0.1	6.1	<0.02	48	<0.05	15	108
19/11/95	QH04A	1.8	1050	310	0.3	210	559	3.9	30.1	2770	<0.05	14.0	<0.05	17.0	<0.1	14	1540	<0.05	<0.1	5.1	<0.02	63	<0.05	9	96
19/11/95	QH06	1.8	830	245	0.3	213	549	4.1	44.6	2370	<0.05	13.4	<0.05	14.0	<0.1	17	1660	<0.05	<0.1	4.8	<0.02	82	<0.05	9	80
19/11/95	QH07	4.9	235	545	0.2	285	367	4.1	15.9	3150	1.8	24.9	4.5	26.5	<0.1	34	2600	<0.05	3.0	2.7	1.20	31	1.50	8	48
19/11/95	QH09	4.8	265	550	0.1	342	434	5.2	33.3	3700	<0.05	35.6	2.0	24.0	<0.1	40	3070	<0.05	<0.1	2.4	<0.02	41	<0.05	<0.3	58
18/11/95	SH05	0.2	132	32	0.0	43	61	0.3	1.1	113	<0.05	0.9	0.3	3.3	<0.1	5	266	<0.05	<0.1	0.4	0.25	4	0.42	<0.3	8
18/11/95	SH06	<0.02	23	<0.5	<0.5	27	43	0.1	<0.001	<1.0	<0.05	<0.02	<0.05	1.4	<0.1	1	86	<0.05	<0.1	<0.1	<0.02	2	<0.05	<0.3	1
18/11/95	SH09A	<0.02	295	3	<0.5	57	122	0.5	1.5	63	<0.05	0.7	<0.05	5.0	<0.1	8	899	<0.05	<0.1	0.3	<0.02	6	<0.05	<0.3	11
18 11/95	SH10A	0.2	282	18	<0.5	59	145	0.7	1.9	75	<0.05	1.1	<0.05	7.2	<0.1	16	1200	<0.05	0.6	0.5	0.28	9	0.28	<0.3	13
18 11/95	SH11	<0.02	91	16	<0.5	50	120	0.6	1.8	108	<0.05	1.3	<0.05	5.4	<0.1	24	1000	<0.05	0.4	0.3	<0.02	6	<0.05	<0.3	15
18/11/95	SH12	3.0	100	371	0.1	235	334	3.0	10.6	2050	1.3	11.5	2.9	20.8	<0.1	18	1770	<0.05	1.7	1.3	1.00	18	<0.05	<0.3	35
18/11/95	SH13	1.2	98	182	<0.5	136	181	1.6	5.9	1180	<0.05	5.7	<0.05	10.0	<0.1	20	1340	<0.05	<0.1	0.5	<0.02	10	<0.05	<0.3	28
18/11/95	SH15	1.0	117	106	0.0	84	143	1.1	4.0	625	<0.05	4.9	0.6	8.3	<0.1	11	773	<0.05	<0.1	0.6	0.42	10	<0.05	3	28
20/11/95	WG01	0.5	20	68	<0.5	57	79	0.6	2.1	445	<0.05	1.4	<0.05	3.5	<0.1	3	389	<0.05	<0.1	0.1	<0.02	4	<0.05	<0.3	17
10/03/96	BB01	0.0	14	6	<0.5	24	39	0.4	0.5	<1.0	<0.05	<0.02	<0.05	0.3	<0.1	1	14	<0.05	<0.1	<0.1	<0.02	1	<0.05	<0.3	<0.2
10/03/96	BB02	0.1	32	13	<0.5	48	85	0.9	0.7	5	<0.05	0.1	<0.05	0.7	<0.1	5	169	<0.05	<0.1	0.1	<0.02	3	<0.05	<0.3	<0.2
14/03/96	HR04	0.3	31	7	0.7	35	88	0.2	1.0	4300	0.3	0.3	0.5	1.5	<0.1	3	1710	<0.05	<0.1	3.1	<0.02	2	<0.05	1	6
14/03/96	HR07	0.3	33	7	1.0	37	113	0.4	1.1	4980	0.5	0.3	0.4	2.3	<0.1	3	3770	<0.05	<0.1	12.3	<0.02	5	<0.05	4	10
14/03/96	HR07A	0.3	48	18	1.1	28	74	0.3	0.9	6360	0.4	1.8	0.4	1.4	<0.1	3	3000	<0.05	<0.1	8.4	<0.02	3	<0.05	3	10
14/03/96	HR08	0.3	60	22	1.7	35	103	0.4	1.1	7330	0.5	1.9	0.3	1.0	<0.1	3	2560	<0.05	<0.1	13.5	<0.02	8	<0.05	3	8
14/03/96	HR09	0.3	60	15	1.8	40	218	0.9	1.3	5790	2.6	1.2	0.3	1.5	<0.1	8	3420	0.2	0.7	18.5	<0.02	58	<0.05	3	7

Date	Sample	Li ng ml^{-1}	Na ng ml^{-1}	K ng ml^{-1}	Be ng ml^{-1}	Mg ng ml^{-1}	Ca ng ml^{-1}	Sr ng ml^{-1}	Ba ng ml^{-1}	Al ng ml^{-1}	La ng ml^{-1}	Ti ng ml^{-1}	V ng ml^{-1}	Cr ng ml^{-1}	Mo ng ml^{-1}	Mn ng ml^{-1}	Fe ng ml^{-1}	Co ng ml^{-1}	Ni ng ml^{-1}	Cu ng ml^{-1}	Ag ng ml^{-1}	Zn ng ml^{-1}	Cd ng ml^{-1}	Pb ng ml^{-1}	P ng ml^{-1}
14/03/96	HR10	0.2	49	34	0.7	49	323	1.8	4.2	2300	1.3	1.1	0.3	1.8	<0.1	15	5170	0.6	1.7	8.0	<0.02	77	<0.05	1	44
14/03 96	HR11	0.5	79	48	0.6	80	401	2.3	5.8	2020	1.0	3.3	0.3	1.5	<0.1	21	5250	0.7	2.5	7.0	<0.02	81	<0.05	1	50
11/03/96	QH02	1.1	1630	262	2.2	261	562	3.0	8.1	8210	1.5	5.6	1.0	3.8	<0.1	15	1180	<0.05	1.3	16.7	0.17	42	<0.05	31	32
15/03/96	QH02	1.0	1900	248	2.2	242	646	3.4	9.9	7970	2.3	4.1	0.8	1.5	<0.1	14	950	<0.05	1.0	18.4	<0.02	43	<0.05	29	24
11/03/96	QH03	0.5	780	118	2.1	115	355	1.9	2.5	7000	1.4	1.3	0.6	2.0	<0.1	7	784	<0.05	0.8	14.4	0.15	38	<0.05	23	19
11/03/96	QH04	0.4	673	108	2.2	102	350	2.0	13.5	6370	2.2	1.6	0.4	0.8	<0.1	7	772	0.2	0.8	15.8	0.17	56	<0.05	23	14
11/03/96	QH05	0.6	583	107	2.3	117	396	3.0	63.6	5620	4.9	3.8	0.7	1.7	<0.1	13	1400	0.6	2.2	17.5	0.13	188	<0.05	22	19
11/03/96	QH06	0.3	463	73	1.4	74	283	1.8	4.1	3280	3.3	1.6	<0.05	1.3	<0.1	8	1150	0.3	1.7	10.0	<0.02	141	<0.05	13	9
11/03/96	QH07	2.3	131	174	0.3	155	389	3.3	7.4	1020	1.6	11.7	1.7	1.8	<0.1	56	1450	1.3	3.9	5.4	<0.02	36	<0.05	2	21
11/03/96	QH09	2.0	188	123	0.6	163	478	4.1	8.9	1340	2.0	5.0	1.4	2.5	<0.1	48	1780	1.1	4.2	6.8	<0.02	89	<0.05	4	22
15/03/96	QHW-I	1.1	1370	203	2.3	226	551	3.3	28.6	8440	2.9	8.1	1.2	1.5	<0.1	13	1080	<0.05	1.2	23.7	0.29	53	<0.05	33	31
15/03/96	QHW-4	0.2	567	49	0.6	43	126	0.6	1.0	2180	0.4	0.2	0.1	0.7	<0.1	3	498	<0.05	0.2	4.7	<0.02	15	0.10	6	4
13/03/96	SH05	<0.02	65	6	0.0	23	39	0.2	0.6	18	<0.05	0.2	<0.05	<0.05	<0.1	1	141	<0.05	<0.1	0.1	<0.02	1	<0.05	<0.3	1
13/03/96	SH06	0.0	28	5	0.0	24	37	0.1	0.5	18	<0.05	0.1	<0.05	<0.05	<0.1	1	153	<0.05	<0.1	0.6	<0.02	0	<0.05	1	1
13/03 96	SH07	0.1	56	8	0.0	26	45	0.1	0.5	23	<0.05	0.1	<0.05	<0.05	<0.1	1	201	<0.05	<0.1	0.3	<0.02	1	<0.05	<0.3	1
13/03/96	SH09	1.5	316	129	0.1	304	495	2.4	8.7	717	0.5	8.9	1.9	2.3	<0.1	22	2090	0.3	1.0	2.9	<0.02	14	<0.05	6	43
13/03/96	SH10	1.6	333	149	0.1	360	633	3.1	10.5	821	0.8	11.9	2.4	3.1	<0.1	27	4890	0.5	1.9	3.2	0.08	21	<0.05	7	45
13/03/96	SH11	0.3	191	28	0.1	117	536	2.9	7.6	158	0.3	1.6	0.5	3.0	<0.1	41	9360	1.0	2.8	1.1	<0.02	21	<0.05	<0.3	36
13/03/96	SH12	0.3	50	42	0.0	54	101	0.6	2.3	183	0.3	1.6	0.4	0.8	<0.1	3	406	<0.05	0.5	0.2	<0.02	2	<0.05	<0.3	6
13/03/96	SH13	0.3	194	49	0.1	128	450	2.3	5.9	175	<0.05	2.4	0.4	1.5	<0.1	24	6510	0.6	1.8	0.8	<0.02	16	<0.05	<0.3	43
13/03/96	SH15	0.5	234	64	0.0	119	327	1.9	6.3	269	<0.05	5.8	0.5	1.6	<0.1	24	3230	0.5	1.3	0.8	<0.02	12	<0.05	<0.3	48
10/03/96	TC01	0.3	76	24	0.0	83	157	1.3	0.4	<1.0	0.2	0.3	<0.05	1.0	<0.1	3	252	<0.05	<0.1	0.4	0.07	3	<0.05	<0.3	4
09/10/96	BB01	0.1	42	7	0.0	21	40	0.3	<0.001	4	0.1	0.4	<0.05	0.1	<0.1	1	<0.5	<0.05	0.2	0.2	0.11	4	0.11	<0.3	1
09 10/96	HR04	1.1	97	12	0.3	121	205	0.4	0.3	1670	<0.05	0.4	0.8	0.4	<0.1	14	1390	<0.05	1.0	1.4	0.21	8	<0.05	<0.3	6
08/10/96	HR07	1.1	270	48	0.1	80	144	0.7	0.9	679	1.3	2.0	0.9	0.7	<0.1	9	754	0.4	1.8	1.7	0.71	14	<0.05	3	17
08/10/96	HR07A	0.5	118	30	0.0	34	62	0.3	0.4	254	0.2	1.0	<0.05	0.4	<0.1	4	271	<0.05	0.6	0.6	0.25	5	<0.05	<0.3	8
08/10/96	HR08	0.3	118	16	1.6	40	139	0.6	0.1	6380	1.6	0.9	<0.05	<0.05	<0.1	10	598	<0.05	0.6	7.0	0.29	28	<0.05	4	5
08/10/96	HR09	0.3	124	19	1.6	50	177	0.7	0.0	5860	2.1	0.7	<0.05	<0.05	<0.1	11	747	<0.05	1.0	7.3	0.21	60	<0.05	4	4
08/10/96	HR10	0.4	303	45	0.1	127	380	1.3	0.5	375	<0.05	0.8	<0.05	<0.05	<0.1	24	473	<0.05	3.0	4.0	0.40	38	<0.05	<0.3	84
08/10/96	HR11	0.2	106	16	0.0	33	84	0.3	<0.001	75	<0.05	0.3	<0.05	<0.05	<0.1	4	135	<0.05	0.8	1.0	0.17	8	<0.05	<0.3	14
09/10/96	QH01	1.0	659	79	3.0	112	309	2.5	14.7	8550	1.2	1.3	0.3	1.3	<0.1	17	936	0.3	1.7	5.4	0.20	42	<0.05	4	6
09/10/96	SH06	0.0	41	5	<0.5	21	38	0.1	<0.001	1	<0.05	0.1	<0.05	<0.05	<0.1	1	130	<0.05	0.2	0.8	0.09	2	<0.05	<0.3	1
09/10/96	BB01 B	0.2	91	13	<0.5	48	81	0.7	<0.001	<1.0	<0.05	0.4	<0.05	0.7	<0.1	1	<0.5	<0.05	0.5	0.2	0.17	4	<0.05	<0.3	1
09/10/96	HR04 B	0.7	47	8	0.0	79	134	0.2	<0.001	43	<0.05	0.2	<0.05	0.5	<0.1	9	70	<0.05	0.7	0.2	0.17	4	<0.05	<0.3	<0.2
08/10/96	HR07 B	0.8	241	23	0.0	70	149	0.3	<0.001	25	1.6	1.2	0.7	1.4	<0.1	7	30	0.7	1.8	0.8	0.93	8	0.54	2	3
08 10/96	HR07A E	0.3	206	23	<0.5	40	102	0.2	<0.001	17	<0.05	0.8	<0.05	1.7	<0.1	3	<0.5	<0.05	1.3	0.5	0.50	6	<0.05	<0.3	<0.2
08/10/96	HR08 B	0.2	60	11	0.0	24	65	0.2	<0.001	29	0.3	0.6	<0.05	0.7	<0.1	2	20	<0.05	0.5	0.4	0.24	7	<0.05	<0.3	2
08 10/96	HR09 B	0.1	54	7	0.0	18	48	0.1	<0.001	16	0.2	0.2	<0.05	<0.05	<0.1	1	91	<0.05	0.5	0.4	0.14	4	<0.05	<0.3	1

Date	Sample	Li ng ml^{-1}	Na ng ml^{-1}	K ng ml^{-1}	Be ng ml^{-1}	Mg ng ml^{-1}	Ca ng ml^{-1}	Sr ng ml^{-1}	Ba ng ml^{-1}	Al ng ml^{-1}	La ng ml^{-1}	Ti ng ml^{-1}	V ng ml^{-1}	Cr ng ml^{-1}	Mo ng ml^{-1}	Mn ng ml^{-1}	Fe ng ml^{-1}	Co ng ml^{-1}	Ni ng ml^{-1}	Cu ng ml^{-1}	Ag ng ml^{-1}	Zn ng ml^{-1}	Cd ng ml^{-1}	Pb ng ml^{-1}	P ng ml^{-1}
08/10/96	HR11 B	0.1	88	14	<0.5	31	73	0.2	<0.001	<1.0	<0.05	0.3	<0.05	1.0	<0.1	<0.05	<0.5	<0.05	0.4	0.2	0.16	4	<0.05	<0.3	1
09/10/96	QH01 B	0.3	367	36	0.0	56	145	0.7	<0.001	36	0.1	0.5	<0.05	0.4	<0.1	4	15	<0.05	0.6	0.3	0.19	7	0.21	<0.3	1
09/10/96	SH06 B	0.2	89	15	0.0	47	137	0.4	<0.001	25	0.6	2.2	0.3	1.5	<0.1	2	53	<0.05	0.8	0.7	0.42	28	0.73	1	3
04/07/97	BB01	<0.02	83	13	<0.5	37	63	0.6	<0.001	<1.0	<0.05	0.2	<0.05	0.4	<0.1	1	<0.5	<0.05	0.4	0.3	0.17	3	<0.05	<0.3	1
05/07/97	EY01	0.2	331	44	0.0	84	266	0.8	0.1	12	0.4	0.4	0.1	1.0	<0.1	3	1680	0.1	0.8	0.4	0.18	4	<0.05	1	3
04/07/97	HR04	0.6	305	54	2.0	70	288	0.9	0.7	12800	1.9	1.3	0.6	1.7	<0.1	5	1240	<0.05	1.1	14.9	0.14	12	<0.05	6	12
04/07/97	HR07	0.8	245	45	0.7	66	212	0.9	1.2	3470	1.3	1.8	0.8	1.5	<0.1	6	1880	<0.05	2.5	15.0	0.60	24	<0.05	5	27
04/07/97	HR07A	1.1	266	88	0.7	90	274	1.1	1.8	3560	1.3	3.9	0.9	3.1	<0.1	7	2190	<0.05	2.5	15.9	0.63	34	<0.05	<0.3	33
05/07/97	SH06	0.1	339	36	0.0	59	141	0.4	1.4	319	<0.05	0.4	<0.05	0.7	<0.1	2	248	<0.05	0.8	2.0	0.10	3	0.10	1	3

IV.iii Stream sediment chemistry

Date	Sample	Li	Na	K	Be	Mg	Ca	Sr	Ba	Al	La	Ti	V	Cr	Mo	Mn	Fe	Co	Ni	Cu	Ag	Zn	Cd	Pb	P
		µg g^{-1}	µg g^{-1}	µg g^{-1}	µg g^{-1}	µg g^{-1}	µg g^{-1}	µg g^{-1}	µg g^{-1}	µg g^{-1}	µg g^{-1}	µg g^{-1}	µg g^{-1}	µg g^{-1}	µg g^{-1}	µg g^{-1}	µg g^{-1}	µg g^{-1}	µg g^{-1}	µg g^{-1}	µg g^{-1}	µg g^{-1}	µg g^{-1}	µg g^{-1}	µg g^{-1}
06/05/95	BB01	8	183	695	4	7350	28800	253	122	7020	15	246	35	<0.4	<0.4	992	422000	16	26	37	0.7	388	2.8	720	458
04/05/95	EY01	1	93	158	3	557	4360	30	21	1020	9	13	7	<0.4	<0.4	243	490000	5	7	4	0.2	92	2.1	<1.2	41
03 05/95	HR01	114	499	9890	7	8080	32300	172	259	64400	31	548	73	340	1	6220	37600	97	225	179	0.4	2430	5.0	119	1090
03 05/95	HR02	2	158	188	0	382	1380	4	6	2960	2	15	12	<0.4	<0.4	45	436000	<0.2	<0.4	22	<0.08	12	1.0	<1.2	213
03/05/95	HR04.1	4	88	123	19	341	1020	4	6	129000	4	15	9	<0.4	6	54	159000	<0.2	7	80	0.3	74	1.5	8	95
03/05/95	HR04.2	5	123	375	7	1860	6100	35	35	52200	6	49	13	<0.4	2	108	334000	1	6	75	1.1	98	<0.2	14	334
03/05/95	HR04.3	5	273	368	12	429	1730	6	12	137000	3	56	10	<0.4	4	50	119000	<0.2	2	45	0.4	25	<0.2	<1.2	106
03/05/95	HR04.4	27	123	1300	16	7560	49800	302	91	92800	31	384	22	<0.4	6	365	63700	10	41	89	0.8	304	4.3	48	258
03 05/95	HR05.1	4	48	388	1	264	471	3	14	6880	3	43	11	<0.4	<0.4	44	446000	<0.2	<0.4	26	0.3	31	<0.2	9	62
03 05 95	HR05.2	4	160	428	1	334	1110	5	35	8950	3	47	12	<0.4	<0.4	52	450000	<0.2	1	71	<0.08	63	2.0	18	82
03/05/95	HR05.3	115	394	9730	3	3510	5780	70	63	68800	27	627	67	401	4	420	118000	10	36	70	0.4	191	<0.2	163	476
03/05/95	HR06	136	511	11000	4	3580	2650	66	96	75700	29	782	69	332	2	477	88800	11	38	70	0.4	197	<0.2	126	435
03/05/95	HR07	3	58	173	10	200	390	2	5	98200	3	24	8	<0.4	3	32	199000	<0.2	<0.4	57	0.4	41	<0.2	8	88
03/05/95	HR09	21	183	2040	15	1320	6550	50	191	56600	34	309	20	<0.4	2	730	259000	21	68	210	0.4	1510	7.8	24	173
01/05/95	LL01	72	1100	5790	5	6890	10900	77	204	44300	29	583	66	325	2	1390	52700	38	63	99	0.3	585	<0.2	154	715
06/05/95	LL01	66	350	7640	2	3620	5470	58	339	44800	33	564	46	223	<0.4	2410	44000	29	46	27	0.2	355	<0.2	510	1300
01/05/95	LL02	35	153	2340	5	1150	1630	27	277	65000	15	452	22	<0.4	3	194	259000	4	13	74	0.3	205	2.3	41	247
06/05/95	LL02	49	160	3420	4	1280	1250	46	272	64200	17	636	31	<0.4	4	162	206000	4	14	88	0.5	273	2.8	74	350
01 05/95	LL04	28	165	3100	1	1670	3390	36	432	20900	18	446	29	<0.4	<0.4	578	236000	12	27	24	0.3	368	2.8	320	1530
06 05/95	LL04	1	65	90	3	536	6160	58	53	9310	8	9	6	<0.4	<0.4	256	490000	4	16	18	0.2	145	2.3	<1.2	157
01 05/95	LL05	56	303	6130	2	3230	3740	45	123	37300	15	752	47	254	1	2900	60000	41	53	44	0.2	475	<0.2	287	1210
04/05/95	QH01	65	911	6600	2	5330	9420	72	231	44600	25	622	81	220	1	324	31300	12	51	89	0.4	228	<0.2	59	373
04 05/95	QH02	77	891	6720	4	8030	12470	73	246	47800	32	573	68	369	2	1700	56400	34	62	94	0.3	572	<0.2	249	866
04/05/95	QH03	54	1460	4160	5	6360	11150	82	207	37850	20	862	91	373	4	3550	65000	60	116	196	0.4	1040	1.8	179	554
04/05/95	QH04	4	1230	625	19	461	2550	37	248	52400	74	38	84	<0.4	22	174	319000	5	35	293	0.4	900	1.3	638	403
04 05/95	QH05	58	940	4300	4	2550	4170	672	17600	35400	18	854	59	254	5	2480	61800	71	101	179	1.0	2350	4.8	293	664
04 05/95	QH06	70	709	3560	5	2050	2990	499	15200	33400	12	579	50	295	5	6280	76200	145	197	238	0.9	3060	5.8	205	472
04/05/95	QH07	18	162	3170	1	1450	1350	21	181	16600	16	404	21	94	<0.4	427	16550	8	17	8	0.1	65	<0.2	17	179
04 05/95	QH08	16	246	3010	1	1340	1190	27	880	15600	19	409	20	110	<0.4	572	16600	10	20	8	0.2	147	<0.2	18	184
04 05/95	QH10	18	180	2840	1	1170	1020	63	673	15800	26	528	23	107	1	459	18400	10	22	13	0.2	220	0.4	27	214
02/05/95	SH01	54	469	9340	3	3120	2690	49	385	46600	26	529	60	239	1	1990	53100	29	80	59	0.3	402	<0.2	88	547
05 05/95	SH01	55	536	11800	3	3810	2840	59	348	51900	30	566	67	281	2	1980	66100	28	84	66	0.4	422	<0.2	86	577
02 05/95	SH02	56	522	10200	3	3430	3100	55	365	50700	28	568	68	282	1	1310	70000	32	85	69	0.4	433	<0.2	94	685
02 05/95	SH03	53	454	12300	3	3350	1950	63	684	59900	29	579	68	361	1	1630	105000	23	56	72	0.4	257	<0.2	89	681
02/05/95	SH04	53	486	14000	2	4080	3300	67	453	63600	35	561	68	388	1	18500	70400	22	92	47	0.2	316	<0.2	53	494
02 05/95	SH05	42	336	8250	2	2890	2410	46	425	40700	25	486	53	316	1	2420	84800	27	58	60	0.2	317	<0.2	63	564

Date	Sample	Li	Na	K	Be	Mg	Ca	Sr	Ba	Al	La	Ti	V	Cr	Mo	Mn	Fe	Co	Ni	Cu	Ag	Zn	Cd	Pb	P
		µg g^{-1}	µg g^{-1}	µg g^{-1}	µg g^{-1}	µg g^{-1}	µg g^{-1}	µg g^{-1}	µg g^{-1}	µg g^{-1}	µg g^{-1}	µg g^{-1}	µg g^{-1}	µg g^{-1}	µg g^{-1}	µg g^{-1}	µg g^{-1}	µg g^{-1}	µg g^{-1}	µg g^{-1}	µg g^{-1}	µg g^{-1}	µg g^{-1}	µg g^{-1}	µg g^{-1}
02/05/95	SH06	9	155	2450	3	1090	2140	22	203	11700	10	202	17	<0.4	<0.4	179	446000	5	20	16	<0.08	145	3.3	15	143
05 05/95	SH06.1	0	113	138	3	578	4790	32	42	3050	5	9	6	<0.4	<0.4	647	491000	11	21	13	0.2	123	1.8	12	62
05/05/95	SH06.2	1	85	170	3	486	4010	29	47	2850	5	13	7	<0.4	<0.4	368	490000	6	17	12	<0.08	137	2.5	9	41
05/05/95	SH06.3	2	123	405	3	688	4050	27	64	3960	6	37	8	<0.4	<0.4	307	493000	5	17	16	0.2	108	4.5	12	59
05/05/95	SH06.4	0	110	115	3	447	3440	19	34	3050	5	9	7	<0.4	<0.4	127	490000	2	10	16	0.2	78	4.0	21	55
05/05/95	SH06.5	2	113	453	3	537	2760	18	63	2730	6	33	8	<0.4	<0.4	137	490000	2	10	6	0.3	124	<0.2	3	65
05/05/95	SH06.6	8	220	2460	3	1170	2890	25	206	12300	11	171	17	<0.4	<0.4	179	433000	6	23	18	0.2	132	0.5	18	161
02/05/95	SH08	7	193	1120	4	1440	9410	69	263	7930	8	122	16	<0.4	<0.4	6450	424000	55	101	27	0.2	356	5.0	17	191
05 05/95	SH08	9	208	1420	3	1630	9220	68	267	9200	10	131	16	<0.4	<0.4	5620	430000	52	100	30	0.3	346	1.0	21	227
05 05/95	SH09	24	358	3530	2	4260	13100	81	305	19300	15	491	40	<0.4	<0.4	4500	285000	45	63	39	0.5	326	2.8	51	474
05 05/95	SH11	29	280	5630	2	2440	4470	48	401	30200	19	455	51	403	2	3830	122000	83	158	54	0.1	362	<0.2	49	528
05/05/95	SH12	24	194	4190	1	1580	1420	29	157	25200	26	426	34	153	<0.4	635	33700	10	18	10	0.2	80	<0.2	33	370
05/05/95	SH13	31	281	5500	2	2530	4930	46	219	30600	26	515	49	248	1	1270	52400	28	55	31	0.2	184	<0.2	56	763
06/05/95	TC01	8	320	620	2	2890	27400	420	211	3460	11	185	17	<0.4	<0.4	945	423000	32	48	38	0.9	204	7.0	233	478
06/05/95	TC01	3	350	438	2	4010	23100	258	460	1810	6	542	12	<0.4	3	14600	257000	254	98	117	0.9	373	8.0	89	1050
06/05/95	TC01	0	113	85	3	547	4470	30	13	685	9	7	7	<0.4	<0.4	268	498000	5	9	3	<0.08	89	3.5	<1.2	36
03/05/95	WG01	10	113	908	1	1610	6020	30	86	5000	7	78	22	<0.4	<0.4	3220	443000	47	71	23	0.3	138	5.0	<1.2	1410
24/07/95	BB01	3	427	146	4	1430	12350	251	93	668	8	14	8	153	2	1040	465500	19	27	2	<0.08	75	<0.2	40	363
24/07/95	BB02	4	303	225	3	1620	21100	438	178	490	7	8	6	150	<0.4	19800	425000	103	49	2	<0.08	34	<0.2	21	189
29/07/95	CM01	35	588	2780	2	2440	43000	319	234	17300	20	438	29	82	1	5010	37700	29	52	86	0.3	129	<0.2	44	471
29/07/95	CM02	20	382	1670	1	1850	29200	184	578	9970	17	371	20	19	1	2970	21700	16	30	25	0.1	81	0.4	34	293
29 07/95	EY01	2	88	238	3	586	4700	34	16	1420	11	21	6	149	<0.4	180	460000	3	9	5	<0.08	75	<0.2	8	68
29/07/95	EY02	27	223	4320	1	2440	19700	53	550	24000	28	546	32	40	1	3480	29800	24	42	19	0.4	166	0.6	31	722
29/07/95	EY03	3	158	363	3	943	12000	89	98	1520	7	35	8	141	<0.4	3260	414000	77	32	11	<0.08	161	<0.2	6	2250
26/07/95	HR02	16	125	1740	1	619	593	10	91	15900	7	163	20	133	<0.4	244	374000	4	9	54	<0.08	77	<0.2	47	246
26/07/95	HR03	6	38	415	6	429	1070	8	22	36600	7	41	14	124	<0.4	320	349000	8	11	89	<0.08	131	<0.2	45	117
26/07/95	HR03A	40	355	3260	10	1450	4820	32	112	51400	15	446	31	113	<0.4	832	260000	21	37	144	0.2	266	<0.2	158	541
26 07/95	HR04	14	180	868	6	1980	12500	72	70	42200	13	173	28	118	<0.4	185	303000	3	15	62	<0.08	123	<0.2	38	244
26 07/95	HR05	4	88	313	0	287	712	4	12	7980	2	32	16	139	<0.4	47	388000	<0.2	<0.4	18	<0.08	20	<0.2	12	98
26/07/95	HR05A	11	253	710	28	2050	16000	117	110	113000	55	111	7	60	<0.4	2730	146000	77	181	238	<0.08	3830	7.5	71	257
26/07/95	HR06	2	243	98	0	329	746	3	2	5440	2	12	16	144	<0.4	56	420000	<0.2	<0.4	12	<0.08	12	<0.2	3	96
26/07/95	HR07	4	88	223	0	308	556	3	8	6210	2	24	15	142	<0.4	53	417000	<0.2	<0.4	10	<0.08	7	<0.2	3	99
26 07 95	HR08	12	198	563	35	998	9640	82	62	138000	63	96	8	53	<0.4	2400	124000	45	73	247	0.3	1930	3.5	74	200
26 07 95	HR09	11	338	1020	23	1840	14450	111	129	87700	48	124	9	72	<0.4	2420	188000	76	186	238	<0.08	3440	8.3	51	458
26 07/95	HR09 siev	15	180	703	36	1650	15300	117	75	151000	66	104	7	33	<0.4	2580	60300	76	175	225	0.5	4310	9.0	93	553
26/07/95	HR10	70	295	4430	5	3240	9540	63	163	41800	25	385	48	39	3	5010	70000	86	165	195	0.3	983	2.1	80	824

Date	Sample	Li	Na	K	Be	Mg	Ca	Sr	Ba	Al	La	Ti	V	Cr	Mo	Mn	Fe	Co	Ni	Cu	Ag	Zn	Cd	Pb	P
		µg g^{-1}	µg g^{-1}	µg g^{-1}	µg g^{-1}	µg g^{-1}	µg g^{-1}	µg g^{-1}	µg g^{-1}	µg g^{-1}	µg g^{-1}	µg g^{-1}	µg g^{-1}	µg g^{-1}	µg g^{-1}	µg g^{-1}	µg g^{-1}	µg g^{-1}	µg g^{-1}	µg g^{-1}	µg g^{-1}	µg g^{-1}	µg g^{-1}	µg g^{-1}	µg g^{-1}
26/07/95	HR11	41	331	4150	10	4670	16000	83	214	57300	29	418	33	24	1	5830	69900	107	206	108	0.2	2090	5.3	109	1550
26/07/95	HR12	42	222	4540	2	3280	6130	46	301	28800	28	460	34	35	1	5470	34800	62	115	48	<0.08	420	1.8	65	637
26/07/95	HR14	46	255	5170	2	2610	3790	40	277	29600	24	522	37	25	1	1520	30900	22	47	30	0.4	214	0.5	58	567
26/07/95	HR15	52	266	5050	3	2750	7380	52	293	30800	24	450	48	31	2	4280	39600	52	111	115	0.4	491	0.9	112	758
27 07/95	LL01	51	265	6330	2	2650	2600	47	343	36300	24	546	41	14	1	1400	36650	22	36	26	0.3	290	0.8	371	1230
27/07/95	LL02	18	113	1350	4	520	1430	21	182	50900	12	233	13	123	<0.4	212	329000	3	6	47	<0.08	151	<0.2	48	197
27/07/95	LL03	18	175	2110	2	792	1630	33	235	31100	17	276	20	129	<0.4	235	357000	2	7	46	0.3	109	<0.2	62	325
27/07/95	LL04	10	80	1080	1	681	2150	21	363	7850	8	172	14	129	<0.4	356	360000	8	18	13	<0.08	416	<0.2	195	815
27/07/95	LL04B	2	213	78	1	640	7260	64	53	1050	4	8	7	150	<0.4	313	449000	8	24	2	<0.08	129	<0.2	6	118
27/07/95	LL05	36	229	3650	6	3000	6630	54	99	35200	38	434	33	21	1	3200	153000	47	47	38	0.4	805	4.9	490	9930
28/07/95	QH01	70	1130	7270	3	9780	12600	88	285	50100	26	824	116	30	3	384	39000	18	81	106	0.6	409	0.8	101	536
28/07/95	QH02	41	768	3290	5	13600	30700	120	187	33900	18	888	80	45	6	1670	99200	30	56	143	0.4	654	<0.2	147	719
28/07/95	QH03	34	584	2690	5	3490	6040	60	41	34250	14	766	64	74	7	963	157000	19	38	110	0.6	351	<0.2	130	430
28/07/95	QH04	6	563	633	9	568	1780	31	208	27400	48	52	59	121	17	527	357000	17	18	160	0.2	448	<0.2	321	267
28/07/95	QH05	66	612	4140	4	3670	6900	196	410	34300	14	799	61	22	4	542	45000	33	78	160	0.5	1300	3.4	95	696
28/07/95	QH06	69	514	2810	6	2200	3430	613	<0.04	32400	21	584	47	18	6	8480	75800	230	158	209	0.5	2830	6.3	189	562
28/07/95	QH07	24	218	3600	1	1580	7910	45	223	18400	21	368	23	17	1	1200	17850	11	27	12	0.2	106	0.8	20	260
28/07/95	QH08	26	289	3000	2	1970	3890	113	1520	18100	11	472	26	14	1	2210	22000	42	67	40	0.1	1070	1.9	50	246
28/07/95	QH09	33	281	3650	1	2040	3370	51	629	20000	18	481	25	15	1	691	19200	14	37	26	0.1	404	0.7	38	227
28/07/95	QHW-4	17	998	1410	2	928	2240	29	115	24500	8	182	27	102	2	158	271000	12	22	150	<0.08	574	<0.2	65	1510
29/07/95	SH05	34	328	6930	3	2460	4350	51	292	31600	20	446	48	78	<0.4	1910	151000	26	52	79	<0.08	435	<0.2	48	538
29 07/95	SH06	2	35	330	2	659	4400	24	33	1920	7	25	5	155	<0.4	165	504000	<0.2	10	3	<0.08	89	<0.2	<1.2	100
29 07/95	SH06 dry	1	40	60	2	577	4340	26	26	1950	4	5	5	150	<0.4	541	465000	10	26	9	<0.08	111	<0.2	23	66
29/07/95	SH07	11	178	1750	2	1510	9800	76	199	8350	7	172	16	140	<0.4	6910	398000	59	71	20	<0.08	322	<0.2	18	173
29/07/95	SH08	6	138	1090	3	1490	11600	86	232	5730	5	91	11	143	<0.4	15100	409000	136	211	17	<0.08	427	<0.2	9	116
29/07/95	SH09	13	395	1800	2	3760	17800	102	238	10200	12	337	26	134	<0.4	7630	336000	61	96	26	0.5	360	<0.2	54	348
29/07/95	SH10	9	288	1390	1	2890	17100	111	325	6740	8	115	14	141	<0.4	21400	426750	174	229	16	<0.08	438	<0.2	18	198
29/07/95	SH11	35	377	5810	2	3470	8950	70	294	31000	19	393	52	25	1	12600	164000	110	174	57	<0.08	417	<0.2	73	869
29 07/95	SH12	34	294	5070	1	2160	1880	36	205	29800	22	403	40	15	1	978	35300	13	23	14	0.2	96	<0.2	42	426
29/07/95	SH13	28	393	4330	2	3440	11300	65	227	24700	22	525	52	30	1	1590	44100	17	43	40	0.1	192	<0.2	67	1170
29/07/95	SH14	23	182	4230	1	1730	2360	35	243	22200	34	394	33	53	1	3100	43000	28	48	21	<0.08	150	<0.2	32	646
29 07/95	SH15	33	324	5920	1	3260	7650	56	294	31900	26	494	46	21	1	2890	45700	27	53	35	0.2	277	0.4	173	1080
29 07/95	SH16	29	231	5640	1	2320	3250	39	373	30000	22	481	36	13	1	3340	39000	23	41	20	0.1	190	<0.2	53	637
24 07/95	TC01	46	528	1390	2	12000	37700	293	458	10900	18	920	32	347	2	2460	257000	63	66	225	5.3	1300	16.8	3630	544
25/07/95	WG01	6	188	333	0	771	1330	5	16	1660	3	39	6	143	<0.4	301	463000	1	4	4	<0.08	9	<0.2	<1.2	202
25 07/95	WG01B	15	100	1240	0	2560	3700	21	77	6940	8	277	17	132	<0.4	1870	373000	33	24	9	<0.08	48	<0.2	20	549

Date	Sample	Li	Na	K	Be	Mg	Ca	Sr	Ba	Al	La	Ti	V	Cr	Mo	Mn	Fe	Co	Ni	Cu	Ag	Zn	Cd	Pb	P
		$\mu g\,g^{-1}$	$\mu g\,g^{-1}$	$\mu g\,g^{-1}$	$\mu g\,g^{-1}$	$\mu g\,g^{-1}$	$\mu g\,g^{-1}$	$\mu g\,g^{-1}$	$\mu g\,g^{-1}$	$\mu g\,g^{-1}$	$\mu g\,g^{-1}$	$\mu g\,g^{-1}$	$\mu g\,g^{-1}$	$\mu g\,g^{-1}$	$\mu g\,g^{-1}$	$\mu g\,g^{-1}$	$\mu g\,g^{-1}$	$\mu g\,g^{-1}$	$\mu g\,g^{-1}$	$\mu g\,g^{-1}$	$\mu g\,g^{-1}$	$\mu g\,g^{-1}$	$\mu g\,g^{-1}$	$\mu g\,g^{-1}$	$\mu g\,g^{-1}$
25 07 95	WG02	30	318	5520	1	3160	4150	41	346	28300	24	536	39	24	1	2350	32300	14	31	27	0.3	153	0.2	92	694
25/07/95	WG03	33	299	5930	1	3250	4780	48	370	30800	24	411	40	20	1	24890	96650	224	91	25	0.2	194	0.3	64	731
22/11/95	EY01	2	115	128	3	495	3850	28	14	895	8	13	7	152	<0.4	164	457000	3	10	3	<0.08	97	<0.2	8	53
22/11/95	EY02	19	116	3080	1	1770	2340	38	562	16700	105	507	36	156	1	1130	31500	16	28	39	0.2	195	0.9	28	510
22/11/95	EY03	19	130	3240	1	1640	1840	28	379	17100	21	360	26	17	1	738	25000	14	26	24	0.1	101	0.8	26	352
21/11/95	HR04	3	85	130	4	294	1210	8	10	34000	5	24	2	97	<0.4	48	490000	<0.2	4	53	<0.08	56	<0.2	14	145
21/11/95	HR07	2	5	113	1	156	268	2	9	4460	2	16	13	141	<0.4	40	405000	<0.2	<0.4	33	<0.08	29	<0.2	9	70
21/11/95	HR07A	16	90	1630	1	581	743	14	115	12000	8	228	21	132	<0.4	242	364000	2	5	67	<0.08	98	<0.2	57	216
21/11/95	HR08	51	234	4820	2	2070	2570	42	173	30500	22	590	38	29	2	1570	50200	22	32	39	0.2	181	<0.2	55	363
21/11/95	HR09	64	220	5170	2	1880	2680	43	101	32500	24	538	41	17	7	19600	61000	245	534	72	<0.08	1290	5.6	56	398
21/11/95	HR09	56	212	4490	7	1800	3620	48	176	48800	31	421	37	24	2	3610	89200	61	104	91	0.2	863	1.5	62	450
21/11/95	HR10	79	390	6180	3	3120	9010	69	157	42250	28	610	65	53	5	5290	59200	65	128	130	0.4	580	1.7	239	1090
19 11/95	QH01	81	978	9540	3	10700	15400	97	94	55600	27	835	125	37	4	449	35800	18	84	134	1.0	587	1.9	151	803
19 11/95	QH02	51	709	4700	4	7550	17000	79	95	44600	25	627	73	33	6	968	120000	20	51	103	0.4	560	<0.2	181	900
19/11/95	QH03	38	758	3120	5	12300	28700	157	1030	29700	25	1390	96	147	9	1450	91100	28	79	132	0.7	611	<0.2	213	648
19 11/95	QH04A	68	647	4990	4	3280	5170	326	776	40100	21	879	69	29	5	1670	53600	38	86	177	1.0	1160	2.4	187	874
19/11/95	QH07	27	173	4270	1	1530	1130	25	215	21850	19	465	27	16	1	604	17900	13	26	17	0.2	79	0.6	23	202
19/11/95	QH09	29	196	4740	1	2020	1710	87	910	24600	19	590	30	16	1	873	23100	15	32	20	0.4	289	1.0	34	260
18/11/95	SH05	49	403	9280	4	2930	2790	54	328	45200	27	411	62	23	4	3740	116000	44	86	89	0.2	474	<0.2	70	648
18 11/95	SH06	2	240	295	1	429	3530	26	27	615	5	7	5	155	<0.4	161	486000	3	15	2	<0.08	141	<0.2	<1.2	44
18/11/95	SH09A	9	658	1280	2	1510	13700	116	299	6290	5	106	17	138	<0.4	8130	378000	65	136	48	<0.08	458	<0.2	17	164
18/11/95	SH10A	16	222	3940	1	1600	2760	36	380	18300	19	298	30	20	1	2060	49500	23	41	19	<0.08	118	4.4	23	346
18/11/95	SH11	31	380	5640	2	2690	7350	61	310	29400	23	403	52	29	3	4760	105000	58	115	60	0.2	296	0.8	74	603
18/11/95	SH13	21	293	3740	1	2300	8320	53	181	20900	20	448	46	17	2	968	36100	11	23	29	0.1	130	1.0	58	524
18/11/95	SH15	18	177	3600	1	1330	2240	29	191	18000	14	286	28	9	1	1280	31100	15	28	18	0.1	141	1.0	46	444
20/11/95	WG01	7	85	925	1	1030	2870	21	106	4990	5	97	25	144	<0.4	6320	432000	170	47	24	<0.08	146	<0.2	6	2530
20 11/95	WG02	21	167	4590	1	1820	1880	31	266	22700	25	414	30	12	1	797	28800	11	21	15	0.2	136	0.8	38	491
20/11/95	WG03	24	160	4510	1	3130	3350	36	325	23500	58	385	35	40	1	2790	43700	35	37	20	0.2	112	0.5	53	644
10 03/96	BB01	2	343	250	3	2150	18000	338	131	1350	9	43	9	149	<0.4	843	459000	10	17	4	<0.08	74	<0.2	102	294
10/03/96	BB02	7	700	675	3	1680	20300	406	344	2100	9	37	9	156	<0.4	45000	371000	236	119	7	<0.08	110	<0.2	107	461
14 03/96	HR04	3	48	128	5	308	1340	9	10	34900	3	23	13	128	<0.4	55	352000	<0.2	5	53	<0.08	62	<0.2	23	145
14 03/96	HR07	2	18	165	6	149	349	2	11	45500	3	23	10	117	<0.4	42	342000	<0.2	<0.4	76	<0.08	41	<0.2	21	137
14 03/96	HR07A	45	242	4970	3	1270	391	31	111	40700	20	526	45	54	1	323	88100	7	17	64	0.2	109	<0.2	67	444
14 03/96	HR08	54	283	5820	8	1630	1070	39	92	58000	27	659	50	65	5	480	84000	12	26	188	0.6	172	<0.2	76	455
14 03/96	HR09	48	266	4520	12	1480	3020	41	151	62200	31	409	39	70	1	1350	112000	24	44	180	0.3	546	<0.2	67	372
14 03/96	HR10	102	436	7960	4	3150	6930	75	205	52700	33	577	67	64	4	3410	70700	61	111	103	0.4	591	1.1	155	695

Date	Sample	Li	Na	K	Be	Mg	Ca	Sr	Ba	Al	La	Ti	V	Cr	Mo	Mn	Fe	Co	Ni	Cu	Ag	Zn	Cd	Pb	P
		µg g^{-1}	µg g^{-1}	µg g^{-1}	µg g^{-1}	µg g^{-1}	µg g^{-1}	µg g^{-1}	µg g^{-1}	µg g^{-1}	µg g^{-1}	µg g^{-1}	µg g^{-1}	µg g^{-1}	µg g^{-1}	µg g^{-1}	µg g^{-1}	µg g^{-1}	µg g^{-1}	µg g^{-1}	µg g^{-1}	µg g^{-1}	µg g^{-1}	µg g^{-1}	µg g^{-1}
14/03/96	HR11	23	205	3780	1	1790	2600	31	358	20100	27	420	29	31	1	796	26900	18	33	21	0.2	164	0.6	42	411
11/03/96	QH02	37	755	3090	11	19100	33800	67	357	47100	35	542	91	118	11	588	159000	16	46	157	<0.08	790	<0.2	489	929
11/03/96	QH03	47	910	3790	9	10700	23100	111	127	41300	36	578	92	104	8	1580	104000	68	62	172	0.8	928	<0.2	292	879
11/03/96	QH05	42	546	2940	5	2160	4980	1485	53100	28850	34	546	45	59	5	2430	78150	62	134	249	1.7	3330	8.7	315	500
11/03/96	QH06	53	457	3220	6	1730	3090	1450	47100	33900	24	660	43	69	5	2420	71500	89	126	230	1.3	3360	8.0	311	496
11/03/96	QH07	22	170	3350	1	1230	1020	23	354	17000	47	436	24	43	0	600	16600	11	22	11	<0.08	78	<0.2	22	206
11/03/96	QH09	21	188	3420	1	1490	1420	64	938	17200	18	419	24	49	1	687	19900	13	26	15	<0.08	216	0.5	27	199
13/03/96	SH05	49	424	10600	3	3220	2310	62	475	48600	31	427	61	77	3	2390	112000	31	73	77	0.4	336	<0.2	65	648
13/03/96	SH06	4	80	960	3	636	2830	19	86	8780	8	69	9	150	<0.4	119	468000	<0.2	12	30	<0.08	78	<0.2	39	84
13/03/96	SH07	31	358	6270	3	2390	4630	55	565	29950	21	508	44	99	<0.4	2880	202500	37	65	66	<0.08	316	<0.2	59	419
13/03/96	SH07B	3	240	455	5	891	8750	58	143	8430	8	33	9	139	<0.4	1190	429000	13	34	52	<0.08	255	<0.2	36	182
13/03/96	SH09	31	1060	5570	2	2650	7490	72	290	26400	19	340	44	95	1	13900	177000	131	343	49	<0.08	408	<0.2	67	447
13/03/96	SH10	26	594	4450	2	2770	8360	64	402	22300	18	329	40	78	1	7220	159000	76	137	43	0.1	345	<0.2	55	496
13/03/96	SH11	33	407	5570	3	2720	6670	62	330	28800	24	346	54	73	2	3690	119000	65	123	60	0.3	365	<0.2	77	663
13/03/96	SH12	18	165	3650	1	1180	920	25	194	19000	36	337	29	62	<0.4	1090	26200	13	16	8	<0.08	63	<0.2	26	268
13/03/96	SH13	23	204	4050	1	1330	1310	30	203	23200	20	443	32	30	1	970	26200	13	21	11	0.1	81	<0.2	35	336
13/03/96	SH15	19	312	3650	1	1430	2860	35	292	18800	19	295	32	31	1	1520	40300	20	35	20	<0.08	179	<0.2	41	441
09/10/96	BB01	1	188	88	3	1120	15800	350	117	350	10	5	1	<0.4	<0.4	789	456000	14	20	1	0.3	30	<0.2	9	251
09/10/96	HR04	10	210	925	6	545	815	11	82	26600	10	154	23	16	<0.4	151	309000	1	8	73	0.3	62	<0.2	60	210
08/10/96	HR07	12	160	1110	1	363	492	8	61	16400	7	155	12	13	<0.4	73	370000	<0.2	2	29	<0.08	20	<0.2	32	160
08/10/96	HR08	26	255	2100	20	1200	6470	66	254	69700	64	329	15	9	<0.4	8990	176000	166	199	249	<0.08	1990	<0.2	54	336
08/10/96	HR09	37	388	2340	20	1600	8490	79	263	81600	51	415	19	10	<0.4	7040	121000	168	227	212	0.3	2800	5.5	68	443
08/10/96	HR10	78	395	4950	8	2940	9500	78	234	52800	33	448	45	27	2	7320	97600	129	236	145	0.5	1700	1.1	142	1170
08/10/96	HR11	42	329	4750	5	3970	10900	67	262	37400	28	402	35	23	<0.4	11300	54000	109	188	71	0.4	1090	1.7	87	1340
09/10/96	QH01	23	700	2050	7	7840	15000	55	292	37700	27	515	66	33	15	402	246000	9	30	122	0.8	457	<0.2	290	665
09/10/96	SH06	1	195	185	2	425	2580	17	30	1660	9	17	<0.2	<0.4	<0.4	171	491000	3	17	6	0.4	148	<0.2	9	60
04/07/97	BB01	1	125	75	4	988	12800	284	99	390	12	5	<0.2	<0.4	<0.4	723	460000	11	18	1	<0.08	41	<0.2	12	300
04/07/97	HR04	10	163	560	6	1280	11000	60	55	40500	11	120	17	96	<0.4	136	321000	<0.2	12	61	<0.08	105	<0.2	27	250
04/07/97	HR07	2	88	188	2	167	282	2	12	18500	4	23	5	9	<0.4	43	376000	<0.2	<0.4	71	<0.08	62	<0.2	15	123
04/07/97	HR07A	16	168	1970	1	644	466	12	95	14800	11	390	19	21	<0.4	152	341000	1	6	36	0.3	54	<0.2	26	285